CORA Cork Open Research Archive
Cartlann Taighde Oscailte Chorcaí

Title	Aiming at the lung microbiota in adult asthma; an asthmatic immune microbe dialogue?
Authors	Sullivan, Ashley
Publication date	2020
Original Citation	Murphy, A. 2020. Aiming at the lung microbiota in adult asthma; an asthmatic immune microbe dialogue?. PhD Thesis, University College Cork.
Type of publication	Doctoral thesis
Rights	© 2020, Ashley Sullivan. - https://creativecommons.org/licenses/by-nc-nd/4.0/
Download date	2026-11-15 11:59:39
Item downloaded from	https://hdl.handle.net/10468/11362

UCC
University College Cork, Ireland
Coláiste na hOllscoile Corcaigh

Ollscoil na hÉireann, Corcaigh

National University of Ireland, Cork



Aiming at the lung microbiota in adult asthma; an asthmatic immune microbe dialogue?

Thesis presented by

Ashley Sullivan, B.Sc

https://orcid.org/0000-0001-7718-9305

for the degree of

Doctor of Philosophy

University College Cork

School of Medicine

Head of School: Prof. Paula O'Leary

Supervisors: Dr John MacSharry and Dr Desmond Murphy

2020

Contents

Acknowlegements 4

Acronyms 6

Chapter 1 - Literature Review - Aiming at the lung microbiota in adult asthma; an asthmatic immune microbe dialogue? 11

Chapter 2 - Study Cohorts' - Asthmatic patient bronchoscopy and patient sample collection protocols. 52

Chapter 3 - Fungi in Asthma - The presence of *Aspergillus fumigatus* in the asthmatic airways is not clearly related to clinical disease severity. 63

Chapter 4 - The Microbiome of the Lung - A study to define microbiome subtypes in the adult asthmatic airway. 105

Chapter 5 - The Effect of Immunomodulation Therapy on the Microbiome of the Adult Asthmatic Lung - An investigation into the effects of anti-IgE (Omalizumab/Xolair) treatment on the lung microbiome in a subset of adult asthmatic patients 190

Chapter 6 - The Microbiome of the Lung - A study into the effect of anti-IL-5 therapy on the lung microbiome in a cohort of adult asthmatic patients 252

Chapter 7 - Epithelial Responses to Inflammatory Stimuli - The response of asthmatic airway bronchial epithelial cells (Beas-2B) to microbial compounds, cytokines and metabolites . 311

Chapter 8 - Bronchial Brushings and Inflammatory Stimuli - Examination of bronchial brushings as a method to investigate the inflammatory response of the asthmatic cohort 374

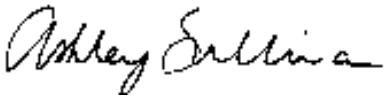
Chapter 9 - Primary Cell Culture Techniques - Future directions in primary cell culture techniques 411

Chapter 10 - Immunoglobulins and Asthma - BAL and serum immunoglobulin profiling in a cohort of asthmatic patients 450

Thesis Summary and Future Directions 488

Appendix 496

This is to certify that the work I am submitting is my own and has not been submitted for another degree, either at University College Cork or elsewhere. All external references and sources are clearly acknowledged and identified within the contents. I have read and understood the regulations of University College Cork concerning plagiarism

Signed: 

Ashley Sullivan

Acknowlegements

I would like to acknowledge and offer my most sincere thanks to the patients who have participated in this study, without whom this research could not have taken place.

I would like to give special acknowledgement to my PhD Supervisors Dr John MacSharry and Dr Desmond Murphy. Thank you both for the amazing opportunity to be a member of your lab group, researching such a novel, exciting and rewarding topic for my PhD. Thank you for your constant guidance and mentorship during the PhD process. Thank you both for always being willing to encourage me and for enabling me to take part in amazing opportunities from presentations, publications, conferences and fellowships to name but a few!

I would like to acknowledge APC Microbiome Ireland for the opportunity to carry out my research within APC Microbiome Ireland, I really enjoyed my time within the institute.

Thank you to Brigita Motuzyte, Dr Susan Lapthorne and Dr Eoin Hunt for welcoming me into the lab group.

Thank you to Dr Katie Dadswell and Dr Bernie Crowley, it was a pleasure to have the opportunity to work with you – thanks for all of your help.

To all in the APC Host – Microbe Dialogue group in lab 4.38, thanks for all of your assistance and guidance which I received during my PhD, it was a pleasure to work with you all.

Thanks to Caroline O'Donovan for all of her kind emails, for keeping me updated with patient bronchoscopy schedules and her amazing help with organising patient data at the end of my research – it is much appreciated!

To the doctors, nurses, porters and all involved in the Endoscopy Unit, Cork University Hospital, thank you for making me welcome every time while I waited to collect samples. A special thanks to Deirdre Flynn for all your help with patient lung function testing and the ACQ-7 questionnaires.

Thanks to Eva McArdle and Grainne Heelan for being ready to help when needed- it is much appreciated.

To Colette Crowley for all of her help with placing any order I needed during my PhD and a special thanks to her for going the extra mile any time I had to ship samples to America – she always calmed my nerves!

A sincere thank you to Dr Chris Ward, Professor Jeff Pearson, Dr Bernard Verdon, Dr Emily Mavin, Dr Matt Wilcox, Dr Vinciane Saint-Criq, Dr Peter Chater, Abdulla Althuwaybi and Livia Delpiano for making me feel so at home during my time at Newcastle University and for the most valued guidance and mentorship which they provided.

To Emma, Brigita, Jenna, Angelikh, Nada, Emily, Jennifer, Ashleigh and Grainne – Thank you for your encouragement and advice over many coffees.

A special thanks to Emma for always being ready to support with any worry or problem I might have had during my PhD, and for being willing to listen to countless poster and presentation run-throughs before each conference!

Thank you to my amazing family and friends at home in Kerry, I appreciate all the help and encouragement you have given me, you are all amazing! A special thank you to my sister Debbie and my brother Thomas for all of your support.

Without two special people I feel I never would have managed to achieved this and therefore it feels right that this thesis be dedicated to them-

To my Mom; words cannot begin to explain how much your constant encouragement, guidance, love, optimism, belief and support means to me. Thank you for everything you have done to help me get to this stage!! Love you x

And in memory of my Gaga (Grandad), Diarmuid Lawlor; thank you for all of the drives to school, the encouragement and advice when needed, or gentle presence in later years, you were one amazing grandfather. I miss you greatly and wish you could have made it to this graduation too!

Acronyms

ABPA – Allergic Bronchopulmonary Aspergillosis

ACQ-7 – Asthma Control Questionnaire 7

ALI – Air Liquid Interface

ANOVA – Analysis of Varience

APC – Antigen Presenting Cell

ASM – Airway Smooth Muscle

ATS – American Thoracic Society

ATTC – American Type Culture Collection

BAL – Bronchoalveolar lavage

Bmal1 – Brain and muscle ARNT-like 1

BMI – Body Mass Index

BP – Bacteria Pellet

CCL20 – C-C motif Ligand 20

CCRF – Cork Clinical Research Facility

CD4+T – T helper cell

CF – Cystic Fibrosis

COPD – Chronic Obstructive Pulmonary Disease

CP – Cellular/Cell Pellet

CRP – C-Reactive Protein

CT – Computed Tomography

Ct/Cp – Cycle Threshold/Crossing Point

CXCL – C-X-C motif Ligand

DAMP – Damage Associated Molecular Pattern

DC – Dendritic Cell

DMSO- Dimethyl Sulfoxide

DNA – Deoxyribonucleic Acid

DPX – Distyrene Plasticizer Xylene

EDTA – Ethylenediaminetetraacetic Acid

ELISA – Enzyme Linked Immunosorbent Assay

EMA – European Medicines Agency

ERS – European Respiratory Society

ESR – Erythrocyte Sedimentation Rate

EGR1 – Early Growth Response

FBS – Foetal Bovine Serum

FDA – Food and Drug Administration

FeNO – Fractional exhaled Nitric Oxide

FEV1 – Forced Expiratory Volume in the first second

FLVR – *Faecalibacterium, Lachnospira, Veillonella, Rothia*

FVC – Forced Vital Capacity

GABA – Gamma-aminobutryic Acid

GINA – Global Initiative for Asthma

GM-CSF – Granulocyte-Macrophage Colony-Stimulation Factor

GOI – Gene of Interest

GOR – Gastro-Oseophageal Reflux

GPR – G-Protein coupled Receptor

Hb – Haemoglobin

HDAC – Histone deacetylase

HDM – House Dust Mite

HK – House Keeper

HS – High Sensitivity

IAA – Indole Acetic Acid

ICS – Inhaled Corticosteroids

ICU – Intensive Care Unit

IFN - Interferon

Ig – Immunoglobulin

IL - Interleukin

ILC – Innate Lymphoid Cell

IPF – Idiopathic Pulmonary Fibrosis

ITS – Internal Transcribed Spacer

LABA – Long Acting Beta Agonist

LPS - Lipopolysaccharide

LDC's – Lung Dendritic Cells

mRNA – Messenger Ribonucleic Acid

MSD – MesoScale Discovery ELISA

NADPH – Nicotinamide Adenine Dinucleotide Phosphate

NFκβ – Nuclear Factor Kappa Beta

NGS – Next Generation Sequencing

NK – Natural Killer Cell

NTC – No Template Control

OCDB – One Codex Data Base

Pa – *Pseudomonas aeruginosa*

PAMP – Pathogen Associated Molecular Pattern

PBEC – Primary Bronchial Epithelial Cells

PBS – Phosphate Buffered Saline

PCoA – Principle Coordinates Analysis

PCR – Polymerase Chain Reaction

PG – *Porphyromonas gingivalis*

PNEC – Primary Nasal Epithelial Cells

PRM – Pathogen Recognition Molecule

PRR – Pathogen Recognition Receptor

PT – Pertussis Toxin

qPCR – quantitative Polymerase Chain Reaction

qRT-PCR – quantitative Reverse Transcriptase-Polymerase Chain Reaction

RML – Right Middle Lobe

RNA – Ribonucleic Acid

rRNA – ribosomal Ribonucleic Acid

RSV – Respiratory Syncytial Virus

RT-PCR – quantitative Reverse Transcriptase-Polymerase Chain Reaction

RV – Respiratory Virus

SA – Sodium Acetate

SABA – Short Acting Beta Agonist

SAFS – Severe Asthma with Fungal Sensitisation

SCFA – Short Chain Fatty Acid

SNP – Single Nucleotide Polymorphism

Sp – Species

TGF – Transforming Growth Factor

Th – T helper

TLR – Toll-Like Receptor

TNF – Tumour Necrosis Factor

TSLP – Thymic Stromal Lymphopoietin

Tregs – Regulatory T cells

WBC – White Blood Cell Count

Abstract

Within this thesis we have reported novel findings which will contribute to a better understanding of the role the microbiome plays within the lungs of clinically diagnosed asthmatic patients. The prevalence of asthma is increasing in the western world with more than 300 million people worldwide believed to affected by this chronic respiratory disorder. Through this thesis we have dissected the immune microbe dialogue at play within the asthmatic lung. The findings within this thesis are novel, and we feel add to recent discoveries within the field of microbiome research, with an emphasis on the potential contribution the lung microbiome may play in the pathogenesis of asthma.

Chapter 1

Literature Review

Aiming at the lung microbiota in adult asthma; an asthmatic immune microbe dialogue?

Author Contributions: Ashley Sullivan wrote the manuscript with significant contribution from Eoin Hunt, John MacSharry and Desmond Murphy.

This chapter has been published in part in Respiratory Medicine

'The Microbiome and the Pathophysiology of Asthma'

https://doi.org/10.1186/s12931-016-0479-4

PMCID: PMC5139145

Abstract 13
Background 14
Microbes and the airway 15
Lung environment 17
Sample collection and the lungs 20
Asthma characteristics 24
Asthma treatment strategies 26
Epithelial development and the role of the microbiota 29
Microbes and the host 31
The virome and asthma 40
The mycobiome and asthma 41
Conclusions 44
References 45

Abstract

Asthma is a chronic respiratory disease whose prevalence is increasing in the western world. Recently research has begun to focus on the role the microbiome plays in asthma pathogenesis in the hope of further understanding this respiratory disorder. Considered sterile until recently, the lungs have revealed themselves to contain a unique microbiota. A shift towards molecular methods for the quantification and sequencing of microbial DNA has revealed that the airways harbour a unique microbiota with apparent, reproducible differences present between healthy and diseased lungs. There is a hope that in classifying the microbial load of the asthmatic airway an insight may be afforded as to the possible role pulmonary microbes may have in propagating an asthmatic airway response. This could potentially pave the way for new therapeutic strategies for the treatment of chronic lung conditions such as asthma.

Background

Asthma has seen a staggering rise in prevalence in recent years with more than 300 million people worldwide believed to be affected by this chronic respiratory disorder[1-3]. The burden of asthma is felt globally, however it is in developed countries that asthma has come to the fore as a health care concern where the incidence rate of asthma and in particular adult onset asthma has risen so dramatically that this respiratory disorder has reached epidemic proportions[4,5]. The incidence of childhood asthma in the western world has also reached worrying levels[6].

Recently research has begun to focus on the role microbes play in this chronic respiratory disorder. Thanks to advances in sequencing technologies it is now possible to dissect the role microbial composition and diversity can play in a multi-factorial disorder such as asthma[7]. It is beginning to become clear that there are clear differences present between asthmatics and non-asthmatics and the microbial load they carry[7,8]. See figure 1. Through gaining an insight into the unique microbiota of asthmatics much may be revealed, as has happened with gastrointestinal research, which could undoubtedly aid in disease prognosis and treatment.

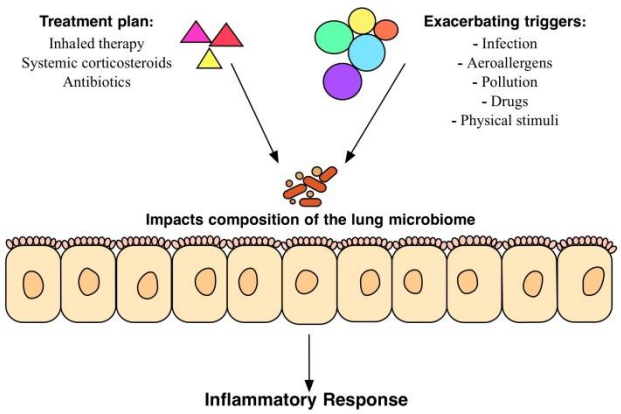


Figure 1 Studies have shown that there are clear differences present between asthmatics and non-asthmatics and the microbial load they carry. Factors such as treatment plans and exacerbating triggers are believed to impact the composition of the lung microbiome[8].

Microbes and the airway

While research into respiratory diseases has rewarded us with pharmacological treatments such as inhaled corticosteroids, leukotriene receptor antagonists, β agonists and more recently targeted monoclonal therapies which have helped alleviate the burden of asthma, it is only since ca. 2010 that research has confirmed that the environment of the lungs are not sterile as had previously been believed[9,10]. Prior to this the prevailing dogma was that if bacteria were detected in the lower respiratory tract it is understood to represent an abnormal health state and that the healthy lung was sterile[11]. This belief arose mainly due to poor, ineffective microbial culturing techniques which were unable to replicate the lung habitat and culture the microbes from respiratory specimens[12]. However it is clear that although the lung contains a smaller bacterial burden than in the upper respiratory tract there is a distinct microbiota present in the lower airways of healthy individuals[13]. This finding that the lungs harbour a unique microbiota irrespective of health or disease has led to the surge of research now taking place in an effort to not only categorise the distinct microbiota of the diseased lung but also that of the healthy lung[14]. Thanks to the advancement of culture independent techniques the unique steady state microbiota of the lungs is being elucidated[7,11]. A change in the microbial composition of the lower airway microbiota may be connected with chronic lung disease such as asthma[2,15].

The development of inexpensive next generation sequencing techniques, developed for the Human Genome Project to sequence the human genome, has made it possible to determine microbial, in particular bacterial, communities in a culture independent manner. By screening the diversity of bacterial ribosomal rRNA genes present in biological nucleic acid samples against sequence databases and development of bioinformatic algorithms have enabled the organisation and interpretation of the huge data sets made available by these sequencing machines[16,17]. Meta-genomic approaches have enabled a far greater understanding of the microbes present at various sites and the role they play in the overall host-microbiome interaction[17]. Thanks to culture independent techniques low levels of

oral bacteria such as *Prevotella* and *Veillonella* have been discovered in the lower airways of healthy individuals[17-19].

It is noted that lifelong microbial exposure can have beneficial effects upon the human host; however, maladaptive microbiota-host interactions have the potential to lead to disease prognosis[20]. Through the exposure to microbial species the hosts immune system can elicit a number of responses, from direct interaction of the hosts immune system and the microbiota to the ability of the microbiota to alter the hosts metabolic functions and the potential of the host to either prevent or promote microbial invasion[20].

In both diseased and non-diseased states the airways provide a mucosal environment with distinct niches and resources for the commensal microbes which have been discovered to be present, leading to a complex and changing host environment for the microbes residing in the lungs[20]. It is known that microbes possess the ability to interact with the human host in a manner so as to alter their host environment, which can provide the microbe with a novel niche environment or the potential to create a barrier to subsequent microbial exposures to their niche, however such an interaction on behalf of the microbes can lead to in certain cases to negative effects for the human host[20].

Overall research with respect to the microbial host interactions present within the respiratory environment will lead to a greater understanding of a site which until ca. 2010 was considered sterile and may lead to major implications for disease prognosis and therapeutic strategies.

Lung environment

With a surface area of 75 m^2 and direct exposure to the environment, the lungs are prime sites for microbial exposure[12]. As the environmental conditions shape the composition of the microbial communities in that habitat it is important to understand the environment of the lungs to fully understand the potential microbes which could inhabit this location, see figure 2.

The anatomy of the airways can in part explain the variances found with respect to microbial density observed. For example the nasal passage is continuously exposed to the environment and as a result, a continuous flow of particle debris and microbes results in leading to a relatively high density of microbes present in this location. The trachea in turn is exposed to debris particles and microbes as well as the potential exposure to oropharynx aspirated microbes. Through the process of mucociliary clearance, the lower airways are in theory protected from particle and microbe invasion, however microbes have been found through advances in sequencing technologies, to reside in the lower respiratory tract[20]. While the upper and lower respiratory tracts may be exposed in theory to the same microbes differences are present with respect to the bacterial abundance[20].

The lungs cannot be viewed as one standard habitat, as they in fact consist of microenvironments in which differences in temperature, pH, mucus production, epithelial specialisation, the motility of the mucociliary escalator, oxygen concentration and nutrient availability all have the potential to influence the variety and type of microorganism present[21,22]. Such physiochemical property gradients may plausibly allow for survival of different microorganisms within varying regions of the airways. It should be noted however that a recent study has concluded that in the lungs of healthy individuals spatial variation in the microbiota appears to be far less significant than the variation present across individuals[23]. The authors also reported that the microbiota of the lungs in health seems to be more influenced by the immigration and elimination of microbes rather than by growth conditions influencing bacterial growth rates. Furthermore, this pattern may be reversed in

patients with advanced lung disease due to alterations in the pulmonary environment induced by disease progression[23].

As the lungs are connected directly to the microbial rich oral and nasal passages, the potential for regular translocation of microbes from these sites to secondary to inspiration and with possible associated micro aspiration, it is therefore not surprising that there may be similarities between the microbial composition of these sites. To investigate this further, Venkataraman *et al.,* utilised a neutral model for community ecology to differentiate members of the lung microbiome whose presence in the lungs is consistent with dispersal from other body sites and the members of the lung microbiome who deviate from this model, suggesting a competitive advantage for these microbes in the lung[24]. From this study dispersal of microbes from the oral cavity would seem to be the main mechanism whereby the lungs become colonised in healthy individuals and as no species constantly deviated from the neutral model one might postulate that it is the constant dispersal that is important for the microbial structure of the lower lungs rather than selective pressure[24]. However, the process could possibly be more complex than suggested in this neutral model, with the possibility that microbes introduced into the airways are killed at the same rate in which they are introduced, creating a homeostatic balance and therefore the perception of a neutral distribution, where in fact the lung environment is highly selective.

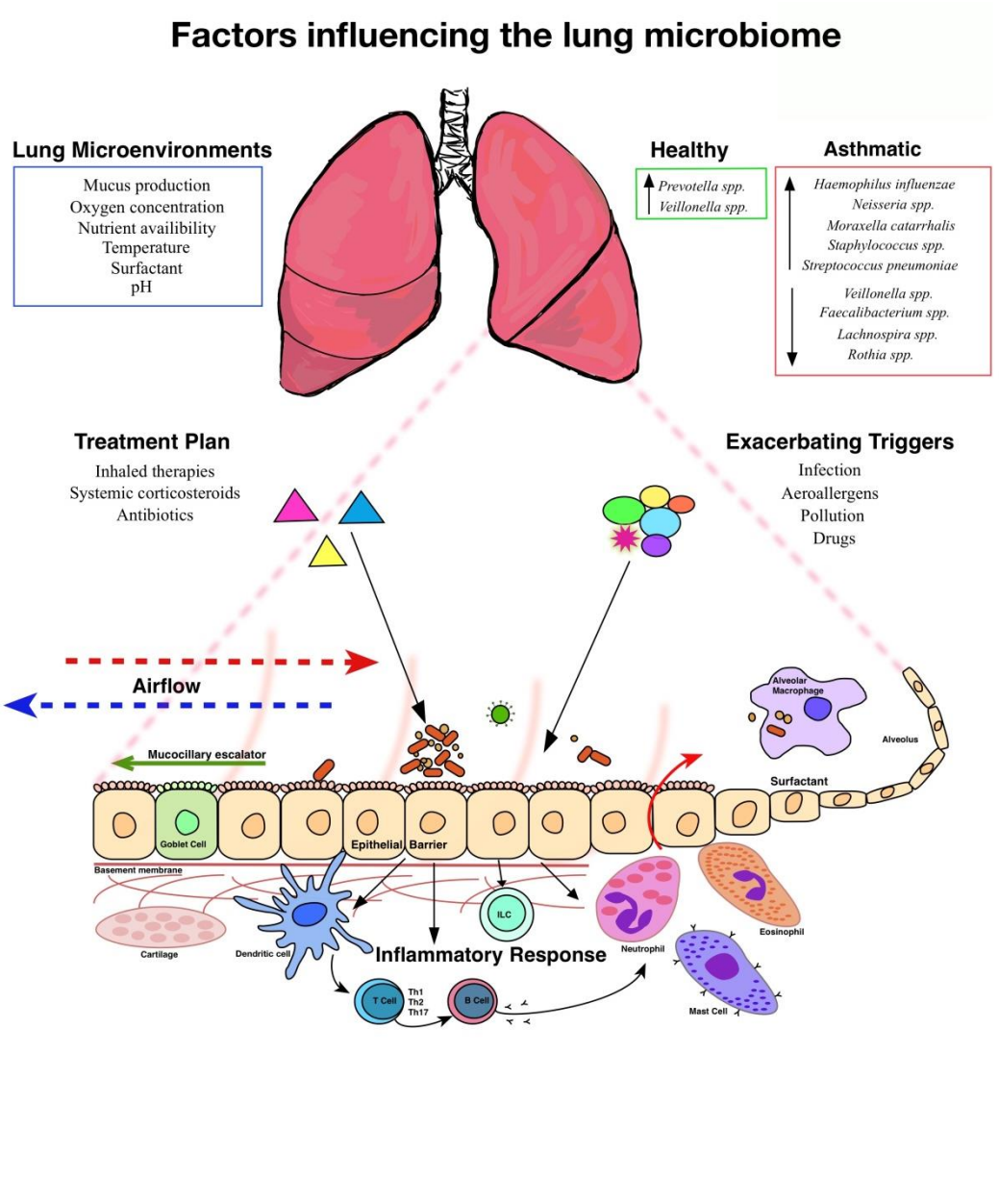


Figure 2 Schematic illustrating the complex factors affecting the lung microbiome in asthma. The lung microenvironment selects for specific microbes which change in asthma due to environmental factors, infection and treatment options which modulate the inflammatory cascade at the epithelial interface and the corresponding microbiome. Asthmatics display a changed microbiome with increased lung microbes such as H*aemophilus*, *Neisseria*, *Moraxella*, *Staphylococcus*, and *Streptoccoccus* with reduced *Veillonella*, *Faecalibacterium*, *Lachospira* and *Rothia* spp.

Sample collection and the lungs

As a consequence of the lower bacterial abundance and the difficulty of acquiring lower respiratory tract samples the study of the lung microbiome is technically challenging[20] Due to the belief that the lungs were sterile and due to the invasive nature of bronchoscope sampling the lower respiratory tract was not, at first, included in the Human Microbiome Project[25].

As recent characterisation of the lung microbiota has revealed, there are definable reproducible differences between healthy and diseased state lungs. It is now accepted that the healthy lung microbiome is diverse and some studies have even shown that the respiratory tract can more rapidly acquire diversity after birth than the intestines[26]. While there is now acceptance that there are microbes present within the airway, the challenge remains in overcoming the difficulty in sampling and culturing these microbes from the lower respiratory tract.

The validity of sampling techniques such as bronchoalveolar lavage (BAL) fluid and bronchial brushes have been subject to debate due to the potential for contamination from the oropharynx during bronchoscopy. Despite such concerns, recent studies have shown that, by comparing the microbial species present in the upper respiratory tract with the microbiota of the lower respiratory tract, the microbiota within the lower respiratory tract are unique. A recent study by Bassis *et al.,* compared samples from healthy subjects collected by oral wash, BAL fluid, nasal swab and gastric aspirates and demonstrated that the oral microbiome did not contaminate BAL samples[25]. The oral cavity and stomach contained high species richness and the highest bacterial signal levels in comparison to both the nasal cavity and lungs which had much lower bacterial signal levels. Whilst it was seen that the bacterial communities present in the healthy lung overlapped with those present in the oropharynx, the concentrations were much lower in the lungs and there was a different community composition in samples from healthy lungs[25].

While the sampling technique is of concern with regards to contamination, caution should also be taken with sample processing and the generation and analysis of complex datasets. Unintentional environmental contamination when processing

can lead to the unintentional identification of contaminants by the powerful sequencing technologies and controlling potential sources of contamination such as reagents is vital. It is also important to avoid bias and extraction protocols are critical. In sequencing of samples it is usually one of the variable regions of the 16S rRNA gene that is targeted by primers, however this is not ideal for the detection of certain species such as fungi where 18S rRNA and internal transcribed spacer sequencing represent a more appropriate target and viral identification requires approaches other than marker-gene-directed PCR analysis[27].

Lung diseases

The effect of the lung microbiome composition on health and disease states is of interest not just in asthma research but for other respiratory diseases such as cystic fibrosis, COPD, pulmonary fibrosis, and bronchiectasis.

In bronchiectasis it is now believed that a change in composition of the lung microbiota through events such as antibiotic therapy and inflammation may have downstream consequences for the function of the immune system, allowing for the formation and preservation of chronic infection lead by microbial pathogens[28].

There is an appreciation that cystic fibrosis is a multisystem disease with involvement of the hepatobiliary and gastrointestinal tracts[29]. While gastro-oesophageal reflux (GOR) affects CF patients, the lung and gastric microbiomes and an inter-dependant relationship between the two is clearly defined. Gastric and sputum cultures have revealed that 73% of patients with CF had one or more microorganism (fungal or bacterial) in common between the two samples and among the bacteria found in the two sites were *Pseudomonas, Streptococcus* and *Achromobacter*. *Pseudomonas aeruginosa* (Pa), a bacteria typically associated with CF was found in the sputum samples of 11 patients of which 4 had identical *P. aeruginosa* isolates in the stomach. In comparison, non CF gastric juice samples revealed a higher diversity. The stomach microbiome in patients with CF may act as a potential pathogen reservoir and the aerodigestive microbiome warrants further research as it may impinge on the pathophysiology of CF[30]. Bile acid aspiration is a comorbidity factor linked to many lung diseases which could plausibly shape the lung microbiome and promote the colonisation of *P. aeruginosa* in CF patients. Using a systems based analysis involving transcriptomics, functional genomics and immunochemistry the network of genes involved in virulence, adaptive metabolism and antibiotic tolerance linked to the bile response of the pathogens and the host cells has been elucidated. Bile acid leakage into the oesophageal tract occurs in up to 80% of CF patients and occurs in up to 35% of COPD patients (although this figure is thought to be underestimated)[31]. Disease progression and antibiotic tolerance in respiratory patients may be linked to bile acid signalling. Bile acids can

elicit biofilm behaviour in *Pseudomonas aeruginosa*, increase polymyxin and macrolide antibiotic tolerance, and reduce microbial biodiversity[31].

COPD research is in its infancy with regards to the microbiota of the COPD lung however some recent studies have demonstrated that as the disease progresses there is a reduction in bacterial diversity however there is no demonstrable outgrowth of a single microorganism as is the case in CF where *Pseudomonas aeruginosa* predominate[32]. Patients with idiopathic pulmonary fibrosis (IPF) are reported to have a higher relative abundance of *Haemophilus, Streptococcus, Neisseria* and *Veillonella* species[33].

Asthma characteristics

Asthma is a chronic inflammatory disease, which is characterised by airway hyper-responsiveness leading to intermittent, repeated bouts of wheezing, chest tightness, breathlessness and coughing[34,35].Asthma has seen a staggering rise in prevalence in recent years and the burden is felt globally with more than 300 million people believed to be impacted by this chronic respiratory disorder which has reached epidemic proportions in the western world[1-5].While the global prevalence of asthma accounts for approximately 300 million people or 4.5% of the global population the prevalence of asthma can be as high as 21.5% within populations[36]. In Europe, around 30 million children and adults under 45 have asthma with the overall financial burden estimated to be 72 billion Euros per year. Ireland has some of the highest rates in the world, representing a huge societal burden[37].

Asthma has a complex heterogeneity with many clinical phenotypes whose varying expression depends on interplay between numerous environmental factors along with many different susceptibility genes[1,38]. The airway epithelium is pivotal in the inflammatory response of the host and is a major source of pro-inflammatory mediators[38]. The airway obstruction which characterises the clinical presentation of asthma runs in cycles of symptom free periods followed by varying periods of exacerbation to which there is usually a trigger or stimuli[39]. These exacerbations result in a worsening in symptoms and lung function and although is generally reversible and followed by a return to normal lung function, in some patients repeated exacerbations may lead to a new, compromised baseline[40,41]. Such exacerbating triggers include infection, aeroallergens, pollution, drugs and physical stimuli[34,42,43]. These exacerbations are often treated with varying combinations of increased inhaled therapy, systemic corticosteroids and antibiotics[10]. One might postulate, therefore, that the exacerbating event and the mode of therapy utilised to treat the event may impact on the composition of the lung microbiome. Indeed recent studies have demonstrated that the gut microbiota can alter circadian rhythms which may open new avenues of research into identifying the cause of asthmatic exacerbations[44,45]. It has been noted that an alteration to the *Bmal 1* (the

clock gene) in bronchiolar cells disrupts the circadian neutrophil recruitment via CXCL5, which in turn leads to an exaggerated host response to LPS and a deficient host immune response to *Streptococcus pneumoniae*[46].

Asthma treatment strategies

The European Respiratory Society (ERS) states in their white book on adult asthma that there are three terms used to describe the clinical course of asthma: asthma control, asthma severity and asthma exacerbations.

Methods such as the Asthma Control Questionnaire-7 (ACQ-7) are used to measure asthma control. The ACQ-7 is a validated questionnaire consisting of 7 items, five questions related to the highest scoring symptoms people with asthma experience, one question related to bronchodilator use and one question which is answered by the medical professional post spirometry testing, related to the FEV_1% of predicted normal[47,48]. Through the scoring of each question on a seven point scale a discriminative method of measuring a patients asthma control is established[49].

The Global Initiative for Asthma (GINA), established to raise asthma awareness among health professionals, authorities and the community is strongly focused on preventing asthma related deaths and severe exacerbations while also focusing on the efficacy and effectiveness of asthma treatment in general. Through their yearly report comprising of the latest scientific research, GINA enables the dissemination of best practice with respect to asthma diagnosis and treatment. Through their classification system GINA enables the grouping of asthma patients into stages or steps of asthma severity from stage 1, mild to stage 5, severe, which aids in the treatment strategy implemented[50-52].

Asthma exacerbations can be experienced as a loss of disease control and the development of acute symptoms[53]. Asthma exacerbations can result in an increased risk of morbidity as well as being a financial burden to health systems[53].

Management of asthma is vital to prevent exacerbations and control symptoms as currently there is no cure for most types of adult asthma[37] Treatment with inhaled steroids and bronchodilators are the mainstay of international asthma treatment guidelines but it is recognised that the pathophysiology is incompletely understood and there is a need for new treatment approaches. In order to control the symptoms of asthma, help improve the function of the lungs and aid in the reduction of exacerbations, asthma patients are frequently prescribed inhaled

corticosteroids (ICS) and/or a combination of long acting beta (β) agonist (LABA) bronchodilators. For the majority of patients this proves to be successful. However in about 10% of the asthmatic population further additional therapy is required in order for these patients to establish control of their asthma symptoms, improve lung function and reduce the number of exacerbations suffered[54]. While accounting for 5-10% of the overall asthma population, severe asthmatics account for 50% of the direct and indirect costs associated with asthma[55]

Monoclonal antibody therapy as a treatment option for certain cohorts of asthma patients has gained traction as it enables the treatment of patients in a highly specific manner and whilst monoclonal antibody therapy is an expensive treatment option the overall cost is outweighed by the benefits[36,56]. For patients with severe asthma where either persistent symptoms or exacerbations occur despite the use of maximal maintenance medications such as inhaled corticosteroids (ICS) and long acting beta agonists (LABA) or rescue medications such as short acting beta agonists (SABA) and oral steroids, monoclonal antibody therapy is an attractive add on treatment[36,57]. In such asthmatic patients monoclonal antibody therapy offers a lifeline[56].

It is believed that approximately 5-10% of asthma patients can be classified as severe asthmatics and it is believed that within this population over 50% can be classified as allergic, IgE-mediated asthmatics[58]. Therefore monoclonal antibody therapies targeting IgE are of increasing interest with recombinant humanised monoclonal antibodies such as Omalizumab (Xolair®) (Novartis-Genentech) proving effective as an adjunctive treatment option for severe, IgE-mediated asthmatics[58]. Omalizumab binds to the IgE antibody at the Fc portion which reduces the amount of free IgE, stopping IgE binding to the inflammatory cell IgE receptors and thus reducing the IgE receptor ($F_{c\varepsilon}RI$ and $F_{c\varepsilon}RII$) density on effector cells, all of which prevent an inflammatory cascade from occurring[58,59].

40-60% of severe asthma patients suffer from eosinophilic airway inflammation, a well-defined endotype of severe asthma[56]. Monoclonal antibodies which target this have recently become available for use as adjunctive therapy options. Three such

monoclonal antibody therapies are Mepolizumab (Nucala®) (GlaxoSmithKline), Relizumab (Cinquero®) (Teva Pharmaceutical Industries) and Benralizumab (Fasenra®) (AstraZeneca). IL-5 is a homodimeric cytokine, secreted by eosinophils, basophils, T cells, mast cells and Type 2 innate lymphoid cells, which binds to the receptor IL-5Rα, activating the high affinity IL-5R to transduce intracellular signals upon binding[56]. The IL-5 cytokine is highly involved in eosinophil development and pathobiology within humans[56]. As about 50% of severe asthma exacerbations are eosinophilic in nature a reduction in eosinophils within severe eosinophilic asthma patients with could potentially reduce exacerbations[60].

Mepolizumab (GlaxoSmithKline) and Reslizumab (Teva Pharmaceutical Industries) are IL-5 antagonist monoclonal antibodies and both bind to soluble IL-5 which inhibits the binding of IL-5 to its corresponding IL-5 surface receptors resulting in the downregulation of the IL-5 eosinophil inflammatory pathway[36,57]. Benralizumab (AstraZeneca) however binds to the IL-5 receptor on the α-chain and prevents IL-5 from binding to its receptor which results in the inhibition of eosinophil differentiation and maturation in the bone marrow[61]. Benralizumab also can bind to the RIIIa region of Fcγ receptor on Natural Killer (NK) cells, macrophages and neutrophils. This results in the induction of cell mediated cytotoxicity for both circulating eosinophils and tissue resident eosinophils[61].

As adjunctive therapy options become more readily available, questions as to their potential effect on the respiratory microbiome are of emerging interest. The diversity of the human microbiome and the role it plays in health and diseased states is of great interest and technological advances have enabled the advancement of such studies[8].

Epithelial development and the role of the microbiota

A wide range of early life environmental exposures, and early lung structural changes represent important risks for subsequent development of asthma[62]. Therefore epigenetic cellular changes may play an under researched and potentially key role. Population studies also show that obesity, insulin resistance and diabetes are associated with worsening disease in airways pathophysiology. These important, increasingly prevalent, co-morbidities have been specifically implicated in asthma[63] and are worthy of further investigations.

Loss of epithelial barrier function, inflammation, obesity and co-morbid diabetes, while being associated with asthma severity have also been seen to lead to dysregulated levels of airway glucose as a final common end point. Normal airway glucose levels are tightly regulated to levels of around 0.4mM[64] and raised levels are associated with infection[65] and potential metabolic effects on airway cells. This indicates the potential for combined airway remodelling, inflammation, dysregulated metabolic homeostasis and the overall airway environment to contribute to asthma pathophysiology.

In the gastrointestinal tract there is a complex interplay between the symbiotic bacteria which are responsible for processes such as nutrient metabolism and the host which in turn provides a nutrient rich, protective environment. This interplay requires strict sequestration of the resident microbes and the host lumen to prevent the triggering of processes such as sepsis and inflammation. Epithelial antimicrobial proteins play a vital role in hindering the contact of resident microbes and the host mucosal surfaces[66]. Germ-free mice and antibiotic treatment of murine models have demonstrated evidence that the microbiota is required for gut epithelia development and function[67]. Cash *et al.,* first identified the role microbes play in inducing antimicrobial peptides and epithelial villus development and maturation[67]. It has been seen that in germ-free mice microbial colonisation induces the expression of RegIIIγ, which is a secreted C-type lectin, known in humans as HIP/PAP. This expression directly correlates with bacterial expression and host epithelial contact, with preferential binding to peptidoglycan which is

present in gram positive bacteria. This highlights how the host-microbial symbiotic relationship is maintained[67]. It is therefore possible that a similar protective mechanism could be involved in the lung mucosal epithelium.

Innate Lymphoid Cells (ILCs) have emerged as a population of innate immune cells derived from an Id2 dependent lymphoid cell progenitor cell population. ILCs share many functional and developmental characteristics with $CD4^{+}$T cell populations. ILCs have been demonstrated to be involved in orchestrating certain host-commensal bacteria relationships[68]. Such an involvement would have implications on immunity, inflammation and tissue homeostasis in the intestines. In the lungs it has been seen that pathogenic ILC responses have been associated with asthma and airway hyperresponsiveness in murine models[68]. As commensal bacteria, epithelial cells and ILCs share close proximity and investigation into the potential impact of this interaction upon the development of ILCs is taking place. Hence ILCs may represent a potential target for numerous human diseases such as asthma[68].

Recent studies focusing on ILCs have also identified the key dialogue between ILCs, epithelia and the microbiota[69]. IgA is the predominant antibody at mucosal surfaces, in particular in the upper respiratory tract. Through its pleiotropic effects IgA induces a tolerizing phenotype at mucosal surfaces and is of critical importance to the maintenance of mucosal homeostasis. IgA is created through the class switch recombination of Ig heavy chains. IgA offers an important role in mucosal homeostasis such as opsonisation and neutralisation of pathogens and toxins. This results in a reduction of antigenic load on the mucosal immune system. In $IgA^{-/-}$ mice the protective role of IgA at mucosal surfaces is highlighted as these mice have an impaired clearance of luminal pathogens such as *Mycobacterium tuberculosis*, *Streptococcus pneumoniae*, *Citrobacter rodentium*, *Giardia muris* and *Giardia lamblia*[69]. It has been demonstrated that the microbiota acts through Toll-like receptors to condition lung dendritic cells (LDCs) to produce TGF-β and this in turn influences the production of IgA in the lung[69]. While research to date has focused mainly on the gut, evidence of bi-directional links between the gut and the lung immune function are increasing[70].

Microbes and the host

A key feature of any microorganism is its ability to be recognised and sampled by the immune system. The ensuing immune response, depending on the microbe, can range from benign tolerance to acute inflammation and injury, with ensuing repair and remodelling in the lungs[3]. Respiratory fungi, bacteria and viruses are recognised by innate receptors including Toll-like receptors (TLRs), RIG-1-like helicases and NOD-like receptors which when stimulated then activate the nuclear factor κ B (NFκB) group transcription factors with the possible resultant induction of more than 100 pro-inflammatory and host response genes[3,71]. Microorganisms can affect the permeability of the epithelium increasing infection risk, affecting epithelial integrity by invasion of the epithelium cells leading to cell death and shedding. By compromising the epithelium, subsequent allergen uptake and the effect of environmental exposure to pollutants may cause an increased possibility for the development of further exacerbations and a heightened immune response increasing the risk of a pathogenic response and asthma development[3,72-74].

Asthma patients have an increased risk of bacterial infection and through culture dependent and independent techniques it has been seen that there is increased carriage of pathogenic respiratory bacteria. Birth cohort studies have shown that increased carriage of bacteria such as *Streptococcus pneumoniae, Haemophilus influenzae* and *Moraxella catarrhalis* in early life can be linked to asthma risk and the development of recurrent wheeze in children born to asthmatic mothers[75]. This study by Bisgaard *et al.,* also revealed that, in children with recurrent wheeze during the first three years of life, that these wheezing episodes are associated with bacterial and viral infections equally, suggesting that bacterial and viral infections may act independently to contribute to asthma symptoms and thereby highlighting the important role of bacterial infection independent of viral infection in the pathogenesis of asthma[76].

In a study by Hilty *et al.,* members of the phylum *Proteobacteria* were associated with airway disease in both asthma and COPD patients. *Haemophilus*, *Moraxella* and *Neisseria* spp. found in the lungs of asthmatic patients had strong correlations

with increased asthma risk when found in the oropharynx of neonates. *Staphylococcus* was found to be present in the airways of children with difficult asthma. *Bacteroidetes* and in particular *Prevotella* and *Veillonella* spp. were found to be most prevalent in healthy controls[2].

While microorganisms can add to the onset and progression of atopic asthma, microorganisms can also have a protective function[3]. The 'hygiene hypothesis' can in part help to explain the disproportionate spread of asthma in the western, industrialised world. It proposed that repeated exposure to diverse common infections and repeated exposure to environmental microbes during childhood can stimulate the immune system in a manner which promotes a protective response against future asthma risk[3].

The so-called 'hygiene hypothesis' contends that exposure to soil, dust, microbes, antibiotics, vaccinations, farm animals and family size in addition to factors such as caesarean section birth versus vaginal birth and exclusive formula feeding versus breastfeeding can all in some part determine asthma risk[77-79]. In one meta-analysis study there was a 20% increase in the subsequent risk of asthma development in children born by caesarean section[80].

The use of anti-inflammatory drugs and antibiotics can significantly alter the lung microbiome[81]. Such a change in the microbiome of the lung may lead to resistance, resilience, functional redundancy, or a permanently altered microbiome[13]. It is seen that even before birth children are exposed to antibiotics, with about half of all pregnant women in America receiving antibiotics which alter their microbiota before transfer to their offspring[13].

Environmental microbial exposure can have a protective effect against asthma development. In the PARSIFAL and GABRIELA studies asthma and atopy prevalence among children living on farms and among children in the reference group (not living on a farm) were examined[82]. In both studies children living on a farm had a lower prevalence of asthma than the reference group. From these two large scale observational studies it would appear that a wider range of microbial exposures offers a protective effect on the development of asthma[82].

The PASTURE study aimed to characterise prenatal exposure to the asthma protecting effects of farm life[83]. Cord blood cells upon analysis showed once again that maternal exposure to multiple types of animal species and barns during pregnancy caused an enhancement in the production of TNFα and IFNγ in children[84]. Newborns' had increased production of TNFα and IFNγ if born to mothers who consumed butter produced from unpasteurised milk during pregnancy[83].

It has been shown that single nucleotide polymorphisms (SNPs) in TNFAIP3 which encodes A20 is linked to the development of asthma in farm dwelling children[85]. A20 is an ubiquitin-modifying enzyme which weakens NFκB activation through the deubiquitination of key signalling intermediates down-stream of IL-1 receptor, Toll-like receptor and TNF family receptors[85]. It is accepted that chronic exposure to low-dose endotoxin or farm dust conveys a protective effect against the development of house dust mite (HDM) induced asthma in mice and loss of A20 is associated with allergy and asthma risk[85]. It has been shown that in mice with an induced absence of A20 there is an increased sensitivity to HDM and the ensuing asthma is seen to be more severe[85].

Children from rural areas in Germany, Austria and Switzerland from farming and non-farming households were involved in a study to determine whether there was a protective effect present upon endotoxin exposure against the risk of asthma and atopic wheeze. Mattress dust, as an indicator for endotoxin exposure, was examined and it was found that environmental exposure to endotoxins was associated with the development of tolerance towards ubiquitous allergens found in natural environments[86]. Muramic acid, a component of bacterial peptidoglycan, is a marker for microbial burden and is a biologically active substance which influences the cellular immune response in a manner different to endotoxin[87]. A high level of muramic acid in a similarly constructed study provided complimentary findings, lending further credence to the notion that asthma could in part be due to inadequate activation, at the appropriate educational time point, of the innate immune responses which are stimulated by certain microbial products[87].

Studies have shown that a decrease in *Akkermansia, Bifobacterium* and *Faecalibacterium* abundance in the gastrointestinal tract of neonates can be linked to later development of asthma and allergy symptoms[88]. Exposure to the bacteria *Moraxella catarrhalis* was shown in murine studies to induce IL-17 and exacerbate allergic inflammation in the lungs through the resulting eosinophil and neutrophil recruitment[20,89]

Recent studies, including the Canadian CHILD cohort study, have highlighted the importance of this window of colonisation in children and long-term side effects such as asthma which can ensue when there is a presence or lack of certain microorganisms in the gastrointestinal system[90]. It was determined that the relative abundance of the bacterial genera *Faecalibacterium, Lachnospira, Veillonella,* and *Rothia* (FLVR) appeared notably decreased in the gut of children who were at risk of developing asthma[90]. These microorganisms appeared to be mostly significantly different between the groups at 3 months and this difference decreased once the children reached 1 year of age, suggesting the presence of a colonisation "window of opportunity"[90,91]. It was also seen that it is not just the prevalence of the gut microbiota that is important but the metabolites that they derive, such as the short chain fatty acids (SCFAs) propionate and acetate which have been demonstrated in a murine model to reduce airway cellular infiltration offering a protective effect from asthma development and differences in SCFA composition at 3 months has been linked to atopy at wheeze development at 1 year[90,92]. This concept of a "window of opportunity" for colonisation, while now generally accepted, requires further investigation. In mice this critical window occurs during the first 2-3 weeks of life and it is expected that in humans the critical window is narrower than first expected and rather than years is likely to merely last for a matter of months[91].

In germ-free mice it has been shown by Olszak *et al*., that there is dysregulation in the development of an immune cell profile when there has been no microbial exposure. However if colonised gastrointestinally during a crucial neonatal period with a microbiome, a protective effect against exaggerated inflammation developed and this effect could not be demonstrated in recolonised adult mice[93]. Hence, one might postulate that if microbial exposure can alleviate or prevent the

immune cascade as seen with allergic disorders such as asthma, could a prebiotic or probiotic have a protective or even preventive role in asthma? Studies have shown that gnotobiotic mice who are in receipt of the FLVR taxa; *Faecalibacterium, Lachnospira, Veillonella,* and *Rothia* (FLVR) displayed signs of protection from allergic airway inflammation when compared to mice who did not receive supplementation with FLVR bacteria[90]

It has been seen that *Lactobacillus reuteri*, when administered to mice demonstrating a normal microbial flora, can abate airway hyperresponsiveness via systemic increase in regulatory T cells, which can therefore alleviate asthma symptoms[94-96]. It was seen also that direct exposure to an innocuous strain of *Escherichia coli* could result in long term protection against allergic disorders in normal mice by reprogramming macrophages and dendritic cells[97]. Dendritic cells bridge the gap between innate and adaptive immunity[77]. In BALB/c ovalbumin challenged mice fed daily with *Bifidobacterium longum* it was noted that airway inflammation was attenuated and a reduction in BAL eosinophilia, BAL fluid IL-4 protein and BAL cell IFN-γ and IL-4 mRNA levels was observed[98].

To test the effect of early life antibiotic exposure to the microbiota and subsequent allergic asthma susceptibility Russell *et al.,* treated neonatal mice with clinical doses of Vancomycin and Streptomycin. Changes in the resident gut microbiota and subsequent asthma susceptibility were documented. In mice treated with Streptomycin there was no significant effect upon the microbiota or asthma risk. However in mice treated with vancomycin it was noted that there was a reduction in microbial diversity and changes in bacterial population composition were observed leading to a heightened risk of asthma development upon allergic challenge. As neither antibiotic had an effect upon adult mice, one might infer that the hygiene hypothesis is of relevance only in neonatal shift in microbial diversity and composition[99]. Russell *et al*., investigated whether or not this effect held true for perinatal antibiotic treated mice and the risk of developing hypersensitivity pneumonitis, a T_H1 – T_H17 mediated lung disease. Contrary to the previous findings severity of the disease increased dramatically with Streptomycin. It was concluded that perinatal antibiotics affect the resident gut microbiota in a highly selective

manner and this then leads to a change in susceptibility to T_H2 or T_H1-T_H17 driven lung inflammatory diseases[100].

The prevalence of *Helicobacter pylori,* which was once the dominant bacteria in the stomach and had strong maternal transmission, is now decreasing and with it possibly the protective effects this bacteria seems to have against asthma development[101]. Studies have shown that childhood acquisition of *H. pylori* reduces the risk of allergy and asthma[101]. In developing countries nearly all adults harbour the gastric bacterium *H. pylori* but in industrialised countries its prevalence is much lower[102]. In industrialised countries such as the United States fewer than 10% of children under 10 years of age are colonised with *H. pylori*[103]. However it should be noted that *H. pylori* acquisition does not appear to be associated with adult onset asthma suggesting that the pathogenic risk factors for adult onset asthma may differ from those for childhood asthma[103].

It is believed that microaspiration, which occurs in healthy individuals but has a higher prevalence in asthmatics, could in part explain the presence of oral microbiota in the lower lung[17]. However this does not fully explain why some individuals have a higher relative abundance of certain bacteria that would be expected had the bacteria originated from the upper respiratory tract[17,104].

In a recent study by Marri *et al.,* induced sputum samples from a mild active asthmatic and non-asthmatic cohort of adults was examined and it was determined that all sputum samples contained the 5 main bacterial genera with *Firmicutes, Proteobacteria* and *Actinobacteria* making up 90% of the sequence reads. It was further shown that *Proteobacteria* levels were elevated in asthmatics and *Firmicutes* and *Actinobacteria* were more common in the non-asthmatic cohort. From this study it was determined that mild asthma was more similar in microbial composition to that of severe asthmatics that to the non-asthmatic group[105].

The “disappearing microbiota” hypothesis contends that as we become less colonised by ancient commensal microorganisms, which aid in a multitude of processes such as vitamin uptake and immunity, we become more susceptible to attack by potential pathogenic microorganisms. A shift in an individual’s microbial

balance may have detrimental consequences. The “disappearing microbiota” hypothesis has been studied in relation to the increased and decreased prevalence of several diseases in developed nations. While the hygiene hypothesis highlights our susceptibility to infection caused by our decreased sampling of microorganisms from the environment the disappearing microbiota hypothesis suggests that our susceptibility is due to a decrease in ancestral microorganisms which offered protection[106].

Lung epithelia and mucosal immune defences

While the role of the gut microbiota in shaping the mucosal immune system, the symbiosis between the gut microbiota and intestinal mucosa, and the importance of barrier function within the gut is well understood, there remains a paucity of information pertaining to the lung[13]. As the lungs are directly exposed to the environment the epithelium is the first line of defence against infection[107,108]. In fact the lungs have the largest epithelial surface of the body[109]. By producing inflammatory products such as cytokines, growth factors, chemokines, lipid mediators, peptide mediators and reactive oxygen/nitrogen species the respiratory epithelial cells regulate the inflammatory response in the airways[110]. The epithelium acts as a barrier which prevents inhaled pathogens gaining access. Club and type II alveolar epithelial cells produce a surfactant which effectively traps pathogens and mucociliary clearance aid pathogen removal. The epithelium can function as a catabolic barrier for proteases and peptides with the epithelium expressing cell surface peptidases and producing protease inhibitors. The epithelium barrier function is further augmented by integral tight junction proteins[110]. The cells of the innate immune response include macrophages, neutrophils and monocytes which utilise pathogen recognition molecules (PRMs) to recognise pathogen association molecular patterns (PAMPs) leading to the production of antimicrobial products[107,110]. Well known cell surface receptors include Toll-like receptors which can recognise a wide variety of viral and bacterial PAMPs such as LPS[107,111].

Asthma is a heterogenous disease, with airway inflammation induced by epithelial exposure to allergens, pollutants and microbes which further stimulate the underlying APC cells inducing an immune response[112]. This epithelial exposure can result in a predominantly eosinophilic or neutrophilic cell influx into the airway. The allergic subtype, which responds to environmental allergens, is characterised by increased eosinophil, basophils, and mast cells along with expansion of the T helper 2 cell (T_H2 cell) subtype. As the epithelial or mucosal barrier is where the allergen presents itself, a breakdown in these physical barriers, the site of allergen presentation, can further propagate allergic, inflammatory response[10]. Indeed fungal spores, which are potent allergens, are postulated to damage the epithelial

barrier by inducing cell shrinkage and subsequent inflammation and barrier breakdown[113].

The interaction of the APC with the epithelium is the critical event in the resulting immune response. Dendritic cells act as sentinels, reacting to the exposure to certain allergens and pathogens from the environment. Dendritic cells activate an appropriate immune response after exposure to an allergen dependent on the appropriate mechanism of action for clearing the invading pathogen. It has been noted that mice lacking in DCs have major deficiencies in their antibacterial, antiviral and antifungal immunity. From recent murine studies it is believed that the epithelium has a key role in the activation of dendritic cells after exposure to an adverse pathogen or allergen and that there is an established epithelia – dendritic cell communication pathway[114].

Alveolar macrophages are the primary microbial sampling and clearance mechanism within the lung lumen and play an integral role in pulmonary host defence positioned at the interface between the mucosa and the external environment[115]. The composition of the microbiome in an asthmatic lung will consequentially affect macrophage sampling. Indeed the function of the alveolar macrophages may also effect what microbes persist in the lung and hence influence the resulting airway microbiome. Studies on alveolar macrophages in smokers have demonstrated that accumulation of tobacco smoke particulates in the lysosome effects migration and response to *Mycobacterium tuberculosis*[116]. These observations should also be noted with regard to asthmatics and their lung microbiota, as failure to efficiently clear certain species may result in persistence and imbalance.

T_H2 cells play a prominent role in allergic disorder pathogenesis leading to B cells isotype switching, generating IgE antibodies which are specific to the particular allergen[10]. T_H2 cells further enlist and enhance survival of eosinophils and mast cells, induce goblet cell hyperplasia and further drive bronchial hyper reactivity[34].

The virome and asthma

Epidemiological studies across five continents spanning three decades have revealed a strong link between respiratory infections and the pathogenesis of asthma[3]. Respiratory Syncytial Virus (RSV), Metapneumovirus, Coronavirus, Parainfluenza and Human Rhinovirus are just some of a plethora of human viruses which are known to be connected with respiratory diseases like asthma[117]. Human rhinoviruses can act as a trigger for asthma exacerbations[110]. Viral respiratory tract infections, most commonly rhinovirus infections, can have a serious effect on asthmatic patients or people at risk of developing asthma, causing exacerbations and worsening disease prognosis[117]. Some emerging evidence has shown that individuals with asthma may have deficiencies in antiviral activity and a dysfunctional epithelial barrier, increasing susceptibility to severe viral respiratory infections with more potential for exacerbations[117]. Sigurs *et al.,* have determined that acute RSV infections, occurring in conjunction with a family history of asthma, synergistically increase the risk of asthma development in an individual, illustrating that this gene-by-environment interaction has prognostic implications in asthma[117,118].

Viruses have been seen to predispose individuals to secondary bacterial infection. Upon exposure to RSV there is an increase in the adherence of *Streptococcus pneumoniae* to human epithelial cells[110,119]. Respiratory virus infection markedly increases emergency room admissions in relation to asthma exacerbations[3]. Wheezing respiratory viral illnesses from birth to 3 years of age, in high risk children (parent who tests positive for respiratory allergies or a history of diagnosed asthma) increase the risk of asthma development 10 fold when the child reaches 6 years of age[120]. It has also been shown that severe respiratory syncytial virus bronchiolitis in infancy, predisposes to the development of adult asthma[121].

Respiratory virus (RV) and Respiratory Syncytial Virus (RSV) are capable of activating a range of proinflammatory cytokines, chemokines, growth factors, adhesion molecules and mucins, relevant to the pathophysiology of asthma[3].

The mycobiome and asthma

The bacterial microbiome of the lungs has been the main focus of research to date, however the fungal microbiome/mycobiome of the lungs warrants investigation[122]. The respiratory tract is constantly exposed, via the atmospheric environment, to hyphal fragments, fungal spores and yeasts[123-126]. Thermotolerant fungi, including *Candida, Aspergillus* and *Penicillium* are sources of allergens, commensals and opportunistic pathogens and can colonise airways with potential clinical ramifications[123,126].

A marker for fungal exposure, extracellular polysaccharides, derived from *Aspergillus* and *Penicillium* are now known to be inversely associated with asthma[127]. A recent investigation of pooled sputum samples from asthma patients and controls identified 136 fungal species of which 90 species were more common in asthmatics. *Psathyrella candolleana, Malassezia pachydermatis, Termitomyces clypeatus* and *Grifola sordulenta* were most commonly found in asthmatics and *Eremothecium sinecaudum, Systenostrema alba, Cladosporium cladosporioides* and *Vanderwaltozyma polyspora* were more prevalent in the sputum samples of the control group[128].

Wheeler *et al.,* have demonstrated that antifungal drugs cause a fungal dysbiosis in mice and this dysbiosis results in an increase in the severity of airway inflammatory diseases such as asthma[129]. It has been well recognised for centuries that mould exposure can lead to an exacerbation of asthma[113]. In certain patients, mould exposure can have detrimental effects leading to increased disease severity, hospital admissions, and increased risk of bronchial reactivity and death[113].

Environmental risk factors such as pollen, animal dander and mould spores and their impact on asthma were examined from 1985 to 1989 in a cohort of asthmatics ranging in age from 5 to 34 years in Chicago, US. It was discovered that there was a 2.16 times greater chance of an asthma related death on days when the mould spore count reached >1000 spores per cubic meter. While factors such as genetics and the patients' socioeconomic situation have important roles, there appears to be a temporal relationship between the high environmental spore count and

subsequent asthma attacks[130]. The summer-autumn period of asthma admissions and deaths corresponds with the peak in environmental mould spores seen at this time[113].

It has been reported by Black *et al.,* in 37 patients admitted to the ICU for an acute asthma attack, that 54% tested positive in a skin test for fungal spores which included *Alternaria tenuis, Cladosporium cladosporides, Epicoccum nigrum and Helminthosporium maydis*[131]*.* O' Driscoll *et al.,* recruited 181 patients, aged between 16 – 60 years of age and divided them into three groups; severe, moderate and mild, dependent on their number of lifetime hospital admissions. 76% of patients with severe asthma tested positive in a skin test to one or more moulds including *Aspergillus fumigatus, Penicillium notatum, Cladosporium herbarum, Alternaria alternata* or the yeast *Candida albicans* in comparison to lower rates of positivity in patients with moderate or mild asthma (16% - 19%)[132].

Exposure to fungal allergens can have a devastating impact on asthmatics. Fungi contain proteins which are detrimental to the airway epithelium, enhance additional reactions and also act as allergens[113]. It is possible that the long term fungal colonisation of an atopic patient may provide a chronic source of allergen exposure, propagate airway inflammation and increase severity of asthma phenotype[113].

Severe asthma studies have suggested that fungi may play a role and the term severe asthma with fungal sensitisation (SAFS) has been used to describe severe asthma patients who demonstrate sensitisation to fungus in the absence of allergic bronchopulmonary aspergillosis (ABPA)[133]. See figure 3.

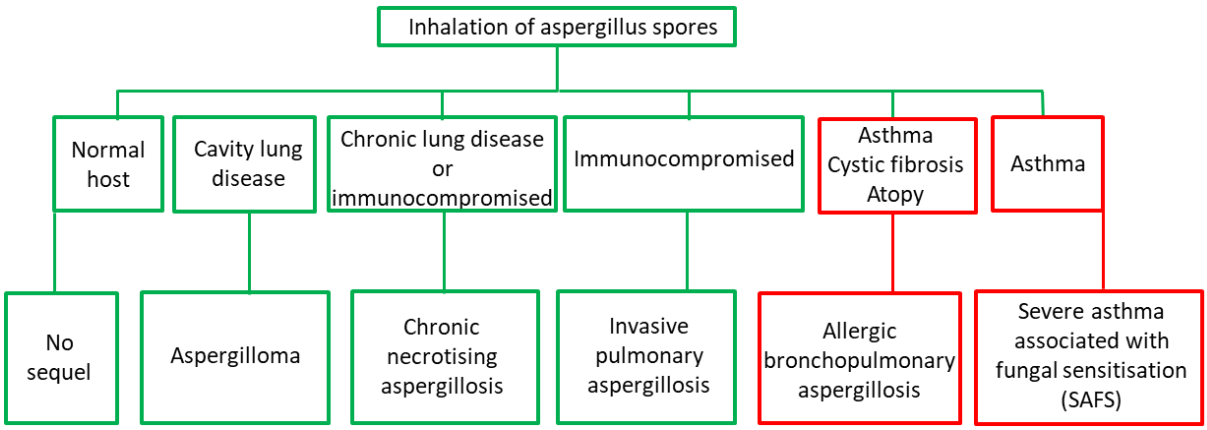


Figure 3 The inhalation of *Aspergillus* spores is believed to result in a number of different sequelae depending on the host. Figure adapted from Kousha et al., Pulmonary aspergillosis: a clinical review[134].

Previously published work carried out by our research group involved a study of the mycobiome in the airways of 69 adult asthmatics[126]. This work included the striking finding that fungal spores and hyphae were detectable microscopically in 70% of BAL obtained from the cohort. Molecular analysis demonstrated that 86% of patients had evidence of fungal presence within their BAL and almost half had detectable *Aspergillus fumigatus* in the airway by qPCR analysis[126]. This work is interrogated in greater detail in *Chapter 4 – Fungi in Asthma*. Our recent work describing striking high levels of fungal detection in asthmatics parallel and resonate with emergent studies showing that exposure to bacterial and fungal components may imprint epigenetic memory in inflammatory cells of the innate immune system with a consequence of this being the dysregulated release of cytokines[135].

Conclusions

There is an emerging consensus that the microbiome potentially plays a critical role in disease development, including in the pathogenesis of airway conditions such as asthma[136]. Asthma rates are increasing and thanks to meta-genomics it is now possible to define the composition of microbes in the lungs and elucidate whether changes in the composition of lower airway microbiota influences the complex pathophysiology of chronic lung disease such as asthma. Emerging data suggests that the role of microbial immune engagement and their metabolites cannot be ignored in studying asthma disease progression. Both Russell *et al*., and more recently Wheeler *et al* found that antibiotics and antimycotics alter the gut microbiota exacerbating allergic asthma symptoms in mice[99,129]. A reduction in microbial diversity and changes in bacterial population composition was found to lead to a heightened risk of asthma development when challenged by allergens. Vancomycin, which is orally administered, targets the gram positive Clostridium bacterial groups in the gut[99]. Clostridia make SCFAs such as butyrate and it possible that these metabolites lead to the observed negative impact on lung function. The "disappearing microbiota" theory, therefore contends that a disrupted microbiota or shift in an individual's microbial balance could possibly have detrimental effects[106]. Further research is now required to fully dissect this role and ultimately pave the way for the emergence of new therapeutic strategies in combating these conditions[8].

References

1. Kim HY, DeKruyff RH, Umetsu DT. The many paths to asthma: phenotype shaped by innate and adaptive immunity. *Nature immunology.* 2010;11(7):577-584.
2. Hilty M, Burke C, Pedro H, et al. Disordered microbial communities in asthmatic airways. *PLoS ONE.* 2010;5(1).
3. Edwards MR, Bartlett NW, Hussell T, Openshaw P, Johnston SL. The microbiology of asthma. *Nat Rev Micro.* 2012;10(7):459-471.
4. Burney P, Jarvis D, Perez-Padilla R. The global burden of chronic respiratory disease in adults. *The International Journal of Tuberculosis and Lung Disease.* 2015;19(1):10-20.
5. Umetsu DT, McIntire JJ, Akbari O, Macaubas C, DeKruyff RH. Asthma: an epidemic of dysregulated immunity. *Nat Immunol.* 2002;3(8):715-720.
6. Noverr MC, Huffnagle GB. Does the microbiota regulate immune responses outside the gut? *Trends Microbiol.* 2004;12(12):562-568.
7. Abdel-Aziz MI, Vijverberg SJH, Neerincx AH, Kraneveld AD, Maitland-van der Zee AH. The crosstalk between microbiome and asthma: Exploring associations and challenges. *Clinical & Experimental Allergy.* 2019;49(8):1067-1086.
8. Sullivan A, Hunt E, MacSharry J, Murphy DM. 'The Microbiome and the Pathophysiology of Asthma'. *Respiratory Research.* 2016;17(1):163.
9. Marsland BJ. Influences of the Microbiome on the Early Origins of Allergic Asthma. *Annals of the American Thoracic Society.* 2013;10(Supplement):S165-S169.
10. Holgate ST, Polosa R. Treatment strategies for allergy and asthma. *Nat Rev Immunol.* 2008;8(3):218-230.
11. Aho VT, Pereira PA, Haahtela T, Pawankar R, Auvinen P, Koskinen K. The microbiome of the human lower airways: a next generation sequencing perspective. *The World Allergy Organization journal.* 2015;8(1):23.
12. Marsland BJ, Gollwitzer ES. Host-microorganism interactions in lung diseases. *Nat Rev Immunol.* 2014;14(12):827-835.
13. Segal LN, Blaser MJ. A brave new world: the lung microbiota in an era of change. *Annals of the American Thoracic Society.* 2014;11 Suppl 1:S21-27.
14. Huffnagle GB, Dickson RP. The bacterial microbiota in inflammatory lung diseases. *Clinical Immunology.* 2015;159(2):177-182.
15. Erb-Downward JR, Thompson DL, Han MK, et al. Analysis of the Lung Microbiome in the "Healthy" Smoker and in COPD. *PLoS ONE.* 2011;6(2):e16384.
16. Turnbaugh PJ, Ley RE, Hamady M, Fraser-Liggett CM, Knight R, Gordon JI. The Human Microbiome Project. *Nature.* 2007;449(7164):804-810.
17. Segal LN, Rom WN, Weiden MD. Lung microbiome for clinicians. New discoveries about bugs in healthy and diseased lungs. *Annals of the American Thoracic Society.* 2014;11(1):108-116.
18. Charlson ES, Bittinger K, Haas AR, et al. Topographical continuity of bacterial populations in the healthy human respiratory tract. *Am J Respir Crit Care Med.* 2011;184(8):957-963.
19. Segal LN, Alekseyenko AV, Clemente JC, et al. Enrichment of lung microbiome with supraglottic taxa is associated with increased pulmonary inflammation. *Microbiome.* 2013;1(1):19.
20. Wilson NG, Hernandez-Leyva A, Kau AL. The ABCs of wheeze: Asthma and bacterial communities. *PLOS Pathogens.* 2019;15(4):e1007645.
21. Salami O, Marsland BJ. Has the airway microbiome been overlooked in respiratory disease? *Genome Medicine.* 2015;7(1):62.

22. Dickson RP, Erb-Downward JR, Huffnagle GB. Towards an ecology of the lung: new conceptual models of pulmonary microbiology and pneumonia pathogenesis. *The Lancet Respiratory medicine.* 2014;2(3):238-246.
23. Dickson RP, Erb-Downward JR, Freeman CM, et al. Spatial Variation in the Healthy Human Lung Microbiome and the Adapted Island Model of Lung Biogeography. *Annals of the American Thoracic Society.* 2015;12(6):821-830.
24. Venkataraman A, Bassis CM, Beck JM, et al. Application of a neutral community model to assess structuring of the human lung microbiome. *mBio.* 2015;6(1).
25. Bassis CM, Erb-Downward JR, Dickson RP, et al. Analysis of the upper respiratory tract microbiotas as the source of the lung and gastric microbiotas in healthy individuals. *mBio.* 2015;6(2):e00037.
26. Madan JC, Koestler DC, Stanton BA, et al. Serial analysis of the gut and respiratory microbiome in cystic fibrosis in infancy: interaction between intestinal and respiratory tracts and impact of nutritional exposures. *mBio.* 2012;3(4).
27. Huang YJ, Charlson ES, Collman RG, Colombini-Hatch S, Martinez FD, Senior RM. The role of the lung microbiome in health and disease. A National Heart, Lung, and Blood Institute workshop report. *Am J Respir Crit Care Med.* 2013;187(12):1382-1387.
28. Boyton RJ, Reynolds CJ, Quigley KJ, Altmann DM. Immune mechanisms and the impact of the disrupted lung microbiome in chronic bacterial lung infection and bronchiectasis. *Clinical & Experimental Immunology.* 2013;171(2):117-123.
29. Ooi CY, Durie PR. Cystic fibrosis from the gastroenterologist's perspective. *Nat Rev Gastroenterol Hepatol.* 2016;13(3):175-185.
30. Al-Momani H, Perry A, Stewart CJ, et al. Microbiological profiles of sputum and gastric juice aspirates in Cystic Fibrosis patients. *Scientific reports.* 2016;6:26985.
31. Reen FJ, Flynn S, Woods DF, et al. Bile signalling promotes chronic respiratory infections and antibiotic tolerance. *Scientific reports.* 2016;6:29768.
32. Sze MA, Hogg JC, Sin DD. Bacterial microbiome of lungs in COPD. *International Journal of Chronic Obstructive Pulmonary Disease.* 2014;9:229-238.
33. Morris A, Gibson K, Collman RG. The Lung Microbiome in Idiopathic Pulmonary Fibrosis. What Does It Mean and What Should We Do about It? *Am J Respir Crit Care Med.* 2014;190(8):850-852.
34. Hammad H, Lambrecht BN. Dendritic cells and epithelial cells: linking innate and adaptive immunity in asthma. *Nat Rev Immunol.* 2008;8(3):193-204.
35. Levy ML, Fletcher M, Price DB, Hausend T, Halbert RJ, Yawn BP. International Primary Care Respiratory Group (IPCRG) Guidelines: Diagnosis of respiratory diseases in primary care. *Primary Care Respiratory Journal.* 2006;15:20.
36. Edris A, De Feyter S, Maes T, Joos G, Lahousse L. Monoclonal antibodies in type 2 asthma: a systematic review and network meta-analysis. *Respiratory Research.* 2019;20(1):179.
37. ERS White Book. 2019; https://www.erswhitebook.org/chapters/adult-asthma/, 2019.
38. Murphy DM, O'Byrne PM. Recent advances in the pathophysiology of asthma. *Chest.* 2010;137(6):1417-1426.
39. Lambrecht BN, Hammad H. The airway epithelium in asthma. *Nat Med.* 2012;18(5):684-692.
40. Dickson RP, Martinez FJ, Huffnagle GB. The role of the microbiome in exacerbations of chronic lung diseases. *Lancet.* 2014;384(9944):691-702.
41. Sanders DB, Hoffman LR, Emerson J, et al. Return of FEV1 after pulmonary exacerbation in children with cystic fibrosis. *Pediatric pulmonology.* 2010;45(2):127-134.

42. Bateman ED, Hurd SS, Barnes PJ, et al. Global strategy for asthma management and prevention: GINA executive summary. *The European respiratory journal.* 2008;31(1):143-178.
43. Holt PG, Macaubas C, Stumbles PA, Sly PD. The role of allergy in the development of asthma. *Nature.* 1999.
44. Joyce SA, MacSharry J, Casey PG, et al. Regulation of host weight gain and lipid metabolism by bacterial bile acid modification in the gut. *Proceedings of the National Academy of Sciences of the United States of America.* 2014;111(20):7421-7426.
45. Liang X, Bushman FD, FitzGerald GA. Rhythmicity of the intestinal microbiota is regulated by gender and the host circadian clock. *Proceedings of the National Academy of Sciences of the United States of America.* 2015;112(33):10479-10484.
46. Gibbs J, Ince L, Matthews L, et al. An epithelial circadian clock controls pulmonary inflammation and glucocorticoid action. *Nat Med.* 2014;20(8):919-926.
47. Juniper EF, Svensson K, Mork AC, Stahl E. Measurement properties and interpretation of three shortened versions of the asthma control questionnaire. *Respir Med.* 2005;99(5):553-558.
48. Juniper EF, O'Byrne PM, Guyatt GH, Ferrie PJ, King DR. Development and validation of a questionnaire to measure asthma control. *The European respiratory journal.* 1999;14(4):902-907.
49. Juniper EF, Bousquet J, Abetz L, Bateman ED. Identifying 'well-controlled' and 'not well-controlled' asthma using the Asthma Control Questionnaire. *Respir Med.* 2006;100(4):616-621.
50. *Global Strategy for Asthma Management and Prevention 2019 Update.* Global Initiative For Asthma2019.
51. *Pocket Guide for Asthma Management and Prevention 2019 Update.* Global Initiative For Asthma 2019.
52. Reddel HK, FitzGerald JM, Bateman ED, et al. GINA 2019: a fundamental change in asthma management. *Treatment of asthma with short-acting bronchodilators alone is no longer recommended for adults and adolescents.* 2019;53(6):1901046.
53. Castillo JR, Peters SP, Busse WW. Asthma Exacerbations: Pathogenesis, Prevention, and Treatment. *J Allergy Clin Immunol Pract.* 2017;5(4):918-927.
54. Al Said A, Cushen B, Costello RW. Targeting patients with asthma for omalizumab therapy: choosing the right patient to get the best value for money. *Ther Adv Chronic Dis.* 2017;8(2-3):31-45.
55. Drick N, Seeliger B, Welte T, Fuge J, Suhling H. Anti-IL-5 therapy in patients with severe eosinophilic asthma - clinical efficacy and possible criteria for treatment response. *BMC pulmonary medicine.* 2018;18(1):119-119.
56. Nixon J, Newbold P, Mustelin T, Anderson GP, Kolbeck R. Monoclonal antibody therapy for the treatment of asthma and chronic obstructive pulmonary disease with eosinophilic inflammation. *Pharmacology & Therapeutics.* 2017;169:57-77.
57. Hom S, Pisano M. Reslizumab (Cinqair): An Interleukin-5 Antagonist for Severe Asthma of the Eosinophilic Phenotype. *P T.* 2017;42(9):564-568.
58. Thomson NC, Chaudhuri R. Omalizumab: clinical use for the management of asthma. *Clin Med Insights Circ Respir Pulm Med.* 2012;6:27-40.
59. Bang LM, Plosker GL. Spotlight on omalizumab in allergic asthma. *BioDrugs : clinical immunotherapeutics, biopharmaceuticals and gene therapy.* 2004;18(6):415-418.
60. O'Byrne PM. Role of monoclonal antibodies in the treatment of asthma. *Can Respir J.* 2013;20(1):23-25.

61. Davila Gonzalez I, Moreno Benitez F, Quirce S. Benralizumab: A New Approach for the Treatment of Severe Eosinophilic Asthma. *Journal of investigational allergology & clinical immunology.* 2019;29(2):84-93.
62. Bush A, Saglani S. Structurally Unsound? Why Airways Become Asthmatic. *Am J Respir Cell Mol Biol.* 2018;59(4):405-406.
63. Schatz M, Sicherer SH, Zeiger RS. The Journal of Allergy and Clinical Immunology: In Practice 2017 Year in Review. *The Journal of Allergy and Clinical Immunology: In Practice.* 2018;6(2):328-352.
64. Bearham J, Garnett JP, Schroeder V, Biggart MGS, Baines DL. Effective glucose metabolism maintains low intracellular glucose in airway epithelial cells after exposure to hyperglycemia. *American journal of physiology Cell physiology.* 2019;317(5):C983-c992.
65. Baker EH, Wood DM, Brennan AL, Clark N, Baines DL, Philips BJ. Hyperglycaemia and pulmonary infection. *The Proceedings of the Nutrition Society.* 2006;65(3):227-235.
66. Pickard JM, Zeng MY, Caruso R, Núñez G. Gut microbiota: Role in pathogen colonization, immune responses, and inflammatory disease. *Immunological reviews.* 2017;279(1):70-89.
67. Cash HL, Whitham CV, Behrendt CL, Hooper LV. Symbiotic bacteria direct expression of an intestinal bactericidal lectin. *Science.* 2006;313(5790):1126-1130.
68. Sonnenberg Gregory F, Artis D. Innate Lymphoid Cell Interactions with Microbiota: Implications for Intestinal Health and Disease. *Immunity.* 2012;37(4):601-610.
69. Ruane D, Chorny A, Lee H, et al. Microbiota regulate the ability of lung dendritic cells to induce IgA class-switch recombination and generate protective gastrointestinal immune responses. *The Journal of Experimental Medicine.* 2016;213(1):53-73.
70. Fujimura KE, Lynch SV. Microbiota in allergy and asthma and the emerging relationship with the gut microbiome. *Cell Host Microbe.* 2015;17(5):592-602.
71. O'Neill LAJ, Bowie AG. The family of five: TIR-domain-containing adaptors in Toll-like receptor signalling. *Nat Rev Immunol.* 2007;7(5):353-364.
72. Bassetti S, Bischoff WE, Walter M, et al. Dispersal of Staphylococcus aureus Into the Air Associated With a Rhinovirus Infection. *Infection Control and Hospital Epidemiology.* 2005;26(2):196-203.
73. Bossios A, Psarras S, Gourgiotis D, et al. Rhinovirus infection induces cytotoxicity and delays wound healing in bronchial epithelial cells. *Respiratory Research.* 2005;6(1):114-114.
74. Message SD, Laza-Stanca V, Mallia P, et al. Rhinovirus-induced lower respiratory illness is increased in asthma and related to virus load and Th1/2 cytokine and IL-10 production. *Proceedings of the National Academy of Sciences of the United States of America.* 2008;105(36):13562-13567.
75. Bisgaard H, Hermansen MN, Buchvald F, et al. Childhood Asthma after Bacterial Colonization of the Airway in Neonates. *New Engl J Med.* 2007;357(15):1487-1495.
76. Bisgaard H, Hermansen MN, xf, et al. Association of bacteria and viruses with wheezy episodes in young children: prospective birth cohort study. *BMJ: British Medical Journal.* 2010;341(7776):770-770.
77. Lambrecht BN, Hammad H. The role of dendritic and epithelial cells as master regulators of allergic airway inflammation. *Lancet.* 2010;376(9743):835-843.
78. Marsland BJ, Salami O. Microbiome influences on allergy in mice and humans. *Current opinion in immunology.* 2015;36:94-100.
79. Dominguez-Bello MG, Blaser MJ. Asthma: Undoing millions of years of coevolution in early life? *Sci Transl Med.* 2015;7(307):307fs339-307fs339.

80. Thavagnanam S, Fleming J, Bromley A, Shields MD, Cardwell CR. A meta-analysis of the association between Caesarean section and childhood asthma. *Clinical and experimental allergy : journal of the British Society for Allergy and Clinical Immunology.* 2008;38(4):629-633.
81. Murk W, Risnes KR, Bracken MB. Prenatal or early-life exposure to antibiotics and risk of childhood asthma: a systematic review. *Pediatrics.* 2011;127(6):1125-1138.
82. Ege MJ, Mayer M, Normand A-C, et al. Exposure to Environmental Microorganisms and Childhood Asthma. *New Engl J Med.* 2011;364(8):701-709.
83. von Mutius E, Schmid S, the PSG. The PASTURE project: EU support for the improvement of knowledge about risk factors and preventive factors for atopy in Europe. *Allergy.* 2006;61(4):407-413.
84. Schaub B, Liu J, Hoppler S, et al. Maternal farm exposure modulates neonatal immune mechanisms through regulatory T cells. *The Journal of allergy and clinical immunology.* 2009;123(4):774-782.e775.
85. Schuijs MJ, Willart MA, Vergote K, et al. Farm dust and endotoxin protect against allergy through A20 induction in lung epithelial cells. *Science.* 2015;349(6252):1106-1110.
86. Braun-Fahrlander C, Riedler J, Herz U, et al. Environmental exposure to endotoxin and its relation to asthma in school-age children. *The New England journal of medicine.* 2002;347(12):869-877.
87. van Strien RT, Engel R, Holst O, et al. Microbial exposure of rural school children, as assessed by levels of N-acetyl-muramic acid in mattress dust, and its association with respiratory health. *The Journal of allergy and clinical immunology.* 2004;113(5):860-867.
88. Fujimura KE, Sitarik AR, Havstad S, et al. Neonatal gut microbiota associates with childhood multisensitized atopy and T cell differentiation. *Nat Med.* 2016;22(10):1187-1191.
89. Alnahas S, Hagner S, Raifer H, et al. IL-17 and TNF-α Are Key Mediators of Moraxella catarrhalis Triggered Exacerbation of Allergic Airway Inflammation. *Front Immunol.* 2017;8(1562).
90. Arrieta MC, Stiemsma LT, Dimitriu PA, et al. Early infancy microbial and metabolic alterations affect risk of childhood asthma. *Sci Transl Med.* 2015;7(307).
91. Pattaroni C, Marsland Benjamin J. Asthma Prevention: Right Bugs, Right Time? *Cell Host & Microbe.* 2015;18(5):523-525.
92. Trompette A, Gollwitzer ES, Yadava K, et al. Gut microbiota metabolism of dietary fiber influences allergic airway disease and hematopoiesis. *Nat Med.* 2014;20(2):159-166.
93. Olszak T, An D, Zeissig S, et al. Microbial exposure during early life has persistent effects on natural killer T cell function. *Science.* 2012;336(6080):489-493.
94. Marsland BJ, Yadava K, Nicod LP. The airway microbiome and disease. *Chest.* 2013;144(2):632-637.
95. Forsythe P, Inman MD, Bienenstock J. Oral treatment with live Lactobacillus reuteri inhibits the allergic airway response in mice. *Am J Respir Crit Care Med.* 2007;175(6):561-569.
96. Karimi K, Inman MD, Bienenstock J, Forsythe P. Lactobacillus reuteri-induced regulatory T cells protect against an allergic airway response in mice. *Am J Respir Crit Care Med.* 2009;179(3):186-193.
97. Nembrini C, Sichelstiel A, Kisielow J, Kurrer M, Kopf M, Marsland BJ. Bacterial-induced protection against allergic inflammation through a multicomponent immunoregulatory mechanism. *Thorax.* 2011;66(9):755-763.

98. MacSharry J, O'Mahony C, Shalaby KH, et al. Immunomodulatory effects of feeding with Bifidobacterium longum on allergen-induced lung inflammation in the mouse. *Pulmonary pharmacology & therapeutics.* 2012;25(4):325-334.
99. Russell SL, Gold MJ, Hartmann M, et al. Early life antibiotic-driven changes in microbiota enhance susceptibility to allergic asthma. *EMBO Rep.* 2012;13(5):440-447.
100. Russell SL, Gold MJ, Reynolds LA, et al. Perinatal antibiotic-induced shifts in gut microbiota have differential effects on inflammatory lung diseases. *J Allergy Clin Immunol.* 2015;135(1):100-109.
101. Chen Y, Blaser MJ. Inverse associations of Helicobacter pylori with asthma and allergy. *Archives of internal medicine.* 2007;167(8):821-827.
102. Banatvala N, Mayo K, Megraud F, Jennings R, Deeks JJ, Feldman RA. The cohort effect and Helicobacter pylori. *The Journal of infectious diseases.* 1993;168(1):219-221.
103. Blaser MJ, Chen Y, Reibman J. Does Helicobacter pylori protect against asthma and allergy? *Gut.* 2008;57(5):561-567.
104. Charlson ES, Bittinger K, Chen J, et al. Assessing Bacterial Populations in the Lung by Replicate Analysis of Samples from the Upper and Lower Respiratory Tracts. *PLoS ONE.* 2012;7(9).
105. Marri PR, Stern DA, Wright AL, Billheimer D, Martinez FD. Asthma-associated differences in microbial composition of induced sputum. *J Allergy Clin Immunol.* 2013;131(2):346-352.e343.
106. Blaser MJ, Falkow S. What are the consequences of the disappearing human microbiota? *Nat Rev Micro.* 2009;7(12):887-894.
107. Uehara A, Fujimoto Y, Fukase K, Takada H. Various human epithelial cells express functional Toll-like receptors, NOD1 and NOD2 to produce anti-microbial peptides, but not proinflammatory cytokines. *Molecular immunology.* 2007;44(12):3100-3111.
108. Gómez MI, Prince A. Airway epithelial cell signaling in response to bacterial pathogens. *Pediatric pulmonology.* 2008;43(1):11-19.
109. Suzuki T, Chow C-W, Downey GP. Role of innate immune cells and their products in lung immunopathology. *The International Journal of Biochemistry & Cell Biology.* 2008;40(6–7):1348-1361.
110. Proud D, Leigh R. Epithelial cells and airway diseases. *Immunological reviews.* 2011;242(1):186-204.
111. Toews GB. Cytokines and the lung. *European Respiratory Journal.* 2001;18(34 suppl):3s-17s.
112. Mitchell PD, O'Byrne PM. Biologics and the lung: TSLP and other epithelial cell-derived cytokines in asthma. *Pharmacology & Therapeutics.*
113. Denning DW, O'Driscoll BR, Hogaboam CM, Bowyer P, Niven RM. The link between fungi and severe asthma: a summary of the evidence. *European Respiratory Journal.* 2006;27(3):615-626.
114. Lambrecht BN, Hammad H. Dendritic Cell and Epithelial Cell Interactions at the Origin of Murine Asthma. *Annals of the American Thoracic Society.* 2014;11(Supplement 5):S236-S243.
115. Byrne AJ, Maher TM, Lloyd CM. Pulmonary Macrophages: A New Therapeutic Pathway in Fibrosing Lung Disease? *Trends in Molecular Medicine.*22(4):303-316.
116. Berg Russell D, Levitte S, O'Sullivan Mary P, et al. Lysosomal Disorders Drive Susceptibility to Tuberculosis by Compromising Macrophage Migration. *Cell.* 2016;165(1):139-152.

117. Busse WW, Lemanske RF, Jr., Gern JE. Role of viral respiratory infections in asthma and asthma exacerbations. *Lancet.* 2010;376(9743):826-834.
118. Sigurs N, Bjarnason R, Sigurbergsson F, Kjellman B. Respiratory syncytial virus bronchiolitis in infancy is an important risk factor for asthma and allergy at age 7. *Am J Respir Crit Care Med.* 2000;161(5):1501-1507.
119. Hament JM, Aerts PC, Fleer A, et al. Enhanced adherence of Streptococcus pneumoniae to human epithelial cells infected with respiratory syncytial virus. *Pediatric research.* 2004;55(6):972-978.
120. Jackson DJ, Gangnon RE, Evans MD, et al. Wheezing rhinovirus illnesses in early life predict asthma development in high-risk children. *Am J Respir Crit Care Med.* 2008;178(7):667-672.
121. Hansel TT, Johnston SL, Openshaw PJ. Microbes and mucosal immune responses in asthma. *Lancet.* 2013;381(9869):861-873.
122. Beigelman A, Weinstock GM, Bacharier LB. The relationships between environmental bacterial exposure, airway bacterial colonization, and asthma. *Curr Opin Allergy Clin Immunol.* 2014;14(2):137-142.
123. Rick EM, Woolnough K, Pashley CH, Wardlaw AJ. Allergic Fungal Airway Disease. *Journal of investigational allergology & clinical immunology.* 2016;26(6):344-354.
124. Underhill DM, Iliev ID. The mycobiota: interactions between commensal fungi and the host immune system. *Nat Rev Immunol.* 2014;14:405.
125. Gauthier GM. Dimorphism in Fungal Pathogens of Mammals, Plants, and Insects. *PLoS Pathogens.* 2015;11(2):e1004608.
126. Sullivan A, Hunt EB, Ward C, et al. The presence of Aspergillus fumigatus in asthmatic airways is not clearly related to clinical disease severity. *Allergy.* 2019.
127. Ege MJ, Frei R, Bieli C, et al. Not all farming environments protect against the development of asthma and wheeze in children. *J Allergy Clin Immunol.* 2007;119(5):1140-1147.
128. van Woerden HC, Gregory C, Brown R, Marchesi JR, Hoogendoorn B, Matthews IP. Differences in fungi present in induced sputum samples from asthma patients and non-atopic controls: a community based case control study. *BMC infectious diseases.* 2013;13:69.
129. Wheeler ML, Limon JJ, Bar AS, et al. Immunological Consequences of Intestinal Fungal Dysbiosis. *Cell Host Microbe.* 2016;19(6):865-873.
130. Targonski PV, Persky VW, Ramekrishnan V. Effect of environmental molds on risk of death from asthma during the pollen season. *The Journal of allergy and clinical immunology.* 1995;95(5 Pt 1):955-961.
131. Black PN, Udy AA, Brodie SM. Sensitivity to fungal allergens is a risk factor for life-threatening asthma. *Allergy.* 2000;55(5):501-504.
132. O'Driscoll BR, Hopkinson LC, Denning DW. Mold sensitization is common amongst patients with severe asthma requiring multiple hospital admissions. *BMC Pulmonary Medicine.* 2005;5(1):1-10.
133. Denning DW, O'Driscoll BR, Hogaboam CM, Bowyer P, Niven RM. The link between fungi and severe asthma: a summary of the evidence. *The European respiratory journal.* 2006;27(3):615-626.
134. Kousha M, Tadi R, Soubani AO. Pulmonary aspergillosis: a clinical review. *European Respiratory Review.* 2011;20(121):156-174.
135. Quintin J. Fungal mediated innate immune memory, what have we learned? *Seminars in Cell & Developmental Biology.* 2019;89:71-77.
136. Herbst T, Sichelstiel A, Schär C, et al. Dysregulation of allergic airway inflammation in the absence of microbial colonization. *Am J Respir Crit Care Med.* 2011;184(2):198-205.

Chapter 2

Study Cohorts'

Asthmatic patient bronchoscopy and patient sample collection protocols

Author Contributions: Ashley Sullivan wrote the manuscript with significant contribution from Desmond Murphy. Ashley Sullivan, Desmond Murphy and John MacSharry read and approved the final manuscript.

1.1. Principles of respiratory investigations....54
1.2 Patient recruitment....54
1.3. Bronchoscopy....55
1.4. Spirometry....56
1.5. FeNO – Fractional exhaled Nitric Oxide....57
1.8. Blood sampling....60
References....62

1.1. Principles of respiratory investigations

The European Respiratory Society (ERS) White Book states that the diagnosis and follow up of respiratory diseases may require the implementation of a number of investigative procedures, implemented in an appropriate and cost effective step-by-step evaluation[1]. A detailed clinical history is first required for each patient, followed by a physical examination which may provide crucial clues as to future diagnostic avenues. The use of microbiological, histological and cytological laboratory procedures may then aid in the diagnosis or rule out the diagnosis of a number of possible diseases. In the case of asthma total and specific immunoglobulin E or skin testing with allergens may be implemented in the laboratory stage of the diagnostic process. The use of respiratory function testing such as spirometry is also vital to the diagnostic process, providing an assessment of disease severity and the monitoring of treatment. When required to carry out further more invasive investigations imaging techniques such as chest radiography or computed tomography (CT) enable visualisation and invasive bronchoscopy and biopsy techniques prove essential when simpler clinical or laboratory processes fail to provide a clear patient diagnosis[1].

1.2 Patient recruitment

All studies within this thesis have been approved by the Clinical Research Ethics Committee of the Cork Teaching Hospitals. Patient study cohorts consist of patients with a history of asthma; either documented change in FEV1 ≥12%/200ml with bronchodilator or a positive inhalation challenge. All patients were recruited through a dedicated asthma clinic in a tertiary referral centre, Cork University Hospital by my clinical supervisor, Dr Des Murphy. Patients were scheduled for bronchoscopy, with spirometry, ACQ-7 and blood sampling performed on the day of bronchoscopy. Written informed consent was obtained from patients on the day of bronchoscopy.

1.3. Bronchoscopy

Patient bronchoscopies were performed by Dr Des Murphy at Cork University Hospital. For many respiratory diseases such as asthma endoscopy and biopsy techniques are vital. Bronchoscopy is the key endoscopic procedure with regards to respiratory medicine and is implemented for both diagnostic and therapeutic purposes[2]. With respect to studies regarding the microbiome of the lung, bronchoscopy is often implemented as a method to sample the airways and is also key with regards to studies on airway inflammation and bronchial remodelling[3]. A rigid or flexible bronchoscope can be used to examine the airways; however for the purpose of these studies a flexible bronchoscope, in which the tube was less than 1cm wide and about 60 cm long, was used. It is accepted that flexible bronchoscopy is the gold standard for the direct visualisation of the airways and allows for various diagnostic and therapeutic interventions[4].

Flexible bronchoscopy using video assisted imaging was generally performed under conscious sedation with local anaesthetic applied topically to the vocal cords, trachea and endobronchial tree[2]. It is required that pharmacological sedatives are administered in a manner of conscious sedation so as to achieve a moderate level of sedation that is sufficient to achieve procedural tolerance on the part of the patient while maintaining a patent airway and ventilatory and cardiovascular function[4]. In order to achieve this manner of sedation pharmacological sedatives are administered incrementally to achieve the required clinical and physiological effect. Two sedatives used commonly in bronchoscopy include benzodiazepines and opioids[4]. The agents utilised in our institution are midazolam and fentanyl. When selecting pharmacological sedatives for bronchoscopy ideally the chosen sedatives will be easy to administer, have a rapid onset and short duration of action and a rapid recovery with rapid return of cognition whilst not being altered by possible interactions with other drugs and the chosen sedatives should be reversible in a predictable manner through the use of antagonists[4].

Benzodiazepines are widely used in bronchoscopy to achieve the required level of sedation. It is known that benzodiazepines enhance the effect of the gamma-

aminobutryic acid (GABA), producing sedative, hyponotic, anxiolytic, anti-convulsant and muscle relaxing properties, with the benzodiazepine midazolam commonly used by bronchoscopists as it has a short half lift and it offers a fast onset of action[4]. The benzodiazepine, midazolam, is often used in bronchoscopy in combination with opiates as their analgesic, antitussive, sedative properties complement benzodiazepines to deliver the desired sedation, improving the patients tolerance to the procedure[4]. Opioids bind to mu (μ), kappa (κ), delta (δ) and sigma (σ) receptors located in the brain, spinal cord and peripheral sensory neurons and the gastrointestinal tract. For the purpose of bronchoscopy opioids which target the μ receptor, such as fentanyl which has a fast onset of action and short half-lift, results in supraspinal analgesia, respiratory depression and muscle rigidity creating an improved bronchoscopy experience[4].

Bronchoalveolar lavage (BAL) is achieved through the instillation of saline via the bronchoscope and it enables the collection of specimen directly from the endobronchial lumen for subsequent cytological or microbiological investigation[2]. Bronchoalveolar lavage (BAL) in these studies was obtained as a standardised 180ml (3x60ml) sample from either the right middle lobe or lingula.

In addition to the collection of Bronchoalveolar lavage (BAL), bronchial brushings were collected during bronchoscopy, by passing a small brush through the sampling channel of the bronchoscope to collect cells from the airway lining of the lung. The bronchial brushings, which are often used in research to establish primary bronchial cell culture, were in this case used for qRT-PCR analysis and so upon collection of the bronchial cells at the completion of the bronchoscopy the brush containing the cells was cut and placed in a sterile sample tube with a preservative for processing.

1.4. Spirometry

Spirometry was performed by research nurses from the Cork Clinical Research Facility – CCRF immediately prior to bronchoscopy. Spirometry is a widely used pulmonary function test which provides an aid in the diagnosis of lung diseases,

differentiating between obstructive and restrictive airway disorders and the monitoring of lung health[5]. Spirometry measures the maximal volume of air an individual can inspire and expire with maximal effort[5]. Forced Vital Capacity (FVC) is the volume of air delivered during an expiration made as forcefully and completely as possible with the time recorded from full inspiration[5]. Forced Expiratory Volume in the first second (FEV_1) is a measurement of the expiratory volume in the first second of the FVC maneuver[5]. The American Thoracic Society and European Respiratory Society state in their Standardisation in Spirometry 2019 report that the key stages of an FVC maneuver include; maximal inspiration, a "blast" of expiration, continued complete expiration for a maximal 15 seconds and inspiration at maximal flow back to maximal lung volume[5]. Maximum flow-volume curves, whereby the expired volume is measured by electrical integration of airflow, are produced by the spirometer[2]. The Irish Thoracic Society states that the use of spirometry to confirm diagnosis and assess responses to treatment in respiratory diseases such as asthma is recommended[6]. The Irish Thoracic Society states that when interpreting the results of a spirometer reading it is noted that in patients with airflow obstruction there is an inability for patients to exhale air quickly, leading to a fall in FEV_1 while FVC remains consistent leading to a FEV_1/FVC ratio below 70%, leading to a diagnosis of respiratory disorders such as asthma[6]. While a FEV_1/FVC ratio that is greater than 70% may represent normal pulmonary function it may at times represent restrictive airway disease, and in cases where the FEV_1 and FVC values are reduced poor technique must be ruled out before a restrictive airway disease can be diagnosed[6]. Spirometry is a useful respiratory function test as the spirometry test measurements complement the Global Initiative for Asthma (GINA) classification system, allowing for guidelines as to best practice with respect to therapy or mode of action[6].

1.5. FeNO – Fractional exhaled Nitric Oxide

Fractional exhaled Nitric Oxide (FeNO) is a non-invasive marker of inflammation and can elucidate how successful inhaled steroids are at supressing a patient's

inflammation[7]. For cases where a patient displays eosinophilic asthma FeNo has been reported to be elevated, while in patients with non-eosinophilic asthma this is not the case. Mast cells and antigen specific Th2 cells are activated in cases of eosinophilic asthma, which results in an upregulation of epithelial inducible nitric oxide[8]. Therefore in asthma patients FeNO has been noted to be a good biomarker for eosinophilic airway inflammation and predictor of poor or good corticosteroid response[8].

In 2011 the American Thoracic Society endorsed the use of FeNO as a diagnostic and decision-support tool for asthma[8]. It has been noted that FeNo can aid in; the detection of eosinophilic airway inflammation, the likelihood of inhaled corticosteroid (ICS) success, the monitoring of airway inflammation for the need to prescribe the patient inhaled corticosteroids and revealing possible patient ICS non-adherence[8]. Patients underwent FeNO measurement using a portable device which measured the level of nitric oxide in parts per billion (ppb) in the air which was exhaled from their lungs slowly.

1.6. ACQ-7 – Asthma Control Questionnaire-7

The Asthma Control Questionnaire (ACQ) was carried out by research nurses from the Cork Clinical Research Facility (CCRF) on the day of bronchoscopy. The ACQ-7 is a validated questionnaire developed and used under the permission of Prof. Elizabeth Juniper and is implemented is the following studies as it is validated for its discriminative properties enabling measurement of patient asthma control[9]. The questionnaire consists of 7 items, 5 questions relate to the highest scoring symptoms people with asthma experience, 1 question related to rescue bronchodilator use and 1 question is answered by the research nurse post spirometry and is related to the FEV_1% of predicted normal[10]. Patients are required to recall their asthma symptoms and behaviour and their bronchodilator use during the previous week and answer each question on a 7 point scale which is provided, whereby 0 = no impairment and 6 = maximum impairment. The questions are as follows:

1. On average, during the past week, how often were you woken by your asthma during the night?
2. On average, during the past week, how bad were your asthma symptoms when you woke up in the morning?
3. In general, during the past week, how limited were you in your activities because of your asthma?
4. In general, during the past week, how much shortness of breath did you experience because of your asthma?
5. In general, during the past week, how many times did you wheeze?
6. On average, during the past week, how many puffs/inhalations of short acting bronchodilator have you used each day?
7. FEV_1 % predicted?

All questions in the ACQ-7 are equally weighted and the mean of the 7 questions is used to calculate the patients ACQ-7 score[11].

1.7. GINA – Global Initiative for Asthma

Established by the World Health Organisation and the National Heart, Lung and Blood Institute in 1993 GINA – The Global Initiative for Asthma was formed to increase asthma awareness among health professionals, authorities and the community[12]. GINA is strongly focused on preventing asthma related deaths and severe exacerbations while also focusing on the efficacy and effectiveness of asthma treatment in general. GINA through the release of their yearly report compiles the most recent understandings in scientific research with respect to asthma and translates this scientific evidence in a manner that will improve patient care. Providing guidance on many aspects of asthma diagnosis and treatment, the GINA report also groups patients into stages or steps of asthma severity, from stage 1; mild to stage 5; severe[13,14]. All patients within the following cohorts have been assigned a GINA ranking of asthma severity by Dr Des Murphy; whereby GINA 1+2 = Mild, GINA 3= Moderate and GINA 4+5 = Severe.

1.8. Blood sampling

Venepuncture was carried out prior to bronchoscopy by the Doctor on duty using aseptic technique and strict adherence to standard precautions. The Vacutainer System was used for blood drawing. The order in which blood containers were filled was in accordance to Cork University Hospital recommendations of blood draw order.

In order to test for *Aspergillus* antibodies blood was collected in a 4ml red capped Vacuette tube with clotting accelerator to ensure blood coagulated and a separator gel to ensure blood fractions separated upon centrifugation. The *Aspergillus* antibodies test was performed by a reference laboratory (Mycology Reference Centre, Leeds, UK).

In order to test patient IgE levels, blood was collected in a plain 4ml red capped Vacuette tube with clotting accelerator and the IgE level test was performed by the Clinical Biochemistry Department at Cork University Hospital. IgE levels above 80 KU/L were considered not normal.

In a patient specific manner, C-reactive protein (CRP), a blood marker for inflammation in the body, was tested for. This required blood to be collected in a 4ml red capped plain tube with clotting accelerator. The test was performed by the Clinical Biochemistry Department at Cork University Hospital. The reference range for CRP is 0.0-5.0 mg/L.

With respect to the patient cohorts involved in the following research studies both serum and plasma samples were required for future analysis at the APC Microbiome Ireland, University College Cork. The required blood samples were collected in serum specific red and yellow capped Vacuette tubes and plasma specific purple capped Vacuette tubes (Greiner Bio-One). The inner wall of the serum specific Vacuette tube was coated with silica particles which activated the coagulation process and a specific separator gel at the base of the tube formed a stable barrier during centrifugation to enable the serum and the blood to remain separated. The plasma specific purple capped Vacuette tube contained a coating of either K2EDTA or K3EDTA which acted as an anticoagulant by binding calcium ions

to prevent the clotting cascade from taking place. Upon return to the laboratory both tubes were centrifuged at 200rpm for 20 minutes and the serum and plasma was removed by pipetting and stored in screw-cap microcentrifuge tubes. All patient serum and plasma isolated samples were then stored at -80^{o}C for future processing and analyses.

Erythrocyte sedimentation rate (ESR) was measured in a patient specific manner. The ESR measurement is a non-specific test of inflammation and tissue damage. Blood was collected in a 3ml purple EDTA containing Vacuette tube. The ESR protocol was carried out by the Haematology Department at Cork University Hospital. The blood specimen must be less than 12 hours old from the time of phlebotomy however the ESR is most accurate within 4 hours of phlebotomy and the minimum sample volume required is 1.4ml. The reference range for males is 0-10 mm/hour and for females is 0-22 mm/hour.

A full blood count including analysis of haemoglobin, red cell count, white blood cell count, eosinophil count, lymphocyte count and neutrophil count was carried out for all patients. Blood was collected in a 3ml purple Vacuette tube with EDTA and the test procedure was carried out by the Haematology Department at Cork University Hospital. The haemoglobin reference range for males >18 years is 13.0-17.0 g/dl and for females >18 years is 11.7-15.9 g/dl. The red cell count reference range for males >18 years is 4.2-5.6 x10^{12}/l and for females >18 years is 3.9-5.3 x10^{12}/l. The reference range for white blood cell count for both males and females >18 years is 4.4-11.3 x10^{9}/l. The reference range for the eosinophil count for both males and females >18 years is 0.04-0.4 x10^{9}/l. The reference range for the lymphocyte count for both males and females >18 years is 0.9-3.2 x10^{9}/l. The reference range for the neutrophil count for both males and females >18 years is 1.4-6.6 x 10^{9}/l.

Glucose levels required the collection of blood in a 4ml sodium fluoride EDTA grey capped Vacuette tube. The protocol to determine glucose concentration was carried out by the Clinical Biochemistry Department at Cork University Hospital and the reference range of blood glucose levels is determined by WHO guidelines, with the normal range below 11.1 mmol/l and the fasting range below 5.5 mmol/l.

References

1. ERS White Book. 2019; https://www.erswhitebook.org/chapters/adult-asthma/, 2019.
2. Principles of respiratory investigation. 2020; https://www.erswhitebook.org/chapters/principles-of-respiratory-investigation/, 2020.
3. Martinsen EMH, Eagan TML, Leiten EO, et al. Motivation and response rates in bronchoscopy studies. *Multidisciplinary Respiratory Medicine.* 2019;14(1):14.
4. José RJ, Shaefi S, Navani N. Sedation for flexible bronchoscopy: current and emerging evidence. *European Respiratory Review.* 2013;22(128):106-116.
5. Graham BL, Steenbruggen I, Miller MR, et al. Standardization of Spirometry 2019 Update. An Official American Thoracic Society and European Respiratory Society Technical Statement. *Am J Respir Crit Care Med.* 2019;200(8):e70-e88.
6. O'Connor T, Manning, P. *Spirometry: Performance and Interpretation - A Guide for General Practitioners.* Irish Thoracic Society Irish Thoracic Society;2005.
7. Gemicioglu B, Musellim B, Dogan I, Guven K. Fractional exhaled nitric oxide (FeNo) in different asthma phenotypes. *Allergy Rhinol (Providence).* 2014;5(3):157-161.
8. Price D, Ryan D, Burden A, et al. Using fractional exhaled nitric oxide (FeNO) to diagnose steroid-responsive disease and guide asthma management in routine care. *Clinical and Translational Allergy.* 2013;3(1):37.
9. Juniper EF, O'Byrne PM, Guyatt GH, Ferrie PJ, King DR. Development and validation of a questionnaire to measure asthma control. *The European respiratory journal.* 1999;14(4):902-907.
10. Juniper EF, Svensson K, Mork AC, Stahl E. Measurement properties and interpretation of three shortened versions of the asthma control questionnaire. *Respir Med.* 2005;99(5):553-558.
11. Juniper EF, Bousquet J, Abetz L, Bateman ED. Identifying 'well-controlled' and 'not well-controlled' asthma using the Asthma Control Questionnaire. *Respir Med.* 2006;100(4):616-621.
12. Reddel HK, FitzGerald JM, Bateman ED, et al. GINA 2019: a fundamental change in asthma management. *Treatment of asthma with short-acting bronchodilators alone is no longer recommended for adults and adolescents.* 2019;53(6):1901046.
13. *Global Strategy for Asthma Management and Prevention 2019 Update.* Global Initiative For Asthma2019.
14. *Pocket Guide for Asthma Management and Prevention 2019 Update.* Global Initiative For Asthma 2019.

Chapter 3

Fungi in Asthma

The presence of *Aspergillus fumigatus* in asthmatic airways is not clearly related to clinical disease severity

Author Contributions: Desmond Murphy, John MacSharry, Chris Ward and Paul O'Byrne were responsible for the study design and concept. Desmond Murphy and Eoin Hunt were responsible for patient recruitment, clinical characterisation and sample acquisition. Sample processing and study assays were primarily performed by Ashley Sullivan with contribution from Eoin Hunt, Susan Lapthorne, Liam Fanning, John MacSharry and Chris Ward. Statistical analysis was performed by the authors in conjunction with biostatistical support from Joseph Eustace and The Clinical Research Facility University College Cork. Analysis and interpretation of data, manuscript preparation and approval were performed by Ashley Sullivan, Eoin Hunt, Chris Ward, Susan Lapthorne, Joseph Eustace, Liam Fanning, Barry Plant, Paul O'Byrne, John MacSharry and Desmond Murphy.

This chapter has been published in Allergy

https://doi.org/10.1111/all.14087

PMID: 31605638

1. Abstract 65
2. Introduction 66
3. Methods 68
    3.1. Patient recruitment 68
    3.2. Total IgE and *Aspergillus fumigatus* IgE detection 69
    3.3. Microscopy 70
    3.4. DNA extraction 70
    3.5. Fungal quantitative PCR 72
    3.6. Platelia *Aspergillus* antigen (Galactomannan assay) 73
    3.7. Cytokine measurement 74
    3.8. Statistical analyses 75
4. Results 76
    4.1. Patient demographics 76
    4.2. Serological detection of fungal sensitisation and presence 82
    4.3. Fungal detection by microscopy 83
    4.4. Molecular detection of fungal presence 84
    4.5. Plasma and BAL cytokine levels correlate with BAL fungal presence 90
5. Discussion 96
6. References 102

1. Abstract

Background: It is thought that airway fungi, in particular *Aspergillus* may impact on the severity of the clinical phenotype in asthma. Indeed the term severe asthma with fungal sensitisation (SAFS) has been coined. We aimed to determine whether the presence of fungi, in particular *Aspergillus fumigatus*, in the airway correlated with asthma severity and control. Furthermore, we aimed to determine if traditional markers of *Aspergillus* sensitisation related to the presence of *Aspergillus* within the airway.

Methods: Sixty-nine patients characterised by asthma severity (GINA) and level of control (ACQ-7) underwent bronchoscopy and bronchoalveolar lavage (BAL). Serum was assessed for *A. fumigatus* specific IgE and total IgE. Galactomannan and relevant cytokine levels were assessed in serum, plasma and BAL. BAL was analysed for the presence of *A. fumigatus.*

Results: In BAL, fungi were visible by microscopy in 70% (n=69) and present by qPCR in 86% of patients, while *A. fumigatus* was detectable by qPCR in 46%. Plasma and BAL IL-4, IL-6, IL-10, IL-13 and TNF-α correlated with BAL fungal presence, while plasma IL-17 correlated with BAL fungal presence. *Aspergillus* positive BAL correlated with increased plasma and BAL IL-6 and BAL IL-13. There was no relationship between fungal airway presence and oral steroid or inhaled corticosteroid dose, asthma severity or control. The presence of *Aspergillus* within the airway also did not relate to serum IgE positivity for *Aspergillus*.

Conclusions: Fungi were present in a large proportion of our asthmatic patients' airways, but their presence was not predicted by traditional markers of sensitisation, nor did it appear to be related to measures of disease severity or control.

2. Introduction

The term severe asthma groups patients with varying pathophysiological and phenotypic characteristics[1]. Studies have suggested roles for fungi in severe asthma and the term severe asthma with fungal sensitisation (SAFS) has been coined; the current definition of which is based on demonstrating sensitisation to fungus in the absence of allergic bronchopulmonary aspergillosis (ABPA)[2]. Therapies aimed at fungal elimination have afforded mixed results[3,4].

The respiratory tract is constantly exposed, via the atmospheric environment, to hyphal fragments, fungal spores and yeasts[5-7]. Thermotolerant fungi, including *Candida, Aspergillus* and *Penicillium* are sources of allergens, commensals and opportunistic pathogens and can colonise airways with potential clinical ramifications[5].

Aspergillus fumigatus, a ubiquitous fungus can elicit a destructive response in a susceptible host[8]. Due to the spherical shape of *A. fumigatus* conidia, typically 2.0-3.0μm in diameter, the conidia can evade mucociliary clearance and reach the lower airways[9]. Pathogen recognition receptors and innate immune cells can subsequently initiate a cascading anti-fungal response, culminating in phagocytosis, removal of the fungal insult and down-regulation of inflammatory cytokine signalling[10,11]. In a healthy host these innate mechanisms ensure that fungal spores are cleared[11]. In a host with a pre-existing disorder, such as asthma, there is a risk that fungal exposure will lead to airway colonisation, and disorders such as severe asthma with fungal sensitisation (SAFS) or ABPA[10,11]. It has been suggested that fungal sensitisation and asthma severity may be related, and a temporal relationship between fungal exposure and clinical outcome has been shown[2,12]. While interest remains in relation to *Aspergillus* colonisation, attention to other fungi is also of interest and a wider group of sensitisation to genera such as *Candida* and *Penicillium* exists and is encompassed within the diagnosis Allergic Bronchopulmonary Mycosis[5].

In this study, we sought to ascertain whether fungi, and in particular *Aspergillus* were present in the airways of asthmatics across the spectrum of disease severity

and determine whether their presence was associated with airway and systemic cytokines, levels of control, disease severity or treatment with steroids. We additionally wished to determine whether or not systemic sensitisation with *Aspergillus* as currently utilised to define SAFS was related to *Aspergillus* presence within the airway.

3. Methods

3.1. Patient recruitment

The study was approved by the Clinical Research Ethics Committee of the Cork Teaching Hospitals. Sixty-nine patients with a history of asthma (either documented change in FEV1 ≥12%/200ml with bronchodilator or a positive inhalation challenge) were recruited through a dedicated asthma clinic in a tertiary referral centre, Cork University Hospital, by my clinical supervisor, Dr Des Murphy. Patients with ABPA were excluded. Patients were scheduled for bronchoscopy, with spirometry, ACQ-7 and blood sampling performed on the day of bronchoscopy. Written informed consent was obtained from patients on the day of bronchoscopy.

Spirometry, a lung function test, was performed according to ATS/ERS guidelines by a research nurse from the Cork Clinical Research Facility – CCRF immediately prior to bronchoscopy[13]. Spirometry measures the maximal volume of air an individual can inspire and expire with maximal effort[14]. The cohort was stratified by both severity [mild (GINA 1+2), moderate (GINA 3) and severe (GINA 4+5)] and asthma control (ACQ-7)[15,16] (Table 2). Asthma severity was determined through the implementation of the Global Initiative for Asthma (GINA) ranking system which groups patients into stages or steps of asthma severity, from stage 1; mild to stage 5; severe[17,18]. In order to group patients by level of control the Asthma Control Questionnaire (ACQ-7) was utilised by a research nurse from the Cork Clinical Research Facility – CCRF prior to bronchoscopy. The ACQ-7 consists of 7 items; 5 questions related to the highest scoring symptoms people with asthma experience, 1 question related to rescue bronchodilator use and 1 question was answered by the research nurse post spirometry and was related to the FEV_1% of predicted normal[19]. All questions in the ACQ-7 are equally weighted and the mean of the 7 questions was used to calculate the patients ACQ-7 score[20].

Venepuncture was carried out prior to bronchoscopy by the doctor on duty using aseptic technique and strict adherence to standard precautions. The Vacutainer System was used for blood drawing and the order in which the blood containers were filled was in accordance to Cork University Hospital recommendations for

blood draw order. Serum was assessed for total IgE and *A.fumigatus* specific IgE and plasma was assessed for cytokines. For further information regarding blood collection and processing please see *Chapter 2 Study Cohorts' – 1.8 Blood sampling*.

Patients underwent bronchoscopy according to standard guidelines[21]. Flexible bronchoscopy using video assisted imaging was performed under conscious sedation with local anaesthetic applied topically to the vocal cords, trachea and endobronchial tree[22]. Bronchoalveolar lavage (BAL) was achieved through the instillation of saline via the bronchoscope enabling the collection of specimen directly from the endobronchial lumen for subsequent cytological or microbiological investigation[22]. Bronchoalveolar lavage (BAL) was obtained as a standardised 180ml (3X60ml) sample from either the right middle lobe or lingula[23].

Further information with regards to asthmatic patient bronchoscopy and patient sample collection protocols can be found in *Chapter 2 Study Cohorts'*.

3.2. Total IgE and *Aspergillus fumigatus* IgE detection

In order to quantitatively assess for circulating total IgE and *Aspergillus fumigatus* specific IgE in human serum ImmunoCAP IgE assays (Thermo Fischer Scientific/Phadia, Uppsala, Sweden) were performed at the clinical laboratories at Cork University Hospital according to the manufacturers protocols. Briefly, the ImmunoCAP solid phase consists of a capsule with a cellulose derivative. In the case of total IgE detection Anti-IgE was covalently coupled to the solid phase ImmunoCAP and a reaction with total IgE within the patient sample occurred. After washing the capsule enzyme labelled antibodies against IgE were added to the capsule and a complex was formed and incubation of the complex occurred. Following the incubation stage unbound enzyme was then washed away and the bound complex was then incubated with the developing agent. Once the reaction was stopped the fluorescence of the eluate was measured and values were transformed using a calibration curve. Fluorescence was directly proportional to the concentration of IgE within the patient sample.

In the case of *A. fumigatus* specific IgE detection the allergen of interest, *A. fumigatus,* covalently coupled to the ImmunoCAP, reacted with the *A. fumigatus* specific IgE in the patient serum. Non-specific IgE was washed away and enzyme labelled anti-IgE antibodies were added and a complex was formed. Upon the completion of the incubation stage any unbound anti-IgE was washed away and further incubation of the bound complex and a developing agent occurred. Once the reaction is stopped the fluorescence values were transformed using a calibration curve to determine the amount of *A. fumigatus* specific IgE present within the serum.

3.3. Microscopy

A differential cell count was performed on BAL cytospin slides, stained with the Kwik-Diff kit (Thermo-Fisher) using light microscopy and Olympus DP software. Immune cell percentage counts were calculated and slides scored for fungal presence by 3 independent observers and microscopic observation of fungus was determined by size and presence of hyphae and/or spores. Samples received a positive or negative fungal score (0/1). A representative positive sample is shown in figure 4 B-C.

3.4. DNA extraction

To reduce contaminating host cell DNA, BAL was centrifuged at 500g for 10 minutes, supernatant collected and centrifuged in 2ml screwcap microcentrifuge tubes at 20,000g for 5 minutes. The supernatant was then removed and the remaining bacteria pellets were recombined for DNA extraction. See figure 1 for patient BAL processing which occurred on the day of patient bronchoscopy.

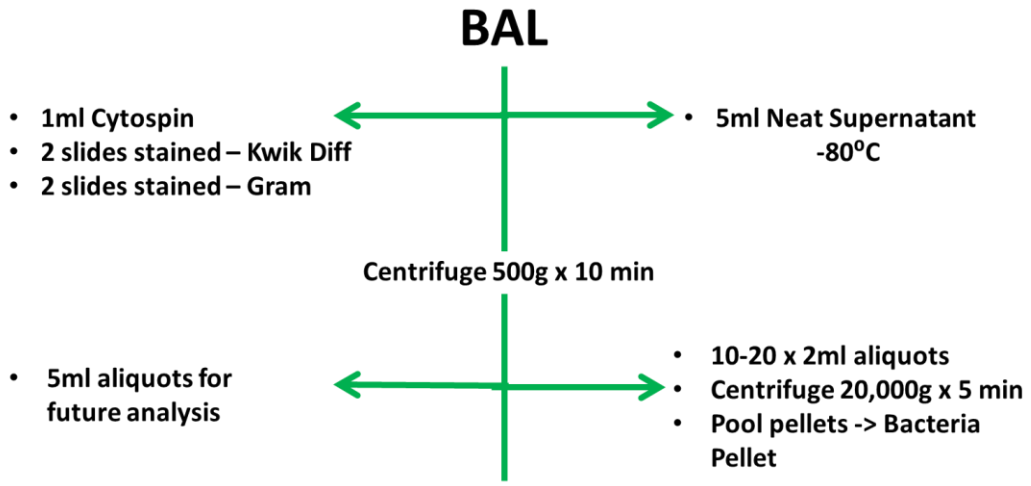


Figure 1. Patient BAL processing schematic. Chart depicting the process the patient BAL underwent once processing began in the laboratory on the day of bronchoscopy.

DNA extraction took place using a QIAamp UPC Pathogen Mini Kit (Qiagen, Manchester, UK). Patient bacteria pellet samples were centrifuged at 20,000g for 5 minutes, supernatant discarded and 500ul buffer ATL was used to resuspend the pellet which was then added to a pathogen lysis tube containing silica beads (Scratech Scientific, UK) and vortexed at 7000rpm for 1 minute using a MagNA Lyser machine. The tube was then centrifuged at 8000g for 30 seconds and supernatant removed to a fresh microcentrifuge tube without disrupting the silica beads. 40µl of Proteinase K was added; the tube was vortexed and incubated at 56^{o}C for 10 minutes. 200µl buffer APL2 then added to the sample, the tube was vortexed and incubated at 70^{o}C for 10 minutes. 300µl of ethanol was added to the lysate and the tube was pulse vortexed for 30 seconds and the lysate was then transferred to a mini spin column placed in a collection tube and centrifuged at 6000g for 1 minute. This was repeated until all of the lysate had been transferred and passed through the mini spin column, discarding the filtrate after each spin. 600µl of Buffer APW1 was added to the mini spin column which was then centrifuged at 6000g for 1 minute, discarding the filtrate afterwards. 750µl of Buffer APW2 was transferred to the mini spin column which was then centrifuged at 20,000g for 3 minutes,

transferring the mini spin column to a new collection tube and repeating centrifugation to eliminate buffer carryover. The mini spin column was then transferred to a new collection tube and incubated at 56^{o}C for 3 minutes to ensure the membrane was dry and was then transferred to a new DNA elution tube and 100µl of Buffer AVE was added to the centre of the membrane and incubated at room temperature for 1 minute before being centrifuged at 20,000g for 1 minute to elute the DNA. DNA quantification was performed using a NanoDrop 2000 Spectrophotometer (Fisher Scientific, Dublin, Ireland) and samples above 5ng/µl were diluted back to 5ng/µl with molecular grade water.

3.5. Fungal quantitative PCR

Primers were designed and validated. qPCR was performed on extracted BAL DNA to determine presence of fungi and *A. fumigatus* using a total fungal primer (Fungi Quant)[24] and an *A. fumigatus* ITS specific primer[25] (Table 1). qPCR's were performed using a 384 well plate layout and LightCycler Probes Master (Roche, Ireland) or LightCycler SYBR Green Master (Roche, Ireland) reagent mix, dependent on the use of hydrolysis probes or SYBR Green primer sets. Water NTCs (No Template Control) were used in each reaction in order to identify reaction set up contamination and to test for the propensity of primers to create primer dimers in the case of reactions which were carried out with SYBR Green Master. Reactions were performed on a LightCycler 480 machine (Roche, Ireland). qPCR conditions were as follows; pre-incubation at 50^{o}C for 2 minutes, ramp rate 4.8^{o}C/s and 95^{o}C for 10 minutes, ramp rate 4.8^{o}C/s. Amplification at 95^{o}C for 10 seconds, ramp rate 4.8^{o}C/s, 60^{o}C for 45 seconds, ramp rate 2.5^{o}C/s and 75^{o}C for 1 second, ramp rate 4.8^{o}C for 45 cycles in total. A melt curve also occurred at 95^{o}C with a ramp rate of 0.11^{o}C/s for any primer which used LightCycler SYBR Green Master. A cooling stage then occurred at 40^{o}C, ramp rate 2^{o}C/s at the end of the process. Fluorescent readings were taken in single acquisition mode. All NTCs did not produce a product and melt curves produced clear peaks indicating that the products produced were not an artefact.

Primer		Sequence	Reference
Fungi Quant	Fungi Quant-F	5'-GGR AAA CTC ACC AGG TCC AG-3'	[24]
	Fungi Quant-R	5'GSW CTA TCC CCA KCA CGA-3'	
Aspergillus fumigatus	OliAFMB-L-pl-103	5'-AGC ACG GCT TGT GTG TTG -3'	**Modification on** *Aspergillus* ITS KT358862 [25]
	OliAFMB-R-pl-103	5'-GGG TGA CAA AGC CCC ATA C-3'	

Table 1. Primer sequences. Validated primer sequences utilised for the detection of total fungi (Fungi Quant) and *Aspergillus fumigatus* (gene OliAFMB). Note: K=G or T, R=A or G, S=G or C, W=A or T, IUPAC code.

3.6. Platelia *Aspergillus* antigen (Galactomannan assay)

Platelia *Aspergillus* antigen immunoenzymatic sandwich microplate assay (Bio-Rad, Dublin, Ireland) was performed on patient serum and BAL to determine presence/absence of *Aspergillus* galactomannan antigen. The assay was performed using the manufacturer's protocol. Briefly, rat derived EBA-2 monoclonal antibodies were used to coat the wells of the microplate, bind the antigen and to detect the antigen bound to the sensitised microplate. The serum or BAL fluid samples to be tested were first heat treated in the presence of EDTA. The treated samples and conjugate reagent (peroxidase-linked anti-galactomannan monoclonal antibodies) were then transferred to the coated microplate and the plate was incubated. A monoclonal antibody-galactomannan-monoclonal antibody/peroxidase complex was formed in the presence of the antigen galactomannan. The microplate was then washed five times to ensure the removal of any potentially unbound material. Chromogen TMB solution was rapidly added in the wells of the microplate ensuring exposure to bright light was avoided and a blue colour reaction took place upon the

reaction with the bound complexes in the wells. A 1N sulfuric acid solution was then added to the wells in order to stop the enzymatic reaction and a colour change from blue to yellow was observed The optical density of each well was read using a spectrophotometer set at 450nm (reference filter 620/630nm) (Synergy HTX Multi Mode Reader, BioTek, USA).

3.7. Cytokine measurement

BAL and plasma cytokines were analysed using a custom MSD proinflammatory panel 1 containing targets for Interleukin (IL)-1β, IL-4, IL-6, IL-8, IL-10, IL-13, Interferon (IFN)-γ and tumour necrosis factor (TNF)-α and a custom MSD cytokine panel 1 containing targets for IL-5 and IL-17A. Reagent preparation consisted of the following; calibrator standards were prepared by resuspension of the lyophilised calibrator with 1000µl of the appropriate diluent (diluent 2 for proinflammatory panel 1 and diluent 43 for cytokine panel 1) and then transferring 100µl of the re-suspended calibrator with 300µl of appropriate diluent. This 4 fold serial dilution was repeated 5 additional times to generate 7 calibrators with the diluent alone used as a zero calibrator. Plasma samples were diluted as follows; 35µl of plasma and 35µl of appropriate diluent, while BAL samples were undiluted. A detection antibody solution was created for the proinflammatory panel by combining 60µl of each SULFO-TAG anti-human IL-1β, IL-4, IL-6, IL-8, IL-10, IL-13 IFN-γ and TNF-α antibody with 2520µl diluent 3 to bring to a final volume of 3000µl. A detection antibody solution for cytokine panel 1 consisted of 60µl each of SULFO-TAG Anti-human IL-5 and IL-17A with 2880µl of diluent 3 for a final volume of 3000µl. Wash buffer consisted of PBS and 0.05% Tween 20. Read buffer for each plate consisted of 10ml of Read Buffer T (4X) and 10ml of deionised water for a 2X working solution. Step 1 of the assay involved washing the plate 3 times with 150µl/well wash buffer 50µl of prepared calibrators or samples was added per well, the plate was sealed before overnight incubation with shaking at 2-8^{o}C. Step 2 involved washing the plate a further 3 times with 150µl/well wash buffer before the addition of 25µl detection antibody solution to each well, the plate sealed and a two hour

room temperature incubation with shaking occurred. Step 3; the plate was washed 3 times as before and 150µl of 2X Read Buffer T was added to each well before analysis of the plate using an electro-chemiluminescence QuickPlex SQ 120 imager from Meso Scale Discovery (Gaithersburg, MD, USA).

3.8. Statistical analyses

Statistical analyses were performed using Graph Pad Prism Software 6. Appropriate tests such as T-test, Spearman and Pearson Correlations were performed, with corrections for parametric/non-parametric data. Results were considered statistically significant when $P<0.05$.

4. Results

4.1. Patient demographics

Of the sixty-nine adult asthmatic patients recruited, 61% were female. The cohort was stratified by asthma severity into 35% mild (GINA 1+2), 22% moderate (GINA 3), 43% severe (GINA 4+5) and level of control (ACQ-7) with 38% controlled (ACQ-7<1.5) and 62% uncontrolled (ACQ-7≥1.5).

Seven patients (10%) were on maintenance oral steroids at the time of testing (7.5mg median; min-max 5-30 mg daily). Ten asthmatics (14%) were newly diagnosed and ICS naïve at the time of sampling.

Of the sixty-nine patients recruited 7 were current smokers, 18 were ex-smokers and 44 patients had never smoked. 65% (45/69) of patients lived in a rural location while 35% (24/69) of patients lived in an urban setting.

Results and patient characteristics are summarised in table 2.

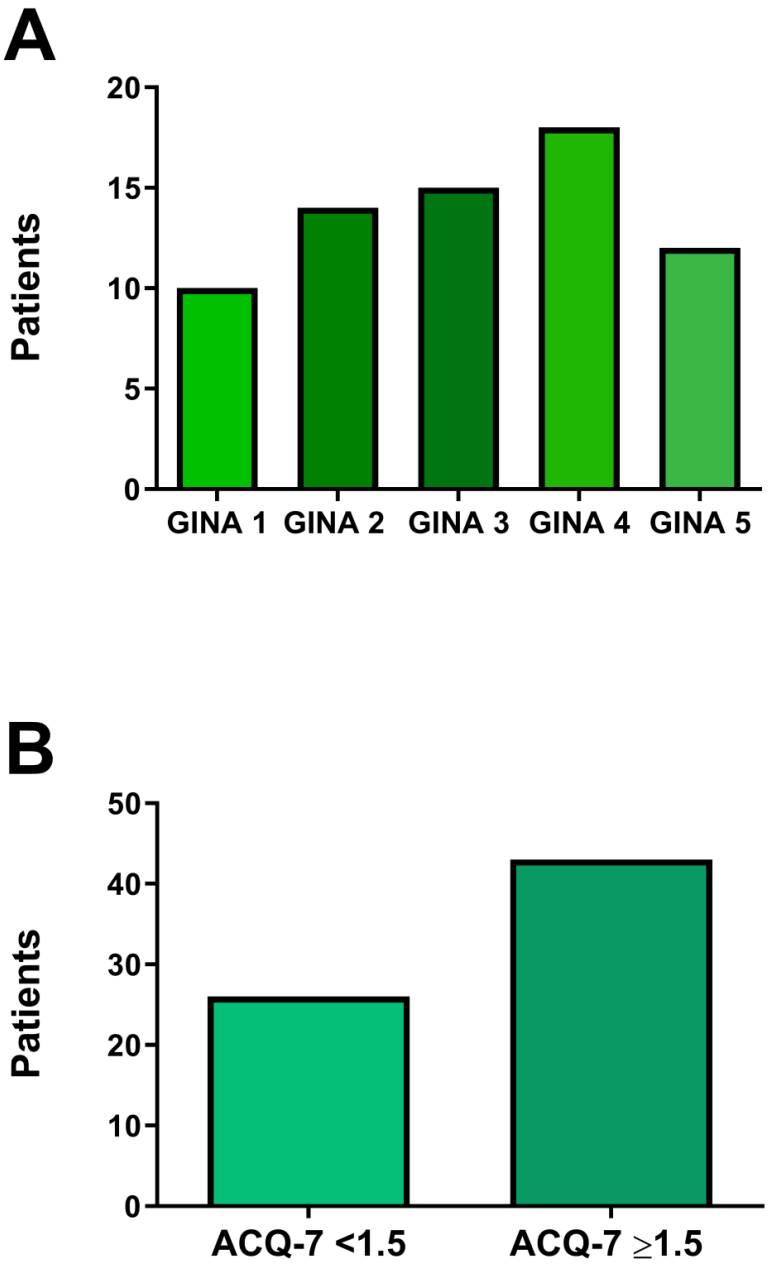


Figure 2. Distribution of patient asthma severity and level of control. The patient cohort was stratified by (A) asthma severity (GINA) into 35% (24/69) mild (GINA 1+2), 22% (15/69) moderate (GINA 3), 43% (30/69) severe (GINA 4+5) and (B) level of control (ACQ-7) with 38% (26/69) controlled (ACQ-7<1.5) and 62% (43/69) uncontrolled (ACQ-7 ≥ 1.5) asthmatics. n=69

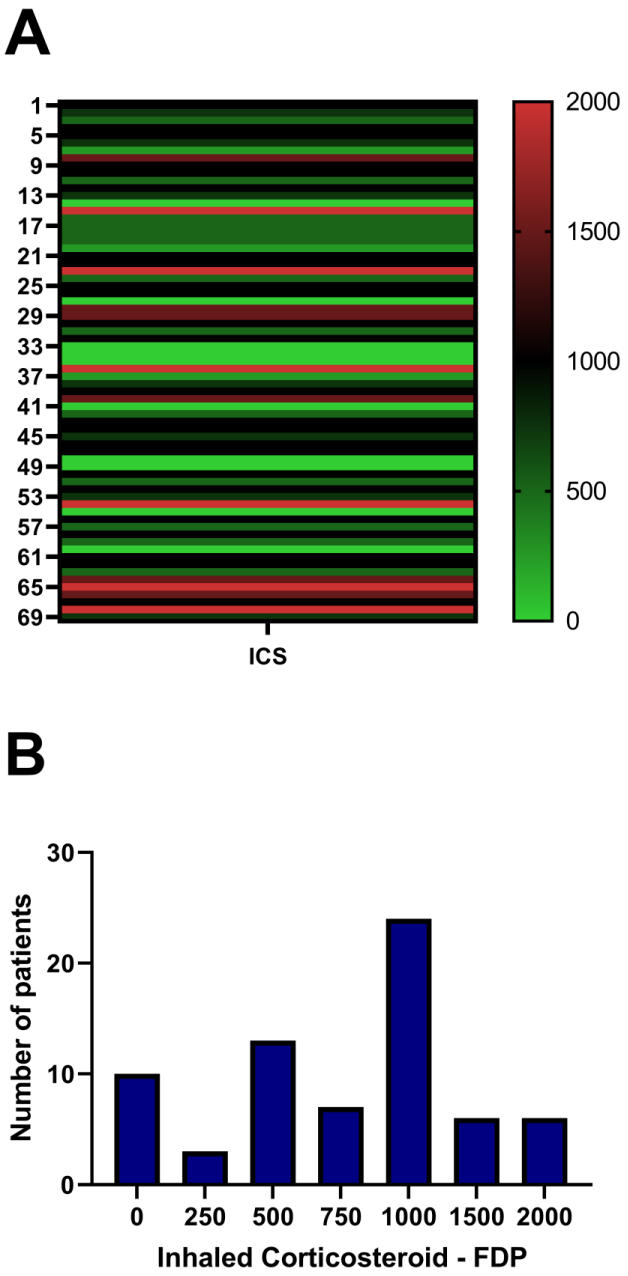


Figure 3. Range of inhaled corticosteroid dose of asthmatic patients. (A) Heatmap visualisation of patient inhaled corticosteroid (ICS) FDP prescribed. (B) Breakdown of patient inhaled corticosteroid (ICS) (FDP) dose. 10 patients within the cohort were newly diagnosed and ICS naïve at the time of sampling. ICS FDP; 0 (10/69), 250 (3/69), 500 (13/69), 750 (7/69), 1000 (24/69), 1500 (6/69), 2000 (6/69).n=69

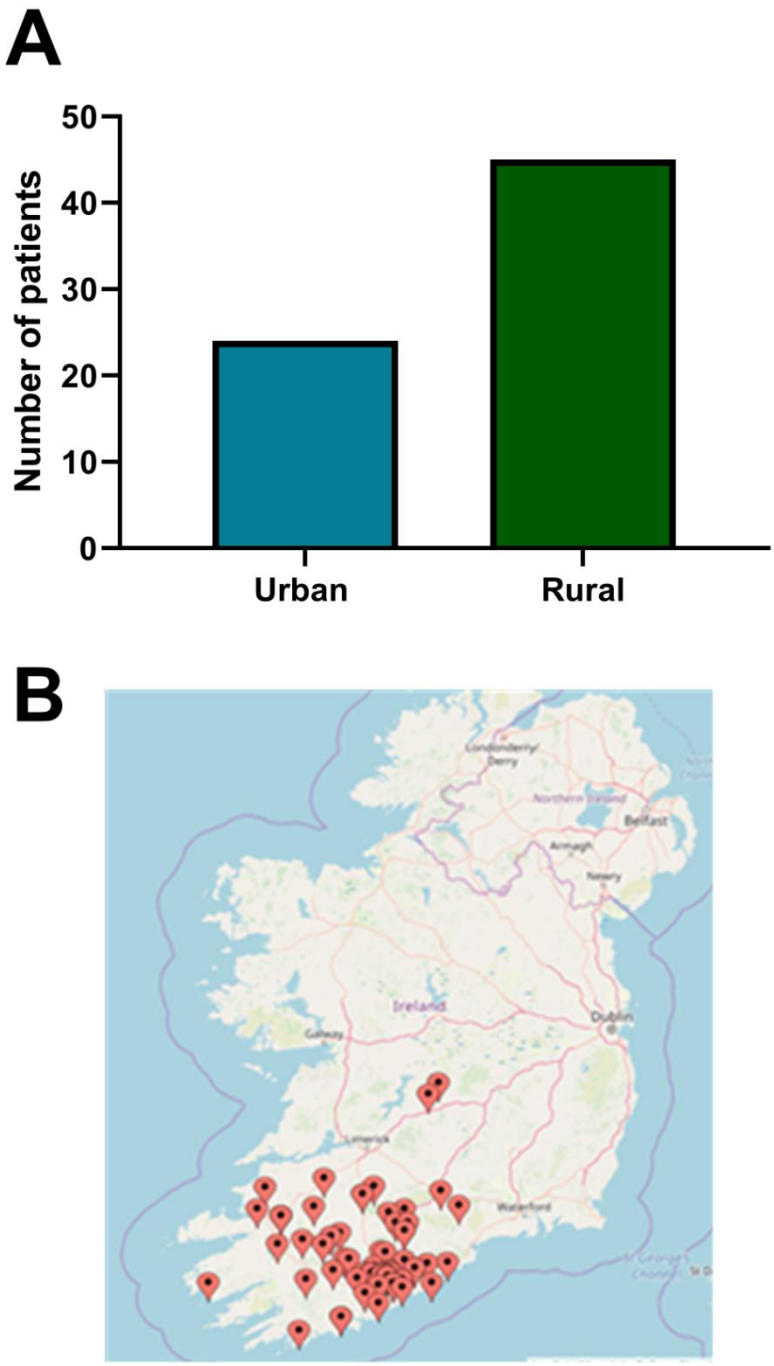


Figure 4. Patient location. When the location of the patients within the cohort was investigated it was found that 35% (24/69) of patients lived in an urban dwelling while 65% (45/69) of patients lived in a rural location (A-B). n=69

Table 2. Asthmatic patient demographics. Patient demographics broken into grouping for mild, moderate and severe asthma as defined by GINA groupings Mild (GINA 1+2), Moderate (GINA 3) and Severe (GINA 4+5). Note † ACQ-7, Asthma Control Questionnaire; ‡ FEV-1, Forced Expiratory Volume in the first second; § FeNO, Fractional exhaled Nitric Oxide; ¶ BMI, Body Mass Index. Table continued on following page.

		Mild (GINA 1-2)	**Moderate (GINA 3)**	**Severe (GINA 4-5)**
Patients	n=69 (%)	24 (35%)	15 (22%)	30 (43%)
Male		11 (46%)	5 (33%)	11 (37%)
Female		13 (54%)	10 (67%)	19 (63%)
Smoker	Current	2	1	4
	Ex-	7	2	9
	Never	15	12	17
IgE (KU/L)	[Mean (SD)]	[354 (654.1)]	[178 (252.3)]	[317 (484.1)]
***A. fumigatus* IgE**	Positive	2	1	3
ACQ-7 †	[Mean (SD)]	(1 (0.6)]	[2 (1.0)]	[3 (1.1)]
FEV-1 (Percent Predicted) ‡	[Mean (SD)]	[86 (13.7)]	[88 (21.7)]	[66 (22.3)]
FeNO (ppb) §	[Mean (SD)]	[25 (24.6)]	[20 (14.0)]	[17 (25.3)]
BMI (kg/m^2) ¶	[Mean (SD)]	[26 (4.5)]	[29 (6.8)]	[31 (6.7)]
BAL Galactomannan	Positive	3	0	2
Serum Galactomannan	Positive	0	0	1
BAL Fungal Microscopy	Positive	18 (75%)	12 (80%)	18 (60%)
BAL Total Fungi (Cp)	Positive	20 (84%)	14 (94%)	25 (84%)
	[Mean (SD)]	[34 (2.2)]	[34 (2.6)]	[36 (2.2)]
BAL *A. fumigatus* (Cp)	Positive	13 (54%)	7 (47%)	12 (40%)
	[Mean (SD)]	[34 (3.4)]	[36 (1.4)]	[34 (2.6)]
BAL Monocyte % count	[Mean (SD)]	[8 (7.6)]	[6 (8.3)]	[4 (4.6)]
BAL Macrophage % count	[Mean (SD)]	[80 (10.20)]	[62 (27.4)]	[75 (20.1)]
BAL Lymphocyte % count	[Mean (SD)]	[7 (5.1)]	[9 (11.4)]	[9 (10.6)]

		Mild (GINA 1-2)	Moderate (GINA 3)	Severe (GINA 4-5)
BAL Eosinophil % count	[Mean (SD)]	[2 (2.1)]	[3 (5.5)]	[3 (8.2)]
BAL Neutrophil % count	[Mean (SD)]	[3 (7.4)]	[14 (20.7)]	[5 (6.9)]
BAL IL-4 (pg/ml)	[Mean (SD)]	[0.5 (1.9)]	[0.1 (0.1)]	[1 (1.9)]
BAL IL-5 (pg/ml)	[Mean (SD)]	[0.2 (0.4)]	[0.7 (2.4)]	[2 (7.4)]
BAL IL-6 (pg/ml)	[Mean (SD)]	[2 (2.9)]	[4 (5.6)]	[10 (20.4)]
BAL IL-8 (pg/ml)	[Mean (SD)]	[397 (843.2)]	[740 (1846)]	[236 (318.1)]
BAL IL-10 (pg/ml)	[Mean (SD)]	[0.7 (2.3)]	[0.2 (0.3)]	[1 (1.4)]
BAL IL-13 (pg/ml)	[Mean (SD)]	[4 (10.7)]	[3 (1.7)]	[6 (6.9)]
BAL IL-1β (pg/ml)	[Mean (SD)]	[8 (30.8)]	[5 (16.2)]	[5 (10.1)]
BAL TNF-α (pg/ml)	[Mean (SD)]	[1 (2.4)]	[0.4 (0.5)]	[2 (2.3)]
Plasma IL-4 (pg/ml)	[Mean (SD)]	[0.6 (1.6)]	[0.2 (0.1)]	[3 (5.1)]
Plasma IL-5 (pg/ml)	[Mean (SD)]	[0.6 (0.8)]	[0.8 (1.6)]	[0.9 (2.0)]
Plasma IL-6 (pg/ml)	[Mean (SD)]	[1 (1.8)]	[0.8 (0.9)]	[3 (4.3)]
Plasma IL-8 (pg/ml)	[Mean (SD)]	[5 (2.4)]	[8 (14.1)]	[13 (28.1)]
Plasma IL-10 (pg/ml)	[Mean (SD)]	[1 (3.0)]	[0.8 (1.2)]	[5(10.0)]
Plasma IL-13 (pg/ml)	[Mean (SD)]	[8 (16.6)]	[5 (4.3)]	[25 (35.9)]
Plasma IL-1β (pg/ml)	[Mean (SD)]	[0.6 (3.0)]	[0.1 (0.2)]	[1 (2.3)]
Plasma TNF-α (pg/ml)	[Mean (SD)]	[5 (11.8)]	[2 (1.3)]	[16 (24.9)]
Plasma IFN-γ (pg/ml)	[Mean (SD)]	[5 (2.4)]	[6 (4.4)]	[7 (8.9)]

4.2. Serological detection of fungal sensitisation and presence

IgE levels above 80 KU/L was considered above the hospitals upper limit of normal. IgE levels were elevated in 38/69 (55%) of patients (mean 299.5; SD 512.1) (Figure 2). 6/69 patients (9%) demonstrated positive IgE reactivity to *A. fumigatus.* The Platelia *Aspergillus* assay for detection of *Aspergillus* galactomannan antigen afforded a positive result in one of the sixty-nine patient's serum. This was not related to elevated IgE.

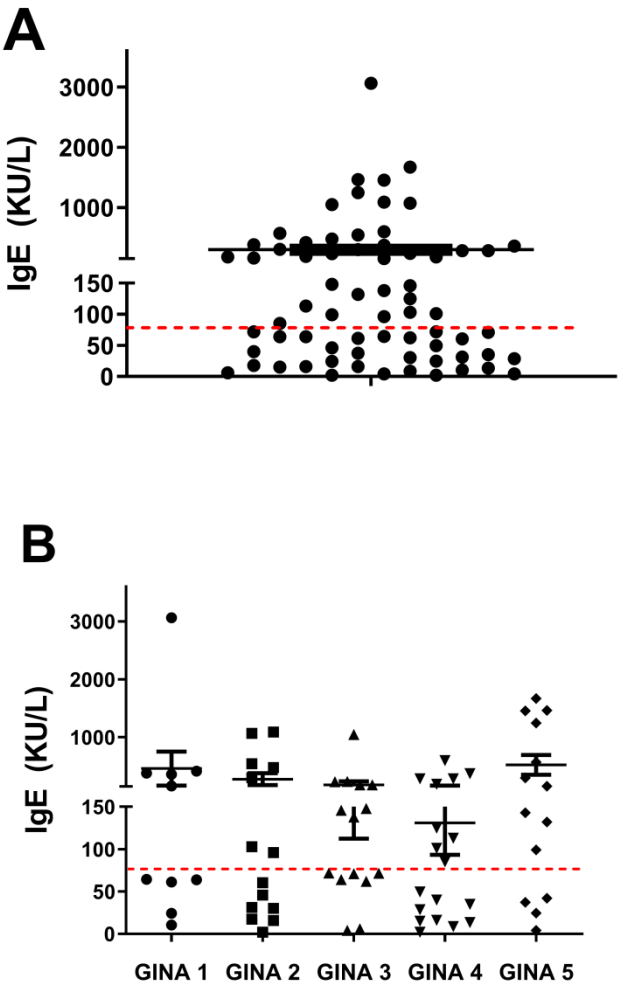


Figure 5. Serological testing of asthmatic patient serum IgE levels. Serum was assessed for total IgE levels (mean 299.5; SE ± 61.64; SD 512.1). (A) 38/69 (55%) of patients displayed total IgE levels above the hospitals upper limit of normal (80KU/L), red dashed line, showing atopic asthma. (B) When grouped by GINA there was no distinctive difference between GINA grouping and total IgE levels. n=69

4.3. Fungal detection by microscopy

BAL cell differential revealed macrophages to be the most dominant immune cell type with varying levels of neutrophils, eosinophils and lymphocytes present (Figure 3). Fungal presence was detectable by microscopy in 48/69 (70%) of cytospins (Figure 3B-C). Presence of fungi in cytospin slides correlated with increased neutrophils ($P<0.05$; rs = 0.275). There was no observed relationship between microscopic fungal presence in BAL and serum IgE levels or BAL eosinophils.

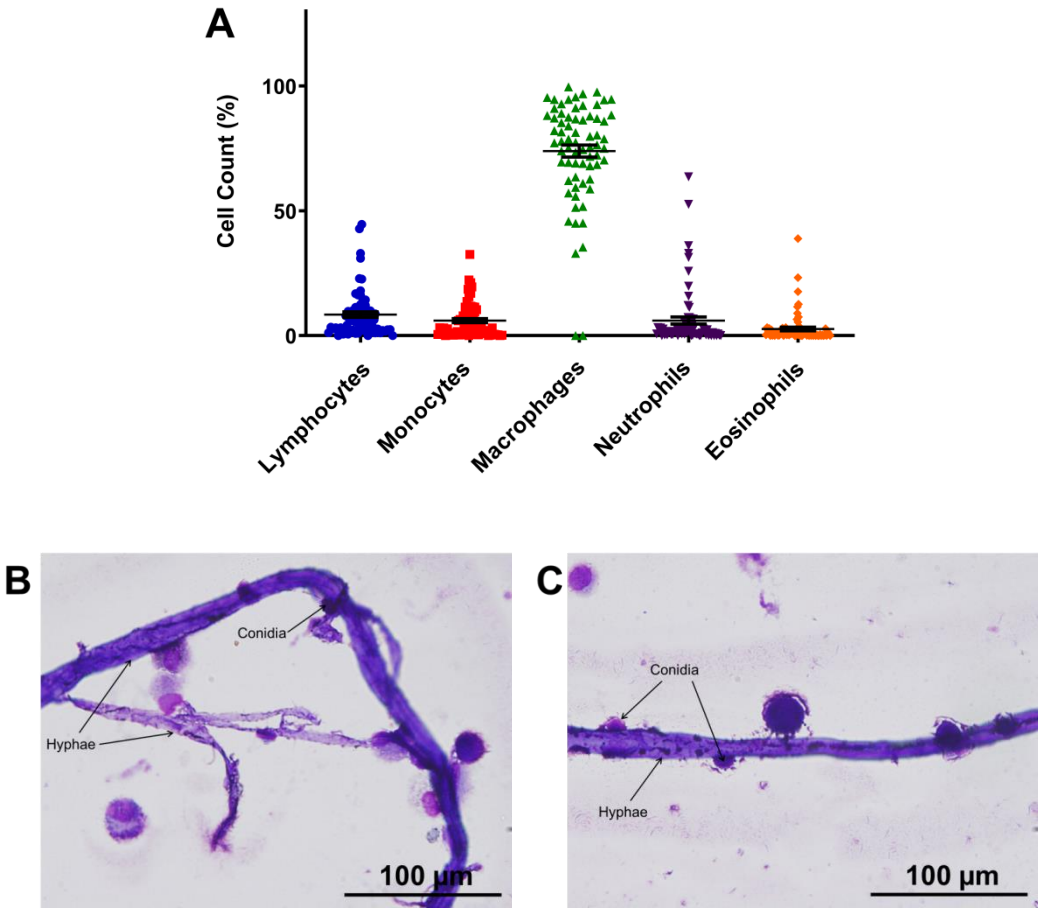


Figure 6. Microscopic evidence of fungal presence in asthmatic patient bronchoalveolar lavage (BAL). (A) BAL immune cell differential counts revealed macrophages to be the most dominant immune cell type present with varying levels of neutrophils and eosinophils present within the patient BAL. (B-C) Representative microscope images of patient BAL fluid stained with a commercial Kwik-Diff stain displaying fungal presence. Fungal hyphae (B) and conidia (C) detected at 40x. n=69.

4.4. Molecular detection of fungal presence

59/69 patients (86%) had detectable presence of fungi (Fungi Quant) and 32/69 (46%) had detectable *A. fumigatus* in BAL (Figure 7.A).

BAL *A. fumigatus* qPCR levels negatively correlated with macrophage counts (*P*<0.01; rs = -0.418) (Figure 7.B). *A. fumigatus* did not correlate with BAL neutrophil or eosinophil counts. Total fungi, Fungi Quant qPCR, correlated with increased BAL neutrophils (*P*<0.05).Interestingly, patients who smoked had lower levels of *A. fumigatus* but not fungi by qPCR (*P*<0.05; rs=0.171). Severe asthmatic patients (GINA 4/5) also had lower levels of detectable fungi (*P*<0.05; rs=0.084) but asthma severity had no relationship with levels of detectable *A. fumigatus.* There was no significant difference in detection of fungi or *A. fumigatus* in patients on high or low dose inhaled corticosteroids (ICS) (250 – 2000 FDP) or on maintenance oral steroids. When grouped by allergic (total IgE>80 KU/L) and non-allergic asthma 34/38 allergic asthma patients had detectable fungi and 17/38 had detectable *A. fumigatus* by qPCR. For non-allergic asthma patients 25/31 had detectable fungi and 15/31 had detectable *A. fumigatus*.

When grouped by eosinophilic and non-eosinophilic asthma 21/23 patients with eosinophilia (peripheral eosinophil count > 0.3) had detectable fungi and 10/23 had detectable *A. fumigatus* by qPCR. In non-eosinophilic asthma patients 38/46 had detectable fungi and 22/46 had detectable *A. fumigatus* by qPCR. There were no statistical differences between detectable fungi or *A. fumigatus* between allergic and non-allergic asthma. There were no statistical differences between detectable fungi and eosinophilic or non-eosinophilic asthma, however there was a statistically significant difference between *A, fumigatus* presence in eosinophilic and non-eosinophilic asthmatics (*P*<0.05).

30 patients had detectable fungi by both qPCR assays (Fungi Quant and *A. fumigatus*) and 22 patients had corresponding positive results for *A. fumigatus* detection by qPCR and detectable fungal presence by microscopy (Figure 8)[26]. 40 patients had corresponding positive total fungal qPCR and detectable fungi by microscopy of which 21 patients had fungi detectable by microscopy and both qPCR

assays (Fungi Quant and *A. fumigatus)*. As expected fungi other than *A. fumigatus* are detectable in BAL, however the identities of these were not investigated further in this study (Figure 8)

5 patients had a positive Galactomannan result for presence of *Aspergillus* in BAL (Figure 9). Only one patient was positive for *A. fumigatus* qPCR, microscopy, BAL Galactomannan and Fungi Quant qPCR (Figure 10). FEV1 negatively correlated with BAL galactomannan ($P<0.05$).

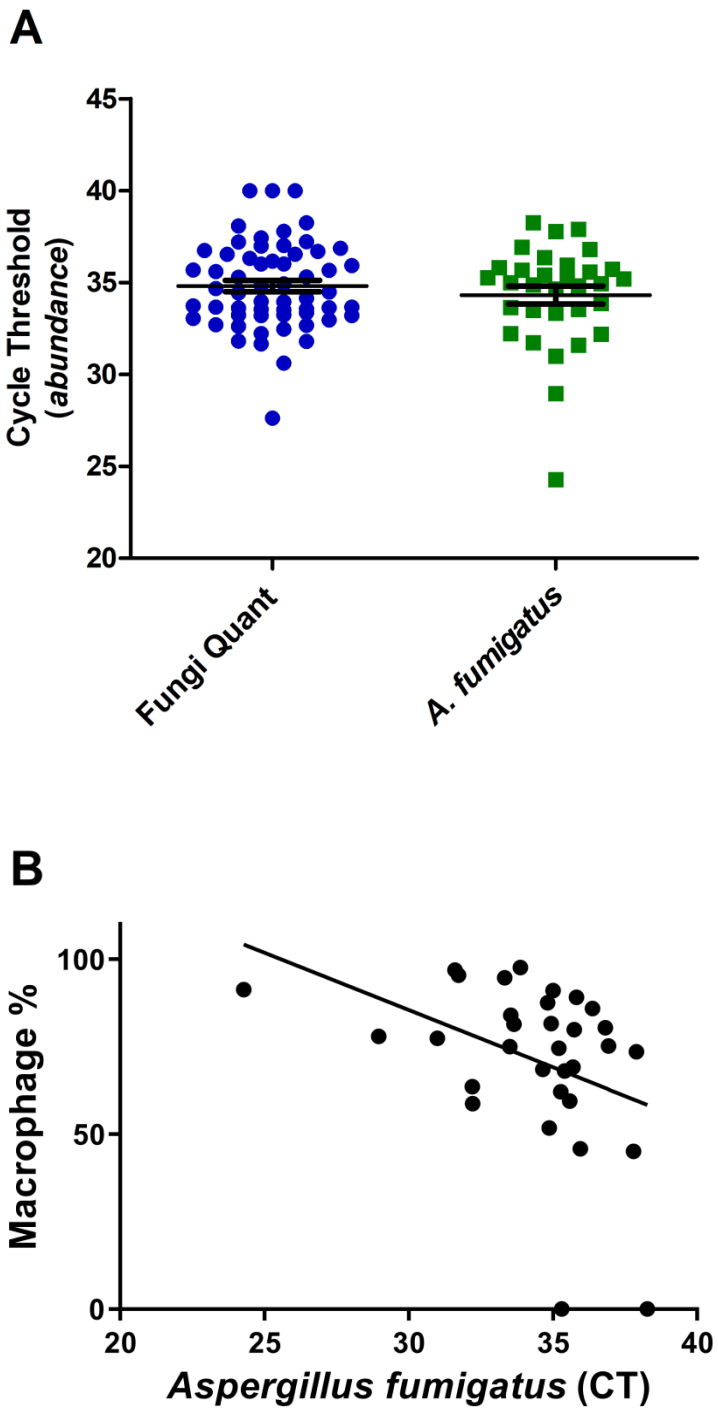


Figure 7 qPCR detection of fungi in asthmatic BAL. (A) qPCR was performed on the extracted BAL DNA using the Fungi Quant and *Aspergillus fumigatus* ITS specific primer; 59 patients (86%) had detectable fungi within their lungs and 32 (46%) had detectable *A. fumigatus* within their lungs. (B) BAL *Aspergillus fumigatus* qPCR levels were seen to correlate with macrophage immune cell percentage count levels ($P<0.05$; Spearman r= -0.4176). n=69.

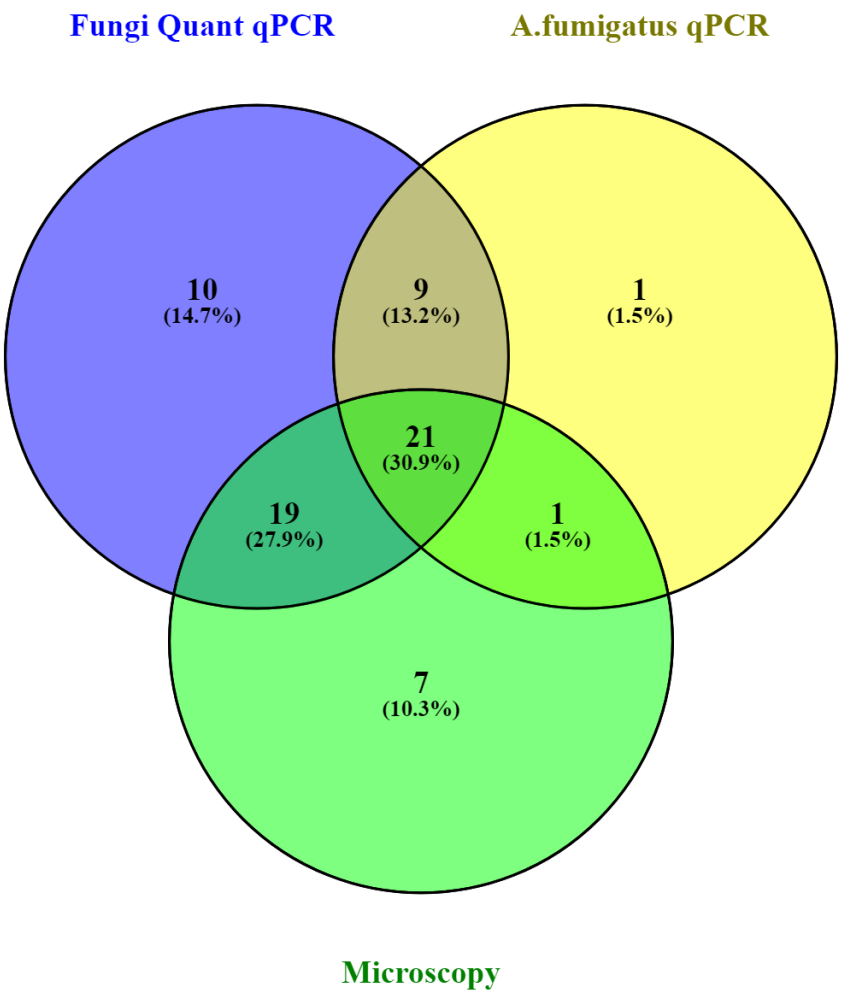


Figure 8 Venn diagram of fungal detection methods. Venn diagram of results of fungal presence using both molecular and microscopy detection methods [26].

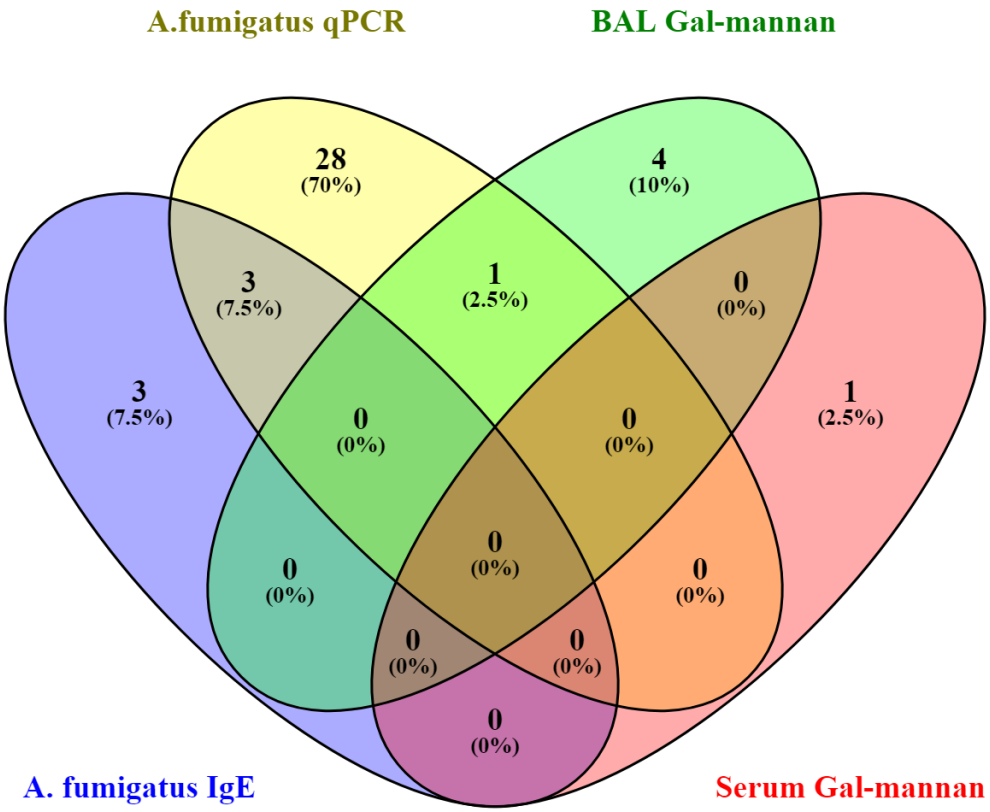


Figure 9 Venn diagram of *A. fumigatus* qPCR, *A. fumigatus* IgE and serum and BAL Galactomannan. Venn diagram showing the comparison of positive results between patients who tested positive to the following; *A. fumigatus* IgE, BAL Galactomannan, *A. fumigatus* qPCR and serum Galactomannan (Gal-mannan).

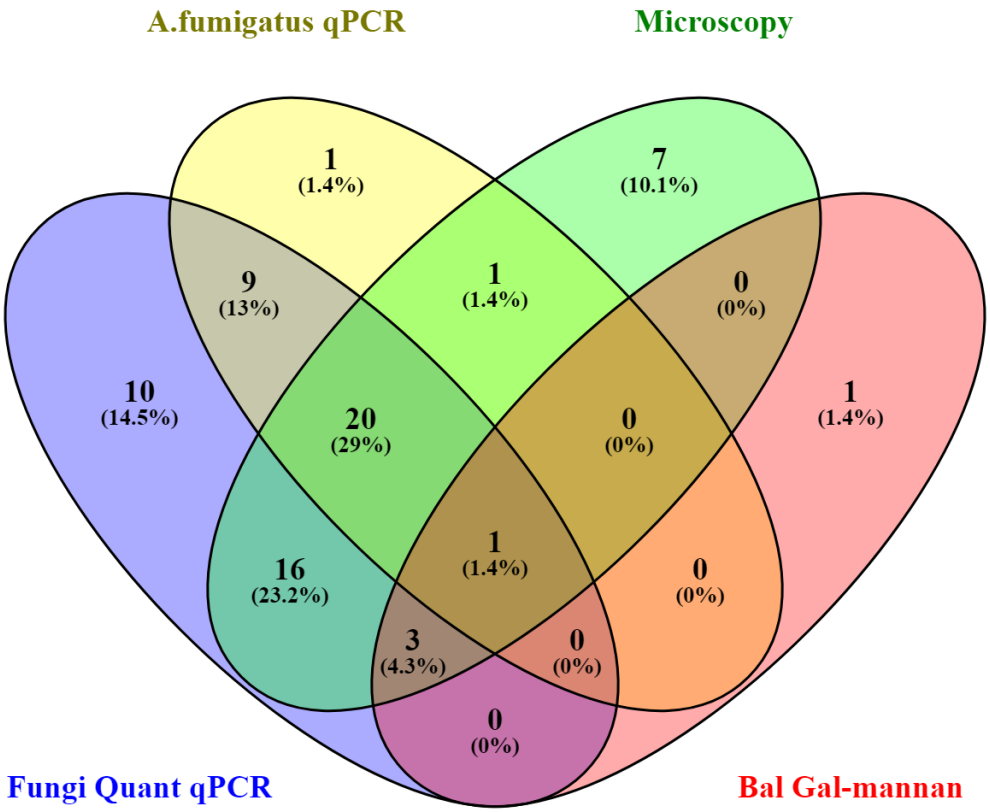


Figure 10 Venn diagram of *A. fumigatus* qPCR, Microscopy, BAL Galactomannan and fungi qPCR. Venn diagram depicting the presence of *A. fumigatus,* fungal presence by microscopy, BAL Galactomannan and fungal presence by qPCR (Fungi Quant) showing comparison of positive results between patients.

4.5. Plasma and BAL cytokine levels correlate with BAL fungal presence

The cytokines Interleukin (IL)-1β, IL-4, IL-5, IL-6, IL-8, IL-10, IL-13, IL-17, IFN-γ and TNF-α were measured in plasma and BAL (Figure 11), n=69. BAL qPCR with the total fungi primer, Fungi Quant, correlated with plasma IL-4 (P<0.001), IL-6 (P<0.05) IL-10 (P<0.01) IL-13 (P<0.05), IL-17 (P<0.01) and TNFα (P<0.001) (Figure 12), n=69. No correlation between total fungi qPCR and IL-1β, IL-5, IL-8 and IFN-γ was observed, n=69. Microscopic detection of fungi in BAL also correlated with patient plasma IL-4 (P<0.05), IL-6 (P<0.01) and TNFα (P<0.01), n=69.

BAL Fungi qPCR correlated with increased BAL IL-4 (P<0.05), IL-6 (P<0.05), IL-10 (P<0.01), IL-13 (P< 0.05) and TNFα (P<0.05) but not IL-1β, IL-5, IL-8 and IL-17 (Figure 10), n=69. Microscopic detection of fungi in BAL correlated with BAL IL-4 (P<0.01) and IL-10 (P<0.01), n=69.

A. fumigatus positive BAL, by qPCR, correlated with increased plasma IL-6 (P<0.001) (Figure 14) and increased BAL IL-6 (P< 0.01) and IL-13 (P<0.05) (Figure 15) but not BAL and plasma IL-1β, IL-4, IL-5, IL-8, IL-10, IL-17, TNF-α or plasma IL-13 and IFN-γ, n=69.

The presence of fungi by microscopy and qPCR also correlated with changes in BAL cell counts, particularly with increased neutrophils (P<0.05; rs=0.296), n=69.

BAL eosinophil percentage counts correlated with plasma IL-5 (P<0.005; rs=0.349) and BAL IL-5 (P<0.05; rs=0.263). Neutrophil cell percentage counts correlated with plasma IL-4 (P<0.05; rs=-0.248) and TNFα (P<0.05; rs=-0.276) and BAL IL-8 (P<0.05; rs=0.278), n=69. Macrophages correlated with BAL IL-6 (P<0.01; rs=-0.296), IL-10 (P<0.01; rs=-0.302) and TNF-α (P<0.05; rs=-0.250), n=69. Monocytes correlated with plasma IL-17 (P<0.001; rs=0.381), TNF-α (P<0.01; rs=0.372) and IFN-γ (P<0.005; rs=0.372) and BAL IL-4 (P<0.01; rs=0.320), n=69. Patient lung function measured by FEV1 negatively correlated with BAL IL-5 presence (P<0.005; rs=-0.352), n=69. However while the correlations were statistically significant the Correlation Coefficient was weak.

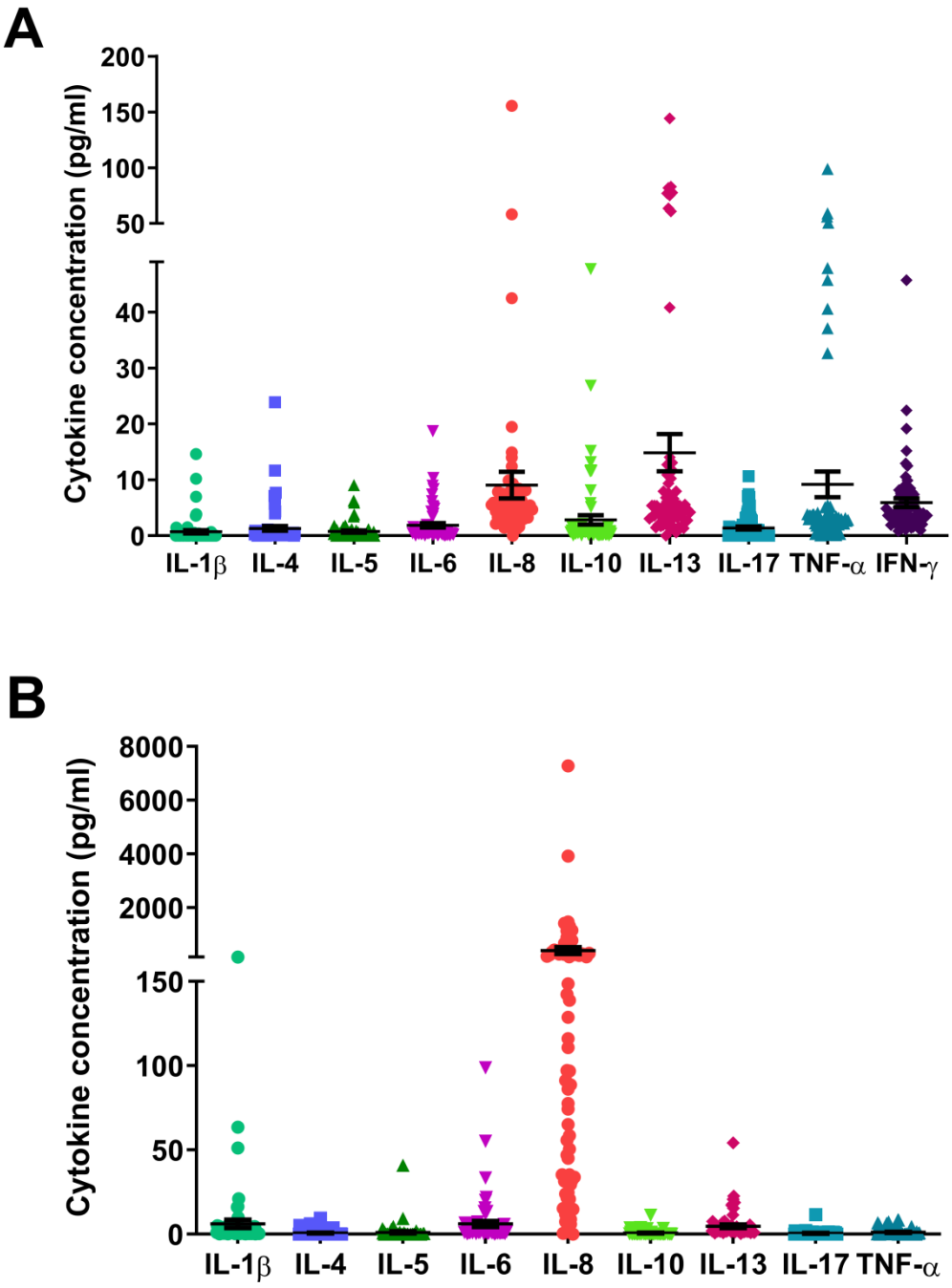


Figure 11 Cytokine levels in patient plasma and BAL Measurement of secreted human cytokines interleukin- 1β (IL-1β), IL-4, IL-5, IL-6, IL-8, IL-10, IL-13, IL-17, interferon-γ (IFN-γ) and tumour necrosis factor-α (TNF-α) in patient plasma and BAL using an electro-chemiluminescence QuickPlex SQ 120 imager from Meso Scale Discovery (Gaithersburg, MD, USA) where antibodies labelled with SULFO-TAG™ reagents emitted light upon electrochemical stimulation. n=69

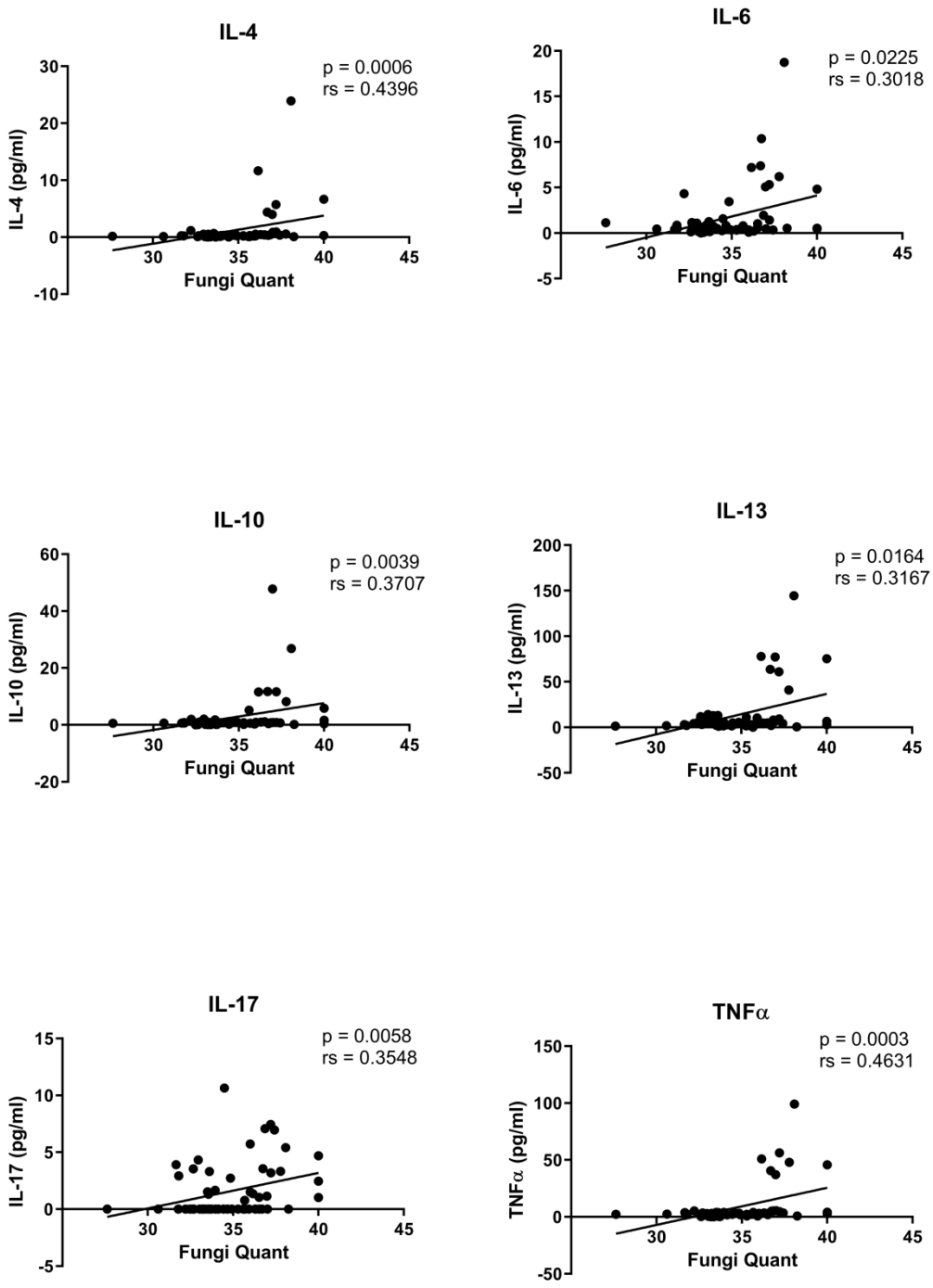


Figure 12 Correlations between BAL qPCR fungal presence (Fungi Quant) and plasma cytokine levels. BAL fungal presence, detected by qPCR using the primer Fungi Quant, correlated with plasma cytokines IL-4 (*P*<0.001; rs=0.440), IL-6 (*P*<0.05; rs=0.302), IL-10 (*P*<0.01; rs=0.371), IL-13 (*P*<0.05; rs=0.318), IL-17 (*P*<0.01; rs=0.355), TNFα (*P*<0.001; rs=0.463). n=69

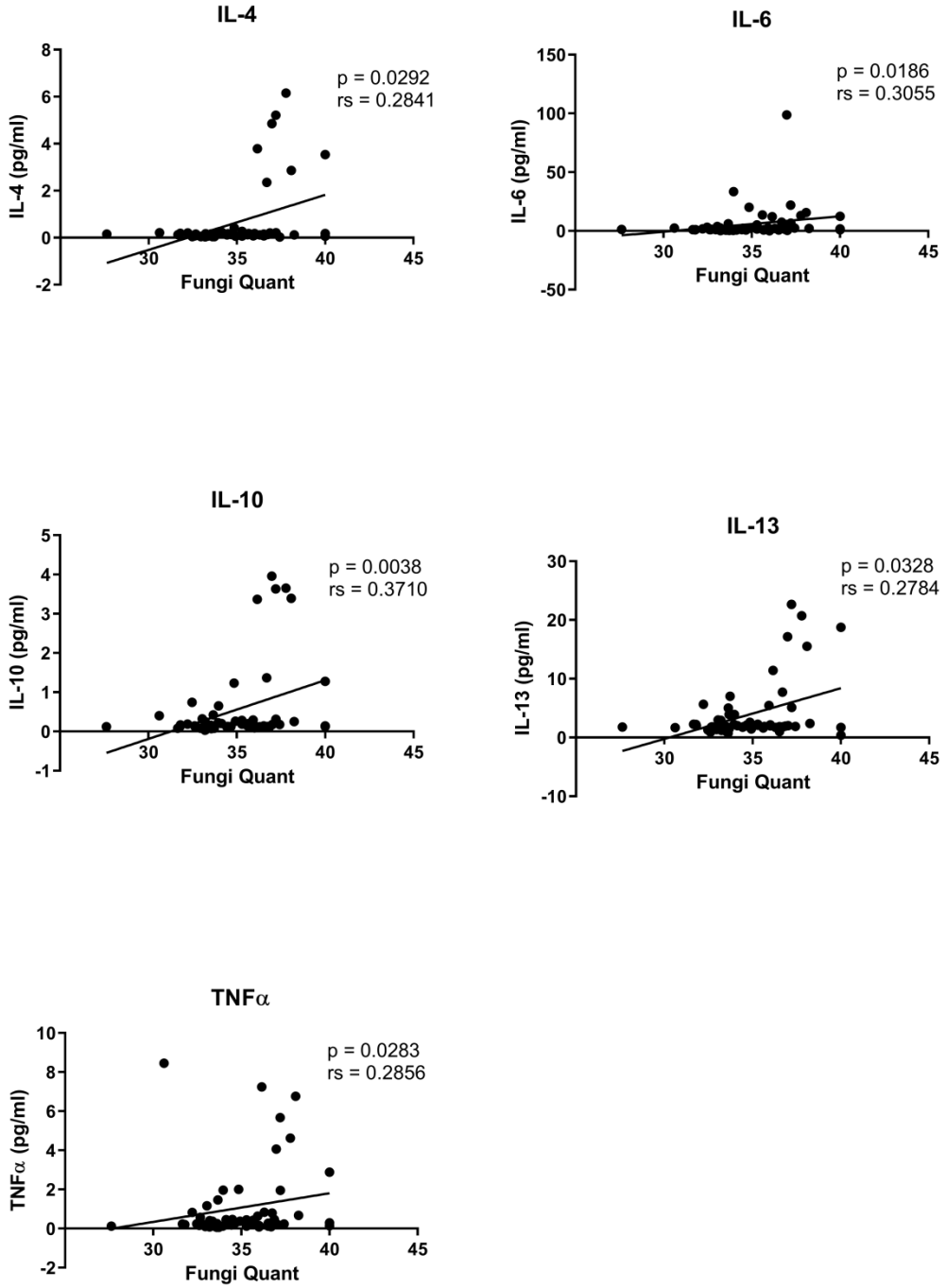


Figure 13 Correlations between BAL qPCR fungal presence (Fungi Quant) and BAL cytokines. BAL fungal presence, detected by qPCR using the primer Fungi Quant, correlated with BAL cytokines IL-4 (*P*<0.05; rs=0.284), IL-6 (*P*<0.05; rs=0.306), IL-10 (*P*<0.01; rs=0.371), IL-13 (*P*<0.05; rs=0.278) and TNFα (*P*<0.05; rs=0.286). n=69

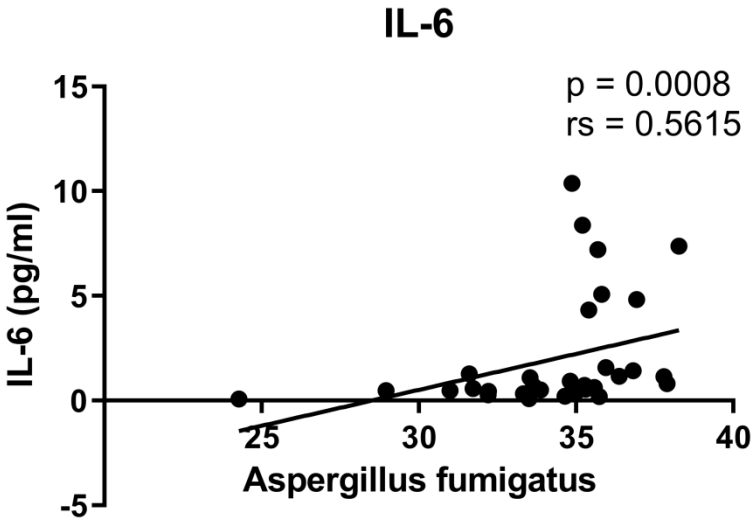


Figure 14 Correlation between BAL qPCR *A. fumigatus* and the plasma cytokine IL-6. *A. fumigatus* BAL qPCR correlated with the plasma cytokine IL-6 (*P*<0.001; rs=0.562). n=69

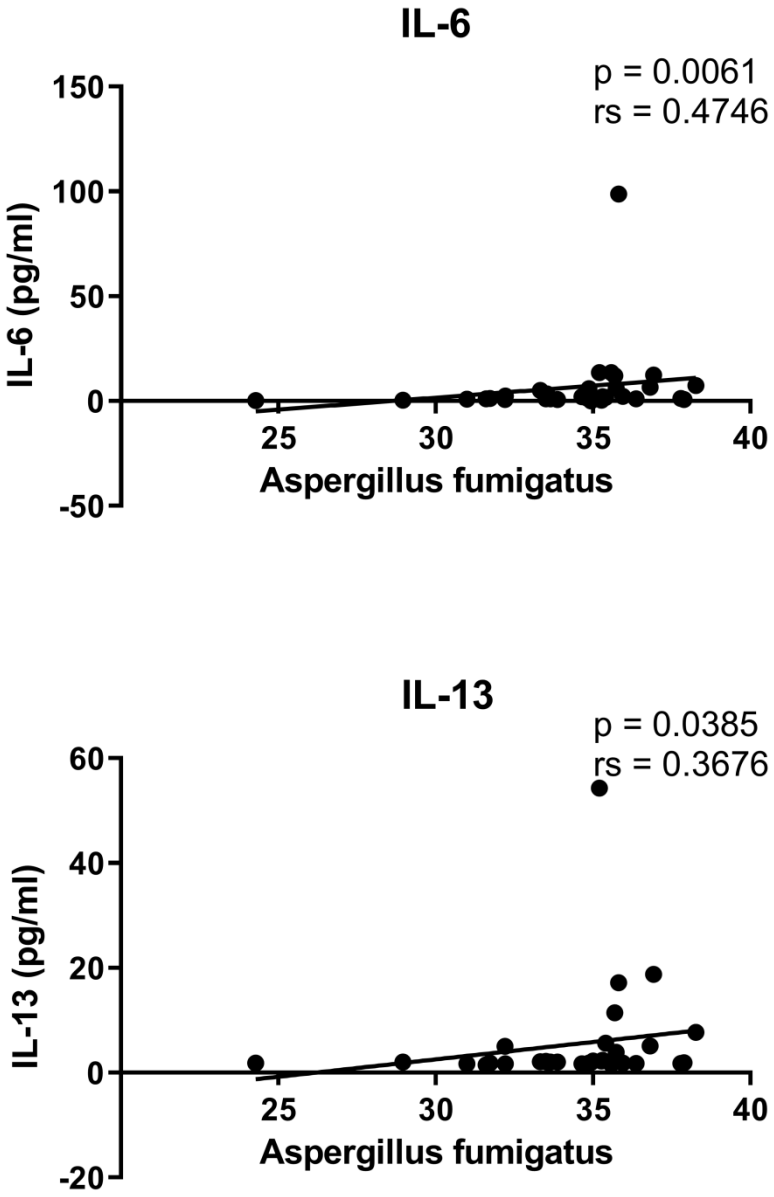


Figure 15 Correlation between BAL *A. fumigatus* presence by qPCR and BAL cytokine levels. BAL *A.fumigatus* qPCR results correlated with the presence of BAL cytokines IL-6 (*P*<0.01; rs=0.475) and IL-13 (*P*<0.05; rs=0.368). n=69

5. Discussion

Our study has demonstrated presence of fungi within the airways of adult asthmatic patients with varying asthma severity and levels of control. Microscopic and nucleic analysis revealed that fungi, including *A.fumigatus*, were detectable in BAL. Microscopy alone revealed spores and hyphae within 70% of the cohort and qPCR analysis demonstrated that 86% of patients have fungal presence within their BAL. Almost half (46%) of the cohort had detectable *A.fumigatus* in their airways. Despite the high frequency of fungi and specifically *A. fumigatus*, we were unable to find any association between its presence and measures of control, severity, or steroid use, in contrast to previous reports, which documented finding higher levels of fungi within severe asthma patients and found corticosteroid treatment to be significantly associated with increased fungal load (P<0.01) and patients in receipt of steroid therapy had significantly increased *A. fumigatus* and total fungus within their BAL[27]. In fact, severe asthmatic patients had less detectable fungi in comparison to mild and moderate GINA grouped patients but there was no relationship between severity and levels of *A. fumigatus*. Asthma severity was associated with BAL neutrophils, however the presence of *A. fumigatus* did not correlate with BAL neutrophil or eosinophils but was associated with reduced BAL macrophages. The detection of fungal DNA (Fungi Quant) in BAL did however correlate with BAL neutrophil counts. This observation of BAL fungal presence associated with BAL neutrophilia, is in keeping with other studies in which *A. fumigatus* alkaline protease 1 levels in sputum correlated with sputum neutrophilia but not eosinophil levels[28].

Plasma IgE levels above 80kU/L is an indicator of an active allergic response and elevated IgE levels were observed in 38/69 patients suggesting that 55% of the cohort has atopic asthma. While qPCR revealed fungi in BAL of 86% and *A. fumigatus* in 46% of patients, serum antibody titres for *A. fumigatus* specific IgE were only positive in 9%. *A. fumigatus* IgE positivity did not indicate an *A. fumigatus* qPCR positive result in 3 patients (Figure 9). Antigen testing for fungi involves detection of specific antigen components present in the fungal cell wall which have been shed into blood or other body fluids. Several of these antigens have been

utilised recently as an aid in detection of fungi, for example, galactomannan antigens in serum or BAL to diagnose invasive *Aspergillus* infection[29]. In our study, galactomannan was detectable in the serum of 1 patient and BAL of 5 patients. However, when these results were analysed for concordance in detection methods, no patient tested positive for all parameters (Figure 9). Antigen testing has restrictions which must be considered when used to diagnose fungal infections. False positive serum *Aspergillus* galactomannan assays may exist in patients presenting with other fungal infections, in those taking β-lactam antibiotics or in presence of penicillium infections because of the possibility of cross-reactivity[29]. However, it is noteworthy that none of our patients were exacerbating or on antibiotics at the time of sample acquisition.

Nucleic analysis was revealed to be a more robust method of detecting presence of fungi and *A. fumigatus* within BAL of our asthmatic cohort. It was discovered that 21 patients tested positive for all criteria; total fungi by qPCR (Fungi Quant), *A. fumigatus* by qPCR and fungal detection by microscopy. 40 patients displayed a positive total fungi qPCR result and fungal presence by microscopy, while 10 displayed fungal presence by qPCR alone. This suggests that while *A. fumigatus* is present within BAL of our asthmatics it is not the only fungal species present, as elucidated by our total fungi and microscopy results (Figure 8).

The results suggest, at present, the best indicator of fungal and *A. fumigatus* presence in BAL is qPCR, which is relatively inexpensive (Figure 8-10). Previous studies have reported *A. fumigatus* detection in sputum was associated with IgE sensitization, airway neutrophilia and reduction in lung function. This study utilised fungal culture of sputum. Furthermore, *Aspergillus* was cultured in 63% of IgE sensitised patients, but also 31% of non sensitised patients. In this study of 79 patients, 89% were classified as GINA 4/5[30]. Our study included less severe asthmatics but higher numbers of mild and moderate asthmatics.

The presence of *A. fumigatus* in BAL, by qPCR, negatively correlated with macrophage counts. Alveolar macrophages are responsible for uptake and removal of inhaled conidia[31]. The ability of macrophages to kill *Aspergillus* species is

dependent on LC3-associated phagocytosis via NADPH oxidase function. In human macrophages *A. fumigatus* has the ability to germinate in the late phagosome resulting in macrophage necrosis. Macrophages play a key role in protection of the host and their alteration or destruction can cause deleterious effects in the host[11]. We are uncertain as to whether the associated reduction in percentage BAL macrophages we observed is reflective of destruction by *Aspergillus* or simply a reciprocal decrease due to increase in neutrophils and fluxes in other cell percentages, but believe this warrants further investigation.

Cytokines, intracellular signalling proteins, target specific cells causing consequences such as cell mediated immunity and allergic responses[32-34]. It was generally believed disequilibrium between pro-inflammatory Th1 and anti-inflammatory Th2 groups plays a role in the pathogenesis of allergic airway responses. However regulatory T cells (Tregs) producing cytokines such as inhibitory IL-10 and IL-17 producing Th17 cells make elucidating the pathogenesis of allergic disorders more complex[33-38]. Cytokines were chosen in order to investigate known cytokines of interest in asthma and to also examine the complex groups of Th1, Th2, Tregs and Th17 representative cytokines.

Within our cohort it was seen that presence of fungi within BAL, as detected by qPCR, correlated positively with levels of a number of cytokines. Fungal presence within the lungs positively correlated with plasma IL-4, IL-6, IL-10, IL-13, IL-17 and TNF-α and BAL IL-4, IL-6, IL-10, IL-13 and TNF-α. The cytokine IL-4 has been linked to allergic inflammation development and plays a role in sudden allergic reactions through the induction of IgE dependent mast cell activation and can induce mucin expression resulting in mucus hypersecretion, a well-known asthma characteristic feature[39]. IL-6 is a pleotrophic cytokine with the ability to act in an anti-inflammatory and pro-inflammatory manner. It is recognised that IL-6 is produced in response to the recognition of microbes by pattern associated molecular patterns[40]. IL-10 plays an important role in regulating asthma control through the regulation of T cell-mediated responses[41]. IL-13 is known to play a role in the pathogenesis and plays a role in features such as bronchial hyper-responsiveness, B cell immunoglobulin class switching from IgM to IgE production and goblet cell

differentiation increases[42]. The pro-inflammatory cytokine IL-17 plays an important role in asthma pathobiology, through its role in neutrophilic inflammation and asthma severity and the promotion of cytokine and chemokine production in bronchial epithelial cells[43]. TNF-α is a cytokine which is mainly produced by lymphocytes, macrophages and mast cells and it is believed that TNF-α may play a sentinel role in inflammatory state maintenance in asthmatics[44].

It is therefore plausible that presence of fungi within the lungs of these patients has triggered an immune response resulting in upregulation of these cytokines[45-47]. Our study focused on detection of fungi rather than specific viable culture. Further studies to culture specific fungal species may be attempted in the future; however there are many difficulties in culturing fungi in clinical laboratories. It has been documented that culture identification can be significantly affected by the starting volume of sample and qPCR has been observed to be the most sensitive method of detection[48]

It is notable within our cohort, that presence of *A.fumigatus* in BAL, as detected by qPCR, positively correlated with BAL IL-6 and IL-13 levels and plasma IL-6, suggesting a systemic response.

Neutrophils are key players implicated in removal of fungal components within the lung through the use of phagocytic oxidative and non-oxidative mechanisms and through release of granules which mediate extracellular killing[46]. Patient BAL neutrophils correlated negatively with plasma IL-4 and TNF-α and positively with BAL levels of the neutrophil chemoattractant IL-8 .Neutrophil presence also correlated with the presence of fungi by microscopy.

Macrophage cell percentage counts negatively correlated with BAL IL-10, IL-6 and TNF-α, and monocytes correlated positively with plasma IL-17, TNF-α, IFN-γ, and BAL IL-4. It is of interest that in our cohort the percentage of macrophages negatively correlated with BAL IL-10. IL-10, an anti-inflammatory cytokine, regulates lung inflammation and a decrease in IL-10 might be expected to be associated with potential worsening in clinical outcome[49].

As in previous studies we found BAL eosinophil levels correlated with plasma and BAL IL-5 levels. IL-5 is essential for maturation of eosinophils in the bone marrow and subsequent release into the blood. Furthermore, IL-5 inhibition through monoclonal antibody therapy has demonstrated clinical effectiveness in treating patients with severe, eosinophilic asthma[50]. IL-17 has been highlighted as a key component of fungal immunity[47]. It is known that pulmonary epithelial cells possess IL-17 receptors which induce antimicrobial peptide and chemokine production and resulting Th17 cell induction and neutrophil recruitment[47]. Members of our group have previously demonstrated ability of IL-17 to upregulate release of several cytokines and chemokines from primary bronchial epithelial cells but in particular those associated with neutrophilia[51]. In our current study, we observed that BAL fungal presence by qPCR correlated with plasma IL-17. Patient BAL monocyte percentage counts positively correlated with plasma IL-17.

It has been recently highlighted by Hernández-Santos *et al*. that ability of innate immune cells to kill fungi is dependent on presence of NF-κB mediated production of chemokines by pulmonary epithelia, which is IL-1R dependent. This chemokine cascade orchestrates Th17 derived IL-17A and GM-CSF signaling which are known to aid phagocytic destruction of fungi[47].

Our results have demonstrated through both rapid microscopy and qPCR methods, that fungi and to a lesser extent *A. fumigatus* are present in lower airways of a large proportion of an adult asthmatic cohort regardless of their disease severity. Serological and antigen testing alone revealed a far lower level of positivity for *Aspergillus.* The presence of serum *A. fumigatus* specific IgE did not always predict presence of *A. fumigatus* by qPCR in patients BAL. Positive *A. fumigatus*-specific IgE was not linked to disease severity or control. It is therefore possible that while there are detectable fungal and *A. fumigatus* communities within the lungs of our cohort, perhaps this presence is not always provoking an active immune response. Furthermore, positivity for serum *A. fumigatus* specific IgE was not associated with a reduction in FEV1. FEV1 is the Forced Expiratory Volume in the first second and is a measurement of the expiratory volume in the first second of the FVC (Forced Vital Capacity) maneuver in spirometry[13]. Our findings appear to differ from previously

published results suggesting that asthma patients sensitised to *Aspergillus* had lower FEV1[30]. FEV1 negatively correlated with BAL IL-5 and BAL galactomannan, however it should be noted that only 5/69 patients showed BAL galactomannan positivity. Of the 5 patients who tested positive for galactomannan only one was *A. fumigatus* qPCR positive. This appears to suggest that BAL Galactomannan may relate to airway fungal presence but not necessarily presence of *A.fumigatus*.

One of the weaknesses of the current study is the lack of control group which we aim to address in future work. This considerable undertaking is suggested by the results of our present study and will require a careful ethics case to be made, that will allows a generally safe but invasive procedure in volunteers. A strength of our study however was that it did include patients of all asthma severity and indeed patients on maintenance oral steroids and patients newly diagnosed and yet to receive any asthma-directed therapy. The decision to exclude patients with ABPA was made in an effort to specifically interrogate the current definition of SAFS which excludes this group. Further studies aimed at addressing this group are planned for the future. Fungal sensitisation is the sudden cutaneous hyperreactivity to fungal antigen or elevation of fungal specific IgE[52]. SAFS is a subphenotype of severe asthma[53]. Fungi are associated with severe asthma through fungal spore inhalation, sensitisation or the causation of Allergic Bronchopulmonary Mycosis[52]. Previous studies revealed numerous fungal species can cause sensitisation in asthmatics, however it is not yet known which is implicated to the greatest degree in SAFS and if it is prevalent within other subgroups of asthma[52]. It would therefore be of interest to investigate this further in order to interrogate the current definition of SAFS.

Further studies are required to assess whether or not *Aspergillus* within the asthmatic airway has a pathological role in the disease. Our study has shown an almost ubiquitous presence of fungi within the asthmatic airway regardless of disease severity, treatment taken and presence of systemic sensitisation. It has become apparent from this study that other fungal species are present within the lungs of our asthmatic cohort. Whether or not these fungi play a pathophysiological role or are mere bystanders has yet to be determined.

6. References

1. Shaw DE, Sousa AR, Fowler SJ, et al. Clinical and inflammatory characteristics of the European U-BIOPRED adult severe asthma cohort. *The European respiratory journal.* 2015;46(5):1308-1321.
2. Denning DW, O'Driscoll BR, Hogaboam CM, Bowyer P, Niven RM. The link between fungi and severe asthma: a summary of the evidence. *The European respiratory journal.* 2006;27(3):615-626.
3. Denning DW, O'Driscoll BR, Powell G, et al. Randomized controlled trial of oral antifungal treatment for severe asthma with fungal sensitization: The Fungal Asthma Sensitization Trial (FAST) study. *Am J Respir Crit Care Med.* 2009;179(1):11-18.
4. Agbetile J, Bourne M, Fairs A, et al. Effectiveness of voriconazole in the treatment of Aspergillus fumigatus-associated asthma (EVITA3 study). *The Journal of allergy and clinical immunology.* 2014;134(1):33-39.
5. Rick EM, Woolnough K, Pashley CH, Wardlaw AJ. Allergic Fungal Airway Disease. *Journal of investigational allergology & clinical immunology.* 2016;26(6):344-354.
6. Underhill DM, Iliev ID. The mycobiota: interactions between commensal fungi and the host immune system. *Nat Rev Immunol.* 2014;14:405.
7. Gauthier GM. Dimorphism in Fungal Pathogens of Mammals, Plants, and Insects. *PLoS Pathogens.* 2015;11(2):e1004608.
8. Hohl TM, Feldmesser M. Aspergillus fumigatus: principles of pathogenesis and host defense. *Eukaryotic cell.* 2007;6(11):1953-1963.
9. Kwon-Chung KJ, Sugui JA. Aspergillus fumigatus—What Makes the Species a Ubiquitous Human Fungal Pathogen? *PLOS Pathogens.* 2013;9(12):e1003743.
10. Kousha M, Tadi R, Soubani AO. Pulmonary aspergillosis: a clinical review. *European Respiratory Review.* 2011;20(121):156-174.
11. van de Veerdonk FL, Gresnigt MS, Romani L, Netea MG, Latge JP. Aspergillus fumigatus morphology and dynamic host interactions. *Nature reviews Microbiology.* 2017;15(11):661-674.
12. Targonski PV, Persky VW, Ramekrishnan V. Effect of environmental molds on risk of death from asthma during the pollen season. *The Journal of allergy and clinical immunology.* 1995;95(5 Pt 1):955-961.
13. Miller MR, Hankinson J, Brusasco V, et al. Standardisation of spirometry. *The European respiratory journal.* 2005;26(2):319-338.
14. Graham BL, Steenbruggen I, Miller MR, et al. Standardization of Spirometry 2019 Update. An Official American Thoracic Society and European Respiratory Society Technical Statement. *Am J Respir Crit Care Med.* 2019;200(8):e70-e88.
15. GINA Report. Global strategy for asthma management and prevention. 2018.
16. Juniper EF, O'Byrne PM, Guyatt GH, Ferrie PJ, King DR. Development and validation of a questionnaire to measure asthma control. *The European respiratory journal.* 1999;14(4):902-907.
17. *Global Strategy for Asthma Management and Prevention 2019 Update.* Global Initiative For Asthma2019.
18. *Pocket Guide for Asthma Management and Prevention 2019 Update.* Global Initiative For Asthma 2019.
19. Juniper EF, Svensson K, Mork AC, Stahl E. Measurement properties and interpretation of three shortened versions of the asthma control questionnaire. *Respir Med.* 2005;99(5):553-558.
20. Juniper EF, Bousquet J, Abetz L, Bateman ED. Identifying 'well-controlled' and 'not well-controlled' asthma using the Asthma Control Questionnaire. *Respir Med.* 2006;100(4):616-621.

21. Du Rand IA, Blaikley J, Booton R, et al. British Thoracic Society guideline for diagnostic flexible bronchoscopy in adults: accredited by NICE. *Thorax.* 2013;68 Suppl 1:i1-i44.
22. Principles of respiratory investigation. 2020; https://www.erswhitebook.org/chapters/principles-of-respiratory-investigation/, 2020.
23. Hunt EB, Ward C, Power S, et al. The Potential Role of Aspiration in the Asthmatic Airway. *Chest.* 2017;151(6):1272-1278.
24. Liu CM, Kachur S, Dwan MG, et al. FungiQuant: A broad-coverage fungal quantitative real-time PCR assay. *BMC Microbiology.* 2012;12(1):255.
25. Cuenca-Estrella M, Meije Y, Diaz-Pedroche C, et al. Value of serial quantification of fungal DNA by a real-time PCR-based technique for early diagnosis of invasive Aspergillosis in patients with febrile neutropenia. *J Clin Microbiol.* 2009;47(2):379-384.
26. Oliveros JC. Venny. An interactive tool for comparing lists with Venn's diagrams. 2007-2015.
27. Fraczek MG, Chishimba L, Niven RM, et al. Corticosteroid treatment is associated with increased filamentous fungal burden in allergic fungal disease. *The Journal of allergy and clinical immunology.* 2018;142(2):407-414.
28. Basu T, Seyedmousavi S, Sugui JA, et al. Aspergillus fumigatus alkaline protease 1 (Alp1/Asp f13) in the airways correlates with asthma severity. *The Journal of allergy and clinical immunology.* 2018;141(1):423-425.e427.
29. Limper AH. The Changing Spectrum of Fungal Infections In Pulmonary and Critical Care Practice. *Proceedings of the American Thoracic Society.* 2010;7(3):163-168.
30. Fairs A, Agbetile J, Hargadon B, et al. IgE sensitization to Aspergillus fumigatus is associated with reduced lung function in asthma. *Am J Respir Crit Care Med.* 2010;182(11):1362-1368.
31. Segal BH. Role of macrophages in host defense against aspergillosis and strategies for immune augmentation. *The oncologist.* 2007;12 Suppl 2:7-13.
32. Chung KF, Barnes PJ. Cytokines in asthma. *Thorax.* 1999;54(9):825-857.
33. Berger A. Th1 and Th2 responses: what are they? *BMJ.* 2000;321(7258):424.
34. Zhang J-M, An J. Cytokines, Inflammation and Pain. *International anesthesiology clinics.* 2007;45(2):27-37.
35. Cosmi L, Liotta F, Maggi E, Romagnani S, Annunziato F. Th17 cells: new players in asthma pathogenesis. *Allergy.* 2011;66(8):989-998.
36. Murphy DM, O'Byrne PM. Recent advances in the pathophysiology of asthma. *Chest.* 2010;137(6):1417-1426.
37. Maes T, Joos GF, Brusselle GG. Targeting Interleukin-4 in Asthma: Lost in Translation? *American Journal of Respiratory Cell and Molecular Biology.* 2012;47(3):261-270.
38. Lambrecht BN, Hammad H, Fahy JV. The Cytokines of Asthma. *Immunity.* 2019;50(4):975-991.
39. Steinke JW, Borish L. Th2 cytokines and asthma. Interleukin-4: its role in the pathogenesis of asthma, and targeting it for asthma treatment with interleukin-4 receptor antagonists. *Respiratory research.* 2001;2(2):66-70.
40. Poynter ME, Irvin CG. Interleukin-6 as a biomarker for asthma: hype or is there something else? *The European respiratory journal.* 2016;48(4):979-981.
41. Coomes SM, Kannan Y, Pelly VS, et al. CD4+ Th2 cells are directly regulated by IL-10 during allergic airway inflammation. *Mucosal immunology.* 2017;10(1):150-161.
42. Corren J. Role of interleukin-13 in asthma. *Current allergy and asthma reports.* 2013;13(5):415-420.

43. Chesne J, Braza F, Mahay G, Brouard S, Aronica M, Magnan A. IL-17 in severe asthma. Where do we stand? *Am J Respir Crit Care Med.* 2014;190(10):1094-1101.
44. Holgate ST, Noonan M, Chanez P, et al. Efficacy and safety of etanercept in moderate-to-severe asthma: a randomised, controlled trial. *European Respiratory Journal.* 2011;37(6):1352-1359.
45. Opal SM, DePalo VA. Anti-inflammatory cytokines. *Chest.* 2000;117(4):1162-1172.
46. Becker KL, Ifrim DC, Quintin J, Netea MG, van de Veerdonk FL. Antifungal innate immunity: recognition and inflammatory networks. *Seminars in immunopathology.* 2015;37(2):107-116.
47. Hernández-Santos N, Wiesner DL, Fites JS, et al. Lung Epithelial Cells Coordinate Innate Lymphocytes and Immunity against Pulmonary Fungal Infection. *Cell Host & Microbe.*23(4):511-522.e515.
48. Fraczek MG, Kirwan MB, Moore CB, Morris J, Denning DW, Richardson MD. Volume dependency for culture of fungi from respiratory secretions and increased sensitivity of Aspergillus quantitative PCR. *Mycoses.* 2014;57(2):69-78.
49. Bordon J, Aliberti S, Fernandez-Botran R, et al. Understanding the roles of cytokines and neutrophil activity and neutrophil apoptosis in the protective versus deleterious inflammatory response in pneumonia. *International Journal of Infectious Diseases.* 2013;17(2):e76-e83.
50. Greenfeder S, Umland SP, Cuss FM, Chapman RW, Egan RW. Th2 cytokines and asthma — The role of interleukin-5 in allergic eosinophilic disease. *Respiratory Research.* 2001;2(2):71-79.
51. Murphy DM, Forrest IA, Corris PA, et al. Simvastatin attenuates release of neutrophilic and remodeling factors from primary bronchial epithelial cells derived from stable lung transplant recipients. *American journal of physiology Lung cellular and molecular physiology.* 2008;294(3):L592-599.
52. Agarwal R, Gupta D. Severe asthma and fungi: current evidence. *Medical Mycology.* 2011;49(Supplement_1):S150-S157.
53. Licari A, Brambilla I, Marseglia A, De Filippo M, Paganelli V, Marseglia GL. Difficult vs. Severe Asthma: Definition and Limits of Asthma Control in the Pediatric Population. *Frontiers in Pediatrics.* 2018;6(170).

Chapter 4

The Microbiome of the Lung

A study to define microbiome subtypes in the adult asthmatic airway

Author Contributions: Desmond Murphy, John MacSharry, Chris Ward and Paul O'Byrne were responsible for the study design and concept. Desmond Murphy and Eoin Hunt were responsible for patient recruitment, clinical characterisation and sample acquisition. Sample processing and study assays were primarily performed by Ashley Sullivan with contribution from Eoin Hunt, Susan Lapthorne, John MacSharry and Chris Ward. Next Generation Sequencing was performed by the APC Microbiome Institute Sequencing Platform. Primary analysis of Next Generation Sequencing data was performed by Ashley Sullivan in conjunction with One Codex, Christopher Smith, Denise Lynch and John MacSharry. Statistical analysis was performed by the authors in conjunction with biostatistical support from Joseph Eustace and The Clinical Research Facility University College Cork. Analysis and interpretation of data, manuscript preparation and approval were performed by Ashley Sullivan, John MacSharry and Desmond Murphy.

1. Abstract 107
2. Introduction 108
3. Methods 110
3.1. Patient recruitment 110
3.2. Sample processing 111
3.3. Microscopy 114
3.4. DNA extraction 114
3.5. DNA quantification 115
3.6. Primers 117
3.7. qPCR – quantitative Polymerase Chain Reaction 117
3.8. REPLI-g 119
3.9. Next Generation Sequencing (NGS) 120
3.10. Primary analysis of the Next Generation Sequencing (NGS) dataset 122
3.11. Cytokine measurement in BAL and plasma samples 123
3.12. Glucose assay 124
3.13. Statistical analyses 125
4. Results 126
4.1. Patient demographics 126
4.2. Serological detection of Immunoglobulin E (IgE) levels 131
4.3. Microscopy and BAL immune cell percentage counts 132
4.4. Molecular detection of microbial presence 134
4.5. BAL and plasma cytokines 136
4.6.qPCR correlations 139
4.7. Next Generation Sequencing 147
5. Discussion 173
6. Supplementary 184
7. References 187

1. Abstract

Background: Molecular methods have recently demonstrated that airways harbour a distinct microbiome. The aim of our study was to characterise the lower airway microbiota in a cohort of well-defined asthmatics.

Methods: 73 patients, stratified by asthma severity (GINA) and level of control (ACQ-7) were recruited. Spirometry, FeNO, serum IgE/RAST and eosinophil levels were documented on the day of bronchoscopy. Bronchoalveolar lavage (BAL) was obtained from either the right middle lobe or lingula. Cell differentials were performed on BAL, which was further evaluated for the presence of microbes by qPCR and next generation sequencing (NGS).

Results: qPCR revealed a wide variety of microbial species present in the lungs of the asthmatic cohort. 93% (68/73) of patients had detectable levels of bacteria. Firmicutes (73% (53/73)), *Pseudomonas aeruginosa* (34% (25/73)), *Pseudomonas fluorescens* (88% (64/73)), *Escherichia* (37% (27/73)), Bordetella (53% (38/73)), *Prevotella* (79% (58/73)), *Veillonella* (80% (59/73)), *Mycoplasma pneumoniae* (62% (45/73)), *Chlamydophilia pneumoniae* (70% (51/73)), *Staphylococcus aureus* (75% (55/73)), *Neisseria bacilliformis* (66% (48/73)), *Moraxella catarrhalis* (78% (57/73), *Neisseria meningitidis* (67% (49/73)), *Streptococcus pneumoniae* (73% (53/73)) *Haemophilus influenzae* (67% (49/73)), *Rothia* (86% (63/73)) and *Micromonospora* (85% (62/73)) were all detectable in the BAL obtained from the asthmatic cohort. Interestingly the WGS data revealed that the *Micromonospora* species were also highly prevalent within the BAL of the asthma cohort a finding not currently widely associated with the microbiome of the lungs.

Conclusions: Our results demonstrate the presence of microbial species within the previously considered sterile airway of asthmatic patients. Thanks to the advancement of culture independent techniques the unique microbiota of the lungs is being elucidated. It is hoped that the novel findings of this study may add to the growing body of research with respect to the microbiome and asthma and may potentially offer insights into asthma susceptibility, pathogenesis and prognosis.

2. Introduction

Until recent years the prevailing dogma with respect to the microbiome of the lungs was that the lungs were a sterile environment and if bacteria were to be detected in the lower lungs this was as a result of an abnormal health state of the host[1]. It has only been since ca. 2010 that advances in research has enabled the confirmation that the lungs were not sterile as has been previously documented[2,3].

In the past, poor ineffective microbial culturing techniques were unable to replicate the lung habitat and culture the microbes from respiratory specimens[4]. Thanks to the advancement of culture independent techniques, the unique steady state microbiota of the lungs is being elucidated[1,5]. It is now established that the lungs harbour a unique microbiota, irrespective of health or disease and although the lung contains a smaller bacterial burden than is present in the upper respiratory tract, there is a distinct microbiota present in the lower airways of healthy individuals[6,7]. A change in the microbial composition of the lower airway microbiota may be connected with chronic lung disease such as asthma[8,9].

Due to the lower bacterial abundance and the difficulty of acquiring lower respiratory tract samples, the study of the lung microbiome is technically challenging[10]. However the findings that the lungs harbour a unique microbiota irrespective of health or disease has led to the surge of research now taking place in an effort to characterise the distinct microbial stated in a variety of lung conditions and that of the healthy lung[1,5,6]. Thanks to advancements in sequencing technologies research with respect to the lung microbiome is a rapidly advancing field[1,5].

Asthma rates are increasing and as a result of meta-genomics it is now possible to define the composition of microbes in the lungs and elucidate whether changes in the composition of lower airway microbiota influences the complex pathophysiology of chronic lung disease such as asthma. There is an emerging consensus that the microbiome potentially plays a critical role in disease development, including in the pathogenesis of airway conditions such as asthma[11].

Research with respect to the microbiota in asthma has the potential to fully dissect the role of the microbiome in this chronic respiratory disorder and can ultimately pave the way for the emergence of new therapeutic strategies to combat this respiratory condition[12].

A key aim of this study is to investigate the presence of microbial species within the previously considered sterile airway of a cohort of well-defined asthmatic patients. The presence of differing species within the airway of asthmatic patients may provide a rationale for personalised therapeutic targeting of microbes within the asthmatic lung. Changes in the microbial composition of the lungs could underlie susceptibility to and progression and chronicity of lung diseases.

3. Methods

3.1. Patient recruitment

The study was approved by the Clinical Research Ethics Committee of the Cork Teaching Hospitals. Seventy-three patients with a history of asthma (either documented change in FEV1 ≥12%/200ml with bronchodilator or a positive inhalation challenge) were recruited through a dedicated asthma clinic in a tertiary referral centre, Cork University Hospital, by my clinical supervisor, Dr Des Murphy. Patients with ABPA were excluded. Patients were scheduled for bronchoscopy, with spirometry, ACQ-7 and blood sampling performed on the day of bronchoscopy. Written informed consent was obtained from patients on the day of bronchoscopy.

Spirometry was performed according to ATS/ERS guidelines under the supervision of a research nurse from the Cork Clinical Research Facility – CCRF immediately prior to bronchoscopy[13]. Spirometry is a widely used pulmonary function test which measures the maximal volume of air an individual can inspire and expire with maximal effort[13,14].

The Asthma Control Questionnaire (ACQ-7) which consists of 7 items, weighted equally, the mean of which is used to calculate the patients ACQ-7 score, enabling the measurement of patient asthma control, was carried out by research nurses from the Cork Clinical Research Facility – CCRF prior to bronchoscopy[15-17].

Venepuncture was carried out prior to bronchoscopy by the doctor on duty using aseptic technique and strict adherence to standard precautions. The Vacutainer System was used for blood drawing and the order in which the blood containers were filled was in accordance to Cork University Hospital recommendations for blood draw order.

Patients underwent bronchoscopy according to standard guidelines[18]. Flexible bronchoscopy using video assisted imaging was performed under conscious sedation with local anaesthetic applied topically to the vocal cords, trachea and endobronchial tree[19]. Bronchoalveolar lavage (BAL) was achieved through the

instillation of saline via the bronchoscope enabling the collection of specimen directly from the endobronchial lumen for subsequent cytological or microbiological investigation[19]. Bronchoalveolar lavage (BAL) was obtained as a standardised 180ml (3X60ml) sample from either the right middle lobe or lingula[20].

Further information with regards to asthmatic patient bronchoscopy and patient sample collection protocols can be found in *Chapter 2 Study Cohorts'*.

The cohort was comprised of 73 patients; 26 males (36%) and 47 females (64%). The cohort was stratified by both severity [mild (GINA 1+2), moderate (GINA 3) and severe (GINA 4+5)] and asthma control (ACQ-7)[15-17,21,22]. See Table 1 for patient demographics. When stratified by asthma severity 36% were classified as mild (GINA 1+2), 22% were moderate (GINA 3) and 42% of the cohort were classified as severe asthmatics (GINA 4+5). When stratified by level of asthma control (ACQ-7), 41% were controlled (ACQ-7 <1.5) while 59% were uncontrolled (ACQ-7 ≥1.5).

3.2. Sample processing

After the bronchoscopy procedure was completed the patient BAL and bloods were processed in a laminar flow hood under strict aseptic technique practices. 5ml of the neat BAL was removed and aliquoted for future downstream processing.

Microscopic processing

Approximately 500-1000µl of neat BAL was also aliquoted into a 2ml screwcap tube for cytocentrifugation, to allow for microscopic examination and scoring of the BAL sample. A Shandon CytoSpin 4 centrifuge (Thermo Scientific) was used and 200µl of BAL was required per microscope slide. The machine was organised with the labelled microscope slides and funnel system, using approximately 2-4 microscope slides per patient. The samples were centrifuged at 400rpm for 2 minutes. The cytocentrifuge deposited the cells into a clearly defined area of the glass microscope while constructively flattening the cells to allow for clear nuclear presentation.

The slides then underwent staining procedures using a Kwik Diff commercial staining kit (Thermo Scientific) and a Gram staining kit (Sigma Aldrich). The Kwik Diff staining kit comprised of 3 reagents; methanol, xanthene dye in buffer salts and thiazine dye in buffer salts. The reagents were added to three separate staining jars and the microscope slides, with the deposited BAL cells were added to a slide rack which was dipped into each of the reagents approximately 10-15 times, ensuring excess reagent was allowed to drain back into the jar before moving to the next staining jar. Upon the completion of the final staining step, the slides were rinsed under deionised water and the slides were then air dried and cover slipped the following day using DPX histology mountant (Sigma Aldrich).

Gram staining (Sigma Aldrich) to differentially stain for Gram positive and negative bacteria took place as follows. The microscope slide with the deposited BAL sample was first flooded with crystal violet for 1 minute before washing the slide gently under an indirect stream of water for 2 seconds. The slide was then flooded with Gram's iodine for 1 minute before washing the stain as before. Acetone-alcohol decolourised was used to flood the slide and allowed to sit for 15 seconds before the slide was then flooded with the counterstain safranin and allowed to sit for 1 minute before the slide was washed gently under an indirect stream of water. The slides were allowed to air dry and were cover slipped the following day using a DPX histology mountant (Sigma).

DNA collection

BAL was centrifuged at 500g for 10 minutes and the supernatant was removed. The BAL supernatant was aliquoted into 2-5ml tubes for future analysis. BAL supernatant was also aliquoted into 10-20 2ml screw cap microcentrifuge tubes (Sarstedt) and centrifuged at 20,000g for 5 minutes. The supernatant of which was aliquoted into 2ml tubes for future cell stimulations and the remaining pellets were re-suspended and pooled together creating the bacteria pellet fraction (BP) for future DNA isolation and analysis

Blood collection

Blood samples were collected in serum specific red and yellow capped Vacuette tubes and plasma specific purple capped Vacuette tubes (Greiner Bio-One). The inner wall of the serum specific tube was coated with silica particles which activated the coagulation process and a specific separator gel at the base of the tube formed a stable barrier during centrifugation to enable the serum and blood cells to remain separate. The plasma specific Vacuette tube contained a coating of either K2EDTA or K3EDTA which acted as an anticoagulant by binding calcium ions to prevent the clotting cascade from taking place. Both tubes were centrifuged at 200rpm for 20 minutes and the serum and plasma were removed by pipetting and stored in screw-cap microcentrifuge tubes.

All BAL and blood isolated samples were stored at -80^{o}C for future processing and analyses.

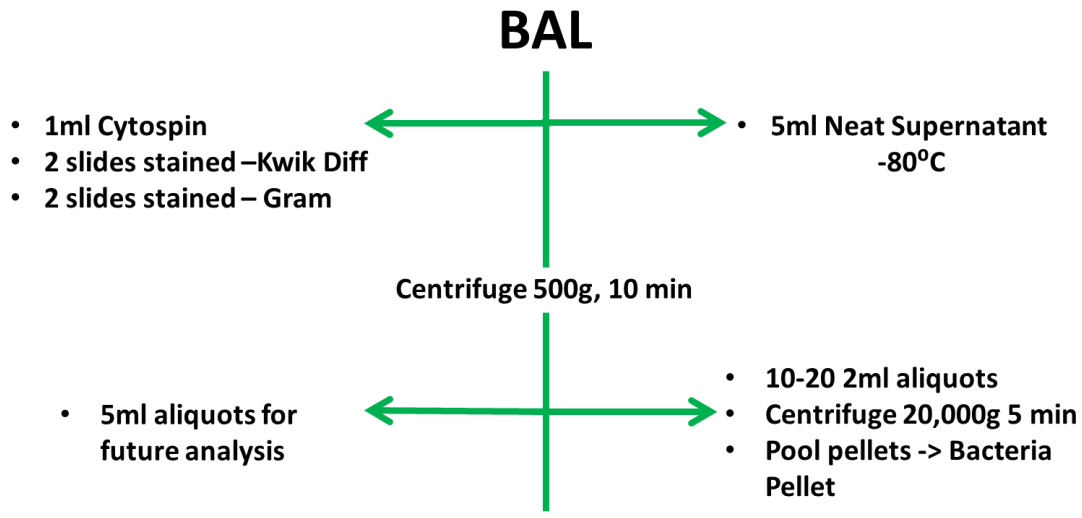


Figure 1 Patient BAL processing. Schematic depicting the processing undertaken with the patient BAL once received in the laboratory on the day of bronchoscopy.

3.3. Microscopy

A differential cell count was performed on BAL cytospin slides, stained with the Kwik-Diff kit (Thermo-Fischer) using a light microscope (Olympus) and Olympus DP software. Immune cell percentage counts for Monocyte, Macrophage, Lymphocyte, Neutrophil and Eosinophil cells were performed in 10 random fields of view for two cytospin Kwik-Diff differentiated slides per patient. Microscopic observation of microbes present within macrophages and outside immune cells occurred while counting the immune cell percentages in certain patient cytospin slides.

3.4. DNA extraction

DNA extraction was carried out on the bacteria pellet isolated from the patient BAL due to differential centrifugation. At sample processing on the day of bronchoscopy to remove host cell DNA, BAL was centrifuged at 500g for 10 minutes, supernatant collected and centrifuged in 2ml screwcap microcentrifuge tubes at 20,000g for 5 minutes. The supernatant was then removed, and the remaining bacteria pellets were recombined for DNA extraction.

DNA extraction took place using a QIAamp UPC Pathogen Mini Kit (Qiagen, Manchester, UK). Patient bacteria pellet samples were centrifuged at 20,000g for 5 minutes, supernatant discarded and 500µl buffer ATL was used to re-suspend the pellet, which was then added to a pathogen lysis tube containing silica beads and vortexed at 7000rpm for 1 minute, using a MagNA Lyser machine. The tube was then centrifuged at 8000g for 30 seconds and supernatant removed to a fresh microcentrifuge tube without disrupting the silica beads. 40µl of Proteinase K was added and the tube was vortexed and incubated at 56^{o}C for 10 minutes. 200µl buffer APL2 then added to the sample, the tube was vortexed and incubated at 70^{o}C for 10 minutes. 300µl of ethanol was added to the lysate and the tube was pulse vortexed for 30 seconds and the lysate was then transferred to a mini spin column placed in a collection tube and centrifuged at 6000g for 1 minute. This was repeated until all of the lysate had been transferred and passed through the mini spin column, discarding the filtrate after each spin. 600µl of Buffer APW1 was

added to the mini spin column, which was then centrifuged at 6000g for 1 minute, discarding the filtrate afterwards. 750µl of Buffer APW2 was transferred to the mini spin column, which was then centrifuged at 20,000g for 3 minutes, transferring the mini spin column to a new collection tube and repeating centrifugation to eliminate buffer carryover. The mini spin column was transferred to a new collection tube and incubated at 56^{o}C for 3 minutes to ensure the membrane was dry and was then transferred to a new elution tube and 100µl of Buffer AVE was added to the centre of the membrane and incubated at room temperature for 1 minute before being centrifuged at 20,000g for 1 minute to elute the DNA. The isolated DNA samples were then stored at -20^{o}C for further downstream processing.

3.5. DNA quantification

Nano Drop spectrophotometer

The concentration and quality of the extracted DNA was analysed using a Nano Drop ND1000 spectrophotometer using the settings nucleic acid; DNA-50 (Thermo Fischer Scientific, Wilmington, Delaware, USA).

The Nano Drop was calibrated using 1µl of DNase/RNase free water. The DNA extracted from the patient bacteria pellet sample was analysed by pipetting 1µl of sample onto the lower measure platform of the machine, closing the sampling arm and initiating spectral measurement using the operating software documenting the ng/µl and 260:280 values and DNA curve graph. In order to standardise the DNA a dilution step was performed whereby the undiluted DNA was diluted with molecular biology grade water (Sigma Aldrich) to ensure a standard value of 5ng/µl (15ng per reaction) of DNA for each patient sample.

Qubit Fluorometer

DNA quantification was also performed using a Qubit dsDNA High Sensitivity (HS) assay kit (Life Technologies, Thermo-Fischer) which consisted of Qubit dsDNA HS assay reagent (200X concentrate in DMSO), Qubit dsDNA HS dilution buffer, Qubit dsDNA HS standard #1 (0ng/µl in TE buffer) and Qubit dsDNA HS standard #2

(10ng/µl in TE buffer) and a Qubit 0.2 Fluorometer (Life Technologies, Thermo Fischer).

The assay was highly selective for double-stranded (dsDNA) and was accurate for initial sample concentrations of 10pg/µl to 10ng/µl. Specialised Qubit thin wall clear 0.5ml assay tubes were sourced (Life Technologies, Thermo-Fischer) and the number of tubes required for the samples and two standards were labelled on the tube lid but not the side as this may interfere with the Qubit Fluorometer reading.

The Qubit working solution was prepared by diluting the Qubit HS reagent 1:200 in Qubit dsDNA HS buffer using a clean plastic tube each time the Qubit working solution was prepared. For each sample the working solution consisted of 200µl of Qubit dsDNA HS buffer and 1µl of Qubit HS assay reagent. The working solution was prepared in batches of 5 reactions, which consisted of 1ml Qubit dsDNA HS buffer and 5µl of Qubit HS assay reagent. For the standards 190µl of working solution was added to each of two standard tubes and 10µl of standard #1 and 10µl of standard #2 was added to the appropriate tube and the tubes were then vortexed for 3 seconds.

In order to prepare for the DNA sample readings 198µl working solution was added to the individual pre-labelled assay tubes and to this 2µl of DNA sample was added to the appropriate assay tubes for a final volume of 200µl. Tubes were vortexed for 3 seconds ensuring no air bubbles were produced. The assay tubes were incubated at room temperature for 2 minutes. The dsDNA High Sensitivity programme was selected for on the Qubit Fluorometer machine and in order to calibrate the machine standard #1 was inserted into the sample chamber and was read before standard #2 was read in the same manner. Once calibration was complete the DNA samples were read. In order to standardise the DNA samples before further analysis such as qPCR and Next Generation Sequencing, samples above 5ng/µl were diluted to 5ng/µl using molecular grade water.

3.6. Primers

Primers were designed through analyses of pre-designed validated primers already present in the literature, through the use of the 16S RNA gene database Greengenes[23] or through literature research to determine specific genes present in the microorganism of interest and using this information to retrieve the sequence coding of that gene. All primers designed in house through Greengenes or gene sequences were formulated using the Universal Probe Library Assay Design Centre platform (Roche Life Science) by copying the sequence of interest to the platform, selecting for other organism and deselecting to automatically select for intron spanning assay. The platform then designed potential primers for the sequence of interest, ranking them by order of suitability. Primer sequences were analysed using the NCBI Blastn platform. Two primers sequences were then selected for each microorganism of interest and were ordered from Sigma.Aldrich (Ireland).

Primers were centrifuged upon arrival to ensure the lyophilised pellet was at the bottom of the primer tube and primers were re-suspended with molecular grade water in accordance to individual primer specification (µl for 100µM). Once re-suspended primers were vortexed and the left and right primer were recombined to a 1 in 10 working solution (20µl L+ 20µl R + 160µl molecular grade water) in a sterile 1.5ml tube. Primers were stored at -20^{o}C.

Probes corresponding to the primers of interest were sourced from Universal Probe Library Probes (Roche Life Sciences) and were available within the laboratory. All primers were validated before use on the individual patient bacteria pellet and cell pellet DNA. See supplementary table 1 for primer sequences

3.7. qPCR – quantitative Polymerase Chain Reaction

Primers once re-suspended were first tested on pooled sample of extracted DNA from various patients bacteria pellet (BP) samples at the following concentrations; neat undiluted, 1:10 and 1:100 diluted in order to validate all primers before they were tested on each individual sample.

qPCR was performed on extracted BAL BP DNA in order to verify the presence of the following bacteria; Total Bacteria, Firmicutes, *Staphylococcus aureus*, *Streptococcus pneumoniae*, *Rothia*, *Micromonospora*, *Pseudomonas aeruginosa*, *Pseudomonas fluorescens*, *Escherichia*, *Bordetella*, *Prevotella*, *Veillonella*, *Mycoplasma pneumoniae*, *Chlamydophilia pneumoniae*, *Neisseria bacilliformis*, *Moraxella catarrhalis*, *Neisseria meningitidis* and *Haemophilus influenzae.* See supplementary table 1 for primer sequences.

qPCR's were performed using a 384 well plate layout and LightCycler Probes Master (Roche, Ireland) or LightCycler SYBR Green Master (Roche, Ireland) reagent mix, dependent on the use of hydrolysis probes or SYBR Green primer sets. Water NTCs (No Template Control) were used in each reaction in order to identify reaction set up contamination and to test for the propensity of primers to create primer dimers in the case of reactions which were carried out with SYBR Green Master.

Reactions were performed on a LightCycler 480 machine (Roche, Ireland). qPCR conditions were as follows; pre-incubation at 50^{o}C for 2 minutes, ramp rate 4.8^{o}C/s and 95^{o}C for 10 minutes, ramp rate 4.8^{o}C/s. Amplification at 95^{o}C for 10 seconds, ramp rate 4.8^{o}C/s, 60^{o}C for 45 seconds, ramp rate 2.5^{o}C/s and 75^{o}C for 1 second, ramp rate 4.8^{o}C for 45 cycles in total. A melt curve also occurred at 95^{o}C with a ramp rate of 0.11^{o}C/s for any primer which used LightCycler SYBR Green Master. A cooling stage then occurred at 40^{o}C, ramp rate 2^{o}C/s at the end of the process. Fluorescent readings were taken in single acquisition mode.

The primers *Neisseria meningitidis*, *Streptococcus pneumoniae* and *Haemophilus influenzae* required a change in the acquisition temperature to 67^{o}C due to the nature of the primer sequences. All NTCs did not produce a product and melt curves produced clear peaks indicating that the products produced were not an artefact.

3.8. REPLI-g

Due to the low volume of DNA (100µl), isolated from the patient bacteria pellet samples during the DNA extraction process, it was decided in order to have enough DNA to carry out the qPCR bacterial analysis of the patient bacteria pellet DNA and whole genome sequencing of patient DNA, it was necessary for patient bacteria pellet DNA to undergo Repli g mini kit (Qiagen) processing in which the whole genome amplification from small samples using Multiple Displacement Amplification (MDA) took place.

The protocol was carried out as per manufacturer's instructions as follows. Briefly, denaturation buffer D1 and neutralisation buffer N1 were prepared for the total number of whole genome amplification reactions to take place. Per every 15 reactions 9µl of reconstituted buffer DLB with 32µl of nuclease-free water was required to prepare Buffer D1. Per every 15 reactions 12µl of stop solution and 68µl of nuclease-free water was required to prepare Buffer N1. 2.5µl of the previously standardised template DNA (5ng/µl) was added to a microcentrifuge tube with 2.5µl of Buffer D1. The microcentrifuge tube was then vortexed and centrifuged briefly before incubation at room temperature occurred for 3 minutes. 5µl of Buffer N1 was then added to the microcentrifuge tube before vortexing and centrifugation occurred. The REPLI-g Mini DNA Polymerase was then thawed on ice while the other kit components were thawed at room temperature before all components were vortexed and centrifuged briefly. A mastermix was then prepared on ice as follows; 10µl of nuclease-free water, 29µl of REPLI-g Mini Reaction Buffer and 1µl of REPLI-g Mini DNA Polymerase per reaction. 10µl of the denatured DNA per sample was then transferred to pre-labelled 96 well un-skirted PCR plate into which 40µl of mastermix was added. The 96 well plate was then sealed using a foil PCR seal and the plate was incubated at 30^{o}C for 16 hours using a benchtop PCR Thermal Cycler machine (Thermo Fischer Scientific) with the lid of the machine set to 70^{o}C. After 16 hours the machine was then heated to 65^{o}C for 3 minutes in order to inactivate REPLI-g Mini DNA Polymerase. For downstream qPCR experiments' the amplified DNA was then diluted to 1:20 and 3µl of this diluted DNA was then required per qPCR reaction. The amplified DNA was stored at -20^{o}C.

3.9. Next Generation Sequencing (NGS)

Prior to sample transfer to the APC Microbiome Institute Sequencing Platform patient DNA samples underwent an assessment of DNA quantity and purity. DNA quantification took place using a fluorometric based method, the Qubit dsDNA High Sensitivity (HS) assay kit (Life Technologies, Thermo-Fischer). A fluorometric based quantification method was preferred for Next Generation Sequencing DNA library preparation. However in order to assess DNA purity the Nano Drop ND1000 spectrophotometer (Thermo-Fischer Scientific) platform was implemented as it enabled the assessment of DNA purity using UV absorbance at 260nm to 280nm to measure the ratio of absorbance with 260/280 absorbance ratio values between 1.8 to 2.0 indicating a pure DNA sample.

Patient DNA samples, ranging from 0.5ng to 580ng were sent for DNA sequencing to the Teagasc Food Research Centre, Ireland. The Illumina Nextera XT Library Preparation Kit (Illumina Inc., San Diego, CA, USA) was used to fragment and add sequencing adaptors to the extracted DNA, as described in the manufacturer's instructions, but with tagmentation time increased to 7 minutes. Following clean-up of the indexed libraries as described in the manufacturer's protocols, libraries were quantified by Qubit High Sensitivity Assay (Life Technologies, Thermo-Fischer) and the average size of the fragments determined by running each sample on the Agilent Bioanalyser using a High Sensitivity Assay (Agilent Technologies). The molarity of each sample was then determined and the samples were then pooled equimolarly. The final pool was quantified by qPCR using the Kapa Library Quantification Kit from Illumina (Roche) and then sequences on the Illumina NextSeq 500 platform using high-output chemistry (2x150bp) according to the manufacturer's instructions. The demultiplexed dataset was uploaded to Illumina Basespace and imported onto One Codex (One Codex, CA, USA). The interpretation of the sequence data occurred through the use of data visualisation software present in the BaseSpace Sequence Hub and through the use of the One Codex microbial reference database

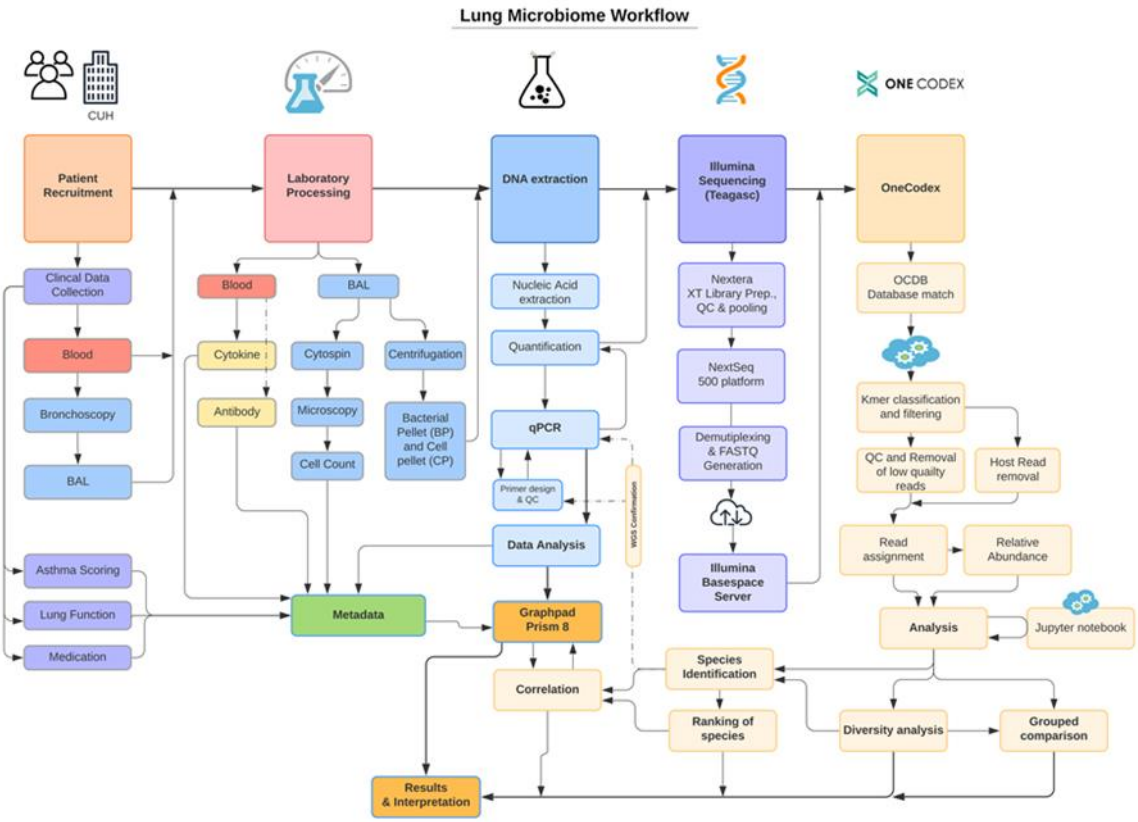


Figure 2. Microbiome analysis workflow. Schematic of the microbiome analysis performed on the patient dataset.

3.10. Primary analysis of the Next Generation Sequencing (NGS) dataset

The primary analysis of the Next Generation Sequencing (NGS) dataset was performed in conjunction with One Codex, Dr Christopher Smith, Dr Denise Lynch and Dr John MacSharry.

All raw sequences were analysed using the One Codex database (OCDB). The One Codex Database consists of ~114K complete microbial genomes, including 62K distinct bacterial genomes, 48K viral genomes, and approximately 4K fungal, archaeal and eukaryotic genomes. The human genome was included to screen out host reads, and a complete list of references is available in the One Codex application at https://app.onecodex.com/references. The database was assembled from both public and private sources, with a combination of automated and manual curation steps to remove low quality or mislabelled records.

Comparing a microbial sample against the One Codex Database consisted of three sequential steps. First, every individual NGS read were compared against the One Codex Database by exact alignment using k-mers where k=31 (see Ames et al., 2014 and Wood et al., 2014 for details on k-mer based classification)[24,25]. The k-mer classification results were filtered based on the relative frequency of unique k-mers in the sample, sequencing artefacts were filtered out of the sample. This filtering only removed probable sequencing or reference genome based artefacts, and does not filter out low abundance or low confidence hits. Finally the relative abundance of each microbial species was estimated based on the depth and coverage of sequencing across every available reference genome.

Alpha diversity

Alpha diversity measures the ecological diversity within each sample. The Chao1 estimator of diversity, the Simpson index, and the Shannon index were calculated for each sample.

Chao1 estimator: The non-bias corrected Chao1 estimator for each sample, which estimated the richness of the sample, was calculated.

Simpson index: The Simpson index for each sample, which is an estimator of evenness of the abundance of all taxa in the sample, was calculated.

Shannon index: The Shannon index for each sample, which is a measure of both richness and evenness of the sample, was calculated.

Beta diversity

Beta diversity is the relative distance or dissimilarity between communities or samples. Pairwise comparisons between all pairs of samples was calculated between all pairs of samples to calculate the dissimilarities, and this data can be then used to identify similar clusters of samples using analyses such as a Principle Component Analysis. The beta diversity was represented using the Bray-Curtis dissimilarity metric.

Bray-Curtis Dissimilarity: An ecological dissimilarity metric that accounts for both the presence/absence and abundance of organisms in a community.

3.11. Cytokine measurement in BAL and plasma samples

BAL and plasma cytokines were analysed using a custom MSD proinflammatory panel 1 containing targets for Interleukin (IL)-1β, IL-4, IL-6, IL-8, IL-10, IL-13, Interferon (IFN)-γ and tumour necrosis factor (TNF)-α and a custom MSD cytokine panel 1 containing targets for IL-5 and IL-17A.

Reagent preparation consisted of the following; calibrator standards were prepared by suspension of the lyophilised calibrator with 1000µl of the appropriate diluent (diluent 2 for proinflammatory panel 1 and diluent 43 for cytokine panel 1) and then transferring 100µl of the re-suspended calibrator with 300µl of appropriate diluent. This 4 fold serial dilution was repeated 5 additional times to generate 7 calibrators with the diluent alone used as a zero calibrator.

Plasma samples were diluted as follows; 35µl of plasma and 35µl of appropriate diluent, while BAL samples were undiluted. A detection antibody solution was

created for the proinflammatory panel by combining 60µl of each SULFO-TAG anti-human IL-1β, IL-4, IL-6, IL-8, IL-10, IL-13 IFN-γ and TNF-α antibody with 2520µl diluent 3 to bring to a final volume of 3000µl. A detection antibody solution for cytokine panel 1 consisted of 60µl each of SULFO-TAG Anti-human IL-5 and IL-17A with 2880µl of diluent 3 for a final volume of 3000µl. Wash buffer consisted of PBS and 0.05% Tween 20. Read buffer for each plate consisted of 10ml of Read Buffer T (4X) and 10ml of deionised water for a 2X working solution.

Step 1 of the assay involved washing the plate 3 times with 150µl/well wash buffer. 50µl of prepared calibrators or samples were then added per well, the plate was sealed before overnight incubation with shaking at 2-8^{o}C occurred. Step 2 involved washing the plate a further 3 times with 150µl/well wash buffer before the addition of 25µl detection antibody solution to each well, the plate sealed and a two hour room temperature incubation with shaking occurred. Step 3; the plate was washed 3 times as before and 150µl of 2X Read Buffer T was added to each well before analysis of the plate using an electro-chemiluminescence QuickPlex SQ 120 imager from Meso Scale Discovery (Gaithersburg, MD, USA).

3.12. Glucose assay

Blood glucose levels were routinely tested for in Cork University Hospital. BAL glucose levels were analysed in the APC Microbiome Ireland using a Glucose Assay Kit (Calbiochem, Merck) with an assay range of 1-200µM. The kit provided direct measurement of glucose in the BAL fluid by utilizing the glucose enzyme mix to specifically oxidase glucose to generate a product that reacts with a dye to generate colour (lambda=570nm) and fluorescence (Ex/Em=535/587nm) with the generated colour and fluorescence being proportional to the amount of glucose present in the sample.

A standard curve for fluorometric analysis was prepared by diluting the glucose standard solution to 0.1nmol/µl by adding 10µl of the Glucose Standard to 990µl of the Glucose Assay Buffer and mixing well. 20µl of this solution was then added to 180µl of Glucose Assay Buffer and mixed well. 0, 2, 4, 6, 8 and 10µl of this was then

added to the wells of the 96 well plate in duplicate and the volume was adjusted to 50µl in the wells with Glucose Assay Buffer generating a standard curve of 0, 0.2, 0.4, 0.6, 0.8 and 1.0nmol/well in duplicate.50µl of the BAL samples to be tested were added to the 96 well plate, corresponding to a pre-determined plate layout. The reaction mix was prepared as follows and each 50µl reaction mix per well contained 46µl of Glucose Assay Buffer, 2µl Glucose Probe and 2µl diluted Glucose Enzyme Mix. 50µl of the reaction mix was added to each well containing the diluted Glucose Standard or test sample and thorough mixing occurred. The plate was then covered in foil and incubated for 30 minutes at 37^{o}C. The absorbance was read using a fluorometric plate reader (Synergy HTX Multi Mode Reader, BioTek, USA) at excitation/emission = 535/590nm. Background noise was corrected for by subtracting the value derived from the zero glucose control from all the standards and test samples. The glucose concentrations were derived from the standard curve generated.

3.13. Statistical analyses

All data was stored in Microsoft Excel files before statistical analyses occurred. Graph Pad Prism 8 software was used to perform all statistical analyses and to provide graphical representation of the data. All data was assessed using normality and lognormality tests and the Shapiro-Wilk test was applied to assess the normality of the data set. Normally distributed data was presented as the mean ± standard deviation (SD) within the text and figures. Normally distributed data sets where both the X and Y values were normally distributed were analysed using Pearson correlation coefficient analysis. Data was considered to be statistically significant when $P<0.05$. Non-normally distributed data was presented as median ± interquartile range (IQR) within the text and figures. Non-normally distributed data sets where both the X and Y values were not both normally distributed were analysed using the non-parametric Spearman correlation[26]. Data was considered to be statistically significant when $P<0.05$.

4. Results

4.1. Patient demographics

The patient cohort consisted of seventy-three adult asthmatic patients, 26 males and 47 females. 62% (45/73) of the asthmatic patients had never smoked, while 27% (20/73) were ex-smokers and 11% (8/73) were current smokers. 64% (47/73) of patients lived in a rural location while 36% (26/73) lived in an urban setting.

When stratified by asthma severity 36% (26/73) were classified as mild (GINA 1+2), 22% (16/73) were moderate (GINA 3) and 42% (31/73) of the cohort were classified as severe asthmatics (GINA 4+5). When stratified by level of asthma control (ACQ-7), 41% (30/73) were controlled (ACQ-7 <1.5) while 59% (43/73) were uncontrolled (ACQ-7 ≥1.5).

8 patients within the cohort were in receipt of oral steroids (mg) at time of bronchoscopy (min 5mg – max 30mg). 14% (10/73) of the asthma cohort were not in receipt of inhaled corticosteroids (ICS) (FDP 250) at time of bronchoscopy while 86% (63/73) of patients were in receipt of inhaled corticosteroids (ICS) (min 250 – max 2000 FDP). See Table 1 for patient demographics at bronchoscopy.

Table 1. Patient demographics at bronchoscopy. Note † FEV-1, Forced Expiratory Volume in the first second; § FeNO, Fractional exhaled Nitric Oxide; ¶ BMI, Body Mass Index; ¥ ESR, Erythrocyte Sedimentation Rate; ‡ CRP, C-reactive protein.

		Mild (GINA 1-2)	**Moderate (GINA 3)**	**Severe (GINA 4-5)**
Patients	n=73 (%)	26 (36%)	16 (22%)	31 (42%)
Male		11 (42%)	4 (25%)	11 (35%)
Female		15 (58%)	12 (75%)	20 (65%)
ACQ-7	[Mean (SD)]	[1.1 (0.6)]	[1.9 (1.0)]	[3.2 (1.1)]
	[Median (IQR)]	[0.9 (0.6-1.5)]	[1.9 (1.0-2.4)]	[3.1 (2.4-4.1)]
IgE (KU/L)	[Mean (SD)]	[374(642)]	[174.9 (244)	[302.5 (450.5)]
	[Median (IQR)]	[96.1 (30.7-447)]	[142 (62.6-180.5)]	[113 (28.5-299)]
FEV-1 (Percent Predicted)†	[Mean (SD)]	[87 (12.8)]	[87.6 (21)]	[65.3 (23.2)]
	[Median (IQR)]	[88 (78.8-96.0)]	[81 (74.3-102.8)]	[68 (50-81)]
FeNO (ppb) §	[Mean (SD)]	[34.1 (27.2)]	[21.7 (11.1)]	[24.4 (27.2)]
	[Median (IQR)]	[23 (12.5-46.5)]	[21.0 (14-30)]	[15 (10-25)]
BMI (kg/m^2) ¶	[Mean (SD)]	[25.8 (4.5)]	[27.2 (7)]	[30.4 (6.5)]
	[Median (IQR)]	[24 (22.4-30.0)]	[25.4 (22.2-30.8)]	[29.8 (25.1-34.1)]
Haemoglobin (Hb) (g/L)	[Mean (SD)]	[14.3 (1.3)]	[13.9 (0.9)]	[13.4 (1.4)]
	[Median (IQR)]	[14.2 (13.2-15.4)	[14.1 (12.9-14.4)]	[13.3 (12.6-14.5)]
White cell count (WBC) (10^9/L)	[Mean (SD)]	[6.8 (1.7)]	[7 (1.7)]	[8.6 (3.4)]
	[Median (IQR)]	[6.8 (5.3-8.0)]	[6.7 (5.6-8.1)]	[8.1 (6.8-8.8)]
Blood Lymphocyte count (10^9/L)	[Mean (SD)]	[2.0 (0.6)]	[2 (0.6)]	[2.3 (1)]
	[Median (IQR)]	[2.0 (1.6-2.6)]	[1.2 (1.5-2.3)]	[2.1 (1.5-2.9)]
Blood Eosinophil count (10^9/L)	[Mean (SD)]	[0.3 (0.2)]	[0.3 (0.4)]	[0.3 (0.3)]
	[Median (IQR)]	[0.2 (0.1-0.3)]	[0.2 (0.1-0.4)]	[0.2 (0.1-0.3)]
Blood Neutrophil count (10^9/L)	[Mean (SD)]	[4.0 (1.4)]	[4.5 (1.0)]	[5.4 (2.8)]
	[Median (IQR)]	[3.9 (3.0-4.7)]	[4.7 (3.6-5.4)]	[5 (3.6-5.9)]
ESR (mm/hr)¥	[Mean (SD)]	[6.3 (4.4)] [n=25}	[8.6 (6.6)] [n=14]	[11.9 (12.8)] [n=28]
	[Median (IQR)]	[5 (2.0-9.5)	[7 (2.8-12.3)]	[7(2.8-13.8)]
CRP (mg/L)‡	[Mean (SD)]	[5.8 (2.0)] [n=26]	[7.9 (4.6)] [n=5]	[10 (15.6)] [n=30]
	[Median (IQR)]	[5 (5-5)]	[6.1 (5.5-11.1)]	[5 (5-8.3)]
Blood glucose (mMol)	[Mean (SD)]	[4.9 (0.4)] [n=24}	[5 (0.5)] [n=16]	[1.8 (0.8)] [n=20]
	[Median (IQR)]	[4.8 (4.6-5.1)]	[4.9 (4.6-5.3)]	[2 (1.0-2.8)]
BAL glucose (µMol)	[Mean (SD)]	[1.8 (2.2)]	[1.3 (2.1)]	[2.7 (2.6)] [n=30]
	[Median (IQR)]	[1 (1-2)	[1 (0-1)]	[2 (1-4)]

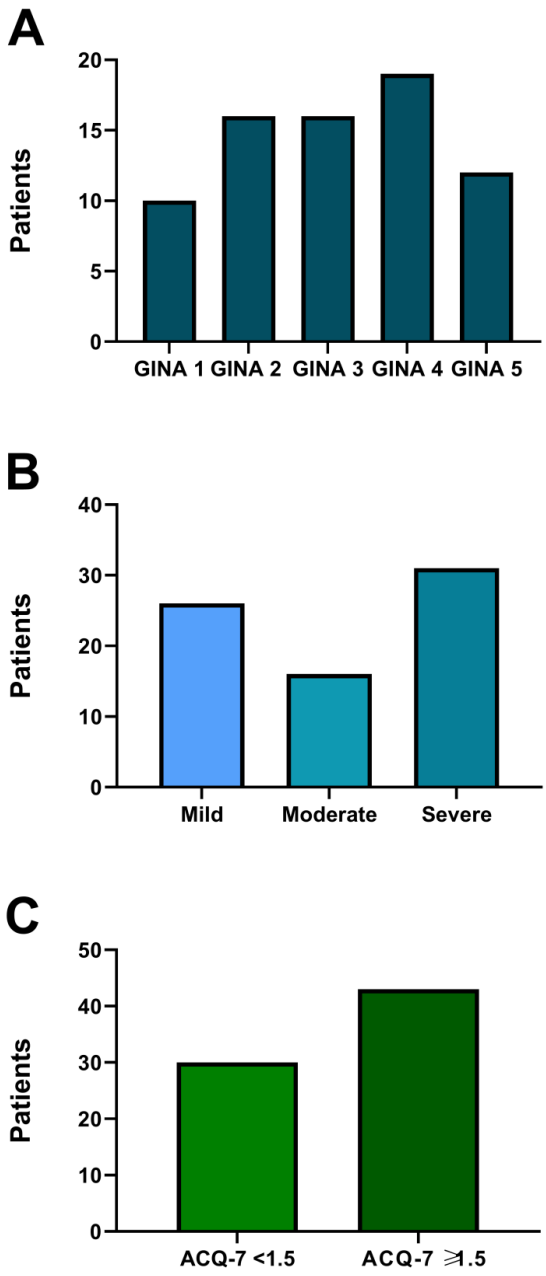


Figure 3. Patient asthma severity and level of control. The patient cohort was stratified by (A) asthma severity (GINA). When GINA stages were grouped into mild (GINA 1+2), moderate (GINA 3) and severe (GINA 4+5) 36% (26/73) of patients were mild (GINA 1+2), 22% (16/73) moderate (GINA 3) and 31% (42%) severe (GINA 4+5) (B). When the patient cohort was stratified by level of control (ACQ-7) 41% (30/73) were controlled (ACQ-7<1.5) and 59% (43/73) were uncontrolled (ACQ-7≥1.5) asthmatics (C). n=73

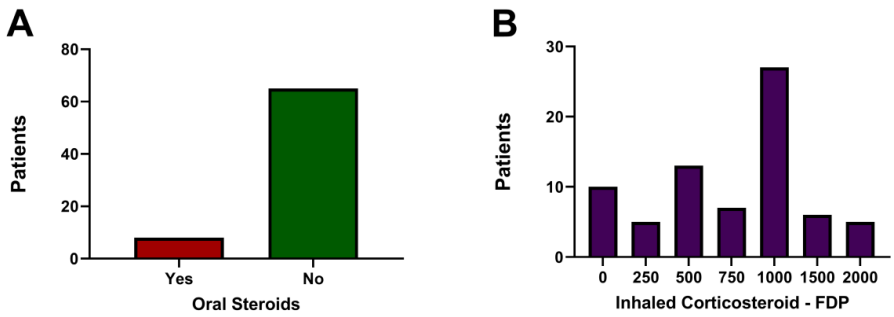


Figure 4. Patient oral steroids and inhaled corticosteroids. (A) 8 patients were in receipt of oral steroids at time of bronchoscopy (5mg min – 30mg max) while 65 patients were not in receipt of oral steroids at time of bronchoscopy. (B) Breakdown of patient inhaled corticosteroid (ICS) (FDP) dose at time of bronchoscopy. 86% (63/73) of patients were in receipt of ICS while 14% (10/73) of patients within the cohort were newly diagnosed and ICS naïve at the time of sampling. n=73

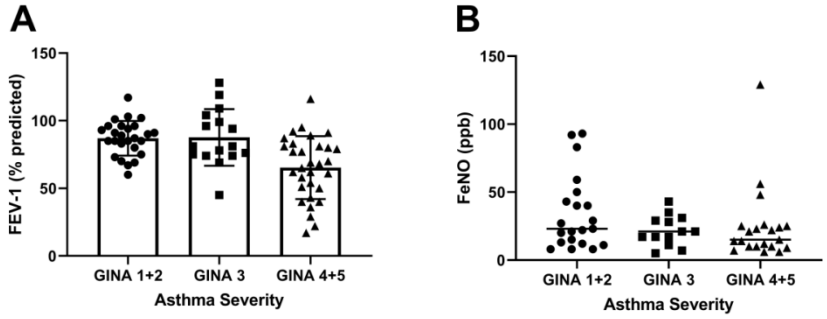


Figure 5. FEV-1 and FeNO at bronchoscopy. Forced Expiratory Volume in the first second (FEV-1) is a measurement of the expiratory volume in the first second of the Forced Vital Capacity (FVC) maneuver. (A) depicts the FEV-1 % predicted measurements obtained from the cohort on the day of bronchoscopy. (B) Fractional exhaled Nitric Oxide (FeNO) is a non-invasive marker of inflammation. Patients underwent FeNO measurements prior to bronchoscopy whereby the level of nitric oxide in parts per billion (ppb) in the air which was exhaled slowly from their lungs was measured using a portable FeNO device.

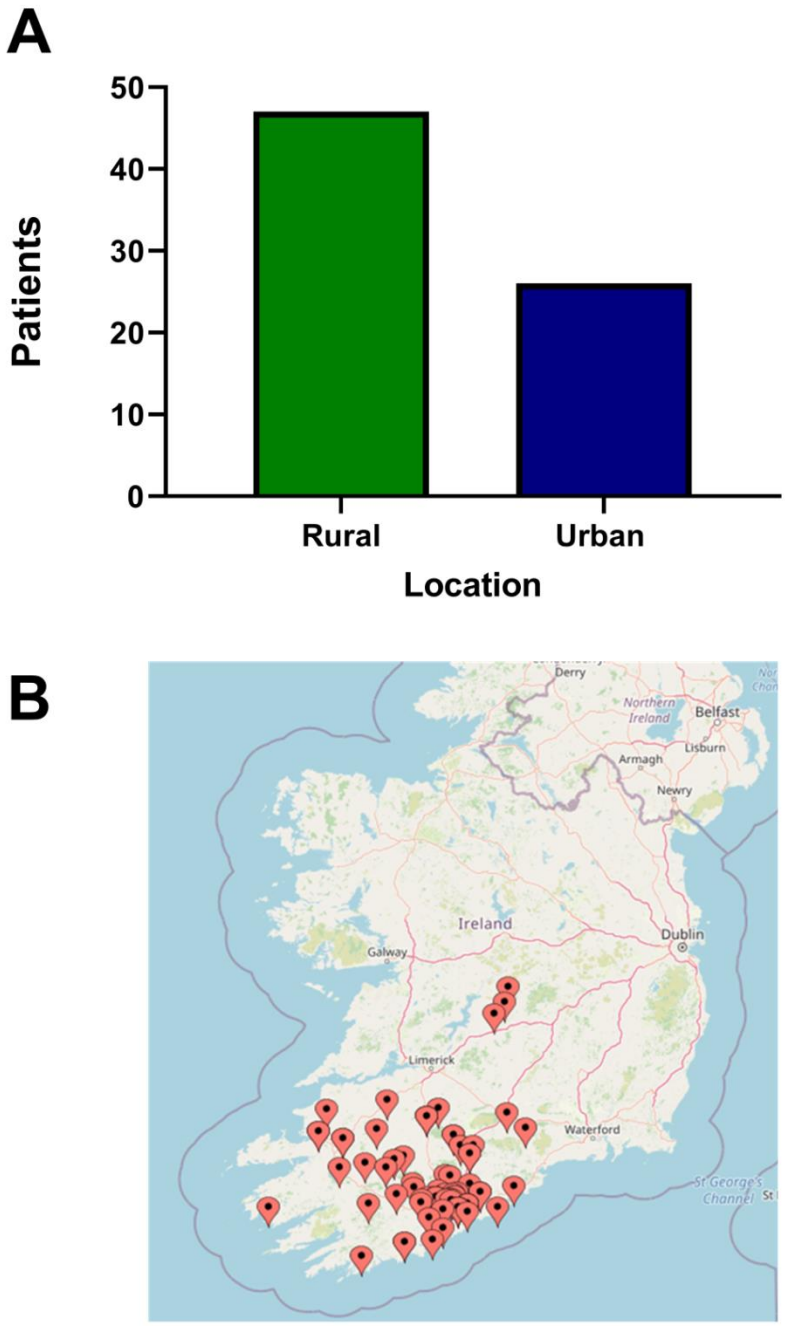


Figure 6. Location of the patient cohort. (A-B) 64% (47/73) of the asthma cohort resided in a rural location whilst 36% (26/73) lived in an urban location.

4.2. Serological detection of Immunoglobulin E (IgE) levels

IgE levels above 80KU/L were considered above the hospitals upper limit of normal. IgE levels were elevated in 56% (41/73) of the patient cohort (median 108.0; IQR 35.5-329.5). See figure 7 for IgE breakdown by patients (A) and by asthma severity (GINA) (B) and level of control (ACQ-7) (C).

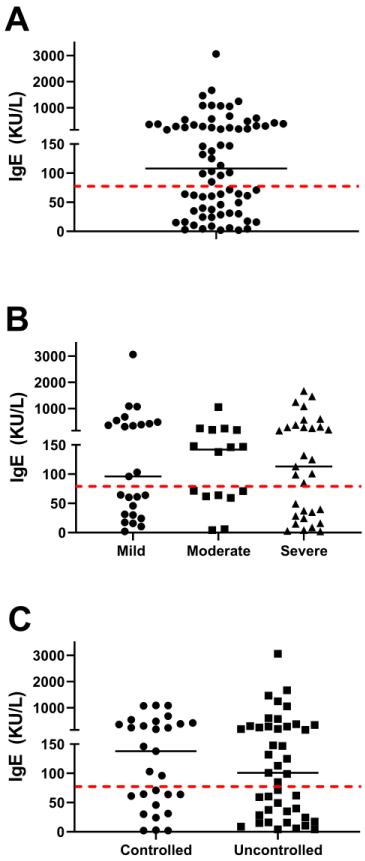


Figure 7. Serological testing of asthmatic patient serum IgE levels. Serum was assessed for total IgE levels (median 108.0; IQR 35.5-329.5). 56% of patients displayed total IgE levels above the hospitals upper limit of normal (80KU/L), red dashed line, showing atopic asthma (A). IgE levels upon grouping patients by GINA stage; mild (GINA 1+2) (median 96.1; IQR 30.7-447.0), moderate (GINA 3) (median 142.0; IQR 62.6-180.5) and severe (GINA 4+5) (median 113.0; IQR 28.5-299.0) (B). IgE levels upon grouping patients by level of asthma control (ACQ-7); controlled (ACQ-7<1.5) (median 138.0; IQR 53.5-399.0) and uncontrolled (ACQ-7≥1.5) (median 101.0; IQR 28.5-282.0).

4.3. Microscopy and BAL immune cell percentage counts

Microscopy enabled the examination of the patient BAL fluid, which had been previously processed onto microscopy slides and stained using the Kwik Diff differential staining method ensuring two BAL cytospin slides were prepared for each patient. BAL immune cell percentage counts were carried out, whereby the percentage of lymphocytes, monocytes, macrophages, neutrophils and eosinophils were recorded for each patient. Ball cell differentials revealed that macrophages were the most dominant immune cell type present within the BAL of the asthmatic cohort with varying levels of lymphocytes, monocytes, neutrophils and eosinophils present. n=73

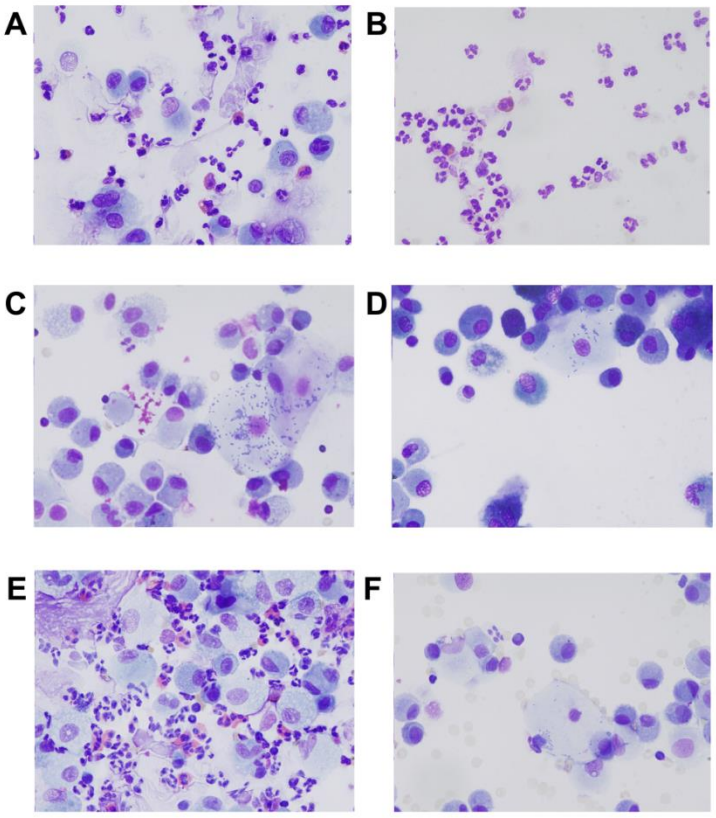


Figure 8. Microscopic examination of patient bronchoalveolar lavage (BAL). (A-F) Representative microscope images of patient BAL fluid stained with a commercial Kwik Diff stain displaying lymphocytes, monocytes, macrophages, neutrophils and eosinophils. All images were taken at 40x magnification where A=patient A27, B=patient A16, C=patient A12, D=patient A11, E=patient A27, F=patient A19.

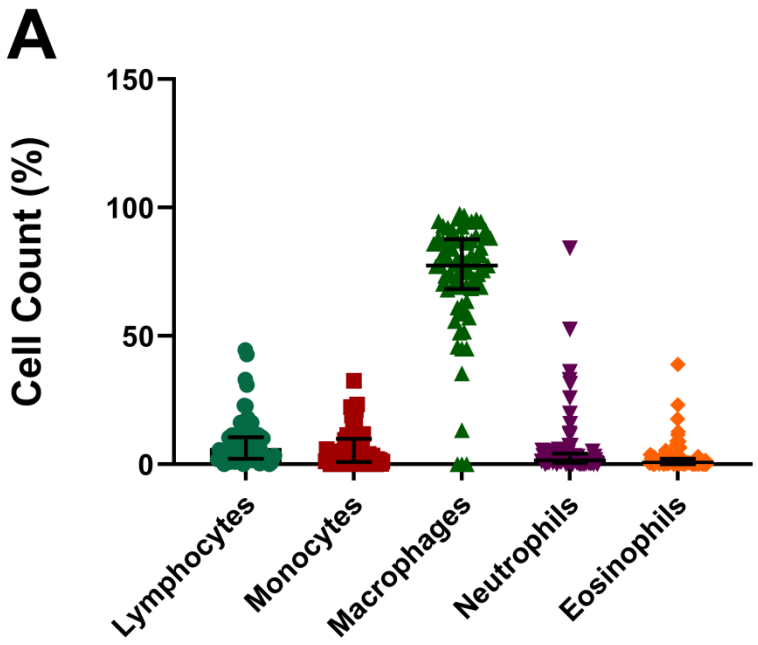


Figure 9. BAL immune cell percentage counts. (A)BAL immune cell differential counts revealed macrophages to be the most dominant immune cell type present with varying levels of lymphocytes, monocytes, neutrophils and eosinophils present within the patient BAL. n=73

Table 2. BAL Immune cell percentage counts. The [Mean (SD)] and [Median (IQR)] of the immune cell percentage counts when patients are stratified by GINA stage where GINA 1+2= Mild, GINA 3= Moderate and GINA 4+5= Severe

		Mild (GINA 1+2)	Moderate (GINA 3)	Severe (GINA 4+5)
BAL Lymphocyte % count	[Mean (SD)]	[6.9 (5.0)]	[9.1 (11.1)]	[8.9 (10.6)]
	[Median (IQR)]	[6.4 (2.9-10.2)]	[5.9 (1.0-13.4)]	[5.6 (2.1-11.4)
BAL Monocyte % count	[Mean (SD)]	[8.8 (7.6)]	[5.7 (8.1)]	[4.2 (5.0)]
	[Median (IQR)]	[6.7 (1.8-15.9)]	[3.2 (1.2-9.1)]	[3.1 (0.6-6.3)]
BAL Macrophage % count	[Mean (SD)]	[79.6 (9.2)]	[61.0 (30.4)]	[73.4 (22.6)]
	[Median (IQR)]	[80.1 (74.3-87.3)]	[71.1 (45.1-85.0)]	[77.3 (63.6-89.1)]
BAL Neutrophil % count	[Mean (SD)]	[2.9 (7.1)]	[8.8 (15.1)]	[7.1 (15.8)]
	[Median (IQR)]	[1.0 (0.6-1.6)]	[2.8 (0.2-6.9)]	[2.6 (0.7-5.2)]
BAL Eosinophil % count	[Mean (SD)]	[1.9 (2.5)]	[2.9 (5.3)]	[3.2 (8.0)]
	[Median (IQR)]	[0.7 (0.1-2.9)]	[0.7 (0.1-1.4)]	[0.5 (0-2.0)

4.4. Molecular detection of microbial presence

qPCR revealed a wide variety of microbial species present in the lungs of the asthmatic cohort, n=73. 93% (68/73) of patients had detectable levels of bacteria using the total bacteria primer[27]. 73% (53/73) of patients had detectable levels of Firmicutes. *Pseudomonas aeruginosa* was detectable in 34% (25/73) of asthmatics. *Pseudomonas fluorescens* was detectable in 88% (64/73). *Escherichia* was detectable in 37% (27/73). *Bordetella* was detectable in 53% (38/73). *Prevotella* was detectable in 79% (58/73). *Veillonella* was detectable in 80% (59/73). *Mycoplasma pneumoniae* was detectable in 62% (45/73). *Chlamydophilia pneumoniae* was detectable in 70% (51/73). *Staphylococcus aureus* was detectable in 75% (55/73). *Neisseria bacilliformis* was detectable in 66% (48/73). *Moraxella catarrhalis* was detectable in 78% (57/73). *Neisseria meningitidis* was detectable in 67% (49/73). *Streptococcus pneumoniae* was detectable in 73% (53/73). *Haemophilus influenzae* was detectable in 67% (49/73). *Rothia* was detectable in 86% (63/73). *Micromonospora* was detectable in 85% (62/73) of BAL from the asthmatic cohort. See Figure 2 for a schematic of the microbiome analysis performed on the patient dataset. See Figure 10 for the qPCR cycle threshold (abundance) values for each primer investigated. n=73.

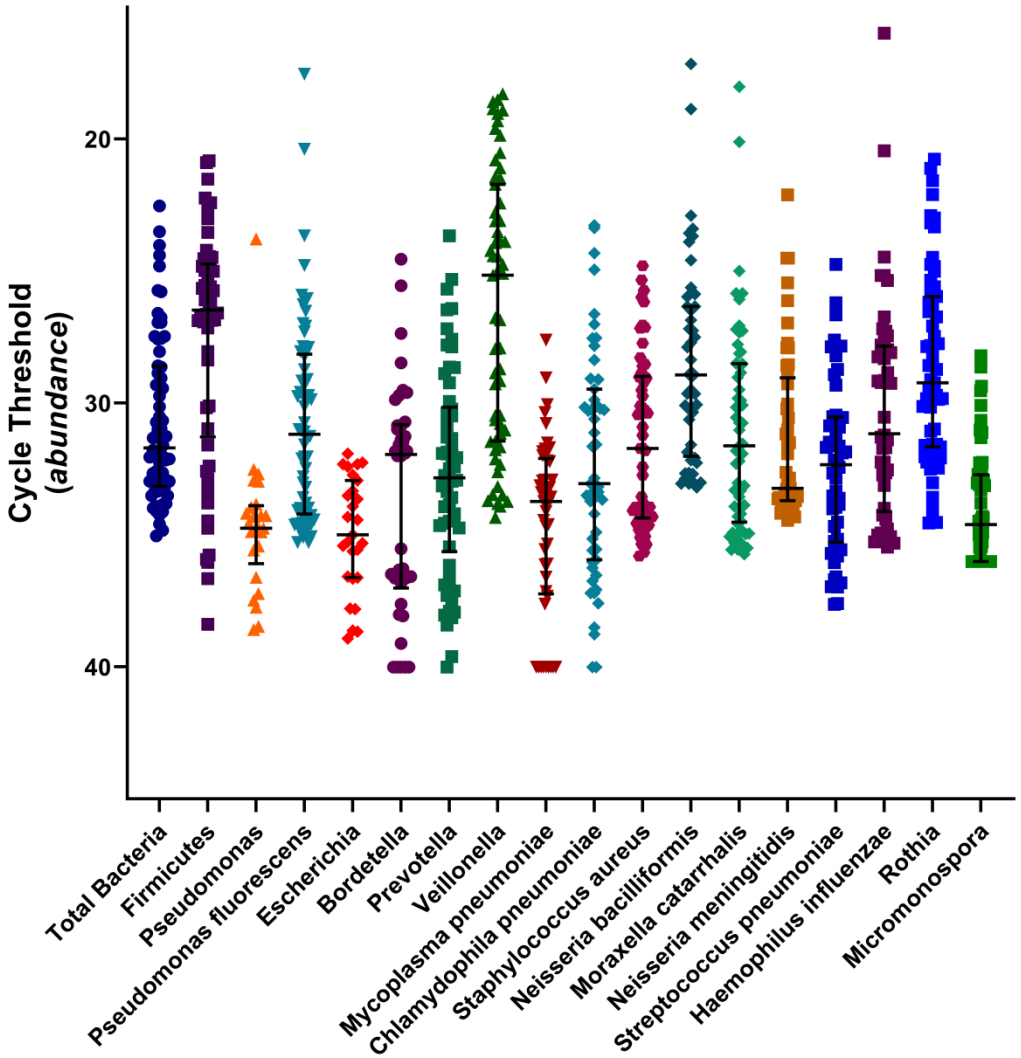


Figure 10. qPCR detection of bacteria species in the asthmatic patient BAL. qPCR was performed on the extracted BAL DNA with respect to a number of microbial species of interest. n=73.

4.5. BAL and plasma cytokines

Measurement of secreted human cytokines Interleukin – 1β (IL-1β), IL-4, IL-5, IL-6, IL-8, IL-10, IL-13, IL-17 and Tumour Necrosis Factor – α (TNF-α) in patient BAL at bronchoscopy and the secreted human cytokines Interleukin – 1β (IL-1β), IL-4, IL-5, IL-6, IL-8, IL-10, IL-13, IL-17, Tumour Necrosis Factor – α (TNF-α) and Interferon – γ (IFN-γ) in patient plasma at bronchoscopy took place using an electro-chemiluminescence Quick Plex SQ 120 imager from Meso Scale Discovery (Gaithersburg, MD, USA) where antibodies labelled with SULFO-TAG™ reagents emitted light upon electrochemical stimulation. See Figure 11 for the cytokine levels in the patient BAL and plasma. See Table 3 for the cytokine levels in the patient BAL and plasma.

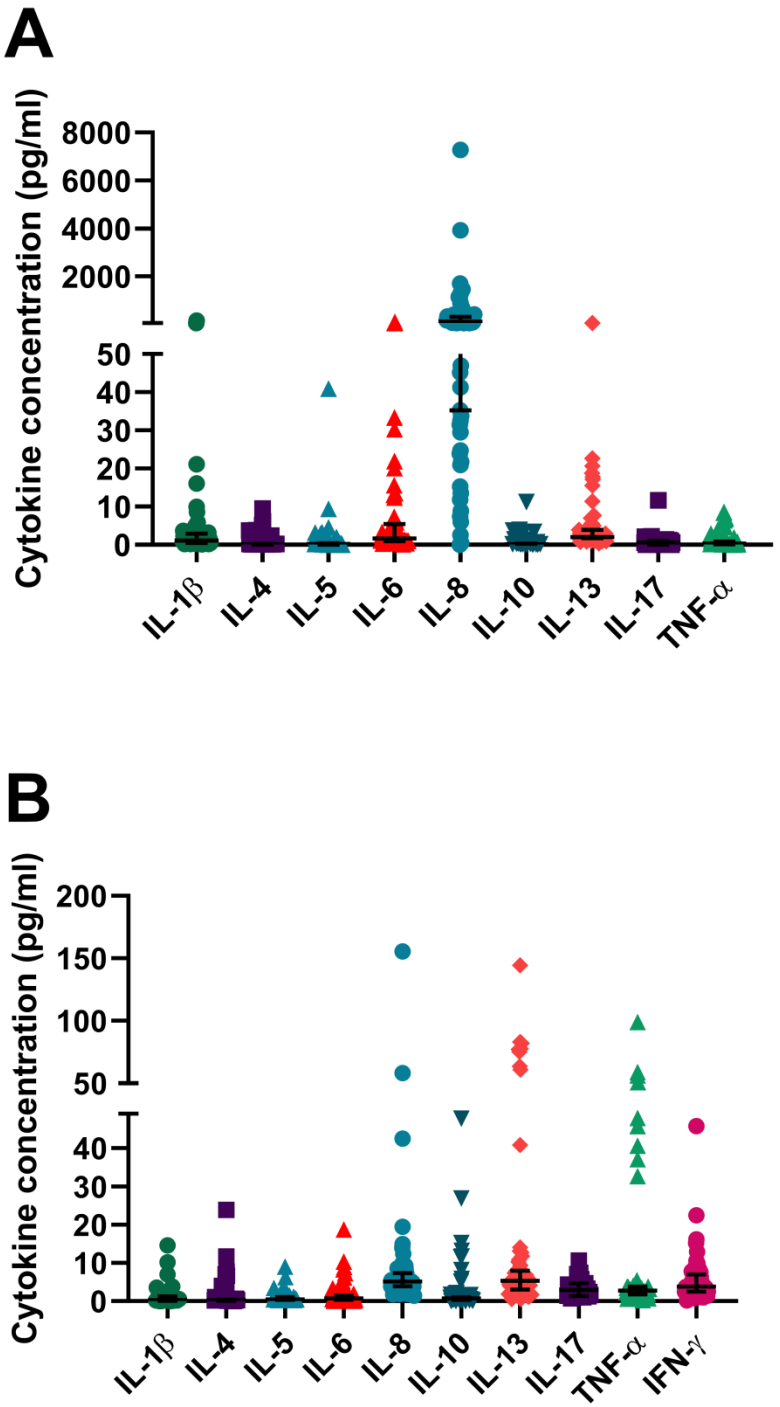


Figure 11. Cytokine levels in patient BAL and plasma. Measurement of secreted human cytokines interleukin- 1β (IL-1β), IL-4, IL-5, IL-6, IL-8, IL-10, IL-13, IL-17, tumour necrosis factor-α (TNF-α) and interferon-γ (IFN-γ) in patient BAL (A) and plasma (B). [Median (IQR)], n=73.

Table 3. Cytokine levels in patient BAL and plasma. Cytokine levels in patient BAL and plasma upon stratification of patients by asthma severity (GINA). n=73.

		Mild (GINA 1-2)	Moderate (GINA 3)	Severe (GINA 4-5)
BAL IL-1β (pg/ml)	[Mean (SD)]	[7.8 (29.6)]	[5.1 (16.2)]	[4.6 (9.9)]
	[Median (IQR)]	[0.7 (0.4-3.2)]	[0.9 (0.4-1.2)]	[1.6 (1.0-3.7)]
BAL IL-4 (pg/ml)	[Mean (SD)]	[0.5 (1.8)]	[0.1 (0.1)]	[1.2 (1.9)]
	[Median (IQR)]	[0.2 (0.1-0.2)]	[0.1 (0.1-0.2)]	[0.2 (0.1-2.5)]
BAL IL-5 (pg/ml)	[Mean (SD)]	[0.3 (0.4)]	[0.9 (2.4)]	[2.1 (7.3)]
	[Median (IQR)]	[0.2 (0.1-0.4)]	[0.2 (0.1-0.4)]	[0.3 (0.04-0.9)]
BAL IL-6 (pg/ml)	[Mean (SD)]	[2.4 (2.9)]	[5.8 (8.7)]	[10.4 (20.4)]
	[Median (IQR)]	[1.1 (0.8-3.1)]	[2.3 (1.0-5.1)]	[1.8 (1.1-12.2)]
BAL IL-8 (pg/ml)	[Mean (SD)]	[441.5 (849.0)]	[812.2 (1837.0)]	[226.0 (318.3)]
	[Median (IQR)]	[114.2 (24.0-306.0)]	[214.3 (86.1-777.0)	[94.1 (31.8-319.2)]
BAL IL-10 (pg/ml)	[Mean (SD)]	[0.6 (2.2)]	[0.2 (0.3)]	[1.0 (1.4)]
	[Median (IQR)]	[0.2 (0.1-0.2)]	[0.1 (0.1-0.3)]	[0.2 (0.1-1.3)]
BAL IL-13 (pg/ml)	[Mean (SD)]	[4.2 (10.3)]	[2.2 (1.0)]	[6.1 (6.9)]
	[Median (IQR)]	[2.0 (1.7-2.2)]	[1.9 (1.8-2.4)]	[2.2 (1.7-8.6)]
BAL IL-17 (pg/ml)	[Mean (SD)]	[0.7 (0.6)]	[0.8 (0.6)]	[0.8 (2.1)]
	[Median (IQR)]	[0.6 (0.1-1.1)]	[0.9 (0.1-1.3)]	[0.2 (0.02-0.8)]
BAL TNF-α (pg/ml)	[Mean (SD)]	[1.0 (2.3)]	[0.4 (0.5)]	[1.6 (2.3)]
	[Median (IQR)]	[0.2 (0.1-0.4)]	[0.3 (0.1-0.6)]	[0.4 (0.2-2.2)]
Plasma IL-1β (pg/ml)	[Mean (SD)]	[2.6 (5.9)]	[0.2 (1.2)]	[1.9 (2.8)]
	[Median (IQR)]	[0.2 (0.06-3.9)]	[0.2 (0.06-0.4)]	[0.7 (0.2-2.6)]
Plasma IL-4 (pg/ml)	[Mean (SD)]	[0.6 (1.5)]	[0.2 (0.1)]	[2.7 (5.2)]
	[Median (IQR)]	[0.3 (0.1-0.5)]	[0.2 (0.07-0.3)]	[0.4 (0.2-4.1)]
Plasma IL-5 (pg/ml)	[Mean (SD)]	[0.7 (0.8)]	[1.8 (1.9)]	[1.6 (2.6)]
	[Median (IQR)]	[0.5 (0.4-0.8)]	[1.3 (0.4-1.8)]	[0.6 (0.3-1.6)]
Plasma IL-6 (pg/ml)	[Mean (SD)]	[1.0 (1.7)]	[0.9 (0.8)]	[3.2 (4.1)]
	[Median (IQR)]	[0.6 (0.3-0.9)]	[0.6 (0.4-1.1)]	[1.2 (0.6-5.1)]
Plasma IL-8 (pg/ml)	[Mean (SD)]	[5.0 (2.3)]	[8.0 (14.0)]	[13.3 (28.4)]
	[Median (IQR)]	[4.8 (3.8-6.4)]	[3.4 (2.9-7.3)]	[5.9 (4.5-9.4)]
Plasma IL-10 (pg/ml)	[Mean (SD)]	[1.2 (2.9)]	[0.8 (1.2)]	[5.1 (10.0)]
	[Median (IQR)]	[0.7 (0.5-0.9)]	[0.6 (0.2-0.8)]	[0.8 (0.4-6.4)]
Plasma IL-13 (pg/ml)	[Mean (SD)]	[8.1 (16.2)]	[4.6 (4.1)]	[24.8 (35.8)]
	[Median (IQR)]	[5.4 (2.3-6.5)]	[3.2 (1.5-6.6)]	[6.5 (3.9-45.9)]
Plasma IL-17 (pg/ml)	[Mean (SD)]	[2.7 (1.7)]	[5.6 (3.3)]	[3.3 (2.4)]
	[Median (IQR)]	[2.1 (1.5-3.7)]	[3.9 (3.1-8.8)]	[2.9 (1.1-5.1)]
Plasma TNF-α (pg/ml)	[Mean (SD)]	[5.1 (11.1)]	[2.1 (1.0)]	[15.6 (24.1)]
	[Median (IQR)]	[3.0 (2.4-3.9)]	[2.2 (1.2-3.0)]	[3.0 (1.7-33.8)]
Plasma IFN-γ (pg/ml)	[Mean (SD)]	[4.7 (2.5)]	[5.5 (3.8)]	[6.6 (8.9)]
	[Median (IQR)]	[3.7 (3.2-6.7)]	[4.5 (2.9-7.2)]	[4.0 (2.1-7.2)]

4.6.qPCR correlations

Statistical analysis of the qPCR results in correlation to ACQ-7, inhaled corticosteroids (ICS), Forced Expiratory Volume (FEV-1), Fractional exhaled Nitric Oxide (FeNO), total IgE levels, Body Mass Index (BMI), Haemoglobin (Hb), White Cell Count (WBC), blood lymphocytes, blood eosinophils, blood neutrophils, Erythrocyte Sedimentation Rate (ESR), C-reactive protein (CRP), blood glucose levels, BAL glucose levels, immune microscopy counts, plasma cytokines and BAL cytokines. Statistical analyses were carried out as described in *3.13. Statistical analyses.*

Upon the examination of the patients' bronchoscopy BAL qPCR data a number of correlations were determined. The presence of qPCR total bacteria correlated with BAL IL-8 cytokine levels ($P<0.05$; $r_s=-0.2971$). The presence of Firmicutes in the BAL by qPCR correlated with plasma cytokine IL-6 levels ($P<0.05$; $r_s=-0.3236$), plasma TNF-α ($P<0.01$; $r_s=-0.3823$), BAL IL-4 ($P<0.05$; $r_s=-0.3446$) and BAL IL-5 ($P<0.05$; $r_s=-0.2955$). *Pseudomonas aeruginosa* presence by qPCR correlated with the White Cell Count (WBC) ($P<0.05$; $r_s=0.4645$) and blood neutrophil levels (10^9/L) ($P<0.05$; $r_s=0.4910$). *Pseudomonas fluorescens* presence correlated with the IL-5 cytokine levels in BAL ($P<0.05$; $r_s=-0.2601$). See Figure 12. n=73

Pseudomonas fluorescens presence correlated with BAL IL-13 cytokine levels ($P<0.05$; $r_s=0.2971$) and the immune cell percentage counts of neutrophils ($P<0.05$; $r_s=-0.2887$). *Escherichia* presence in the BAL by qPCR correlated with plasma IL-5 ($P<0.05$; $r_s=0.3994$), plasma IL-6 ($P<0.01$; $r_s=0.5238$), plasma IL-10 ($P<0.05$; $r_s=0.4450$), IL-17 BAL ($P<0.05$; $r_s=-0.4230$), and the immune cell percentage count of neutrophils ($P<0.05$; $r_s=-0.4278$). *Bordetella* correlated with the presence of IL-1β in the plasma ($P<0.05$; $r_s=-0.5963$). See Figure 13. n=73

Bordetella correlated with plasma IL-4 levels ($P<0.05$; $r_s=-0.3523$), plasma IL-8 levels ($P<0.05$; $r_s=0.3266$), plasma IL-10 levels ($P<0.05$; $r_s=-0.3507$), plasma TNF-α levels ($P<0.0005$; $r_s=-0.5560$), BAL IL-4 levels ($P<0.05$; $r_s=-0.4134$), BAL IL-17 levels ($P<0.001$; $r_s=-0.5774$) and the immune cell percentage count of monocytes ($P<0.005$; $r_s=-0.4893$). *Prevotella* presence by qPCR correlated with plasma IL-10 levels ($P<0.05$; $r_s=-0.2709$). See Figure 14. n=73

Prevotella also correlated with plasma TNF-α levels (P<0.05; r_s=-0.3256) and BAL IL-17 levels (P<0.05; r_s=-0.2709). *Veillonella* correlated with plasma IL-8 levels (P<0.05; r_s=-0.2639). *Chlamydophilia pneumoniae* presence by qPCR correlated with BAL IL-8 levels (P<0.05; r_s=-0.2826) and BAL IL-13 levels (P<0.05; r_s=-0.3380). *Staphylococcus aureus* presence correlated with plasma IL-17 levels (P<0.05; r_s=0.3994) and BAL IL-1β (P<0.01; r_s=-0.3777). *Neisseria bacilliformis* correlated with BAL IL-1β levels (P<0.05; r_s=-0.3373). See Figure 15. n=73

Moraxella catarrhalis presence by qPCR correlated with BAL IL-13 levels (P<0.05; r_s=0.3141) and the immune cell percentage count of neutrophils (P<0.05; r_s=-0.2639). *Neisseria meningitidis* presence correlated with plasma IL-8 levels (P<0.05; r_s=-0.3086). *Streptococcus pneumoniae* presence by qPCR correlated with the immune cell percentage count of macrophages (P<0.05; r_s=0.3424). *Rothia* correlated with FEV-1 (percent predicted) (P<0.05; r_s=0.2697) and plasma IL-6 (P<0.05; r_s=-0.4592). *Micromonospora* correlated with FeNO (ppb) (P<0.05; r_s=0.3004) and plasma IL-1β levels (P<0.05; r_s=-0.4703). See Figure 16. n=73

Micromonospora also correlated with plasma IL-6 (P<0.05; r_s=-0.3018) and BAL IL-1β (P<0.05; r_s=-0.2737). See Figure 17. n=73

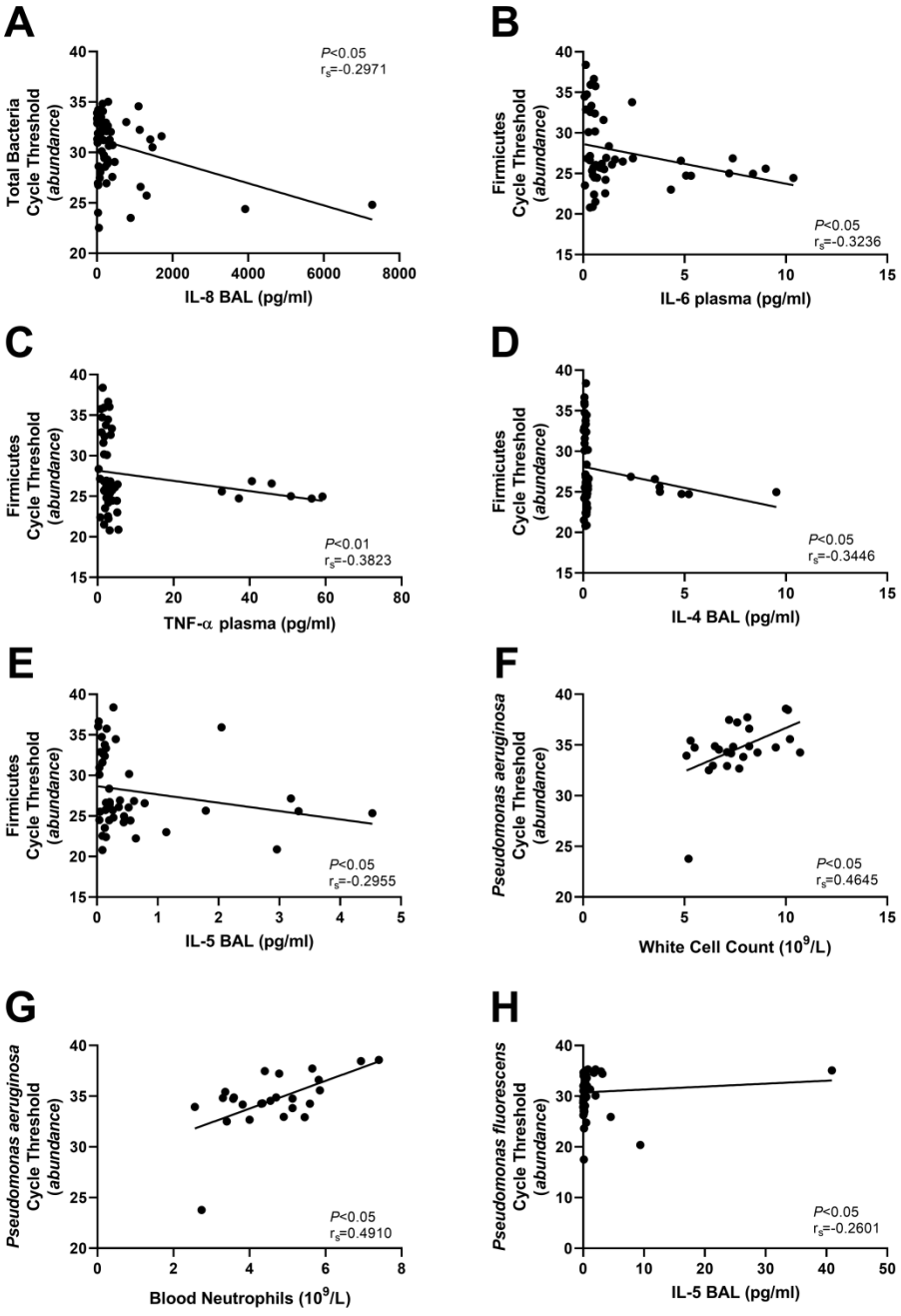


Figure 12. BAL qPCR correlations. Total bacteria correlated with BAL IL-8 cytokine levels (P<0.05; r_s=-0.2971) (A). The presence of Firmicutes in the BAL by qPCR correlated with plasma cytokine IL-6 levels (P<0.05; r_s=-0.3236) (B), plasma TNF-α (P<0.01; r_s=-0.3823) (C), BAL IL-4 (P<0.05; r_s=-0.3446) (D) and BAL IL-5 (P<0.05; r_s=-0.2955) (E). *Pseudomonas aeruginosa* presence by qPCR correlated with the White Cell Count (WBC) (P<0.05; r_s=0.4645) (F) and blood neutrophil levels (10^9/L) (P<0.05; r_s=0.4910) (G). *Pseudomonas fluorescens* presence correlated with the IL-5 cytokine levels in BAL (P<0.05; r_s=-0.2601) (H).

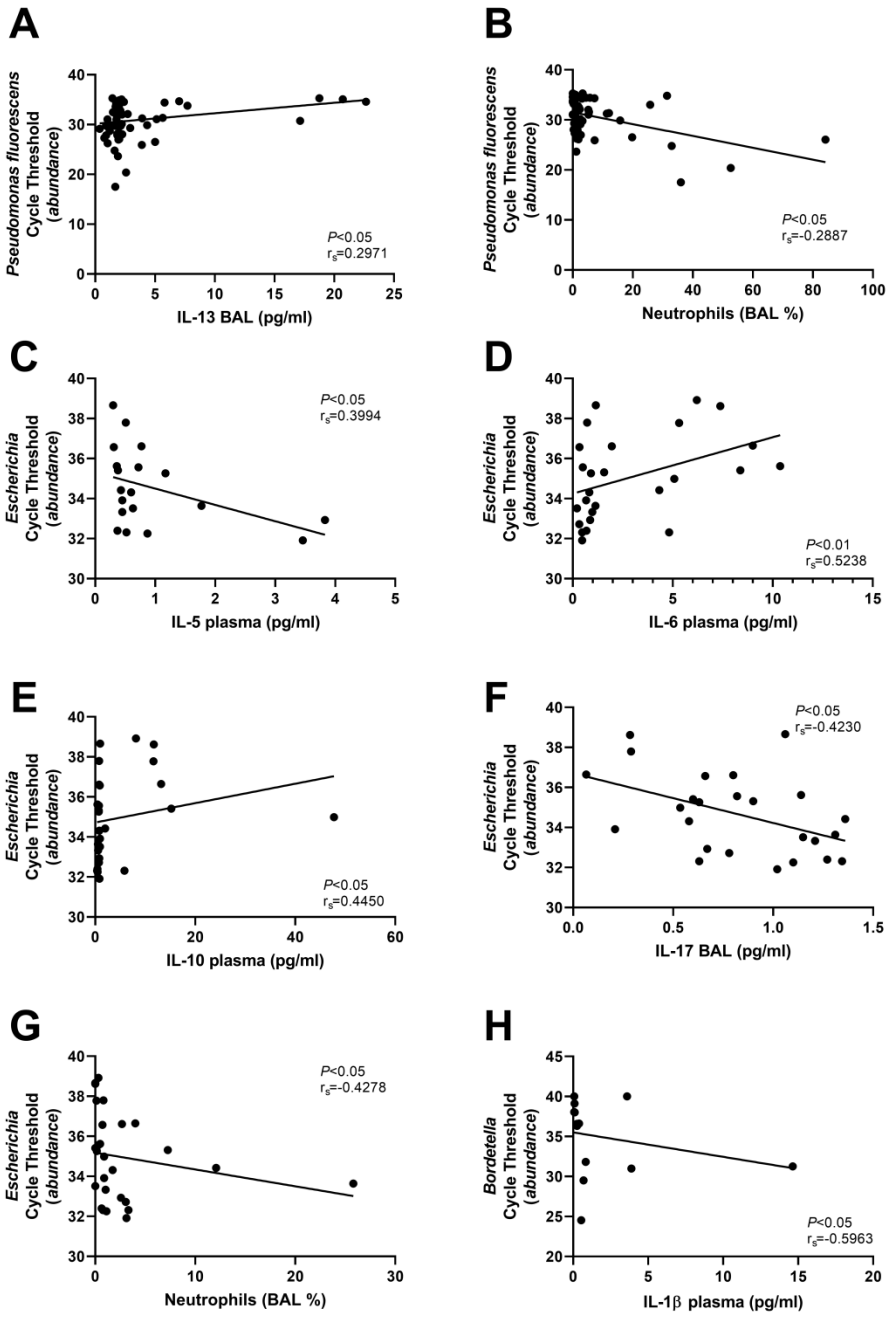


Figure 13. BAL qPCR correlations. *Pseudomonas fluorescens* presence correlated with BAL IL-13 cytokine levels ($P<0.05$; $r_s=0.2971$) (A) and the immune cell percentage counts of neutrophils ($P<0.05$; $r_s=-0.2887$) (B). *Escherichia* presence in the BAL by qPCR correlated with plasma IL-5 ($P<0.05$; $r_s=0.3994$) (C), plasma IL-6 ($P<0.01$; $r_s=0.5238$) (D), plasma IL-10 ($P<0.05$; $r_s=0.4450$) (E), IL-17 BAL ($P<0.05$; $r_s=-0.4230$) (F), and the immune cell percentage count of neutrophils ($P<0.05$; $r_s=-0.4278$) (G). *Bordetella* correlated with the presence of IL-1β in the plasma ($P<0.05$; $r_s=-0.5963$) (H). n=73

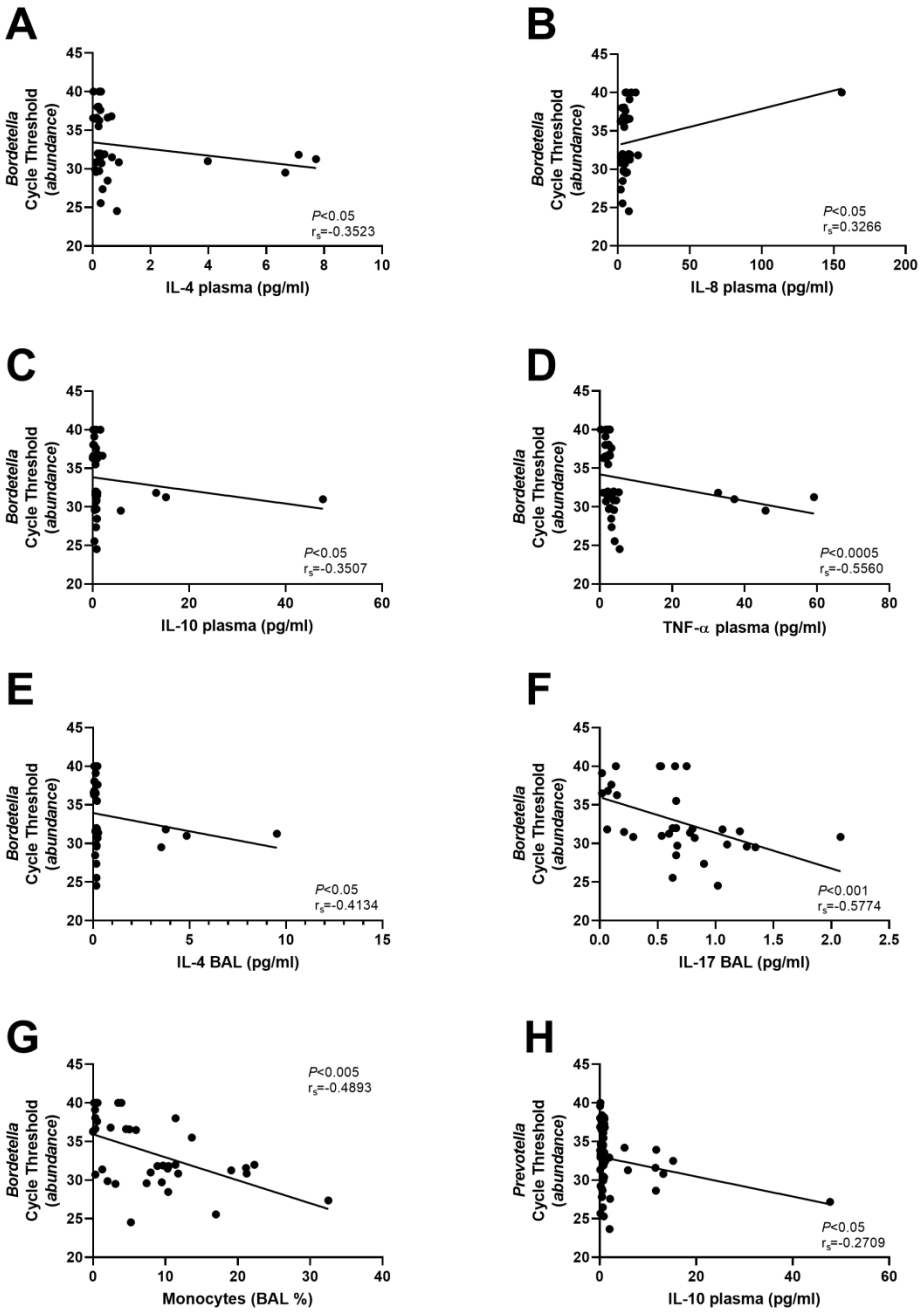


Figure 14. BAL qPCR correlations. *Bordetella* correlated with plasma IL-4 levels ($P<0.05$; $r_s=-0.3523$), plasma IL-8 levels ($P<0.05$; $r_s=0.3266$), plasma IL-10 levels ($P<0.05$; $r_s=-0.3507$), plasma TNF-α levels ($P<0.0005$; $r_s=-0.5560$), BAL IL-4 levels ($P<0.05$; $r_s=-0.4134$), BAL IL-17 levels ($P<0.001$; $r_s=-0.5774$) and the immune cell percentage count of monocytes ($P<0.005$; $r_s=-0.4893$). *Prevotella* presence by qPCR correlated with plasma IL-10 levels ($P<0.05$; $r_s=-0.2709$). n=73

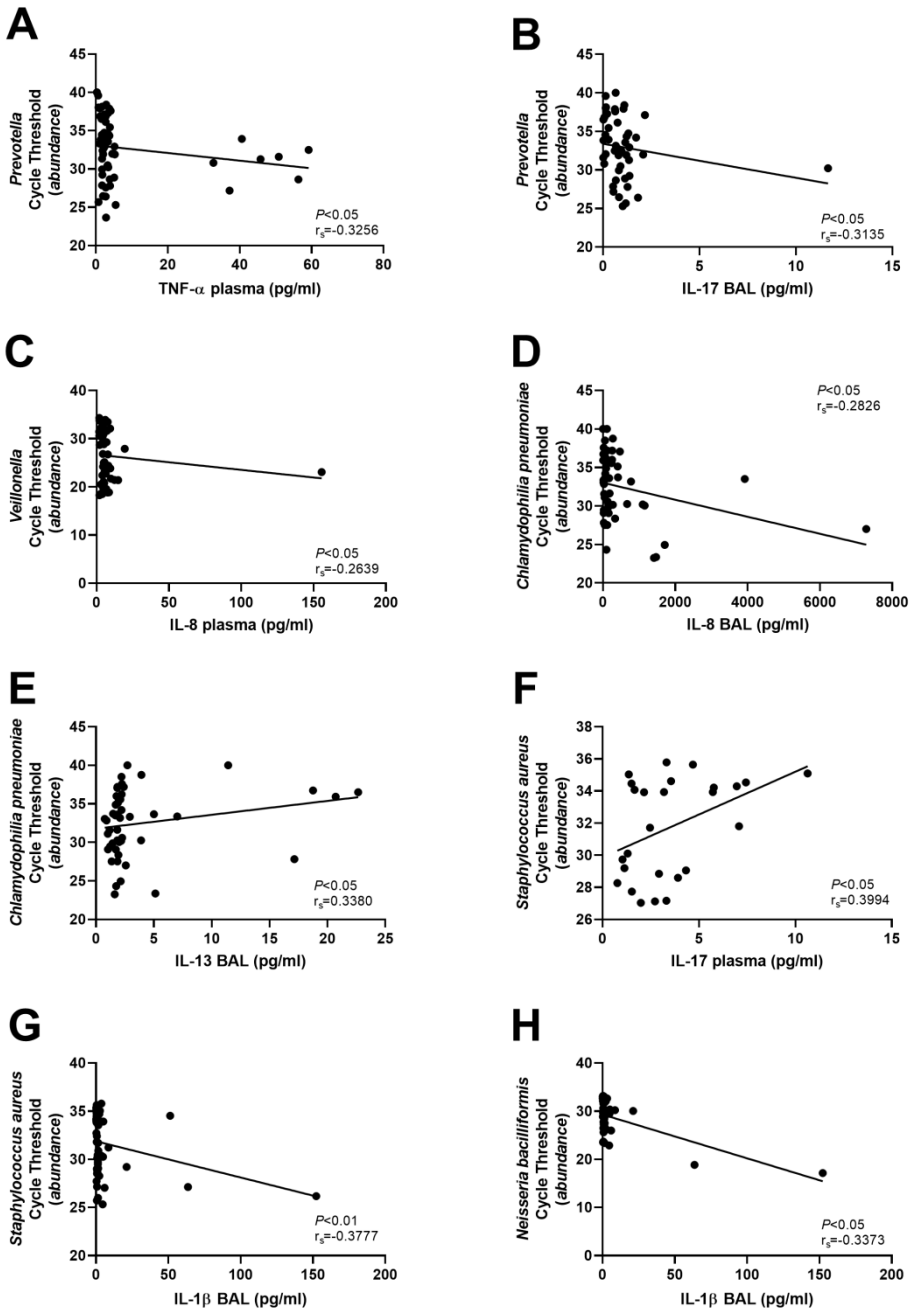


Figure 15. BAL qPCR correlations. *Prevotella* correlated with plasma TNF-α levels (P<0.05; r_s=-0.3256) (A) and BAL IL-17 levels (P<0.05; r_s=-0.2709) (B). *Veillonella* correlated with plasma IL-8 levels (P<0.05; r_s=-0.2639) (C). *Chlamydophilia pneumoniae* presence by qPCR correlated with BAL IL-8 levels (P<0.05; r_s=-0.2826) (D) and BAL IL-13 levels (P<0.05; r_s=-0.3380) (E). *Staphylococcus aureus* presence correlated with plasma IL-17 levels (P<0.05; r_s=0.3994) (F) and BAL IL-1β (P<0.01; r_s=-0.3777) (G). *Neisseria bacilliformis* correlated with BAL IL-1β levels (P<0.05; r_s=-0.3373) (H). n=73

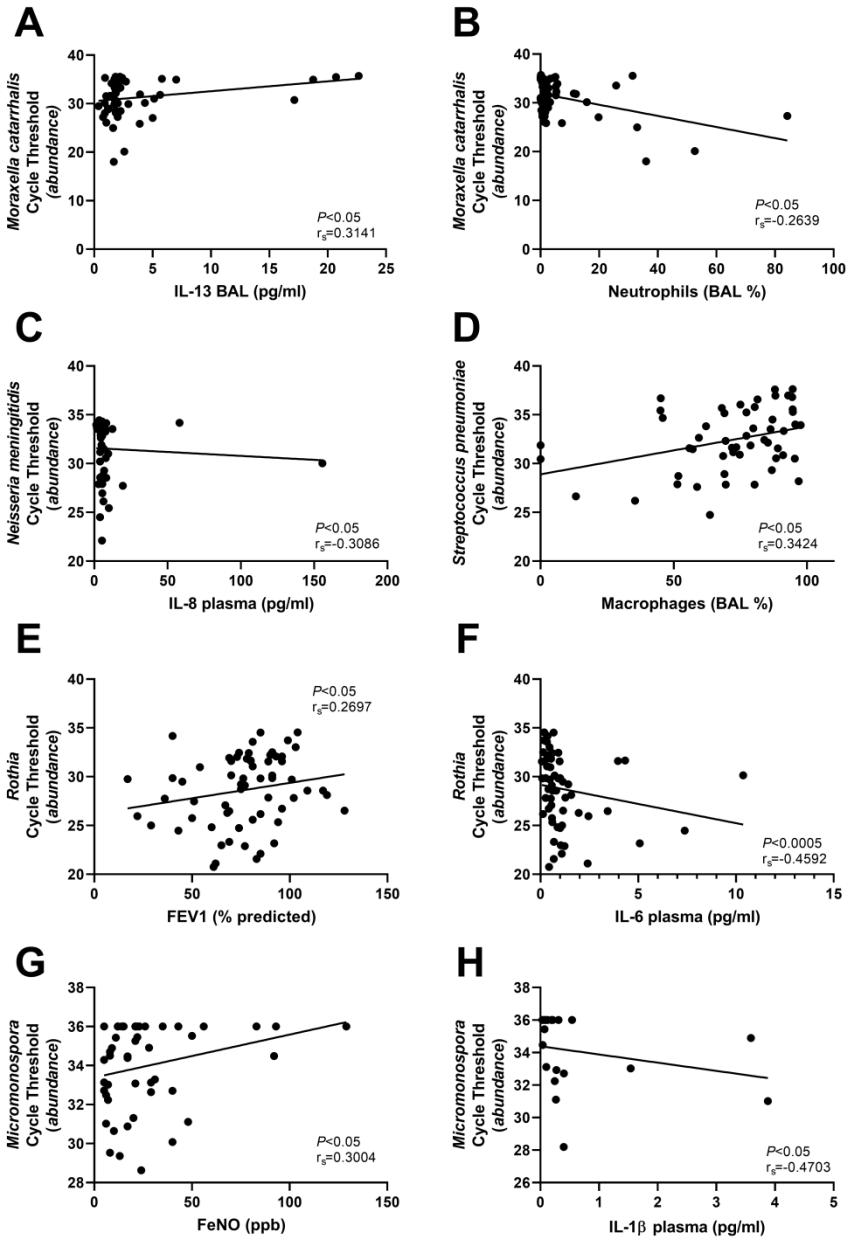


Figure 16. BAL qPCR correlations. *Moraxella catarrhalis* presence by qPCR correlated with BAL IL-13 levels ($P<0.05$; $r_s=0.3141$) (A) and the immune cell percentage count of neutrophils ($P<0.05$; $r_s=-0.2639$) (B). *Neisseria meningitidis* presence correlated with plasma IL-8 levels ($P<0.05$; $r_s=-0.3086$) (C). *Streptococcus pneumoniae* presence by qPCR correlated with the immune cell percentage count of macrophages ($P<0.05$; $r_s=0.3424$) (D). *Rothia* correlated with FEV-1 (percent predicted) ($P<0.05$; $r_s=0.2697$) (E) and plasma IL-6 ($P<0.05$; $r_s=-0.4592$) (F). *Micromonospora* correlated with FeNO (ppb) ($P<0.05$; $r_s=0.3004$) (G) and plasma IL-1β levels ($P<0.05$; $r_s=-0.4703$) (H). n=73

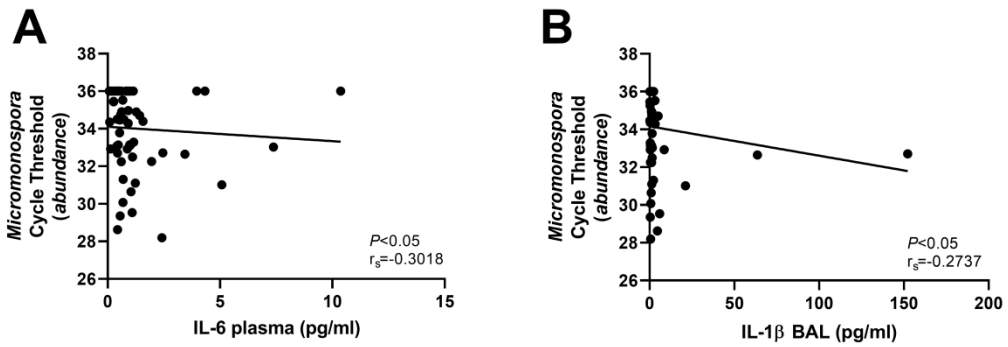


Figure 17. BAL qPCR correlations. *Micromonospora* correlated with plasma IL-6 (*P*<0.05; r_s=-0.3018) (A) and BAL IL-1β (*P*<0.05; r_s=-0.2737) (B). n=73

4.7. Next Generation Sequencing

The One Codex database identifies microbial and host reads and allows for filtering of the data, removal of host reads and known kit contaminants, and easy download for use on third party software such as MS Excel and GraphPad Prism. See Figure 18 below for an example of the interface where matched reads, and corresponding number, abundances and % are calculated. As is evident and expected due to the sample nature there is a high level of host reads which are filtered out.

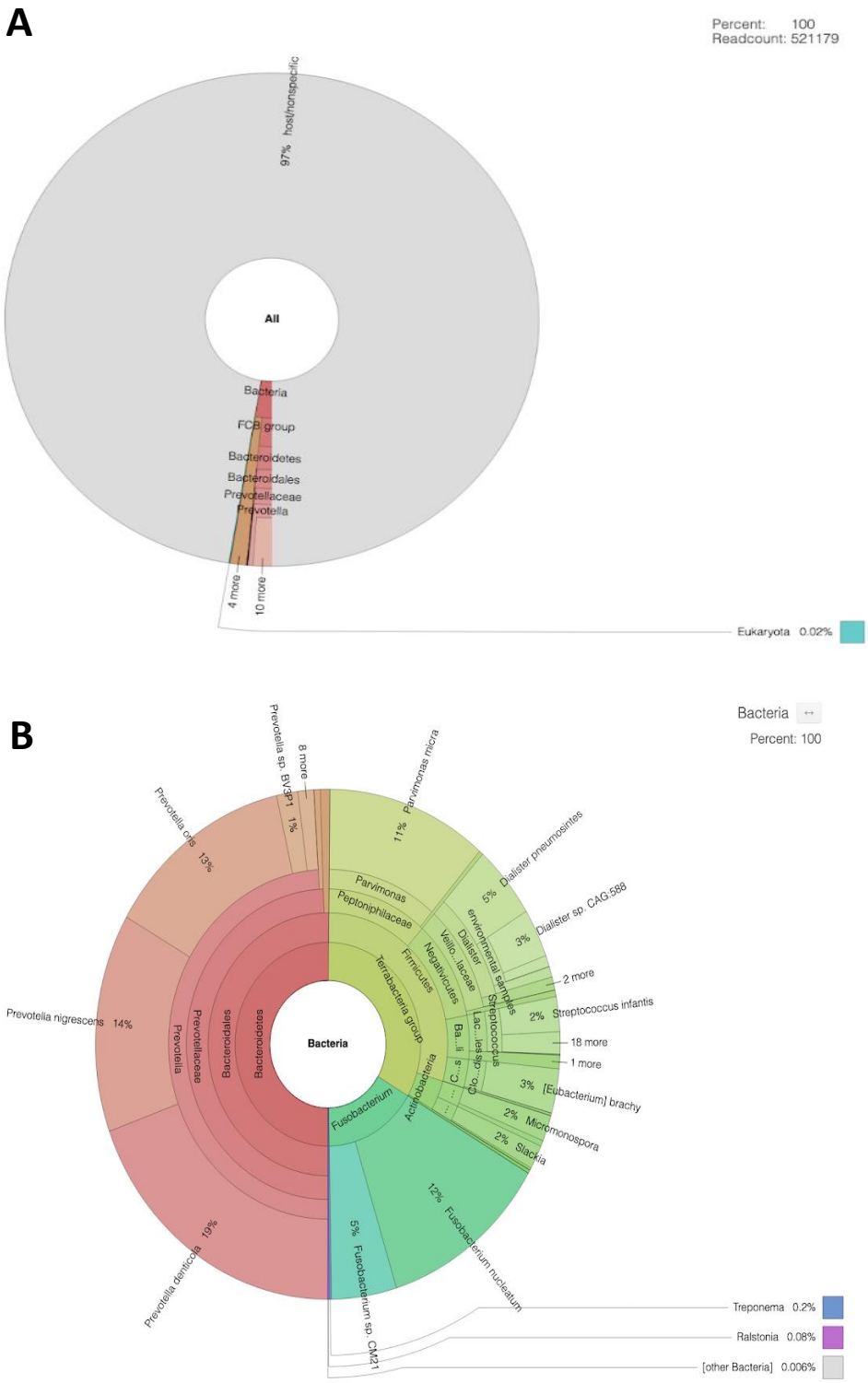
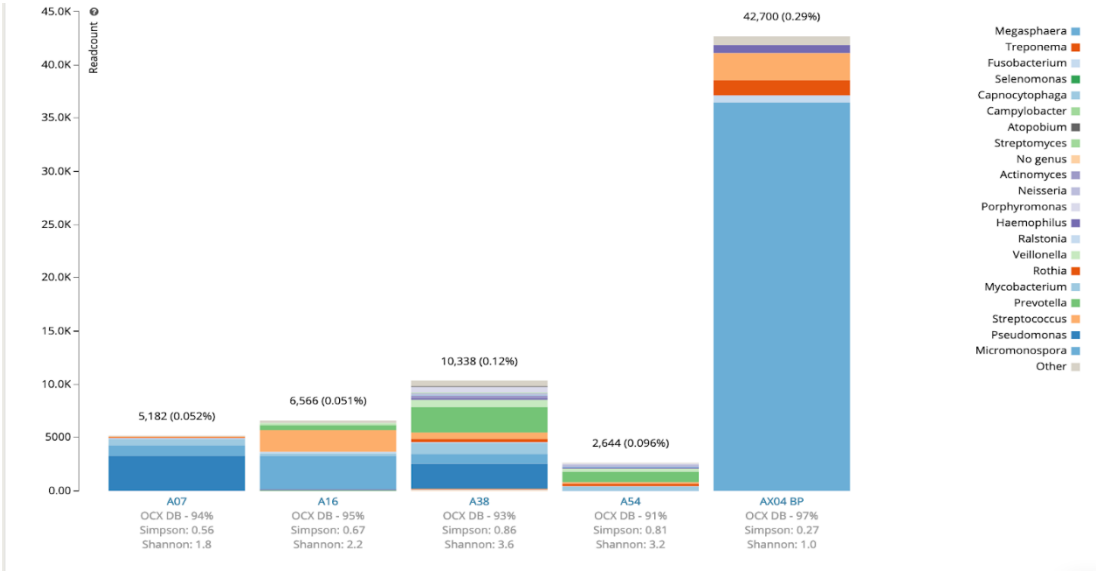


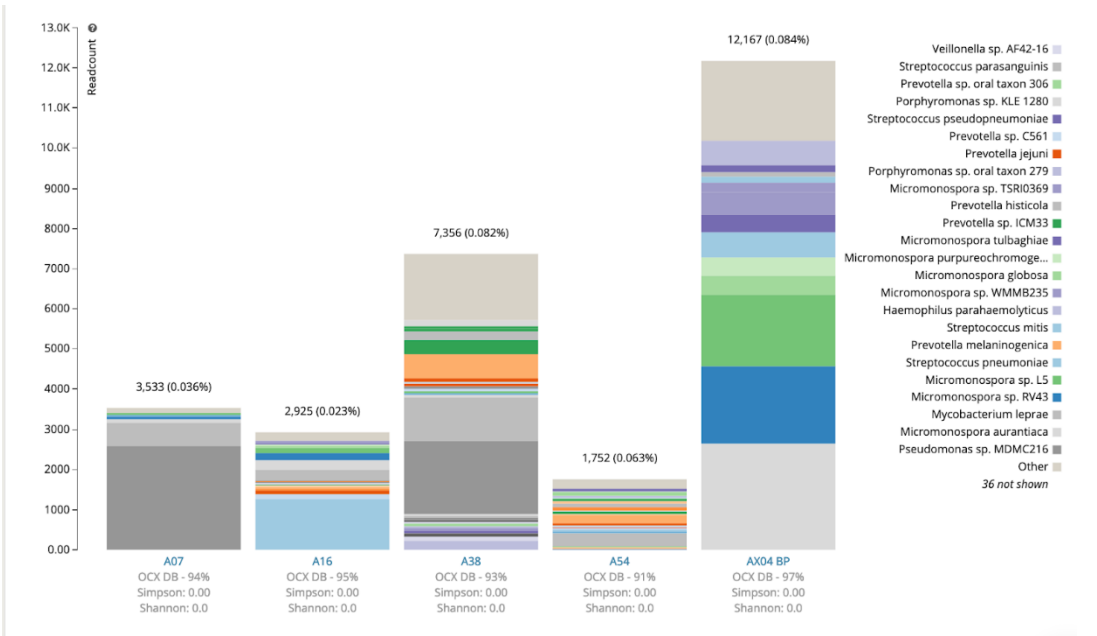
Figure 18. Next Generation Sequencing analyses. Examples of the OneCodex interface for shotgun sequence analysis of one sample allowing identification of the dominant microbial species (a) high host reads relative to microbial reads and (b) percentage microbial reads present in the samples.

The database allows for analyses at the associated microbial samples at read level and counts reads with children (reads associated with phylum and subsequently class, order, family, genus and species) and then calculates the relative abundance of the microbial species and therefore the diversity. Figure 19 demonstrates the interface for Bacterial reads by count, normalisation and relative abundance. It is interesting to note that several of the samples have quite varied biomass (reads) prior to normalisation and at the genus level there are several dominant genera including *Micromonospora* which has hitherto been unreported in lung washes or BALs.

A



B



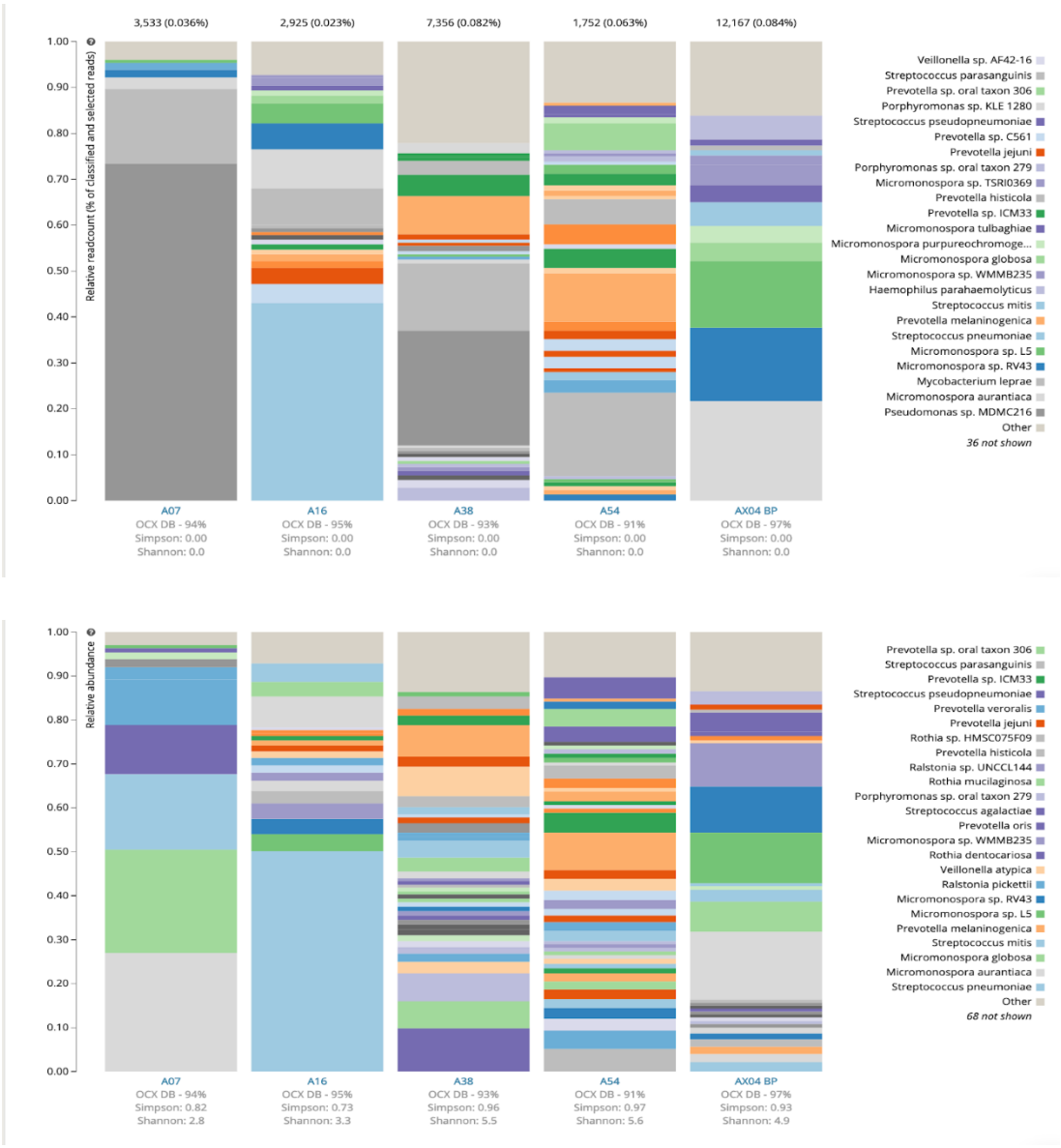


Figure 19. Next Generation Sequencing analyses. The One Codex interface allowing visual comparison of several samples on bacterial read count and taxonomic levels such as (a) genera, (b) species with (c) read normalisation and (d) relative abundance. (n=5)

It is however important to note that relative abundance cannot be calculated for some samples where the databases may be weaker/less populated, such as with fungal genomes. As is evident in figure 20 below while there are several fungal reads associated with the samples as the taxonomic selection is more refined, reads are not assigned and at the species level there are very few detectable species.

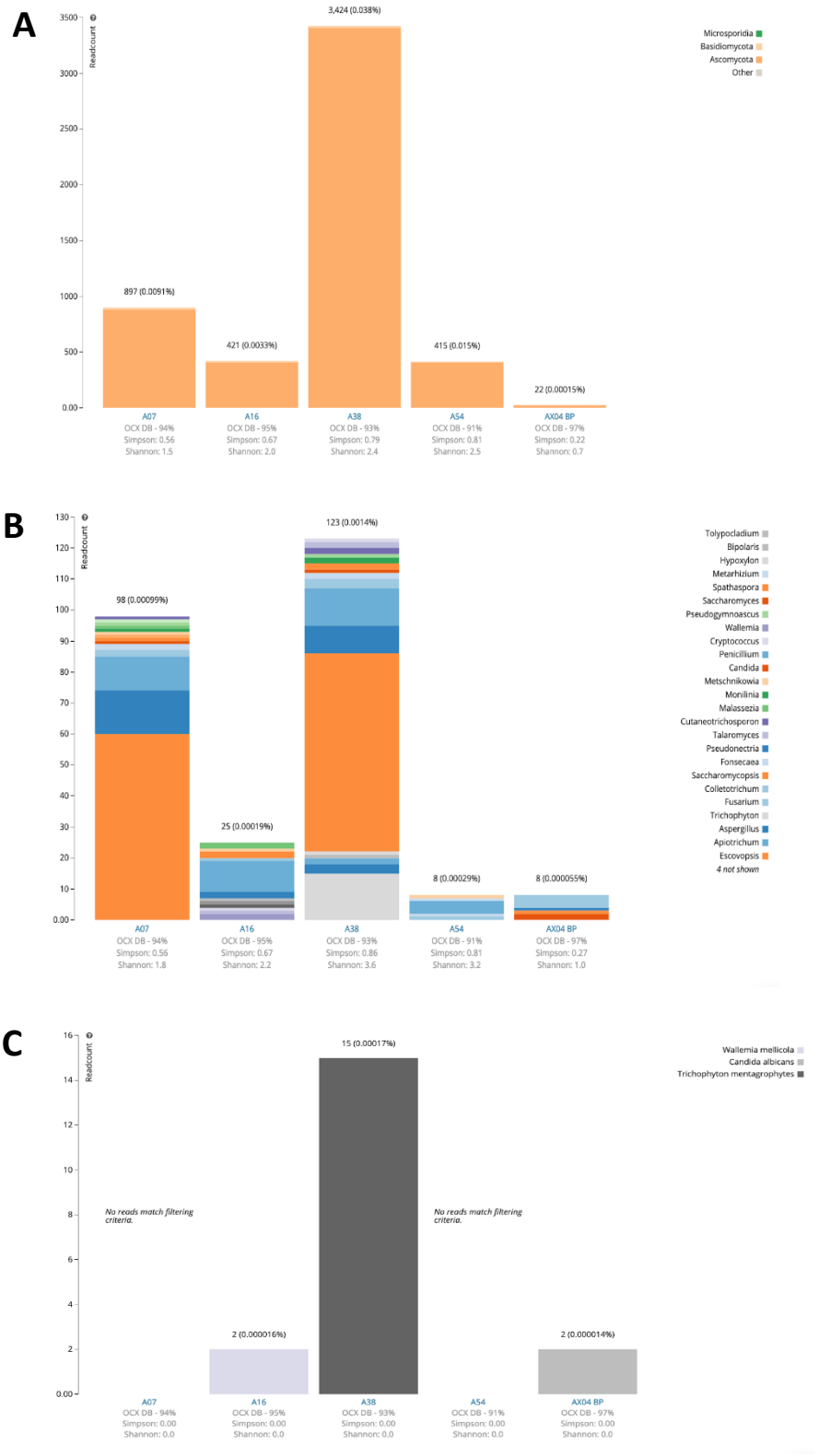


Figure 20. Next Generation Sequencing analyses – fungal genomes. OneCodex interface allowing visual comparison of several samples on fungal read count and taxonomic levels such as (a) phylum, (b) genus and (c) species. (n=5)

OneCodex also have a specific viral database which allows for detection of host and microbial viruses (phage); however this is quite limited for several of the phage genomes, see figure 21, but does detect several phage associated with dominant microbial strains.

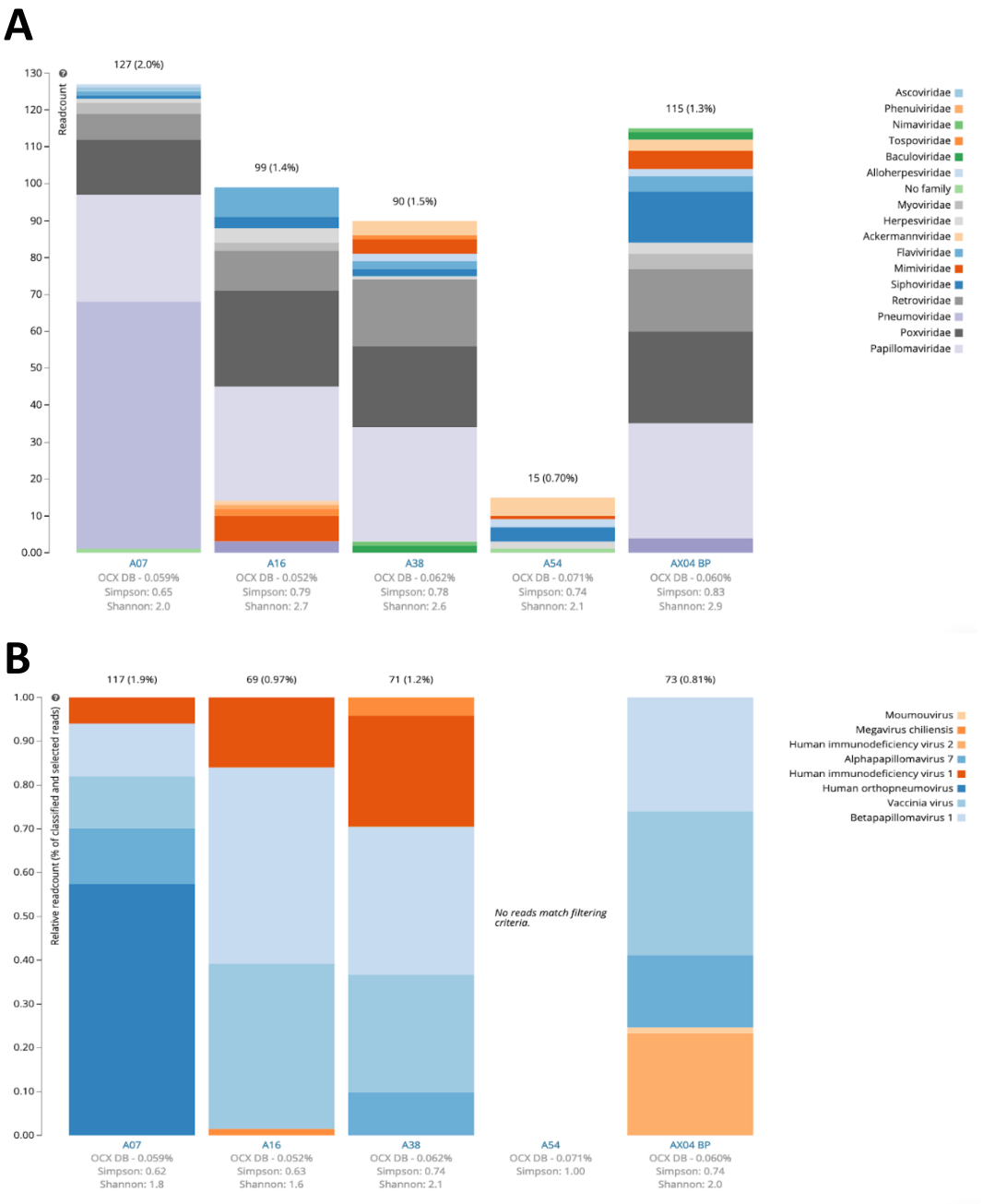


Figure 21. Next Generation Sequencing analyses –viral genomes. OneCodex interface allowing visual comparison of several samples on viral read counts at the family (a) and species (b) level. n=5.

Analysis of the entire 70 shotgun data samples shows that the majority of non-host reads detected in the lung BALs are from the bacterial kingdom, as was also evident by the qPCR data, see previous figure 10 and figure 22 below. The main focus of the subsequent analysis was on the bacterial signals which also allowed to measure relative abundance of the species present, due to the sequencing and database depth. There is also evidence of fungal (including dikarya), viral but also other eukaryota reads present, see figure 22 below.

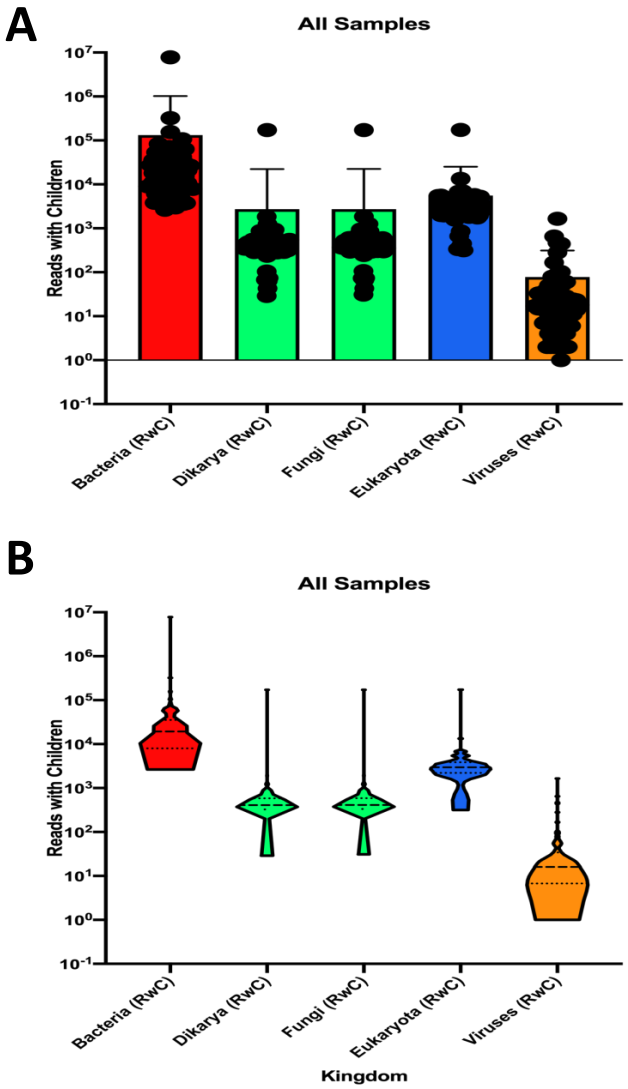


Figure 22. Next Generation Sequencing analyses – relative abundance. Analysis of the Kingdom level of distribution of reads with children matched to the One Codex database (a) bar plot (b) violin plot level. n=70

The relative abundances of the top taxa with the greatest mean abundance across these samples at the species level was determined. All abundances are calculated from the filtered results of the One Codex Database classification. The most abundant strains were determined beginning with a filter from the top 50 to the top species, see figures 23 and 24 below.

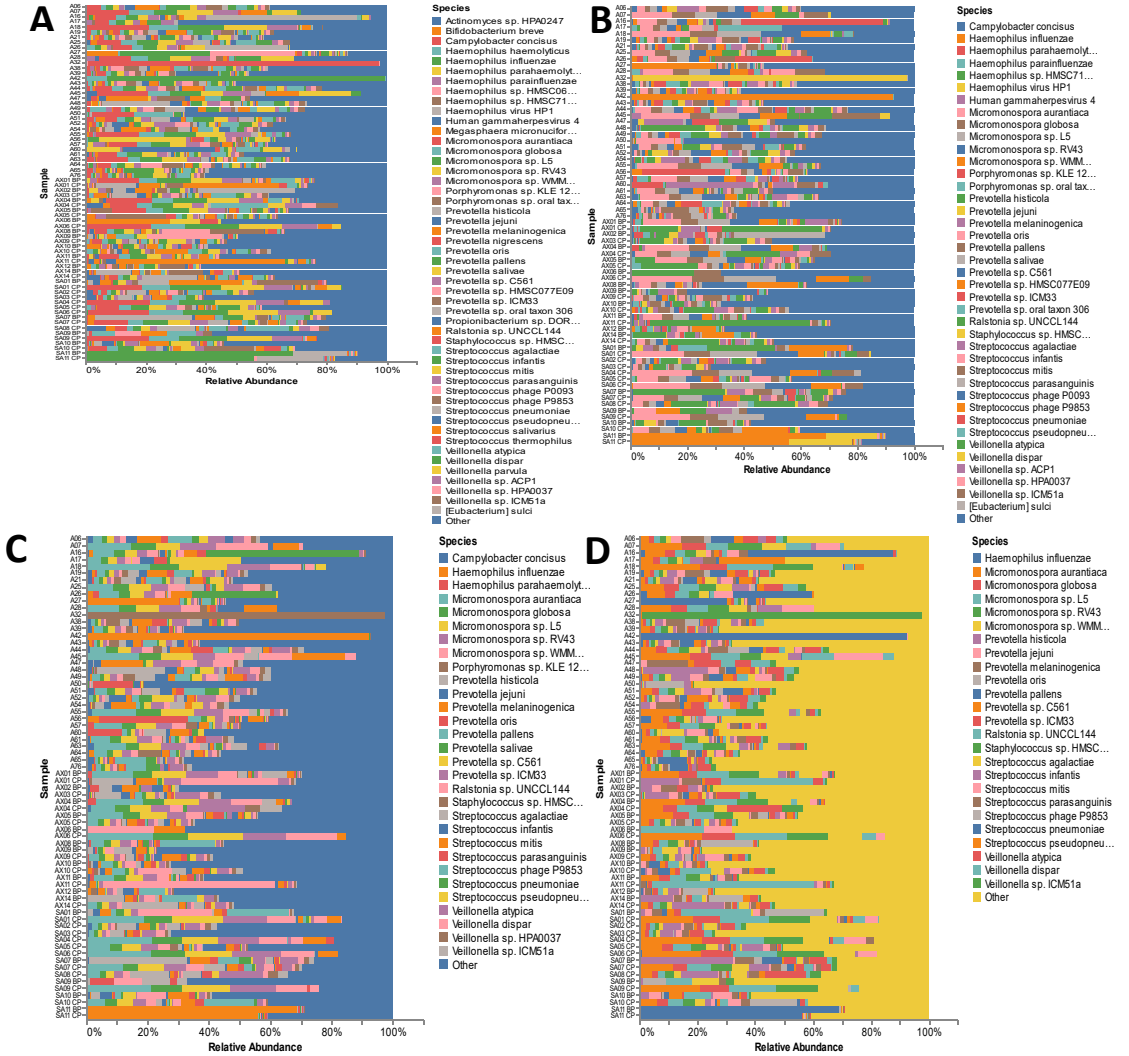


Figure 23. Next Generation Sequencing –relative abundance charts. Relative abundance chart for all samples at the species taxonomic level. Samples are sorted alphabetically from top to bottom. As part of the post-hoc filtering process, abundances are proportionalized such that the above plots are adjusted for variable sequencing depth. (a) top 50, (b) top 40, (c) top 30 and (d) top 25 species. n=70.

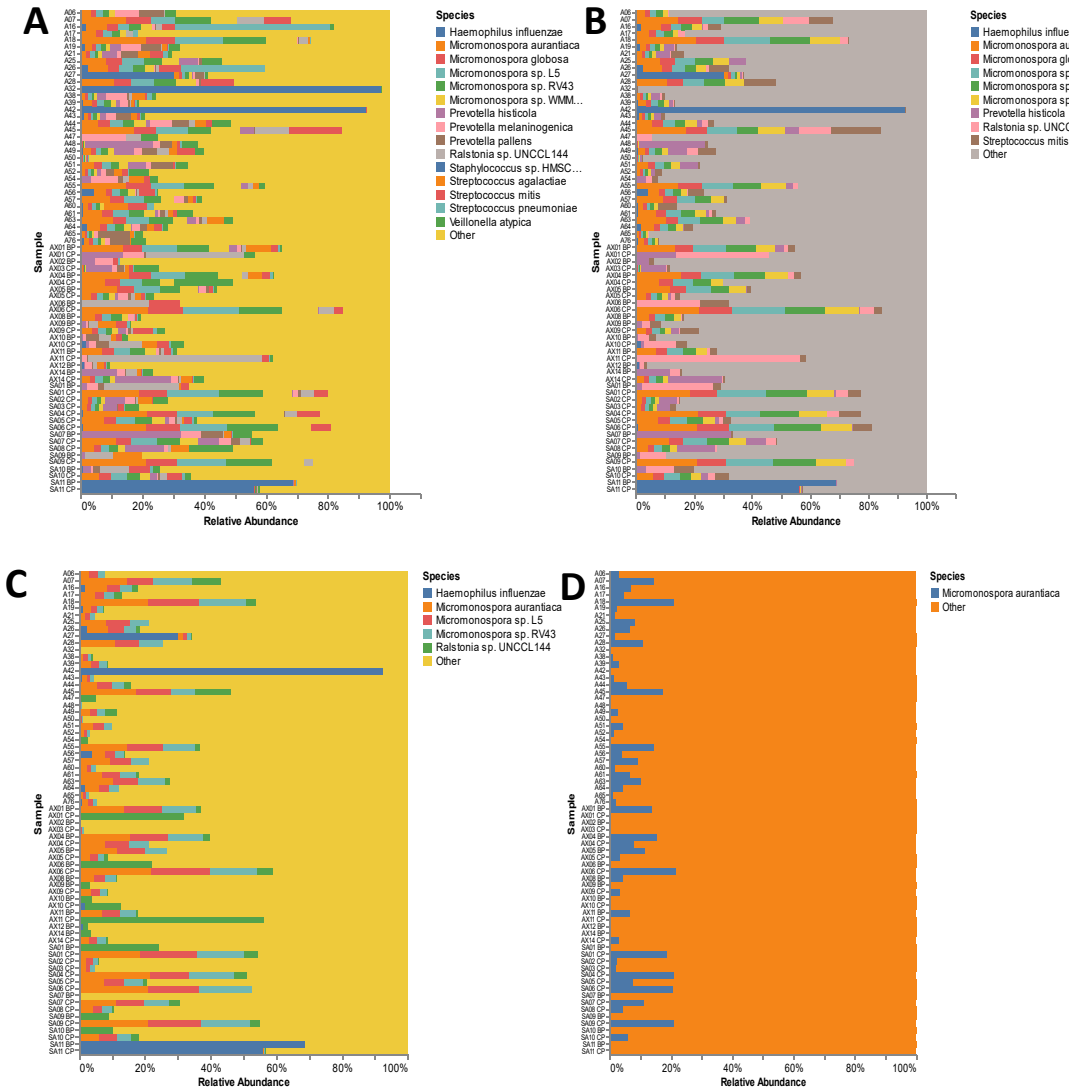


Figure 24. Whole Genome Sequencing analyses – relative abundance of samples at the taxonomic level. Relative abundance chart for all samples at the species taxonomic level. Samples are sorted alphabetically from top to bottom. As part of the post-hoc filtering process, abundances are proportionalized such that the above plots are adjusted for variable sequencing depth. (a) top 15 species, (b) top 10, (c) top 5 and (d) the top species. n=70.

The gram-positive spore forming aerobe actinobacteria *Micromonospora aurantica* was the most abundant species present. Subsequent analysis focussed on the top 10-20 abundant microbial species. *Micromonospora aurantica* is the dominant microbe present in 51/70 of the samples, followed by *Veillonella atypica*, *M. globosa* and *Streptococcus mitis*, see table 4 for further details. Many of the top 20 species detected were part of similar genera and some phage specifically targeting the species were evident see figure 25 and 26. Phage specific for *Haemophilus influenzae*, several *Streptococcus* species and human viruses such as human gammaherpesvirus 4 (Epstein Barr Virus) were also detectable at high levels in the BAL, see figure 25 and 26 below.

Table 4. Top 20 relative abundance species present in the asthmatic patient samples. n=70

Species	*Micromonospora aurantiaca*	*Micromonospora globosa*	*Ralstonia pickettii*	*Prevotella histicola*	*Haemophilus influenzae*
Number of values (70)	51	43	30	38	13
Minimum	0.0008419	0.0003859	0.004	0.001197	0.005269
Median	0.06653	0.04959	0.028	0.02945	0.02593
Maximum	0.4954	0.4027	0.472	0.3134	0.9249
Mean	0.1087	0.09012	0.06557	0.0539	0.2045
Std. Deviation	0.1179	0.09767	0.1019	0.06545	0.3151
Std. Error of Mean	0.01651	0.01489	0.01861	0.01062	0.08738
Species	Human gammaherpesvirus 4 (EBV)	*Micromonospora sp. L5*	*Micromonospora sp. RV43*	*Micromonospora sp. WMMB235*	*Porphyromonas sp. KLE 1280*
Number of values (70)	8	26	22	22	10
Minimum	0.007573	0.0006116	0.0004913	0.000357	0.0001
Median	0.01214	0.0312	0.03549	0.03328	0.0285
Maximum	0.3049	0.1713	0.1418	0.09998	0.072
Mean	0.05193	0.04749	0.04992	0.03845	0.03001
Std. Deviation	0.1028	0.04398	0.04205	0.02937	0.01918
Std. Error of Mean	0.03635	0.008626	0.008964	0.006262	0.006064
Species	*Porphyromonas sp. oral taxon 279*	*Prevotella melaninogenica*	*Ralstonia sp. UNCCL144*	*Rothia mucilaginosa*	*Streptococcus infantis*
Number of values (70)	15	42	13	17	25
Minimum	0.0002	0.0002754	0.01415	0.011	0.007161
Median	0.029	0.02483	0.02568	0.034	0.0221
Maximum	0.047	0.1422	0.2447	0.136	0.09449
Mean	0.02495	0.03548	0.04887	0.04682	0.02715
Std. Deviation	0.01266	0.029	0.06225	0.03174	0.02114
Std. Error of Mean	0.00327	0.004475	0.01727	0.007698	0.004228
Species	*Streptococcus mitis*	*Streptococcus parasanguinis*	*Streptococcus pseudopneumoniae*	*Streptococcus thermophilus*	*Veillonella atypica*
Number of values (70)	46	33	19	17	49
Minimum	0.0002057	0.0003633	0.0001	0.011	0.0002937
Median	0.03034	0.02271	0.019	0.029	0.03651
Maximum	0.1319	0.0487	0.229	0.071	0.2977
Mean	0.04002	0.02344	0.03053	0.02941	0.05085
Std. Deviation	0.03012	0.01157	0.04907	0.0149	0.05326
Std. Error of Mean	0.004441	0.002014	0.01126	0.003615	0.007608

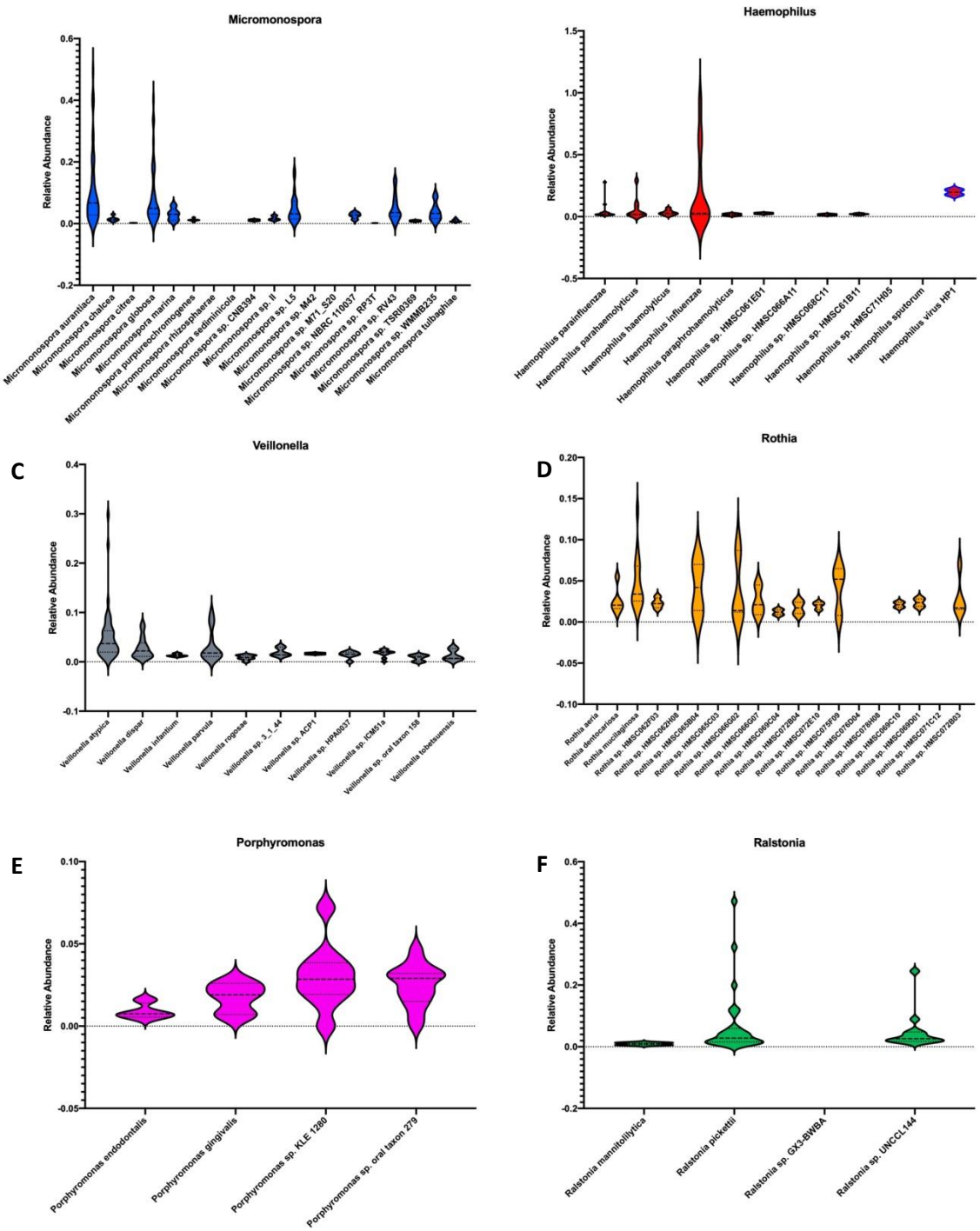


Figure 25. Next Generation Sequencing analyses – top 20 relative abundance species by genera. Top 20 relative abundance species by genera in present in the asthma patient samples. n=70. (a) Micromonospora, (b) Haemophilus, including specific phage HP1(blue border, far right), (c) Veillonella, (d) Rothia, (e) Porphyromonas, (f) Ralstonia. n=70.

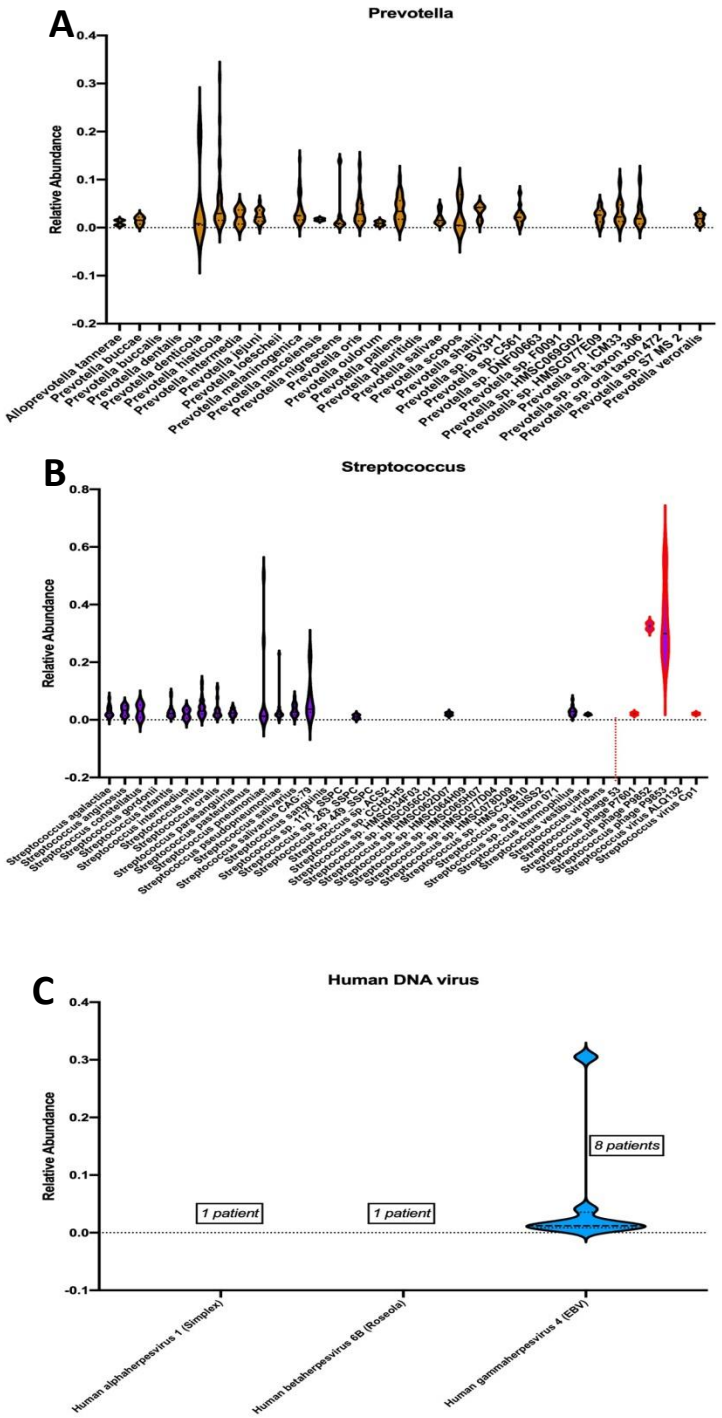


Figure 26. Next Generation Sequencing analyses – top 20 relative abundance species by genera. Top 20 relative abundance species by genera in present in the asthma patient samples. n=70. (a) Prevotella, (b) Streptococcus including specific phages (red, far right) (c) Veillonella, (c) human DNA viruses, Herpes family (Simplex, Roseola, EBV). n=70.

Shannon alpha diversity index was calculated for each sample against abundance this allowed to identify the richness and evenness of the microbial population. The average diversity was 2.55 with a minimum of 0.2 and 4.248 maximum. The Micromonospora genera is the predominant species present and that high diversity within the sample, calculated using the Shannon diversity index, reflects low bacterial counts while some samples with very high numbers of bacteria have reduced Shannon diversity, See figure 27 below. Of note, several patient samples showed blooms of *Haemophilus influenzae* as is evident in figure 27 below which had a corresponding Shannon diversity due to the dominance of the species. Shannon diversity was also grouped via GINA status, however there was no distinct difference, see figure 28.

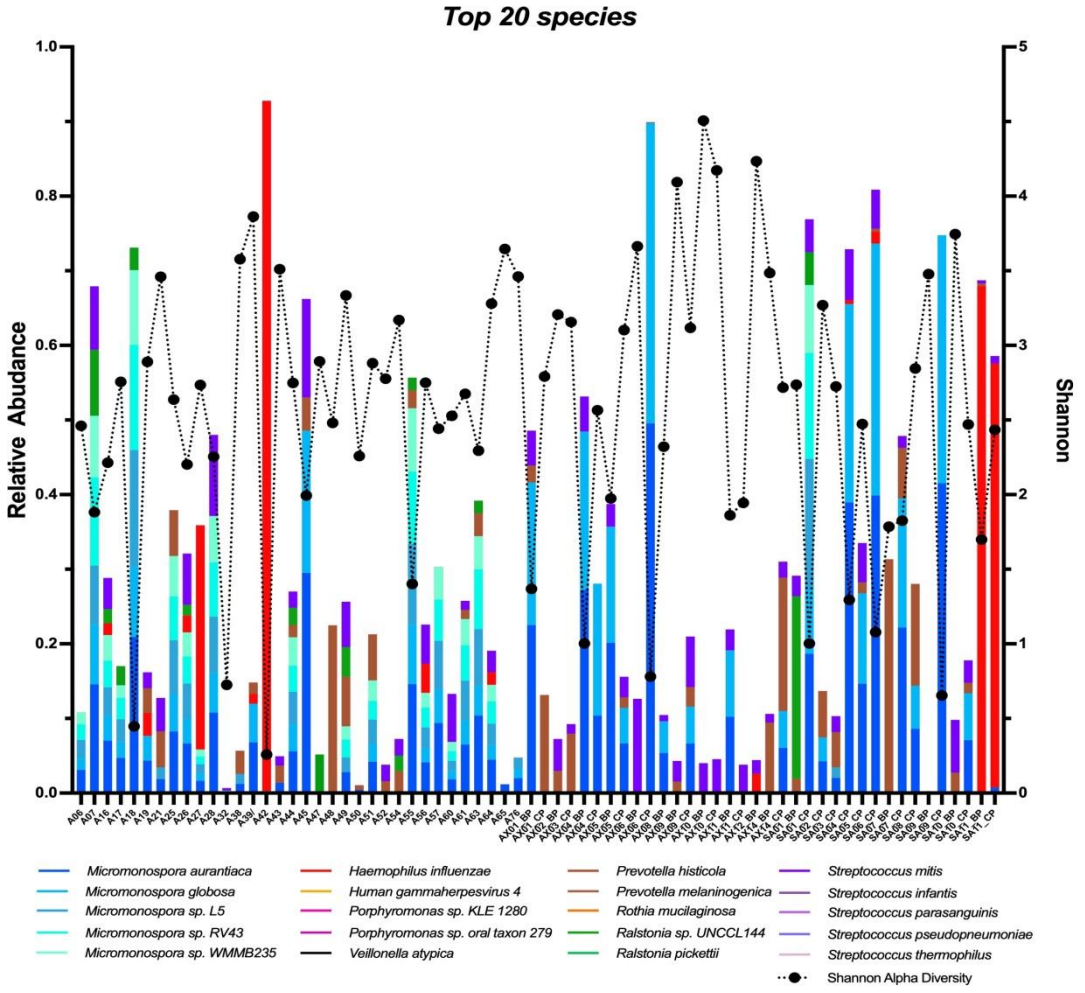


Figure 27. Next Generation Sequencing analyses. Top 20 relative abundance species present in the asthma samples overlaid with Shannon diversity score. n=70.

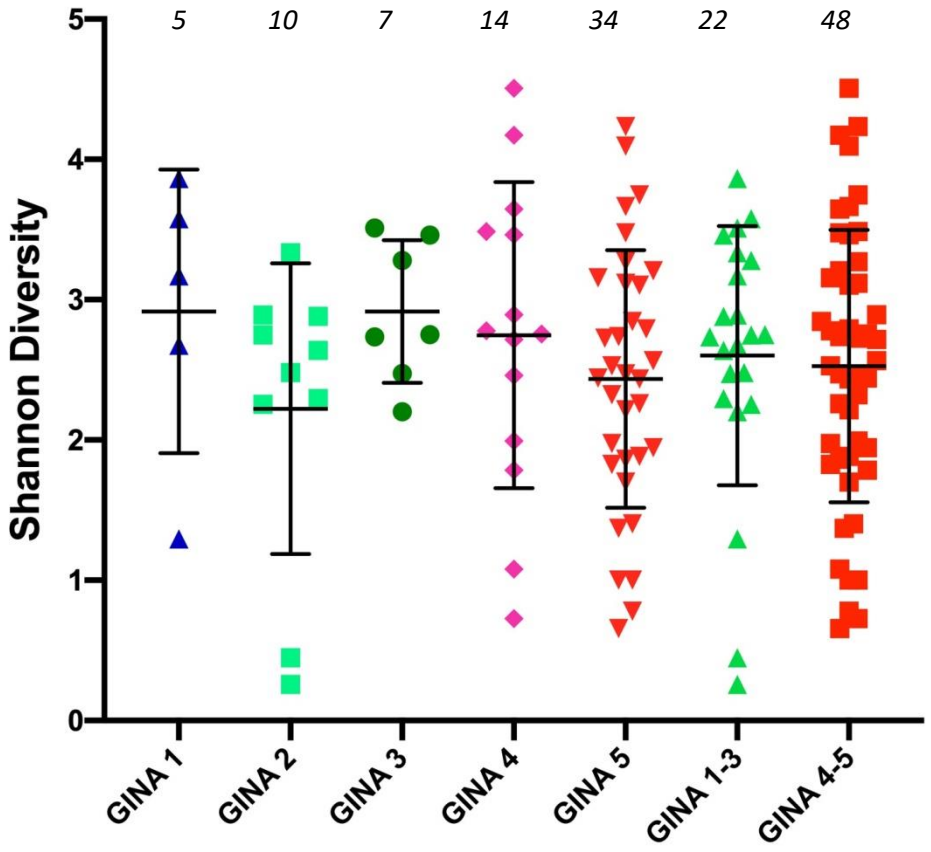


Figure 28. Next Generation Sequencing analyses. Shannon alpha diversity plotted corresponding to patient GINA status, with the distribution highlighted above the scatter plot. n=70.

Beta Diversity was calculated using the Bray Curtis Dissimilarity matrix for all samples. This was performed to compare the samples for similarity and dissimilarity. This ecological dissimilarity metric accounts for both the presence/absence and abundance of organisms in a community and allows subsequent principal component analysis and correlation analysis. As is evident below several samples were quite similar and in a clear example those which represent the bloom of *Haemophilus influenzae* cluster together, see figure 29 (A) below. Principal Coordinates Analysis (PCoA) was also generated of all samples. As is evident the *H. influenzae* cluster also is associated with high BAL TNFα levels, see figure 29 (B-C).

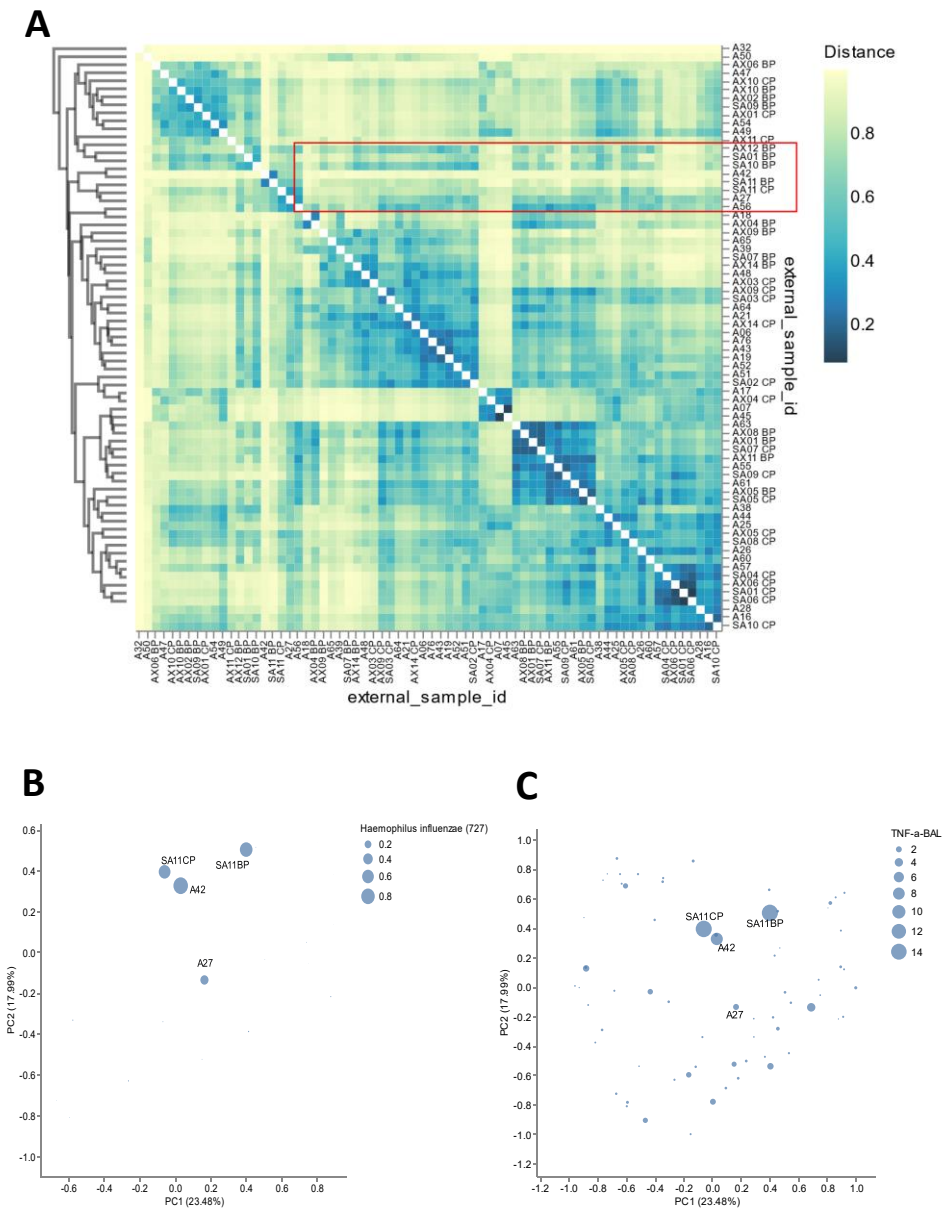


Figure 29. Next Generation Sequencing analyses – Diversity and Principal Coordinates Analysis (PCoA) plot of all samples. (A) Heatmap of Bray-Curtis dissimilarity between all samples using readcounts at the species level. Samples are clustered hierarchically. As is evident several samples clustered together (red box) (B) PCoA, for *Haemophilus influenzae,* the first and second principal components are plotted on the x and y axes, respectively. Each dot represents one sample, and dots are coloured based on the metadata group. PCoA was performed on the estimated relative abundances at the species level. Percentages on each axis label are the proportion of variation explained by each respective principal component. (C) PCoA for BAL TNF-α concentration. n=70

Correlation analysis was performed on the samples that were uniquely dominated by *Haemophilus influenzae*, to identify the metadata variables that were associated with this effect. A handful of factors were all positively associated with the relative abundance of *H. influenzae*, most notably BAL TNF-α, IL-1β, IL-8 and Neutrophils, See figure 30 below. Indeed the HP1 Haemophilus phage was also correlated with the presence of *H. influenzae* and the BAL cytokines and neutrophils.

A	***Haemophilus influenzae***		***Haemophilus virus HP1***
Factor			
TNF-α BAL	0.857	**IL-1β BAL**	1
IL-1β BAL	0.814	**IL-10 BAL**	0.991
IL-8 BAL	0.681	**TNF-α BAL**	0.984
Neutrophils BAL	0.648	***Haemophilus influenzae***	0.978
		Neutrophils BAL	0.947

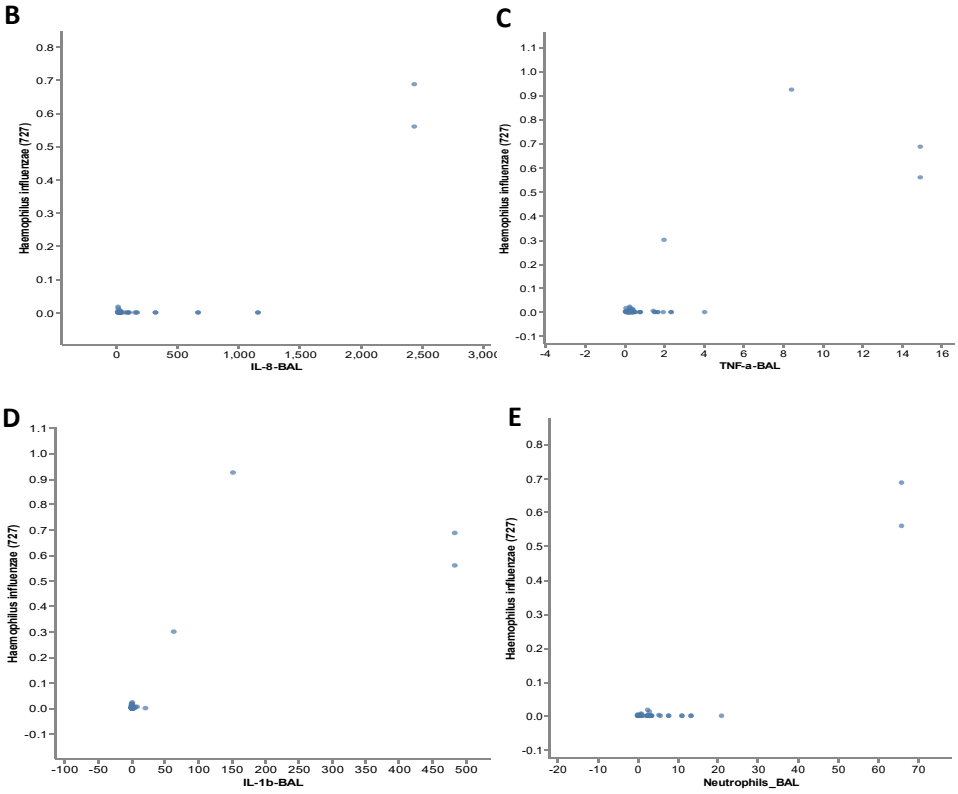


Figure 30. Next Generation Sequencing analyses - correlations and abundance plots of the relative abundance *Haemophilus influenzae* blooms. (a) Correlation analysis linking BAL *Haemophilus influenzae* and HP1 Phage abundance to BAL (b) IL-8, (c) TNF-α , (d) IL1-β and (e) Neutrophils.

Further correlations were performed using GraphPad Prism and the One Codex Jupyter notebook server to evaluate the patient metadata. Both Pearson's and Spearman's correlations were performed using GraphPad Prism. To visualise the correlations and for ease of viewing analysis was split into three components; (1) Patient metadata to compare the microbiome to the patient clinical scoring, (2) Microbiome vs qPCR for correlation of the NGS data to the qPCR analysis and (3) Microbiome immune to correlate the microbiome data to the host immune factors.

See figures 31-34 for correlation analysis data. With respect to patient metadata to compare the microbiome to the patient clinical scoring the correlation analysis shows that a number of correlations are present. See figure 31. GINA class correlated with BMI (P<0.05), oral steroids (P<0.05), inhaled corticosteroids (P<0.0001) and FeNO (P<0.0001).

Comparing Microbiome vs qPCR for correlation of the NGS data to the qPCR analysis shows that a number of correlations are present qPCR total bacteria correlated with NGS *Micromonospora aurantiaca* (P<0.05). qPCR *Pseudomonas aeruginosa* correlated with NGS *Ralstonia* sp. UNCCL144 (P<0.05). qPCR *Pseudomonas fluorescens* correlated with NGS *Micromonospora aurantiaca* (P<0.005), *Micromonospora globosa* (P<0.05), *Haemophilus influenzae* (P<0.05), Human gammaherpesvirus 4 (P<0.005), *Micromonospora* sp. RV43 (P<0.05), *Streptococcus parasangiunis* (P<0.05) and *Veillonella atypica* (P<0.05).

qPCR *Veillonella* correlated with NGS *Micromonospora aurantiaca* (P<0.05), *Ralstonia pickettii* (P<0.05) and *Streptococcus mitis* (P<0.005). qPCR *Veillonella* correlated with NGS *Micromonospora aurantiaca* (P<0.005) and *Micromonospora globosa* (P<0.0005). qPCR *Neisseria bacilliformis* correlated with NGS *Micromonospora aurantiaca* (P<0.005) and *Micromonospora globosa* (P<0.05), Human gammaherpesvirus 4 (P<0.005) and *Veillonella Atypica* (P<0.05).

qPCR *Moraxella catarrhalis* correlated with NGS *Micromonospora aurantiaca* (P<0.005) and *Micromonospora globosa* (P<0.05), *Haemophilus influenzae* (P<0.005) and *Streptococcus parasanguinis* (P<0.005). *Neisseria meningitidis* qPCR correlated with NGS *Veillonella atypica* (P<0.005). qPCR *Streptococcus pneumoniae*

correlated with NGS *Micromonospora aurantiaca* (*P*<0.05) and *Porphyromonas* sp. oral taxon 279 (*P*<0.05). qPCR *Haemophilus influenzae* correlated with NGS *Haemophilus influenzae* (*P*<0.0005), *Micromonospora* sp RV43 (*P*<0.05), *Micromonospora* sp. WMMB235 (*P*<0.05), *Porphyromonas* sp. oral taxon 279 (*P*<0.005), *Ralstonia* sp. UNCCL144 (*P*<0.05) and *Streptococcus parasanguinis* (*P*<0.05).

qPCR *Rothia* correlated with NGS *Micromonospora aurantiaca* (*P*<0.05) and *Micromonospora globosa* (*P*<0.05). qPCR *Micromonospora* correlated with NGS *Micromonospora aurantiaca* (*P*<0.05), *Micromonospora globosa* (*P*<0.05) and Human gammaherpesvirus 4 (*P*<0.05).

Correlations were present with respect to the microbiome data and the host immune factors. See figure 33 and figure 34. The BAL monocyte percentage counts correlated with NGS *Streptococcus parasanguinis* (*P*<0.05) and *Veillonella atypica* (*P*<0.0005). BAL lymphocyte percentage counts correlated with *Streptococcus pseudopneumoniae* (*P*<0.05). BAL eosinophil percentage counts correlated with NGS *Rothia mucilaginosa* (*P*<0.005) and *Streptococcus infantis* (*P*<0.05). BAL neutrophil percentage counts correlated with NGS Human gammaherpesvirus 4 (*P*<0.0001) and *Porphyromonas* sp. oral taxon 279 (*P*<0.05).

BAL cytokine IL-1β correlated with NGS *Haemophilus influenzae* (*P*<0.01) and *Porphyromonas* sp. oral taxon 279 (*P*<0.05). BAL cytokine IL-4 correlated with NGS *Haemophilus influenzae* (*P*<0.05), *Porphyromonas* sp. KLE 1280 (*P*<0.05) and *Streptococcus pseudopneumoniae* (*P*<0.05). BAL IL-5 correlated with NGS *Streptococcus infantis* (*P*<0.05) and *Streptococcus mitis* (*P*<0.05). BAL IL-10 correlated with NGS *Haemophilus influenzae* (*P*<0.05) and *Porphyromonas* sp. KLE1280 (*P*<0.05). BAL IL-13 correlated with NGS *Micromonospora globosa* (*P*<0.05) and *Ralstonia* sp.UNCCL114 (*P*<0.05). BAL IL-17 correlated with NGS *Micromonospora aurantiaca* (*P*<0.05) and *Micromonospora globosa* (*P*<0.05) and *Porphyromonas* sp. KLE1280 (*P*<0.05). BAL TNF-α levels correlated with NGS *Haemophilus influenzae* (*P*<0.01) and *Porphyromonas* sp. oral taxon 279 (*P*<0.05).

Blood IgE levels correlated with NGS *Ralstonia pickettii* (P<0.01), human gammaherpesvirus 4 (P<0.05), *Porphyromonas* sp. oral taxon 279 (P<0.05) and *Streptococcus thermophilus* (P<0.05). Blood haemoglobin levels correlated with NGS *Haemophilus influenzae* (P<0.05). Blood eosinophil levels correlated with NGS *Ralstonia* sp. (P<0.05) and *Streptococcus influenzae* (P<0.005). C-reactive protein (CRP) correlated with human gammaherpesvirus (P<0.05). Blood glucose levels correlated with NGS *Prevotella histicola* (P<0.05).

Plasma cytokine IL-1β correlated with NGS *Micromonospora aurantiaca* (P<0.05), *Micromonospora globosa* (P<0.05), *Porphyromonas* sp. KLE1280 (P<0.05), *Ralstonia* sp. UNCCL144 (P<0.005) and *Streptococcus mitis* (P<0.005). Plasma IL-4 correlated with NGS *Ralstonia* sp. UNCCL144 (P<0.0005). Plasma IL-5 correlated with NGS *Streptococcus infantis* (P<0.0005). Plasma IL-6 correlated with NGS *Ralstonia* sp. UNCCL144 (P<0.005). Plasma IL-8 correlated with *Micromonospora aurantiaca* (P<0.0005), *Micromonospora globosa* (P<0.0001), *Ralstonia* sp. UNCCL144 (P<0.01) and *Streptococcus mitis* (P<0.05). Plasma IL-10 correlated with *Ralstonia* sp. UNCCL144 (P<0.01). Plasma IL-13 correlated with *Ralstonia* sp. UNCCL144 (P<0.005). Plasma IL-17 correlated with *Streptococcus pseudopneumoniae* (P<0.05). TNF-α levels in the plasma correlated with *Ralstonia* sp. UNCCL144 (P<0.005) and *Streptococcus pseudopneumoniae* (P<0.05). IFN-γ plasma levels correlated with *Haemophilus influenzae* (P<0.01).

Patient Correlations

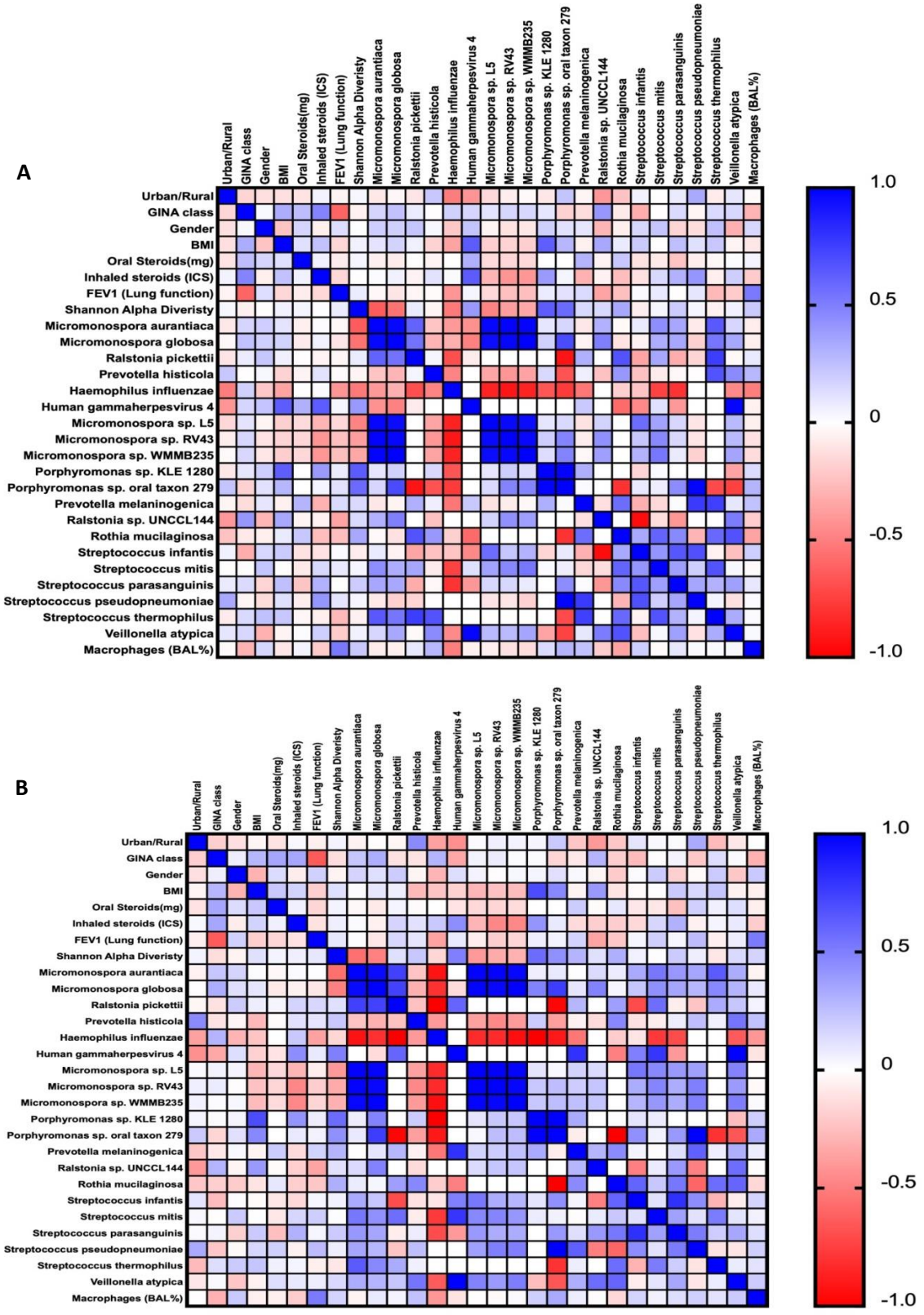


Figure 31 Correlations of relative abundance versus patient metadata. (a) Pearson r correlation (b) Spearman r correlation. n=70

qPCR Correlations

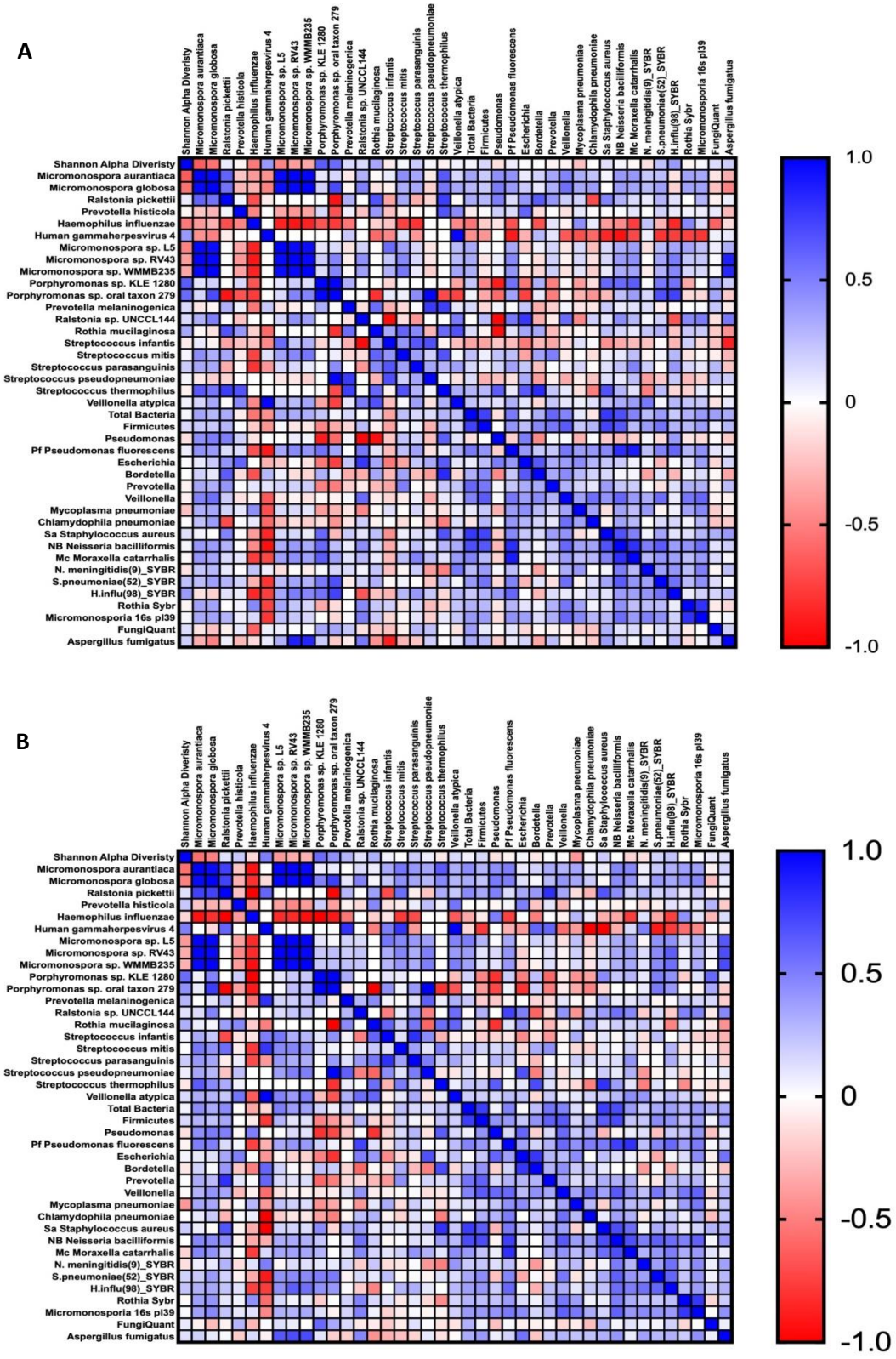


Figure 32 Correlations of relative abundance versus qPCR data. (a) Pearson r correlation (b) Spearman r correlation. n=70

Immune Correlations-I

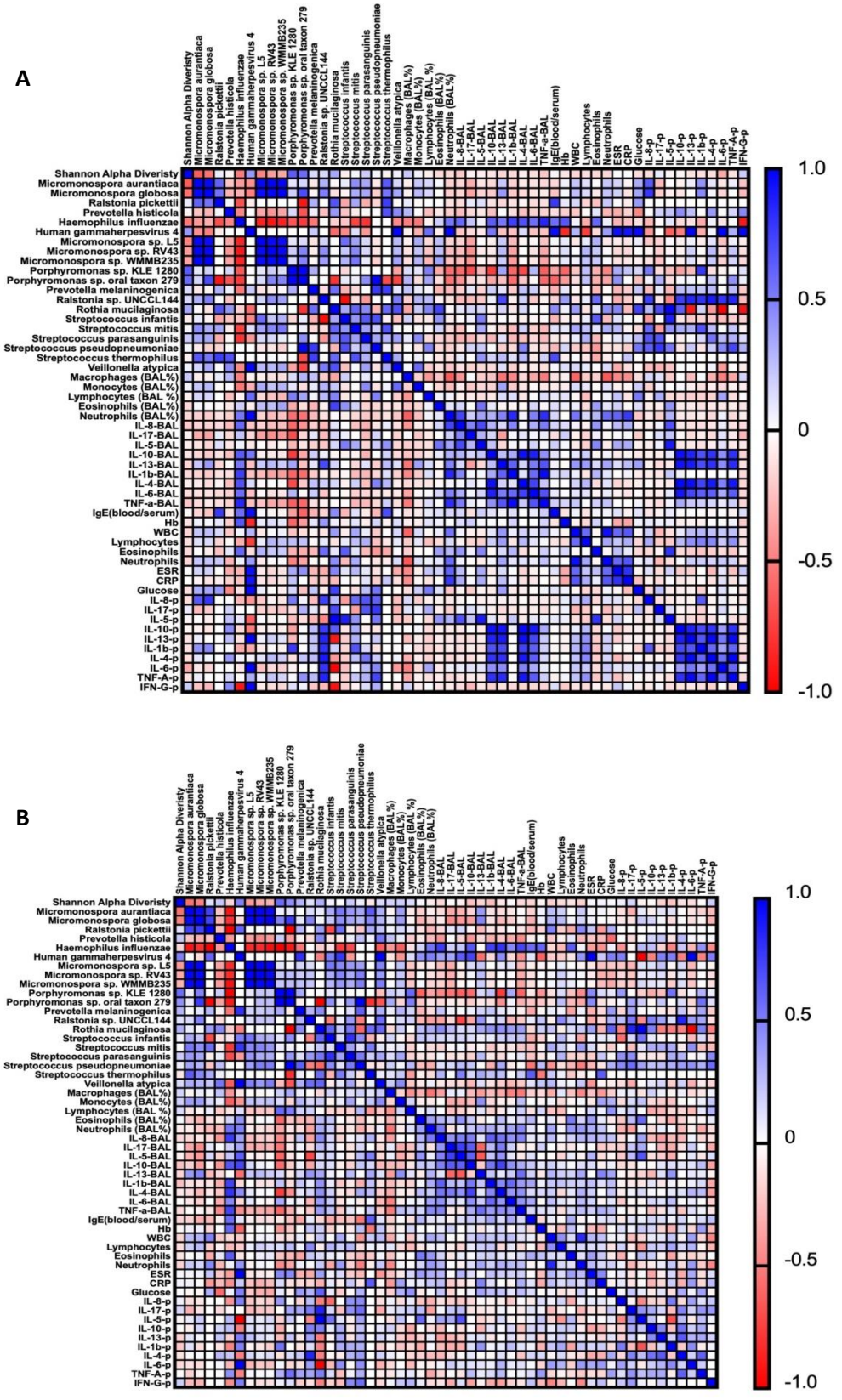


Figure 33. Correlations of relative abundance versus immune cell and cytokine data. (a) Pearson r correlation (b) Spearman r correlation. n=70

Immune Correlations-II

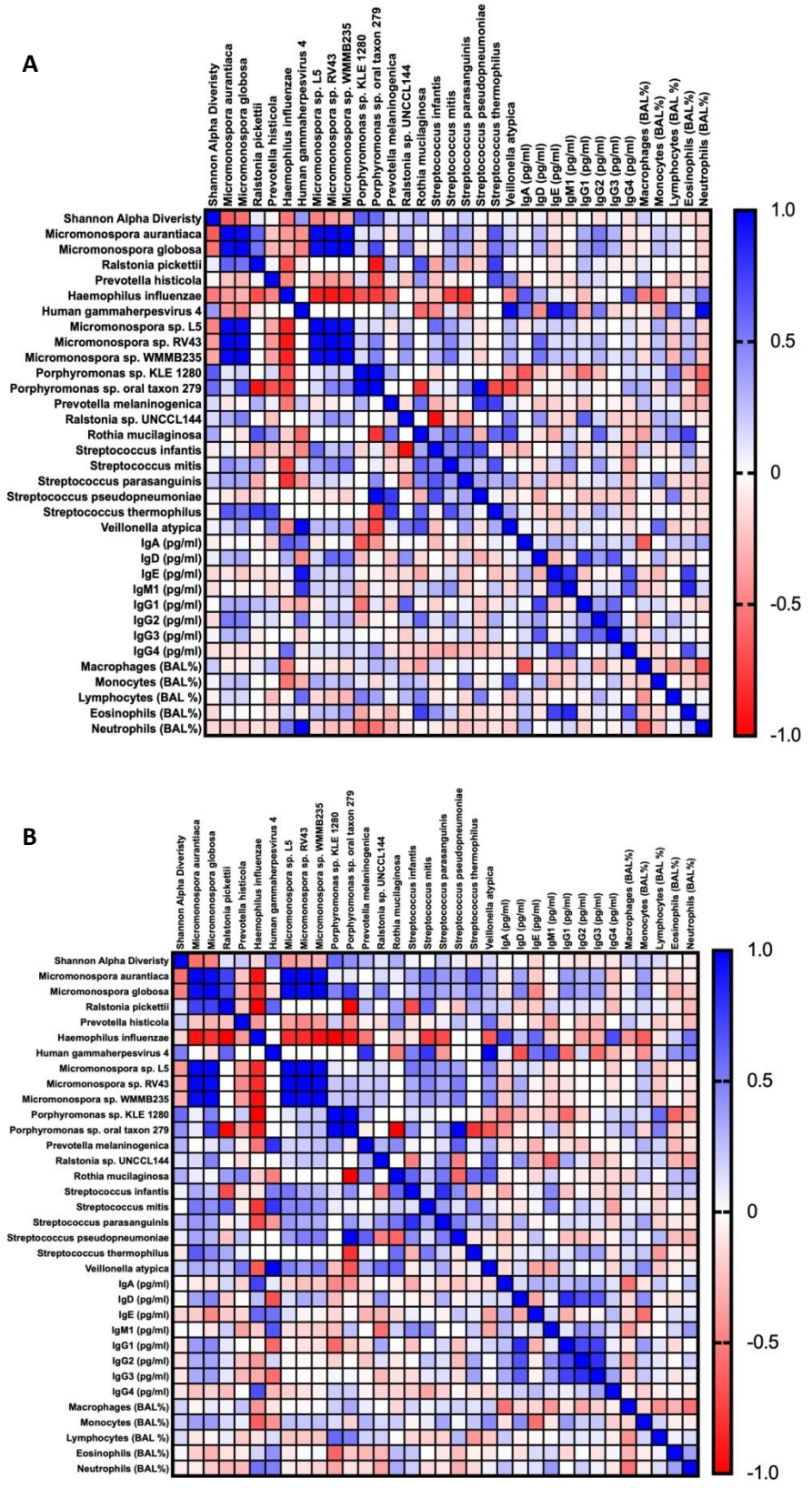


Figure 34. Correlations of relative abundance versus immune antibody and cell data. (A) Pearson r correlation (B) Spearman r correlation. n=70

5. Discussion

Background

Asthma rates are increasing and as a result of meta-genomics it is now possible to define the composition of microbes in the lungs and elucidate whether changes in the composition of lower airway microbiota influences the complex pathophysiology of chronic lung disease such as asthma[1,5]. There is an emerging consensus that the microbiome potentially plays a critical role in disease development, including in the pathogenesis of airway conditions such as asthma[11].

A key aim of this study is to investigate the presence of microbial species within the previously considered sterile airway of a cohort of well-defined asthmatic patients. The presence of differing species within the airway of asthmatic patients may provide a rationale for personalised therapeutic targeting of microbes within the asthmatic lung. Changes in the microbial composition of the lungs could underlie susceptibility to and progression and chronicity of lung diseases.

The asthma cohort

The asthma cohort consisted of 73 adult asthmatic patients. When stratified by asthma severity 36% (26/73) were classified as mild (GINA 1+2), 22% (16/73) were moderate (GINA 3) and 42% (31/73) of the cohort were classified as severe asthmatics (GINA 4+5). When stratified by level of asthma control (ACQ-7), 41% (30/73) were controlled (ACQ-7 <1.5) while 59% (43/73) were uncontrolled (ACQ-7 ≥1.5), see figure 3.

The availability of a well-defined asthma cohort enabled the investigation into the presence of microbial species within a previously considered sterile environment, the lungs, and provided the opportunity to investigate if the airway microbiome may play a critical role in the pathogenesis of asthma.

Microscopy and immune cell percentage counts

Through the implementation of various staining protocols such as Kwik Diff it was possible to differently score the immune cells present within the patient BAL. This presented valuable insights with respect to the overall immune cell percentage of lymphocytes, monocytes, macrophages, neutrophils and eosinophils within the patient BAL and macrophages were found to be the most dominant immune cell present within the BAL, with varying levels of lymphocytes, monocytes, neutrophils and eosinophils. See figure 8 and figure 9.

When the patients were stratified by GINA it was observed that the patients classified as (GINA 1+2) mild asthmatics had lower levels of BAL neutrophils and eosinophils. Mild asthmatics (GINA 1+2) had eosinophil levels of [Mean (SD)] [2.9 (7.1)] and [Median (IQR)] [1.0 (0.6-1.6) compared to moderate (GINA 3) asthmatics [8.8 (15.1)]; [2.8 (0.2-6.9)] and severe (GINA 4+5) asthmatics [7.1 (15.8)]; [2.6 (0.7-5.2)]. Mild asthmatics also overall had lower BAL eosinophil percentage counts [1.9 (2.5)]; [0.7 (0.1-2.9)] compared to moderate asthmatics [2.9 (5.3)]; [0.7 (0.1-1.4)] and severe asthmatics [3.2 (0.8)]; [0.5 (0-2.0)]. See table 2.

Implementation of molecular detection methods; qPCR and WGS; to investigate microbial species

Thanks to the advancement of culture independent techniques, the unique steady state microbiota of the lungs is being elucidated[1,5]. Both quantitative Polymerase Chain Reaction (qPCR) and Next Generation Sequencing (NGS) were implemented in this study in order to develop a robust model system to investigate the presence of both microbial species of interest, in the case of qPCR, and the overall abundance of microbial species within the BAL DNA of the asthma cohort, n=73.

qPCR revealed a wide variety of microbial species present in the lungs of the asthmatic cohort. See figure 10. Through the analyses of the qPCR results a number of statistically significant correlations to various patient demographics and patient immune profiles were found.

Total bacteria

93% (68/73) of patients had detectable levels of bacteria using the total bacteria primer[27]. The presence of qPCR total bacteria correlated with BAL IL-8 cytokine levels (P<0.05; r_s=-0.2971). IL-8 is also known as CXCL8; chemokine (C-X-C motif) ligand 8. The significant correlation existing between qPCR total bacteria presence and IL-8 is of interest. The IL-8 cytokine is a neutrophil and mast cell chemoattractant which is known in asthma to function in inflammatory cell regulation[28].

Firmicutes

73% (53/73) of patients had detectable levels of the mainly gram-positive containing phyla; Firmicutes. The presence of Firmicutes in the BAL by qPCR correlated with plasma cytokine IL-6 levels (P<0.05; r_s=-0.3236), plasma TNF-α (P<0.01; r_s=-0.3823), BAL IL-4 (P<0.05; r_s=-0.3446) and BAL IL-5 (P<0.05; r_s=-0.2955).

Streptococcus pneumoniae, Staphylococcus aureus, Moraxella catarrhalis, Haemophilus influenzae* and *Pseudomonas aeruginosa

Studies have previously shown that within a cohort of asthma patients, who at the time of sputum collection were displaying symptoms of an asthma exacerbation, the bacteria *Streptococcus pneumoniae, Moraxella catarrhalis* and *Haemophilus influenzae* were reported within 27% of the cohort[29]. Within our asthma cohort no patients were experiencing an asthma exacerbation at the time of bronchoscopy.

However other studies also have detected the same genera of bacteria, *Streptococcus pneumoniae, Moraxella catarrhalis* and *Haemophilus influenzae* within 15% of patients whereby samples, in the form of induced sputum, were obtained during a time when the asthma patients were not experiencing an exacerbation[30].

Studies have also documented that within a cohort of 56 stable, severe asthmatics, from whom sputum was cultured from, *Haemophilus influenzae, Pseudomonas aeruginosa* and *Staphylococcus aureus* were the main strains present within the 29 asthmatics with positive bacterial cultures[31].

Within our study cohort all samples were obtained during a time when patients were not experiencing an exacerbation and all samples were obtained as BAL from the right middle lobe (RML) or lingula. While the aforementioned studies obtained an asthmatic patient bacterial profile through the use of culture techniques our study instead focused on the implementation of molecular techniques to investigate the presence of bacterial species in the lungs of a well-defined asthma cohort, n=73.

Streptococcus pneumoniae was detectable in 73% (53/73) of patients by qPCR. *Streptococcus pneumoniae* presence by qPCR correlated with the immune cell percentage count of macrophages ($P<0.05$; $r_s=0.3424$). See figure 16.

Staphylococcus aureus was detectable in 75% (55/73) of patients BAL by qPCR. *Staphylococcus aureus* presence correlated with plasma IL-17 levels ($P<0.05$; $r_s=0.3994$) and BAL IL-1β ($P<0.01$; $r_s=-0.3777$). See figure 15.

Moraxella catarrhalis was detectable in 78% (57/73) of patients BAL by qPCR. *Moraxella catarrhalis* presence by qPCR correlated with BAL IL-13 levels ($P<0.05$; $r_s=0.3141$) and the immune cell percentage count of neutrophils ($P<0.05$; $r_s=-0.2639$). See figure 16.

Haemophilus influenzae was detectable in 67% (49/73) of patients BAL by qPCR. While *Haemophilus influenzae* presence by qPCR did not significantly correlated to patient demographics or immune profiles the detection of *Haemophilus influenzae* by Next Generation Sequencing (NGS) did correlate with a number of factors. qPCR *Haemophilus influenzae* correlated with NGS *Haemophilus influenzae* ($P<0.0005$), *Micromonospora* sp RV43 ($P<0.05$), *Micromonospora* sp. WMMB235 ($P<0.05$), *Porphyromonas* sp. oral taxon 279 ($P<0.005$), *Ralstonia* sp. UNCCL144 ($P<0.05$) and *Streptococcus parasanguinis* ($P<0.05$).

Pseudomonas aeruginosa was detectable in 34% (25/73) of asthmatics. *Pseudomonas aeruginosa* presence by qPCR correlated with the White Cell Count (WBC) ($P<0.05$; $r_s=0.4645$) and blood neutrophil levels (10^9/L) ($P<0.05$; $r_s=0.4910$). See figure 12.

Pseudomonas fluorescens

Pseudomonas fluorescens was detectable in 88% (64/73) of patients BAL by qPCR. *Pseudomonas fluorescens* presence correlated with the IL-5 cytokine levels in BAL ($P<0.05$; $r_s=-0.2601$). See figure 12. *Pseudomonas fluorescens* presence also correlated with BAL IL-13 cytokine levels ($P<0.05$; $r_s=0.2971$) and the immune cell percentage counts of neutrophils ($P<0.05$; $r_s=-0.2887$). See figure 13.

Escherichia

Escherichia was detectable in 37% (27/73) of patients BAL by qPCR. *Escherichia* presence in the BAL by qPCR correlated with plasma IL-5 ($P<0.05$; $r_s=0.3994$), plasma IL-6 ($P<0.01$; $r_s=0.5238$), plasma IL-10 ($P<0.05$; $r_s=0.4450$), IL-17 BAL ($P<0.05$; $r_s=-0.4230$), and the immune cell percentage count of neutrophils ($P<0.05$; $r_s=-0.4278$). See figure 13. *Escherichia* when classified by gram stain falls within a gram negative bacteria group[32]. *Escherichia* activates a host innate immune response due to the signal transduction mediated by Toll-like Receptor 4 (TLR-4)[32].

Bordetella

Bordetella is a small gram negative coccobacilli bacterium. While *Bordetella pertussis* the respiratory pathogen that is the causative agent for whooping cough would be generally considered to be the most well documented of the *Bordetella* species, the *Bordetella* genus consists of many other species which do not possess the pertussis toxin (PT) and therefore do not have the virulence factor associated

with whooping cough in patients[33]. *Bordetella* was detectable in 53% (38/73) of patients BAL by qPCR. *Bordetella* correlated with the presence of IL-1β in the plasma (P<0.05; r_s=-0.5963). See figure 13. *Bordetella* correlated with plasma IL-4 levels (P<0.05; r_s=-0.3523), plasma IL-8 levels (P<0.05; r_s=0.3266), plasma IL-10 levels (P<0.05; r_s=-0.3507), plasma TNF-α levels (P<0.0005; r_s=-0.5560), BAL IL-4 levels (P<0.05; r_s=-0.4134), BAL IL-17 levels (P<0.001; r_s=-0.5774) and the immune cell percentage count of monocytes (P<0.005; r_s=-0.4893). See figure 14.

Prevotella

A member of the *Bacteroidetes* phylum *Prevotella* species can be classified as gram negative anaerobic bacteria, classically considered as commensal bacteria[34]. Generally considered to be prevalent within mucosal sites as commensal bacteria, studies have demonstrated that *Prevotella* is commonly found within the respiratory system[8,34,35]. Studies have documented that while considered a commensal bacteria; *Prevotella* can in fact, dependent on the conditions faced and the strain present, be considered as a pathobiont; promoting chronic inflammation[34]. *Prevotella* was detectable in 79% (58/73) of patients BAL by qPCR. *Prevotella* presence by qPCR correlated with plasma IL-10 levels (P<0.05; r_s=-0.2709). See figure 14. *Prevotella* also correlated with plasma TNF-α levels (P<0.05; r_s=-0.3256) and BAL IL-17 levels (P<0.05; r_s=-0.2709). See figure 15.

Veillonella

Veillonella was detectable in 80% (59/73) of patients BAL by qPCR. *Veillonella* presence by qPCR correlated with plasma IL-8 levels (P<0.05; r_s=-0.2639). See figure 15. The IL-8 cytokine is a neutrophil and mast cell chemoattractant which is known in asthma to function in inflammatory cell regulation[28].

Mycoplasma pneumoniae

Mycoplasma pneumoniae was detectable in 62% (45/73) of patients BAL by qPCR. With regards to the presence of *Mycoplasma pneumoniae* by qPCR no statistically significant correlation was found with respect to *Mycoplasma pneumoniae* presence and patient demographics and immune profile of the cohort. *Mycoplasma pneumoniae* infection is thought to be often underestimated within a population. *Mycoplasma pneumoniae* is believed to be a key etiologic agent in patients who present with community-acquired pneumoniae[36].

Chlamydophilia pneumoniae

Chlamydophilia pneumoniae was detectable in 70% (51/73) of patients BAL by qPCR. *Chlamydophilia pneumoniae* presence by qPCR correlated with BAL IL-8 levels ($P<0.05$; $r_s=-0.2826$) and BAL IL-13 levels ($P<0.05$; $r_s=-0.3380$). See figure 15. Studies have investigated the hypothesis that *Chlamydophilia pneumoniae* infection in patients may in fact preceed asthma onset or exacerbation[37]. Studies have documented that when patients experienced repeated or prolonged exposure to *Chlamydophilia pneumoniae* a causal relationship may exist with symptoms such as wheezing or a diagnosis or asthma or asthma bronchitis[38]

Neisseria meningitidis

Neisseria meningitidis was detectable in 67% (49/73) of patients BAL by qPCR and its presence correlated with plasma IL-8 levels ($P<0.05$; $r_s=-0.3086$). See figure 14

Neisseria bacilliformis

Neisseria bacilliformis was detectable in 66% (48/73) of patients BAL by qPCR. *Neisseria bacilliformis* correlated with BAL IL-1β levels ($P<0.05$; $r_s=-0.3373$). See figure 15.

It is of interest that *Neisseria bacilliformis* correlated with IL-1β presence within the patient BAL. The cytokine IL-1β is interesting as it is considered pleiotropic, capable of both pro- and anti- inflammatory effects. It is believed that IL-1β is critical in the pathobiology of asthma and has been an important player in driving the inflammatory response and subsequent changes in airway smooth muscle (ASM) responsiveness making its modulation an attractive therapeutic target[39].

Rothia

Rothia was detectable in 86% (63/73) of patients BAL by qPCR. *Rothia* correlated with FEV-1 (percent predicted) (P<0.05; r_s=0.2697) and plasma IL-6 (P<0.05; r_s=-0.4592). See figure 16. IL-6 is a pleotrophic cytokine with the ability to act in an anti-inflammatory and pro-inflammatory manner. It is recognised that IL-6 is produced in response to the recognition of microbes by pattern associated molecular patterns[40].

Micromonospora

Perhaps one of the most surprising discoveries of this study was the presence of *Micromonospora* within the lungs of the asthmatic cohort by both qPCR and NGS detection methods. *Micromonospora* was found by NGS first and its presence was confirmed by qPCR while NGS analyses was underway. To our knowledge there is an absence of studies which have demonstrated the presence of *Micromonospora* within the lungs of asthma patients. *Micromonospora* is an interesting bacteria; known to be widely distributed in many different locations in nature[41]. In nature *Micromonospora* is known to produce both antimicrobial and antifungal agents and as a bacteria *Micromonospora* possesses a complex lifecycle; possessing the ability to differentiate into both substrate mycelia and spores[41].

With respect to the qPCR detection of *Micromonospora* it was detectable in 85% (62/73) of BAL from the asthmatic cohort. *Micromonospora* correlated with FeNO

(ppb) (P<0.05; r_s=0.3004) and plasma IL-1β levels (P<0.05; r_s=-0.4703). See figure 16. *Micromonospora* also correlated with plasma IL-6 (P<0.05; r_s=-0.3018) and BAL IL-1β (P<0.05; r_s=-0.2737). See figure 17.

Looking at the Next Generation Sequencing data *Micromonospora* was also highly prevalent within the BAL samples from the asthma cohort. The gram-positive spore forming aerobe actinobacteria *Micromonospora aurantica* was the most abundant species present. Subsequent analysis focussed on the top 10-20 abundant microbial species. *Micromonospora aurantica* is the dominant microbe present in 51/70 of the samples, followed by *Veillonella atypica*, *Micromonospora globosa* and *Streptococcus mitis*, see table 4 for further details.

Haemophilus influenzae NGS detection

Phage specific for Haemophilus influenzae, several *Streptococcus* species and human viruses such as human gammaherpesvirus 4 (Epstein Barr Virus) were also detectable at high levels in the BAL, see figure 25 and 26.

Correlation analysis was performed on the samples that were uniquely dominated by *Haemophilus influenzae*, to identify the metadata variables that were associated with this effect. A handful of factors were all positively associated with the relative abundance of *H. influenzae*, most notably BAL TNF-α, IL-1β, IL-8 and Neutrophils. See figure 30. Indeed the HP1 Haemophilus phage was also correlated with the presence of *H. influenzae* and the BAL cytokines and neutrophils.

Of note, several patient samples showed blooms of *Haemophilus influenzae* as is evident in figure 27 which had a corresponding Shannon diversity due to the dominance of the species.

Beta Diversity was calculated using the Bray Curtis Dissimilarity matrix for all samples. This was performed to compare the samples for similarity and dissimilarity. This ecological dissimilarity metric accounts for both the presence/absence and abundance of organisms in a community and allows

subsequent principal component analysis and correlation analysis. As is evident below several samples were quite similar and in a clear example those which represent the bloom of *Haemophilus influenzae* cluster together, see figure 29 (A). Principal Coordinates Analysis (PCoA) was also generated of all samples. As is evident the *H. influenzae* cluster also is associated with high BAL TNFa levels, see figure 29 (B-C).

Haemophilus influenzae is present as a commensal bacterium within the nasopharynx of most healthy adults. Colonisation of the upper respiratory tract begins in infancy and at least 75% of adults are colonised by this bacteria, with constant turnover of different *Haemophilus influenzae* strains during life. *Haemophilus influenzae* can be grouped into polysaccharide encapsulated strains and non-encapsulated strains with non-encapsulated strains considered to be primarily respiratory pathogens. *Haemophilus influenzae* can be transmitted by aerosol droplets and through contact with secretions. The nasopharynx is a potential reservoir for the pathogen which can spread to the lower respiratory tract in certain individuals dependent on host defence mechanisms and bacteria mechanisms and virulence factors such as adhesins, pili, Hia and Hap proteins which can help the bacteria attach to mucosal surfaces and after attachment, the bacterium possesses mechanisms to aid persistence within the host such as proteases. Non encapsulated strains of *Haemophilus influenzae* are known to invade tissue and target macrophages and epithelial cells increasing their ability to survive within a susceptible individual[42]

The implementation of both qPCR and Next Generation Sequencing

The use of molecular technologies such as qPCR and Next Generation Sequencing offered the encapsulation of a deeper insight into the microbes present within the lungs of a cohort of asthma patients than the implementation of only one of the techniques would have. A fuller picture as to the microbes present within the lungs of the asthmatic cohort was gained and the two methods were complementary of each other. In fact correlations were found to exist between the microbial species

detected by qPCR means and the detection of species through the implementation of Next Generation Sequencing platforms.

Asthma rates are increasing and as a result of meta-genomics it is now possible to define the composition of microbes in the lungs and elucidate whether changes in the composition of lower airway microbiota influences the complex pathophysiology of chronic lung disease such as asthma[1,5].

Conclusions

Thanks to the advancement of culture independent techniques, the unique steady state microbiota of the lungs is being elucidated[1,5]. Poor, ineffective microbial culturing techniques which created a hurdle when trying to investigate the lung microbiome due to the difficulties in replicating the lung habitat are no longer a stumbling block when investigating the microbiome of the lung[4]. While due to the lower bacterial abundance and the difficulty of acquiring lower respiratory tract samples, the study of the lung microbiome is technically challenging the possibilities of the lung microbiome playing a potentially critical role in disease development and pathogenesis highlights the importance of research into the lung microbiome and in fact thanks to advancements in sequencing technologies, lung microbiome research is rapidly advancing[1,5,10,11]. It is hoped that the novel findings of this study may add to the growing body of research with respect to the microbiome and asthma and may potentially offer insights into asthma susceptibility, pathogenesis and prognosis.

6. Supplementary

Supplementary table 1: Validated primer sequences utilised for the detection of microorganisms of interest. Note K=G or T, R=A or G, S=G or C, W=A or T following IUPAC code.

Primer		**Sequence**	**Reference**
Total Bacteria	F-Bact-1369	5'-CGGTGAATACGTTCCCGG-3'	[27]
	R-Prok-1492	5'-TACGGCTACCTTGTTACGACTT-3'	
Total Bacteria Probe	P-TM1389F	5'-CTTGTACACACCGCCCGTC-3'	
Firmicutes	Firm-L	5'-GGAGYATGTGGTTTAATTCGAAGCA-3'	[43]
	Firm-R	5'- AGCTGACGACAACCATGCAC-3'	
Staphylococcus aureus	Sa-pl-47-L	5'-ATGCATAGCCGACCTGAGAG-3'	NCBI:txid1280
	Sa-pl-47-R	5'- AGGAGTCTGGACCGTGTCTC-3'	
Streptococcus pneumoniae	S.pneu-pl-52-L	5'-GCAAGGTATGCAGGAATCGT-3'	Modification on *Streptococcus pneumoniae* alpha fucosidase gene NCBI:txid488222
	S.pneu-pl-52-R	5'-TCGCTTGAGTATGAACCAACC-3'	
Rothia	Rothia-Spp-L	5'-GCCTGGGAAACTGGGTCTAAT-3'	[44]
	Rothia-Spp-R	5'-CAAGCTGATAGGCCGTGAG-3'	
Micromonospor ia	Mimo16S-pl-39-L	5'-GGTACAATGGGCTGCGATAC-3'	Modification on *Micromonospori a* strain ATCC 27029 NCBI:NR_074415 .1
	Mimo16S-pl-39-R	5'-CGAACTGAGACCGGCTTTT-3'	

Pseudomonas aeruginosa	ORPL-pl-11-L	5’-CCAGAGCCATGTTGTACTCG-3’	[45] [46] Modification on *Pseudomonas aeruginosa* Outer Membrane Protein L NCBI:txid205922
	ORPL-pl-11-R	5’-ACACGCGAAAGACCTGAAAG-3’	
Pseudomonas fluorescens	Pf-pl-66-L	5’-GACAGAATAAGCACCGGCTAA-3’	NCBI:txid294
	Pf-pl-66-R	5’-ACGCTTGCACCCTCTGTATT-3’	
Escherichia	UidA405-pl-9-L	5’-CTGATAGCGCGTGACAAAAA-3’	Modification on Beta-glucuronidase protein, Uid A405 gene NCBI:txid83333
	UidA405-pl-9-R	5’-CGGTTCGTTGGCAATACTC-3’	
Bordetella	Bordetella-pl-45-L	5’-GAGCCATTGTCGGTGAGC-3’	NCBI:txid517
	Bordetella-pl-45-R	5’-CGCAGTGGCCTACTACCAG-3’	
Prevotella	Prevotella-pl-66-L	5’-TGCAGGTACCGCATGAATAA-3’	NCBI:txid838
	Prevotella-pl-66-R	5’-CCGGACCTTCCGTATTACC-3’	
Veillonella	Veillonella-L	5’-CCGTGATGGGATGGAAACTGC-3’	[47]
	Veillonella-R	5’-CCTTCGCCACTGGTGTTCTTC-3’	
Mycoplasma pneumoniae	Myco.pneu-pl-16-L	5’-AGACACGGCCCATACTCCTA-3’	Greengenes GenBank: CP017343.1
	Myco.pneu-pl-16-R	5’-CAAGCTTTCGCTCATTGTGA-3’	
Chlamydophilia pneumoniae	C.pneu-pl-45-L	5’-CGTGAGATGGAGCAAATCCTA-3’	Greengenes GenBank: CP001713.1

	C.pneu-pl-45-R	5’-ACTTCATGTAGTCGAGTTGCAGA-3’	
Neisseria bacilliformis	Nb-pl-8-L	5’-TGCGTAGAGATGTGGAGGAAT-3’	Greengenes NCBI:txid267212
	Nb-pl-8-R	5’-CTGTTTGCTACCCACGCTTT-3’	
Moraxella catarrhalis	Mc-pl-66-L	5’-CACAGAATAAGCACCGGCTAA-3’	Greengenes GenBank: CP010573.1
	Mc-pl-66-R	5’-ACGCTTGCACCCTCTGTATT-3’	
Neisseria meningitidis	N.meningitidis-pl-9-L	5’-ATTCCACTACGGCAAACACC-3’	[48] Modification on *Neisseria meningitidis* SodC gene NCBI:txid487
	N.meningitidis-pl-9-R	5’-TCGGTGCCTTTGATTTGATT-3’	
Haemophilus influenzae	H.influ-pl-98-L	5’-AGCTGGTAAAGGTGTTGATGC-3’	Modification on Peptidoglycan associated outer membrane lipoprotein-OMP P6 NC_000907.1
	H.influ-pl-98-R	5’-GCAGGTTTTTCTTCACCGTAA-3’	
Fungi Quant	Fungi Quant-F	5’-GGRAAACTCACCAGGTCCAG-3’	[49]
	Fungi Quant-R	5’GSW CTA TCC CCA KCA CGA-3’	
Aspergillus fumigatus	OliAFMB-L-pl-103	5’-AGC ACG GCT TGT GTG TTG -3’	Modification on *Aspergillus* ITS KT358862 [50]
	OliAFMB-R-pl-103	5’-GGG TGA CAA AGC CCC ATA C-3’	

7. References

1. Aho VT, Pereira PA, Haahtela T, Pawankar R, Auvinen P, Koskinen K. The microbiome of the human lower airways: a next generation sequencing perspective. *The World Allergy Organization journal.* 2015;8(1):23.
2. Marsland BJ. Influences of the Microbiome on the Early Origins of Allergic Asthma. *Annals of the American Thoracic Society.* 2013;10(Supplement):S165-S169.
3. Holgate ST, Polosa R. Treatment strategies for allergy and asthma. *Nat Rev Immunol.* 2008;8(3):218-230.
4. Marsland BJ, Gollwitzer ES. Host-microorganism interactions in lung diseases. *Nat Rev Immunol.* 2014;14(12):827-835.
5. Abdel-Aziz MI, Vijverberg SJH, Neerincx AH, Kraneveld AD, Maitland-van der Zee AH. The crosstalk between microbiome and asthma: Exploring associations and challenges. *Clinical & Experimental Allergy.* 2019;49(8):1067-1086.
6. Huffnagle GB, Dickson RP. The bacterial microbiota in inflammatory lung diseases. *Clinical Immunology.* 2015;159(2):177-182.
7. Segal LN, Blaser MJ. A brave new world: the lung microbiota in an era of change. *Annals of the American Thoracic Society.* 2014;11 Suppl 1:S21-27.
8. Hilty M, Burke C, Pedro H, et al. Disordered microbial communities in asthmatic airways. *PLoS ONE.* 2010;5(1).
9. Erb-Downward JR, Thompson DL, Han MK, et al. Analysis of the Lung Microbiome in the "Healthy" Smoker and in COPD. *PLoS ONE.* 2011;6(2):e16384.
10. Wilson NG, Hernandez-Leyva A, Kau AL. The ABCs of wheeze: Asthma and bacterial communities. *PLOS Pathogens.* 2019;15(4):e1007645.
11. Herbst T, Sichelstiel A, Schär C, et al. Dysregulation of allergic airway inflammation in the absence of microbial colonization. *Am J Respir Crit Care Med.* 2011;184(2):198-205.
12. Sullivan A, Hunt E, MacSharry J, Murphy DM. 'The Microbiome and the Pathophysiology of Asthma'. *Respiratory Research.* 2016;17(1):163.
13. Miller MR, Hankinson J, Brusasco V, et al. Standardisation of spirometry. *The European respiratory journal.* 2005;26(2):319-338.
14. Graham BL, Steenbruggen I, Miller MR, et al. Standardization of Spirometry 2019 Update. An Official American Thoracic Society and European Respiratory Society Technical Statement. *Am J Respir Crit Care Med.* 2019;200(8):e70-e88.
15. Juniper EF, O'Byrne PM, Guyatt GH, Ferrie PJ, King DR. Development and validation of a questionnaire to measure asthma control. *The European respiratory journal.* 1999;14(4):902-907.
16. Juniper EF, Svensson K, Mork AC, Stahl E. Measurement properties and interpretation of three shortened versions of the asthma control questionnaire. *Respir Med.* 2005;99(5):553-558.
17. Juniper EF, Bousquet J, Abetz L, Bateman ED. Identifying 'well-controlled' and 'not well-controlled' asthma using the Asthma Control Questionnaire. *Respir Med.* 2006;100(4):616-621.
18. Du Rand IA, Blaikley J, Booton R, et al. British Thoracic Society guideline for diagnostic flexible bronchoscopy in adults: accredited by NICE. *Thorax.* 2013;68 Suppl 1:i1-i44.
19. Principles of respiratory investigation. 2020; https://www.erswhitebook.org/chapters/principles-of-respiratory-investigation/, 2020.
20. Hunt EB, Ward C, Power S, et al. The Potential Role of Aspiration in the Asthmatic Airway. *Chest.* 2017;151(6):1272-1278.

21. *Global Strategy for Asthma Management and Prevention 2019 Update.* Global Initiative For Asthma2019.
22. *Pocket Guide for Asthma Management and Prevention 2019 Update.* Global Initiative For Asthma 2019.
23. DeSantis TZ, Hugenholtz P, Larsen N, et al. Greengenes, a Chimera-Checked 16S rRNA Gene Database and Workbench Compatible with ARB. *Applied and Environmental Microbiology.* 2006;72(7):5069-5072.
24. Ames SK, Hysom DA, Gardner SN, Lloyd GS, Gokhale MB, Allen JE. Scalable metagenomic taxonomy classification using a reference genome database. *Bioinformatics.* 2013;29(18):2253-2260.
25. Wood DE, Salzberg SL. Kraken: ultrafast metagenomic sequence classification using exact alignments. *Genome biology.* 2014;15(3):R46.
26. Kowalski CJ. On the Effects of Non-Normality on the Distribution of the Sample Product-Moment Correlation Coefficient. *Journal of the Royal Statistical Society Series C (Applied Statistics).* 1972;21(1):1-12.
27. Suzuki MT, Taylor LT, DeLong EF. Quantitative analysis of small-subunit rRNA genes in mixed microbial populations via 5'-nuclease assays. *Applied and environmental microbiology.* 2000;66(11):4605-4614.
28. John AE, Zhu YM, Brightling CE, Pang L, Knox AJ. Human airway smooth muscle cells from asthmatic individuals have CXCL8 hypersecretion due to increased NF-kappa B p65, C/EBP beta, and RNA polymerase II binding to the CXCL8 promoter. *J Immunol.* 2009;183(7):4682-4692.
29. Cazzola M, Matera MG, Rossi F. Bronchial hyperresponsiveness and bacterial respiratory infections. *Clinical therapeutics.* 1991;13(1):157-171.
30. Wood LG, Simpson JL, Hansbro PM, Gibson PG. Potentially pathogenic bacteria cultured from the sputum of stable asthmatics are associated with increased 8-isoprostane and airway neutrophilia. *Free radical research.* 2010;44(2):146-154.
31. Zhang Q, Illing R, Hui CK, et al. Bacteria in sputum of stable severe asthma and increased airway wall thickness. *Respiratory research.* 2012;13(1):35-35.
32. Bang DW, Yang HJ, Ryoo E, et al. Asthma and risk of non-respiratory tract infection: a population-based case–control study. *BMJ Open.* 2013;3(10):e003857.
33. Connelly CE, Sun Y, Carbonetti NH. Pertussis toxin exacerbates and prolongs airway inflammatory responses during Bordetella pertussis infection. *Infect Immun.* 2012;80(12):4317-4332.
34. Larsen JM. The immune response to Prevotella bacteria in chronic inflammatory disease. *Immunology.* 2017;151(4):363-374.
35. Charlson ES, Bittinger K, Haas AR, et al. Topographical continuity of bacterial populations in the healthy human respiratory tract. *Am J Respir Crit Care Med.* 2011;184(8):957-963.
36. Bajantri B, Venkatram S, Diaz-Fuentes G. Mycoplasma pneumoniae: A Potentially Severe Infection. *J Clin Med Res.* 2018;10(7):535-544.
37. Harju TH, Leinonen M, Nokso-Koivisto J, et al. Pathogenic bacteria and viruses in induced sputum or pharyngeal secretions of adults with stable asthma. *Thorax.* 2006;61(7):579-584.
38. Hahn DL, Dodge RW, Golubjatnikov R. Association of Chlamydia pneumoniae (strain TWAR) infection with wheezing, asthmatic bronchitis, and adult-onset asthma. *Jama.* 1991;266(2):225-230.
39. Whelan R, Kim C, Chen M, Leiter J, Grunstein MM, Hakonarson H. Role and regulation of interleukin-1 molecules in pro-asthmatic sensitised airway smooth muscle. *The European respiratory journal.* 2004;24(4):559-567.

40. Poynter ME, Irvin CG. Interleukin-6 as a biomarker for asthma: hype or is there something else? *The European respiratory journal.* 2016;48(4):979-981.
41. Hirsch AM, Valdés M. Micromonospora: An important microbe for biomedicine and potentially for biocontrol and biofuels. *Soil Biology and Biochemistry.* 2010;42(4):536-542.
42. King P. Haemophilus influenzae and the lung (Haemophilus and the lung). *Clin Transl Med.* 2012;1(1):10-10.
43. Guo X, Xia X, Tang R, Zhou J, Zhao H, Wang K. Development of a real-time PCR method for Firmicutes and Bacteroidetes in faeces and its application to quantify intestinal population of obese and lean pigs. *Letters in applied microbiology.* 2008;47(5):367-373.
44. Keisuke N, Hiroshi M, Hideaki I, Norimasa T. Simple and rapid detection of Rothia mucilaginosa by loop-mediated isothermal amplification method. *日本口腔検査学会雑誌 = Journal of Japanese Society for Evidence and the Dental Professional : JJSEDP.* 2018;10(1):44-52.
45. Rao AR, Laxova A, Farrell PM, Barbieri JT. Proteomic identification of OprL as a seromarker for initial diagnosis of Pseudomonas aeruginosa infection of patients with cystic fibrosis. *Journal of clinical microbiology.* 2009;47(8):2483-2488.
46. Le Gall F, Le Berre R, Rosec S, et al. Proposal of a quantitative PCR-based protocol for an optimal Pseudomonas aeruginosa detection in patients with cystic fibrosis. *BMC Microbiology.* 2013;13(1):143.
47. Chalmers NI, Palmer RJ, Cisar JO, Kolenbrander PE. Characterization of a Streptococcus sp.-Veillonella sp. Community Micromanipulated from Dental Plaque. *Journal of Bacteriology.* 2008;190(24):8145-8154.
48. Dolan Thomas J, Hatcher CP, Satterfield DA, et al. sodC-based real-time PCR for detection of Neisseria meningitidis. *PLoS ONE.* 2011;6(5):e19361-e19361.
49. Liu CM, Kachur S, Dwan MG, et al. FungiQuant: A broad-coverage fungal quantitative real-time PCR assay. *BMC Microbiology.* 2012;12(1):255.
50. Cuenca-Estrella M, Meije Y, Diaz-Pedroche C, et al. Value of serial quantification of fungal DNA by a real-time PCR-based technique for early diagnosis of invasive Aspergillosis in patients with febrile neutropenia. *J Clin Microbiol.* 2009;47(2):379-384.

Chapter 5

The Effect of Immunomodulation Therapy on the Microbiome of the Adult Asthmatic Lung

An investigation into the effects of anti-IgE (Omalizumab/Xolair) treatment on the lung microbiome in a subset of adult asthmatic patients

Author Contributions: Desmond Murphy, John MacSharry, Chris Ward and Paul O'Byrne were responsible for the study design and concept. Desmond Murphy was responsible for patient recruitment, clinical characterisation and sample acquisition. Deirdre Flynn was responsible for spirometry and FeNO testing and ACQ-7 questionnaires. Sample processing and study assays were primarily performed by Ashley Sullivan with contribution from Eoin Hunt, Susan Lapthorne, Bernie Crowley and John MacSharry. Statistical analysis was performed by the authors. Analysis and interpretation of data and manuscript preparation was performed by Ashley Sullivan, John MacSharry and Desmond Murphy. Manuscript approval were performed by all authors; Ashley Sullivan, Deirdre Flynn, Eoin Hunt, Chris Ward, Susan Lapthorne, Joseph Eustace, Bernie Crowley, Barry Plant, Paul O'Byrne, John MacSharry and Desmond Murphy.

1. Abstract 192
2. Introduction 193
3. Methods 195
    3.1. Patient recruitment 195
    3.2. Sample processing 196
    3.3. Microscopy 199
    3.4. DNA extraction 199
    3.5. DNA quantification 200
    3.6. Primers 201
    3.7. Quantitative polymerase chain reaction (qPCR) 202
    3.8. Cytokine measurement 203
    3.9. Post-Omalizumab treatment BAL and plasma cytokine analysis 204
    3.10. Statistical analyses 205
4. Results 206
    4.1. Patient demographics 206
    4.2. Microscopy and immune cell percentage counts 210
    4.3. BAL cytokine levels 213
    4.4. Plasma cytokine levels 214
    4.5. Molecular detection of microbial species 215
    4.6. Microbial and fungal species pre- and post- Omalizumab treatment 221
    4.7 Bacterial and fungal qPCR species correlations 226
5. Discussion 238
6. Supplementary 247
7. References 249

1. Abstract

Background: Severe asthma accounts for 5-10% of the asthma population, of which 50% of severe asthmatics can be classified as having allergic IgE mediated asthma. While inhaled corticosteroids (ICS) and long acting beta agonist (LABA) bronchodilators are effective in 90% of the asthma population, the remaining 10% require additional therapy to control their asthma. Omailzumab (Xolair®) is an effective add on therapy for the treatment of severe allergic IgE mediated asthma. Little is known as to its effect on the lung microbiome. Our aim was to elucidate potential differences in microbial diversity in a cohort of well-defined severe asthmatics after treatment with Omalizumab.

Methods: Nine well characterised severe asthmatic patients underwent bronchoscopy with broncholaveolar lavage (BAL) pre- and post- Omalizumab treatment. Cell differentials and cytokine levels were determined and DNA extraction performed. BAL cell pellet (CP, phagocytosed bacteria) and bacteria pellet (BP, free bacteria) derived DNA underwent qPCR to determine the presence and identity of microbes pre- and post- Omalizumab.

Results: Microbes such as *Prevotella, Veillonella, N. bacilliformis* and *M. catharralis* remained at consistent levels within the patient cohort irrespective of treatment. Following Omalizumab therapy there was an increased detection of *Bordetella* (CP) (0% to 89%), *C. pneumoniae* (CP) (11% to 89%) and (BP) (22% to 67%), *N. meningitidis* (CP) (22% to 100%) and (BP) (11% to 78%), *S. pneumoniae* (CP) (33% to 89%), *H. influenzae* (CP) (44% to 100%) and *S. aureus* (BP) (0% to 78%). A decrease in the detection of microbes such as *Bordetella* (BP) (56% to 22%), *M. pneumoniae* (BP) (44% to 22%) and *H. influenzae* (BP) (78% to 55%) was observed.

Conclusions: These findings suggest monoclonal asthma treatments such as Omalizumab may affect lung microbial diversity.

2. Introduction

Asthma has seen a staggering rise in prevalence in recent years and the burden is felt globally with more than 300 million people believed to be impacted by this chronic respiratory disorder which has reached epidemic proportions in the western world[1-6]. In order to control the symptoms of asthma, help improve the function of the lungs and aid in the reduction of exacerbations asthma patients are frequently prescribed inhaled corticosteroids (ICS) and/or a combination of long acting beta (β) agonist (LABA) bronchodilators. For the majority of patients this proves to be successful. However in about 10% of the asthmatic population further additional therapy is required in order for these patients to establish control of their asthma symptoms, improve lung function and reduce the number of exacerbations suffered[7]. It is believed that approximately 5-10% of asthma patients can be classified as severe asthmatics and it is believed that within this population over 50% can be classified as allergic IgE mediated asthmatics[8].

The phenotype of allergic asthma is intrinsically linked to the pathophysiology specific cellular and molecular mechanisms or endotypes, which include the exposure and response generated to an allergen to which the patient is sensitised[7] Complex multifactorial mechanisms including genetic and environmental factors are at play within individuals leading to sensitisation to an allergen or exogenous peptide. The exposure to this exogenous peptide results in responses typical of asthma and is often in association with other responses such as atopic eczema and systemic allergic responses[7]

As IgE plays such a pivotal role in allergic asthma therapies targeting IgE are of interest in the advancement of asthma care. Upon allergen exposure, circulating allergen specific IgE binds to the $F_{c\varepsilon}RI$ receptors, on immune cells such as mast cells and basophils, leading to crosslinking and release of inflammatory mediators[8]. Omalizumab (Xolair®) (Novartis-Genentech), the recombinant humanised monoclonal antibody, binds to the IgE antibody at the Fc portion which reduces the amount of free IgE, stops IgE from binding to inflammatory cell IgE receptors and

reduces IgE receptor ($F_{c\varepsilon}RI$ and $F_{c\varepsilon}RII$) density on effector cells, all of which prevent an inflammatory cascade from occurring[8,9]

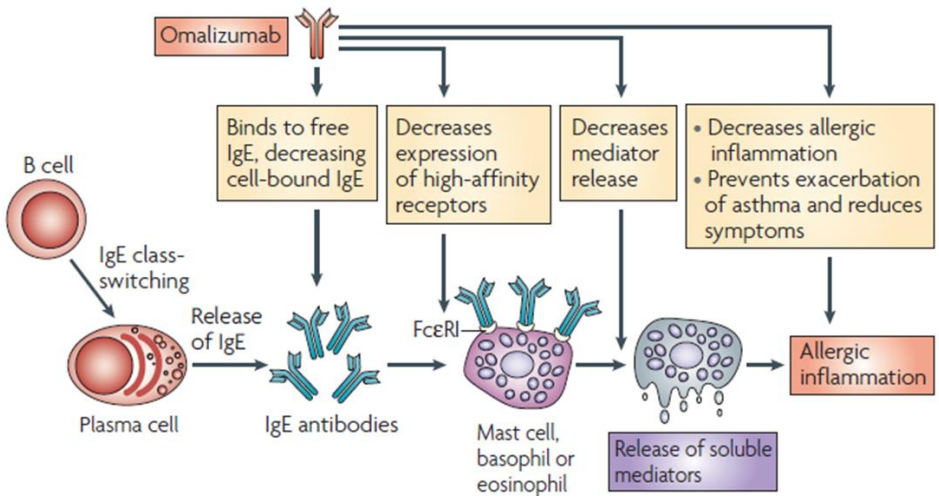


Figure 1. Mechanism of action of Omalizumab monoclonal antibody on allergic responses. The proposed effects of the monoclonal anti-IgE specific antibody Omalizumab on IgE levels, receptor binding and inflammatory mediators on the allergic inflammation cascade. Figure adapted from Holgate et al.,[10].

Omalizumab was approved by the US Food and Drug Administration (FDA) in 2003 in America, to be used subcutaneously in adults and adolescents over 12 years of age whose symptoms are not controlled by inhaled corticosteroids and who display moderate to severe persistent asthma, a positive skin prick test or *in vitro* reactivity to an allergen. In 2005 the European Medicines Agency (EMA) approved Omalizumab for use in Europe as an add on therapy for patients who require additional treatment to their prescribed high dose inhaled corticosteroids and/or long acting β agonists, which was amended in 2009 to include children aged 6 and over[7].

While long term clinical trials have demonstrated the validity of using Omalizumab as an add on therapy for the treatment of moderate to severe allergic asthma few studies have focused on the effects an anti-IgE human monoclonal antibody therapy may have on the lung microbiome present in adult asthmatics. In this study we hope to elucidate potential differences in microbial diversity after treatment with Omalizumab.

3. Methods

3.1. Patient recruitment

The study was approved by the Clinical Research Ethics Committee of the Cork Teaching Hospitals. Nine adult patients with a history of asthma (either documented change in FEV1 ≥12%/200ml with bronchodilator or a positive inhalation challenge) were recruited through a dedicated asthma clinic in a tertiary referral centre, Cork University Hospital by my clinical supervisor, Dr Des Murphy. Baseline bronchoscopy and bronchoscopy post Omalizumab treatment were performed by Dr Des Murphy.

Patients were scheduled for baseline bronchoscopy, with spirometry and ACQ-7 performed on the day of bronchoscopy. Written informed consent was obtained from patients on the day of bronchoscopy. Spirometry was performed according to ATS/ERS guidelines by research nurses from the Cork Clinical Research Facility – CCRF immediately prior to bronchoscopy[11]. Spirometry is a widely used pulmonary function test which provides an aid in the diagnosis of lung diseases, differentiating between obstructive and restrictive airway disorders and the monitoring of lung health[12]. Spirometry measures the maximal volume of air an individual can inspire and expire with maximal effort[12]. The Asthma Control Questionnaire (ACQ-7) was carried out by research nurses from the Cork Clinical Research Facility – CCRF on the day of bronchoscopy. The ACQ-7 consists of 7 items and all questions in the ACQ-7 are equally weighted and the mean of the 7 questions is used to calculate the patients ACQ-7 score which enables the measurement of patient asthma control[13].

Patients underwent bronchoscopy according to standard guidelines[14]. Flexible bronchoscopy using video assisted imaging was performed under conscious sedation with local anaesthetic applied topically to the vocal cords, trachea and endobronchial tree. Bronchoalveolar lavage (BAL) was achieved through the instillation of saline via the bronchoscope and this enabled the collection of specimen directly from the endobronchial lumen for subsequent cytological and

microbiological investigation. Bronchoalveolar lavage (BAL) was obtained as a standardised 180ml (3X60ml) sample from either the right middle lobe or lingula[15].

Patients were then prescribed the biologic anti-IgE humanised monoclonal antibody Omalizumab (Xolair®) which was delivered subcutaneously in a dedicated setting at Cork University Hospital. Patients were scheduled for follow up bronchoscopy with spirometry, ACQ-7 and bloods taken of the day of bronchoscopy. Spirometry was performed according to ATS/ERS guidelines[11]. Patients underwent bronchoscopy according to standard guidelines[14]. Bronchoalveolar lavage (BAL) was obtained as a standardised 180ml (3X60ml) sample from either the right middle lobe or lingula as we have previously described[15]. Further information with regards to asthmatic patient bronchoscopy and patient sample collection protocols can be found in *Chapter 2 Study Cohorts'*.

3.2. Sample processing

Patient BAL was processed on the day of bronchoscopy in a laminar flow hood and strict aseptic technique was observed. 5ml of the neat BAL was removed and aliquoted for downstream processing.

Microscopic processing

Approximately 500µl of neat BAL was aliquoted for microscopic examination and scoring of the BAL sample. To do this a Shandon CytoSpin 4 centrifuge (Thermo Scientific) was used and 200µl of BAL was required per microscope slide. Approximately 2-4 slides were prepared per patient. The samples were centrifuged at 400rpm for 2 minutes. The cytocentrifuge deposited the cells into a clearly defined area of the glass microscope slide while constructively flattening the cells to allow for clear nuclear presentation.

The slides then underwent differential staining using a Kwik Diff commercial staining kit (Thermo Scientific) which comprised of staining the slide with 3 reagents; methanol, xanthene dye in buffer salts and thiazine dye in buffer salts. The reagents were added to three separate staining jars and the microscope slides were added to a slide rack which was dipped into each of the reagents approximately 10-15 times, ensuring the excess reagent was allowed to drain back into the jar before moving to the next staining jar. Upon the completion of the final staining step the slides were rinsed under deionised water and slides were then air dried and cover slipped the following day using DPX histology mountant (Sigma Aldrich).

Slides were also stained using Gram staining; a differential stain for Gram positive and negative bacteria (Sigma Aldrich); whereby the slide was first flooded with crystal violet for 1 minute before washing the slide gently under an indirect stream of water for 2 seconds. The slide was then flooded with Gram's iodine for 1 minute before washing the stain as before. Acetone-alcohol decolouriser was used to flood the slide and allowed to sit for 15 seconds before the slide was then flooded with the counterstain safranin and allowed to sit for 1 minute before the slide was washed gently under an indirect stream of water. The slides were allowed to air dry and were cover slipped the following day using a DPX histology mountant (Sigma)

DNA collection

BAL was centrifuged at 500g for 10 minutes and the supernatant was removed and the remaining cell pellet was re-suspended creating the cell pellet fraction (CP) for future DNA isolation and analysis. The BAL supernatant was aliquoted into 2-5ml tubes for future analysis. BAL supernatant was also aliquoted into 10-20 x 2ml screw cap microcentrifuge tubes (Sarstedt) and centrifuged at 20,000g for 5 minutes in a microcentrifuge. The supernatant of which was aliquoted into 2ml tubes for future cell stimulations and the remaining pellets were re-suspended and pooled together creating the bacteria pellet fraction (BP) for future DNA isolation and analysis.

Blood cytokine collection

Blood samples were collected in serum specific red and yellow capped Vacuette tubes and plasma specific purple capped Vacuette tubes (Greiner Bio-One). The inner wall of the serum specific tube was coated with silica particles which activated the coagulation process and a specific separator gel at the base of the tube formed a stable barrier during centrifugation to enable the serum and blood cells to remain separate. The plasma specific Vacuette tube contained a coating of either K2EDTA or K3EDTA which acted as an anticoagulant by binding calcium ions to prevent the clotting cascade from taking place. Both tubes were centrifuged at 200g for 20 minutes and the serum and plasma was removed by pipetting and stored in screw-cap microcentrifuge tubes.

All BAL and blood isolated samples were stored at -80^{o}C for future processing and analyses.

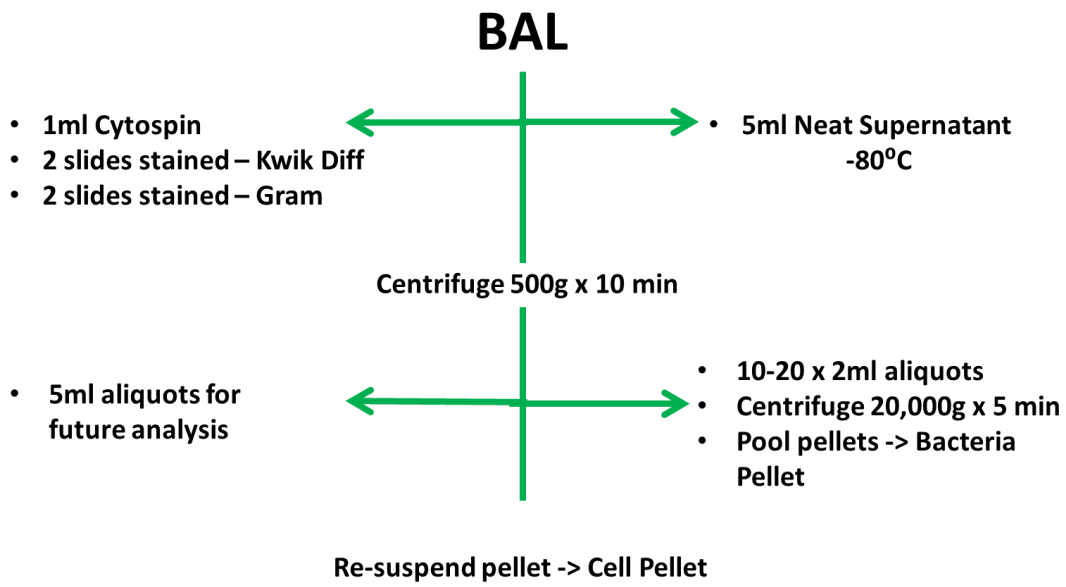


Figure 2. BAL sampling schematic. The processing steps undertaken with the patient BAL once received in the laboratory on day of bronchoscopy.

3.3. Microscopy

A differential cell count was performed on BAL cytospin slides, stained with the Kwik-Diff kit (Thermo-Fischer) using a light microscope (Olympus) and Olympus DP software. Immune cell percentage counts for Monocyte, Macrophage, Lymphocyte, Neutrophil and Eosinophil cells were performed in 10 random fields of view for two cytospin Kwik-Diff differentiated slides per patient. Microscopic observation of microbes present within macrophages and outside immune cells occurred while counting the immune cell percentages in certain patient cytospin slides.

3.4. DNA extraction

DNA extraction was carried out for both the BAL isolated bacteria pellet sample and the BAL isolated cell pellet sample in order to investigate if there was potential differences in bacteria free within the BAL sample and bacteria potentially within the macrophage cell population. The DNA isolation protocol was carried out the same way for both the BAL isolated bacteria pellet and the BAL isolated cell pellet.

As described above to reduce host cell DNA, BAL was centrifuged at 500g for 10 minutes, supernatant collected and centrifuged in 2ml screwcap microcentrifuge tubes at 20,000g for 5 minutes. The supernatant was then removed and the remaining bacteria pellets were recombined for DNA extraction. DNA extraction took place using a QIAamp UPC Pathogen Mini Kit (Qiagen, Manchester, UK). Patient bacteria pellet samples were centrifuged at 20,000g for 5 minutes, supernatant discarded and 500µl buffer ATL was used to re-suspend the pellet which was then added to a pathogen lysis tube containing silica beads and vortexed at 7000rpm for 1 minute using a MagNA Lyser machine. The tube was then centrifuged at 8000g for 30 seconds and supernatant removed to a fresh microcentrifuge tube without disrupting the silica beads. 40µl of Proteinase K was added and the tube was vortexed and incubated at 56^{o}C for 10 minutes. 200µl buffer APL2 then added to the sample, the tube was vortexed and incubated at 70^{o}C for 10 minutes. 300µl of ethanol was added to the lysate and the tube was pulse vortexed for 30 seconds and the lysate was then transferred to a mini spin

column placed in a collection tube and centrifuged at 6000g for 1 minute. This was repeated until all of the lysate had been transferred and passed through the mini spin column, discarding the filtrate after each spin. 600µl of Buffer APW1 was added to the mini spin column which was then centrifuged at 6000g for 1 minute, discarding the filtrate afterwards. 750µl of Buffer APW2 was transferred to the mini spin column which was then centrifuged at 20,000g for 3 minutes, transferring the mini spin column to a new collection tube and repeating centrifugation to eliminate buffer carryover. The mini spin column was transferred to a new collection tube and incubated at 56^{o}C for 3 minutes to ensure the membrane was dry and was then transferred to a new elution tube and 100µl of Buffer AVE was added to the centre of the membrane and incubated at room temperature for 1 minute before being centrifuged at 20,000g for 1 minute to elute the DNA. The isolated DNA samples were then stored at -20^{o}C for further downstream processing.

3.5. DNA quantification

DNA quantification was performed using a Qubit dsDNA High Sensitivity (HS) assay kit (Life Technologies, Thermo-Fischer) which consisted of Qubit dsDNA HS assay reagent (200X concentrate in DMSO), Qubit dsDNA HS dilution buffer, Qubit dsDNA HS standard #1 (0ng/µl in TE buffer) and Qubit dsDNA HS standard #2 (10ng/µl in TE buffer) and a Qubit 0.2 Fluorometer (Life Technologies, Thermo Fischer). The assay was highly selective for double-stranded (dsDNA) and was accurate for initial sample concentrations of 10pg/µl to 10ng/µl. Specialised Qubit thin wall clear 0.5ml assay tubes were sourced (Life Technologies, Thermo-Fischer) and the number of tubes required for the samples and two standards were labelled on the tube lid but not the side as this may interfere with the Qubit Fluorometer reading. The Qubit working solution was prepared by diluting the Qubit HS reagent 1:200 in Qubit dsDNA HS buffer using a clean plastic tube each time the Qubit working solution was prepared. For each sample the working solution consisted of 200µl of Qubit dsDNA HS buffer and 1µl of Qubit HS assay reagent. The working solution was prepared in batches of 5 reactions, which consisted of 1ml Qubit dsDNA HS buffer

and 5µl of Qubit HS assay reagent. For the standards 190µl of working solution was added to each of two standard tubes and 10µl of standard #1 and 10µl of standard #2 was added to the appropriate tube and the tubes were then vortexed for 3 seconds. In order to prepare for the DNA sample readings 198µl working solution was added to the individual pre-labelled assay tubes and to this 2µl of DNA sample was added to the appropriate assay tubes for a final volume of 200µl. Tubes were vortexed for 3 seconds ensuring no air bubbles were produced. The assay tubes were incubated at room temperature for 2 minutes. The dsDNA High Sensitivity programme was selected for on the Qubit Fluorometer machine and in order to calibrate the machine standard #1 was inserted into the sample chamber and was read before standard #2 was read in the same manner. Once calibration was complete the DNA samples were read. In order to standardise the DNA samples before further analyses such as qPCR and Whole Genome Sequencing, samples above 5ng/µl were diluted to 5ng/µl using molecular grade water.

3.6. Primers

Primers were designed through analyses of pre-designed validated primers in the literature, through the use of the 16S RNA gene database Greengenes[16] or through literature research to determine specific genes to the microorganism of interest and using this information to retrieve the sequence coding of that gene. All primers designed in house through Greengenes or gene sequences were formulated using the Universal Probe Library Assay Design Centre platform (Roche Life Science) by copying the sequence of interest to the platform, selecting for other organism and deselecting to automatically select for intron spanning assay. The platform then designed potential primers for the sequence of interest, ranking them by order of suitability. Primer sequences were analysed using the NCBI Blastn platform. Two primers sequences were then selected for each microorganism of interest and were ordered from Sigma.Aldrich (Ireland). Primers were centrifuged upon arrival to ensure the lyophilised pellet was at the bottom of the primer tube and primers were re-suspended with molecular grade water in accordance to individual primer

specification (µl for 100µM). Once re-suspended primers were vortexed and the left and right primer were recombined by adding 20µl of the left and 20µl of the right primer with 160µl of molecular grade water in a sterile 1.5ml tube. Primers were stored at -20^{o}C. Probes corresponding to the primers of interest were sourced from Universal Probe Library Probes (Roche Life Sciences) and were available within the laboratory. All primers were validated before use on the individual patient bacteria pellet and cell pellet DNA. See supplementary table 1 for primer sequences

3.7. Quantitative polymerase chain reaction (qPCR)

Primers were first validated on a pool of bacterial DNA isolated from the bacteria pellet (BP) and a pool of DNA isolated from the cell pellet (CP) undiluted, 1:10 diluted and 1:100 diluted and primers deemed to be viable by qPCR analyses were then carried forward and tested on the isolated bacteria and cell pellet DNA from each individual patient. qPCR was performed on extracted BAL BP and CP DNA pre and post Omalizumab (Xolair®) treatment to determine presence of Total Bacteria, Firmicutes, *Staphylococcus aureus*, *Streptococcus pneumoniae*, *Rothia*, *Micromonospora*, *Pseudomonas aeruginosa*, *Pseudomonas fluorescens*, *Escherichia*, *Bordetella*, *Prevotella*, *Veillonella*, *Mycoplasma pneumoniae*, *Chlamydophilia pneumoniae*, *Neisseria bacilliformis*, *Moraxella catarrhalis*, *Neisseria meningitidis* and *Haemophilus influenzae* and the fungal primers Fungi Quant and *Aspergillus fumigatus.* See supplementary table 1 for primer sequences.

qPCR's were performed using a 384 well plate layout and LightCycler Probes Master (Roche, Ireland) or LightCycler SYBR Green Master (Roche, Ireland) reagent mix, dependent on the use of hydrolysis probes or SYBR Green primer sets. Water NTCs (No Template Control) were used in each reaction in order to identify reaction set up contamination and to test for the propensity of primers to create primer dimers in the case of reactions which were carried out with SYBR Green Master. Reactions were performed on a LightCycler 480 machine (Roche, Ireland). qPCR conditions were as follows; pre-incubation at 50^{o}C for 2 minutes, ramp rate 4.8^{o}C/s and 95^{o}C

for 10 minutes, ramp rate 4.8^{o}C/s. Amplification at 95^{o}C for 10 seconds, ramp rate 4.8^{o}C/s, 60^{o}C for 45 seconds, ramp rate 2.5^{o}C/s and 75^{o}C for 1 second, ramp rate 4.8^{o}C for 45 cycles in total. A melt curve also occurred at 95^{o}C with a ramp rate of 0.11^{o}C/s for any primer which used LightCycler SYBR Green Master. A cooling stage then occurred at 40^{o}C, ramp rate 2^{o}C/s at the end of the process. Fluorescent readings were taken in single acquisition mode. The primers *Neisseria meningitidis*, *Streptococcus pneumoniae* and *Haemophilus influenzae* required a change in the acquisition temperature to 67^{o}C due to the nature of the primer sequences. All NTCs did not produce a product and melt curves produced clear peaks indicating that the products produced were not an artefact.

3.8. Cytokine measurement

BAL cytokines were analysed using a custom MSD proinflammatory panel 1 containing targets for Interleukin (IL)-1β, IL-4, IL-6, IL-8, IL-10, IL-13 and tumour necrosis factor (TNF)-α and a custom MSD cytokine panel 1 containing targets for IL-5 and IL-17A. Reagent preparation consisted of the following; calibrator standards were prepared by suspension of the lyophilised calibrator with 1000µl of the appropriate diluent (diluent 2 for proinflammatory panel 1 and diluent 43 for cytokine panel 1) and then transferring 100µl of the re-suspended calibrator with 300µl of appropriate diluent. This 4 fold serial dilution was repeated 5 additional times to generate 7 calibrators with the diluent alone used as a zero calibrator. Plasma samples were diluted as follows; 35µl of plasma and 35µl of appropriate diluent, while BAL samples were undiluted. A detection antibody solution was created for the proinflammatory panel by combining 60µl of each SULFO-TAG anti-human IL-1β, IL-4, IL-6, IL-8, IL-10, IL-13 IFN-γ and TNF-α antibody with 2520µl diluent 3 to bring to a final volume of 3000µl. A detection antibody solution for cytokine panel 1 consisted of 60µl each of SULFO-TAG Anti-human IL-5 and IL-17A with 2880µl of diluent 3 for a final volume of 3000µl. Wash buffer consisted of PBS and 0.05% Tween 20. Read buffer for each plate consisted of 10ml of Read Buffer T (4X) and 10ml of deionised water for a 2X working solution. Step 1 of the assay

involved washing the plate 3 times with 150µl/well wash buffer 50µl of prepared calibrators or samples was added per well, the plate was sealed before overnight incubation with shaking at 2-8^{o}C. Step 2 involved washing the plate a further 3 times with 150µl/well wash buffer before the addition of 25µl detection antibody solution to each well, the plate sealed and a two hour room temperature incubation with shaking occurred. Step 3; the plate was washed 3 times as before and 150µl of 2X Read Buffer T was added to each well before analysis of the plate using an electro-chemiluminescence QuickPlex SQ 120 imager from Meso Scale Discovery (Gaithersburg, MD, USA). The MSD lower limit of detection for the cytokines tested was as follows; IL-1β=0.04pg/ml, IL-4=0.02pg/ml, IL-5=0.22pg/ml, IL-6=0.06pg/ml, IL-8=0.04pg/ml, IL-10=0.03pg/ml, IL-13=0.24pg/ml, IL-17A=0.74pg/ml, TNF-α=0.04pg/ml and IFN-γ=0.20pg/ml.

3.9. Post-Omalizumab treatment BAL and plasma cytokine analysis

The cytokine levels present within the BAL and plasma samples, obtained at the follow-up bronchoscopy post-Omalizumab treatment, were analysed by RayBiotech (RayBiotech, Georgia, USA) using a custom RayBiotech Quantibody Human Cytokine Array containing targets for Interleukin (IL)-1β, IL-4,IL-5, IL-6, IL-8, IL-10, IL-13, IL-17A, tumour necrosis factor (TNF)-α and Interferon-(IFN)-γ. Testing was carried out according to in-house procedures at RayBiotech which consisted of the following protocol. A capture antibody was bound to a glass surface and incubation occurred with the BAL and plasma samples, which were diluted to a dilution factor of 2. After sample incubation was carried out a target cytokine was trapped to the glass solid surface. A second biotin-labelled detection antibody was added to recognise a specific epitope of the target cytokines. The cytokine-antibody-biotin complex was then visualised by the addition of a streptavidin-conjugated Cy3 equivalent dye and laser scanner. For cytokine quantification, the array specific cytokine standards with predetermined concentrations were implemented to generate standard curves. Through simultaneously running the standard cytokines and samples in each array using the described assay procedure it was possible to compare unknown samples

to the standard curve thus determining the cytokine concentration of the patient BAL and plasma samples. The RayBiotech Quantibody array limit of detection for the cytokines tested was as follows; IL-1β=1.8pg/ml, IL-4=4.7pg/ml, IL-5=3.4pg/ml, IL-6=4.2pg/ml, IL-8=46.8pg/ml, IL-10=1.3pg/ml, IL-13=0.7pg/ml, IL-17A=2.6pg/ml, TNF-α=225.9pg/ml and IFN-γ=56.0pg/ml.

3.10. Statistical analyses

Graph Pad Prism 8 software was used to perform all statistical analyses and to provide graphical representation of the data. All data was assessed using normality and lognormality tests and the Shapiro-Wilk test was applied to assess the normality of the data set.

Normally distributed data was presented as the mean ± standard deviation (SD) within the text and figures. Normally distributed data sets where both the X and Y values were normally distributed were analysed using Pearson correlation coefficient analysis. Data was considered to be statistically significant when $P<0.05$.

Non-normally distributed data was presented as median ± interquartile range (IQR) within the text and figures. Non-normally distributed data sets where both the X and Y values were not both normally distributed were analysed using the non-parametric Spearman correlation[17]. Data was considered to be statistically significant when $P<0.05$.

4. Results

4.1. Patient demographics

The cohort of nine adult asthma patients was stratified by both severity (GINA) and level of control (ACQ-7). The nine patients were grouped as GINA 5 as per normal guidelines for Omalizumab. The cohort consisted of 7 females and 2 males.

5 patients were in receipt of oral steroids (median 15; min 7.5 – max 20mg) at time of baseline bronchoscopy and 4 patients were in receipt of oral steroids (median 15; min 5 – max 15mg) at follow-up bronchoscopy displaying an overall reduction in the number of patients requiring oral steroids and a marked reduction in the prescribed mg volume per patients still in receipt of oral steroids.

Within the cohort at baseline bronchoscopy there was 1 current smoker and 4 ex-smokers while 4 patients had never smoked and this remained consistent at the follow-up bronchoscopy post-Omalizumab treatment.

All 9 patients were in receipt of inhaled corticosteroids at baseline bronchoscopy (median 1000 FDP; min 800 – max 1000 FDP) and at follow-up bronchoscopy (median 1000 FDP; min 800 – max 1000 FDP). The number of patients in receipt of inhaled corticosteroids (FDP) remained consistent at baseline and follow-up bronchoscopy and the inhaled corticosteroid (FDP) dose prescribed also remained the same for patients when comparing their prescribed ICS (FDP) dose at baseline bronchoscopy and at their follow-up bronchoscopy.

Within the cohort 4 patients lived within an urban setting and 5 patients lived within a rural setting.

Upon analysis of the patient ACQ-7 data it was revealed that at follow-up bronchoscopy those who underwent the ACQ-7 survey still considered themselves to be uncontrolled asthmatics (ACQ-7≥1.5) [mean (SD)] [2.9 (0.8)]; [median (IQR)] [2.9 (2.2-3.5)]. However when patients FEV-1 % predicted results were analysed at baseline [mean (SD)] [51.6 (22.7)] ; [median (IQR)] [49.0 (28.3-75.0)] and at follow-up bronchoscopy after patients were in receipt of the anti-IgE monoclonal antibody

Omalizumab there was an increase in the FEV-1 % predicted [mean (SD)] [54.9 (18.0)]; [median (IQR)] [59.0 (38.0-66.5)]. So while interpreting these spirometry results in accordance to Irish Thoracic Society guidelines the patients FEV_1/FVC ratio is below 70%, leading to a diagnosis of respiratory disorders such as asthma there is an improvement overall in the patients ability to exhale air quickly[18].

Patient BMI remained consistent at baseline bronchoscopy [mean (SD)] [33.5 (8.4)]; [median (IQR)] [35.1 (25.5-41.7)] and at follow-up bronchoscopy post Omalizumab treatment [mean (SD)] [33.5 (8.3)]; [median (IQR)] [34.4 (25.7-41.2)].

See Table 1 for patient demographics at baseline bronchoscopy and at follow up bronchoscopy post- Omalizumab treatment.

Table 1. Patient demographics. Patient demographics taken at baseline bronchoscopy and patient demographics taken at follow-up bronchoscopy after patients were prescribed the anti IgE biologic drug Omalizumab (Xolair). Note † ICS, Inhaled Corticosteroids; § FEV-1, Forced Expiratory Volume in the first second; ‡ FeNO, Forced exhaled Nitric Oxide; ¶ BMI, Body Mass Index; ¥ ACQ-7, Asthma Control Questionnaire.

		Baseline	**Treatment**
		Severe – GINA 5	Severe – GINA 5
Patients	n=9 (%)	9	9
Male		2 (22%)	2 (22%)
Female		7 (78%)	7 (78%)
Smoker	Current	1	1
	Ex-	4	4
	Never	4	4
Oral Steroids (mg)	Positive	5	4
	[Mean (SD)]	[13.5 (4.9)]	[12.5 (5)]
	[Median (IQR)]	[15 (8.8-17.5)]	[15 (7.5-15)]
ICS (FDP) †	Positive	9	9
	[Mean (SD)]	[933 (100)]	[933.3 (100)]
	[Median (IQR)]	[1000 (800-1000)]	[1000 (800-1000)]
FEV-1 (% Predicted) §	[Mean (SD)]	[51.6 (22.7)]	[54.9 (18)]
	[Median (IQR)]	[49 (28.3-75.0)]	[59 (38.0-66.5)]
FeNO (ppb) ‡	Readings from	0	3
	[Mean (SD)]		[14.3 (3.8)]
	[Median (IQR)]		[10 (10-17)]
BMI (kg/m^2) ¶	[Mean (SD)]	[33.5 (8.4)]	[33.3 (8.3)]
	[Median (IQR)]	[35.1 (22.5-41.7)]	[34.5 (25.7-41.2)]
ACQ-7 ¥	[Mean (SD)]		[2.9 (0.8)]
	[Median (IQR)]		[2.9 (2.2-3.5)]
IgE (KU/L)	[Mean (SD)]	[505 (683.1)]	
	[Median (IQR)]	[222 (85.5-697.0)]	
BAL Monocyte % count	[Mean (SD)]	[13.4 (6.7)]	[15.7 (10.4)]
	[Median (IQR)]	[14.5 (8.1-17.2)]	[19.0 (4.0-23.8)]
BAL Macrophage % count	[Mean (SD)]	[71.5 (18.4)]	[64.4 (21.4)]
	[Median (IQR)]	[79 (64.8-84.5)]	[74.8 (55.2-78.6)]
BAL Lymphocyte % count	[Mean (SD)]	[10.2 (12.1)]	[5.6 (5.6)]
	[Median (IQR)]	[4.2 (3.3-15.4)]	[3.7 (1.9-8.5)]
BAL Eosinophil % count	[Mean (SD)]	[1.2 (2.2)]	[1.1 (1.5)]
	[Median (IQR)]	[0.2 (0.1-1.4)]	[0.2 (0-3.7)]
BAL Neutrophil % count	[Mean (SD)]	[3.8 (4.0)]	[13.2 (20.6)]
	[Median (IQR)]	[3 (1.0-4.8)]	[7.8 (1-15)]

		Baseline	Treatment
IL-1β BAL (pg/ml)	[Mean (SD)]	[1.6 (1.7)]	[54.1 (161.4)]
	[Median (IQR)]	[1.2 (0.5-1.7)]	[0 (0-1)]
IL-4 BAL (pg/ml)	[Mean (SD)]	[0.02 (0.06)]	[3.2 (4.6)]
	[Median (IQR)]	[0 (0-0)]	[0 (0.0-9.1)]
IL-5 BAL (pg/ml)	[Mean (SD)]	[0 (0)]	[2.6 (3.7)]
	[Median (IQR)]	[0 (0-0)]	[0 (0.0-4.7)]
IL-6 BAL (pg/ml)	[Mean (SD)]	[1.8 (1.4)]	[10.8 (18.2)]
	[Median (IQR)]	[2.0 (0.5-2.5)]	[5.2 (0.0-12.6)]
IL-8 BAL (pg/ml)	[Mean (SD)]	[214 (232.3)]	[378.2 (773.5)]
	[Median (IQR)]	[92.5 (18.0-372.3)]	[133.3 (82.7-176.0)
IL-10 BAL (pg/ml)	[Mean (SD)]	[0 (0)]	[1 (1)]
	[Median (IQR)]	[0 (0-0)]	[1.1 (0.0-1.9)]
IL-13 BAL (pg/ml)	[Mean (SD)]	[12.9 (6.5)]	[9.1 (12.2)]
	[Median (IQR)]	[12.2 (7.2-17.5)]	[5.4 (3.2-10.0)]
IL-17 BAL (pg/ml)	[Mean (SD)]	[0 (0)]	[0 (0)]
	[Median (IQR)]	[0 (0-0)]	[0 (0-0)]
TNF-α BAL (pg/ml)	[Mean (SD)]	[0.7 (0.6)]	[1.7 (5.0)]
	[Median (IQR)]	[0.4 (0.4-1.3)]	[0 (0-0)]
Haemoglobin (HB) (g/L)	[Mean (SD)]	[13.3 (0.6)]	
	[Median (IQR)]	[13.6 (12.7-13.8)]	
White cell count (WBC) (10^9/L)	[Mean (SD)]	[8.1 (3.5)]	
	[Median (IQR)]	[7.6 (5.2-10.7)]	
Blood Lymphocyte count (10^9/L)	[Mean (SD)]	[2.3 (0.8)]	
	[Median (IQR)]	[2 (1.9-2.7)]	
Blood Eosinophil count (10^9/L)	[Mean (SD)]	[0.3 (0.3)]	
	[Median (IQR)]	[0.2 (0.1-0.6)]	
Blood Neutrophil count (10^9/L)	[Mean (SD)]	[5.2 (2.8)]	
	[Median (IQR)]	[4.1 (3.2-7.5)]	

4.2. Microscopy and immune cell percentage counts

BAL cell differential counts were carried out for all n=9 patient samples pre and post treatment with the humanised monoclonal antibody, Omalizumab, commercially know as Xolair (Figure 3 A-D). It was observed that macrophages were the dominant cell type irrespective of therapy (Figure 4 A-B), however differences in cell type percentages were observed within certain individual patients leading to the analyses of the immune cell percentage counts pre and post therapy at an individual level (Figure 5 A-I).

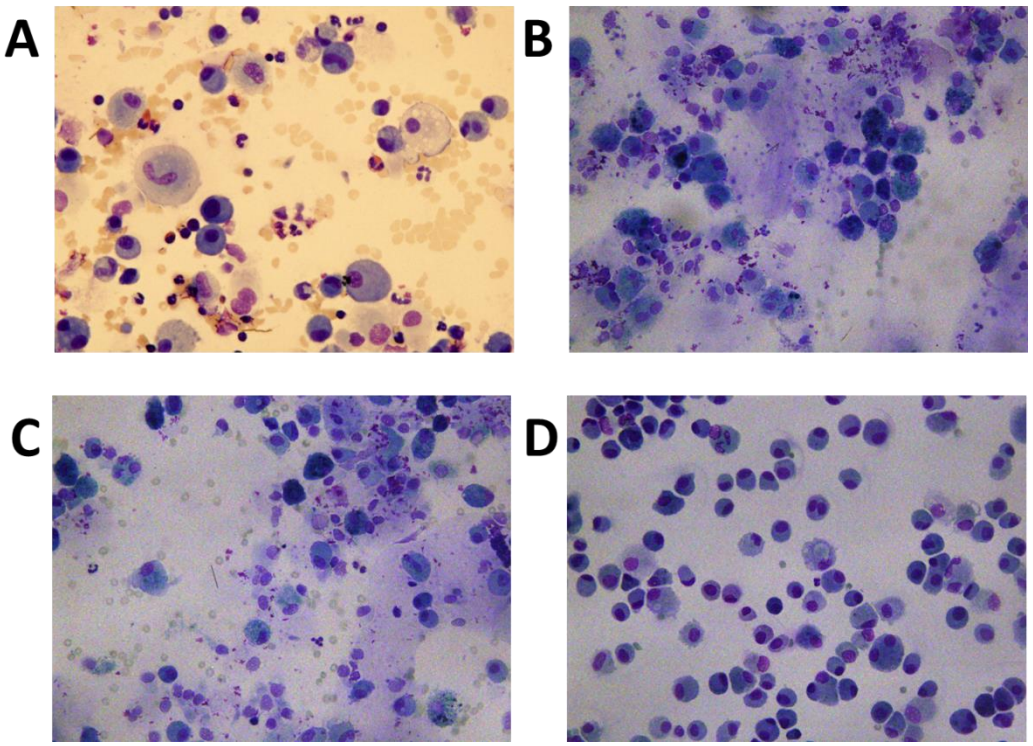


Figure 3. Microscopic examination of asthmatic patient bronchoalveolar lavage (BAL). (A-D) Representative microscopic images of patient BAL stained with a commercial Kwik Diff stain displaying the immune cells present within the BAL of the adult asthmatic cohort (A-D). (A) patient 1,60x magnification, (B) patient 2 40x magnification, (C) patient 2, 40X magnification, (D) patient 5, 40x magnification. All images were taken using an Olympus Microscope, with photos taken using Olympus DP software.

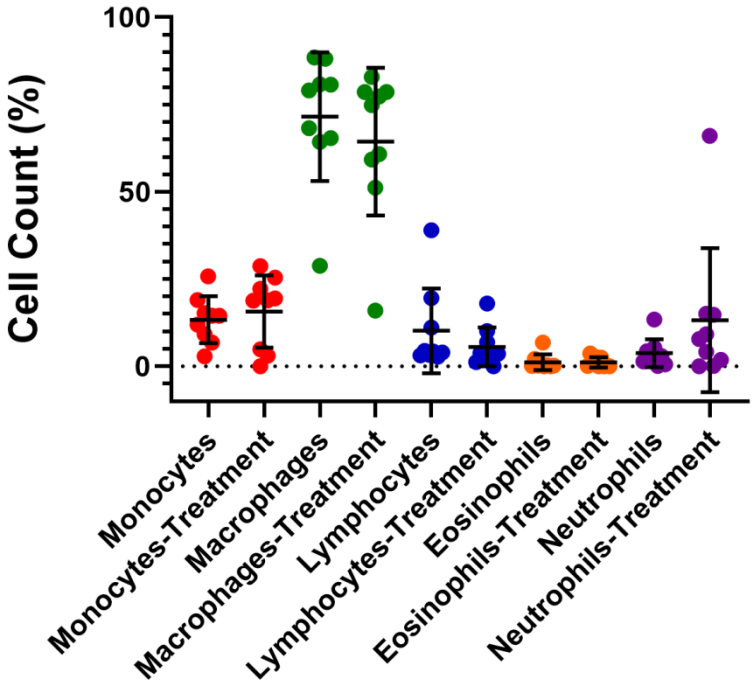


Figure 4. BAL cytospin counts pre- and post-Omalizumab treatment. BAL immune cell differential counts from the bronchoscopy patients prior to and post anti-IgE Omalizumab (Xolair) treatment. n=9

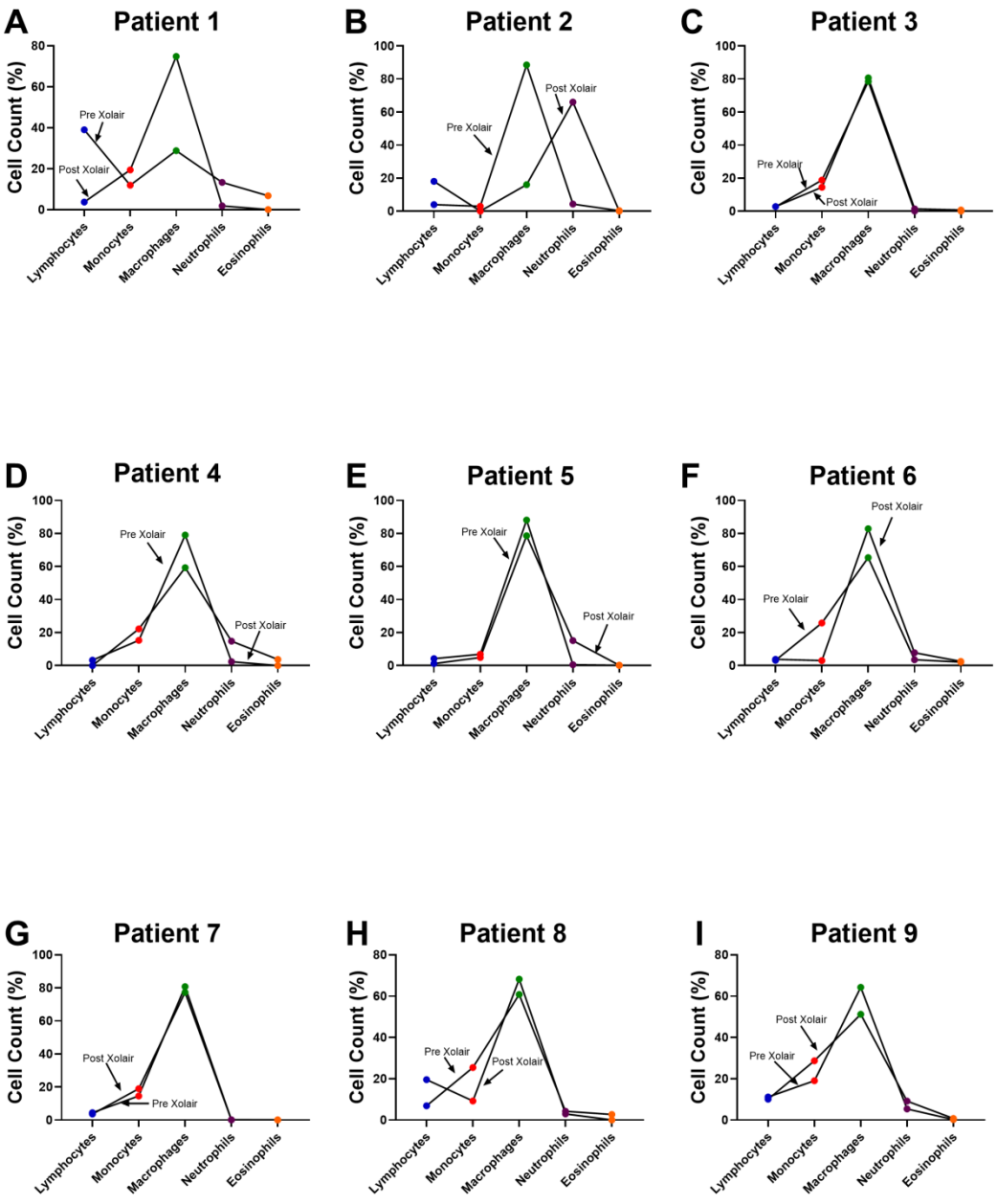


Figure 5. Immune cell differential counts pre- and post- Omalizumab (Xolair) therapy of individual patients. In order to further investigate the differences in cell type percentage counts observed within the cohort pre and post Omalizumab (Xolair) therapy the individual patient immune cell percentage count pre and post Omalizumab (Xolair) therapy were analysed.

4.3. BAL cytokine levels

Cytokines interleukin -1β (IL-1β), IL-4, IL-5, IL-6, IL-8, IL-10, IL-13, IL-17 and Tumour Necrosis Factor-α (TNF-α) were measured in BAL samples obtained at baseline bronchoscopy and at follow-up bronchoscopy after patients were in receipt of the anti-IgE monoclonal antibody, Omalizumab.

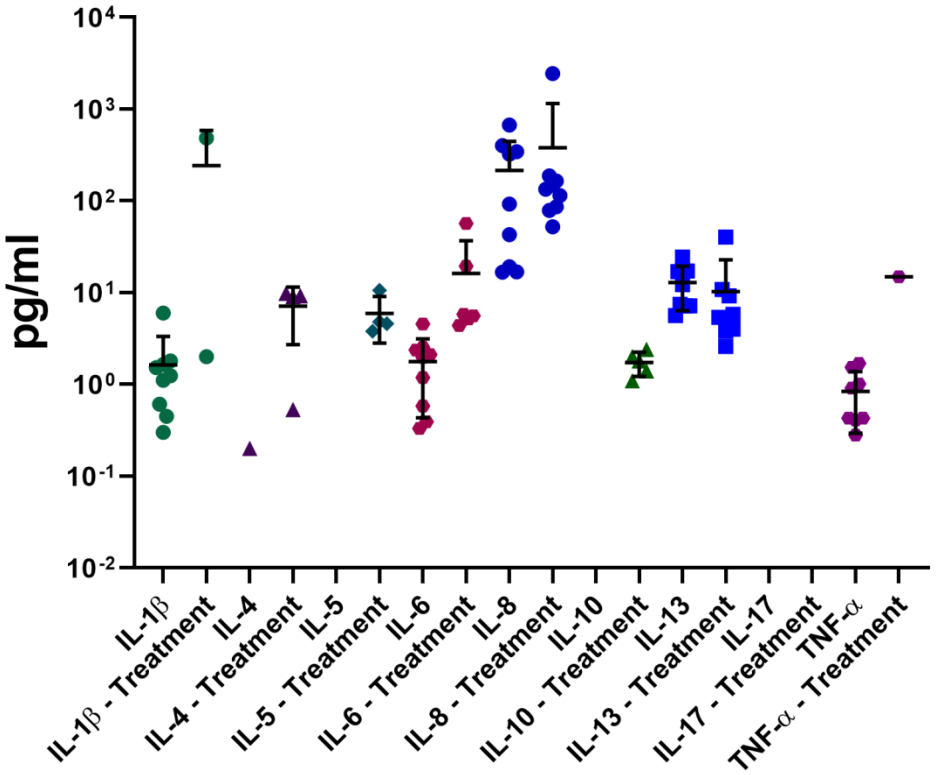


Figure 6. Cytokine levels in the patient BAL at baseline bronchoscopy and at follow-up bronchoscopy after patients received anti-IgE (Omalizumab) treatment. Measurement of secreted human cytokines Interleukin – 1β (IL-1β), IL-4, IL-5, IL-6, IL-8, IL-10, IL-13, IL-17 and Tumour Necrosis Factor – α (TNF-α) in patient BAL at baseline bronchoscopy occurred using an electro-chemiluminescence Quick Plex SQ 120 imager from Meso Scale Discovery (Gaithersburg, MD, USA) where antibodies labelled with SULFO-TAG™ reagents emitted light upon electrochemical stimulation. Measurement of secreted human cytokines Interleukin – 1β (IL-1β), IL-4, IL-5, IL-6, IL-8, IL-10, IL-13, IL-17 and Tumour Necrosis Factor – α (TNF-α) in patient BAL at follow-up bronchoscopy occurred using RayBiotech (Georgia, USA) custom human cytokine Quantibody arrays. [Mean (SD)] n=9.

4.4. Plasma cytokine levels

Cytokines interleukin -1β (IL-1β), IL-4, IL-5, IL-6, IL-8, IL-10, IL-13, IL-17 and Tumour Necrosis Factor-α (TNF-α) were measured in plasma samples obtained at follow-up bronchoscopy after patients were in receipt of the anti-IgE monoclonal antibody, Omalizumab.

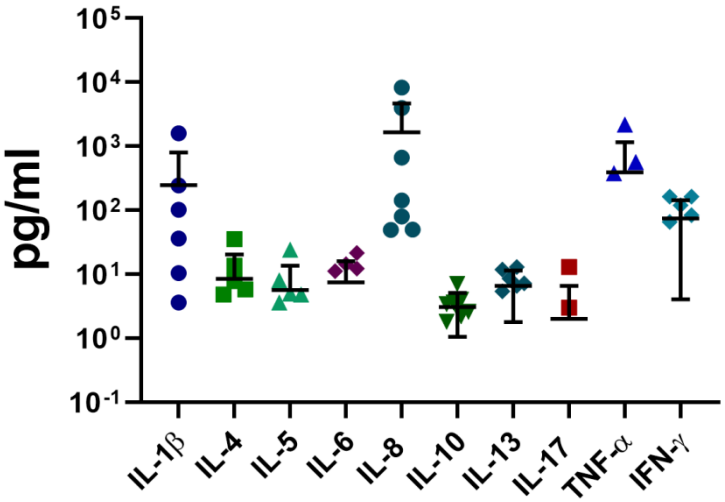


Figure 7. Cytokine levels in the patient plasma at follow-up bronchoscopy after patients received anti-IgE (Omalizumab) treatment. Measurement of secreted human cytokines Interleukin – 1β (IL-1β), IL-4, IL-5, IL-6, IL-8, IL-10, IL-13, IL-17, Tumour Necrosis Factor – α (TNF-α) and Interferon (IFN) –γ in patient plasma at follow-up bronchoscopy occurred using RayBiotech (Georgia, USA) custom human cytokine Quantibody arrays. [Mean (SD)] n=9.

4.5. Molecular detection of microbial species

Upon microscopic examination of the BAL samples, cytocentrifuged onto microscope slides and differentially stained using the commercial Kwik Diff stain it was observed that bacteria was present freely within the immune cell population but was also observable within the macrophages of certain patient samples (Figure 8). This lead to the differential centrifugation of the BAL sample during patient processing on the day of bronchoscopy leading to bacteria pellet (BP) and cell pellet (CP) specific BAL which was later analysed by qPCR for microbial species of interest.

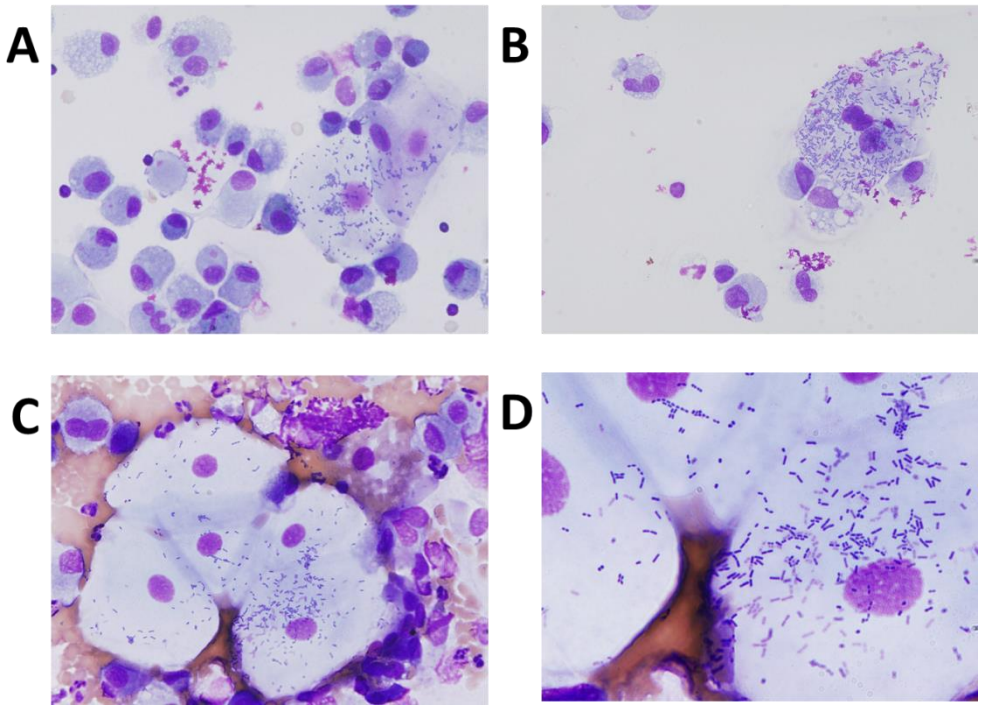


Figure 8. Presence of microbial species evident by microscopy. Immune cell percentage counts revealed that within the BAL of a number of patients there were observable bacterial species present (A-D). (A-B) 40x magnification, (C) 60x magnification, (D) 100x oil immersion magnification.

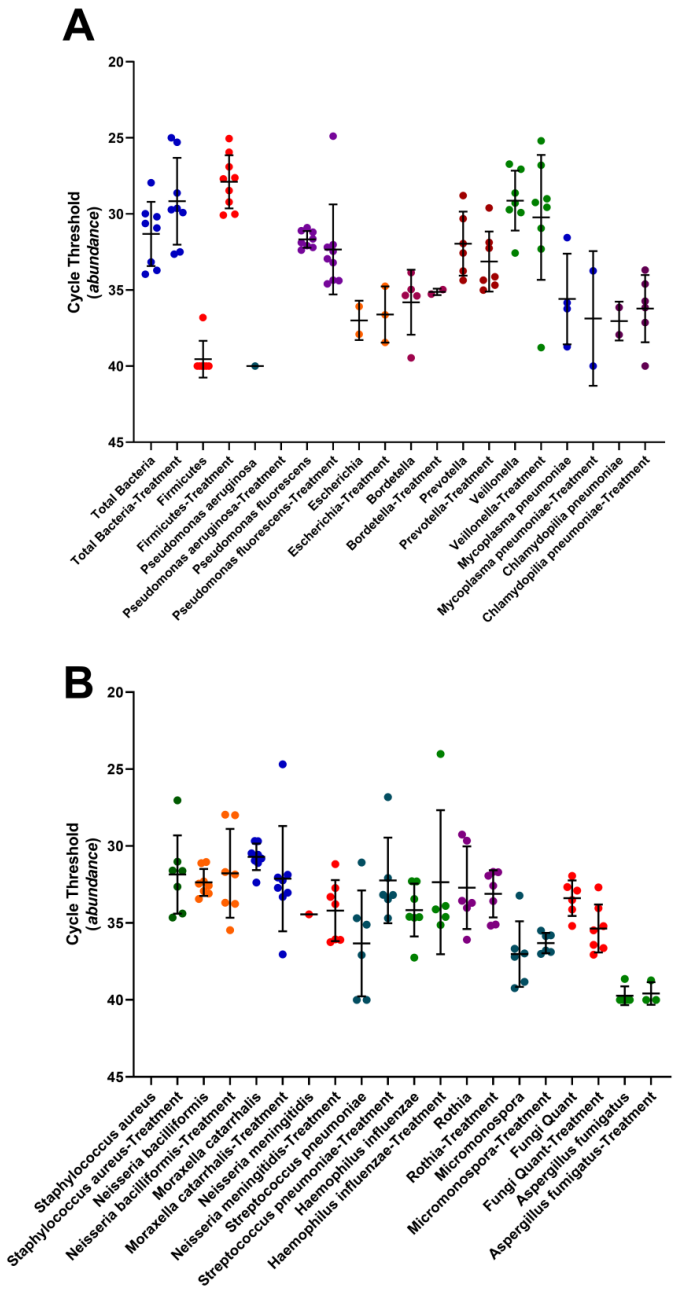


Figure 9 qPCR detection of bacteria and fungi species in asthmatic BAL bacteria pellet at baseline bronchoscopy and follow-up bronchoscopy post anti-IgE (Omalizumab) treatment. qPCR was performed on the extracted baseline bronchoscopy and post Omalizumab treatment bronchoscopy BAL bacteria pellet (BP) DNA (A-B).*Firmicutes* (P<0.0001), *S. pneumoniae* (P<0.05) and Fungi Quant (P<0.05) expression were significantly different at baseline and follow-up bronchoscopy using unpaired t-test with Welch's correction analysis. [Mean (SD)], n=9

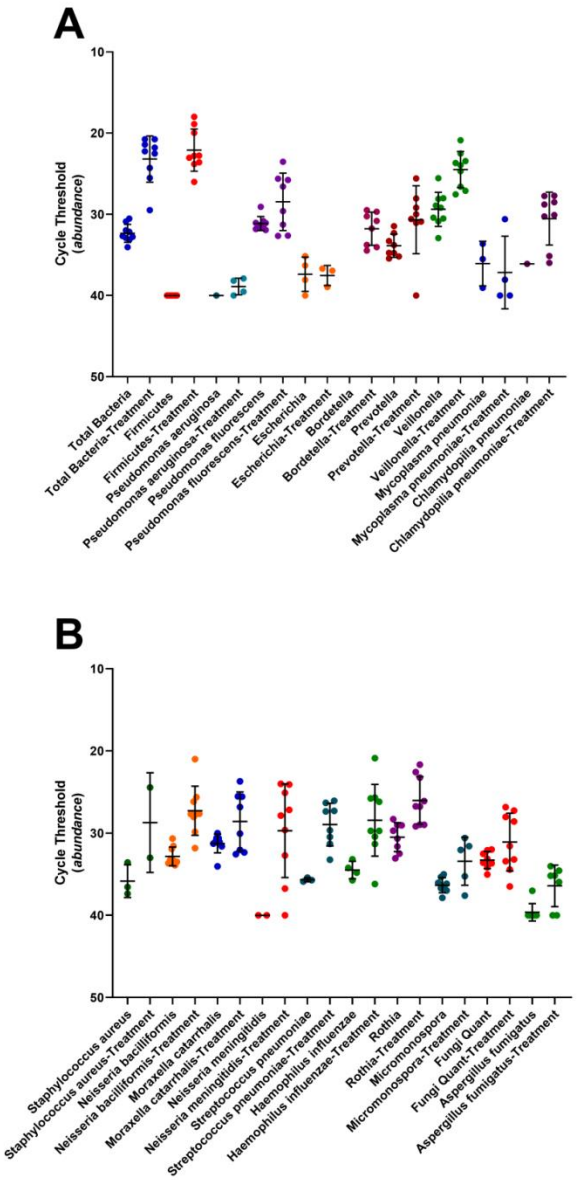


Figure 10. qPCR detection of bacteria and fungi species in the asthmatic BAL cell pellet (intracellular) fraction at baseline bronchoscopy and follow-up bronchoscopy post anti-IgE (Omalizumab) treatment. qPCR was performed on the extracted baseline bronchoscopy and post-Omalizumab treatment bronchoscopy BAL cell pellet (CP) DNA (A-B).When analysed using unpaired t-test with Welch's correction significance was found between the baseline and follow-up BAL CP samples with respect to the prevalence of Total bacteria (P<0.0001), Firmicutes (P<0.0001), *Veillonella* (P<0.0005), *N. bacilliformis* (P<0.0005), *N. meningitidis* (P<0.001), *S. pneumoniae* (P<0.0005), *H. influenzae* (P<0.005), *Rothia* (P<0.005) and *A. fumigatus* (P<0.05). [Mean (SD)], n=9.

Table 2. Molecular analysis of baseline and post-Omalizumab therapy BAL. Pre- and post- Omalizumab (Xolair) anti IgE therapy BAL bacteria pellet (BP) and cell pellet (CP) DNA samples were analysed by qPCR for a variety of bacterial and fungal targets of interest.

n=9		**Baseline**	**Treatment**
		Severe –GINA 5	
Total bacteria BP (CT)	Positive	8	8
	[Mean (SD)]	[31.3 (2.1)]	[29.2 (2.9)]
	[Median (IQR)]	[30.8 (30.0-33.6)]	[29.7 (26.1-31.9)]
Total bacteria CP (CT)	Positive	9	9
	[Mean (SD)]	[32.3 (1.1)]	[23.2 (2.8)]
	[Median (IQR)]	[32.7 (31.4-33.0)]	[22.2 (21.1-24.9)]
***Firmicutes* BP (CT)**	Positive	7	9
	[Mean (SD)]	[39.5 (1.2)]	[27.9 (1.8)]
	[Median (IQR)]	[40 (40-40)]	[27.7 (26.4-29.6)]
***Firmicutes* CP (CT)**	Positive	9	9
	[Mean (SD)]	[40 (0)]	[22.1 (2.6)]
	[Median (IQR)]	[40 (40-40)]	[22.8 (19.4-23.7)]
***Pseudomonas aeruginosa* BP (CT)**	Positive	1	0
	[Mean (SD)]	[40 (0)]	
	[Median (IQR)]	[40 (40-40)]	
***Pseudomonas aeruginosa* CP (CT)**	Positive	1	4
	[Mean (SD)]	[40 (0)]	[38.9 (1)]
	[Median (IQR)]	[40 (40-40)]	[38.9 (38-40)]
***Pseudomonas fluorescens* BP (CT)**	Positive	8	9
	[Mean (SD)]	[31.7 (0.6)]	[32.3 (3)]
	[Median (IQR)]	[31.8 (31.1-32.2)]	[33 (32.1-34.4)]
***Pseudomonas fluorescens* CP (CT)**	Positive	9	8
	[Mean (SD)]	[31.1 (0.9)]	[28.5 (3.5)]
	[Median (IQR)]	[31.3 (31.0-31.7)]	[28.1 (25.7-32.3)]
***Escherichia* BP (CT)**	Positive	2	3
	[Mean (SD)]	[37 (1.3)]	[36.6 (1.9)]
	[Median (IQR)]	[37 (36.1-37.9)]	[36.6 (34.8-38.4)]
***Escherichia* CP (CT)**	Positive	4	3
	[Mean (SD)]	[37.4 (2.1)]	[37.5 (1.2)]
	[Median (IQR)]	[37.2 (35.5-39.5)]	[37 (36.7-39)]
***Bordetella* BP (CT)**	Positive	5	2
	[Mean (SD)]	[35.8 (2.1)]	[35.1 (0.2)]
	[Median (IQR)]	[35.4 (34.4-37.4)]	[35.1 (35.0-35.3)]
***Bordetella* CP (CT)**	Positive	0	8
	[Mean (SD)]		[31.8 (2)]
	[Median (IQR)]		[31.3 (29.8-34.0)]
***Prevotella* BP (CT)**	Positive	6	7
	[Mean (SD)]	[32 (2.1)]	[33.1 (2)]
	[Median (IQR)]	[32.3 (29.9-33.9)]	[34.1 (31.9-34.7)]
***Prevotella* CP (CT)**	Positive	8	8
	[Mean (SD)]	[33.9 (1.4)]	[30.7 (4.2)]
	[Median (IQR)]	[34.3 (32.6-35.1)]	[30.3 (28.3-31.0)]
***Veillonella* BP (CT)**	Positive	7	8
	[Mean (SD)]	[29.1 (2)]	[30.2 (4.1)]
	[Median (IQR)]	[29.3 (27.1-29.9)]	[29.4 (27.4-32.0)]
***Veillonella* CP (CT)**	Positive	9	9
	[Mean (SD)]	[29.4 (2.1)]	[24.5 (2.2)]
	[Median (IQR)]	[29.2 (28.1-30.7)]	[24 (23.0-26.9)]

		Baseline	Treatment
***Mycoplasma pneumoniae* BP (CT)**	Positive	4	2
	[Mean (SD)]	[35.6 (3)]	[36.9 (4.4)]
	[Median (IQR)]	[36 (32.6-38.1)]	[36.9 (33.7-40)]
***Mycoplasma pneumoniae* CP (CT)**	Positive	3	4
	[Mean (SD)]	[36.1 (2.8)]	[37.2 (4.5)]
	[Median (IQR)]	[35.5 (33.6-39.1)]	[39.0 (32.5-40.0)]
***Chlamydophila pneumoniae* BP (CT)**	Positive	2	6
	[Mean (SD)]	[37 (1.3)]	[36.2 (2.2)]
	[Median (IQR)]	[37 (36.1-37.9)]	[36 (34.4-37.9)]
***Chlamydophila pneumoniae* CP (CT)**	Positive	1	8
	[Mean (SD)]	[36.1 (0)]	[30.5 (3.2)]
	[Median (IQR)]	[36.1 (36.1-36.1)]	[29.5 (27.9-33.9)]
***Staphylococcus aureus* BP (CT)**	Positive	0	7
	[Mean (SD)]		[31.9 (2.6)]
	[Median (IQR)]		[31.6 (31.0-34.4)]
***Staphylococcus aureus* CP (CT)**	Positive	3	2
	[Mean (SD)]	[35.8 (2)]	[28.7 (6.1)]
	[Median (IQR)]	[36.6 (33.6-37.4)]	[28.7 (24.4-33.0)]
***Neisseria bacilliformis* BP (CT)**	Positive	8	7
	[Mean (SD)]	[32.4 (0.9)]	[31.8 (2.9)]
	[Median (IQR)]	[32.5 (31.4-33.0)]	[31.8 (28.0-33.8)]
***Neisseria bacilliformis* CP (CT)**	Positive	9	9
	[Mean (SD)]	[32.8 (1.1)]	[27.3 (3)]
	[Median (IQR)]	[33.3 (31.7-33.6)]	[27.7 (25.9-28.9)]
***Moraxella catarrhalis* BP (CT)**	Positive	8	8
	[Mean (SD)]	[30.7 (0.9)]	[32.1 (3.4)]
	[Median (IQR)]	[30.7 (29.9-31.1)]	[32.5 (31.9-33.2)]
***Moraxella catarrhalis* CP (CT)**	Positive	9	8
	[Mean (SD)]	[31.3 (1.1)]	[28.6 (3.6)]
	[Median (IQR)]	[31.1 (30.6-31.4)]	[28.4 (25.5-32.3)]
***Neisseria meningitidis* BP (CT)**	Positive	1	7
	[Mean (SD)]	[34.4 (0)]	[34.2 (2)]
	[Median (IQR)]	[34.4 (34.4-34.4)]	[33.8 (32.7-36.1)]
***Neisseria meningitidis* CP (CT)**	Positive	2	9
	[Mean (SD)]	[40 (0)]	[29.7 (5.7)]
	[Median (IQR)]	[40 (40-40)]	[27.9 (24.6-34.7)]
***Streptococcus pneumoniae* BP (CT)**	Positive	6	6
	[Mean (SD)]	[36.3 (3.5)]	[32.2 (2.8)]
	[Median (IQR)]	[36.1 (33.8-40.0)]	[33.2 (30.8-33.8)]
***Streptococcus pneumoniae* CP (CT)**	Positive	3	8
	[Mean (SD)]	[35.7 (0.2)]	[29 (2.6)]
	[Median (IQR)]	[35.7 (35.4-35.9)]	[28.5 (26.6-31.1)]
***Haemophilus influenzae* BP (CT)**	Positive	7	5
	[Mean (SD)]	[34.2 (1.7)]	[32.4 (4.7)]
	[Median (IQR)]	[34.6 (32.3-34.7)]	[34.1 (29.0-34.9)]
***Haemophilus influenzae* CP (CT)**	Positive	4	9
	[Mean (SD)]	[34.5 (1.1)]	[28.4 (4.4)]
	[Median (IQR)]	[34.5 (33.5-35.5)]	[29.7 (25.7-30.9)]
***Rothia* BP (CT)**	Positive	6	7
	[Mean (SD)]	[32.7(2.7)]	[33.1 (1.5)]
	[Median (IQR)]	[33.6 (29.6-34.5)]	[32.6 (31.7-35.1)]
***Rothia* CP (CT)**	Positive	8	9
	[Mean (SD)]	[30.5 (1.8)]	[26 (2.9)]
	[Median (IQR)]	[30.2 (29.0-32.3)]	[26.7 (22.9-29.0)]
***Micromonospora* BP (CT)**	Positive	6	6
	[Mean (SD)]	[37 (2.1)]	[36.3 (0.7)]
	[Median (IQR)]	[37.1 (35.8-38.9)]	[36.3 (35.7-36.9)]

		Baseline	Treatment
***Micromonospora* CP (CT)**	Positive	8	5
	[Mean (SD)]	[36.3 (0.9)]	[33.4 (2.9)]
	[Median (IQR)]	[36.4 (35.5-36.9)]	[32 (31.1-36.4)]
Fungi Quant BP (CT)	Positive	6	7
	[Mean (SD)]	[33.4 (1.2)]	[35.4 (1.6)]
	[Median (IQR)]	[33.2 (32.5-34.4)]	[35.5 (34.0-36.6)]
Fungi Quant CP (CT)	Positive	8	9
	[Mean (SD)]	[33.3 (1.1)]	[31.1 (3.5)]
	[Median (IQR)]	[33.4 (32.2-34.1)]	[31.6 (27.6-33.9)]
***Aspergillus fumigatus* BP (CT)**	Positive	5	3
	[Mean (SD)]	(39.7 (0.6)]	[39.6 (0.7)]
	[Median (IQR)]	[40 (39.3-40.0)	[40 (38.7-40)]
***Aspergillus fumigatus* CP (CT)**	Positive	8	7
	[Mean (SD)]	[39.6 (1.1)]	[36.4 (2.5)]
	[Median (IQR)]	[40 (40-40)]	[35.2 (34.6-40.0)]

4.6. Microbial and fungal species pre- and post- Omalizumab treatment

At baseline bronchoscopy, pre-Omalizumab treatment, qPCR analyses revealed that 89% of patients had detectable bacteria, using the primer Total Bacteria, within the bacteria pellet (BP) BAL sample. At follow-up bronchoscopy, post Omalizumab treatment, qPCR analyses revealed that 89% of patients had detectable bacteria within the bacteria pellet (BP) BAL sample. 100% of patients had detectable bacteria within the BAL cell pellet (CP) sample using the bacterial specific Total Bacteria primer at baseline bronchoscopy and post-Omalizumab bronchoscopy. When analysed using unpaired t-test with Welch's correction significance was found between the baseline and follow-up BAL CP samples with respect to the prevalence of Total Bacteria (P<0.0001).

Firmicutes were detectable within 78% of BAL bacteria pellet samples prior to Omalizumab treatment while post-Omalizumab 100% of patients had detectable Firmicutes. The prevalence of BAL bacteria pellet *Firmicutes* (P<0.0001) was significantly different at baseline and follow-up bronchoscopy using unpaired t-test with Welch's correction analysis. Within the BAL cell pellet samples 100% of patients has detectable levels of Firmicutes both prior to and post-Omalizumab treatment. When analysed using unpaired t-test with Welch's correction significance was found between the baseline and follow-up BAL CP samples with respect to the prevalence of Firmicutes (P<0.0001).

Escherichia was detectable in 22% of patient BP samples pre-Omalizumab treatment and was detectable in 33% of patient BP samples post-Omalizumab treatment. 44% of patient CP samples had detectable levels of *Escherichia* pre-Omalizumab treatment while 33% of patient CP samples had detectable levels post-Omalizumab treatment.

Bordetella was detectable in 56% of patient BP samples prior to Omalizumab treatment while it was only detectable within 22% of patient BP samples post-Omalizumab treatment. While *Bordetella* was undetectable within the patient CP samples prior to Omalizumab treatment, post-Omalizumab treatment 89% of patients had detectable levels of *Bordetella* within the BAL CP samples.

Prevotella was detectable within 67% of patient BP samples prior to Omalizumab treatment and within 78% of patient BP samples post-Omalizumab treatment. 89% of patient CP samples had detectable *Prevotella* both prior to and post-Omalizumab treatment.

Veillonella was detectable within 78% of patient BP samples prior to Omalizumab treatment and within 89% of BP samples post-Omalizumab treatment. 100% of patient CP samples had detectable levels of *Veillonella* both prior to and post-Omalizumab treatment. When analysed using unpaired t-test with Welch's correction significance was found between the baseline and follow-up BAL CP samples with respect to the prevalence of *Veillonella* ($P<0.0005$).

Rothia was detectable within 67% of patient BP samples prior to Omalizumab treatment and within 78% of BP samples post-Omalizumab treatment. 89% of patient CP samples had detectable levels of *Rothia* prior to Omalizumab treatment while 100% had detectable levels post-Omalizumab. When analysed using unpaired t-test with Welch's correction significance was found between the baseline and follow-up BAL CP samples with respect to the prevalence of *Rothia* ($P<0.005$).

Micromonospora was detectable within 67% of patient BP samples both prior to and post-Omalizumab treatment. 89% of patient CP samples had detectable *Micromonospora* prior to Omalizumab treatment while 55% of patient CP samples had detectable levels post-Omalizumab treatment.

The ITS fungal primer Fungi Quant for the detection of Fungal species was detectable within 67% of patient BP samples prior to Omalizumab treatment and within 78% post-Omalizumab treatment. The prevalence of Fungi Quant ($P<0.05$) within the BAL BP samples was significantly different at baseline and follow-up bronchoscopy using unpaired t-test with Welch's correction analysis. 89% of patient CP samples had detectable fungi prior to Omalizumab treatment while 100% had detectable levels within their CP sample post-Omalizumab treatment.

11% had detectable *Pseudomonas aeruginosa* within bacteria pellet prior to Omalizumab treatment, however, post-Omalizumab treatment *P. aeruginosa* was

undetectable within the patient BP samples. While 11% of patients had detectable levels of *P. aeruginosa* within their CP sample prior to Omalizumab treatment 44% had detectable levels post-Omalizumab treatment.

89% of patient BP samples taken prior to Omalizumab treatment had detectable *P. fluorescens* while 100% had detectable levels post-Omalizumab treatment. *P. fluorescens* was detectable in 100% of patient BAL cell pellet samples prior to Omalizumab treatment and within 87% post-Omalizumab treatment.

Mycoplasma pneumoniae was detectable in 44% of patient BP samples prior to Omalizumab treatment and within 22% of BP samples post-Omalizumab treatment. 33% of patient CP samples had detectable levels of *M. pneumoniae* prior to Omalizumab treatment while 44% of patient CP samples had detectable levels post-Omalizumab treatment.

Chlamydophilia pneumoniae was detectable within 22% of patient BP samples prior to Omalizumab treatment while post-Omalizumab treatment *C. pneumoniae* was detectable within 67% of patient BP samples. 11% of patient CP samples had detectable levels prior to Omalizumab treatment while 89% of patient CP samples had detectable levels of *C. pneumoniae* post-Omalizumab treatment.

Staphylococcus aureus was undetectable within the patient BP samples prior to Omalizumab treatment, however, post-Omalizumab treatment 79% of patients had detectable levels within their BAL bacteria pellet sample. 33% of patients had detectable *S. aureus* within their CP sample prior to Omalizumab treatment while post-Omalizumab treatment 22% of patients had detectable levels within their CP sample.

89% of patients had detectable *Neisseria bacilliformis* detectable within the BP sample prior to Omalizumab treatment while it was detectable in 78% of patient BP samples post-Omalizumab treatment. 100% of patients had detectable levels of *N. bacilliformis* both prior to and post-Omalizumab treatment within their CP sample. When analysed using unpaired t-test with Welch's correction significance was

found between the baseline and follow-up BAL CP samples with respect to the prevalence of *N. bacilliformis* (*P*<0.0005).

Moraxella catarrhalis was detectable within 89% of patient BP samples prior to Omalizumab treatment and within 89% of patient BP samples post-Omalizumab treatment. 100% of patient CP samples had detectable levels of *M. catarrhalis* prior to Omalizumab treatment while 89% had detectable levels post-Omalizumab treatment.

Neisseria meningitidis was detectable within 11% of patient BP samples prior to Omalizumab treatment, however post-Omalizumab treatment, *N. menigitidis* was detectable within 78% of patients BP samples. Prior to Omalizumab treatment 22% of patient CP samples had detectable levels of *N. meningitidis* while post-Omalizumab treatment 100% of patients had detectable levels within their BAL CP sample. When analysed using unpaired t-test with Welch's correction significance was found between the baseline and follow-up BAL CP samples with respect to the prevalence of *N. meningitidis* (*P*<0.001).

Streptococcus pneumoniae was detectable within 67% of patient BP samples both prior to and post-Omalizumab treatment. The prevalence of bacteria pellet *Streptococcus pneumoniae* (*P*<0.05) was significantly different at baseline and follow-up bronchoscopy using unpaired t-test with Welch's correction analysis. While *S. pneumoniae* was detectable in only 33% of patient CP samples prior to Omalizumab treatment, post-Omalizumab treatment 89% of patients had detectable levels within their CP sample. When analysed using unpaired t-test with Welch's correction significance was found between the baseline and follow-up BAL CP samples with respect to the prevalence of *S. pneumoniae* (*P*<0.0005).

Haemophilus influenzae was detectable within 78% of patient BP samples prior to Omalizumab treatment and within 55% of patient BP samples prior to Omalizumab treatment. 44% of patient CP samples had detectable *H. influenzae* levels prior to Omalizumab treatment while 100% of patients had detectable levels within their CP sample post-Omalizumab treatment. When analysed using unpaired t-test with

Welch's correction significance was found between the baseline and follow-up BAL CP samples with respect to the prevalence *H. influenzae* (P<0.005).

Looking specifically at the fungi *Aspergillus fumigatus* 56% of patients BP samples had detectable levels prior to Omalizumab treatment while 33% had detectable levels post-Omalizumab treatment. 89% of patient CP samples had detectable levels of *A. fumigatus* prior to receiving Omalizumab treatment while 78% of patients had detectable levels within their CP sample post-Omalizumab treatment. When analysed using unpaired t-test with Welch's correction significance was found between the baseline and follow-up BAL CP samples with respect to the prevalence of *A. fumigatus* (P<0.05).

4.7 Bacterial and fungal qPCR species correlations

Statistical analyses of qPCR results in correlation to immune cell percentage counts, total IgE, BMI, FEV-1, FeNo, Oral steroids, Inhaled corticosteroids, Haemoglobin (Hb), White Cell Count (WBC), Blood lymphocyte, neutrophil and eosinophil counts and cytokine levels where relevant occurred. Statistical analyses were carried out as described in *3.10. Statistical analyses.*

Upon the examination of patients' baseline bronchoscopy BAL qPCR data and patient demographics at baseline bronchoscopy a number of correlations were determined. Within the baseline analyses the presence of Total bacteria (BP) correlated with BAL macrophage percentage counts (P<0.01; r_s=-0.8571). Total Bacteria (BP) correlated with BAL neutrophil percentage counts (P<0.05; r_s=0.8333). See Figure 11 (A-B). *Escherichia* (CP) correlated with FEV-1 (P<0.05; r=-0.9540). See Figure 11 (C). *Bordetella* (BP) correlated with BAL IL-6 levels (P<0.05; r=0.8793). See Figure 11 (D). *Prevotella* (BP) levels correlated with BAL lymphocyte percentage counts (P<0.05; r_s=-0.8857). See Figure 11 (E). *Prevotella* (CP) correlated with BAL neutrophil percentage counts (P<0.05; r_s=-0.8333). See Figure 11 (F).

The presence of *Prevotella* (CP) correlated with blood eosinophil counts (P<0.0005; r=-0.9968). See Figure 12 (A). The presence of *Prevotella* (CP) correlated with the presence of the cytokine IL-1β in the BAL (P<0.005; r_s=-0.9048). See Figure 12 (B). The presence of *Rothia* (BP) correlated with FEV-1 (P<0.05; r=0.9110). See Figure 12 (C). *Micromonospora* (BP) correlated with total blood IgE levels (KU/L) (P<0.05; r_s=0.8857). See Figure 12 (D). Fungal presence as determined by the qPCR primer Fungi Quant correlated with total oral steroids (mg) (P<0.05; r=-0.9990). See Figure 12 (E).

Pseudomonas fluorescens (BP) (P<0.05; r=0.9250) presence and *Pseudomonas fluorescens* (CP) (P<0.05, r_s=0.8407) presence correlated with blood eosinophil counts (10^9/L). See Figure 13 (A-B). *Pseudomonas fluorescens* (BP) presence correlated with the presence of the cytokine IL-6 in the BAL (P<0.05; r=0.7398). See Figure 13 (C). *Pseudomonas fluorescens* (CP) presence correlated with the presence of the cytokine IL-8 in the BAL (P<0.05; r_s=0.8167). See Figure 13 (D). *Pseudomonas*

fluorescens (CP) presence correlated with the presence of the cytokine TNF-α in the BAL (P<0.05; r_s=0.7364). See Figure 13 (E). *Mycoplasma pneumoniae* (CP) presence correlated with BAL monocyte percentage counts (P<0.05; r=-0.9975). See Figure 13 (F).

The presence of *Neisseria bacilliformis* (CP) correlated with total blood IgE levels (P<0.05; r_s=0.7667). See Figure 14 (A). *Moraxella catarrhalis* (BP) presence correlated with the presence of the cytokine IL-8 in the BAL (P<0.05; r=0.7116). See Figure 14 (B).The presence of *Streptococcus pneumoniae* (CP) correlated with patient BMI levels (P<0.05; r=0.9996). See Figure 14 (C).

The presence of *Haemophilus influenzae* (BP) correlated with patient BMI (P<0.005; r=-0.9425) while *Haemophilus influenzae* (CP) correlated with patient BMI (P<0.05; r=0.9848). See Figure 15 (A-B). The presence of *Haemophilus influenzae* (BP) correlated with the presence of the cytokine IL-1β in the BAL (P<0.05; r_s=-0.8214). See Figure 15 (C).The presence of *Haemophilus influenzae* (BP) correlated with the presence of the cytokine TNF-α in the BAL (P<0.05; r=-0.8021). See Figure 15 (D).

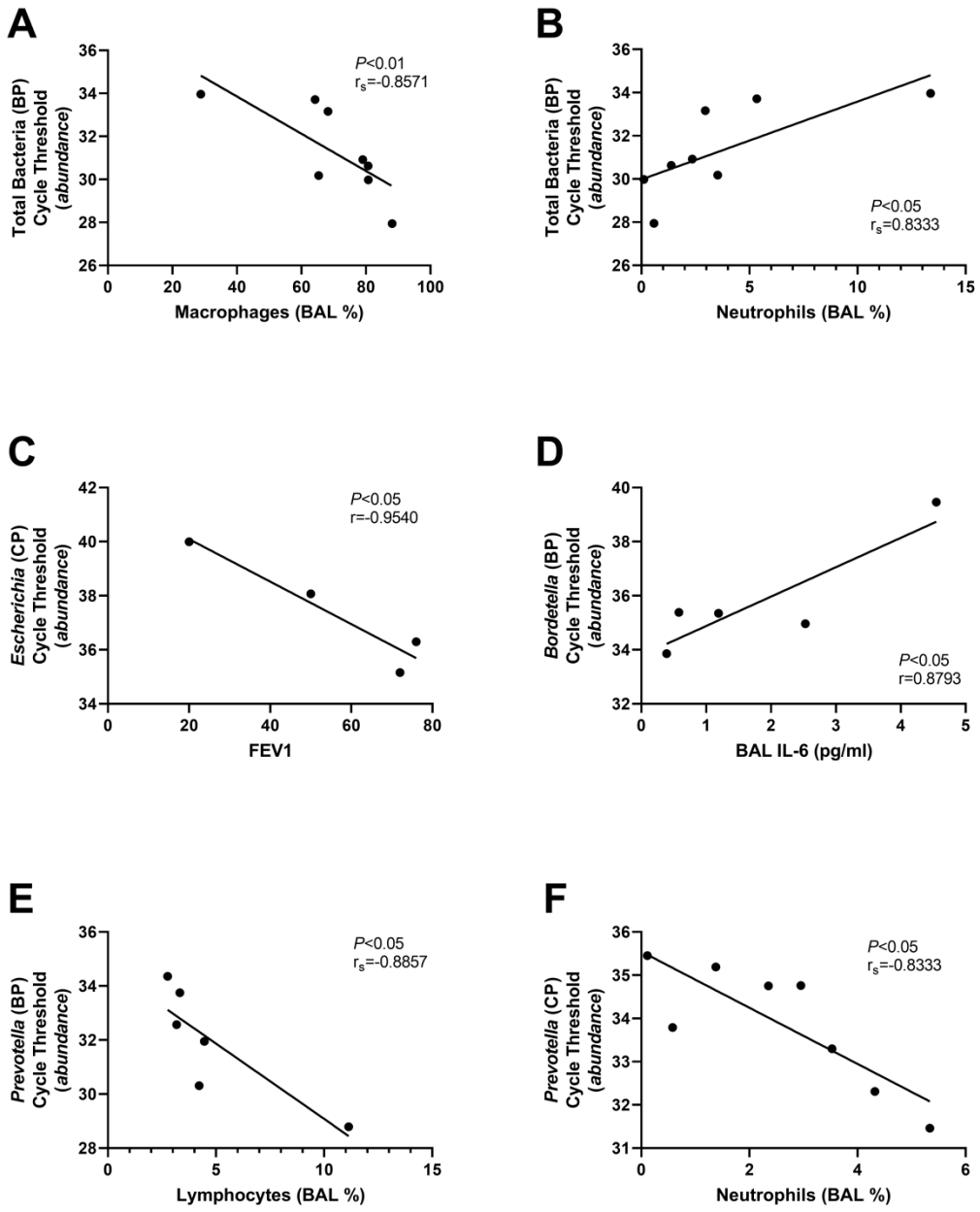


Figure 11. Baseline BAL qPCR correlations. (A) Total bacteria (BP) levels correlated with BAL macrophage percentage counts (P<0.01; r_s=-0.8571). (B) Total Bacteria (BP) correlated with BAL neutrophil percentage counts (P<0.05; r_s=0.8333). (C) *Escherichia* (CP) correlated with FEV-1 (P<0.05; r=-0.9540). (D) *Bordetella* (BP) correlated with BAL IL-6 levels (P<0.05; r=0.8793). (E) *Prevotella* (BP) levels correlated with BAL lymphocyte percentage counts (P<0.05; r_s=-0.8857). (F) *Prevotella* (CP) levels correlated with BAL neutrophil percentage counts (P<0.05; r_s=-0.8333).

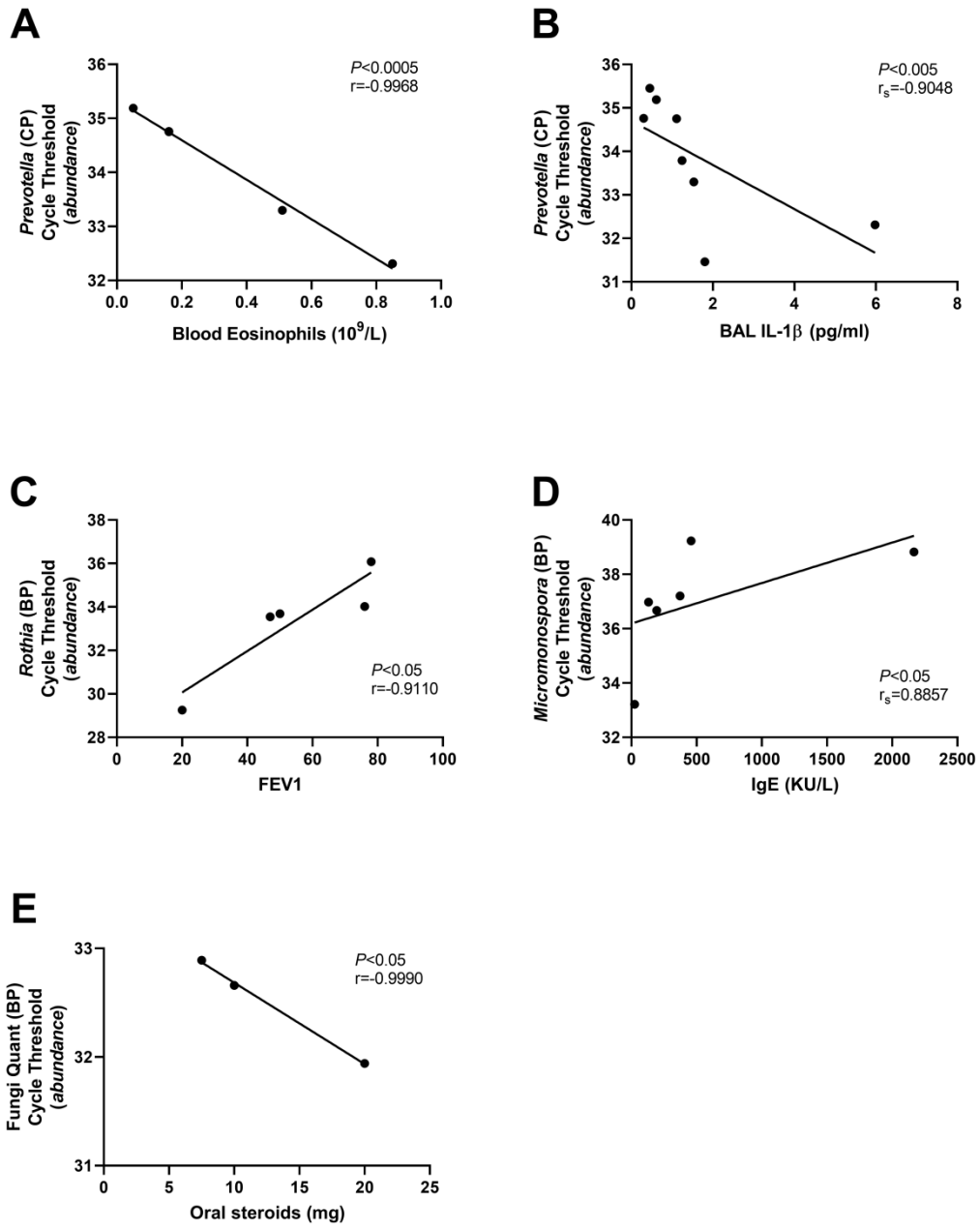


Figure 12. Baseline BAL qPCR correlations. (A) *Prevotella* (CP) correlated with blood eosinophil counts (*P*<0.0005; r=-0.9968). (B) *Prevotella* (CP) correlated with IL-1β in the BAL (*P*<0.005; r_s=-0.9048). (C) *Rothia* (BP) correlated with FEV-1 (*P*<0.05; r=0.9110). (D) *Micromonospora* (BP) correlated with total blood IgE levels (KU/L) (*P*<0.05; r_s=0.8857). (E) Fungal presence as determined by the qPCR primer Fungi Quant correlated with oral steroids (mg) (*P*<0.05; r=-0.9990).

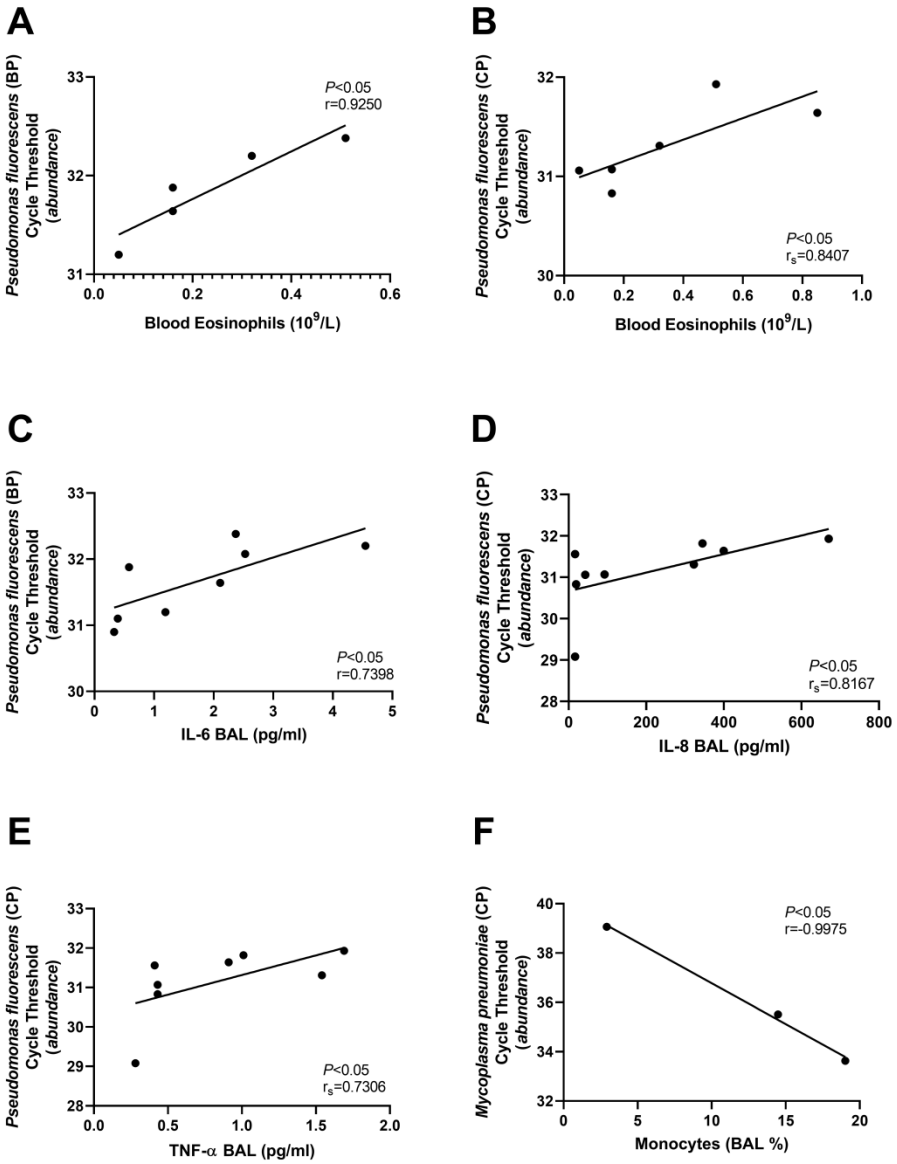


Figure 13. Baseline BAL qPCR correlations. *Pseudomonas fluorescens* (BP) presence correlated with blood eosinophil counts (10^9/L) (*P*<0.05; r=0.9250) (A). *P. fluorescens* (CP) presence correlated with blood eosinophil counts (10^9/L) (*P*<0.05, r_s=0.8407) (B). *P. fluorescens* (BP) presence correlated with the presence of the cytokine IL-6 in the BAL (*P*<0.05; r=0.7398) (C). *P. fluorescens* (CP) presence correlated with the presence of the cytokine IL-8 in the BAL (*P*<0.05; r_s=0.8167) (D). *P. fluorescens* (CP) presence correlated with the presence of the cytokine TNF-α in the BAL (*P*<0.05; r_s=0.7306) (E). *Mycoplasma pneumoniae* (CP) presence correlated with BAL monocyte percentage counts (*P*<0.05; r=-0.9975) (F).

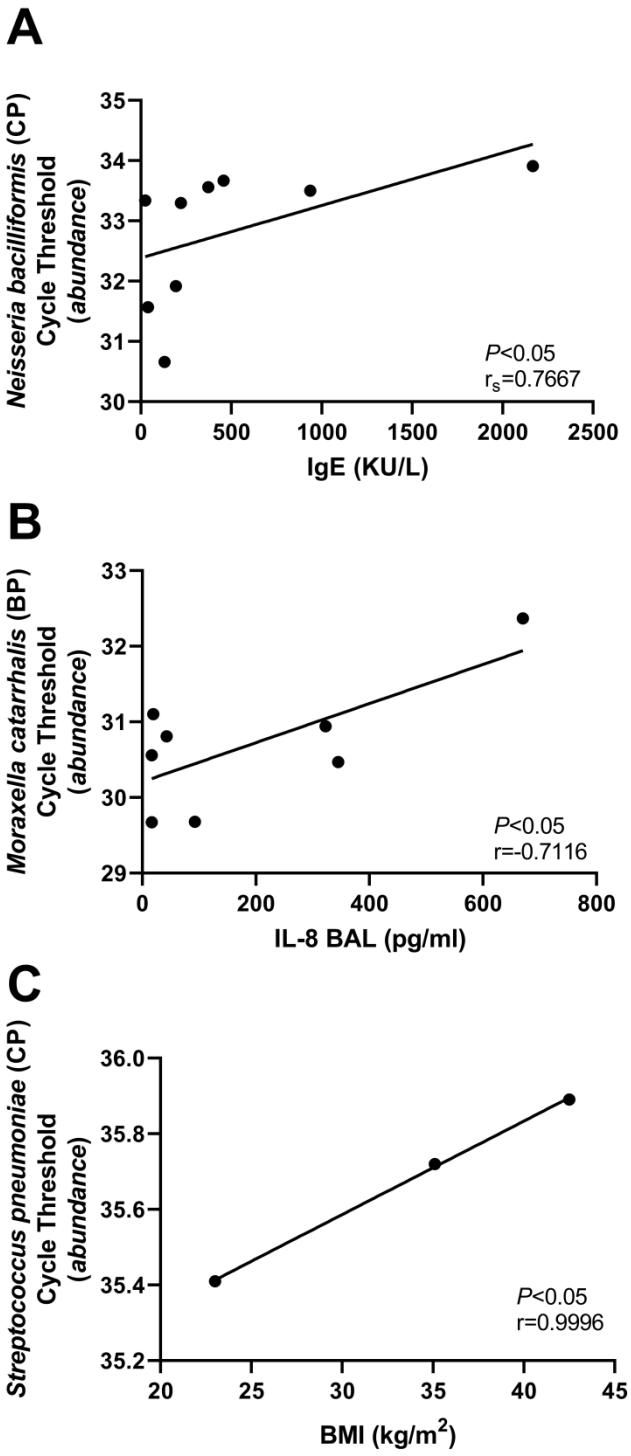


Figure 14. Baseline BAL qPCR correlations. *Neisseria bacilliformis* (CP) correlated with total blood IgE levels (P<0.05; r_s=0.7667) (A). *Moraxella catarrhalis* (BP) presence correlated with the presence of the cytokine IL-8 in the BAL (P<0.05; r=0.7116) (B).The presence of *Streptococcus pneumoniae* (CP) correlated with patient BMI levels (P<0.05; r=0.9996) (C).

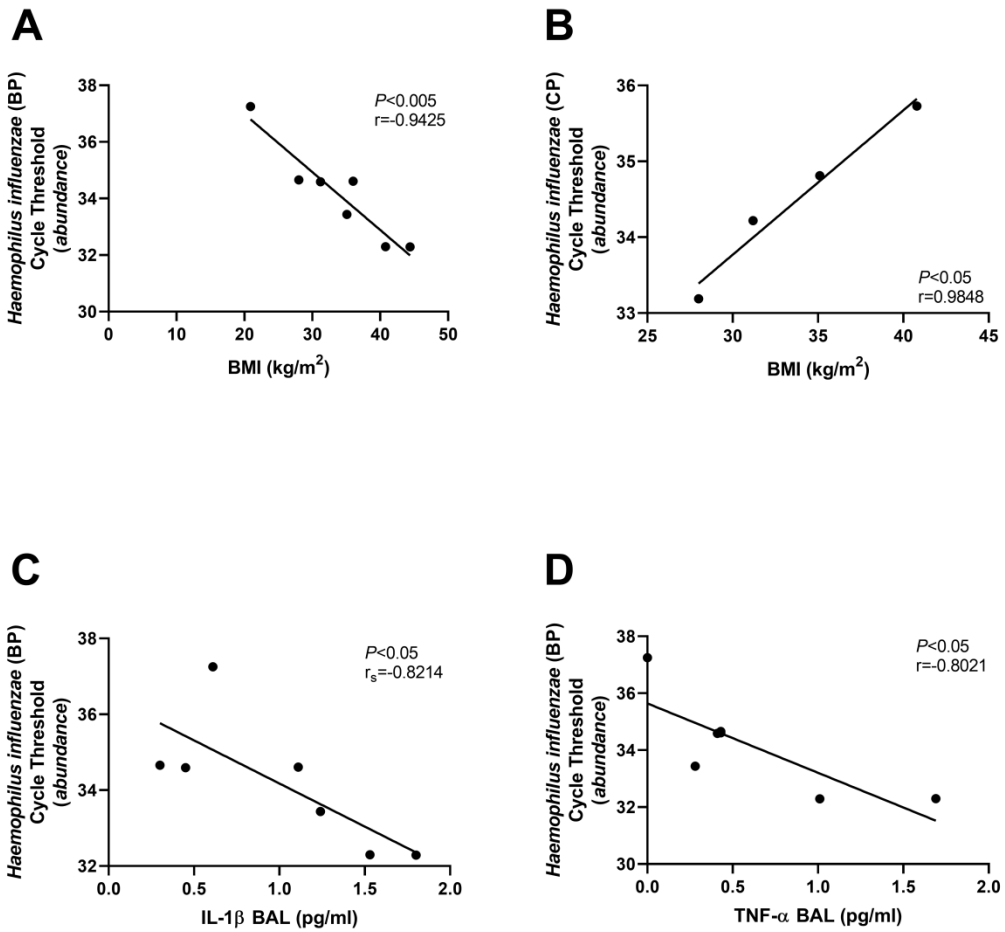


Figure 15. Baseline BAL qPCR correlations. The presence of *Haemophilus influenzae* (BP) correlated with patient BMI (*P*<0.005; r=-0.9425) (A). *Haemophilus influenzae* (CP) correlated with patient BMI (*P*<0.05; r=0.9848) (B). The presence of *Haemophilus influenzae* (BP) correlated with the presence of the cytokine IL-1β in the BAL (*P*<0.05; r_s=-0.8214) (C). The presence of *Haemophilus influenzae* (BP) correlated with the presence of the cytokine TNF-α in the BAL (*P*<0.05; r=-0.8021) (D).

Focusing on BAL obtained post Omalizumab treatment it was observed that the presence of Total Bacteria correlated with BAL neutrophil percentage counts (P<0.05; r_s=-0.7619). See Figure 16 (A). Total bacteria also correlated with BAL IL-6 cytokine levels (P<0.05; r_s=-1). See Figure 16 (B). **T**he presence of Firmicutes (BP) correlated with BAL IL-6 cytokine levels (P<0.05; r_s=-0.9429). See Figure 16 (C). The presence of *Bordetella* (CP) correlated with the BAL neutrophil percentage counts (P<0.05; r_s=0.8095). See Figure 16 (D). The presence of *Prevotella* (BP) correlated with BAL neutrophil percentage counts (P<0.0005; r_s=-1). See Figure 16 (E). The presence of *Prevotella* (BP) correlated with the cytokine IL-6 in the BAL (P<0.05; r_s=-0.9429). See Figure 16 (F). The presence of *Veillonella* (BP) correlated with BAL cytokine IL-6 levels (P<0.05; r_s=-0.9429). See Figure 16 (G). The presence of *Micromonospora* (CP) correlated with BAL monocyte percentage counts (P<0.05; r=-0.9502). See Figure 16 (H).

Pseudomonas fluorescens (BP) correlated with patient BMI (P<0.005; r_s=0.8833) as did *Pseudomonas fluorescens* (CP) (P<0.05; r_s=0.7269). See Figure 17 (A-B). *P. fluorescens* (BP) presence correlated with the BAL cytokine IL-8 (P<0.005; r_s=-0.8667). See Figure 17 (C). *P. fluorescens* (CP) correlated with the BAL cytokine IL-8 (P<0.05; r_s=-0.7857). See Figure 17 (D). *P. fluorescens* (BP) correlated with BAL IL- 13 cytokine levels (P<0.05; r_s=-0.7619). See Figure 17 (E). *Staphylococcus aureus* (BP) correlated with BAL lymphocyte percentage counts (P<0.05; r=-0.7620). See Figure 17 (F).

Both *Moraxella catarrhalis* (BP) (P<0.05; r_s=0.8571) and *Moraxella catarrhalis* (CP) (P<0.05; r=0.7104) *c*orrelated with patient BMI levels. See Figure 18 (A-B). *Moraxella catarrhalis* (BP) (P<0.05; r_s=-0.8571) and *Moraxella catarrhalis* (CP) (P<0.05; r_s=-0.7619) correlated with the levels of BAL cytokine IL-8. See Figure 18 (C-D).

Haemophilus influenzae (CP) correlated with patient BMI (P<0.05; r=0.7340). See Figure 19 (A). *Haemophilus influenzae* (BP) (P<0.05; r_s=-1) and *Haemophilus influenzae* (CP) (P<0.05; r_s=-0.7500) correlated with the BAL cytokine IL-8. See Figure 19 (B-C).

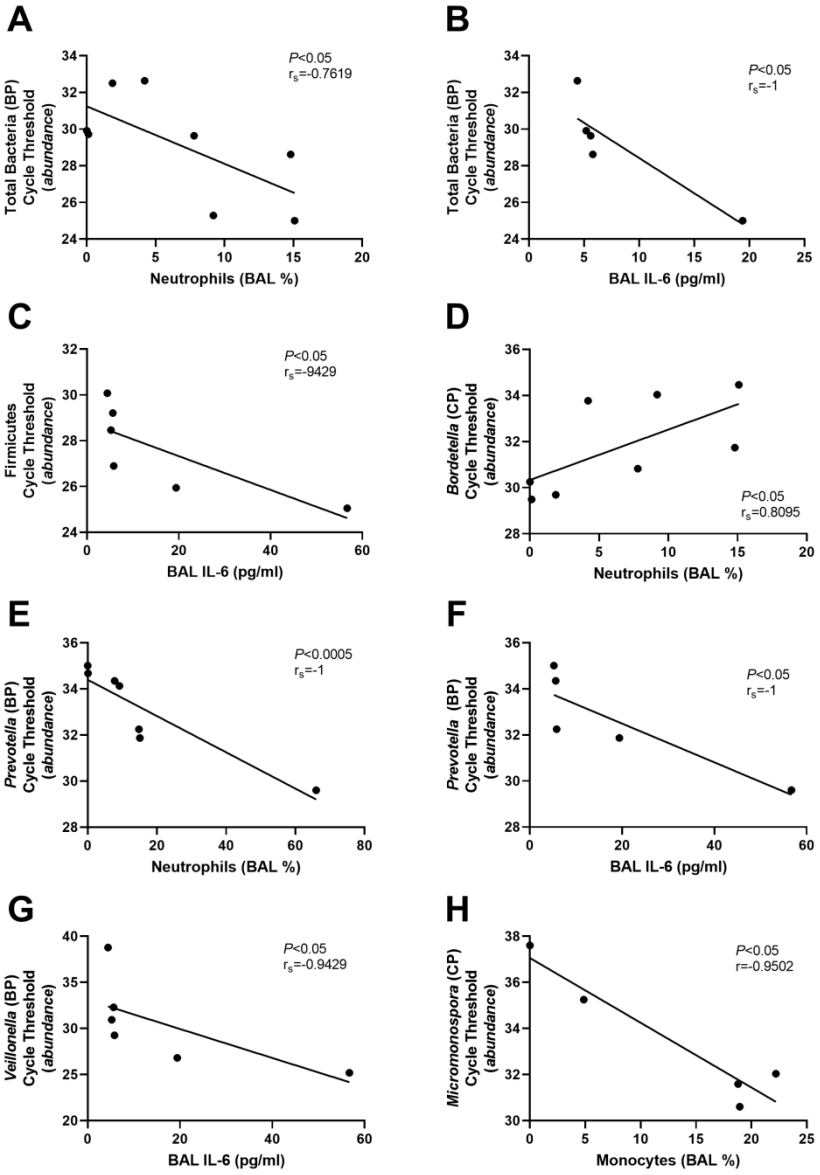


Figure 16. Post-Omalizumab BAL qPCR correlations. Total Bacteria correlated with BAL neutrophil percentage counts (P<0.05; r_s=-0.7619) (A) and BAL IL-6 cytokine levels (P<0.05; r_s=-1) (B). The presence of Firmicutes (BP) correlated with BAL IL-6 cytokine levels (P<0.05; r_s=-0.9429) (C). The presence of *Bordetella* (CP) correlated with the BAL neutrophil percentage counts (P<0.05; r_s=0.8095) (D). The presence of *Prevotella* (BP) correlated with BAL neutrophil percentage counts (P<0.0005; r_s=-1) (E). *Prevotella* (BP) correlated with the cytokine IL-6 in the BAL (P<0.05; r_s=-0.9429) (F). The presence of *Veillonella* (BP) correlated with BAL cytokine IL-6 levels (P<0.05; r_s=-0.9429) (G). The presence of *Micromonospora* (CP) correlated with BAL monocyte percentage counts (P<0.05; r=-0.9502) (H).

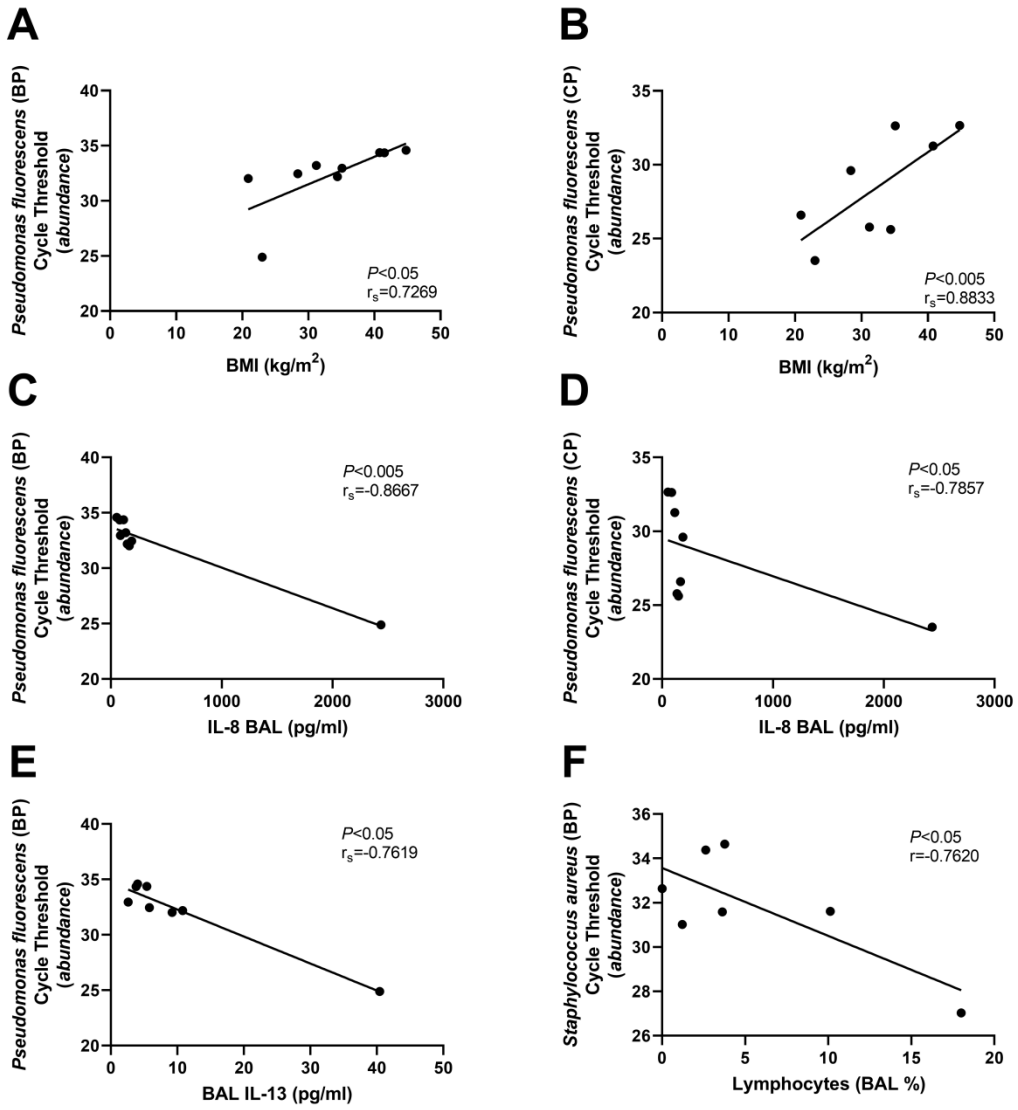


Figure 17. Post-Omalizumab BAL qPCR correlations. *Pseudomonas fluorescens* (BP) correlated with patient BMI (P<0.005; r_s=0.8833) as did *Pseudomonas fluorescens* (CP) (P<0.05; r_s=0.7269) (A-B). *P. fluorescens* (BP) presence correlated with the BAL cytokine IL-8 (P<0.005; r_s=-0.8667) (C). *P. fluorescens* (CP) correlated with the BAL cytokine IL-8 (P<0.05; r_s=-0.7857) (D). *P. fluorescens* (BP) correlated with BAL IL- 13 cytokine levels (P<0.05; r_s=-0.7619) (E). *Staphylococcus aureus* (BP) correlated with BAL lymphocyte percentage counts (P<0.05; r=-0.7620) (F).

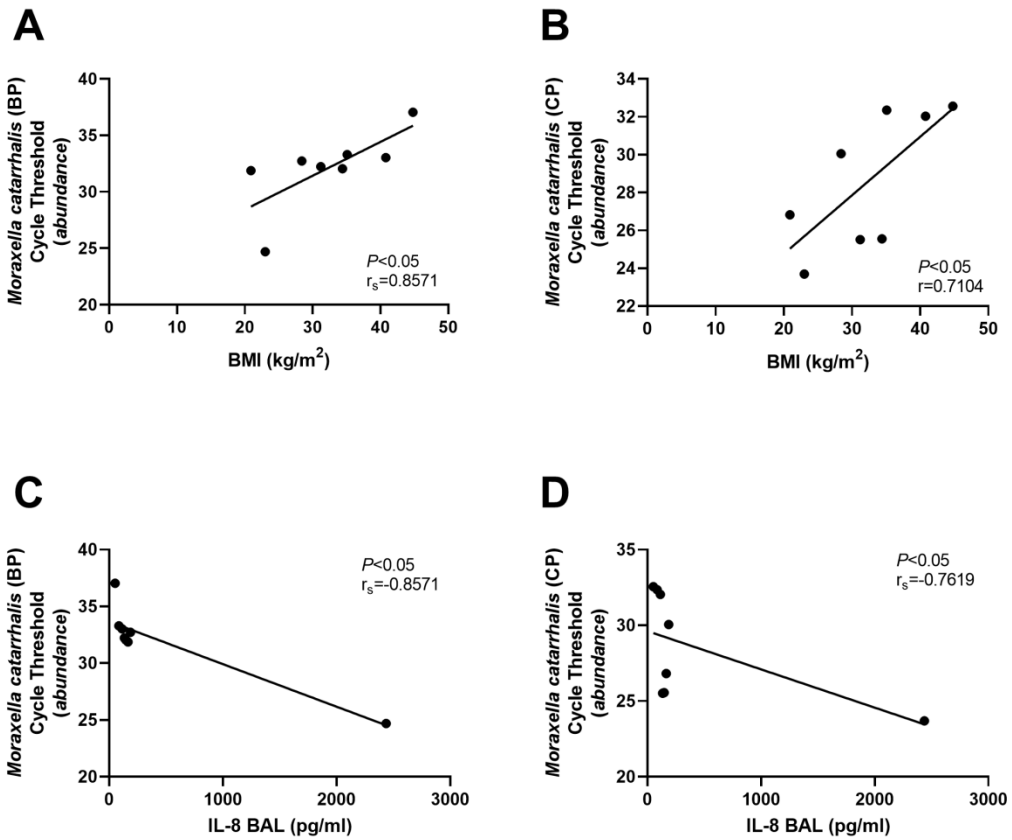


Figure 18. Post-Omalizumab BAL qPCR correlations. *Moraxella catarrhalis* (BP) (*P*<0.05; r_s=0.8571) and *Moraxella catarrhalis* (CP) (*P*<0.05; r=0.7104) correlated with patient BMI levels (A-B). *Moraxella catarrhalis* (BP) (*P*<0.05; r_s=-0.8571) and *Moraxella catarrhalis* (CP) (*P*<0.05; r_s=-0.7619) correlated with BAL cytokine IL-8 (C-D).

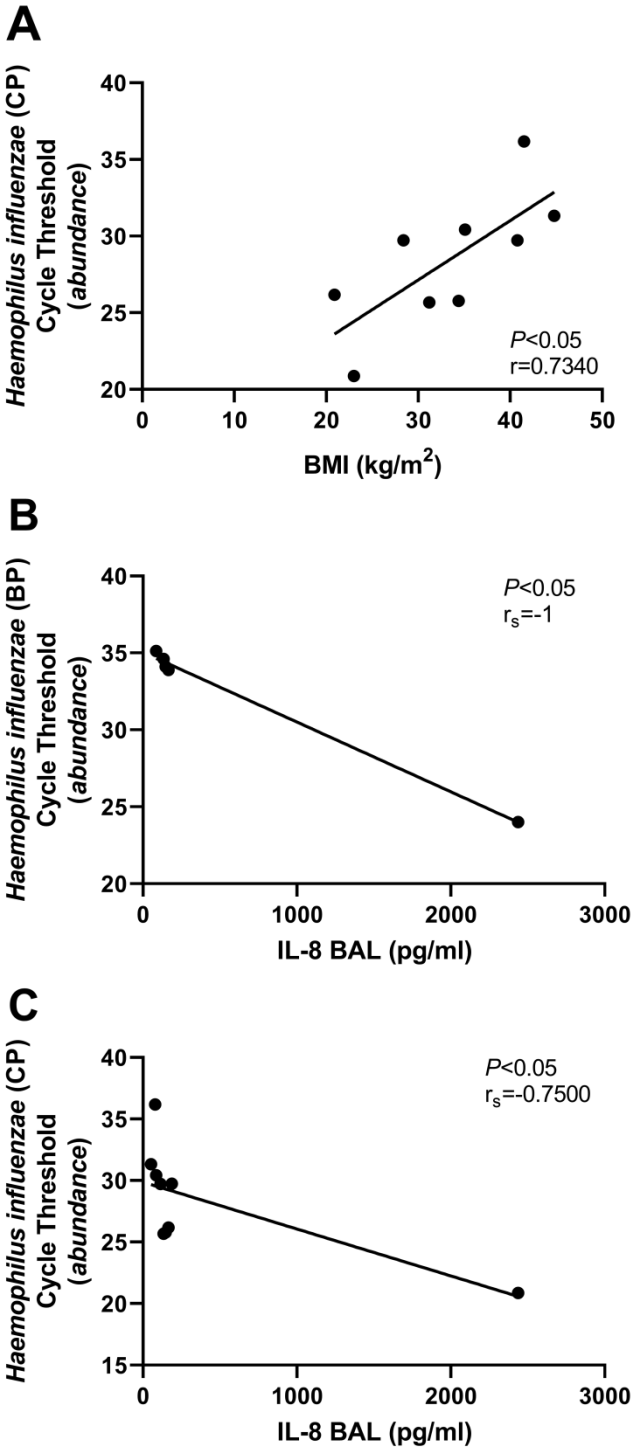


Figure 19. Post-Omalizumab BAL qPCR correlations. *Haemophilus influenzae* (CP) correlated with patient BMI (*P*<0.05; r=0.7340) (A). *Haemophilus influenzae* (BP) (*P*<0.05; r_s=-1) and *Haemophilus influenzae* (CP) (*P*<0.05; r_s=-0.7500) correlated with the BAL cytokine IL-8 (B-C).

5. Discussion

Asthma treatment

Asthma patients are frequently prescribed inhaled corticosteroids (ICS) and/or a combination of long acting β-agonist (LABA) bronchodilators. However within approximately 10% of the asthmatic population further additional therapy is required in order for these patients to establish control of their asthma symptoms, improve lung function and reduce the number of exacerbations suffered[7]. It is believed that approximately 5-10% of asthma patients can be classified as severe asthmatics and it is believed that within this population over 50% can be classified as allergic IgE mediated asthmatics[8]. As IgE plays such a pivotal role in allergic asthma therapies targeting IgE are of interest in the advancement of asthma care. Upon allergen exposure, circulating allergen specific IgE binds to the $F_{c\varepsilon}RI$ receptors, on immune cells such as mast cells and basophils, leading to crosslinking and release of inflammatory mediators[8]

Monoclonal antibody therapy

Monoclonal antibodies has emerged as a promising therapeutic strategy for asthma patients who suffer from difficult to control asthma symptoms despite the use of treatment options such as inhaled corticosteroids and long acting beta agonists[19]. The humanised monoclonal antibody against immunoglobulin E (IgE) (Omalizumab; Xolair®, Novartis) shows promise as an emerging treatment strategy for severe, poorly controlled asthmatics[20]. Our study consisted of a well-defined severe asthma cohort in which bronchoscopy was carried out pre and post treatment with the humanised monoclonal antibody Omalizumab (Xolair®, Novartis) which binds to the constant region of circulating IgE molecules, preventing the free IgE from binding to high and low affinity IgE receptors present in certain inflammatory cells[7]. Little is known as to its effect on the lung microbiome. Our aim was to elucidate potential differences in microbial diversity in a cohort of well-defined severe asthmatics after treatment with Omalizumab.

Omalizumab and its effect on patient clinical parameters

The study cohort consisted of nine adult GINA 5 asthma patients; 7 females and 2 males. With respect to systemic steroids 5 patients were in receipt of oral steroids (median 15; min 7.5 – max 20mg) at time of baseline bronchoscopy and 4 patients were in receipt of oral steroids (median 15; min 5 – max 15mg) at follow-up bronchoscopy displaying an overall reduction in the number of patients requiring oral steroids and a marked reduction in the prescribed mg volume per patients still in receipt of oral steroids. While systemic steroids, often prescribed in the form of oral treatment, are utilised for the management of severe asthma exacerbations and long term management of severe, difficult to treat asthma there are risk factors associated with their use[21]. Longitudinal studies by Bourdin *et al.,* have documented a cohort of moderate to severe asthmatics over a period of twenty years and have found links between systemic steroid use and the increased risk of mortality[22]. While Lee *et al.,* have demonstrated a significant finding that a potential dose-response relationship exists whereby there is an increase in mortality risk with an increase in the prescribed dose of systemic steroids in asthma patients[23]. Therefore due to increased risk associated with long term systemic steroids and the increasing risk dependent on prescribed dose it is promising to see data from this cohort of severe, adult asthmatics whereby upon receipt of the monoclonal antibody Omalizumab there was a marked overall reduction in oral steroid use. Results from this study cohort align with a recent statement released by the European Respiratory Society and the European Academy of Allergy and Clinical Immunology recommending that systemic steroid use is avoided in favour of high dose inhaled corticosteroids, long acting beta agonists and long acting muscarinic antagonist combinations as well as the use of biologicals[24].

With respect to the use of inhaled corticosteroids within this severe asthma cohort all 9 patients were in receipt of inhaled corticosteroids at baseline bronchoscopy (median 1000 FDP; min 800 – max 1000 FDP) and at follow-up bronchoscopy (median 1000 FDP; min 800 – max 1000 FDP). The number of patients in receipt of inhaled corticosteroids (FDP) remained consistent at baseline and follow-up bronchoscopy and the inhaled corticosteroid (FDP) dose prescribed also remained

the same for patients when comparing their prescribed ICS (FDP) dose at baseline bronchoscopy and at their follow-up bronchoscopy indicating that the use of the anti-IgE monoclonal antibody did not result in a change in the patients prescribed inhaled corticosteroid dose.

Upon analysis of the patient ACQ-7 data it was revealed that at follow-up bronchoscopy those who underwent the ACQ-7 survey still considered themselves to be uncontrolled asthmatics (ACQ-7≥1.5) [mean (SD)] [2.9 (0.8)]; [median (IQR)] [2.9 (2.2-3.5)]. However when patients FEV-1 % predicted results were analysed at baseline [mean (SD)] [51.6 (22.7)] ; [median (IQR)] [49.0 (28.3-75.0)] and at follow-up bronchoscopy after patients were in receipt of the anti-IgE monoclonal antibody Omalizumab there was an increase in the FEV-1 % predicted [mean (SD)] [54.9 (18.0)]; [median (IQR)] [59.0 (38.0-66.5)]. So while interpreting these spirometry results in accordance to Irish Thoracic Society guidelines the patients FEV_1/FVC ratio is below 70%, leading to a diagnosis of respiratory disorders such as asthma there is an improvement overall in the patients ability to exhale air quickly[18].

With respect to patient BMI it was observed that patient BMI remained consistent at baseline bronchoscopy [mean (SD)] [33.5 (8.4)]; [median (IQR)] [35.1 (25.5-41.7)] and at follow-up bronchoscopy post Omalizumab treatment [mean (SD)] [33.5 (8.3)]; [median (IQR)] [34.4 (25.7-41.2)].

See Table 1 for the further breakdown of the patient cohort demographics.

Omalizumab and the immune cells of the BAL

Through the use of differential staining methods and microscopy it was possible to comprehensively determine the immune cell percentage counts of monocytes, macrophages, lymphocytes, eosinophils and neutrophils at baseline bronchoscopy and at follow-up bronchoscopy post-anti-IgE therapy. Upon analysis of the immune cell percentage counts it was found that while differences may exist with respect to individual patient's percentage of specific immune cells prior to and post-anti-IgE therapy when the overall patient cohort was examined no statistically significant

difference was observed post-anti-IgE therapy when compared to the cohorts immune cell percentage counts prior to therapy. See Figure 4 for overall BAL immune cells pre- and post- anti-IgE therapy. See Figure 5 for immune cell differential counts pre- and post- anti-IgE therapy for patients individually.

BAL immune cells and BAL microbes

The BAL immune cell percentage counts were analysed with respect to the BAL qPCR microbiome data and it was revealed that correlations were present at baseline bronchoscopy with regards to macrophages and Total Bacteria (P<0.01; r_s=-0.8571), monocytes and *Mycoplasma pneumoniae* (P<0.05; r=-0.9975), lymphocytes and *Prevotella* (P<0.05; r_s=-0.8857) and neutrophils and Total Bacteria (P<0.05; r_s=0.8333) and *Prevotella* (P<0.05; r_s=-0.8333). See Figure 11 and Figure 13. At follow-up bronchoscopy correlations were found with regards to the immune cell percentage of monocytes and *Micromonospora* (P<0.05; r=-0.9502), lymphocytes and *Streptococcus aureus* (P<0.05; r=0.7620) and neutrophils and Total Bacteria (P<0.05; r_s=-0.7619), *Bordetella* (P<0.05; r_s=0.8095) and *Prevotella* (P<0.0005; r_s=-1). See Figure 16 and Figure 17.

Investigating the potential differences in the bacteria pellet and cellular pellet microbiota

An interesting observation of bacteria present both freely and within macrophages while carrying out immune cell percentage count on the differentially stained BAL cytospin slides lead to an alteration on previous patient sample processing. The cell pellet from the 500g 10 minute original BAL centrifugation was saved for DNA isolation and qPCR analysis in order to investigate the potential intracellular microbiota of the BAL. This addition to the protocol has led to many interesting observations. For example, bacterial species which may have been poorly expressed within the bacteria pellet sample which is the 'free bacteria' within the BAL sample may be highly expressed within the cell pellet sample or vice versa.

Baseline qPCR microbiota bacteria pellet and cellular pellet differences

Bacteria pellet and cellular pellet fraction microbiota differences were observed within the baseline qPCR results in many cases, especially in case of *Bordetella* where 56% (5/9) of patients had detectable *Bordetella* by qPCR within the bacteria pellet (BP) sample, however within the cell pellet (C) sample no patient had detectable *Bordetella.* See Table 2. The reverse was observed in *Staphylococcus aureus* qPCR detection where no patients had detectable *Staphylococcus aureus* within their bacteria pellet (BP) sample however it was detectable within 33% (3/9) of patients cell pellet (CP) samples. See Table 2. Focusing on fungal species it was observed that within the bacteria pellet (BP) samples 56% (5/9) of patients had detectable *Aspergillus fumigatus* however within the cell pellet (CP) *Aspergillus fumigatus* was detectable in 89% (8/9) of patients.

Omalizumab treated patient BAL qPCR bacteria pellet and cellular pellet differences

Within the BAL samples obtained at the post-Omalizumab treatment bronchoscopy there were once again differences between the bacteria detected within the bacteria pellet (BP) DNA samples and within the cell pellet (CP) DNA samples. For example, *Pseudomonas aeruginosa* was undetectable within the Omalizumab treated patient BAL BP samples however it was detectable in 44% (4/9) of patients CP samples. See Table 2. *Haemophilus influenzae* was detectable in 56% (5/9) of patient BP samples however it was detectable in 100% (9/9) of patient CP samples. See Table 2. Investigating the fungal species *Aspergillus fumigatus* post-Omalizumab treatment it was seen that within patient BP 33% (3/9) had detectable *Aspergillus fumigatus* while within the CP it was detectable in 78% (7/9) of patients. While the study cohort of n=9 is a moderate cohort number the importance of investigating both the bacteria pellet and cellular pellet fractions of the BAL is highlighted. See Table 2. See Figure 9 and Figure 10 for qPCR detection of bacteria and fungi species within the asthmatic patient BAL bacteria pellet and cellular pellet fractions at baseline and follow-up bronchoscopy.

The role of macrophages in the microbe immune response

Macrophages, major immune sentinel cells, play a key role in promoting the immune response to microorganisms through the release of cytokines, shaping the immune cascade of other cells and physically sensing and eradicating invading microbes, thus protecting the host with a wide range of antimicrobial defence mechanisms[25]. Macrophages possess the ability to phagocytose bacteria, creating a highly acidic organelle with strong antimicrobial effects[26].

Bacteria however have developed mechanisms to survive within this hostile cell environment, for example *Staphylococcus aureus* uses the GraXRS regulatory system to sense and adapt to the hostile, acidic phagolysosome environment present within macrophages[26]. Extracellular bacteria are fully exposed to the immune cells in a host and the resulting immune protection mechanisms. Intracellular bacteria however have the ability to evade host immune cell detection by hiding within the host immune cells such as macrophages, colonising two distinct regions of the host cell, the cytosol or the vacuole and even possess the mechanisms required to replicate within macrophages. While host cells possess mechanisms such as apoptosis, programmed necrosis and pyroptosis to destroy this replication niche of the intracellular bacteria, the intracellular bacteria can block, delay or hijack immune cell death as a means of escape into the host, while reducing the numbers of immune cells available to fight against infection. This unique replication niche awards intracellular bacteria an competitive advantage over extracellular bacteria, thus pathogenic intracellular bacteria can significantly contribute to morbidity and mortality in a wide range of diseases[25].

With regards to fungal species it has recently been shown that macrophages can inhibit *Aspergillus fumigatus* germination and neutrophil-mediated fungal killing[27]. Studies have utilised zebrafish larvae to visualise and quantify the behaviour of macrophages and neutrophils with respect to the inoculation of fungal *Aspergillus fumigatus* spores. While strains which were fast germinators were cleared quickly, slower growing *Aspergillus fumigatus* strains persisted longer. Macrophages can inhibit *Aspergillus* spore germination by forming tight clusters around the spores

thus preventing neutrophil recruitment and neutrophil mediated killing of the *A. fumigatus* as without spore germination of the *Aspergillus fumigatus* neutrophils are not recruited which results in the macrophages acting as a protective niche for the *A. fumigatus* by preventing fungal germination in this case and awarding *Aspergillus fumigatus* virulence factors. The authors of this paper describe this development as being similar to aspergillomas found in human patients. It should be noted however that further research into this phenomenon is required as the authors of the study have at present only utilised zebrafish model systems to investigate the effect of fungal spores on neutrophil and macrophage action[27].

While it is acknowledged that the cohort of nine patients is a moderate cohort number this study has highlighted the fact that through carrying out differential centrifugation of the BAL samples to isolate the bacteria and cell DNA pellets more novel insights into the mechanisms both the host and the microorganism employ in their daily interactions will be further elucidated.

The microbiome pre- and post-anti-IgE Omalizumab therapy

Focusing on the differences in microbial populations pre and post treatment with the monoclonal antibody Omalizumab (Xolair®) it has been noted in this study that there are clear differences pre and post treatment within the diversity of certain microbes. While many microbes such as *Prevotella, Veillonella* and *Neisseria bacilliformis* remained at consistent levels within the patient cohort irrespective of treatment other microbes were present at altered amounts at follow up bronchoscopy.

Pseudomonas aeruginosa detection in the cell pellet samples increased from 11% (1/9) in the baseline BAL samples to 44% (4/9) in the post treatment BAL samples. *Bordetella* decreased from 56% (5/9) to 22% (2/9) patient detection in the bacteria pellet samples however *Bordetella* in the cell pellet samples which was undetectable at baseline bronchoscopy was detectable in 89% (8/9) of the post treatment bronchoscopy samples. *Chlamydophilia pneumoniae* detection increased

from 22% (2/9) to 67% (6/9) in the BP samples and from 11% (1/9) to 87% (8/9) in the CP samples. *Staphylococcus aureus* also increased in the post treatment bronchoscopy samples from no detection at baseline BP to 78% (7/9) BP detection post treatment. *Neisseria meningitidis* also dramatically increased post treatment, with an increase from 11% (1/9) to 78% (7/9) in the BP samples and 22% (2/9) to 100% (9/9) in the CP samples. *Streptococcus pneumoniae* increased in the CP samples from 33% (3/9) to 89% (8/9) while the BP detection remained the same irrespective of treatment. *Micromonospora* decreased in the CP samples post treatment with detection falling from 89% (8/9) to 56% (5/9) and *Aspergillus fumigatus* was also seen to decrease in the BP samples from 56% (5/9) to 33% (3/9).

The increased prevalence of bacteria such as *Pseudomonas aeruginosa, Bordetella, Chlamydophilia pneumoniae, Staphylococcus aureus, Neisseria meningitidis,* and *Streptococcus pneumoniae* within the cohort at follow up bronchoscopy post treatment with the monoclonal antibody Omalizumab is of great interest as a number of these bacteria are responsible for causing lung infections such as pneumoniae[28,29]. However it should also be noted that a reduction of *Haemophilus influenzae, Mycoplasma pneumoniae* and BAL bacteria pellet detected *Bordetella* was found at follow-up bronchoscopy prior to Omalizumab treatment. Overall patients appear to respond positively to treatment with Omalizumab, notably with respect to a reduction in the requirement of oral steroids as part of the patient treatment plan and an overall improvement in the patient FEV1 percent predicted value at follow-up bronchoscopy. Therefore further research with respect to the potential interaction or effect Omalizumab may play with regards to the overall microbial diversity observed within the lungs of asthmatic patients is needed and questions as to whether an improvement in asthma symptoms may lead to potential changes in the microbial diversity observed within such patients BAL is an interesting avenue of future research. Previously published studies have demonstrated significant differences within the bronchial microbiome dependent upon asthma clinical grouping with Th-2 high asthma patients displaying a lower bronchial bacterial diversity when compared to other asthma groups[30].

Comparing the statistically significant correlations present between BAL qPCR data and data such as patient demographics it was seen that while FEV-1 correlated with *Escherichia* (CP) and *Rothia* (BP) and oral steroids correlated with fungal presence (Fungi Quant) both FEV-1 and oral steroids did not correlated with microbial qPCR species post Omalizumab treatment. Inhaled corticosteroids did not correlate with microbial qPCR results before or after Omalizumab treatment. With respect to macrolide therapy there was no statistically significant difference between the qPCR microbiome results for patients in receipt of Azithromycin and patients who did not receive Azithromycin.

The microbiome of the lung is of increasing interest in the field of respiratory research. Overall this study highlights the importance of investigating the effects asthma treatments such as Omalizumab may have on lung microbial diversity. Investigating both the bacteria pellet and cell pellet DNA samples led to interesting observations which should be investigated further.

6. Supplementary

Supplementary table 1 Validated primer sequences utilised for the detection of microorganisms of interest. Note K=G or T, R=A or G, S=G or C, W=A or T following IUPAC code.

Primer		Sequence	Reference
Total Bacteria	F-Bact-1369	5'-CGGTGAATACGTTCCCGG-3'	[31]
	R-Prok-1492	5'-TACGGCTACCTTGTTACGACTT-3'	
Total Bacteria Probe	P-TM1389F	5'-CTTGTACACACCGCCCGTC-3'	
Firmicutes	Firm-L	5'- GGAGYATGTGGTTTAATTCGAAGCA-3'	[32]
	Firm-R	5'- AGCTGACGACAACCATGCAC-3'	
Staphylococcus aureus	Sa-pl-47-L	5'-ATGCATAGCCGACCTGAGAG-3'	NCBI:txid1280
	Sa-pl-47-R	5'- AGGAGTCTGGACCGTGTCTC-3'	
Streptococcus pneumoniae	S.pneu-pl-52-L	5'-GCAAGGTATGCAGGAATCGT-3'	Modification on *Streptococcus pneumoniae* alpha fucosidase gene NCBI:txid488222
	S.pneu-pl-52-R	5'-TCGCTTGAGTATGAACCAACC-3'	
Rothia	Rothia-Spp-L	5'-GCCTGGGAAACTGGGTCTAAT-3'	[33]
	Rothia-Spp-R	5'-CAAGCTGATAGGCCGTGAG-3'	
Micromonospora	Mimo16S-pl-39-L	5'-GGTACAATGGGCTGCGATAC-3'	Modification on *Micromonospora* strain ATCC 27029 NCBI:NR_074415.1
	Mimo16S-pl-39-R	5'-CGAACTGAGACCGGCTTTT-3'	
Pseudomonas aeruginosa	ORPL-pl-11-L	5'-CCAGAGCCATGTTGTACTCG-3'	[34 35] Modification on *Pseudomonas aeruginosa* Outer Membrane Protein L NCBI:txid205922
	ORPL-pl-11-R	5'-ACACGCGAAAGACCTGAAAG-3'	
Pseudomonas fluorescens	Pf-pl-66-L	5'-GACAGAATAAGCACCGGCTAA-3'	NCBI:txid294
	Pf-pl-66-R	5'-ACGCTTGCACCCTCTGTATT-3'	
Escherichia	UidA405-pl-9-L	5'-CTGATAGCGCGTGACAAAAA-3'	Modification on Beta-glucuronidase protein, Uid A405 gene NCBI:txid83333
	UidA405-pl-9-R	5'-CGGTTCGTTGGCAATACTC-3'	
Bordetella	Bordetella-pl-45-L	5'-GAGCCATTGTCGGTGAGC-3'	NCBI:txid517
	Bordetella-pl-45-R	5'-CGCAGTGGCCTACTACCAG-3'	
Prevotella	Prevotella-pl-66-L	5'-TGCAGGTACCGCATGAATAA-3'	NCBI:txid838
	Prevotella-pl-66-R	5'-CCGGACCTTCCGTATTACC-3'	
Veillonella	Veillonella-L	5'-CCGTGATGGGATGGAAACTGC-3'	[36]
	Veillonella-R	5'-CCTTCGCCACTGGTGTTCTTC-3'	
Mycoplasma pneumoniae	Myco.pneu-pl-16-L	5'-AGACACGGCCCATACTCCTA-3'	Greengenes GenBank: CP017343.1
	Myco.pneu-pl-16-R	5'-CAAGCTTTCGCTCATTGTGA-3'	

Chlamydophilia pneumoniae	C.pneu-pl-45-L	5'-CGTGAGATGGAGCAAATCCTA-3'	Greengenes GenBank: CP001713.1
	C.pneu-pl-45-R	5'-ACTTCATGTAGTCGAGTTGCAGA-3'	
Neisseria bacilliformis	Nb-pl-8-L	5'-TGCGTAGAGATGTGGAGGAAT-3'	Greengenes NCBI:txid267212
	Nb-pl-8-R	5'-CTGTTTGCTACCCACGCTTT-3'	
Moraxella catarrhalis	Mc-pl-66-L	5'-CACAGAATAAGCACCGGCTAA-3'	Greengenes GenBank: CP010573.1
	Mc-pl-66-R	5'-ACGCTTGCACCCTCTGTATT-3'	
Neisseria meningitidis	N.meningitidis-pl-9-L	5'-ATTCCACTACGGCAAACACC-3'	[37] Modification on *Neisseria meningitidis* SodC gene NCBI:txid487
	N.meningitidis-pl-9-R	5'-TCGGTGCCTTTGATTTGATT-3'	
Haemophilus influenzae	H.influ-pl-98-L	5'-AGCTGGTAAAGGTGTTGATGC-3'	Modification on Peptidoglycan associated outer membrane lipoprotein-OMP P6 NC_000907.1
	H.influ-pl-98-R	5'-GCAGGTTTTTCTTCACCGTAA-3'	
Fungi Quant	Fungi Quant-F	5'-GGRAAACTCACCAGGTCCAG-3'	[38]
	Fungi Quant-R	5'GSW CTA TCC CCA KCA CGA-3'	
Aspergillus fumigatus	OliAFMB-L-pl-103	5'-AGC ACG GCT TGT GTG TTG -3'	Modification on *Aspergillus* ITS KT358862 [39]
	OliAFMB-R-pl-103	5'-GGG TGA CAA AGC CCC ATA C-3'	

7. References

1. Sullivan A, Hunt E, MacSharry J, Murphy DM. The Microbiome and the Pathophysiology of Asthma. *Respiratory Research.* 2016;17(1):163.
2. Kim HY, DeKruyff RH, Umetsu DT. The many paths to asthma: phenotype shaped by innate and adaptive immunity. *Nature immunology.* 2010;11(7):577-584.
3. Hilty M, Burke C, Pedro H, et al. Disordered microbial communities in asthmatic airways. *PLoS ONE.* 2010;5(1).
4. Edwards MR, Bartlett NW, Hussell T, Openshaw P, Johnston SL. The microbiology of asthma. *Nat Rev Micro.* 2012;10(7):459-471.
5. Burney P, Jarvis D, Perez-Padilla R. The global burden of chronic respiratory disease in adults. *The International Journal of Tuberculosis and Lung Disease.* 2015;19(1):10-20.
6. Umetsu DT, McIntire JJ, Akbari O, Macaubas C, DeKruyff RH. Asthma: an epidemic of dysregulated immunity. *Nat Immunol.* 2002;3(8):715-720.
7. Al Said A, Cushen B, Costello RW. Targeting patients with asthma for omalizumab therapy: choosing the right patient to get the best value for money. *Ther Adv Chronic Dis.* 2017;8(2-3):31-45.
8. Thomson NC, Chaudhuri R. Omalizumab: clinical use for the management of asthma. *Clin Med Insights Circ Respir Pulm Med.* 2012;6:27-40.
9. Bang LM, Plosker GL. Spotlight on omalizumab in allergic asthma. *BioDrugs : clinical immunotherapeutics, biopharmaceuticals and gene therapy.* 2004;18(6):415-418.
10. Holgate ST, Polosa R. Treatment strategies for allergy and asthma. *Nat Rev Immunol.* 2008;8(3):218-230.
11. Miller MR, Hankinson J, Brusasco V, et al. Standardisation of spirometry. *The European respiratory journal.* 2005;26(2):319-338.
12. Graham BL, Steenbruggen I, Miller MR, et al. Standardization of Spirometry 2019 Update. An Official American Thoracic Society and European Respiratory Society Technical Statement. *Am J Respir Crit Care Med.* 2019;200(8):e70-e88.
13. Juniper EF, Bousquet J, Abetz L, Bateman ED. Identifying 'well-controlled' and 'not well-controlled' asthma using the Asthma Control Questionnaire. *Respir Med.* 2006;100(4):616-621.
14. Du Rand IA, Blaikley J, Booton R, et al. British Thoracic Society guideline for diagnostic flexible bronchoscopy in adults: accredited by NICE. *Thorax.* 2013;68 Suppl 1:i1-i44.
15. Hunt EB, Ward C, Power S, et al. The Potential Role of Aspiration in the Asthmatic Airway. *Chest.* 2017;151(6):1272-1278.
16. DeSantis TZ, Hugenholtz P, Larsen N, et al. Greengenes, a Chimera-Checked 16S rRNA Gene Database and Workbench Compatible with ARB. *Applied and Environmental Microbiology.* 2006;72(7):5069-5072.
17. Kowalski CJ. On the Effects of Non-Normality on the Distribution of the Sample Product-Moment Correlation Coefficient. *Journal of the Royal Statistical Society Series C (Applied Statistics).* 1972;21(1):1-12.
18. O'Connor T, Manning, P. *Spirometry: Performance and Interpretation - A Guide for General Practitioners.* Irish Thoracic Society Irish Thoracic Society;2005.
19. Drick N, Seeliger B, Welte T, Fuge J, Suhling H. Anti-IL-5 therapy in patients with severe eosinophilic asthma - clinical efficacy and possible criteria for treatment response. *BMC pulmonary medicine.* 2018;18(1):119-119.
20. O'Byrne PM. Role of monoclonal antibodies in the treatment of asthma. *Can Respir J.* 2013;20(1):23-25.

21. Gaga M, Zervas E. Oral steroids in asthma: a double-edged sword. *European Respiratory Journal.* 2019;54(5):1902034.
22. Bourdin A, Molinari N, Vachier I, Pahus L, Suehs C, Chanez P. Mortality: a neglected outcome in OCS-treated severe asthma. *European Respiratory Journal.* 2017;50(5):1701486.
23. Lee H, Ryu J, Nam E, et al. Increased mortality in patients with corticosteroid-dependent asthma: a nationwide population-based study. *European Respiratory Journal.* 2019;54(5):1900804.
24. Bourdin A, Bjermer L, Brightling C, et al. ERS/EAACI statement on severe exacerbations in asthma in adults: facts, priorities and key research questions. *European Respiratory Journal.* 2019;54(3):1900900.
25. Mitchell G, Chen C, Portnoy DA. Strategies Used by Bacteria to Grow in Macrophages. *Microbiol Spectr.* 2016;4(3):10.1128/microbiolspec.MCHD-0012-2015.
26. Flannagan RS, Kuiack RC, McGavin MJ, Heinrichs DE. Staphylococcus aureus Uses the GraXRS Regulatory System To Sense and Adapt to the Acidified Phagolysosome in Macrophages. *mBio.* 2018;9(4):e01143-01118.
27. Rosowski EE, Raffa N, Knox BP, Golenberg N, Keller NP, Huttenlocher A. Macrophages inhibit Aspergillus fumigatus germination and neutrophil-mediated fungal killing. *PLOS Pathogens.* 2018;14(8):e1007229.
28. Winstead JM, McKinsey DS, Tasker S, De Groote MA, Baddour LM. Meningococcal Pneumonia: Characterization and Review of Cases Seen Over the Past 25 Years. *Clinical Infectious Diseases.* 2000;30(1):87-94.
29. Feldman C, Anderson R. Recent advances in our understanding of Streptococcus pneumoniae infection. *F1000Prime Rep.* 2014;6:82-82.
30. Durack J, Lynch SV, Nariya S, et al. Features of the bronchial bacterial microbiome associated with atopy, asthma, and responsiveness to inhaled corticosteroid treatment. *J Allergy Clin Immunol.* 2017;140(1):63-75.
31. Suzuki MT, Taylor LT, DeLong EF. Quantitative analysis of small-subunit rRNA genes in mixed microbial populations via 5'-nuclease assays. *Applied and environmental microbiology.* 2000;66(11):4605-4614.
32. Guo X, Xia X, Tang R, Zhou J, Zhao H, Wang K. Development of a real-time PCR method for Firmicutes and Bacteroidetes in faeces and its application to quantify intestinal population of obese and lean pigs. *Letters in applied microbiology.* 2008;47(5):367-373.
33. Keisuke N, Hiroshi M, Hideaki I, Norimasa T. Simple and rapid detection of Rothia mucilaginosa by loop-mediated isothermal amplification method. *日本口腔検査学会雑誌 = Journal of Japanese Society for Evidence and the Dental Professional : JJSEDP.* 2018;10(1):44-52.
34. Rao AR, Laxova A, Farrell PM, Barbieri JT. Proteomic identification of OprL as a seromarker for initial diagnosis of Pseudomonas aeruginosa infection of patients with cystic fibrosis. *Journal of clinical microbiology.* 2009;47(8):2483-2488.
35. Le Gall F, Le Berre R, Rosec S, et al. Proposal of a quantitative PCR-based protocol for an optimal Pseudomonas aeruginosa detection in patients with cystic fibrosis. *BMC Microbiology.* 2013;13(1):143.
36. Chalmers NI, Palmer RJ, Cisar JO, Kolenbrander PE. Characterization of a Streptococcus sp.-Veillonella sp. Community Micromanipulated from Dental Plaque. *Journal of Bacteriology.* 2008;190(24):8145-8154.
37. Dolan Thomas J, Hatcher CP, Satterfield DA, et al. sodC-based real-time PCR for detection of Neisseria meningitidis. *PLoS ONE.* 2011;6(5):e19361-e19361.

38. Liu CM, Kachur S, Dwan MG, et al. FungiQuant: A broad-coverage fungal quantitative real-time PCR assay. *BMC Microbiology.* 2012;12(1):255.
39. Cuenca-Estrella M, Meije Y, Diaz-Pedroche C, et al. Value of serial quantification of fungal DNA by a real-time PCR-based technique for early diagnosis of invasive Aspergillosis in patients with febrile neutropenia. *J Clin Microbiol.* 2009;47(2):379-384.

Chapter 6

The Microbiome of the Lung

A study into the effect of anti-IL-5 therapy on the lung microbiome in a cohort of adult asthmatic patients

Author Contributions: Desmond Murphy, John MacSharry, Chris Ward and Paul O'Byrne were responsible for the initial study design and concept. Desmond Murphy was responsible for patient recruitment, clinical characterisation and sample acquisition. Deirdre Flynn was responsible for spirometry and FeNO testing and ACQ-7 questionnaires. Sample processing and study assays were primarily performed by Ashley Sullivan with contribution from Eoin Hunt, Susan Lapthorne, Bernie Crowley and John MacSharry. Statistical analysis was performed by the authors. Analysis and interpretation of data and manuscript preparation was performed by Ashley Sullivan, John MacSharry and Desmond Murphy. Manuscript approval were performed by all authors; Ashley Sullivan, Deirdre Flynn, Eoin Hunt, Chris Ward, Susan Lapthorne, Joseph Eustace, Bernie Crowley, Barry Plant, Paul O'Byrne, John MacSharry and Desmond Murphy.

1. Abstract 254
2. Introduction 255
3. Methods 259
3.1. Patient recruitment 259
3.2. Sample processing 260
3.3. Microscopy 263
3.4. DNA extraction 263
3.5. DNA quantification 264
3.6. Primers 265
3.7. qPCR – quantitative Polymerase Chain Reaction 266
3.8. BAL cytokine measurement 267
3.9. Post anti-IL-5 treatment BAL and plasma cytokine analyses. 268
3.10. Statistical analyses 269
4. Results 270
4.1. Patient demographics 270
4.2. Microscopy 274
4.3. Cytokine analyses 277
4.4. Molecular detection of microbial and fungal species 280
4.5 Anti-IL-5 monoclonal antibody therapy changes the lung microbiota 286
4.6. Bacterial and fungal species patient correlations 289
5. Discussion 297
6. Supplementary 306
7. References 308

1. Abstract

Background: The cytokine IL-5 is highly involved in eosinophilic development. IL-5 monoclonal antibodies result in downregulation of the eosinophilic inflammatory pathway and have demonstrated clinical benefit in patients with severe, eosinophilic asthma. Our aim was to investigate if anti-IL-4 treatment induced changes in the airway microbiome in severe asthmatics.

Methods: Eight well characterised severe asthmatic patients underwent bronchoscopy with broncholaveolar lavage (BAL) pre-anti-IL-5 monoclonal antibody therapy with follow up bronchoscopy within 2 years of first starting anti-IL-5 monoclonal therapy (Reslizumab). Molecular analyses of the BAL composition by qPCR pre- and post- anti-IL-5 therapy was performed.

Results: Anti-IL-5 therapy reduced BAL eosinophil counts (7.1% to 0.4%). Differences were also observed in the detection of bacterial strains after anti-IL-5 therapy. The largest increases were seen in *M. pneumoniae* (25% to 75%), *N. meningitidis* (38% to 100%) and *H. influenzae* (63% to 100%) in BAL by qPCR. At follow up bronchoscopy BAL monocyte cell counts positively correlated with *M. pneumoniae* presence ($P<0.01$; $r_s=0.9856$). At baseline *N. meningitidis* negatively correlated with monocyte cell counts ($P<0.05$; r=-0.9991), positively with lymphocyte cell counts ($P<0.05$; r=0.9979) and negatively with eosinophil counts ($P<0.05$; r=-0.9994) but not at follow up. Decreased levels of *S. aureus* (100% to 50%) and *N. bacilliformis* (88% to 50%) were also observed following therapy.

Conclusions: Anti-IL-5 therapy modulated the composition of the lung microbiota in severe asthma. Monitoring of the lung microbiome during treatment may allow for identification of therapeutic benefit but also susceptibility to respiratory tract infections. Further understanding of the lung microbiota may aid in the improvement of outcomes for patients diagnosed with respiratory conditions such as asthma.

2. Introduction

Monoclonal antibody therapy offers a highly specific means of treatment for a vast array of diseases and has greatly gained traction within the last thirty years becoming successful treatment options for patients with autoimmune and inflammatory diseases[1]. Monoclonal antibodies have a long serum half-life which allows for the therapy to be administered at a less frequent rate as would be the case with other treatment options making the administration of monoclonal antibodies an attractive means of treatment for a number of diseases[1]. While the use of monoclonal antibodies as a treatment option is expensive the resultant benefit of such therapies in inflammatory diseases such as severe asthma can often outweigh the cost of the treatment as patients who have their asthma symptoms under control are likely to experience less exacerbations, are likely to experience less time missed from work, less doctor and hospital admissions and overall patients often experience a better quality of life[2]. Severe asthma, while affecting 5-10% of the overall asthma population, accounts for approximately 50% of the direct and indirect costs associated with asthma[3].

The global prevalence of asthma in adults is approximately 4.5% which translates to 300 million people worldwide with asthma and the prevalence of asthma is often seen to be increased in western countries where the prevalence rate can be as high as 21.5% within a population[2]. While patients can experience specific symptom fluctuations such as triggers like allergens or cold air or a general worsening of symptoms at night or early morning, most asthmatic patients are equipped to keep such occurrences under control thanks to inhaled corticosteroids (ICS)and long acting beta agonists (LABA) which can improve lung function and reduce the rate of exacerbations[2,4].

However within the asthma population 5-10% of patients can be defined as having severe asthma where either persistent symptoms or exacerbations occur despite the use of maximal maintenance medications such as inhaled corticosteroids and long acting beta agonists or rescue medications such as short acting beta agonists and oral steroids[2,5]. In severe asthma where a marked reduction in the burden of

the disease is not often seen and in consequence risk of morbidity and mortality is higher treatment options such as monoclonal antibodies can offer a lifeline[1].

Several endotypes are recognised within severe asthma which can then be characterised by the shared presence of cellular and molecular biomarkers which can be beneficial in the development of novel therapies for this population and at present several monoclonal antibodies targeting inflammatory pathways are commercially available[1,2]. 40-60% of severe asthma patients suffer from eosinophilic airway inflammation, a well-defined endotype of severe asthma[1]. Monoclonal antibodies which target this have recently become available for use as adjunctive therapy options. Three such monoclonal antibody therapies which have received FDA (USA) and EMA (Europe) approval are Nucala®/Mepolizumab (GlaxoSmithKline) and Cinqaero®/Reslizumab (Teva Pharmaceutical Industries) which can be described as anti-IL-5 monoclonal antibodies and Fasenra®/Benralizumab (AstraZeneca) which can be described as an anti-IL-5R monoclonal antibody, targeting the α chain of the IL-5 receptor[2,6].

IL-5 is a homodimeric cytokine, secreted by eosinophils, basophils, T cells, mast cells and Type 2 innate lymphoid cells, which binds to the receptor IL-5Rα, activating the high affinity IL-5R to transduce intracellular signals upon binding[1]. The IL-5 cytokine is highly involved in eosinophil development and pathobiology within humans[1]. As about 50% of severe asthma exacerbations are eosinophilic in nature a reduction in eosinophils within severe eosinophilic asthma patients with could potentially reduce exacerbations[7].

Mepolizumab (GlaxoSmithKline) and Reslizumab (Teva Pharmaceutical Industries) are IL-5 antagonist monoclonal antibodies and both bind to soluble IL-5 which inhibits the binding of IL-5 to its corresponding IL-5 surface receptors resulting in the downregulation of the IL-5 eosinophil inflammatory pathway. Mepolizumab is administered to patients subcutaneously or intravenously while Reslizumab is administered to patients intravenously[2,5]. A schematic depicting monoclonal antibody interaction in the case of Mepolizumab and Reslizumab can be seen in figure 1.

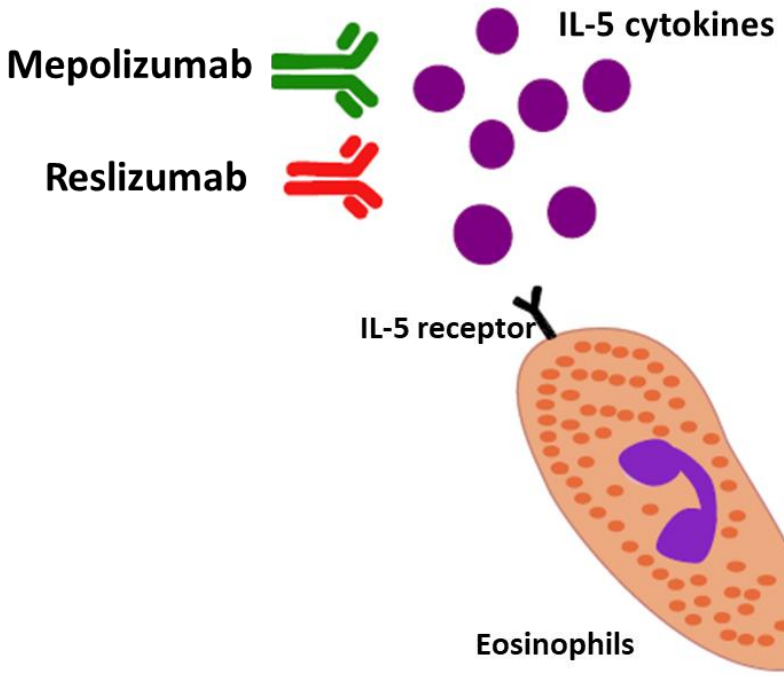


Figure 1. Monoclonal antibody interaction. Mepolizumab and Reslizumab are two monoclonal antibodies recently released for the treatment of asthma. Mepolizumab and Reslizumab target free IL-5 cytokines, binding to the IL-5 cytokine molecules in order to prevent IL-5 cytokines binding to the IL-5 receptor present on eosinophils, thus preventing the downstream effects of growth activation and differentiation of eosinophils, a consequence of IL-5 binding to the IL-5 receptor on these immune cells. Figure adapted from Edris *et al*., Respiratory Research, 2019[2].

Benralizumab (AstraZeneca) binds to the IL-5 receptor on the α-chain and prevents IL-5 from binding to its receptor which results in the inhibition of eosinophil differentiation and maturation in the bone marrow[6]. Benralizumab also can bind to the RIIIa region of Fcγ receptor on Natural Killer (NK) cells, macrophages and neutrophils. This results in the induction of cell mediated cytotoxicity for both circulating eosinophils and tissue resident eosinophils[6]. Benralizumab is administered to patients subcutaneously[6]. A schematic depicting monoclonal antibody interaction in the case of Benralizumab can be seen in figure 2.

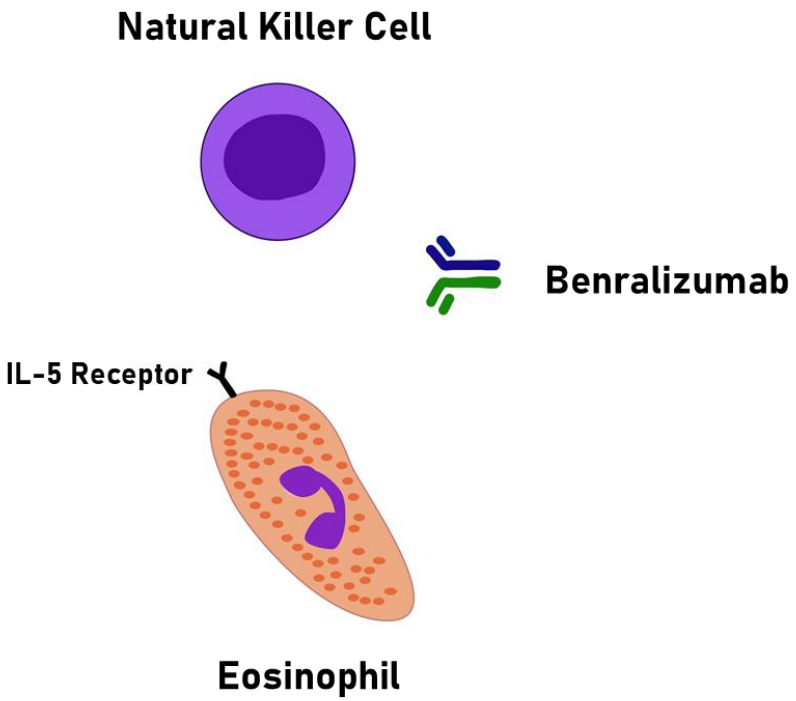


Figure 2. Interaction of the monoclonal antibody Benralizumab. The monoclonal antibody Benralizumab binds to the alpha (α) chain of the IL-5 receptor which enables the prevention of signal transduction. Benralizumab is also capable of binding to Natural Killer Cells at the FcγIIIRa receptor which enables the induction of eosinophil apoptosis. Figure adapted from Edris *et al*., Respiratory Research, 2019[2]

Study of the human lung microbiome in the context of pulmonary health and disease is an area of emerging research interest that is being driven by several contributing factors. These factors include increased recognition of the diversity of human-associated microbiota, their roles in health and in disease associated with chronic inflammation and advancements in technologies and tools that have facilitated such discoveries about the microbiota in organ systems outside of the lung[8]. Therefore through this study the microbiota of the asthma cohort will be investigated with an emphasis on potential differences in the lung microbiome of patients with severe asthma receiving novel treatment protocols.

3. Methods

3.1. Patient recruitment

This study was approved by the Clinical Research Ethics Committee of the Cork Teaching Hospitals. Eight adult patients with a history of asthma (either documented change in FEV1 ≥12%/200ml with bronchodilator or a positive inhalation challenge) were recruited through a dedicated asthma clinic in a tertiary referral centre, Cork University Hospital, by my clinical supervisor, Dr Des Murphy. Baseline bronchoscopy and bronchoscopy post anti-IL-5 monoclonal antibody treatment were performed by Dr Des Murphy.

Patients were scheduled for baseline bronchoscopy, with spirometry and ACQ-7 performed on the day of bronchoscopy. Written informed consent was obtained from patients on the day of bronchoscopy. Spirometry, a widely used pulmonary function test which measures the maximal volume of air an individual can inspire and expire with maximal effort was performed according to ATS/ERS guidelines by research nurses from the Cork Clinical Research Facility – CCRF immediately prior to bronchoscopy[9,10]. The Asthma Control Questionnaire (ACQ-7) consists of 7 items, weighted equally, the mean of which is used to calculate the patients ACQ-7 score, enabling the measurement of patient asthma control was carried out by research nurses from the Cork Clinical Research Facility – CCRF prior to bronchoscopy[11-13].

Patients underwent bronchoscopy according to standard guidelines[14]. Flexible bronchoscopy using video assisted imaging was performed under conscious sedation with local anaesthetic applied topically to the vocal cords, trachea and endobronchial tree. Bronchoalveolar lavage (BAL) was achieved through the instillation of saline via the bronchoscope and this enabled the collection of specimen directly from the endobronchial lumen for subsequent cytological and microbiological investigation. Bronchoalveolar lavage (BAL) was obtained as a standardised 180ml (3X60ml) sample from either the right middle lobe or lingula[15].

Patients were prescribed an anti-IL-5 monoclonal antibody as an adjunctive therapy as part of their asthma treatment plan. Patients in this cohort were prescribed the

anti-IL-5 monoclonal antibody Reslizumab (Cinqaero®, Teva Pharmaceutical Industries). Reslizumab was administered intravenously at a dedicated setting at Cork University Hospital.

Patients were scheduled for follow-up bronchoscopy, with spirometry, ACQ-7 and bloods taken on the day of bronchoscopy. Spirometry was performed according to ATS/ERS guidelines [9]. Bronchoscopy was performed according to standard guidelines[14]. Bronchoalveolar lavage (BAL) was obtained as a standardised 180ml (3X60ml) sample from either the right middle lobe or lingula as we have previously described[15]. Further information with regards to asthmatic patient bronchoscopy and patient sample collection protocols can be found in *Chapter 2 Study Cohorts'*.

3.2. Sample processing

After the bronchoscopy procedure was completed the patient BAL and bloods were processed in a laminar flow hood under strict aseptic technique practices. 5ml of the neat BAL was removed and aliquoted for future downstream processing.

Microscopic processing

Approximately 500-1000µl of neat BAL was also aliquoted into a 2ml screwcap tube for cyto-centrifugation, to allow for microscopic examination and scoring of the BAL sample. A Shandon CytoSpin 4 centrifuge (Thermo Scientific) was used and 200µl of BAL was required per microscope slide. The machine was organised with the labelled microscope slides and funnel system, using approximately 2-4 microscope slides per patient. The samples were centrifuged at 400rpm for 2 minutes. The cytocentrifuge deposited the cells into a clearly defined area of the glass microscope while constructively flattening the cells to allow for clear nuclear presentation.

The slides then underwent staining procedures using a Kwik Diff commercial staining kit (Thermo Scientific) and a Gram staining kit (Sigma Aldrich). The Kwik Diff staining kit comprised of 3 reagents; methanol, xanthene dye in buffer salts and thiazine dye in buffer salts. The reagents were added to three separate staining jars and the microscope slides, with the deposited BAL cells were added to a slide rack which was dipped into each of the reagents approximately 10-15 times, ensuring excess reagent was allowed to drain back into the jar before moving to the next staining jar. Upon the completion of the final staining step, the slides were rinsed under deionised water and the slides were then air dried and cover slipped the following day using DPX histology mountant (Sigma Aldrich).

Gram staining (Sigma Aldrich) to differentially stain for Gram positive and negative bacteria took place as follows. The microscope slide with the deposited BAL sample was first flooded with crystal violet for 1 minute before washing the slide gently under an indirect stream of water for 2 seconds. The slide was then flooded with Gram's iodine for 1 minute before washing the stain as before. Acetone-alcohol decolourised was used to flood the slide and allowed to sit for 15 seconds before the slide was then flooded with the counterstain safranin and allowed to sit for 1 minute before the slide was washed gently under an indirect stream of water. The slides were allowed to air dry and were cover slipped the following day using a DPX histology mountant (Sigma).

DNA collection

Neat BAL was centrifuged at 500g for 10 minutes and the supernatant was removed. While this did not occur for 4 baseline bronchoscopy BAL samples it was decided that the cell pellet remaining after the BAL centrifugation should also be analysed and so for following samples this procedure was adopted and the pellet was re-suspended creating the cell pellet fraction (CP) for future DNA isolation and analysis. The BAL supernatant was aliquoted into 2-5ml tubes for future analysis. BAL supernatant was also aliquoted into 10-20 2ml screw cap microcentrifuge tubes (Sarstedt) and centrifuged at 20,000g for 5 minutes. The supernatant of which was

aliquoted into 2ml tubes for future cell stimulations and the remaining pellets were re-suspended and pooled together creating the bacteria pellet fraction (BP) for future DNA isolation and analysis

Blood cytokine collection

Blood samples were collected in serum specific red and yellow capped Vacuette tubes and plasma specific purple capped Vacuette tubes (Greiner Bio-One). The inner wall of the serum specific tube was coated with silica particles which activated the coagulation process and a specific separator gel at the base of the tube formed a stable barrier during centrifugation to enable the serum and blood cells to remain separate. The plasma specific Vacuette tube contained a coating of either K2EDTA or K3EDTA which acted as an anticoagulant by binding calcium ions to prevent the clotting cascade from taking place. Both tubes were centrifuged at 200rpm for 20 minutes and the serum and plasma was removed by pipetting and stored in screw-cap microcentrifuge tubes.

All BAL and blood isolated samples were stored at -80^{o}C for future processing and analyses.

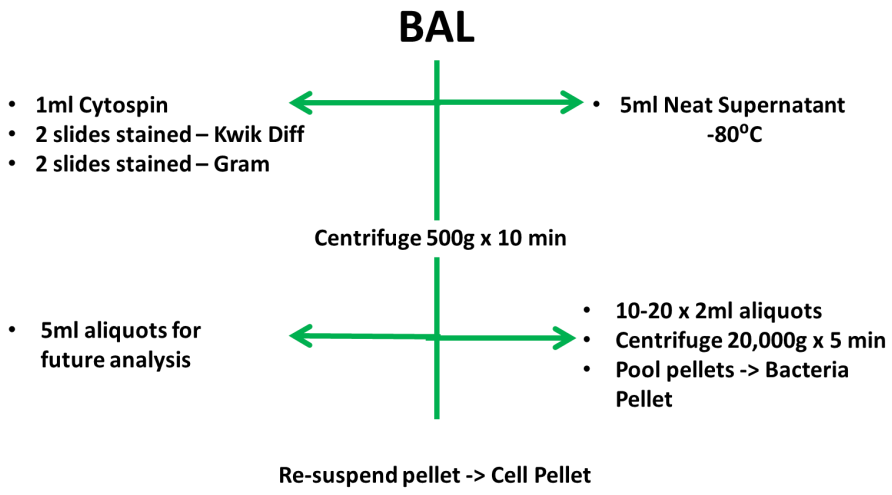


Figure 3. Patient BAL processing schematic BAL processing began in the laboratory on the day of bronchoscopy.

3.3. Microscopy

BAL cytospin slides which were stained with the commercial differentiation staining kit Kwik Diff (Thermo-Fischer) underwent differential cell counts using a light microscope (Olympus or Leica DM750). Microscope slides were pictured using Olympus DP software. Immune cell percentage counts of monocytes, macrophages, lymphocytes, eosinophils and neutrophils took place over 10 random fields of view per microscope slide, n=2 slides per patient. Microbes were visibly present within a number of stain differentiated patient microscope slides both freely among the immune cells and within the macrophages in certain cases.

3.4. DNA extraction

DNA extraction was carried out for both the BAL isolated bacteria pellet (BP) sample and the BAL isolated cell pellet (CP) sample in order to investigate if there was potential differences in bacteria free within the BAL sample and bacteria potentially within the macrophage cell population. The DNA isolation protocol was carried out the same way for both the BAL isolated bacteria pellet and the BAL isolated cell pellet. To remove host cell DNA, BAL was centrifuged at 500g for 10 minutes, supernatant collected and centrifuged in 2ml screwcap microcentrifuge tubes at 20,000g for 5 minutes. The supernatant was then removed and the remaining bacteria pellets were recombined for DNA extraction.

DNA extraction took place using a QIAamp UPC Pathogen Mini Kit (Qiagen, Manchester, UK). Patient bacteria pellet samples were centrifuged at 20,000g for 5 minutes, supernatant discarded and 500ul buffer ATL was used to re-suspend the pellet which was then added to a pathogen lysis tube containing silica beads and vortexed at 7000rpm for 1 minute using a MagNA Lyser machine. The tube was then centrifuged at 8000g for 30 seconds and supernatant removed to a fresh microcentrifuge tube without disrupting the silica beads. 40µl of Proteinase K was added and the tube was vortexed and incubated at 56^{o}C for 10 minutes. 200µl buffer APL2 then added to the sample, the tube was vortexed and incubated at

70°C for 10 minutes. 300µl of ethanol was added to the lysate and the tube was pulse vortexed for 30 seconds and the lysate was then transferred to a mini spin column placed in a collection tube and centrifuged at 6000g for 1 minute. This was repeated until all of the lysate had been transferred and passed through the mini spin column, discarding the filtrate after each spin. 600µl of Buffer APW1 was added to the mini spin column which was then centrifuged at 6000g for 1 minute, discarding the filtrate afterwards. 750µl of Buffer APW2 was transferred to the mini spin column which was then centrifuged at 20,000g for 3 minutes, transferring the mini spin column to a new collection tube and repeating centrifugation to eliminate buffer carryover. The mini spin column was transferred to a new collection tube and incubated at 56°C for 3 minutes to ensure the membrane was dry and was then transferred to a new elution tube and 100µl of Buffer AVE was added to the centre of the membrane and incubated at room temperature for 1 minute before being centrifuged at 20,000g for 1 minute to elute the DNA. The isolated DNA samples were then stored at -20°C for further downstream processing.

3.5. DNA quantification

DNA quantification was performed using a Qubit dsDNA High Sensitivity (HS) assay kit (Life Technologies, Thermo-Fischer) which consisted of Qubit dsDNA HS assay reagent (200X concentrate in DMSO), Qubit dsDNA HS dilution buffer, Qubit dsDNA HS standard #1 (0ng/µl in TE buffer) and Qubit dsDNA HS standard #2 (10ng/µl in TE buffer) and a Qubit 0.2 Fluorometer (Life Technologies, Thermo Fischer). The assay was highly selective for double-stranded (dsDNA) and was accurate for initial sample concentrations of 10pg/µl to 10ng/µl. Specialised Qubit thin wall clear 0.5ml assay tubes were sourced (Life Technologies, Thermo-Fischer) and the number of tubes required for the samples and two standards were labelled on the tube lid but not the side as this may interfere with the Qubit Fluorometer reading.

The Qubit working solution was prepared by diluting the Qubit HS reagent 1:200 in Qubit dsDNA HS buffer using a clean plastic tube each time the Qubit working

solution was prepared. For each sample the working solution consisted of 200µl of Qubit dsDNA HS buffer and 1µl of Qubit HS assay reagent. The working solution was prepared in batches of 5 reactions, which consisted of 1ml Qubit dsDNA HS buffer and 5µl of Qubit HS assay reagent. For the standards 190µl of working solution was added to each of two standard tubes and 10µl of standard #1 and 10µl of standard #2 was added to the appropriate tube and the tubes were then vortexed for 3 seconds.

In order to prepare for the DNA sample readings 198µl working solution was added to the individual pre-labelled assay tubes and to this 2µl of DNA sample was added to the appropriate assay tubes for a final volume of 200µl. Tubes were vortexed for 3 seconds ensuring no air bubbles were produced. The assay tubes were incubated at room temperature for 2 minutes.

The dsDNA High Sensitivity programme was selected for on the Qubit Fluorometer machine and in order to calibrate the machine standard #1 was inserted into the sample chamber and was read before standard #2 was read in the same manner. Once calibration was complete the DNA samples were read. In order to standardise the DNA samples before further analyses such as qPCR and Whole Genome Sequencing, samples above 5ng/µl were diluted to 5ng/µl using molecular grade water.

3.6. Primers

Primers were designed through analyses of pre-designed validated primers already present in the literature, through the use of the 16S RNA gene database Greengenes[16] or through literature research to determine specific genes present in the microorganism of interest and using this information to retrieve the sequence coding of that gene.

All primers designed in house through Greengenes or gene sequences were formulated using the Universal Probe Library Assay Design Centre platform (Roche

Life Science) by copying the sequence of interest to the platform, selecting for other organism and deselecting to automatically select for intron spanning assay. The platform then designed potential primers for the sequence of interest, ranking them by order of suitability. Primer sequences were analysed using the NCBI Blastn platform. Two primers sequences were then selected for each microorganism of interest and were ordered from Sigma.Aldrich (Ireland).

Primers were centrifuged upon arrival to ensure the lyophilised pellet was at the bottom of the primer tube and primers were re-suspended with molecular grade water in accordance to individual primer specification (µl for 100µM). Once re-suspended primers were vortexed and the left and right primer were recombined (20µl L+ 20µl R + 160µl molecular grade water) in a sterile 1.5ml tube. Primers were stored at -20^{o}C.

Probes corresponding to the primers of interest were sourced from Universal Probe Library Probes (Roche Life Sciences) and were available within the laboratory. All primers were validated before use on the individual patient bacteria pellet and cell pellet DNA. See supplementary table 1 for primer sequences

3.7. qPCR – quantitative Polymerase Chain Reaction

Initial qPCRs took place on a pool of the isolated bacterial DNA from both cell pellet (CP) BAL samples isolated DNA and bacteria pellet (BP) BAL samples isolated DNA at neat undiluted, 1:10 and 1:100 diluted concentrations in order to validate all primers before they were tested on each individual sample.

qPCR was performed on extracted BAL BP DNA pre and post anti-IL-5 treatment, on extracted BAL CP DNA post anti-IL-5 treatment and on a subset of BAL CP DNA pre anti-IL-5 treatment, as unfortunately cell pellet DNA was not extracted from earlier BAL samples, as it was not included in earlier protocols. qPCRs took place in order to determine the presence of Total Bacteria, Firmicutes, *Staphylococcus aureus*, *Streptococcus pneumoniae*, *Rothia*, *Micromonospora*, *Pseudomonas aeruginosa*,

Pseudomonas fluorescens, *Escherichia*, *Bordetella*, *Prevotella*, *Veillonella*, *Mycoplasma pneumoniae*, *Chlamydophilia pneumoniae*, *Neisseria bacilliformis*, *Moraxella catarrhalis*, *Neisseria meningitidis* and *Haemophilus influenzae* and the fungal primers Fungi Quant and *Aspergillus fumigatus.* See supplementary table 1 for primer sequences.

qPCR's were performed using a 384 well plate layout and LightCycler Probes Master (Roche, Ireland) or LightCycler SYBR Green Master (Roche, Ireland) reagent mix, dependent on the use of hydrolysis probes or SYBR Green primer sets. Water NTCs (No Template Control) were used in each reaction in order to identify reaction set up contamination and to test for the propensity of primers to create primer dimers in the case of reactions which were carried out with SYBR Green Master. Reactions were performed on a LightCycler 480 machine (Roche, Ireland). qPCR conditions were as follows; pre-incubation at 50^{o}C for 2 minutes, ramp rate 4.8^{o}C/s and 95^{o}C for 10 minutes, ramp rate 4.8^{o}C/s. Amplification at 95^{o}C for 10 seconds, ramp rate 4.8^{o}C/s, 60^{o}C for 45 seconds, ramp rate 2.5^{o}C/s and 75^{o}C for 1 second, ramp rate 4.8^{o}C for 45 cycles in total. A melt curve also occurred at 95^{o}C with a ramp rate of 0.11^{o}C/s for any primer which used LightCycler SYBR Green Master. A cooling stage then occurred at 40^{o}C, ramp rate 2^{o}C/s at the end of the process. Fluorescent readings were taken in single acquisition mode. The primers *Neisseria meningitidis*, *Streptococcus pneumoniae* and *Haemophilus influenzae* required a change in the acquisition temperature to 67^{o}C due to the nature of the primer sequences. All NTCs did not produce a product and melt curves produced clear peaks indicating that the products produced were not an artefact.

3.8. BAL cytokine measurement

BAL cytokines were analysed using a custom MSD pro-inflammatory panel 1 containing targets for Interleukin (IL)-1β, IL-4, IL-6, IL-8, IL-10, IL-13, and tumour necrosis factor (TNF)-α and a custom MSD cytokine panel 1 containing targets for IL-5 and IL-17A. Reagent preparation consisted of the following; calibrator

standards were prepared by suspension of the lyophilised calibrator with 1000µl of the appropriate diluent (diluent 2 for pro-inflammatory panel 1 and diluent 43 for cytokine panel 1) and then transferring 100µl of the re-suspended calibrator with 300µl of appropriate diluent. This 4 fold serial dilution was repeated 5 additional times to generate 7 calibrators with the diluent alone used as a zero calibrator. BAL samples were tested undiluted. A detection antibody solution was created for the pro-inflammatory panel by combining 60µl of each SULFO-TAG anti-human IL-1β, IL-4, IL-6, IL-8, IL-10, IL-13 and TNF-α antibody with 2580µl diluent 3 to bring to a final volume of 3000µl. A detection antibody solution for cytokine panel 1 consisted of 60µl each of SULFO-TAG Anti-human IL-5 and IL-17A with 2880µl of diluent 3 for a final volume of 3000µl. Wash buffer consisted of PBS and 0.05% Tween 20. Read buffer for each plate consisted of 10ml of Read Buffer T (4X) and 10ml of deionised water for a 2X working solution. Step 1 of the assay involved washing the plate 3 times with 150µl/well wash buffer 50µl of prepared calibrators or samples was added per well, the plate was sealed before overnight incubation with shaking at 2-8^{o}C. Step 2 involved washing the plate a further 3 times with 150µl/well wash buffer before the addition of 25µl detection antibody solution to each well, the plate sealed and a two hour room temperature incubation with shaking occurred. Step 3; the plate was washed 3 times as before and 150µl of 2X Read Buffer T was added to each well before analysis of the plate using an electro-chemiluminescence QuickPlex SQ 120 imager from Meso Scale Discovery (Gaithersburg, MD, USA).

3.9. Post anti-IL-5 treatment BAL and plasma cytokine analyses.

BAL and plasma cytokines were analysed using a test service provided by RayBiotech (RayBiotech, Georgia, USA) using a custom RayBiotech Quantibody Human Cytokine Array containing targets for Interleukin (IL)-1β, IL-4,IL-5, IL-6, IL-8, IL-10, IL-13, IL-17A, tumour necrosis factor (TNF)-α and Interferon-(IFN)-γ. Testing was carried out according to in-house procedures at RayBiotech. What occurred was briefly as follows; a capture antibody was bound to a glass surface and incubation occurred with the BAL and plasma samples, which were diluted to a dilution factor of 2. After sample incubation was carried out a target cytokine was

trapped to the glass solid surface. A second biotin-labelled detection antibody was added to recognise a specific epitope of the target cytokines. The cytokine-antibody-biotin complex was then visualised by the addition of a streptavidin-conjugated Cy3 equivalent dye and through the use of a laser scanner. For cytokine quantification, the array specific cytokine standards with predetermined concentrations are implemented to generate standard curves. Through simultaneously running the standard cytokines and samples in each array using the described assay procedure it was possible to compare unknown samples to the standard curve thus determining the cytokine concentration of the patient BAL and plasma samples.

3.10. Statistical analyses

Graph Pad Prism 8 software was used to perform all statistical analyses and to provide graphical representation of the data. All data was assessed using normality and lognormality tests and the Shapiro-Wilk test was applied to assess the normality of the data set.

Normally distributed data was presented as the mean ± standard deviation (SD) within the text and figures. Normally distributed data sets where both the X and Y values were normally distributed were analysed using Pearson correlation coefficient analysis. Data was considered to be statistically significant when $P<0.05$.

Non-normally distributed data was presented as median ± interquartile range (IQR) within the text and figures. Non-normally distributed data sets where both the X and Y values were not both normally distributed were analysed using the non-parametric Spearman correlation[17]. Data was considered to be statistically significant when $P<0.05$.

4. Results

4.1. Patient demographics

The patient cohort consisted of eight adult asthmatic patients, 2 males and 6 females. 7/8 patients (87.5%) had never smoked while one patient (12.5%) was an ex-smoker. 6/8 patients (75%) lived in a rural setting while 2/8 patients (25%) lived in an urban location.

At baseline bronchoscopy patient demographics were as follows. When stratified by asthma severity using GINA groupings of mild (GINA 1-2), moderate (GINA 3) and severe (GINA 4-5) one patient (12.5%) was grouped as a moderate asthmatic (GINA 3) while 7/8 patients (87.5%) were stratified as severe asthmatics (GINA 4-5). 2/8 patients (25%) were in receipt of oral steroids (min 5mg- max 10mg). All eight patients were in receipt of inhaled corticosteroids (ICS) (FDP) (min 800 – max 2000 FDP) [Mean (SD)] [1188 (387.1)]; [Median (IQR)] [1000 (1000-1425)].

At follow up bronchoscopy after anti-IL-5 treatment patient demographics were as follows. Stratified by asthma severity (GINA) all patients were classified as GINA 5 and were grouped as severe asthmatics (GINA 4-5). Using ACQ-7 as a means of determining asthma control 4 patients were grouped as (ACQ-7<1.5) controlled while 4 patients were grouped as (ACQ-7≥1.5) uncontrolled. 2 patients at follow up bronchoscopy were in receipt of oral steroids (min 5mg – max 10mg). All eight patients were in receipt of inhaled corticosteroids (ICS) (min 800 – max 2400 FDP) [Mean (SD)] [1125 (523.0)]; [Median (IQR)] [1000 (850-1000)] at time of follow up bronchoscopy.

While oral steroid dose remained consistent irrespective of anti-IL-5 therapy patients required inhaled corticosteroid (ICS) (FDP) dose reduced upon treatment with the monoclonal antibody Reslizumab. Inhaled corticosteroid dose reduced overall from [Mean (SD)] [1188 (387.1)]; [Median (IQR)] [1000 (1000-1425)].to [Mean (SD)] [1125 (523.0)]; [Median (IQR)] [1000 (850-1000)] at time of follow up bronchoscopy indicating a positive clinical improvement for patients.

Taking into account the patient spirometry results an increase in the FEV-1 was documented overall upon receipt of anti-IL-5 therapy. Patients FEV-1 (percent predicted) increased from [Mean (SD)] [60.3 (19.5)]; [Median (IQR)] [50 (45-83)] to [Mean (SD)] [75.3 (21.7)]; [Median (IQR)] [80 (53.3-95.8)]. Focusing on patients Fractional exhaled Nitric Oxide (FeNO) (ppb) an increase from [Mean (SD)] [22.8 (7.4)]; [Median (IQR)] [25 (15.3-28.0)] to [Mean (SD)] [38.8 (23)]; [Median (IQR)] [30 (22.8-64.0)] was observed on the day of follow-up bronchoscopy after patients were in receipt of the anti-IL-5 monoclonal antibody Reslizumab.

As Reslizumab is an IL-5 antagonist monoclonal antibody, binding to soluble IL-5 inhibiting subsequent binding of IL-5 to its corresponding IL-5 surface receptors thus resulting in the downregulation of the IL-5 eosinophil inflammatory pathway, patient BAL was examined by microscopy to determine the percentage of BAL eosinophils at both baseline bronchoscopy and at follow-up bronchoscopy. At baseline bronchoscopy patient BAL eosinophil counts revealed a mean of 7.1 (SD 7.8) eosinophils while at follow-up bronchoscopy patient BAL eosinophil counts revealed a mean of 0.4 (SD 0.4) eosinophils. Comparing the eosinophil counts pre- and post- anti-IL-5 therapy using an unpaired t-test with Welch's correction revealed a statistically significant difference in eosinophil counts ($P<0.05$). See Figure 4 for BAL Immune cell counts pre- and post- anti-IL-5 therapy. See Figure 5 for immune cell differential counts pre- and post- anti-IL-5 monoclonal antibody treatment.

See Table 1 for patient demographics at baseline bronchoscopy and at follow-up bronchoscopy post-anti-IL-5 (Reslizumab) treatment.

Table 1 Patient demographics. Patient demographics at baseline bronchoscopy before patients were prescribed anti-IL-5 monoclonal antibody treatment and patient demographics taken at follow-up bronchoscopy after patients received the anti-IL-5 monoclonal antibody Reslizumab (Cinqaero). Note † ICS, Inhaled Corticosteroids; ‡ FeNO, Fractional exhaled Nitric Oxide; § FEV-1, Forced Expiratory Volume in the first second; ¶ BMI, Body Mass Index. n=8

n=8		Baseline	Treatment
Male		2 (25%)	2 (25%)
Female		6 (75%)	6 (75%)
Smoker	Current	0	0
	Ex-	1	1
	Never	7	7
Oral Steroids (mg)	Positive	2	2
	[Mean (SD)]	[1.9 (3.7)]	[1.9 (3.7)]
	[Median (IQR)]	[0 (0-3.8)]	[0 (0-3.8)]
ICS (µg) FDP 250 †	Positive	8	8
	[Mean (SD)]	[1188 (387.1)]	[1125 (523)]
	[Median (IQR)]	[1000 (1000-1425)]	[1000 (850-1000)]
FeNO (ppb) ‡	[Mean (SD)]	[22.8 (7.4)]	[38.8 (23)]
	[Median (IQR)]	[25 (15.3-28.0)]	[30 (22.8-64)]
FEV-1 (Percent Predicted) §	[Mean (SD)]	[60.3 (19.5)]	[75.3 (21.7)]
	[Median (IQR)]	[50 (45-83)]	[80 (53.3-95.8)]
BMI (kg/m^2) ¶	[Mean (SD)]	[31.8 (5.7)]	[32.6 (5.3)]
	[Median (IQR)]	[31.5 (28.1-36.4)]	[31 (29.9-36.3)]
IgE (KU/L)	[Mean (SD)]	[205.8 (353.6)]	n/a
	[Median (IQR)]	[67.7 (16.2-247.5)]	n/a
BAL Monocyte % count	[Mean (SD)]	[5.2 (6.1)]	[10.3 (10.3)]
	[Median (IQR)]	[3.3 (0.4-10.3)]	[9.3 (3.2-11.1)]
BAL Macrophage % count	[Mean (SD)]	[64.3(17.5)]	[75 (9.6)]
	[Median (IQR)]	[63.1 (54.3-78.5)]	[77.6 (67.4-88.3)]
BAL Lymphocyte % count	[Mean (SD)]	[6.9 (6.2)]	[7.6 (4.7)]
	[Median (IQR)]	[5.6 (1.9-10.6)]	[5.9 (4.1-12.1)]
BAL Eosinophil % count	[Mean (SD)]	[7.1 (7.8)]	[0.4 (0.4)]
	[Median (IQR)]	[4.1 (1.3-12)]	[0.4 (0.05-0.7)]
BAL Neutrophil % count	[Mean (SD)]	[16.7 (18.3)]	[6.7 (8.6)]
	[Median (IQR)]	[13.4 (0.9-28.8)]	[2.5 (0.3-16.9)]
IL-1β BAL (pg/ml)	[Mean (SD)]	[9.6 (21.9)]	[0.7 (2.1)]
	[Median (IQR)]	[[1.8 (0.8-4.3)]	[0 (0-0)]
IL-4 BAL (pg/ml)	[Mean (SD)]	[0.6 (1.3)]	[3.5 (6.8)]
	[Median (IQR)]	[0.2 (0-0.4)]	[0 (0-7.7)]
IL-5 BAL (pg/ml)	[Mean (SD)]	[1.3 (3.3)]	(1.2 (3.4)]
	[Median (IQR)]	[0 (0-0.5)]	[0 (0-0)]
IL-6 BAL (pg/ml)	[Mean (SD)]	[5.6 (7.1)]	[8.5 (15.4)]
	[Median (IQR)]	[1.5 (1.2-10.8)]	[0 (0-13.6)]
IL-8 BAL (pg/ml)	[Mean (SD)]	[1123 (2527)]	[247.8 (308.7)]
	[Median (IQR)]	[84.9 (30-1024)]	[126.9 (29.9-486.9)]

		Baseline	Treatment
IL-10 BAL (pg/ml)	[Mean (SD)]	[0.7 (1.2)]	[1.5 (2.1)]
	[Median (IQR)]	[1.3 (0-1.2)]	[0 (0-3.5)]
IL-13 BAL (pg/ml)	[Mean (SD)]	[8 (4.4)]	[5.3 (3.9)]
	[Median (IQR)]	[8.9 (3.0-11.8)]	[6.6 (0.7-8.2)]
IL-17 BAL (pg/ml)	[Mean (SD)]	[0.2 (0.5)]	[0 (0)]
	[Median (IQR)]	[0 (0-0)]	[0 (0-0)]
TNF-α BAL (pg/ml)	[Mean (SD)]	[1.5 (2.4)]	[0 (0)]
	[Median (IQR)]	[0.5 (0.4-1.8)]	[0 (0-0)]
Haemoglobin (HB) (g/L)	[Mean (SD)]	[14.1 (1.8)]	[49.3 (65.3)]
	[Median (IQR)]	[14.3 (12.1-15.5)]	[5.9 (0-121.2)]
White cell count (WBC) (10^9/L)	[Mean (SD)]	[8.3 (3.1)]	
	[Median (IQR)]	[7.4 (6.3-8.6)]	
Blood Lymphocyte count (10^9/L)	[Mean (SD)]	[2.1 (1.0)]	
	[Median (IQR)]	[1.7 (1.5-2.8)]	
Blood Eosinophil count (10^9/L)	[Mean (SD)]	[0.6 (0.3)]	
	[Median (IQR)]	[0.7 (0.4-0.9)]	
Blood Neutrophil count (10^9/L)	[Mean (SD)]	[5.3 (1.9)]	
	[Median (IQR)]	[5 (4.0-5.4)]	
IL-1β plasma (pg/ml)	n=	4	8
	[Mean (SD)]	[0.4 (0.6)]	[150.1 (183)]
	[Median (IQR)]	[0.1 (0.1-1.1)]	[55.6 (1.7-340.3)]
IL-4 plasma (pg/ml)	n=	4	8
	[Mean (SD)]	[6.1 (8.0)]	[9.6 (13)]
	[Median (IQR)]	[6.1 (0.4-11.7)]	[5.2 (0-15.9)]
IL-5 plasma (pg/ml)	n=	4	8
	[Mean (SD)]	[7.5 (2.3)]	[1.2 (3.3)]
	[Median (IQR)]	[7.5 (5.9-9.1)]	[0 (0-0)]
IL-6 plasma (pg/ml)		4	8
	[Mean (SD)]	[3.1 (3.0)]	[0 (0)]
	[Median (IQR)]	[2.2 (0.7-6.3)]	[0 (0-0)]
IL-8 plasma (pg/ml)	n=	4	8
	[Mean (SD)]	[5.2 (2.2)]	[964.9 (1708)]
	[Median (IQR)]	[4.8 (3.3-7.4)]	[359.7 (129.5-853.8)]
IL-10 plasma (pg/ml)	n=	4	8
	[Mean (SD)]	[3.3 (5.5)]	[3.1 (3.0)]
	[Median (IQR)]	[0.7 (0.4-8.9)]	[3.1 (0-5)]
IL-13 plasma (pg/ml)	n=	4	8
	[Mean (SD)]	[24.7 (35.4)]	[7.8 (6.5)]
	[Median (IQR)]	[7.8 (6.0-66.3)]	[5.8 (2.9-14.6)]
IL-17 plasma (pg/ml)	n=	4	8
	[Mean (SD)]	[2.1 (0.9)]	[0 (0)]
	[Median (IQR)]	[2.1 (1.4-2.7)]	[0 (0-0)]
TNF-α plasma (pg/ml)	n=	4	8
	[Mean (SD)]	[14.3 (24.4)]	[116.8 (330.3)]
	[Median (IQR)]	[2.4 (1.6-38.9)]	[0 (0-0)]
IFN-γ plasma (pg/ml)	n=	4	8
	[Mean (SD)]	[5.3 (2.4)]	[17.4 (49.1)]
	[Median (IQR)]	[4.3 (3.9-7.8)]	[0 (0-0)]

4.2. Microscopy

Microscope examination took place for the two microscope slides per patient at the pre-treatment time-point and then again at the post-treatment time-point, n=8 patients. Immune cell percentage counts took place for all patients, pre-anti-IL-5 treatment and post-anti-IL-5 treatment and the percentage of monocytes, macrophages, lymphocytes, neutrophils and eosinophils were calculated for each patient at each time-point.

When the BAL immune cell percentage counts were compared pre- and post-anti-IL-5 treatment the percentage of eosinophils present in the BAL slides by microscopy decreased after patients were in receipt of anti-IL-5 therapy. At baseline bronchoscopy patient BAL eosinophil counts revealed a mean of 7.1 (SD 7.8) eosinophils while at follow-up bronchoscopy patient BAL eosinophil counts revealed a mean of 0.4 (SD 0.4) eosinophils. Comparing the eosinophil counts pre- and post- anti-IL-5 therapy using an unpaired t-test with Welch's correction revealed a statistically significant difference in eosinophil counts ($P<0.05$). See Figure 4 for BAL Immune cell counts pre- and post- anti-IL-5 therapy. See Figure 5 for immune cell differential counts pre- and post- anti-IL-5 monoclonal antibody treatment.

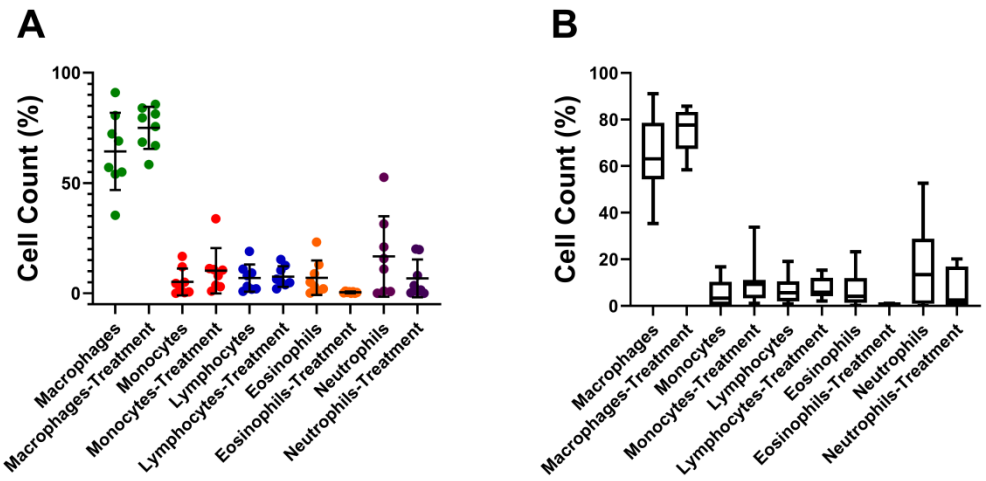


Figure 4. BAL immune cell counts pre- and post- anti-IL-5 therapy. BAL immune cell differential counts took place for n=8 patients at baseline and follow-up bronchoscopy before and after patients received the monoclonal anti-IL-5 antibody therapy. (A) The differences in immune cell differential counts represented in the form of a scatter plot graph with values represented in the form of mean and standard deviation. (B) The overall difference in immune cell differential counts at baseline and follow-up bronchoscopy represented as a box and whiskers graph plotting the min to max. Eosinophils were significantly reduced within the follow-up bronchoscopy BAL samples ($P<0.05$). n=8.

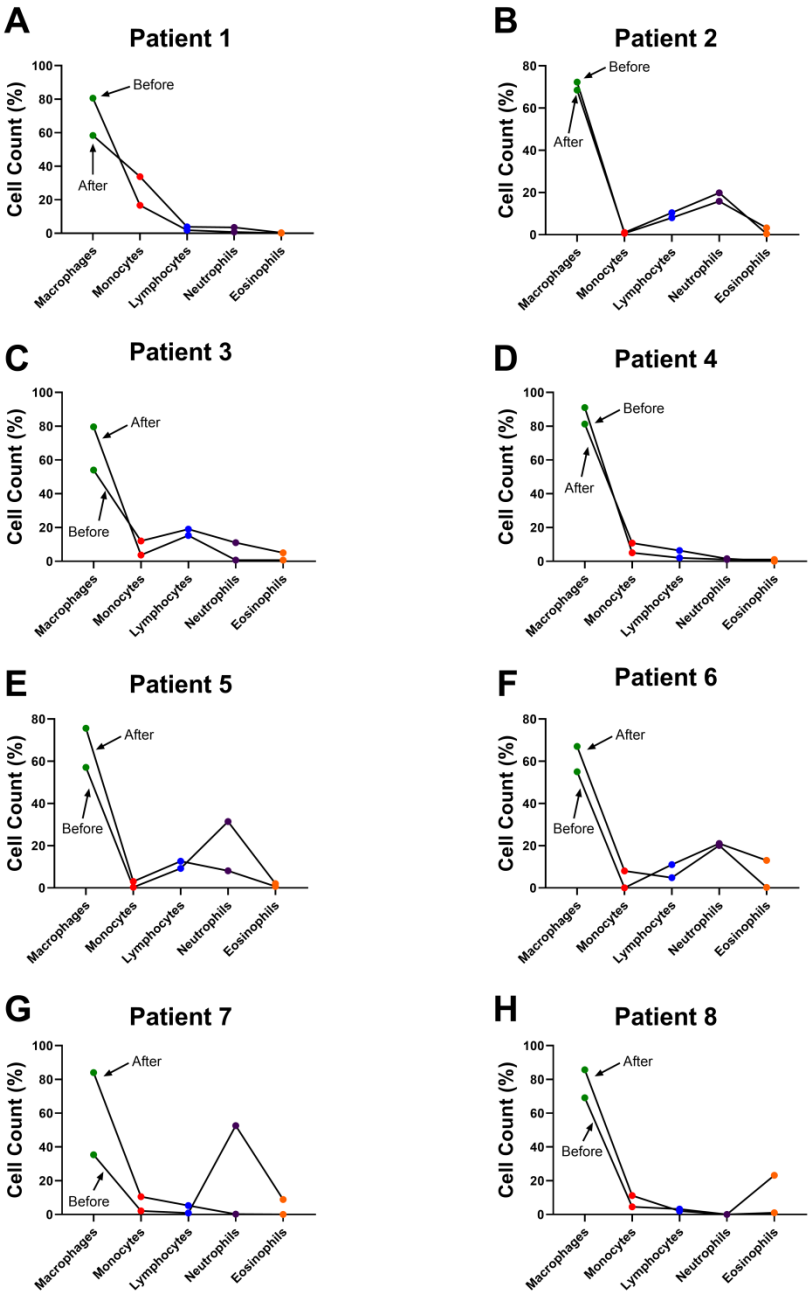


Figure 5. Immune cell differential counts pre and post anti-IL-5 monoclonal antibody treatment. BAL immune cell differential counts for each patient at baseline bronchoscopy and at the follow-up bronchoscopy after patients received treatment with the anti-IL-5 monoclonal antibody.

4.3. Cytokine analyses

Cytokines interleukin -1β (IL-1β), IL-4, IL-5, IL-6, IL-8, IL-10, IL-13, IL-17 and Tumour Necrosis Factor-α (TNF-α) were measured in BAL samples obtained at baseline bronchoscopy. BAL baseline cytokines were measured using an electro-chemiluminescence Quick Plex SQ 120 imager from Meso Scale Discovery (Gaithersburg, MD, USA) where antibodies labelled with SULFO-TAG™ reagents emitted light upon electrochemical stimulation. n=8. The cytokines Interleukin – 1β (IL-1β), IL-4, IL-5, IL-6, IL-8, IL-10, IL-13, IL-17, Tumour Necrosis Factor (TNF)– α and Interferon (IFN) - γ were measured in patient plasma samples obtained at baseline bronchoscopy using an electro-chemiluminescence Quick Plex SQ 120 imager from Meso Scale Discovery (Gaithersburg, MD, USA) where antibodies labelled with SULFO-TAG™ reagents emitted light upon electrochemical stimulation. n=4.

Secreted human cytokines Interleukin – 1β (IL-1β), IL-4, IL-5, IL-6, IL-8, IL-10, IL-13, IL-17, Tumour Necrosis Factor (TNF)– α and Interferon (IFN) - γ were measured in patient plasma and BAL samples obtained at follow up bronchoscopy following anti-IL-5 monoclonal antibody therapy. Cytokines were measured by RayBiotech (Georgia, USA) using Quantibody human cytokine arrays. n=8.

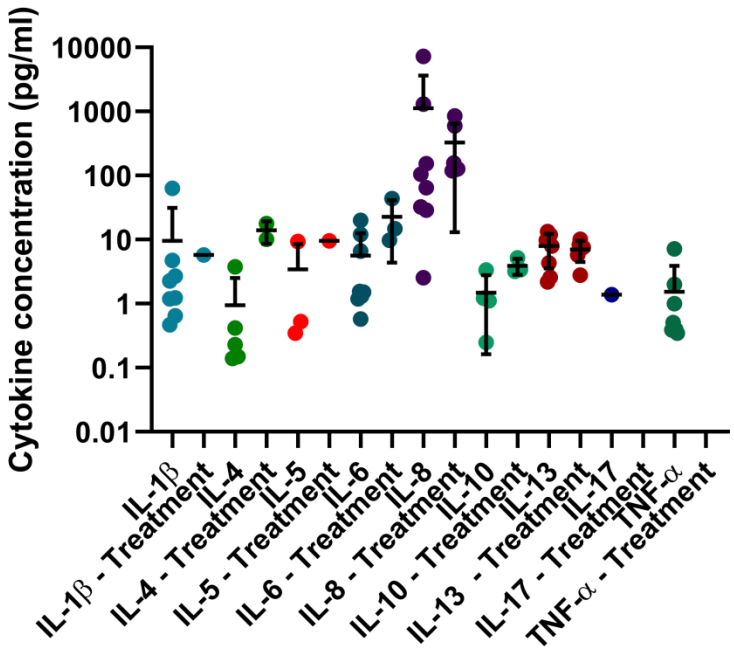


Figure 6. Cytokine levels in the patient BAL at baseline bronchoscopy and at follow-up bronchoscopy after patients received anti-IL-5 (Reslizumab) therapy. Measurement of secreted human cytokines Interleukin – 1β (IL-1β), IL-4, IL-5, IL-6, IL-8, IL-10, IL-13, IL-17 and Tumour Necrosis Factor – α (TNF-α) in patient BAL at baseline bronchoscopy occurred using an electro-chemiluminescence Quick Plex SQ 120 imager from Meso Scale Discovery (Gaithersburg, MD, USA) where antibodies labelled with SULFO-TAG™ reagents emitted light upon electrochemical stimulation. Measurement of secreted human cytokines Interleukin – 1β (IL-1β), IL-4, IL-5, IL-6, IL-8, IL-10, IL-13, IL-17 and Tumour Necrosis Factor – α (TNF-α) in patient BAL at follow-up bronchoscopy occurred using RayBiotech (Georgia, USA) custom human cytokine Quantibody arrays. [Mean (SD)] n=8.

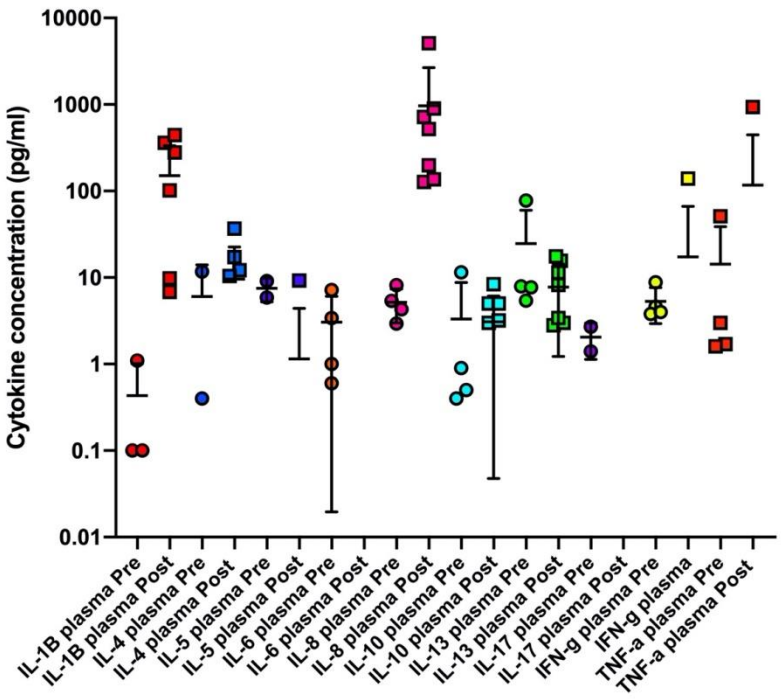


Figure 7 Cytokine levels in patient plasma at baseline bronchoscopy and at follow—up bronchoscopy after patients received anti-IL-5 (Reslizumab) therapy. Measurement of secreted human cytokines Interleukin – 1β (IL-1β), IL-4, IL-5, IL-6, IL-8, IL-10, IL-13, IL-17, Tumour Necrosis Factor – α (TNF-α) and Interferon – γ (IFN-γ) in patient plasma at baseline bronchoscopy occurred using an electro-chemiluminescence Quick Plex SQ 120 imager from Meso Scale Discovery (Gaithersburg, MD, USA) where antibodies labelled with SULFO-TAG™ reagents emitted light upon electrochemical stimulation. [Mean (SD)] n=4. (B) Measurement of secreted human cytokines Interleukin – 1β (IL-1β), IL-4, IL-5, IL-6, IL-8, IL-10, IL-13, IL-17, Tumour Necrosis Factor - α (TNF–α) and Interferon - γ (IFN-γ) in patient plasma at follow up bronchoscopy following anti-IL-5 monoclonal antibody therapy. Cytokines were measured by RayBiotech (Georgia, USA) using Quantibody human cytokine arrays Circles are pre-, squares are post. [Mean (SD)] n=8.

4.4. Molecular detection of microbial and fungal species

Microscopy analysis of BAL samples revealed that within certain samples it was possible to detect microbes present within the macrophage cells. In order to investigate this further the cell pellet remaining after the BAL centrifugation at 500g was retained and underwent the same protocols as the BAL bacteria pellet in order to investigate if there was an observable difference between the bacterial and fungal DNA isolated from the BAL bacteria pellet fraction sample to the bacterial and fungal DNA isolated through the BAL cell pellet fraction. BAL bacteria pellet qPCR data exists for all n=8 patients at baseline and follow-up while BAL cell pellet qPCR data exists for n=4 patients at baseline and n=8 patients at follow up.

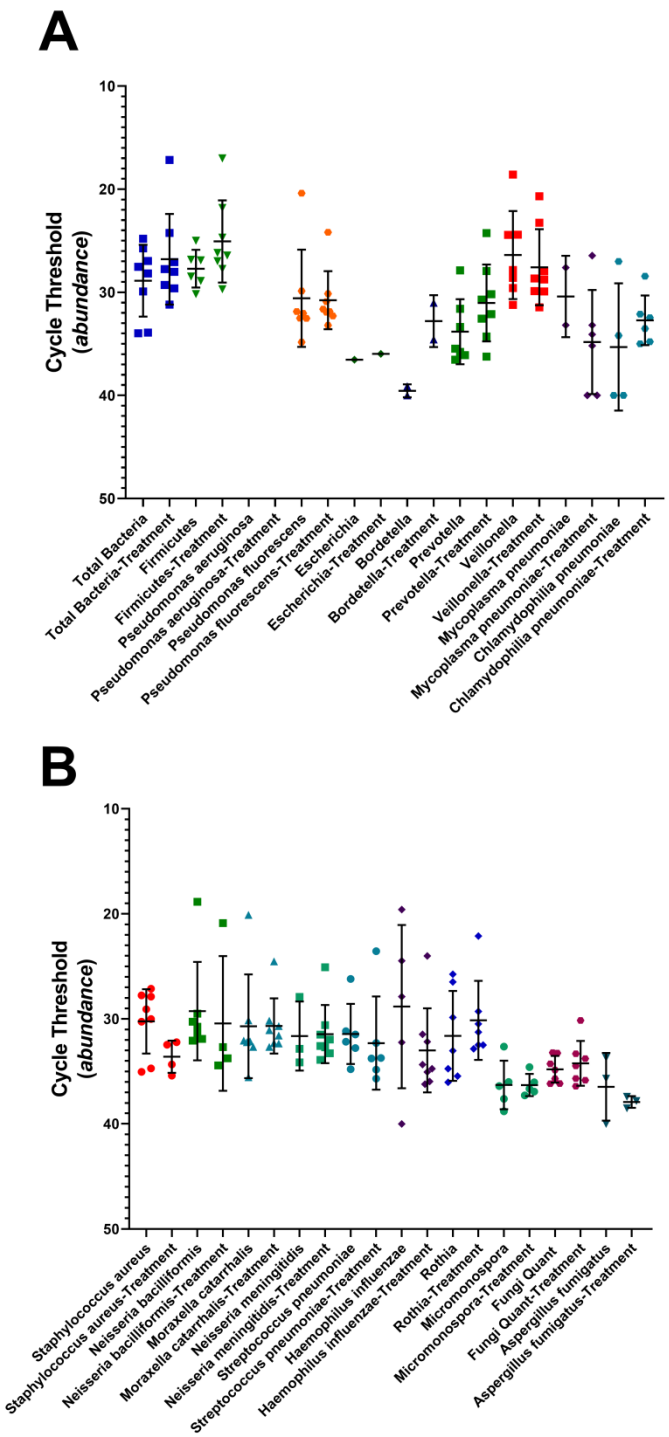


Figure 8 qPCR detection of bacteria and fungi species in the asthmatic BAL bacteria pellet (BP) at baseline bronchoscopy and follow-up bronchoscopy post-anti-IL-5 (Reslizumab) treatment. qPCR was performed on the extracted baseline BAL bacteria pellet (BP) DNA and post-anti-IL-5 treatment bronchoscopy BAL bacteria pellet (BP) DNA. [Mean (SD)], n=8.

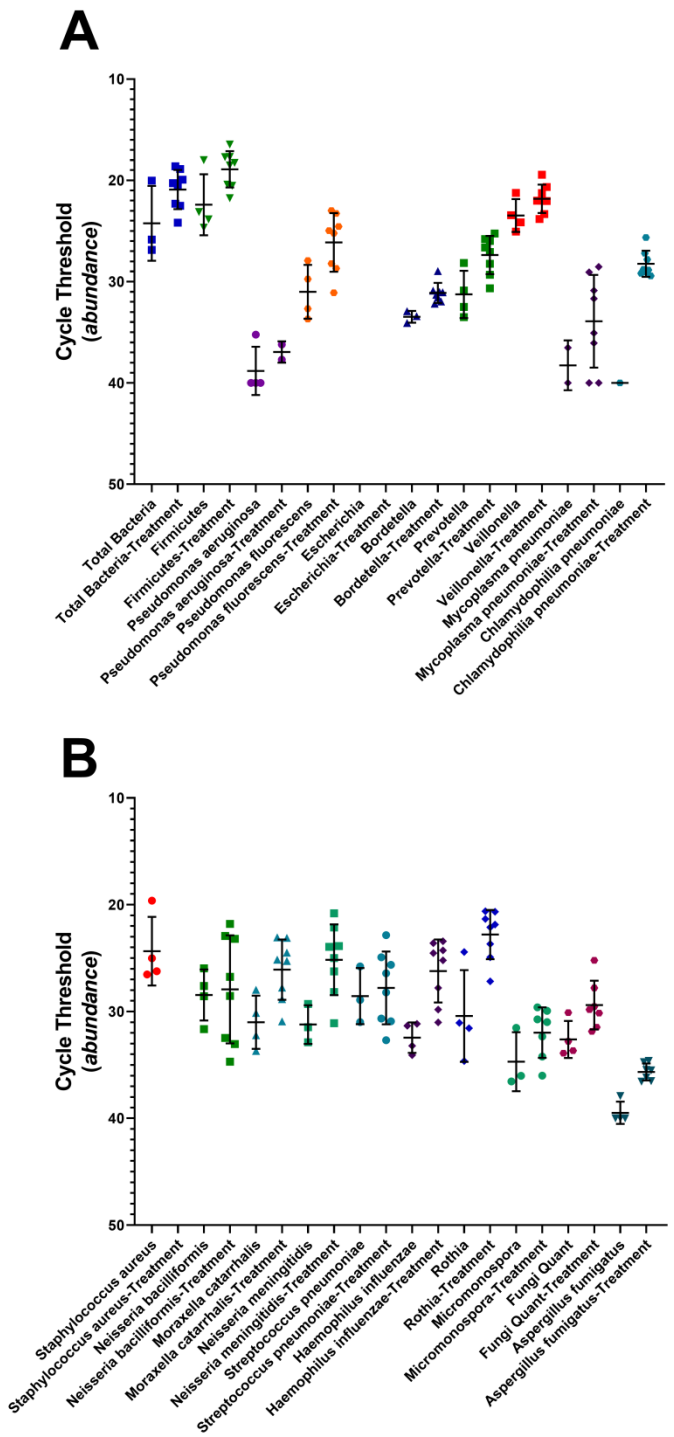


Figure 9 qPCR detection of bacteria and fungi species in the asthmatic BAL cell pellet fraction at baseline bronchoscopy and follow-up bronchoscopy post- anti-IL-5 treatment. qPCR was performed on the extracted baseline BAL cell pellet (CP) fraction DNA, n=4 and on the post-anti-IL-5 treatment bronchoscopy BAL cell pellet (CP) fraction DNA, n=8. [Mean (SD)].

Table 2 Baseline and follow-up bronchoalveolar lavage (BAL) bacteria pellet and cellular pellet molecular analyses. Baseline and follow-up bronchoscopy BAL isolated DNA from the bacteria pellet (BP) samples analysed by qPCR for a variety of bacterial and fungal targets of interest, whereby baseline BAL BP; n=8, baseline BAL CP; n=4, follow-up BAL BP; n=8, follow-up BAL CP; n=8. Note CT=Cycle Threshold

		Baseline	**Treatment**
Total bacteria BP (CT)	Positive	8/8	8/8
	[Mean (SD)]	[28.9 (3.5)]	[26.8 (4.4)]
	[Median (IQR)]	[27.9 (26.0-32.9)]	[27.9 (25.0-29.5)]
Total bacteria CP (CT)	Positive	¾	8/8
	[Mean (SD)]	[24.2 (3.7)]	[20.9 (1.9)]
	[Median (IQR)]	[25.8 (20.0-26.9)]	[20.4 (19.1-22.5)]
***Firmicutes* BP (CT)**	Positive	6/8	8/8
	[Mean (SD)]	[27.7 (1.8)]	[25.1 (4.0)]
	[Median (IQR)]	[27.7 (26.4-29.2)]	[26.3 (22.5-27.5)]
***Firmicutes* CP (CT)**	Positive	4/4	8/8
	[Mean (SD)]	[22.4 (3)]	[18.9 (1.8)]
	[Median (IQR)]	[23.5 (19.3-24.5)]	[18.4 (17.7-20.5)]
***Pseudomonas aeruginosa* BP (CT)**	Positive	0/8	0/8
***Pseudomonas aeruginosa* CP (CT)**	Positive	4/4	2/8
	[Mean (SD)]	[38.8 (2.4)]	[37 (1.1)]
	[Median (IQR)]	[40 (36.4-40.0)]	[37 (36.2-37.7)]
***Pseudomonas fluorescens* BP (CT**	Positive	7/8	8/8
	[Mean (SD)]	[30.6 (4.7)]	[30.8 (2.8)]
	[Median (IQR)]	[32 (29.9-32.5)]	[31.8 (30.3-32.2)]
***Pseudomonas fluorescens* CP (CT)**	Positive	4/4	8/8
	[Mean (SD)]	[31 (2.7)]	[26.1 (2.9)]
	[Median (IQR)]	[31.2 (28.4-33.4)]	[25.1 (23.6-28.6)]
***Escherichia* BP (CT)**	Positive	1/8	1/8
	[Mean (SD)]	[36.5 (0)]	[36 (0)]
	[Median (IQR)]	[36.5 (36.5-36.5)]	[36 (36-36)]
***Escherichia* CP (CT)**	Positive	0/4	0/8
	[Mean (SD)]		
	[Median (IQR)]		
***Bordetella* BP (CT)**	Positive	2/8	2/8
	[Mean (SD)]	[39.6 (0.6)]	[32.8 (2.5)]
	[Median (IQR)]	[39.6 (39-40)]	[32.8 (31.0-34.6)]
***Bordetella* CP (CT)**	Positive	3/4	8/8
	[Mean (SD)]	[33.5 (0.6)]	[31.1 (1)]
	[Median (IQR)]	[33.4 (32.9-34.1)]	[31.2 (30.9-31.9)]
***Prevotella* BP (CT)**	Positive	7/8	8/8
	[Mean (SD)]	[33.8 (3.2)]	[31 (3.7)]
	[Median (IQR)]	[35.5 (31.6-36.1)]	[31.4 (28.5-33.9)]
***Prevotella* CP (CT)**	Positive	4/4	8/8
	[Mean (SD)]	[31.3 (2.3)]	[27.4 (1.9)]
	[Median (IQR)]	[31.7 (28.8-33.3)]	[26.9 (25.9-29.0)]

		Baseline	Treatment
***Veillonella* BP (CT)**	Positive	7/8	8/8
	[Mean (SD)]	[26.4 (4.3)]	[27.6 (3.7)]
	[Median (IQR)]	[27.8 (24.4-29.6)]	[28.7 (24.4-29.9)]
***Veillonella* CP (CT)**	Positive	4/4	8/8
	[Mean (SD)]	[23.5 (1.6)]	[21.8 (1.4)]
	[Median (IQR)]	[23.8 (21.8-24.8)]	[22 (20.8-23.0)]
***Mycoplasma pneumoniae* BP (CT)**	Positive	2/8	6/8
	[Mean (SD)]	[30.4(4)]	[34.8 (5.0)]
	[Median (IQR)]	[30.4 (27.6-33.2)]	[34.6 (31.5-40.0)]
***Mycoplasma pneumoniae* CP (CT)**	Positive	2/4	8/8
	[Mean (SD)]	[38.3 (2.5)]	[33.9 (4.6)]
	[Median (IQR)]	[38.3 (36.5-40.0)]	[33.4 (29.5-39.0)]
***Chlamydophila pneumoniae* BP (CT)**	Positive	4/8	6/8
	[Mean (SD)]	[35.3 (6.2)]	[32.7 (2.4)]
	[Median (IQR)]	[37.1 (28.8-40.0)	[33 (31.2-34.8)]
***Chlamydophila pneumoniae* CP (CT)**	Positive	1/4	8/8
	[Mean (SD)]	[40 (0)]	[28.2 (1.3)]
	[Median (IQR)]	[40 (40-40)]	[28.8 (27.4-29.1)]
***Staphylococcus aureus* BP (CT)**	Positive	8/8	4/8
	[Mean (SD)]	[30.2 (3.1)]	[33.6 (1.5)]
	[Median (IQR)]	[29.6 (27.8-33.6)]	[33.4 (32.3-35.1)]
***Staphylococcus aureus* CP (CT)**	Positive	4/4	0/8
	[Mean (SD)]	[24.4 (3.2)]	
	[Median (IQR)]	[25.6 (21.0-26.5)]	
***Neisseria bacilliformis* BP (CT)**	Positive	7/8	4/8
	[Mean (SD)]	[29.3 (4.7)]	[30.4 (6.4)]
	[Median (IQR)]	[30.8 (29.5-31.9)]	[33.2 (23.8-34.3)]
***Neisseria bacilliformis* CP (CT)**	Positive	4/4	8/8
	[Mean (SD)]	[28.4 (2.4)]	[27.9 (5.1)]
	[Median (IQR)]	[28.1 (26.4-30.9)]	[27.6 (23.0-32.9)]
***Moraxella catarrhalis* BP (CT)**	Positive	7/8	8/8
	[Mean (SD)]	[30.7 (4.9)]	[30.7 (2.6)]
	[Median (IQR)]	[32.1 (30.2-32.7)]	[31.3 (30.3-32.3)]
***Moraxella catarrhalis* CP (CT)**	Positive	4/4	8/8
	[Mean (SD)]	[31 (2.5)]	[26.1 (2.8)]
	[Median (IQR)]	[31.2 (28.5-33.3)]	[25.2 (23.5-28.6)]
***Neisseria meningitidis* BP (CT)**	Positive	3/8	8/8
	[Mean (SD)]	[31.6 (3.3)]	[31.4 (2.8)]
	[Median (IQR)]	[32.8 (27.9-34.1)]	[32.3 (30.8-33.1)]
***Neisseria meningitidis* CP (CT)**	Positive	3/4	8/8
	[Mean (SD)]	[31.2 (1.8)]	[25.2 (3.3)]
	[Median (IQR)]	[31.5 (29.3-32.9)]	[24.5 (22.6-27.7)]
***Streptococcus pneumoniae* BP (CT)**	Positive	6/8	6/8
	[Mean (SD)]	[31.4 (2.9)]	[32.3 (4.4)]
	[Median (IQR)]	[31.8 (29.9-33.3)]	[33.7 (30.1-35.0)]
***Streptococcus pneumoniae* CP (CT)**	Positive	3/4	8/8
	[Mean (SD)]	[28.6 (2.6)]	[27.8 (3.4)]
	[Median (IQR)]	[28.9 (25.8-31.0)]	[27.3 (25.1-30.9)]
***Haemophilus influenzae* BP (CT)**	Positive	5/8	8/8
	[Mean (SD)]	[28.8 (7.8)]	[33 (4)]
	[Median (IQR)]	[27.9 (22.0-36.1)]	[34.5 (31.6-35.7)]

		Baseline	Treatment
***Haemophilus influenzae* CP (CT)**	Positive	4/4	8/8
	[Mean (SD)]	[32.4 (1.4)]	[26.2 (3)]
	[Median (IQR)]	[32.3 (31.2-33.9)]	[24.9 (23.8-29.3)]
***Rothia* BP (CT)**	Positive	7/8	7/8
	[Mean (SD)]	[31.6 (4.3)]	[30.1 (3.8)]
	[Median (IQR)]	[33 (26.5-35.4)]	[31.3 (29.3-32.5)]
***Rothia* CP (CT)**	Positive	4/4	8/8
	[Mean (SD)]	[30.4 (4.3)]	[22.8 (2.3)]
	[Median (IQR)]	[31.3 (26.1-33.9)]	[22 (20.8-24.6)]
***Micromonospora* BP (CT)**	Positive	5/8	5/8
	[Mean (SD)]	[36.3 (2.3)]	[36.3 (1.1)]
	[Median (IQR)]	[36.4 (34.3-38.2)]	[36.7 (35.3-37.1)]
***Micromonospora* CP (CT)**	Positive	3/4	7/8
	[Mean (SD)]	[34.7 (2.8)]	[32 (2.4)]
	[Median (IQR)]	[36 (31.5-36.5)]	[31 (29.9-34.2)]
Fungi Quant BP (CT)	Positive	7/8	7/8
	[Mean (SD)]	[34.8 (1.3)]	[34.2 (2.1)]
	[Median (IQR)]	[34.9 (33.3-36.2)]	[34.5 (33.3-35.8)]
Fungi Quant CP (CT	Positive	4/4	7/8
	[Mean (SD)]	[32.6 (1.7)]	[29.4 (2.3)]
	[Median (IQR)]	[33.2 (30.8-33.8)]	[29.8 (27.8-31.5)]
***Aspergillus fumigatus* BP (CT)**	Positive	3	3/8
	[Mean (SD)]	[36.5 (3.2)]	[37.9 (0.6)]
	[Median (IQR)]	[35.7 (33.7-40.0)]	[37.8 (37.4-38.5)]
***Aspergillus fumigatus* CP (CT)**	Positive	4	7/8
	[Mean (SD)]	[39.5 (1.1)]	[35.7 (0.8)]
	[Median (IQR)]	[40 (38.4-40.0)]	[35.5 (34.7-36.5)]

4.5 Anti-IL-5 monoclonal antibody therapy changes the lung microbiota

At baseline bronchoscopy, before patients received Reslizumab (Cinqaero,Teva Pharmaceutical Industries), qPCR analysis of extracted bacterial DNA from the BAL bacteria pellet (n=8) or BAL cell pellet (n=4) revealed the presence of bacteria and fungi within the lungs of the asthma cohort. At follow-up bronchoscopy, after patients received Reslizumab, qPCR analysis of extracted DNA from the BAL bacteria pellet (n=8) or BAL cell pellet (n=8) revealed the presence of bacteria and fungi in varying amounts in comparison to those found at baseline bronchoscopy.

Investigating the qPCR analysis of the BAL bacteria pellet (BP) samples at baseline bronchoscopy, n=8, and follow-up bronchoscopy, n=8, revealed the presence of microbes within the lung. The bacterial primer used to detect for bacterial presence; Total Bacteria primer set, revealed that 100% of patients had detectable bacteria within the bacteria pellet at baseline bronchoscopy and at follow-up bronchoscopy.

At baseline bronchoscopy 75% of patients had detectable levels of Firmicutes within the BAL bacteria pellet while at follow-up bronchoscopy 100% of patients had detectable levels of Firmicutes. *Escherichia* was detectable in only one patient at baseline bronchoscopy and at follow-up bronchoscopy. *Bordetella* was detectable within 25% of patients at baseline bronchoscopy and at follow-up bronchoscopy *Bordetella* remained at similar levels (25%). *Prevotella* was detectable within 88% of patients BAL BP samples at baseline bronchoscopy and within 100% at follow-up bronchoscopy.

Veillonella was detectable within 88% of patients BAL BP samples at baseline bronchoscopy and within 100% at follow-up bronchoscopy. *Rothia* was detectable within 88% of patients BAL BP samples at baseline bronchoscopy and at follow-up bronchoscopy. *Micromonospora* was detectable within 63% of patients BAL BP samples at baseline bronchoscopy and at follow-up bronchoscopy.

Fungal presence, as determined by the ITS specific fungal primer Fungi Quant, was detectable within 88% of patients at baseline bronchoscopy and within the same percentage at follow-up bronchoscopy.

Pseudomonas aeruginosa was not detectable within the BAL BP samples of the cohort at baseline sampling or at follow-up bronchoscopy sampling. At baseline bronchoscopy *Pseudomonas fluorescens* was detectable within 88% of patient BAL BP samples while at follow-up bronchoscopy *P. fluorescens* was detectable within 100% of patient BAL BP samples. *Mycoplasma pneumoniae* was only detectable within 25% of patients at baseline bronchoscopy, however at follow-up bronchoscopy; *M. pneumoniae* was detectable within 75% of patient BAL BP samples. *Chlamydophilia pneumoniae* was detectable within 50% of patients BAL BP at baseline bronchoscopy and within 75% at follow-up bronchoscopy.

Staphylococcus aureus was detectable in 100% of patient BAL BP samples at baseline bronchoscopy and within 50% at follow-up bronchoscopy. *Neisseria bacilliformis* was detectable within 88% of patients BAL BP at baseline bronchoscopy and within 50% at follow-up bronchoscopy. *Moraxella catarrhalis* was detectable within 88% of patients BAL BP at baseline bronchoscopy and within 100% at follow-up bronchoscopy.

Neisseria meningitidis was detectable within 38% of BAL BP samples at baseline bronchoscopy, however, at follow-up bronchoscopy 100% of patients displayed detectable levels of *N. meningitidis* within their BAL BP sample. *Streptococcus pneumoniae* was present within 75% of patient BAL BP at baseline bronchoscopy and within the same percentage of patients at follow-up bronchoscopy.

Haemophilus influenzae was detectable within 63% of patients BAL BP at baseline bronchoscopy and within 100% at follow-up bronchoscopy. The fungi *Aspergillus fumigatus* was detectable within 38% of patients BAL BP at baseline bronchoscopy and at follow-up bronchoscopy.

Investigation of the intracellular bacteria; the cell pellet (CP), was incorporated into the analysis at a later time-point, therefore CP specific data exists for n=4 patients within this study cohort. Within this 100% had detectable bacterial presence of Firmicutes, *Pseudomonas aeruginosa, Pseudomonas fluorescens, Prevotella, Veillonella, Staphylococcus aureus, Neisseria bacilliformis, Moraxella catarrhalis, Haemophilus influenzae, and Rothia* by qPCR. All had detectable fungi and *Aspergillus fumigatus.* 75% had detectable Total bacteria, *Bordetella, Neisseria meningitidis, Streptococcus pneumoniae* and *Micromonospora.* 50% had detectable *Mycoplasma pneumoniae* while 25% had detectable *Chlamydophila pneumoniae* while *Escherichia* was undetectable in the patient BAL CP samples at baseline bronchoscopy.

At follow-up bronchoscopy the investigation of the intracellular bacteria, the cell pellet, was carried out for all eight patients, n=8. 100% of patients had detectable Total Bacteria, Firmicutes, *Pseudomonas fluorescens*, *Prevotella*, *Veillonella*, *Moraxella catarrhalis*, *Neisseria meningitidis* and *Haemophilus influenzae* within their BAL CP by qPCR. *Pseudomonas aeruginosa* was detectable within 25% of the patient BAL CP by qPCR while *Escherichia* and *Staphylococcus aureus* were undetectable. *Bordetella, Mycoplasma pneumoniae, Chlamydophila pneumonaie, Neisseria bacilliformis, Rothia* and *Streptococcus pneumoniae* were all detectable in 100% of patient BAL CP samples at follow-up bronchoscopy. Micromonospora was detectable within 88% of patients BAL CP samples at follow-up bronchoscopy.

Using ITS specific primers for the detection of fungal species it was seen that fungi was detectable in 88% of patient CP samples using the primer Fungi Quant, while *Aspergillus fumigatus* was detectable in 88% of CP samples by qPCR.

4.6. Bacterial and fungal species patient correlations

At baseline readings monocyte cell percentage counts correlated with *Neisseria meningitidis* (BP) qPCR results (*P*<0.05; r=-0.9991), lymphocyte cell percentage counts correlated with qPCR *Neisseria meningitidis* (BP) (*P*<0.05; r=0.9979) presence, eosinophil percentage counts correlated with the presence of *Neisseria meningitidis* (BP) (*P*<0.05; r=-0.9994) while neutrophil percentage counts correlated with qPCR *Veillonella* (BP) (*P*<0.01; r=-0.8838), *Chlamydophilia pneumoniae* (BP) (*P*<0.05; r=-0.9889) and *Streptococcus pneumoniae* (BP) (*P*<0.005; r=-0.9441) presence. See Figure 10.

At follow up bronchoscopy BAL monocytes correlated with the presence of *Veillonella* (BP) (*P*<0.05; r_s=0.7381), *Mycoplasma pneumoniae* (BP) (*P*<0.01; r_s=0.9856) *Mycoplasma pneumoniae* (CP) (*P*<0.05; r_s=0.8264), and *Streptococcus pneumoniae* (BP) (*P*<0.05; r_s=0.8857). BAL macrophage cell percentage counts correlated with *Streptococcus pneumoniae* (BP) (*P*<0.05; r_s=0.9429) presence. BAL lymphocyte cell percentage counts correlated with the presence of *Pseudomonas fluorescence* (BP) (*P*<0.05; r_s=-0 7857) and BAL neutrophil cell percentage counts with qPCR *Bordetella* (CP) (*P*<0.05; r_s=-0.7381) and *Chlamydophilia pneumoniae* (CP) *(P*<0.05; r_s=-0.7381). See Figure 11.

Oral steroids and inhaled corticosteroids (ICS) did not correlate with qPCR bacterial and fungal presence. Baseline Haemoglobin (HB) levels did correlate with *Haemophilus influenzae* (BP) (*P*<0.05; r=-0.9815) and *Rothia* (BP) (*P*<0.05; r=0.8150). At baseline readings BMI levels were seen to correlate with Firmicutes (BP) (*P*<0.05; r=0.8701) and *Moraxella catarrhalis* (BP) (*P*<0.05; r_s=0.7857). See Figure 12. At follow up bronchoscopy readings BMI levels were seen to correlate with fungal presence (Fungi Quant) (CP) (*P*<0.05; r=-0.7790). See Figure 13.

At baseline bronchoscopy BAL cytokines IL-4, IL-5, IL-8, IL-10, IL-13 and IL-17 levels did not correlate with bacterial or fungal qPCR presence. IL-1β BAL cytokine levels

correlated with qPCR *Veillonella* levels (P<0.05; r_s=-0.8214). BAL IL-6 cytokine levels correlated with qPCR *Veillonella* levels (P<0.005; r_s=-0.9643). TNF-α cytokine levels correlated negatively with *Prevotella* qPCR levels (P<0.05; r_s=-0.8108). See Figure 14.

At follow up bronchoscopy it was seen that the BAL cytokines IL-1β, IL-4, IL-5, IL-6, IL-10, IL-13, IL-17, TNF-α and IFN-γ did not significantly correlate with bacteria or fungi qPCR levels.

Total bacteria (CP) presence by qPCR correlated with BAL IL-8 cytokine levels (P<0.05; r_s=-0.8857). See Figure 15 (A). Firmicutes (CP) correlated with BAL IL-8 cytokine levels (P<0.05; r_s=-0.8857). See Figure 15 (B). *Streptococcus pneumoniae* (CP) correlated with BAL IL-8 cytokine levels (P<0.05; r_s=-0.9429). See Figure 15 (C). *Haemophilus influenzae* (CP) correlated with BAL IL-8 cytokine levels (P<0.05; r_s=-0.9429). See Figure 15 (D).

Plasma cytokine levels of IL-1β, IL-5, IL-6, IL-13, IL-17, TNF-α and IFN-γ did not correlate with qPCR levels of bacteria and fungi at follow up bronchoscopy. *Rothia* (CP) presence correlated with plasma IL-4 cytokine levels (P<0.005; r=0.9962). See Figure 16 (A). *Bordetella* (CP) presence correlated with plasma IL-8 cytokine levels (P<0.05; r_s=-0.8571). See Figure 16 (B). Total bacteria (BP) (P<0.05; r=0.9537), *Firmicutes* (BP) (P<0.05; r=0.9317), *Veillonella* (BP) (P<0.05; r=0.9307) and *Mycoplasma pneumoniae* (CP) (P<0.05; r=0.8967) correlated with plasma IL-10 cytokine levels. See Figure 16 (C-F).

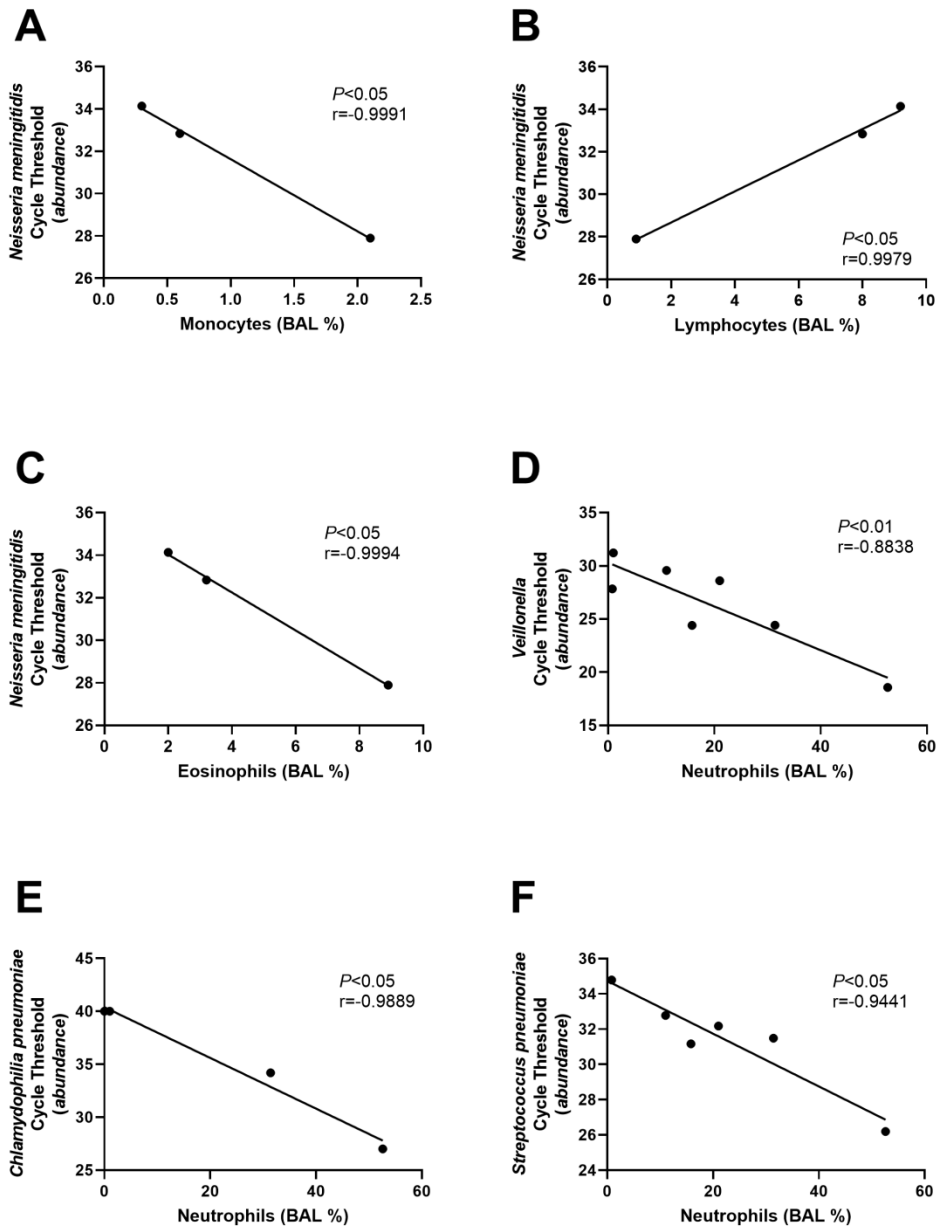


Figure 10 Baseline BAL qPCR – immune cell percentage count correlations. Monocyte BAL cell percentage counts correlated with *Neisseria meningitidis* presence by qPCR (*P*<0.05; r=-0.9991) (A). Lymphocyte cell percentage counts correlated with qPCR *Neisseria meningitidis* presence (*P*<0.05; r=0.9979) (B). Eosinophil percentage counts correlated with qPCR *Neisseria meningitidis* presence (*P*<0.05; r=-0.9994) (C). Neutrophil percentage counts correlated with qPCR *Veillonella* presence (*P*<0.01; r=-0.8838)(D), *Chlamydophilia pneumoniae* presence (*P*<0.05; r=-0.9889) (E) and *Streptococcus pneumoniae* presence (*P*<0.005; r=-0.9441) (F).

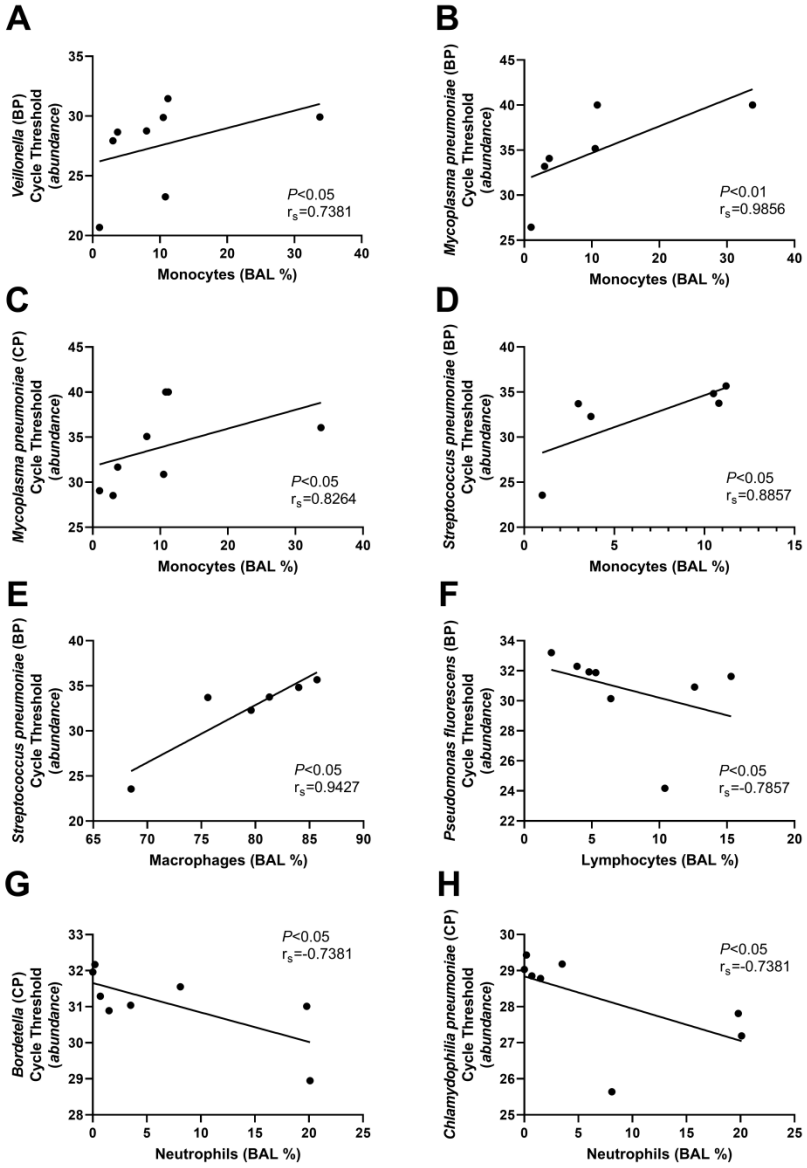


Figure 11 Follow-up bronchoscopy BAL qPCR – immune cell percentage count correlations. BAL Monocytes (%) correlated with the presence of *Veillonella* (BP) (*P*<0.05; r_s=0.7381) (A), *Mycoplasma pneumoniae* (BP) (*P*<0.01; r_s=0.9856) (B) *Mycoplasma pneumoniae* (CP) (*P*<0.05; r_s=0.8264) (C), and *Streptococcus pneumoniae* (BP) (*P*<0.05; r_s=0.8857) (D). Macrophage cell percentage counts correlated with *Streptococcus pneumoniae* (BP) (*P*<0.05; r_s=0.9429) (E), Lymphocyte cell percentage counts correlated with *Pseudomonas fluorescence* (BP) (*P*<0.05; r_s=-0 7857) (F). Neutrophil cell percentage counts correlated with the presence of *Bordetella* (CP) (*P*<0.05; r_s=-0.7381) (G) and *Chlamydophilia pneumoniae* (CP) *(P*<0.05; r_s=-0.7381) (H).

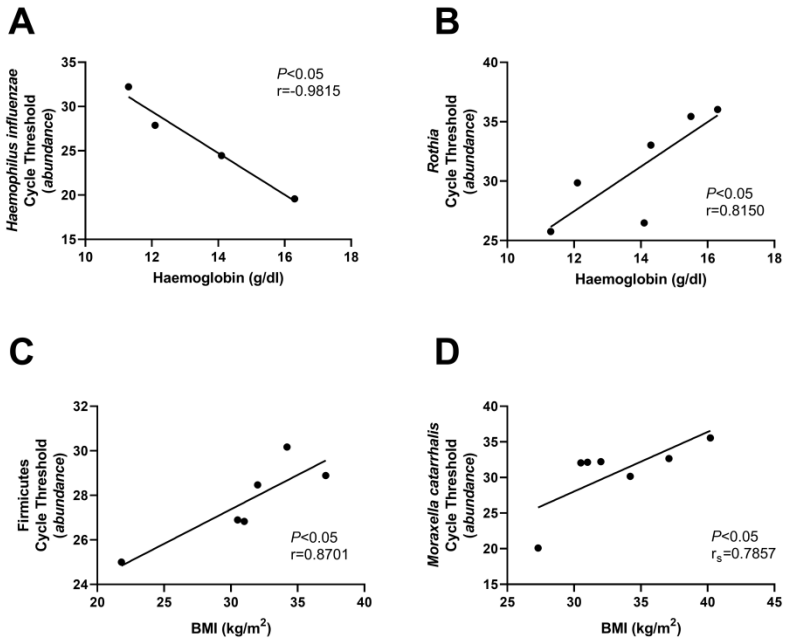


Figure 12 Baseline BAL qPCR – patient demographics correlations. Baseline Haemoglobin (HB) (g/dl) levels correlated with *H. influenzae* (*P*<0.05; r=-0.9815) (A) and *Rothia* (*P*<0.05; r=0.8150) (B) presence. BMI levels correlated with Firmicutes (*P*<0.05; r=0.8701) (C) and *M. catarrhalis* (*P*<0.05; r_s=0.7857) (D).

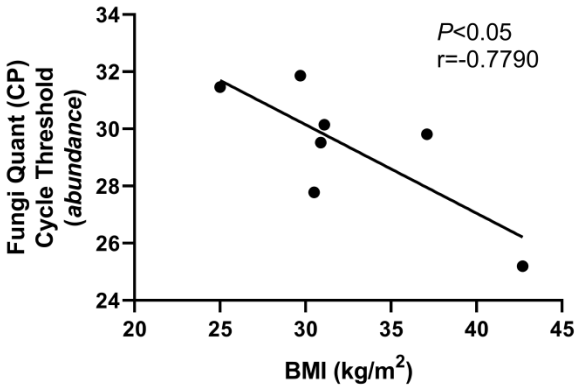


Figure 13 Follow-up bronchoscopy BAL qPCR – patient demographics correlations. At follow up bronchoscopy BMI levels correlated with fungal presence (Fungi Quant) (CP) (*P*<0.05; r=-0.7790).

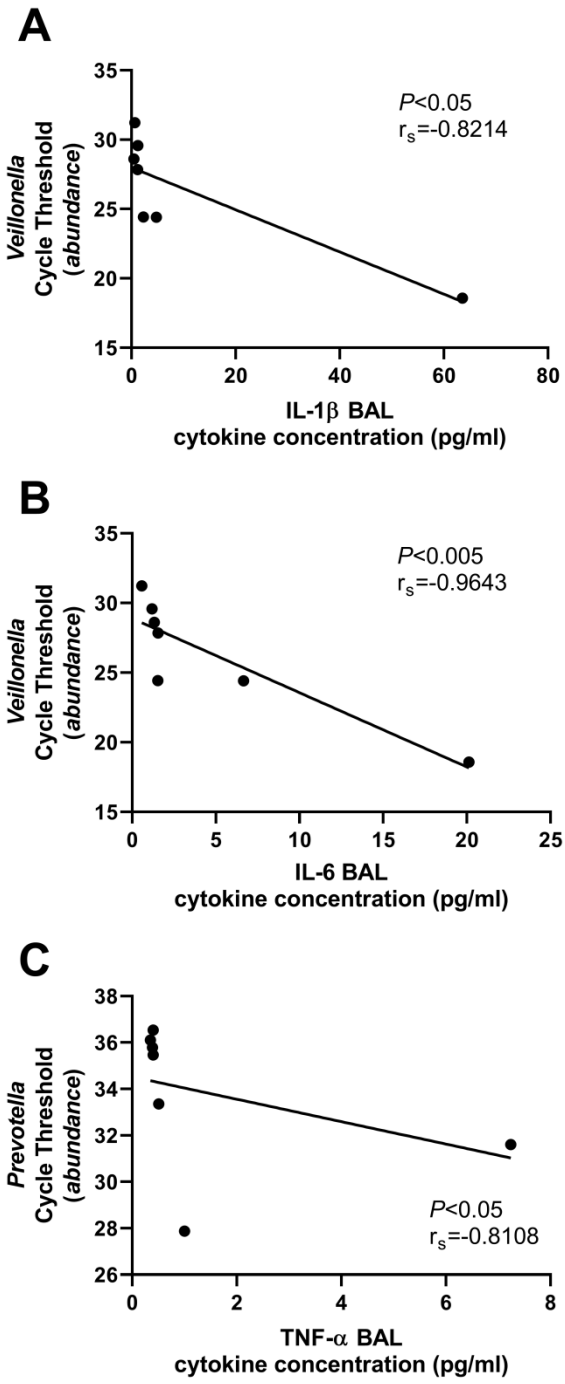


Figure 14 Baseline BAL qPCR – BAL cytokine correlations. IL-1β BAL cytokine levels negatively correlated with the presence of *Veillonella* (*P*<0.05; r_s=-0.8214) (A). BAL IL-6 cytokine levels correlated with qPCR *Veillonella* levels (*P*<0.005; r_s=-0.9643) (B). TNF-α cytokine levels correlated with *Prevotella* qPCR levels (*P*<0.05; r_s=-0.8108) (C).

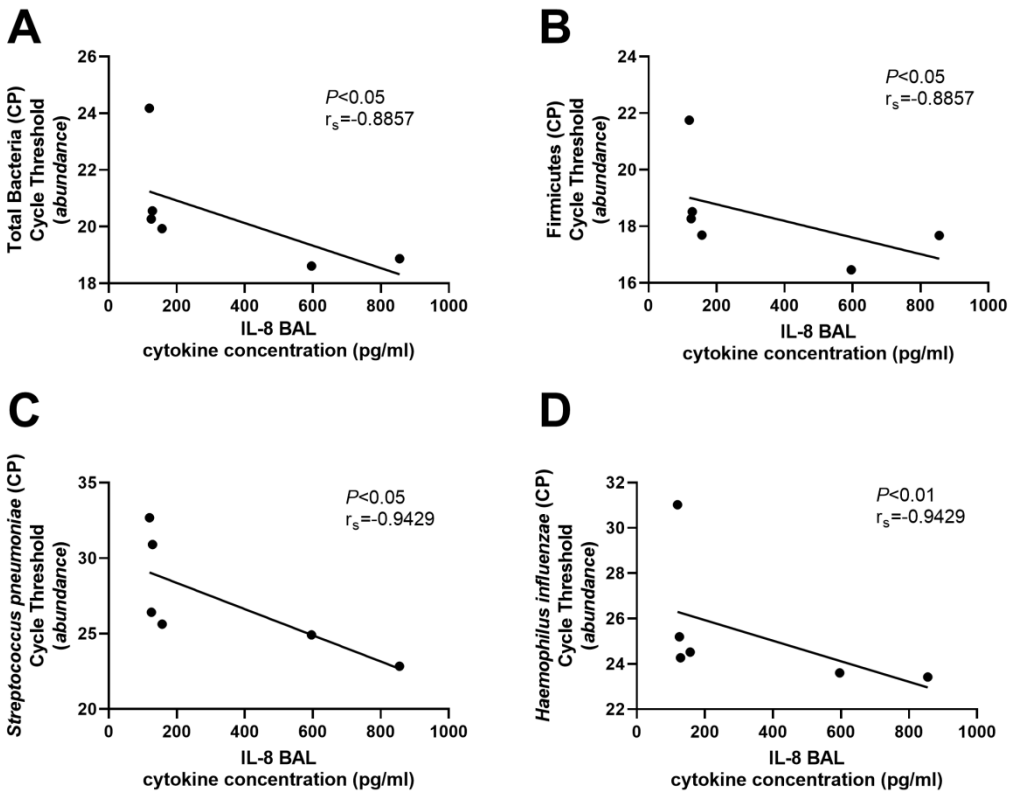


Figure 15 Follow-up bronchoscopy BAL qPCR – BAL cytokine correlations. Total bacteria (CP) presence by qPCR correlated with BAL IL-8 cytokine levels (P<0.05; r_s=-0.8857) (A). Firmicutes (CP) correlated with BAL IL-8 cytokine levels (P<0.05; r_s=-0.8857) (B). *Streptococcus pneumoniae* (CP) correlated with BAL IL-8 cytokine levels (P<0.05; r_s=-0.9429) (C). *Haemophilus influenzae* (CP) correlated with BAL IL-8 cytokine levels (P<0.05; r_s=-0.9429) (D).

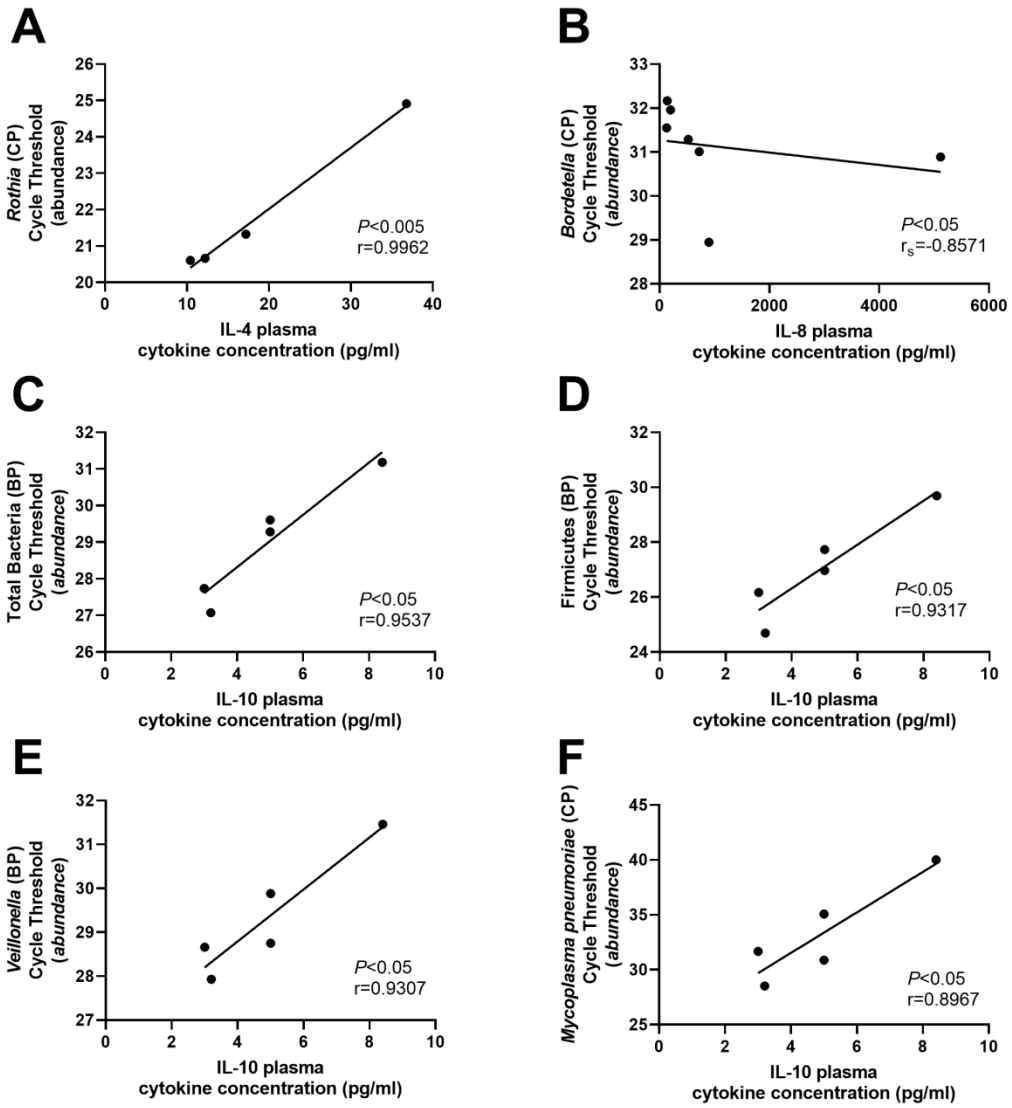


Figure 16 Follow-up bronchoscopy BAL qPCR – plasma cytokine correlations.
Rothia (CP) presence correlated with plasma IL-4 cytokine levels (*P*<0.005; r=0.9962) (A). *Bordetella* (CP) presence correlated with plasma IL-8 cytokine levels (*P*<0.05; r_s=-0.8571) (B). Total bacteria (BP) (*P*<0.05; r=0.9537), *Firmicutes* (BP) (*P*<0.05; r=0.9317), *Veillonella* (BP) (*P*<0.05; r=0.9307) and *Mycoplasma pneumoniae* (CP) (*P*<0.05; r=0.8967) correlated with plasma IL-10 cytokine levels (C-F).

5. Discussion

Monoclonal antibody therapy and asthma

Asthma is a common condition, which is generally well controlled with currently available treatment such as Inhaled corticosteroids and long acting beta agonists. Unfortunately, subsets of patients have asthma that is difficult to control despite the use of these therapies[3] . Monoclonal antibodies have emerged as a promising therapeutic for such patients. Humanised monoclonal antibodies against immunoglobulin E (IgE) as seen with Omalizumab (Xolair, Novartis) or monoclonal antibodies which target specific cytokines of importance such as the IL-5 antagonist group of monoclonal antibodies, Mepolizumab (Nucala®, GlaxoSmithKline) and Reslizumab (Cinqaero®, Teva Pharmaceutical Industries) or Benralizumab (AstraZeneca) which binds to the IL-5 receptor preventing IL-5 from binding to its receptor show promise in the treatment of severe, poorly controlled asthma[6,7].

Investigating the lung microbiome

A shift towards molecular methods has led to insights into the overall microbial load of the lungs and has shown that there are clear and reproducible differences present between the microbes present in the healthy and diseased lungs[8]. Therefore a key goal of this study was to elucidate key microbial players in a cohort of well-defined asthmatics in order to investigate potential changes in the microbial load of patients undergoing established treatment protocols, which could aid in providing a rationale for targeted treatment interventions.

Comparison of patient clinical parameters pre- and post- anti-IL-5 therapy

The patient cohort consisted of eight adult asthmatic patients, 2 males and 6 females. 25% (2/8) patients were in receipt of oral steroids at the time of baseline bronchoscopy and this did not change upon receipt of the anti-IL-5 monoclonal antibody Reslizumab (min 5mg – max 10mg). However the was a reduction in the

prescribed inhaled corticosteroid (ICS) dose (FDP) required by patients at follow-up bronchoscopy.

At baseline bronchoscopy inhaled corticosteroid (ICS) dose (FDP) was as follows; (min 800 – max 2000 FDP) [Mean (SD)] [1188 (387.1)]; [Median (IQR)] [1000 (1000-1425)]; at follow-up bronchoscopy upon treatment with the anti-IL-5 therapy Reslizumab there was a observable reduction in the overall prescribed inhaled corticosteroid dose (FDP) required by patients; (min 800 – max 2400 FDP) [Mean (SD)] [1125 (523.0)]; [Median (IQR)] [1000 (850-1000)] at time of follow up bronchoscopy indicating a positive clinical improvement for patients.

Spirometry is a widely utilised pulmonary function test providing an aid in the diagnosis of lung diseases and the overall monitoring of lung health[10]. Forced Vital Capacity (FVC) is the volume of air delivered during an expiration made as forcefully and completely as possible with the time recorded from full inspiration[10]. Forced Expiratory Volume in the first second (FEV_1) is a measurement of the expiratory volume in the first second of the FVC maneuver[10]. Taking into account the patient spirometry results an increase in the FEV-1 (percent predicted) was documented overall upon receipt of anti-IL-5 therapy. Patients FEV-1 (percent predicted) increased from [Mean (SD)] [60.3 (19.5)]; [Median (IQR)] [50 (45-83)] to [Mean (SD)] [75.3 (21.7)]; [Median (IQR)] [80 (53.3-95.8)].

Focusing on patients Fractional exhaled Nitric Oxide (FeNO) (ppb) an increase from [Mean (SD)] [22.8 (7.4)]; [Median (IQR)] [25 (15.3-28.0)] to [Mean (SD)] [38.8 (23)]; [Median (IQR)] [30 (22.8-64.0)] was observed on the day of follow-up bronchoscopy after patients were in receipt of the anti-IL-5 monoclonal antibody Reslizumab. Fractional exhaled Nitric Oxide (FeNO) is a non-invasive marker of inflammation and can elucidate how successful inhaled steroids are at supressing a patient's inflammation[18]. For cases where a patient displays eosinophilic asthma FeNo has been reported to be elevated which is apparent in the case of this patient cohort. Mast cells and antigen specific Th2 cells are activated in cases of eosinophilic asthma, which results in an upregulation of epithelial inducible nitric oxide[19]. Therefore in asthma patients FeNO has been noted to be a good biomarker for

eosinophilic airway inflammation and predictor of poor or good corticosteroid response[19].

The effect of Reslizumab on patient BAL eosinophil levels

As Reslizumab is an IL-5 antagonist monoclonal antibody, binding to soluble IL-5 inhibiting subsequent binding of IL-5 to its corresponding IL-5 surface receptors thus resulting in the downregulation of the IL-5 eosinophil inflammatory pathway, patient BAL was examined by microscopy to determine the percentage of BAL eosinophils at both baseline bronchoscopy and at follow-up bronchoscopy[2]. Within the cohort at the immune cell level, through the use of microscopy to count the percentage of immune cells within a patient BAL it was clear that after receiving anti-IL-5 monoclonal antibody therapy percentage levels of eosinophils had clearly reduced. At baseline bronchoscopy patient BAL eosinophil counts revealed a mean of 7.1 (SD 7.8) eosinophils while at follow-up bronchoscopy patient BAL eosinophil counts revealed a mean of 0.4 (SD 0.4) eosinophils. Comparing the eosinophil counts pre- and post- anti-IL-5 therapy using an unpaired t-test with Welch's correction revealed a statistically significant difference in eosinophil counts (P<0.05). The cytokine IL-5 is a vital component needed for the maturation and maintenance of eosinophils[2]. After the patients within the cohort received treatment with IL-5 antagonist humanized monoclonal antibodies it was seen that there was a reduction in eosinophil levels.

Molecular analyses of patient bacterial and fungal species within the patient BAL

At a molecular level qPCRs focusing on bacterial and fungal targets of interest were carried out. Unfortunately as study protocols were amended after four patients to include the extraction of the cell pellet from the BAL it was not possible to examine the difference baseline and follow up with regards to the cell pellet bacteria. However it is possible to compare BAL bacteria pellets prior and post anti-IL-5 treatment and it is also possible to compare difference between bacterial and

fungal levels within the bacteria pellet (BP) and cell pellet (CP) at follow up bronchoscopy.

The presence of the bacteria *Pseudomonas aeruginosa* (0%), *Escherichia* (13%), *Bordetella* (25%), *Streptococcus pneumoniae* (75%), *Rothia* (88%), *Micromonospora* (63%), and at the fungal level, Total fungal presence (Fungi Quant) (88%) and *Aspergillus fumigatus* (38%) remained at the same levels prior and post anti-IL-5 treatment.

Staphylococcus aureus reduced from 100% prevalence to 50% at follow up bronchoscopy upon further analysis of the qPCR cycle threshold values it was determined that there was a statistically significant difference by unpaired t-test with Welch's correction with respect to the baseline cycle threshold qPCR *S. aureus* in comparison to the follow-up bronchoscopy *S. aureus* qPCR cycle threshold values ($P<0.05$). *Neisseria bacilliformis* prevalence also decreased from 88% to 50% at follow up bronchoscopy.

However levels of Firmicutes (75% to 100%), *Pseudomonas fluorescens* (88% to 100%), *Prevotella* (88% to 100%), *Veillonella* (88% to 100%), *Chlamydophila pneumoniae* (50% to 75%), *Moraxella catarrhalis* (88% to 100%) all increased in prevalence within the follow up BAL DNA. Perhaps the largest increases were seen in terms of *Mycoplasma pneumoniae* (25% to 75%), *Neisseria meningitidis* (38% to 100%) and *Haemophilus influenzae* (63% to 100%) detection by qPCR.

Mycoplasma pneumoniae detection by qPCR increased within the patient cohort from 25% at initial bronchoscopy to 75% at follow up bronchoscopy. After treatment at follow up bronchoscopy BAL monocytes positively correlated with qPCR (bacteria pellet) *Mycoplasma pneumoniae* (BP) ($P<0.01$; $r_s=0.9856$) and (cell pellet) *Mycoplasma pneumoniae* (CP) ($P<0.05$; $r_s=0.8264$) *Mycoplasma pneumoniae* has been seen to align with a variety of clinical cases including acute and chronic lung infections which in turn is responsible for a wide array of pulmonary and extra-pulmonary sequelae[20,21]. *Mycoplasma pneumoniae* is believed to be the pathogen of interest in 20-40% of community acquired pneumoniae cases[20]. Within asthma populations *Mycoplasma pneumoniae* it is believed to be associated with airway

complications and exacerbations and is a significant source of morbidity[21]. *Mycoplasma pneumoniae* is known to possess a Community-Acquired Respiratory Distress Syndrome (CARDS) toxin which in murine and primate studies has been shown to induce inflammatory cytokines among other effects[22,23]. Therefore its increased prevalence in asthma patients post anti-IL-5 monoclonal antibody therapy is of great interest and required greater examination within a larger cohort of anti-IL-5 recipients.

Neisseria meningitidis detection increased from 38% to 100% within the patient cohort at follow up bronchoscopy. *Neisseria meningitidis* while a commensal ismost commonly associated with meningitis in human's, is also responsible for meningococcal pneumoniae. Meningococcal pneumoniae, the most common non-neurological organ disease caused by *Neisseria meningitidis* accounts for 5-10% of cases in which people are colonised with *Neisseria meningitidis.* Clinically it is indistinguishable in its symptoms from pneumoniae caused by other pathogens and is also indistinguishable through laboratory or radiological features[24]. Known to colonise the oro-nasopharyngeal tract, *Neisseria meningitidis* been found in healthy and diseased individuals and colonisation is mediated by virulence factors such as IgA1 protease, a polysaccharide capsule, and epithelial binding bacterial adhesins. *Neisseria meningitidis* can translocate to the lower airways via the blood stream, aerosol droplets and microaspiration of *Neisseria meningitidis* enclosed in biofilms. It is believed that an initial viral infection within a host can trigger meningococcal bacteraemia and once *Neisseria meningitidis* has become established within the lower airways through its virulence factors it can both supress and divert the host defence mechanisms leading to pulmonary damage and severe infection within a susceptible host[24]. Within the patient cohort *Neisseria meningitidis* was negatively correlated with monocyte cell percentage counts ($P<0.05$; r=-0.9991), lymphocyte cell percentage counts positively correlated with qPCR *Neisseria meningitidis* ($P<0.05$; r=0.9979) and eosinophil percentage counts negatively correlated with qPCR *Neisseria meningitidis* ($P<0.05$; r=-0.9994).

Haemophilus influenzae increased from 63% detection by qPCR to 100% detection within the patient cohort at follow up bronchoscopy. *Haemophilus influenzae* is present as a commensal bacterium within the nasopharynx of most healthy adults. Colonisation of the upper respiratory tract begins in infancy and at least 75% of adults are colonised by this bacteria, with constant turnover of different *Haemophilus influenzae* strains during life. *Haemophilus influenzae* can be grouped into polysaccharide encapsulated strains and non-encapsulated strains with non-encapsulated strains considered to be primarily respiratory pathogens. *Haemophilus influenzae* can be transmitted by aerosol droplets and through contact with secretions. The nasopharynx is a potential reservoir for the pathogen which can spread to the lower respiratory tract in certain individuals dependent on host defence mechanisms and bacteria mechanisms and virulence factors such as adhesins, pili, Hia and Hap proteins which can help the bacteria attach to mucosal surfaces and after attachment, the bacterium possesses mechanisms to aid persistence within the host such as proteases. Non encapsulated strains of *Haemophilus influenzae* are known to invade tissue and target macrophages and epithelial cells increasing their ability to survive within a susceptible individual[25].

The investigation of the bacteria pellet and cell pellet fractions of BAL

The isolation of DNA from both the free BAL bacteria (Bacteria Pellet; BP) and from the intracellular bacteria (Cell Pellet; CP), is an important additional aspect of patient processing as it can lead to subsequent downstream variations in detection for example within the follow-up bronchoscopy qPCR analysis *Bordetella* was present by qPCR in 25% of patients bacteria pellet (BP) BAL sample. However by qPCR *Bordetella* was detectable in 100% of patients cell pellet (CP) samples for the same BAL sample highlighting the importance of differential centrifugation when processing the BAL sample for microbial analyses. *Bordetella* species such as *Bordetella pertussis* the causative agent for pertussis; whooping cough, is predominately an extracellular bacterium however evidence now suggests *Bordetella* can survive within respiratory epithelial cells in order to evade the host

immune defence system, allowing the bacterium to repopulate in the extracellular environment when conditions are favourable[26].

BAL and plasma cytokine detection and the correlation to BAL qPCR microbial and fungal species

At the cytokine level IL-1β, IL-6 and TNF-α correlated with the following bacteria at baseline bronchoscopy BAL. IL-1β BAL cytokine levels correlated with qPCR *Veillonella* levels ($P<0.05$; $r_s=-0.8214$).IL-1β is a pleiotropic cytokine, capable of both pro- and anti- inflammatory effects. IL-1β is believed to be critical in the pathobiology of asthma, playing a role in driving the inflammatory response and the subsequent changes in airway smooth muscle (ASM) responsiveness[27]. BAL IL-6 cytokine levels correlated with qPCR *Veillonella* levels ($P<0.005$; $r_s=-0.9643$). IL-6 is a pleiotropic cytokine with the ability to act in an anti-inflammatory and pro-inflammatory manner. It is recognised that IL-6 is produced in response to the recognition of microbes by pattern associated molecular patterns[28]. *Veillonella* is recognised as a biofilm forming commensal identified in a wide array of locations within the human body including the lungs, mouth and gastrointestinal tract[29]. While recognised as a commensal microbe *Veillonella* has also been associated with several diseased states. In fact *Veillonella* species are known to play a prominent role within the microbial ecology of oral biofilms and are a prevalent member of the oral flora associated with dental plaque and the oral mucosa[30].

TNF-α cytokine levels correlated negatively with *Prevotella* qPCR levels ($P<0.05$; $r_s=-0.8108$). TNF-α has been implicated in systemic inflammation and is classified as a pro-inflammatory cytokine which has been implicated in asthma. Upon binding to its receptors, P55 and P75, TNF-α is capable of activating a number of cellular responses within the host, including activation, differentiation and release of pro-inflammatory mediatiors and it is noted that one of the most powerful activatiors of TNF-α production is the presence of lipopolysaccharides[31]. *Prevotella* is a commensal bacteria found in many locations within the human host including the lungs. *Prevotella* contains lipopolysaccharide on their outer membrane. *Prevotella*

has been found in the lungs of healthy individuals. In fact studies have shown that increased corticosteroid use can lead to a decrease in the relative abundance of *Prevotella* species within the lungs[32].

At follow-up bronchoscopy the chemokine IL-8 correlated with bacterial qPCR targets of interest. BAL IL-8 cytokine levels correlated with qPCR Total Bacteria (CP) *(P*<0.05; r_s=-0.8857), Firmicutes (CP) (*P*<0.05; r_s=-0.8857), *Streptococcus pneumoniae* (CP) (*P*<0.05; r_s=-0.9429) and *Haemophilus influenzae* (CP) (*P*<0.01; r_s=-0.9429) IL-8 (CXCL8) is a CXC chemokine and a neutrophil chemoattractant. It is recognised that IL-8 plays a key role in the innate immune response to bacterial infection. IL-8 inflammation upon bacterial pathogen exposure is a well-known key host immune response, however, in many cases of lung disease such bacterial exposure and subsequent IL-8 activation can in fact result in damaging the lungs through overactive inflammation and remodelling of the lungs which can result in an overall impairment of lung function[33]. Studies have demonstrated that upon challenge with bacterial stimuli the subsequent innate and adaptive immune response including the over-activation of Il-8 can in fact lead to an increase in inflammation, remodelling and mucus hypersecretion[33].

Plasma cytokine levels of IL-1β, IL-5, IL-6, IL-13, IL-17, TNF-α and IFN-γ did not correlate with BAL qPCR levels of bacteria and fungi at follow up bronchoscopy. However the pleiotropic cytokine IL-4 correlated with BAL *Rothia* (CP) (*P*<0.005; r=0.9965). The cytokine IL-4 is known to be associated with the development of allergic inflammation by driving differentiation of naïve T helper type 0 (T_H0) lymphocytes to a T helper type 2 (T_H2) response[34]. The pro-inflammatory chemokine IL-8 correlated with *Bordetella* (CP) (*P*<0.05; r_s=0.8571). The anti-inflammatory plasma IL-10 cytokine levels correlated with Total Bacteria (BP) (*P*<0.05; r=0.9537), Firmicutes (BP) (*P*<0.05; r=0.9317), *Veillonella* (BP) (*P*<0.05; r=0.9307) and *Mycoplasma pneumoniae* (CP) (*P*<0.05; r=0.8967). The cytokine IL-10 is expressed by many immune cells and is known for its anti-inflammatory

properties. The cytokine IL-10 plays a pivotal role in the hosts immune response to pathogens and in turn protects the host from an over-active immune response to a pathogenic stimuli, playing a critical role in the prevention of inflammatory and auto-immune diseased states[35].

Conclusions

Overall this study investigated potential changes in microbial composition within the lungs of a cohort of adult asthmatics after they receive monoclonal antibody therapy, anti-IL-5 biologics. Anti-IL-5 therapy modulated the composition of the lung microbiota in severe asthma. Bacterial respiratory tract infections have been linked to an a worsening in clinical outcome for patients with conditions such as asthma[36]. Therefore it is of growing interest, thanks to advancements in molecular techniques, to investigate the microbiome of patients with diseases such as asthma as it may allow for identification of therapeutic benefit but also susceptibility to respiratory tract infections and may aid in the improvement of outcomes for patients diagnosed with respiratory conditions such as asthma.

6. Supplementary

Supplementary table 1 Validated primer sequences utilised for the detection of microorganisms of interest. Note K=G or T, R=A or G, S=G or C, W=A or T following IUPAC code.

Primer		Sequence	Reference
Total Bacteria	F-Bact-1369	5'-CGGTGAATACGTTCCCGG-3'	[37]
	R-Prok-1492	5'-TACGGCTACCTTGTTACGACTT-3'	
Total Bacteria Probe	P-TM1389F	5'-CTTGTACACACCGCCCGTC-3'	
Firmicutes	Firm-L	5'- GGAGYATGTGGTTTAATTCGAAGCA-3'	[38]
	Firm-R	5'- AGCTGACGACAACCATGCAC-3'	
Staphylococcus aureus	Sa-pl-47-L	5'-ATGCATAGCCGACCTGAGAG-3'	NCBI:txid1280
	Sa-pl-47-R	5'- AGGAGTCTGGACCGTGTCTC-3'	
Streptococcus pneumoniae	S.pneu-pl-52-L	5'-GCAAGGTATGCAGGAATCGT-3'	Modification on *Streptococcus pneumoniae* alpha fucosidase gene NCBI:txid488222
	S.pneu-pl-52-R	5'-TCGCTTGAGTATGAACCAACC-3'	
Rothia	Rothia-Spp-L	5'-GCCTGGGAAACTGGGTCTAAT-3'	[39]
	Rothia-Spp-R	5'-CAAGCTGATAGGCCGTGAG-3'	
Micromonospora	Mimo16S-pl-39-L	5'-GGTACAATGGGCTGCGATAC-3'	Modification on *Micromonospora* strain ATCC 27029 NCBI:NR_074415.1
	Mimo16S-pl-39-R	5'-CGAACTGAGACCGGCTTTT-3'	
Pseudomonas aeruginosa	ORPL-pl-11-L	5'-CCAGAGCCATGTTGTACTCG-3'	[40 41] Modification on *Pseudomonas aeruginosa* Outer Membrane Protein L NCBI:txid205922
	ORPL-pl-11-R	5'-ACACGCGAAAGACCTGAAAG-3'	
Pseudomonas fluorescens	Pf-pl-66-L	5'-GACAGAATAAGCACCGGCTAA-3'	NCBI:txid294
	Pf-pl-66-R	5'-ACGCTTGCACCCTCTGTATT-3'	
Escherichia	UidA405-pl-9-L	5'-CTGATAGCGCGTGACAAAAA-3'	Modification on Beta-glucuronidase protein, Uid A405 gene NCBI:txid83333
	UidA405-pl-9-R	5'-CGGTTCGTTGGCAATACTC-3'	
Bordetella	Bordetella-pl-45-L	5'-GAGCCATTGTCGGTGAGC-3'	NCBI:txid517
	Bordetella-pl-45-R	5'-CGCAGTGGCCTACTACCAG-3'	
Prevotella	Prevotella-pl-66-L	5'-TGCAGGTACCGCATGAATAA-3'	NCBI:txid838
	Prevotella-pl-66-R	5'-CCGGACCTTCCGTATTACC-3'	
Veillonella	Veillonella-L	5'-CCGTGATGGGATGGAAACTGC-3'	[42]
	Veillonella-R	5'-CCTTCGCCACTGGTGTTCTTC-3'	
Mycoplasma pneumoniae	Myco.pneu-pl-16-L	5'-AGACACGGCCCATACTCCTA-3'	Greengenes GenBank: CP017343.1
	Myco.pneu-pl-16-R	5'-CAAGCTTTCGCTCATTGTGA-3'	

Chlamydophilia pneumoniae	C.pneu-pl-45-L	5′-CGTGAGATGGAGCAAATCCTA-3′	Greengenes GenBank: CP001713.1
	C.pneu-pl-45-R	5′-ACTTCATGTAGTCGAGTTGCAGA-3′	
Neisseria bacilliformis	Nb-pl-8-L	5′-TGCGTAGAGATGTGGAGGAAT-3′	Greengenes NCBI:txid267212
	Nb-pl-8-R	5′-CTGTTTGCTACCCACGCTTT-3′	
Moraxella catarrhalis	Mc-pl-66-L	5′-CACAGAATAAGCACCGGCTAA-3′	Greengenes GenBank: CP010573.1
	Mc-pl-66-R	5′-ACGCTTGCACCCTCTGTATT-3′	
Neisseria meningitidis	N.meningitidis-pl-9-L	5′-ATTCCACTACGGCAAACACC-3′	[43] Modification on *Neisseria meningitidis* SodC gene NCBI:txid487
	N.meningitidis-pl-9-R	5′-TCGGTGCCTTTGATTTGATT-3′	
Haemophilus influenzae	H.influ-pl-98-L	5′-AGCTGGTAAAGGTGTTGATGC-3′	Modification on Peptidoglycan associated outer membrane lipoprotein-OMP P6 NC_000907.1
	H.influ-pl-98-R	5′-GCAGGTTTTTCTTCACCGTAA-3′	
Fungi Quant	Fungi Quant-F	5′-GGRAAACTCACCAGGTCCAG-3′	[44]
	Fungi Quant-R	5′GSW CTA TCC CCA KCA CGA-3′	
Aspergillus fumigatus	OliAFMB-L-pl-103	5′-AGC ACG GCT TGT GTG TTG -3′	Modification on *Aspergillus* ITS KT358862 [45]
	OliAFMB-R-pl-103	5′-GGG TGA CAA AGC CCC ATA C-3′	

7. References

1. Nixon J, Newbold P, Mustelin T, Anderson GP, Kolbeck R. Monoclonal antibody therapy for the treatment of asthma and chronic obstructive pulmonary disease with eosinophilic inflammation. *Pharmacology & Therapeutics.* 2017;169:57-77.
2. Edris A, De Feyter S, Maes T, Joos G, Lahousse L. Monoclonal antibodies in type 2 asthma: a systematic review and network meta-analysis. *Respiratory Research.* 2019;20(1):179.
3. Drick N, Seeliger B, Welte T, Fuge J, Suhling H. Anti-IL-5 therapy in patients with severe eosinophilic asthma - clinical efficacy and possible criteria for treatment response. *BMC pulmonary medicine.* 2018;18(1):119-119.
4. Al Said A, Cushen B, Costello RW. Targeting patients with asthma for omalizumab therapy: choosing the right patient to get the best value for money. *Ther Adv Chronic Dis.* 2017;8(2-3):31-45.
5. Hom S, Pisano M. Reslizumab (Cinqair): An Interleukin-5 Antagonist for Severe Asthma of the Eosinophilic Phenotype. *P T.* 2017;42(9):564-568.
6. Davila Gonzalez I, Moreno Benitez F, Quirce S. Benralizumab: A New Approach for the Treatment of Severe Eosinophilic Asthma. *Journal of investigational allergology & clinical immunology.* 2019;29(2):84-93.
7. O'Byrne PM. Role of monoclonal antibodies in the treatment of asthma. *Can Respir J.* 2013;20(1):23-25.
8. Sullivan A, Hunt E, MacSharry J, Murphy DM. The Microbiome and the Pathophysiology of Asthma. *Respiratory Research.* 2016;17(1):163.
9. Miller MR, Hankinson J, Brusasco V, et al. Standardisation of spirometry. *The European respiratory journal.* 2005;26(2):319-338.
10. Graham BL, Steenbruggen I, Miller MR, et al. Standardization of Spirometry 2019 Update. An Official American Thoracic Society and European Respiratory Society Technical Statement. *Am J Respir Crit Care Med.* 2019;200(8):e70-e88.
11. Juniper EF, O'Byrne PM, Guyatt GH, Ferrie PJ, King DR. Development and validation of a questionnaire to measure asthma control. *The European respiratory journal.* 1999;14(4):902-907.
12. Juniper EF, Svensson K, Mork AC, Stahl E. Measurement properties and interpretation of three shortened versions of the asthma control questionnaire. *Respir Med.* 2005;99(5):553-558.
13. Juniper EF, Bousquet J, Abetz L, Bateman ED. Identifying 'well-controlled' and 'not well-controlled' asthma using the Asthma Control Questionnaire. *Respir Med.* 2006;100(4):616-621.
14. Du Rand IA, Blaikley J, Booton R, et al. British Thoracic Society guideline for diagnostic flexible bronchoscopy in adults: accredited by NICE. *Thorax.* 2013;68 Suppl 1:i1-i44.
15. Hunt EB, Ward C, Power S, et al. The Potential Role of Aspiration in the Asthmatic Airway. *Chest.* 2017;151(6):1272-1278.
16. DeSantis TZ, Hugenholtz P, Larsen N, et al. Greengenes, a Chimera-Checked 16S rRNA Gene Database and Workbench Compatible with ARB. *Applied and Environmental Microbiology.* 2006;72(7):5069-5072.
17. Kowalski CJ. On the Effects of Non-Normality on the Distribution of the Sample Product-Moment Correlation Coefficient. *Journal of the Royal Statistical Society Series C (Applied Statistics).* 1972;21(1):1-12.
18. Gemicioglu B, Musellim B, Dogan I, Guven K. Fractional exhaled nitric oxide (FeNo) in different asthma phenotypes. *Allergy Rhinol (Providence).* 2014;5(3):157-161.

19. Price D, Ryan D, Burden A, et al. Using fractional exhaled nitric oxide (FeNO) to diagnose steroid-responsive disease and guide asthma management in routine care. *Clinical and Translational Allergy.* 2013;3(1):37.
20. Defilippi A, Silvestri M, Tacchella A, et al. Epidemiology and clinical features of Mycoplasma pneumoniae infection in children. *Respiratory Medicine.* 2008;102(12):1762-1768.
21. Medina JL, Coalson JJ, Brooks EG, et al. Mycoplasma pneumoniae CARDS Toxin Induces Pulmonary Eosinophilic and Lymphocytic Inflammation. *American Journal of Respiratory Cell and Molecular Biology.* 2012;46(6):815-822.
22. Kannan TR, Baseman JB. ADP-ribosylating and vacuolating cytotoxin of Mycoplasma pneumoniae represents unique virulence determinant among bacterial pathogens. *Proceedings of the National Academy of Sciences.* 2006;103(17):6724-6729.
23. Ramasamy K, Balasubramanian S, Manickam K, et al. Mycoplasma pneumoniae Community-Acquired Respiratory Distress Syndrome Toxin Uses a Novel KELED Sequence for Retrograde Transport and Subsequent Cytotoxicity. *mBio.* 2018;9(1):e01663-01617.
24. Winstead JM, McKinsey DS, Tasker S, De Groote MA, Baddour LM. Meningococcal Pneumonia: Characterization and Review of Cases Seen Over the Past 25 Years. *Clinical Infectious Diseases.* 2000;30(1):87-94.
25. King P. Haemophilus influenzae and the lung (Haemophilus and the lung). *Clin Transl Med.* 2012;1(1):10-10.
26. Lamberti Y, Gorgojo J, Massillo C, Rodriguez ME. Bordetella pertussis entry into respiratory epithelial cells and intracellular survival. *Pathogens and disease.* 2013;69(3):194-204.
27. Whelan R, Kim C, Chen M, Leiter J, Grunstein MM, Hakonarson H. Role and regulation of interleukin-1 molecules in pro-asthmatic sensitised airway smooth muscle. *The European respiratory journal.* 2004;24(4):559-567.
28. Poynter ME, Irvin CG. Interleukin-6 as a biomarker for asthma: hype or is there something else? *The European respiratory journal.* 2016;48(4):979-981.
29. Poppleton DI, Duchateau M, Hourdel V, et al. Outer Membrane Proteome of Veillonella parvula: A Diderm Firmicute of the Human Microbiome. *Front Microbiol.* 2017;8(1215).
30. Knapp S, Brodal C, Peterson J, Qi F, Kreth J, Merritt J. Natural Competence Is Common among Clinical Isolates of Veillonella parvula and Is Useful for Genetic Manipulation of This Key Member of the Oral Microbiome. *Front Cell Infect Microbiol.* 2017;7(139).
31. Babu KS, Davies DE, Holgate ST. Role of tumor necrosis factor alpha in asthma. *Immunol Allergy Clin North Am.* 2004;24(4):583-597, v-vi.
32. Chung KF. Airway microbial dysbiosis in asthmatic patients: A target for prevention and treatment? *The Journal of allergy and clinical immunology.* 2017;139(4):1071-1081.
33. Reynolds CJ, Quigley K, Cheng X, et al. Lung Defense through IL-8 Carries a Cost of Chronic Lung Remodeling and Impaired Function. *Am J Respir Cell Mol Biol.* 2018;59(5):557-571.
34. Steinke JW, Borish L. Th2 cytokines and asthma. Interleukin-4: its role in the pathogenesis of asthma, and targeting it for asthma treatment with interleukin-4 receptor antagonists. *Respiratory research.* 2001;2(2):66-70.
35. Saraiva M, O'Garra A. The regulation of IL-10 production by immune cells. *Nat Rev Immunol.* 2010;10(3):170-181.

36. Earl CS, An S-q, Ryan RP. The changing face of asthma and its relation with microbes. *Trends Microbiol.* 2015;23(7):408-418.
37. Suzuki MT, Taylor LT, DeLong EF. Quantitative analysis of small-subunit rRNA genes in mixed microbial populations via 5'-nuclease assays. *Applied and environmental microbiology.* 2000;66(11):4605-4614.
38. Guo X, Xia X, Tang R, Zhou J, Zhao H, Wang K. Development of a real-time PCR method for Firmicutes and Bacteroidetes in faeces and its application to quantify intestinal population of obese and lean pigs. *Letters in applied microbiology.* 2008;47(5):367-373.
39. Keisuke N, Hiroshi M, Hideaki I, Norimasa T. Simple and rapid detection of Rothia mucilaginosa by loop-mediated isothermal amplification method. *日本口腔検査学会雑誌 = Journal of Japanese Society for Evidence and the Dental Professional : JJSEDP.* 2018;10(1):44-52.
40. Rao AR, Laxova A, Farrell PM, Barbieri JT. Proteomic identification of OprL as a seromarker for initial diagnosis of Pseudomonas aeruginosa infection of patients with cystic fibrosis. *Journal of clinical microbiology.* 2009;47(8):2483-2488.
41. Le Gall F, Le Berre R, Rosec S, et al. Proposal of a quantitative PCR-based protocol for an optimal Pseudomonas aeruginosa detection in patients with cystic fibrosis. *BMC Microbiology.* 2013;13(1):143.
42. Chalmers NI, Palmer RJ, Cisar JO, Kolenbrander PE. Characterization of a Streptococcus sp.-Veillonella sp. Community Micromanipulated from Dental Plaque. *Journal of Bacteriology.* 2008;190(24):8145-8154.
43. Dolan Thomas J, Hatcher CP, Satterfield DA, et al. sodC-based real-time PCR for detection of Neisseria meningitidis. *PLoS ONE.* 2011;6(5):e19361-e19361.
44. Liu CM, Kachur S, Dwan MG, et al. FungiQuant: A broad-coverage fungal quantitative real-time PCR assay. *BMC Microbiology.* 2012;12(1):255.
45. Cuenca-Estrella M, Meije Y, Diaz-Pedroche C, et al. Value of serial quantification of fungal DNA by a real-time PCR-based technique for early diagnosis of invasive Aspergillosis in patients with febrile neutropenia. *J Clin Microbiol.* 2009;47(2):379-384.

Chapter 7

Epithelial Response to Inflammatory Stimuli

The response of asthmatic airway bronchial epithelial cells (BEAS-2B) to microbial compounds, cytokines and metabolites

Author Contributions: Desmond Murphy, John MacSharry and Ashley Sullivan were responsible for the study design and concept. Experimental protocols were performed by Ashley Sullivan with contribution from John MacSharry. Statistical analysis was performed by Ashley Sullivan. Analysis and interpretation of data and manuscript preparation and approval was performed by Ashley Sullivan, John MacSharry and Desmond Murphy.

1. Abstract 313
2. Introduction 314
3. Methods 316
    3.1. Epithelial cell culture 316
    3.2. Removal of cells from cryopreservation 316
    3.3. Cell culture maintenance 317
    3.4. Cryopreservation of cell lines 318
    3.5. Preparation of cell stimulants 318
    3.6. Stimulation of submerged Beas-2B cells grown in 24 well plates 319
    3.7. RNA extraction 321
    3.8. RNA quantification and dilution 322
    3.9. Reverse transcriptase PCR 322
    3.10. Primers 323
    3.11. qRT-PCR 324
    3.12. Statistical analyses 324
4. Results 326
    4.1. Analysis of microbial compounds and cytokine stimulations 326
    4.2. Analysis of microbial compounds and metabolite stimulations 341
5. Discussion 349
6. Supplementary 363
7. References 372

1. Abstract

Background: Asthma is a highly heterogeneous disease with numerous phenotypes and symptoms in individuals can be triggered by a wide range of stimuli including allergens, airborne pollutants and infection. Dietary, genetic, microbial and environmental factors can be contributors to asthma risk.

Methods: BEAS-2B cells were stimulated with TLR2 (Pam3CSK4) and TLR4 (*Escherichia coli* LPS, *Porphyromonas gingivalis* LPS and *Pseudomonas aeruginosa* LPS) agonists alone or in combination with the cytokines IL-1β, IL-4, IL-7 and IL-17A or in combination with the metabolites Indole Acetic Acid and Sodium Acetate. qRT-PCR was performed to in order investigate the genes of interest; IL-6, CXCL8, CCL20, EGR1, IFNγ, TGFβ-1, TGFβ-2, TGFβ-3, TSLP, HDAC6, IL-36γ, GPR41, GPR109A and GPR109B and the relative expression of the genes of interest was calculated against the housekeeper gene, β-actin.

Results: Microbial compounds including LPS derived from *Escherichia coli*, *Porphyromonas gingivalis* and *Pseudomonas aeruginosa* and Pam3CSK4, cytokines including IL-1β, IL-4, IL-7 and IL-17A and metabolites including Indole Acetic Acid and Sodium Acetate alone or in combination resulted in a significant change in the relative expression of an array of targets of interest including IL-6, CXCL8, EGR1, IFN-γ, TGFβ, TSLP, HDAC6, IL-36γ, GPR41, GPR109A and GPR109B**.**

Conclusions: Many facets of allergic sensitisation are controlled by the airway epithelium and it in turn plays a key role in allergic inflammation, remodelling and bronchial hyper-reactivity. Therefore experiments targeting the airway epithelium with the goal of further understanding the pathophysiology of asthma could have many beneficial ramifications in terms of targets for new therapies and advancements in general asthma understanding and management. Overall the research aim to investigate the response of bronchial epithelial cells to microbial compounds, cytokines and metabolites individually and in combination and to investigate the resulting immune reaction upon stimulation was carried out.

2. Introduction

Airway epithelial cells are the frontline defence mechanism between the host and the environment and offer a defensive barrier against allergens, microorganisms and environmental pollutants[1]. The airway epithelium is further comprised of ciliated, club, goblet and basal cells which can transdifferentiate[1]. Airway epithelial cells are considered key controllers of inflammatory, immune and regenerative responses. Epithelial cells express pattern recognition receptors (PRRs) such as Toll like receptors (TLRs), NOD-like receptors, C-type lectins and protease-activated receptors, which respond to the detection of pathogen-associated molecular patterns (PAMPs) present in microorganisms, and to damage-associated molecular patterns (DAMPs), which are released upon tissue damage, cell death or cellular stress[1]. Upon exposure to pathogen-associated molecular patterns (PAMPs) and damage-associated molecular patterns (DAMPs) the pattern recognition receptors (PRRs) are turned on which then leads to modulatory compounds, such as cytokine, chemokine and antimicrobial peptides, to be released which then attract and activate innate and adaptive immune cells[1-3].

The airway epithelium offers a barrier function and mucociliary clearance mechanisms in order to prevent the invasion of allergens. The epithelial barrier integrity is dependent on apical tight junctions and adherens junctions, however in many leading respiratory diseases both the structure and function of the epithelial cells can be altered and it has been documented that in the airways of individuals with asthma the epithelium can be fragile[1,4].

Patients with chronic asthma can be subject to a progressive decline in lung function believed to be as a result of structural remodelling of the airways which is characterised by sub-epithelial fibrosis and smooth muscle hyperplasia leading to a compromised airway epithelium[1]. It has been noted that in asthma there is a change in the normal airway epithelium composition and goblet cell metaplasia, caused by the transdifferentiation of club cells and ciliated cells to goblet cells, resulting in an increase in the production of mucus within these patients leads to a progressive deterioration in lung function[1].

Many facets of allergic sensitisation are controlled by the airway epithelium and it in turn plays a key role in allergic inflammation, remodelling and bronchial hyper-reactivity. Therefore experiments targeting the airway epithelium with the goal of further understanding the pathophysiology of asthma could have many beneficial ramifications in terms of targets for new therapies and advancements in general asthma understanding and management[5].

Asthma is a highly heterogeneous disease with numerous phenotypes and symptoms in individuals can be triggered by a wide range of stimuli including allergens, airborne pollutants and infection[1,6-8]. Dietary, genetic, microbial and environmental factors can be contributors to asthma risk[9]. Airway epithelial cells play their part in both the innate and adaptive immune responses through activation of antimicrobial molecules and pro-inflammatory factors[3]. Studies have shown that respiratory pathogens, viruses, fungi and bacteria can play a role in asthma pathophysiology[10,11]. Intestinal metabolites; small molecules derived from the host, microbiota or exogenous sources such as the diet; have been shown to play a part in diseases such as asthma. Clinically relevant metabolites can contribute to pathogenic changes and it has recently been shown that intestinal bacterial taxa correlate with intestinal metabolites and childhood asthma[9].

It is therefore of interest to investigate the response of bronchial epithelial cells to microbial compounds, cytokines and metabolites individually and in combination and to investigate the resulting immune reaction upon stimulation. Microbial compounds including LPS derived from *Escherichia coli*, *Porphyromonas gingivalis* and *Pseudomonas aeruginosa* (TLR4 agonists) and Pam3CSK4 (TLR2 agonist), cytokines including IL-1β, IL-4, IL-7 and IL-17A and metabolites including Indole Acetic Acid and Sodium Acetate were utilised to investigate their effect upon asthmatic bronchial epithelial cells and the subsequent immune response was examined.

3. Methods

3.1. Epithelial cell culture

Beas-2B human bronchial epithelial cells immortalised through the infection of a replication defective SV40/adenovirus 12 hybrid were acquired from the American Type Culture Collection (ATCC number CRL-9609) (ATCC, Virginia, USA). Airway Epithelial Cell Growth Basal Medium supplemented with SupplementMix (Promo Cell, Brennan & Company, Ireland) was prepared and final supplement concentrations after addition to the serum free cell culture medium were as follows; Bovine Pituitary Extract 0.004ml/ml, Epidermal Growth Factor (recombinant human) 10ng/ml, Insulin (recombinant human) 5µg/ml, Hydrocortisone 0.5µg/ml, Epinephrine 0.5µg/ml, Triiodo-L-thyronine 6.7ng/ml, Transferrin (recombinant human) 10µg/ml, and Retinoic Acid 0.1ng/ml.

3.2. Removal of cells from cryopreservation

Beas-2B human epithelial cells were stored in aliquots in liquid nitrogen cell bank 1, rack 1.5. Cryovials containing $1x10^6$ Beas-2B cells per vial were removed from the cell bank and placed in a 37^{o}C water bath. Once defrosted cells were aliquoted into 15ml falcon tubes which contained 5mls of warmed Airway Epithelial Cell Growth Basal Medium (Promo Cell; Brennan & Company, Ireland) ensuring all cells were removed from the cryovial. The 15ml falcon tube was inverted several times, centrifuged at 200g for 10 minutes, supernatant removed and cell pellet re-suspended with cell culture media pre-warmed in Greiner CELLSTAR 75cm^2 cell culture flasks with red filter screw caps (Cruinn, Ireland). Flasks containing 12mls of medium and cells were then incubated at 37^{o}C with 5% CO_2.

3.3. Cell culture maintenance

Cell culture growth was monitored daily using an inverted microscope (Olympus). Cell medium was changed every 2-3 days to replenish nutrients and ensure correct pH was maintained. This involved removal of 90% of the medium by aspiration and the addition of 12mls of Airway Epithelial Cell Growth Basal Medium. In order to avoid squamous terminal differentiation the cells had to be subcultured before reaching confluence. Once 60-70% cell confluence was reached cell culture medium was removed and the cells were washed with Ca^{2+}/Mg^{2+} Phosphate Buffered Saline (PBS) (Sigma Aldrich). 2ml of trypsin which consisted of 0.05% Trypsin and EDTA in PBS (Gibco, Thermo Fisher Scientific)and 2ml of 1x Cell Dissociation Solution (Sigma Aldrich) was added to the cells in the T75 flask, ensuring all cells were coated. The flask was then incubated at 37^{o}C, 5% CO_2 for 5-10 minutes, and cells were checked regularly under an inverted microscope for dispersal of the cell layer. Once this was observed 5ml of Airway Epithelial Cell Growth Basal Medium was added and cells were aspirated by gentle pipetting. The cell suspension was then transferred to a 15ml falcon tube and centrifuged at 200g for 10 minutes. The supernatant was removed and the cell pellet re-suspended in 10ml of fresh cell medium. Trypan Blue (Invitrogen, UK) was utilised to determine cell viability and cell numbers. Healthy cells have ability to exclude Trypan Blue however non-viable cells cannot and are stained blue. Briefly 10µl of cell suspension and 10µl of Trypan Blue was combined in an Eppendorf tube and 10µl of this suspension was pipetted uniformly into one of the two chambers of the cover-slipped Brightline Haemocytometer (Sigma Aldrich) and 4 squares per chamber were counted under an inverted microscope (Olympus) at 10x objective. When counting a system was employed whereby cells were only counted when they were within the set of 16 squares and on the right hand boundary line of the overall large square. The average cell count from each of the 4 sets of the 16 corner squares was calculated. This value was then multiplied by the volume of the cell suspension, the trypan blue dilution factor of 2 and 10,000. The value obtained from this calculation was then divided by 4 to account for the 4 squares of the haemocytometer chamber counted to obtain the total cells

per ml value. T75 flasks had a seeding density of $2.1x10^6$ and 24 well culture plates (Corning Life Sciences, NY, USA) had a seeding density of $0.05x10^6$ per well.

3.4. Cryopreservation of cell lines

Cell cultures can be frozen indefinitely to preserve the cells and ensure a backup of cells are available. Before cells are frozen they were maintained in an actively growing state to ensure that cells were at maximum health and had the best chance of recovery. Beas-2 cells underwent the same protocol as to subculture the cells and the cell suspension was counted and viability noted in the same manner using a Haemocytometer. The viability of the cells should be 90% in order to ensure the cells survive the freezing process. The cell suspension was centrifuged for 10 minutes at 200g and supernatant was discarded. 10% DMSO which consisted of 9ml Foetal Bovine Serum (FBS) (Sigma Aldrich) and 1ml Dimethylsulfoxide (DMSO) (Sigma Aldrich) was prepared. 10% DMSO was used to re-suspend the cell pellet; the volume used was determined by the cell count number in order that each cryovial contained $1x10^6$ cells per ml. The labelled cryovials were gradually frozen by first freezing the cryovials in a bio-freezing vessel stored at -80^{o}C for 24 hours before transferring the cryovials to liquid nitrogen for long term storage.

3.5. Preparation of cell stimulants

Stock concentrations of the microbial compounds *Escherichia coli* LPS 100µg/ml (Invivogen) (TLR4 agonist), *Porphyromonas gingivalis* LPS 1mg/ml (Invivogen) (TLR4 agonist), *Pseudomonas aeruginosa* LPS 5mg/ml (Sigma Aldrich) (TLR4 agonist), Pam3CYSK4 1000ng/µl (Invivogen) (TLR2 agonist), the cytokines IL-1β 2µg, (Peprotech), IL-4 5µg (Peprotech), IL-7 2µg (Peprotech), IL-17 5µg (Peprotech) and the metabolites Sodium Acetate 3M (Invitrogen, Thermo Fischer Scientific), Indole 3 Acetic Acid 5g (Sigma Aldrich) were diluted to working stock concentrations as per manufacturer's instructions. Concentrations used were determined by best practice from previous cell experiments within the laboratory group and through literature review. Briefly BEAS-2B cells were exposed to 100ng/µl *Escherichia coli* LPS,

100ng/µl *Porphyromonas gingivalis* LPS, 100ng/µl *Pseudomonas aeruginosa* LPS, 1000ng/µl Pam3CSK4, 10ng/µl IL-1β, 10ng/µl IL-4, 10ng/µl IL-7, 50ng/µl IL-17, 2mM (20µl/ml) Sodium Acetate and 2mM (20µl/ml) Indole 3 Acetic Acid.

3.6. Stimulation of submerged Beas-2B cells grown in 24 well plates

24 well culture plates (Corning Life Sciences, NY, USA) were seeded with Beas-2B cells at a density of $0.05x10^6$ cells per well and cells were maintained in a 37^{o}C 5% CO_2 incubator and were fed every two days. Once cells were confluent cells were stimulated with various combinations of microbial compounds, cytokines and metabolites of interest. BEAS-2B cells were exposed the following concentrations; 100ng/µl *Escherichia coli* LPS (TLR4 agonist), 100ng/µl *Porphyromonas gingivalis* LPS (TLR4 agonist), 100ng/µl *Pseudomonas aeruginosa* LPS (TLR4 agonist), 1000ng/µl Pam3CSK4 (TLR2 agonist), 10ng/µl IL-1β, 10ng/µl IL-4, 10ng/µl IL-7, 50ng/µl IL-17, 2mM (20µl/ml) Sodium Acetate and 2mM (20µl/ml) Indole 3 Acetic Acid. See layout 1-4 for plate design. Cells were stimulated with components in triplicate within each 24 well plate and each plate layout was repeated in triplicate.

Unstimulated	LPS E.coli
LPS P. aeruginosa	LPS P. gingivalis
PAM3CSK4	IL-1B
IL-4	IL-7

Layout 1: Plate layout 1, in which cells were stimulated with *Escherichia coli* LPS (TLR4 agonist), *Pseudomonas aeruginosa* LPS (TLR4 agonist), *Porphyromonas gingivalis* LPS (TLR4 agonist), Pam3CSK4 (TLR2 agonist), IL-1β, IL-4 and IL-7 in triplicate. Three wells of Beas-2B cells remained unstimulated as the study control.

IL17	LPS PA + IL-1B
LPS PA + IL-4	LPS PA + IL-7
LPS PA + IL-17	LPS PG + IL-1B
LPS PG + IL-4	LPS PG + IL-7

Layout 2: Plate layout 2, in which cells were stimulated with IL-17, and the following combinations of compounds; *Pseudomonas aeruginosa* LPS and IL-1β, *Pseudomonas aeruginosa* LPS and IL-4, *Pseudomonas aeruginosa* LPS and IL-7, *Pseudomonas aeruginosa* LPS and IL-17, *Porphyromonas gingivalis* LPS and IL-1β, *Porphyromonas gingivalis* LPS and IL-4, *Porphyromonas gingivalis* LPS and IL-7 in triplicate.

LPS PG + IL-17A	PAM3CSK4 + IL-1B
PAM3CSK4 + IL-4	PAM3CSK4 + IL-7
PAM3CSK4 + IL-17	

Layout 3: Plate layout 3, in which cells were stimulated with *Porphyromonas gingivalis* LPS and IL-17, Pam3CSK4 and IL-1β, Pam3CSK4 and IL-4, Pam3CSK4 and IL-7 and Pam3CSK and IL-17 in triplicate.

Indole Acetic Acid	IAA + LPS PA
IAA + LPS PG	IAA + PAM3CSK4
Sodium Acetate	Sodium Acetate + LPS PA
Sodium Acetate + LPS PG	Sodium Acetate + PAM3CSK4

Layout 4: Plate layout 4, in which cells were stimulated with Indole 3 Acetic Acid, Indole 3 Acetic Acid and *Pseudomonas aeruginosa* LPS, Indole 3 Acetic Acid and *Porphyromonas gingivalis* LPS, Indole 3 Acetic Acid and Pam3CSK4, Sodium Acetate, Sodium Acetate and *Pseudomonas aeruginosa* LPS, Sodium Acetate and *Porphyromonas gingivalis* LPS and Sodium Acetate and Pam3CSK4.

Plates were stimulated for 24 hours in a 37^{o}C 5% CO_2 incubator. After 24 hours cells were visualised by microscopy and stimulation was stopped removing the supernatant and by lysing the cells with Solution TR1 and β-mercaptoethanol from the RNeasy PowerLyzer Tissue and Cells Kit (Qiagen).

3.7. RNA extraction

RNA was extracted using the RNeasy PowerLyzer Tissue and Cells Kit (Qiagen). After Beas-2B cells in a 24 well plate were stimulated for 24 hours the stimulation was stopped by lysing the cells. The cell culture medium was removed from each of the 24 wells. Solution TR1 was prepared by adding 10µl of β-mercaptoethanol for every 1ml of Solution TR1, therefore for 24 samples 120µl of β-mercaptoethanol in 12ml of Solution TR1 was required, 500µl of which was added to each well of the plate ensuring the cells were thoroughly homogenised by vigorous pipetting of the solution 15-20 times in the well, ensuring the pipette tip was changed after each well. The 24 well cell culture plate containing the homogenised samples in Solution TR1 was then carefully sealed and stored at -80^{o}C until ready. Once ready to complete the RNA extraction protocol the 24 well cell culture plate was defrosted and 500µl of Solution TR2 was added to the lysate in each well and was mixed thoroughly by pipetting. Solution TR2 consisted of 70% ethanol, ensuring optimal binding conditions were prepared for RNA capture on the MB RNA spin column filter membrane. 600µl of the lysate was then transferred to the corresponding labelled MB RNA spin column in a 2ml collection tube and centrifuged at 10,000g for 1 minute. The flow through was discarded and this step was repeated with the remaining lysate. The RNA was bound to the membrane of the spin column. The spin column was washed with 500µl of Solution WB, centrifuged at 10,000g for 1 minute and the spin column was placed in a new collection tube. This step removed proteins from the spin column membrane. The spin column membrane was then washed with 500µl of Solution RW, centrifuged at 10,000g for 1 minute. The flow through was discarded and the spin column was washed again with 500µl Solution RW, centrifuged at 10,000g for 1 minute ensuring that the ethanol in Solution RW removed salts present in Solution WB. The spin column was then placed in a new collection tube and centrifuged for 2 minutes at 13,000g to completely dry the membrane so the RNA may be released efficiently in the next step. The spin column was placed in a new collection tube and 100µl RNase-free water was directly added to the membrane and incubated at room temperature for 1 minute before being

centrifuged at 10,000g for 1 minute to elute the RNA which was then stored at -80^{o}C until required for further downstream processing.

3.8. RNA quantification and dilution

The concentration and quality of the extracted RNA was analysed using a Nano Drop ND1000 spectrophotometer using the settings nucleic acid; RNA-40 (Thermo Fischer Scientific, Wilmington, Delaware, USA). The Nano Drop was calibrated using 1µl of DNase/RNase free water. The RNA extracted from the Beas-2B cell stimulations was analysed by pipetting 1µl of sample onto the lower measure platform of the machine, closing the sampling arm and initiating spectral measurement using the operating software documenting the ng/µl and 260:280 values and RNA curve graph. See Supplementary Table S1, S2 and S3. In order to standardise the RNA a dilution step was performed where the undiluted RNA was diluted with DEPC treated molecular biology grade water (Calbiochem, Sigma Aldrich) to ensure a standard value of 20ng/µl (200ng per reaction) of RNA for each patient sample.

3.9. Reverse transcriptase PCR

The mRNA isolated from the Beas-2B cell stimulations and diluted to 20ng/µl was reverse transcribed to cDNA. Mastermix per sample reaction consisted of 4µl 5X Transcriptor Buffer, 2µl dNTP (ATGC) 10mM, 1µl Transcriptor RT/RNAsin mix which consisted of Reverse Transcriptase and Protector RNase Inhibitor in a 1:1 volume ratio and 3µl of Random Primer (Roche, Merck-Sigma Aldrich, Germany). A No RT Mastermix consisted of 4µl 5X Transcriptor Buffer, 2µl dNTP (ATGC) 10mM, 3µl Random Primer and 1µl DEPC treated molecular biology grade water (Calbiochem, Sigma Aldrich, Germany). 10µl of Mastermix or no RT Mastermix was pipetted into a 96 well unskirted PCR plate (Thermo Fisher Scientific, Bio Sciences, Ireland) and 10µl of 20ng/µl mRNA, extracted from the Beas-2B cell stimulations, was pipetted into the wells to ensure the mRNA from each stimulation was transcribed to cDNA. The 96 well plate was sealed with a foil plate seal and spun using a microplate

centrifuge (VWR, Dublin, Ireland) to ensure the mastermix and RNA is dispersed to the bottom of the wells. A benchtop 2720 Thermal Cycler machine (Applied Biosystems, Thermo Fisher Scientific, Ireland) was programmed to include 10 minutes at 25^{o}C, 30 minutes at 55^{o}C and 5 minutes at 85^{o}C before cooling to 4^{o}C while the PCR lid was heated to 100^{o}C to prevent reagent loss. Once the Reverse Transcriptase PCR cycles were complete the cDNA was diluted by adding 80µl DEPC treated molecular biology grade water to each well. The cDNA was then stored at -20^{o}C for further downstream applications.

3.10. Primers

Primers were designed using the Universal Probe Library Assay Design Centre (Roche Life Sciences) programme. See Supplementary Table S4 for primer sequences and corresponding probe numbers. Primers were chosen based on scientific literature with an emphasis on cytokines and chemokines in relation to bronchial epithelial cells. When designing the primers using the Universal Probe Library Assay Design Centre *Homo sapiens* was selected as the organism of choice and the target gene of interest was entered by name leading to the design of numerous primer pairs for that gene. Two primer pairs were designed for each gene of interest based on the software ranking system. Primers were supplied by Eurofins Genomics (Ireland) or Sigma Aldrich (Ireland). Primers were centrifuged upon arrival to ensure the lyophilized pellet remained at the bottom of the 2ml screw-cap tube and then were re-suspended with molecular grade water according to individual primer specification (µl for 100µM). Once primers were re-suspended they were then vortexed and combined by adding 20µl of right primer and 20µl of left primer and 160µl of molecular grade water to a sterile labelled Eppendorf tube. Primers were then stored at -20^{o}C. Universal Probe Library (PL) Probes sets (Roche Life Sciences) were available within the laboratory. Primers for which there was not a corresponding probe available for underwent SYBR green qRT-PCR conditions. Primers were tested on a pool of Beas-2B cDNA and primers were considered viable depending on Absolute Quantification/2nd Derivative Max Cp values and Tm calling analysis.

3.11. qRT-PCR

qRT-PCR's were performed using a 384 well plate layout and LightCycler Probes Master (Roche, Ireland) or LightCycler SYBR Green Master (Roche) reagent mix, dependent on the use of hydrolysis probes or SYBR Green primer sets. Water NTCs (No Template Control) were used in each reaction in order to identify reaction set up contamination and to test for the propensity of primers to create primer dimers in the case of reactions which were carried out with SYBR Green Master. Reactions were performed on a LightCycler 480 machine (Roche). qRT-PCR conditions were as follows; pre-incubation at 50^{o}C for 2 minutes, ramp rate 4.8^{o}C/s and 95^{o}C for 10 minutes, ramp rate 4.8^{o}C/s. Amplification at 95^{o}C for 10 seconds, ramp rate 4.8^{o}C/s, 60^{o}C for 45 seconds, ramp rate 2.5^{o}C/s and 75^{o}C for 1 second, ramp rate 4.8^{o}C for 45 cycles in total. A melt curve also occurred at 95^{o}C with a ramp rate of 0.11^{o}C/s for any primer which used LightCycler SYBR Green Master. A cooling stage then occurred at 40^{o}C, ramp rate 2^{o}C/s at the end of the process. Fluorescent readings were taken in single acquisition mode. All NTCs did not produce a product and melt curves produced clear peaks indicating that the products produced were not an artefact. qRT-PCR was carried out on stimulated Beas-2B cDNA with a focus on the following genes of interest; β-actin (pl11), IL-6 (pl16), IL-17F (SYBR), CXCL8 (SYBR), CCL11 (SYBR), CCL20 (SYBR), EGR1 (SYBR), IFN-γ (SYBR), TSLP (SYBR), TGFβ1 (pl31), TGFβ2 (pl44), TGFβ3 (pl38), GPR41 (SYBR), GPR109A (pl23), GRP109B (pl62), IL36-γ (pl54) and HDAC6 (SYBR).

3.12. Statistical analyses

qRT-PCR raw data was analysed using ddCT analysis using Microsoft Excel software. The housekeeper gene, beta (β)-actin raw qPCR data was compared to the raw qPCR Ct (Cycle threshold) data for the gene of interest. To do this, the average of the Ct values for the housekeeping gene (HK), beta (β)-actin was calculated for both the control (unstimulated Beas-2B samples) and the qPCR Ct beta (β)-actin results for all the samples tested in that qRT-PCR run. The average of the Ct values for the gene of interest (GOI) qPCR Ct raw data was also calculated with regards to the average Ct value for the gene of interest (GOI) from the unstimulated Beas-2B

samples and also from the average of the GOI Ct values for all samples tested in that qRT-PCR run. Four averages were generated; the GOI average experimental Ct value, the GOI average control Ct value, the HK average experimental Ct value and the HK average control Ct value.

The difference between the GOI average experimental Ct value and the HK average experimental Ct value was calculated and the difference between the GOI average control Ct value and HK average control Ct value was also calculated. This created the delta Ct (ΔCt) values. Either the delta Ct control or delta Ct experimental value was then used as a calibrator control to calculate the difference between it and the delta Ct of each individual sample, creating the delta delta Ct (ΔΔCt) value for each individual sample. The fold change of the samples was then calculated by 2^-ΔΔCt.

The graphical representation and statistical analysis of data was then carried out using GraphPad Prism 8 software. Results were considered statistically significant when $P<0.05$. An unpaired t test with welch's correction was used to analyse the relative expression data as the standard deviation between the two conditions was not equal.

4. Results

4.1. Analysis of microbial compounds and cytokine stimulations

qRT-PCR analyses of the *in vitro* gene expression in Beas-2B; immortalized human bronchial epithelial cells, using an unstimulated control and the stimulants *Escherichia coli* LPS (TLR4 agonist), *Pseudomonas aeruginosa* (PA) LPS (TLR4 agonist), *Porphyromonas gingivalis* (PG) LPS (TLR4 agonist), Pam3CSK4 (TLR2 agonist), IL-1β, IL-4 and IL-7, IL-17A, *Pseudomonas aeruginosa* (PA) LPS and IL-1β, *Pseudomonas aeruginosa* (PA) LPS and IL-4, *Pseudomonas aeruginosa* (PA) LPS and IL-7, *Pseudomonas aeruginosa* (PA) LPS and IL-17, *Porphyromonas gingivalis* (PG) LPS and IL-1β, *Porphyromonas gingivalis* (PG) LPS and IL-4, *Porphyromonas gingivalis* (PG) LPS and IL-7, *Porphyromonas gingivalis* (PG) LPS and IL-17, Pam3CSK4 and IL-1β, Pam3CSK4 and IL-4, Pam3CSK4 and IL-7 and Pam3CSK4 and IL-17 took place in order to investigate if the stimulants alone or a combination of stimulants induced a significant immune response. All cell stimulation conditions were examined, n=3 per stimulation experiment and all experiments were carried out in triplicate.

IL-6, CXCL8, CCL20, EGR1, IFN-γ, TGFβ-1, TGFβ-2, TGFβ-3, TSLP, HDAC-6, IL-36γ, GPR41, GPR109A and GPR109B levels were analysed using relative expression (2^{-} ddCT) analysis and statistical significance was calculated and graphs were generated using GraphPad Prism 8 software. See Figure 1 – Figure 14 for graphical representation of results. Values are expressed as mean ± SD, n=3, with the asterisk indicative of the level of significance. All cell stimulation conditions were examined, n=3, per stimulation experiment and all experiments were carried out in triplicate.

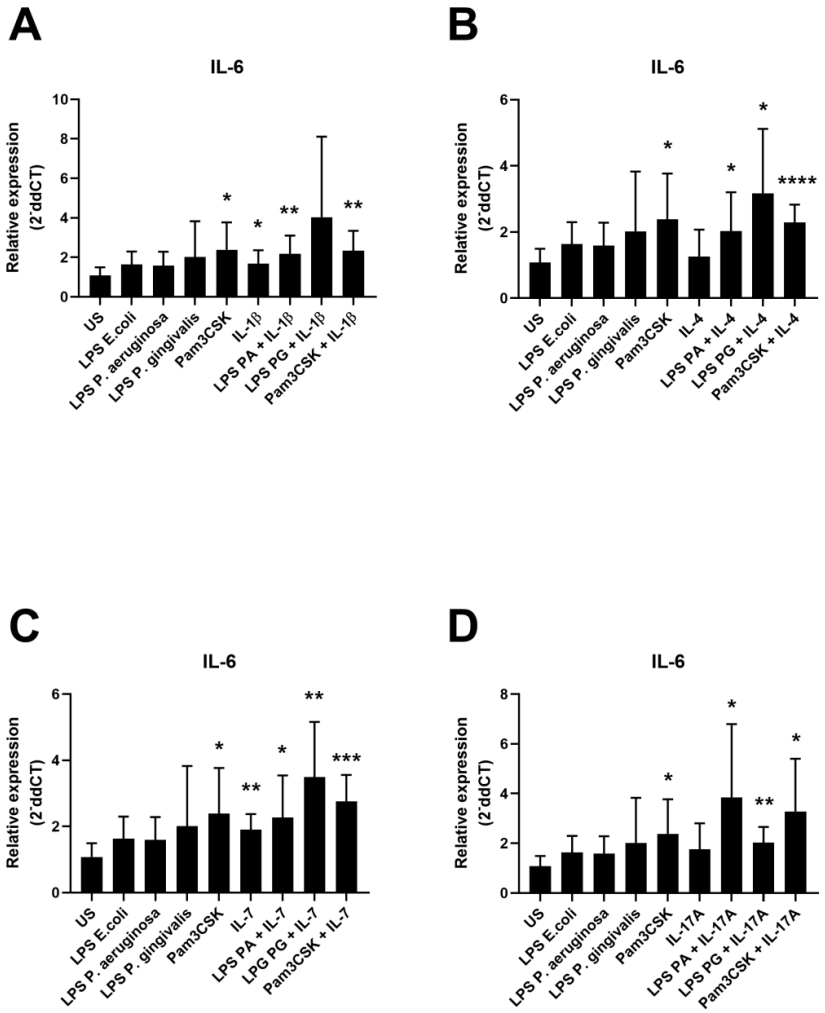


Figure 1. IL-6 mRNA Expression following cytokine and microbial component stimulations for 24 hours. (A) Cells stimulated with the ligand Pam3CSK (*P*<0.05), the cytokine IL-1β (*P*<0.05) and a combination of LPS PA+IL-1β (*P*<0.01) and Pam3CSK+IL-1β (*P*<0.01) had significant increase in the levels of cytokine IL-6 compared to unstimulated Beas-2B cells (US), n=3. (B) Pam3CSK (*P*<0.05) and a combination of LPS PA+IL-4 (*P*<0.05), LPS PG+IL-4 (*P*<0.05) and Pam3CSK+IL-4 (*P*<0.0001) had a significant increase in IL-6 compared to US cells, however IL-4 alone did not have an effect, n=3. (C) Pam3CSK (*P*<0.05), the cytokine IL-7 (*P*<0.005) and a combination of LPS PA+IL-7 (*P*<0.05), LPS PG+IL-7 (*P*<0.005) and Pam3CSK+IL-7 (*P*<0.0005) had a significant increase in IL-6 compared to US cells, n=3. (D) Pam3CSK (*P*<0.05) and a combination of LPS PA+IL-17A (*P*<0.05), LPS PG+IL-17A (*P*<0.005) and Pam3CSK+IL-17A (*P*<0.05) had a significant increase in IL-6 compared to US cells, n=3.

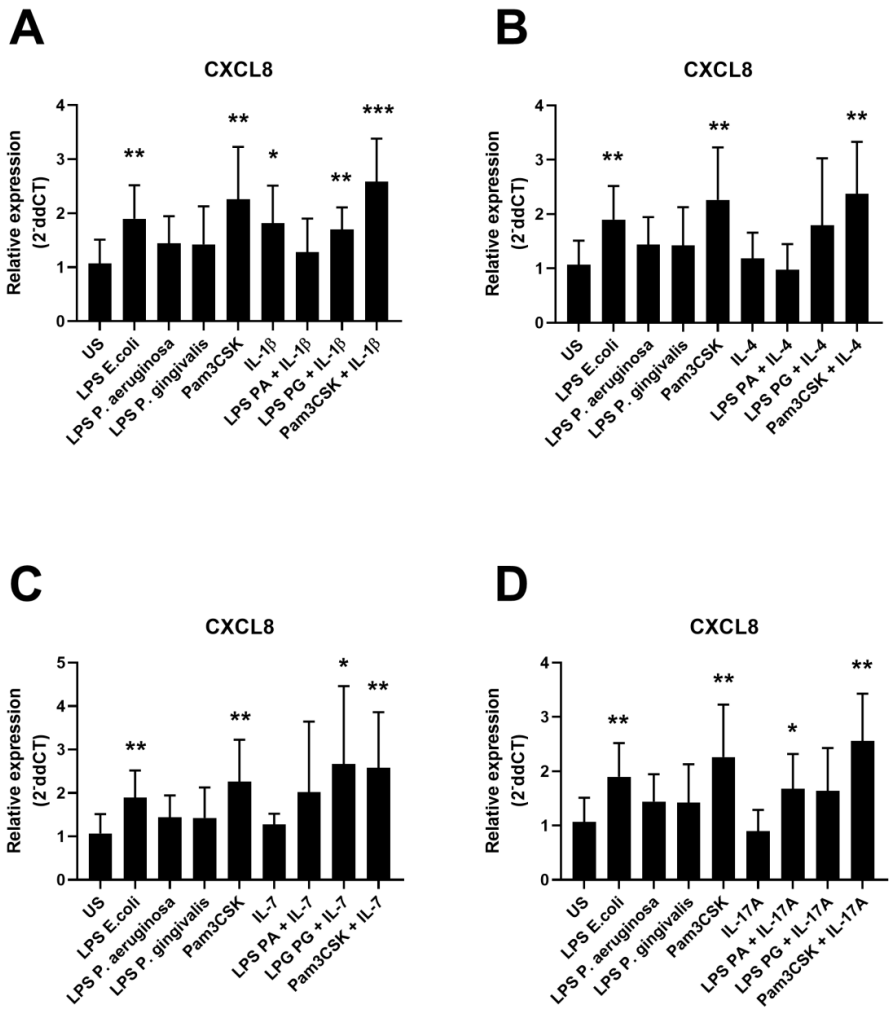


Figure 2. CXCL8 mRNA Expression following cytokine and microbial component stimulations for 24 hours. Beas-2B cells stimulated with *Escherichia coli* derived LPS (*P*<0.01), and the TLR2 agonist Pam3CSK (*P*<0.01) showed a significant level of the chemokine CXCL8 (IL-8) compared to unstimulated (US) cells (A-D). (A) Cells stimulated with the cytokine IL-1β (*P*<0.05) and with a combination of LPS PG+IL-1β (*P*<0.01) and Pam3CSK+IL-1β (*P*<0.0005) showed a significant CXCL8 response however when cells were stimulated with a combination of LPS PA+IL-1β there was not a significant CXCL8 difference. (B) Cells stimulated with a combination of Pam3CSK+IL-4 (*P*<0.005) had a significant increase in CXCL8 compared to US cells, but there was no significance found in IL-4 stimulation alone or in combination with LPS PA or LPS PG. (C) Stimulation with LPS PG+IL-7 (*P*<0.05) and Pam3CSK+IL-7 (*P*<0.01) showed a significant CXCL8 response as did cells stimulated with LPS PA+17-17A (*P*<0.05) and Pam3CSK+IL-17A (*P*<0.005) (D). n=3.

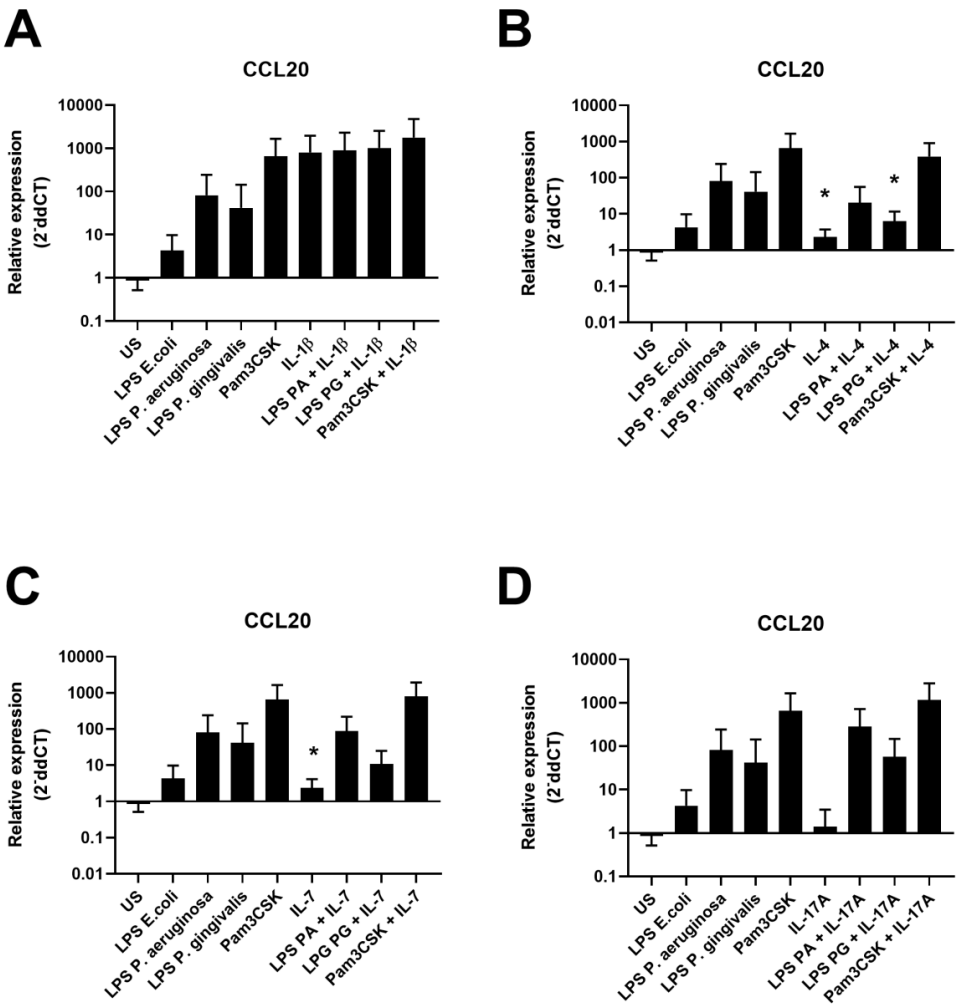


Figure 3. CCL20 mRNA Expression following cytokine and microbial component stimulations for 24 hours. Beas-2 cells when stimulated with various bacterial compounds and cytokines had little statistical significance in CCL20 expression; however this may be due to the large variation observed in expression levels between the 3 individual experiments where the cells were stimulated with the various compounds of interest. Statistical significance was observed when cells were stimulated with IL-4 (P<0.05), IL-7 (P<0.05) and a combination of *Porphyromonas gingivalis* (PG) derived LPS and IL-4 (P<0.05). n=3.

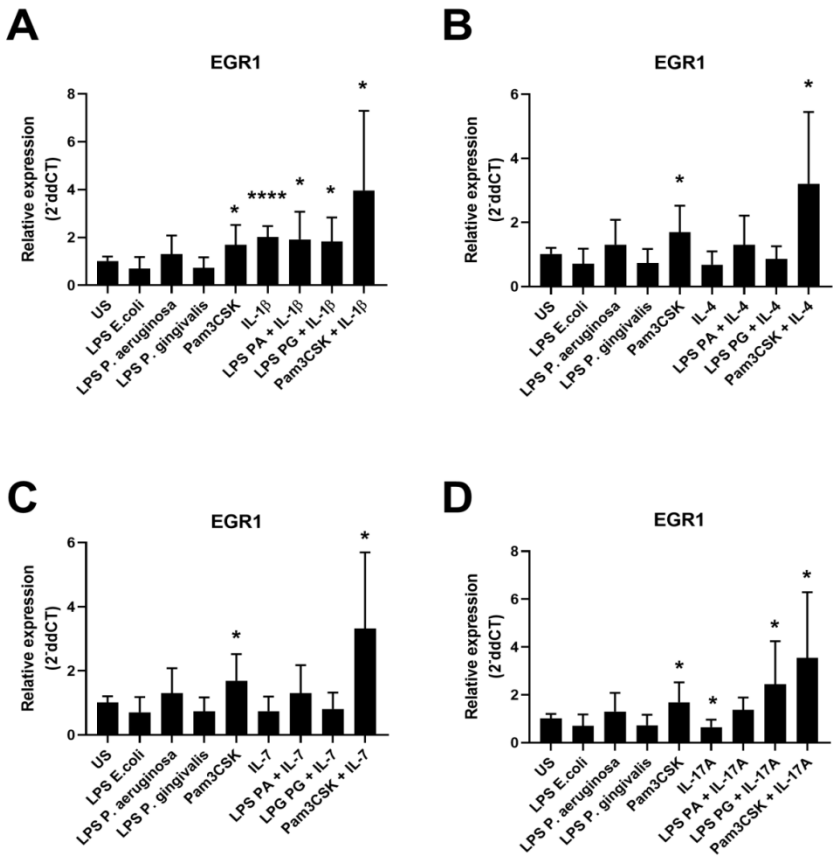


Figure 4. EGR1 mRNA Expression following cytokine and microbial component stimulations for 24 hours. Beas-2B cells stimulated with the TLR2 agonist Pam3CSK (*P*<0.05) showed a significant increase in EGR1 levels in comparison to the unstimulated (US) Beas-2B cells (A-D). (A) Cells stimulated with the cytokine IL-1β (*P*<0.0001) and with combinations of LPS PA+IL-1β (*P*<0.05), LPS PG+IL-1β (*P*<0.05) and Pam3CSK+IL-1β (*P*<0.05) showed a significant EGR1 response when compared to US cells. (B) Cells stimulated with IL-4 alone showed no significance however a combination of Pam3CSK+IL-4 (*P*<0.05) had a significant increase in EGR1 levels compared to US cells. (C) Stimulation with Pam3CSK+IL-7 (*P*<0.01) showed a significant difference in EGR1 expression in comparison to the unstimulated Beas-2B cells. (D) Cells stimulated with IL-17A alone had a statistically significant difference in EGR-1 expression in comparison to unstimulated cells and expression level in the IL-17A stimulated cells was lower on average than the expression in the unstimulated cells. Cells stimulated with LPS PG+IL-17A (*P*<0.05) and Pam3CSK+IL-17A (*P*<0.05) has a statistically significant rise in expression compared to the US cells. n=3.

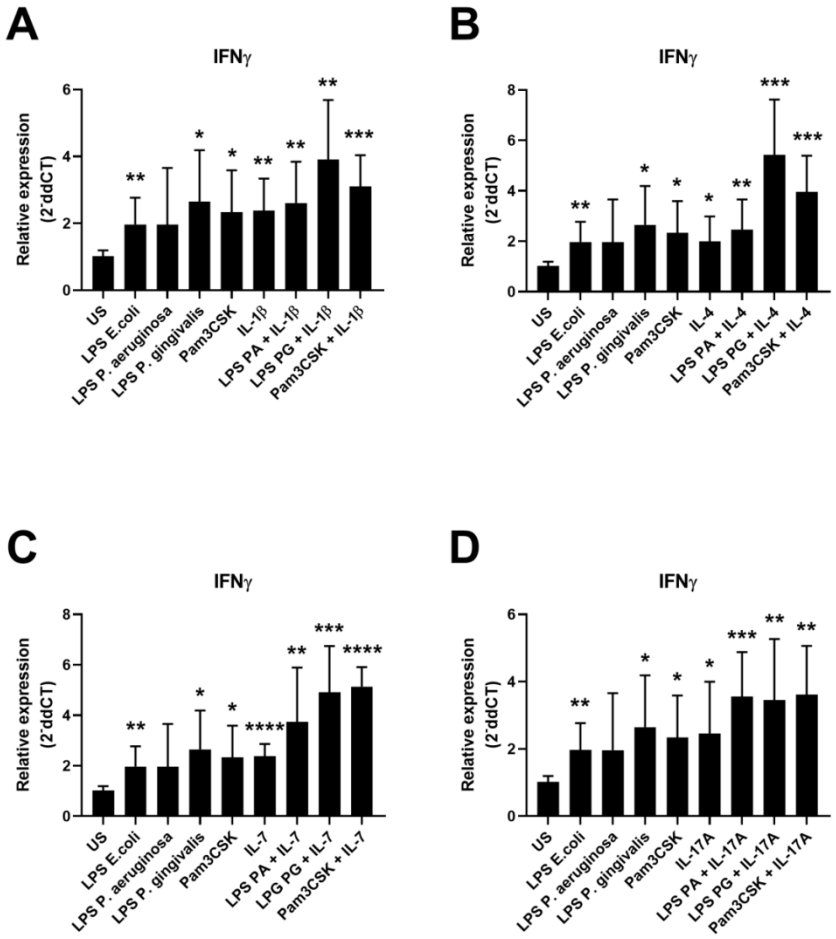


Figure 5. IFNγ Expression following cytokine and microbial component stimulations for 24 hours. Upon stimulation with the bacterial components; *E. coli* derived LPS (*P*<0.01), *P. gingivalis* derived LPS (*P*<0.05) and the TLR2 agonist Pam3CSK (*P*<0.05) there were statistically significant increases in IFNγ expression levels when compared to unstimulated cells (A-D). (A) IL-1β (*P*<0.005) stimulation alone increased IFNγ expression levels as did a combination of LPS PA+IL-1β (*P*<0.005), LPS PG+IL-1β (*P*<0.005) and Pam3CSK+IL-1β (*P*<0.0005). (B) Cells stimulated with IL-4 alone (*P*<0.05) and in combination, LPS PA+IL-4 (*P*<0.01) LPS PG+IL-4 (*P*<0.0005) and Pam3CSK+IL-4 (*P*<0.0005) showed significant IFNγ expression. (C) Cells stimulated with IL-7 (*P*<0.0001), LPS PA+IL-7 (*P*<0.01), LPS PG+IL-7 (*P*<0.0005) and Pam3CSK+IL-7 (*P*<0.0001) all displayed significant IFNγ expression. (D) IL-17A (*P*<0.05), LPS PA+IL-17A (*P*<0.0005), LPS PG+IL-17A (*P*<0.005) and Pam3CSK+IL-17A (*P*<0.005) stimulated Beas-2 cells displayed significant IFNγ expression. n=3.

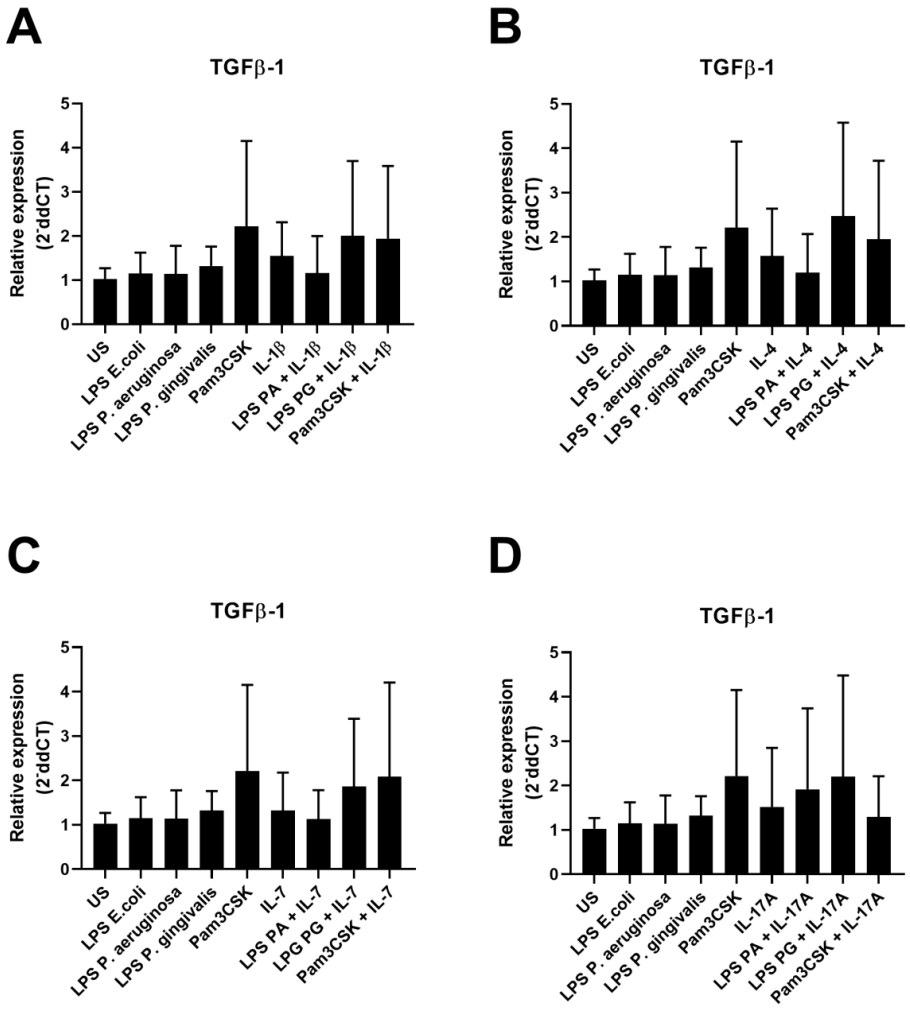


Figure 6. TGFβ-1 mRNA Expression following cytokine and microbial combonent stimulations for 24 hours. When the stimulated Beas-2B airway epithelial cells were analysed for TGFβ-1 expression no significance was found in comparison to the unstimulated Beas-2B cells using an unpaired t-test with Welch's correction as the SD between stimulations was not equal (A-D). n=3

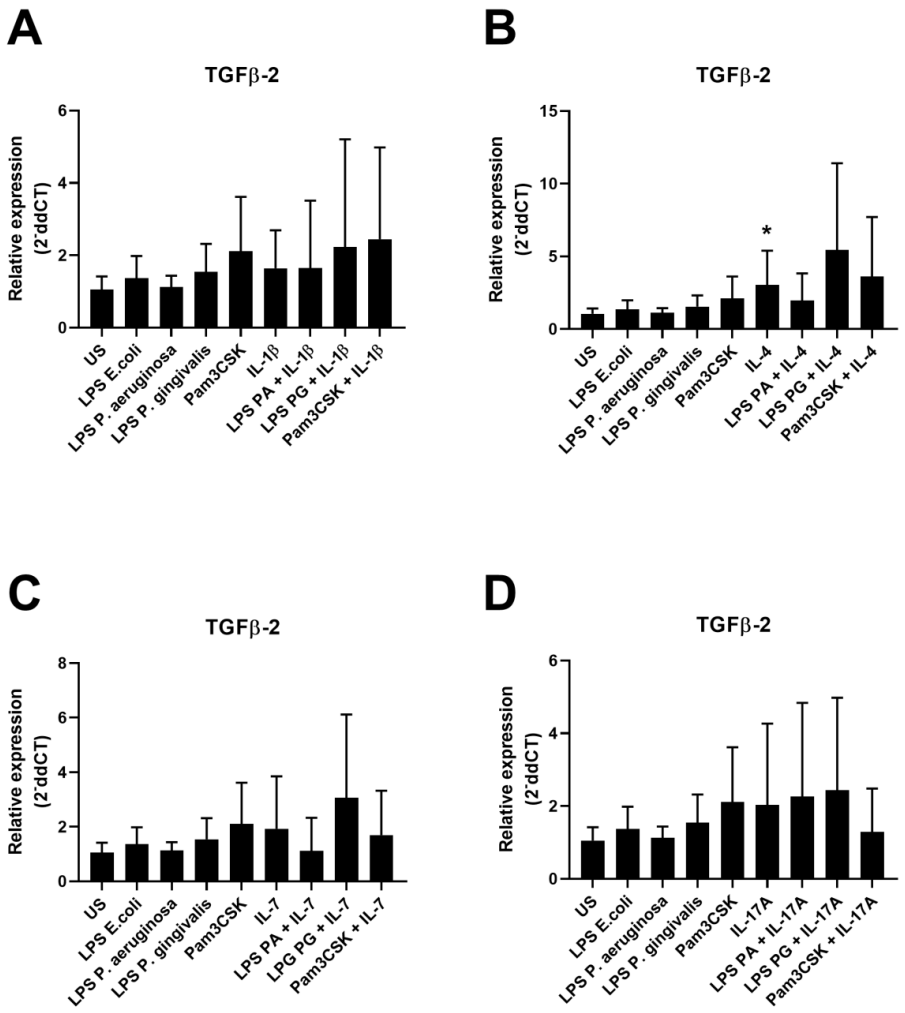


Figure 7. TGFβ-2 mRNA Expression following cytokine and microbial component stimulations for 24 hours. It was found that upon stimulation of the Beas-2B cells with the various microbial components and cytokines only the cytokine IL-4 had a statistically significant increase in TGFβ-2 ($P<0.05$) expression (B). n=3.

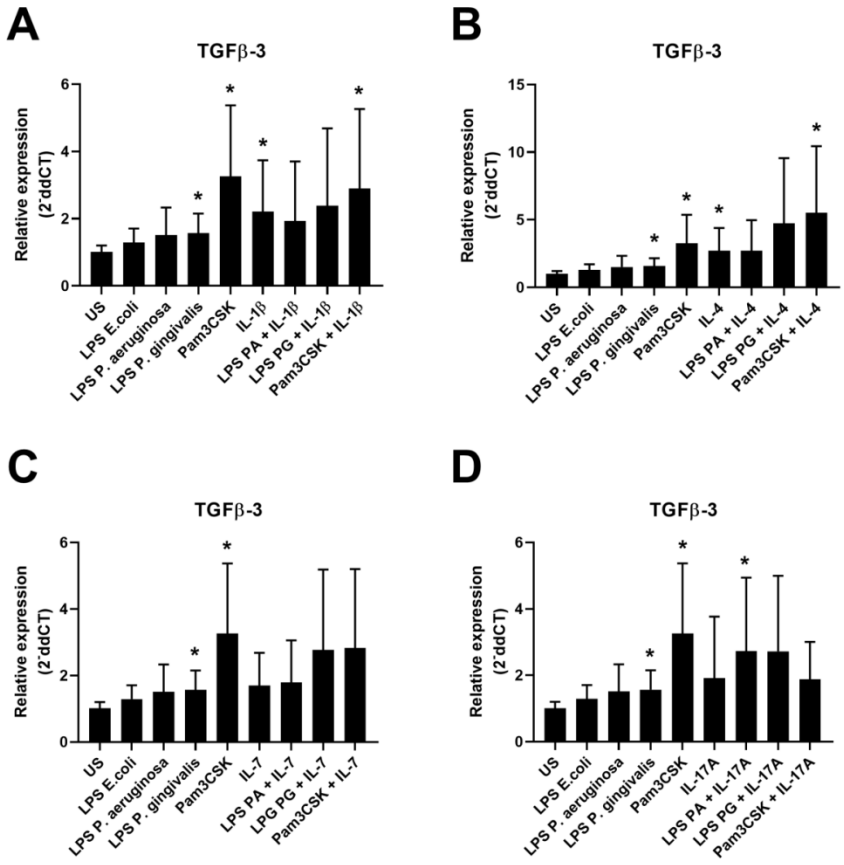


Figure 8. TFGβ-3 mRNA Expression following cytokine and microbial component stimulations for 24 hours. Overall Beas-2B cells stimulated with the TLR4 agonist *P. gingivalis* LPS (P<0.05) and the TLR2 agonist Pam3CSK (P<0.05) resulted in a statistically significant expression level of TGFβ-3 when compared to expression level of TGFβ-3 produced by the unstimulated Beas-2B cells. (A) Cells stimulated with IL-1β (P<0.05) resulted in a statistically significant level of TGFβ-3. While IL-1β when combined with *P. aeruginosa* LPS or with *P. gingivalis* LPS did not result in a statistically significant expression level of TGFβ-3 cells stimulated with Pam3CSK+IL-1β did result in the significant expression of TGFβ-3 (P<0.05). (B) The same was seen for cells stimulated with IL-4 (P<0.05) and Pam3CSK+IL-4 (P<0.05). (C) Cells stimulated with IL-7 alone or in combination did not produce significant TGFβ-3 expression.(D) Cells stimulated with IL-17A alone did not result in statistically significant TGFβ-3 expression however when combined with *P. aeruginosa* LPS it was observed that statistically significant expression levels of TGFβ-3 was produced (P<0.05).n=3.

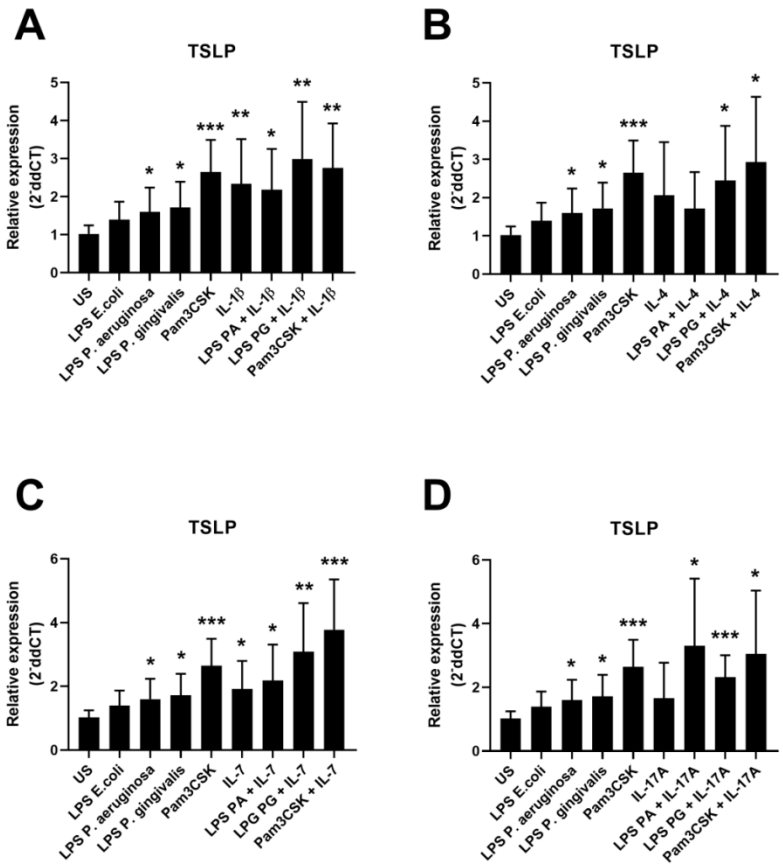


Figure 9. TSLP mRNA Expression following cytokine and microbial component stimulations for 24 hours. *E. coli* LPS (TLR4 agonist) did not produce a statistically significant relative expression of the cytokine TSLP when compared to unstimulated Beas-2B cells. However cells stimulated with *P. aeruginosa* LPS (*P*<0.05) or *P. gingivalis* LPS (*P*<0.05) (TLR4 agonists) or Pam3CSK (*P*<0.0005) (TLR2 agonist) did produce a significant TSLP response (A-D). (A) IL-1β alone (*P*<0.01) or in combination; LPS PA+IL-1β (*P*<0.05), LPS PG+IL-1β (*P*<0.005) and Pam3CSK+IL-1β (*P*<0.005) displayed statistically significant TSLP expression. (B) While cells stimulated with IL-4 and LPS PA+IL-4 did not display significant TSLP expression, cells stimulated with LPS PG+IL-4 (*P*<0.05) and Pam3CSK+IL-4 (*P*<0.05) did display significant TSLP expression. (C) Cells stimulated with IL-7 alone (*P*<0.05), or in combination with LPS PA+IL-7 (*P*<0.05), LPS PG+IL-7 (*P*<0.005) or Pam3CSK+IL-7 (*P*<0.001) had significant TSLP expression. (D) Cells stimulated with IL-17A alone was not significant however when combined; LPS PA+IL-17A (*P*<0.05), LPS PG+IL-17A (*P*<0.0005), Pam3CSK+IL-17A (*P*<0.05) significance in TLSP expression was observed. n=3.

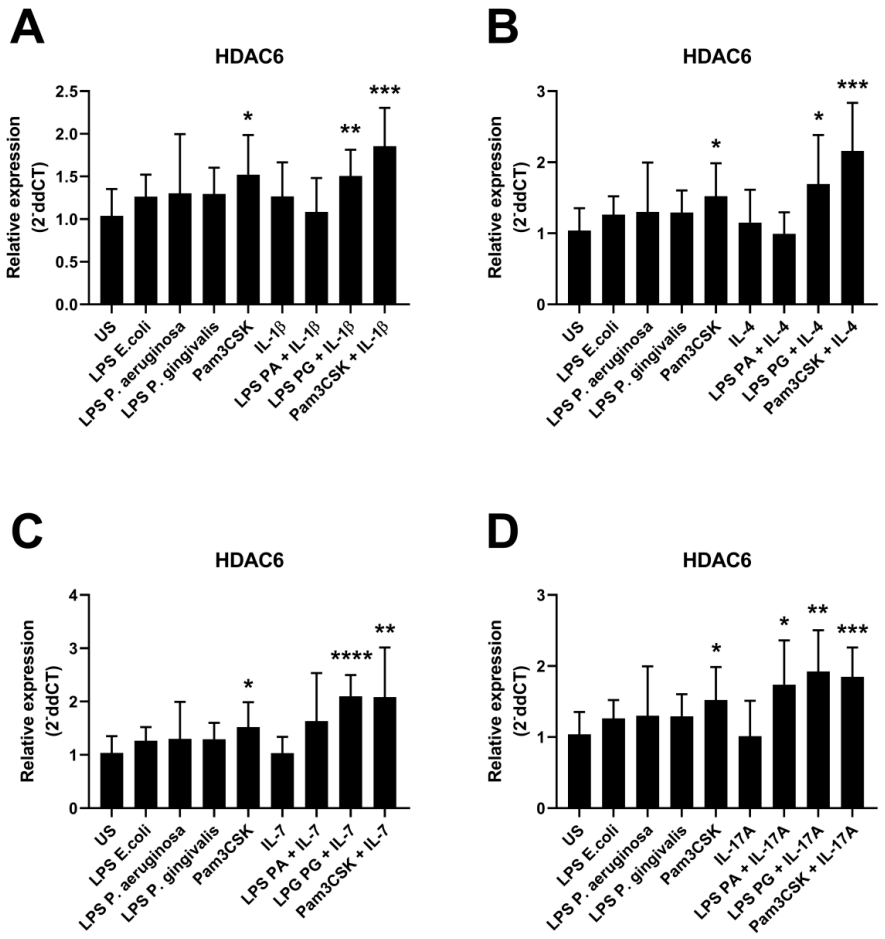


Figure 10 HDAC6 mRNA Expression following cytokine and microbial component stimulations for 24 hours. Pam3CSK alone was seen to produce a statistically significant rise in HDAC6 expression (*P*<0.05) (A-D). While cells stimulated with IL-1β alone did not result in a significant change in HDAC6 expression combinations of LPS PG+IL-1β (*P*<0.01) and Pam3CSK+IL-1β (*P*<0.001) resulted in a significance in HDAC6 expression (A). A similar observation was seen with cells stimulated with IL-4 alone resulted in no statistical significant change however cells stimulated with LPS PG+IL-4 (*P*<0.05) and Pam3CSK+IL-4 (*P*<0.001) resulted in significance (B). This was also observed in IL-7 stimulations where LPS PG+IL-7 (*P*<0.0001) and Pam3CSK+IL-7 (*P*<0.01) resulted in a significant change in HDAC6 expression (C). Stimulation with IL-17A alone did not result in a statistically significant change in HDAC6 expression however combinations of LPS PA+IL-17A (*P*<0.05), LPS PG+IL-17A (*P*<0.005) and Pam3CSK+IL-17A (*P*<0.001) resulted in significant changes in HDAC6 expression in comparison to unstimulated cells (D). n=3.

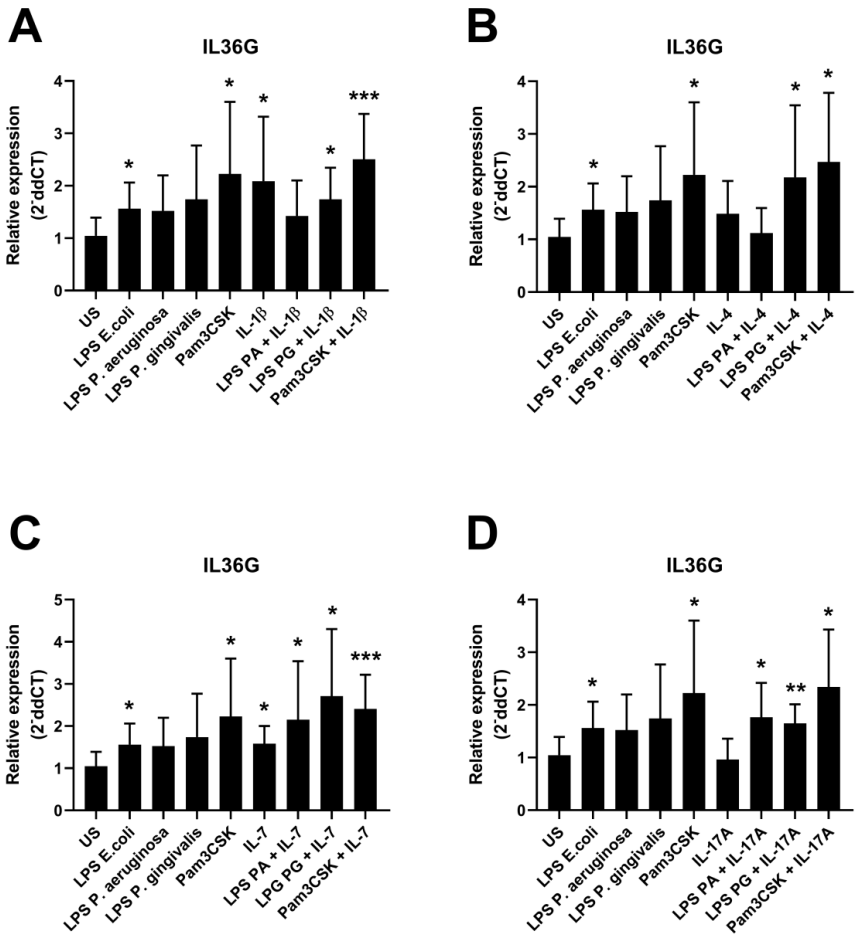


Figure 11. IL-36γ mRNA Expression following cytokine and microbial component stimulations for 24 hours. Cells stimulated with *E. coli* derived LPS produces a statistically significant change in IL-36γ expression levels ($P<0.05$) as did cells stimulated with Pam3CSK ($P<0.05$) (A-D). IL-1β stimulated cells resulted in significant IL-36γ expression ($P<0.05$) as did cells stimulated with LPS PG+IL-1β ($P<0.05$) and Pam3CSK+IL-1β ($P<0.001$) (A). Cells stimulated with IL-4 alone or LPS PA+IL-4 did not result in a significant IL-36γ response, however cells stimulated with LPS PG+IL-4 ($P<0.05$) and Pam3CSK+IL-4 ($P<0.05$) did result in significant IL-36γ expression (B). Cells stimulated with IL-7 ($P<0.05$), LPS PA+IL-7 ($P<0.05$), LPS PG+IL-7 ($P<0.05$) and Pam3CSK+IL-7 ($P<0.001$) resulted in significant IL-36γ expression (C). Cells stimulated with IL-17A alone produced no significant response however combinations of LPS PA+IL17A ($P<0.05$), LPS PG+IL17A ($P<0.005$) and Pam3CSK+IL-17A ($P<0.05$) resulted in significant IL-36γ expression (D). n=3.

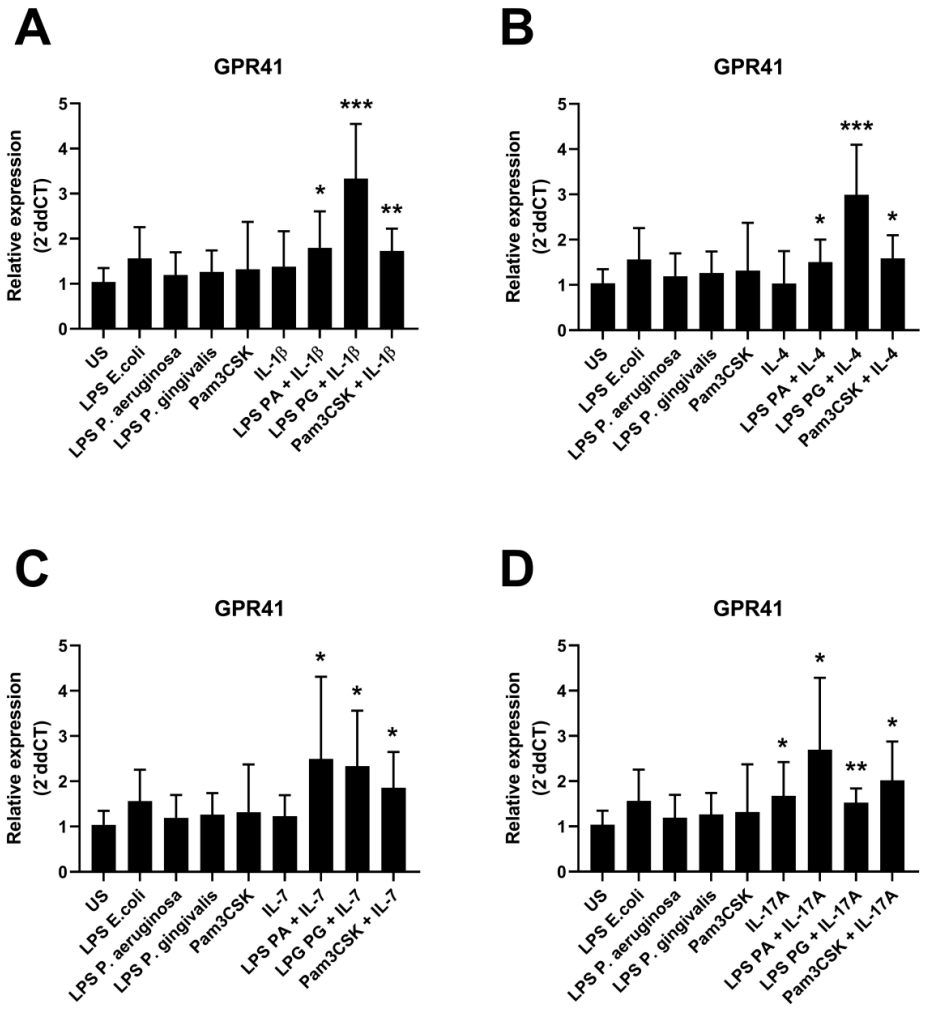


Figure 12. GPR41 mRNA Expression following cytokine and microbial stimulations for 24 hours. (A) Cells stimulated with microbial components or IL-1β alone did not produce a significant GPR41 response, however stimulations with LPS PA+IL-1β (*P*<0.05), LPS PG+IL-1β (*P*<0.0005) and Pam3CSK+IL1β (*P*<0.005) were significant. (B) Similar observations were seen with respect to IL-4 where LPS PA+IL-4 (*P*<0.05), LPS PG+IL-4 (*P*<0.001) and Pam3CSK+IL-4 (*P*<0.05) resulted in significant GPR41 expression while IL-4 alone did not result in a significant response. (C) Cells stimulated with microbial components or IL-7 alone did not result in a significant change in GPR41 expression, however cells stimulated with LPS PA+IL-7 (*P*<0.05), LPS PG+IL-7 (*P*<0.05) and Pam3CSK+IL-7 (*P*<0.05) resulted in significant GPR41 expression. (D) IL-17A (*P*<0.05), LPS PA+IL17A (*P*<0.05), LPS PG+IL-17A (*P*<0.005) and Pam3CSK+IL-17A (*P*<0.05) resulted in a statistically significant GPR41 expression. n=3.

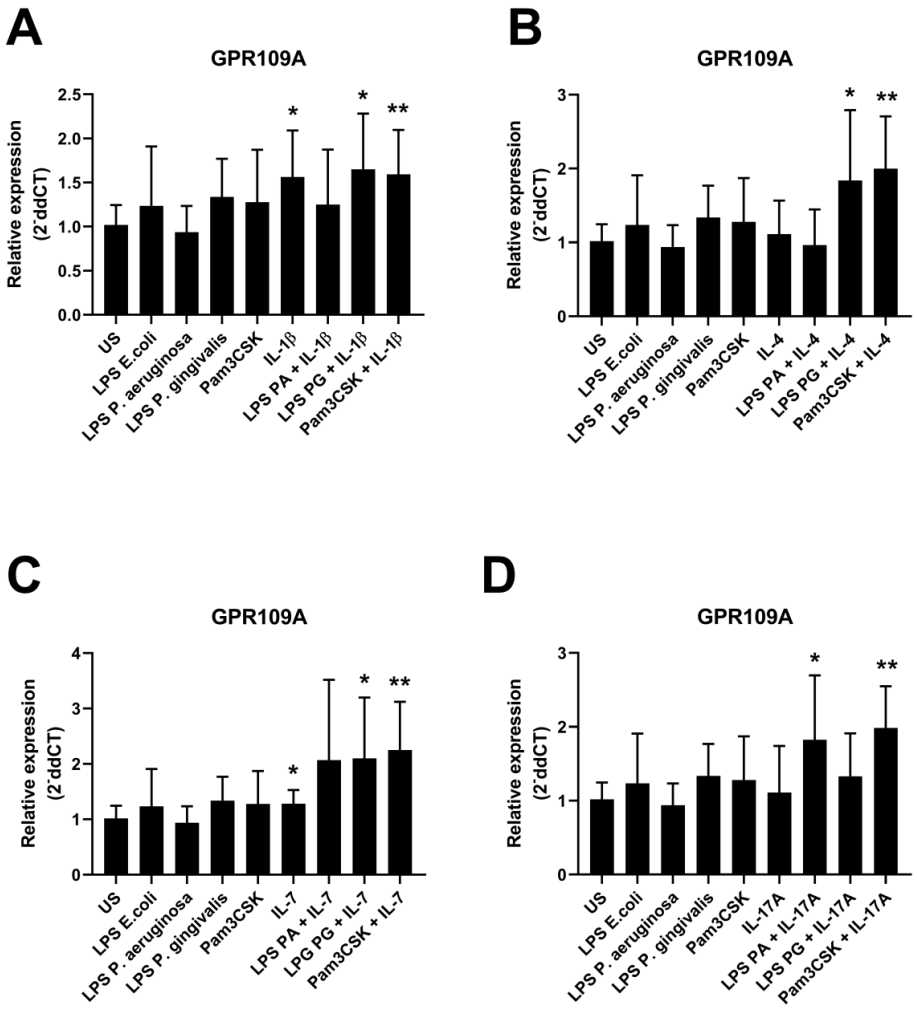


Figure 13. GPR109A mRNA Expression following cytokine and microbial component stimulations for 24 hours. It was observed at that stimulation with microbial components alone did not result in significant GPR109A expression (A-D). (A) Stimulation with IL-1β (*P*<0.05), LPS PG+IL-1β (*P*<0.05) and Pam3CSK+IL-1β (*P*<0.01) resulted in significant GPR109A expression. (B) Stimulation with IL-4 or LPS PA+IL-4 did not result in significant expression of GPR109A however stimulation with LPS PG+IL-4 (*P*<0.05) and Pam3CSK+IL-4 (*P*<0.005) resulted in significant GPR109A expression. (C) Stimulation with IL-7 (*P*<0.05), LPS PG+IL-7 (*P*<0.05) and Pam3CSK+IL-7 (*P*<0.005) resulted in significant expression of GPR109A. (D) Stimulation with LPS PA+IL-17A (*P*<0.05) and Pam3CSK+IL-17A (*P*<0.005) resulted in significant GPR109A expression. n=3.

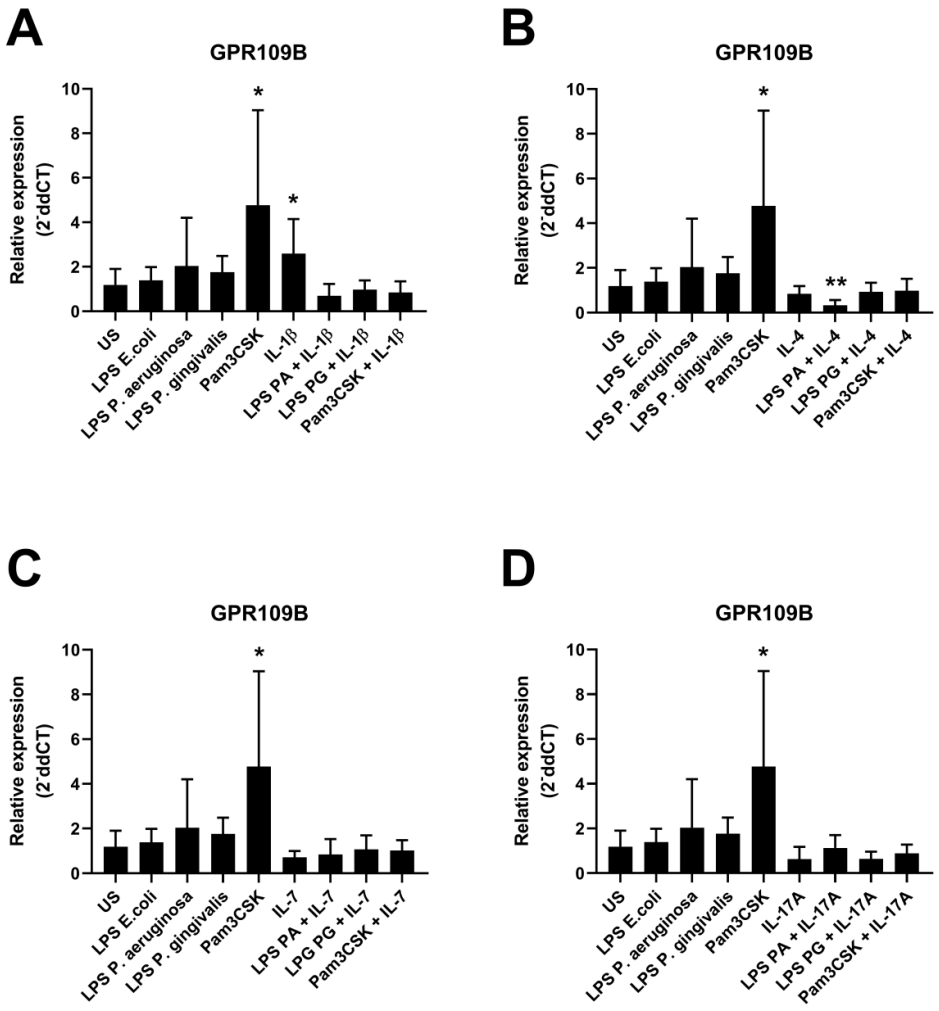


Figure 14. GPR109B mRNA Expression following cytokine and microbial component stimulations for 24 hours. Pam3CSK (*P*<0.05) stimulated cells resulted in an upregulated expression in GPR109B (A-D). (A) Cells stimulated with IL-1β alone resulted in significant GPR109B expression (*P*<0.05) however when combined with the various microbial combinations no significant expression was observed. (B) When cells were stimulated with a combination of LPS PA+ IL-4 GPR109B expression was seen to significantly down regulate (*P*<0.01). (C) Cells stimulated with IL-7 alone or in combination with various microbial components produced no significant response. (D) Similar findings were observed in cells stimulated with IL-17A alone or in combination with microbial components. n=3.

4.2. Analysis of microbial compounds and metabolite stimulations

qRT-PCR analyses of the *in vitro* gene expression in Beas-2B; immortalized human bronchial epithelial cells, using an unstimulated control and the stimulants *Escherichia coli* LPS (TLR4 agonist), *Pseudomonas aeruginosa* (PA) LPS (TLR4 agonist), *Porphyromonas gingivalis* (PG) LPS (TLR4 agonist), Pam3CSK4 (TLR2 agonist), Indole Acetic Acid (IAA), *Pseudomonas aeruginosa* (PA) LPS and Indole Acetic Acid (IAA), *Porphyromonas gingivalis* (PG) LPS and Indole Acetic Acid (IAA), Pam3CSK4 and Indole Acetic Acid (IAA), Sodium Acetate (SA), *Pseudomonas aeruginosa* (PA) LPS and Sodium Acetate (SA), *Porphyromonas gingivalis* (PG) LPS and Sodium Acetate (SA) and Pam3CSK and Sodium Acetate (SA) took place in order to investigate if the stimulants alone or in combination induced a significant immune response. All cell stimulation conditions were examined, n=3, per stimulation experiment and all experiments were carried out in triplicate.

IL-6, CXCL8, CCL20, EGR1, IFN-γ, TGFβ-1, TGFβ-2, TGFβ-3, TSLP, HDAC-6, IL-36γ, GPR41, GPR109A and GPR109B expression levels were analysed using relative expression (2^{-}ddCT) analysis with Microsoft Excel software and statistical significance was calculated and graphs were generated using GraphPad Prism 8 software. See Figure 15 – Figure 28 for graphical representation of results. Values are expressed as mean ± SD, n=3, with the asterisk indicative of the level of significance. All cell stimulation conditions were examined, n=3, per stimulation experiment and all experiments were carried out in triplicate.

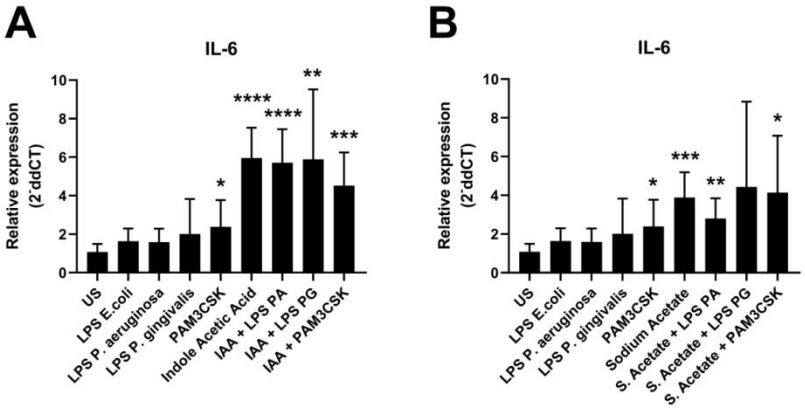


Figure 15. IL-6 mRNA Expression following microbial and metabolite stimulations (24 hours). (A-B) Cells stimulated with *Escherichia coli* derived LPS, *Pseudomonas aeruginosa* (PA) derived LPS and *Porphyromonas gingivalis* (PG) derived LPS did not result in a significant change in IL-6 expression however cells stimulated with Pam3CSK resulted in a significant increase in IL-6 expression (*P*<0.005). (A) Indole Acetic Acid (IAA) alone resulted in a significant increase in IL-6 expression (*P*<0.0001) as did combinations of IAA+LPS PA (*P*<0.0001), IAA+LPS PG (*P*<0.005) and IAA+Pam3CSK (*P*<0.0005). (B) Sodium acetate (SA) stimulated cells resulted in an increased IL-6 expression (*P*<0.0001) as did cells stimulated with SA+LPS PA (*P*<0.005) and SA+Pam3CSK (*P*<0.05). n=3.

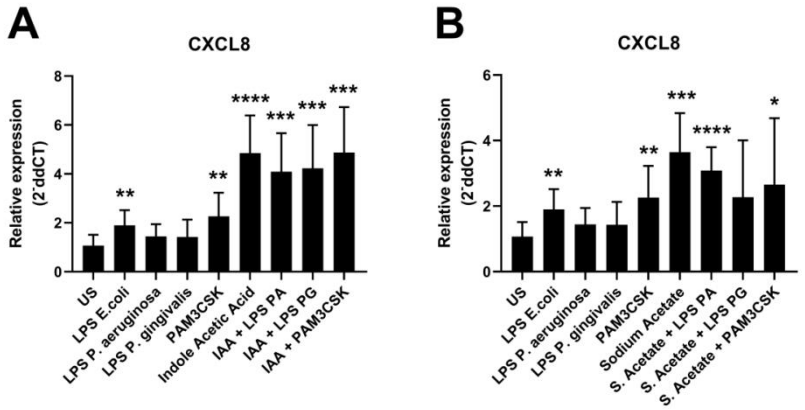


Figure 16. CXCL8 mRNA Expression following microbial and metabolite stimulations (24 hours). (A-B) Cells stimulated with *Escherichia coli* derived LPS (*P*<0.01) and Pam3CSK (*P*<0.005) resulted in an upregulation of CXCL8. (A) IAA alone (*P*<0.0001) and in combination with LPS PA (*P*<0.0005), LPS PG (*P*<0.001) and Pam3CSK (*P*<0.0005) resulted in increased CXCL8 expression. (B) Cells stimulated with SA alone (*P*<0.0005) and in combination with LPS PA (*P*<0.0001) and Pam3CSK (*P*<0.05) resulted in an increased CXCL8 expression. n=3.

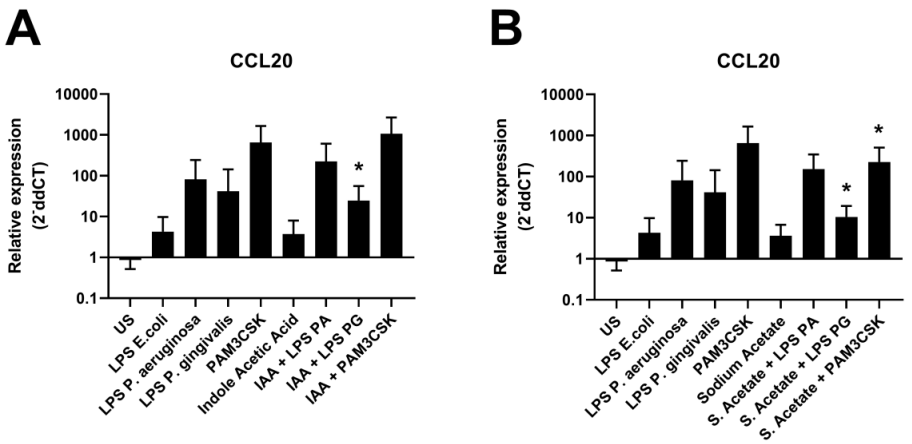


Figure 17. CCL20 mRNA Expression following microbial and metabolite stimulations (24 hours). While microbial components or metabolites alone did not elicit a CCL20 response the combination of IAA+LPS PG (*P*<0.05) (A) and SA+LPS PG (*P*<0.05) and SA+Pam3CSK (*P*<0.05) resulted in a statistically significant difference. n=3.

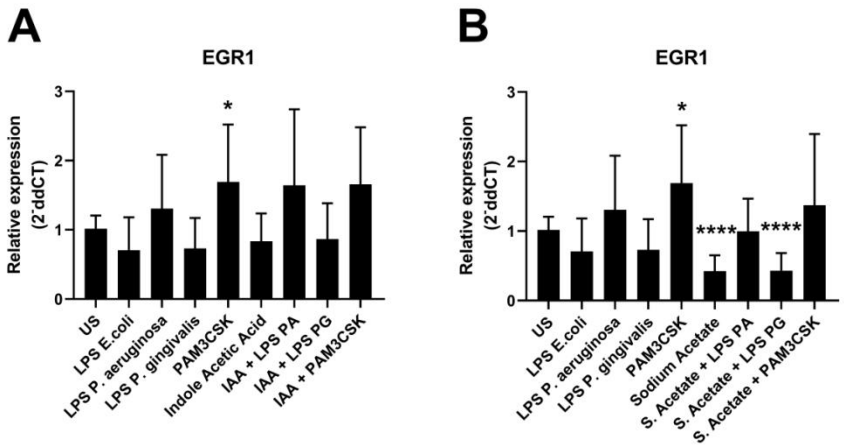


Figure 18. EGR1 mRNA Expression following microbial and metabolite stimulations (24 hours). Cells stimulated with Pam3CSK (*P*<0.05) resulted in a significant change in EGR1 expression (A-B). Indole Acetic Acid alone or in combination with microbial components did not result in a statistically significant change in EGR1 expression levels (A). Cells stimulated with Sodium Acetate resulted in a significant downregulation of EGR1 expression (*P*<0.0001) (B). Cells stimulated with a combination of Sodium Acetate and LPS PG resulted in a significant change in EGR1 expression (*P*<0.0001). n=3.

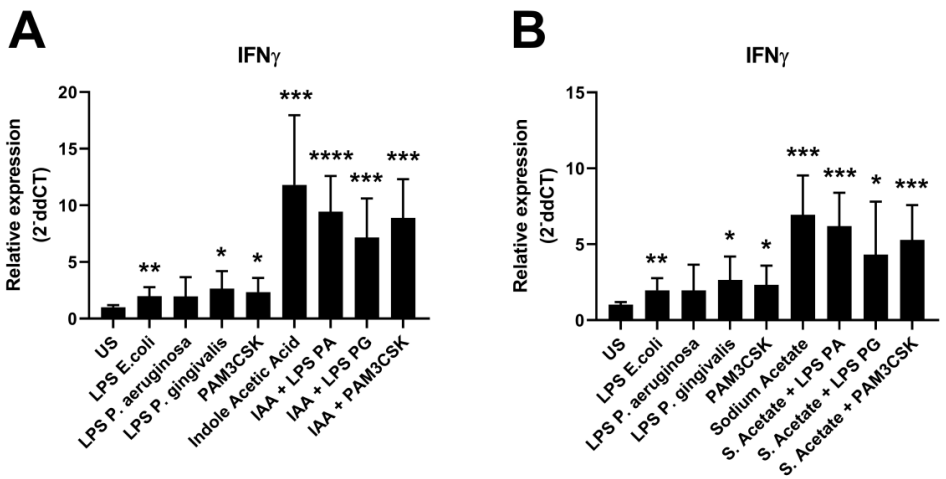


Figure 19: IFN-γ mRNA Expression following microbial and metabolite stimulations (24 hours). Cells stimulated with *E. coli* derived LPS (*P*<0.01), *P. gingivalis* derived LPS (*P*<0.05) and Pam3CSK (*P*<0.05) all resulted in a significant change in IFNγ expression. Indole Acetic Acid (IAA) (*P*<0.001), IAA+LPS PA (*P*<0.0001), IAA+LPS PG (*P*<0.001) and IAA+Pam3CSK (*P*<0.0005) resulted in significant changes to IFNγ expression (A). Sodium Acetate (SA) (*P*<0.0005), SA+LPS PA (*P*<0.0005), SA+LPS PG (*P*<0.05) and SA+Pam3CSK (*P*<0.001) resulted in significant changes to IFNγ expression (B). n=3.

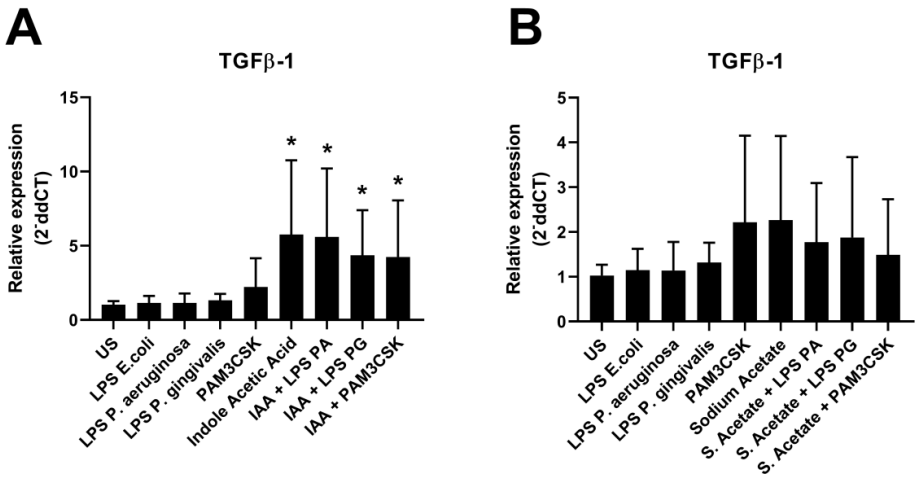


Figure 20. TGFβ-1 mRNA Expression following microbial and metabolite stimulations (24 hours). Cells stimulated with microbial components alone did not result in a significant change in TGFβ-1 expression (A-B). Indole Acetic Acid (IAA) (*P*<0.05), IAA+LPS PA (*P*<0.05), IAA+LPS PG (*P*<0.05) and IAA+Pam3CSK (*P*<0.05) all resulted in a significant change in TGFβ-1 expression (A). Sodium Acetate alone or in combination with microbial components did not result in a statistically significant change in TGFβ-1 expression. n=3.

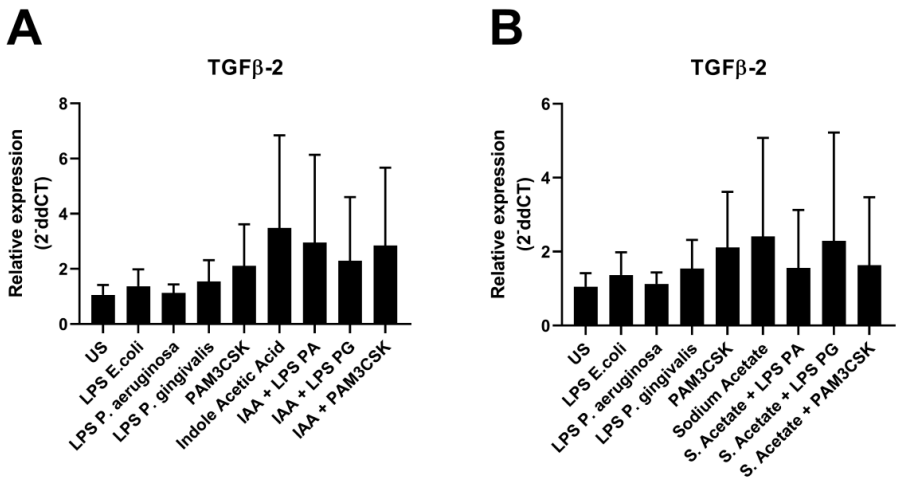


Figure 21. TGFβ-2 mRNA Expression following microbial and metabolite stimulations (24 hours). No statistically significant difference in TGFβ-2 expression was found upon stimulation with various microbial components and metabolites. n=3.

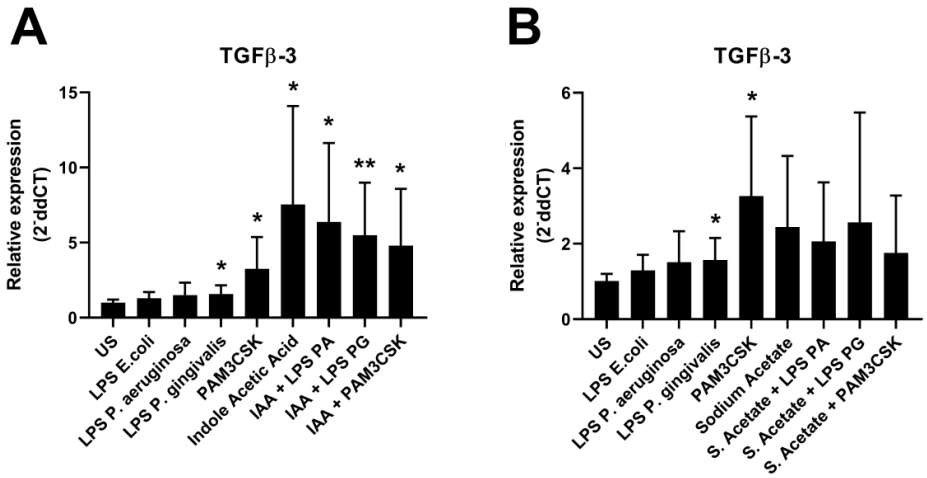


Figure 22. TGFβ-3 mRNA Expression following microbial and metabolite stimulations (24 hours). Stimulation of cells with *P. gingivalis* derived LPS (*P*<0.05) and Pam3CSK (*P*<0.05) resulted in a significant change in TGFβ-3 expression (A-B). Indole Acetic Acid (IAA) (*P*<0.05), IAA+LPS PA (*P*<0.05), IAA+LPS PG (*P*<0.005), IAA+Pam3CSK (*P*<0.05) resulted in a significant change in TGFβ-3 expression (A). Sodium Acetate alone or in combination with microbial components did not result in a significant change in expression of TGFβ-3. n=3.

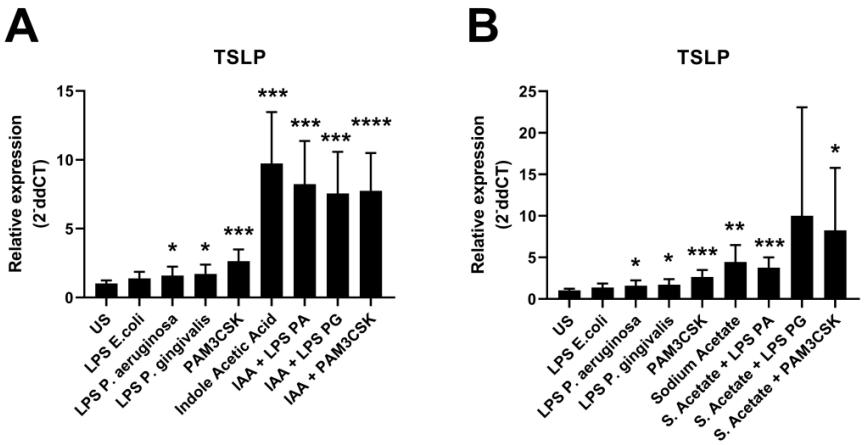


Figure 23. TSLP mRNA Expression following microbial and metabolite stimulations (24 hours). When cells were stimulated with the microbial components LPS PA (*P*<0.05), LPS PG (*P*<0.05) and Pam3CSK (*P*<0.0005) expression of TSLP significantly increased (A-B). When cells were stimulated with Indole Acetic Acid (IAA) alone (*P*<0.0005), IAA+LPS PA (*P*<0.0005), IAA+LPS PG (*P*<0.0005) and IAA+Pam3CSK (*P*<0.0001) a significant increase in TSLP expression was seen (A). When cells were stimulated with Sodium Acetate (SA) (*P*<0.005), SA+LPS PA (*P*<0.0005) and SA+Pam3CSK (*P*<0.05) a significant increase in TSLP was observed (B). n=3.

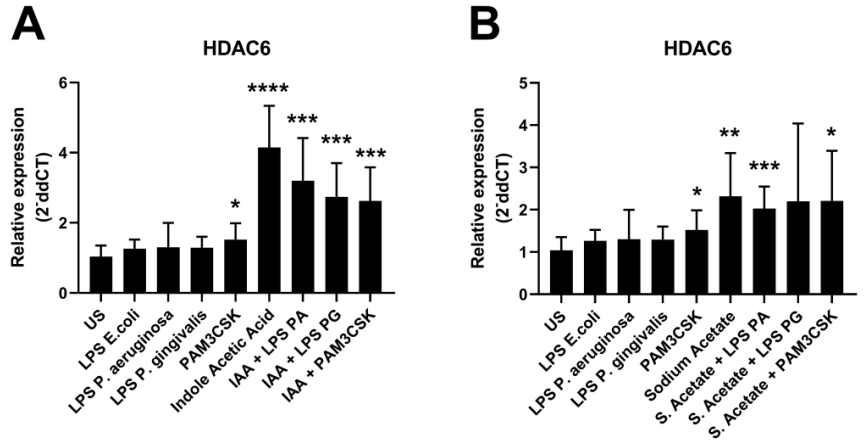


Figure 24. HDAC6 mRNA Expression following microbial and metabolite stimulations (24 hours). Cells stimulated with LPS *E. coli* LPS *P. aeruginosa* and LPS *P. gingivalis* did not result in a statistically significant change in HDAC6 expression levels, however cells stimulated with Pam3CSK resulted in a significant increase in HDAC6 expression (*P*<0.05) (A-B). Indole Acetic Acid (IAA) alone (*P*<0.0001) or in combinations of IAA+LPS PA (*P*<0.001), IAA+LPS PG (*P*<0.001) or IAA+Pam3CSK (*P*<0.001) resulted in a significant increase in HDAC6 expression (A). Sodium Acetate (SA) alone (*P*<0.01), or in combinations of SA+LPS PA (*P*<0.001) or SA+Pam3CSK (*P*<0.05) resulted in a significant increase in HDAC6 expression (B). n=3.

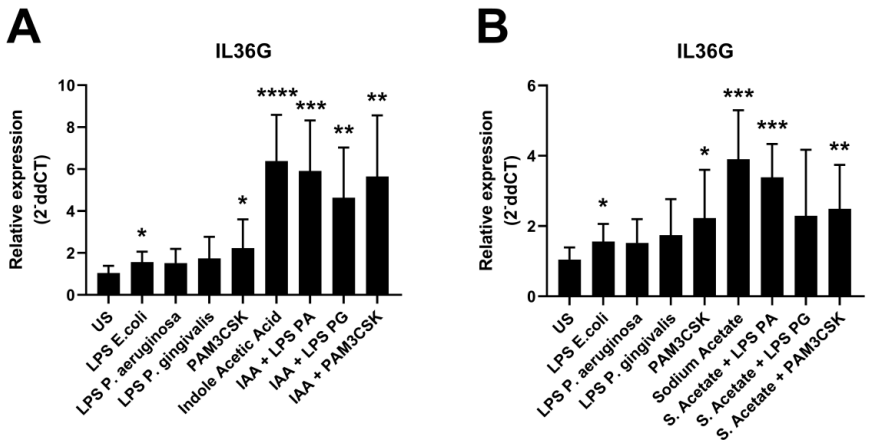


Figure 25. IL-36γ mRNA Expression following microbial and metabolite stimulations (24 hours). *E.coli* derived LPS (*P*<0.05) and Pam3CSK (*P*<0.05) resulted in significant IL-36γ expression levels (A-B). Cells stimulated with Indole Acetic Acid (IAA) (*P*<0.0001), IAA+LPS PA (*P*<0.001), IAA+LPS PG (*P*<0.005) and IAA+Pam3CSK (*P*<0.005) resulted in a significant upregulation in IL-36γ expression (A). Sodium Acetate (SA) (*P*<0.0005), SA+LPS PA (*P*<0.0005) and SA+Pam3CSK (*P*<0.01) resulted in a significant increase in IL-36γ expression (B). n=3.

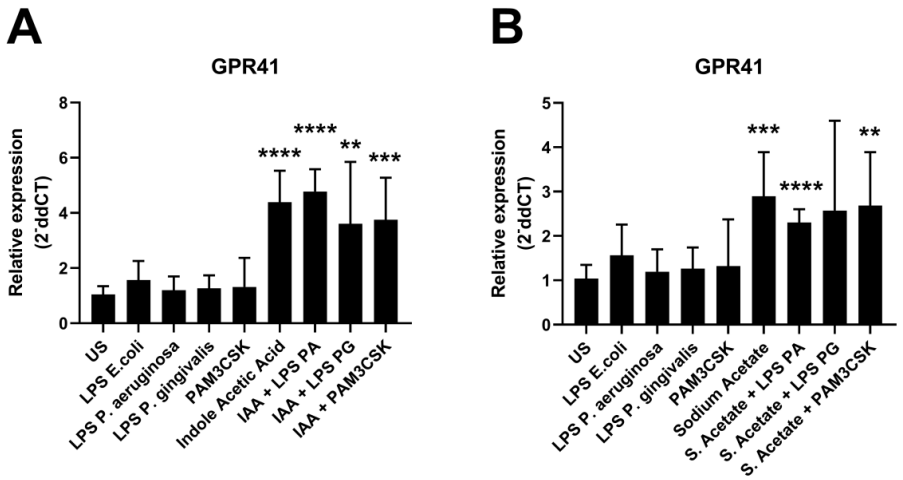


Figure 26. GPR41 mRNA Expression following microbial and metabolite stimulations (24 hours). Microbial stimulants alone did not appear to result in a significant change in GPR41 expression levels (A-B). Indole Acetic Acid (IAA) (*P*<0.0001), IAA+LPS PA (*P*<0.0001), IAA+LPS PG (*P*<0.01) and IAA+Pam3CSK (*P*<0.001) resulted in a significant increase in GPR41 expression levels (A). Sodium Acetate (SA) (*P*<0.0005), SA+LPS PA (*P*<0.0001) and SA+Pam3CSK (*P*<0.005) resulted in a significant increase in GPR41 expression (B). n=3.

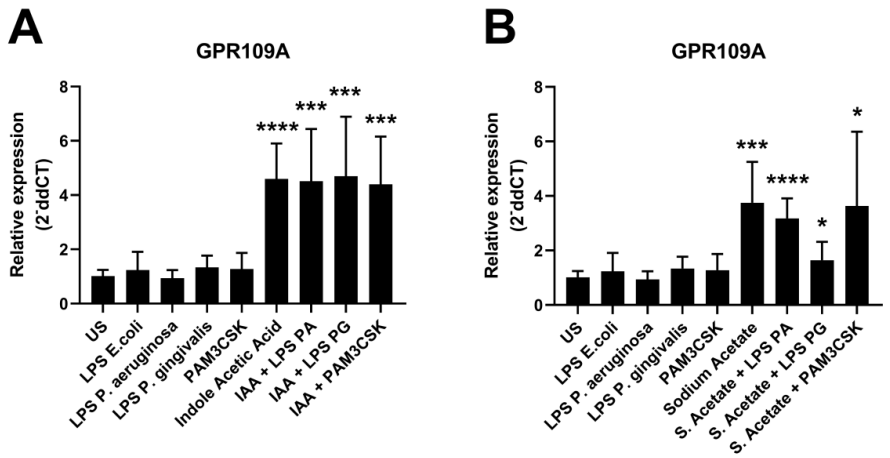


Figure 27. GPR109A mRNA Expression following microbial and metabolite stimulations (24 hours). Microbial components alone did not result in a significant change in GPR109A expression (A-B). Indole Acetic Acid (IAA) (*P*<0.0001), IAA+LPS PA (*P*<0.001), IAA+LPS PG (*P*<0.005) and IAA+Pam3CSK (*P*<0.001) resulted in significant increases in GPR109A expression (A). Sodium Acetate (SA) (*P*<0.001), SA+LPS PA (*P*<0.0001) SA+LPS PG (*P*<0.05) and SA+Pam3CSK (*P*<0.05) resulted in significant GPR109A expression (B). n=3.

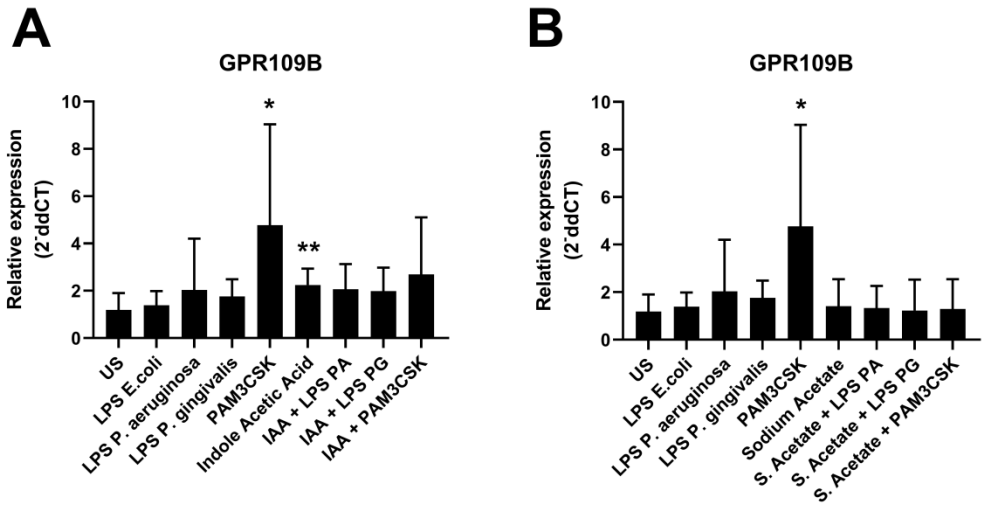


Figure 28. GPR109B mRNA Expression following microbial and metabolite stimulations (24 hours). Pam3CSK (*P*<0.05) resulted in a significant increase in GPR109B expression (A-B). Indole Acetic Acid (IAA) (*P*<0.01) alone resulted in a significant increase in GPR109B expression, however no statistically significant difference was seen when Indole Acetic Acid was used in combination with microbial components (A). No significant was found in GPR109B expression upon stimulation with Sodium Acetate (SA) alone or in combination with microbial components (B). n=3.

5. Discussion

Epithelial cell structure and function

Epithelial cells present upon airway and alveolar surfaces are the first defensive mechanism available to the host upon exposure to inhaled contaminants such as microorganisms, allergens and gases[1]. Functionally the lungs are responsible for gas exchange whereby oxygen containing inhaled air is transported to the alveoli and carbon dioxide is transported away from the alveoli while it is possible that during this process toxic compounds and potentially pathogenic microorganisms may also be transported within the inspired air[12]. The epithelial layer, comprised of epithelial cells and positioned on a basal membrane and tightly connected by intracellular junction complexes forming a barrier, is responsible for protecting the body from such inhaled contaminants[12]. The pseudostratified airway epithelium is comprised of a number of different cell types including goblet cells, ciliated cells, club cells, neuroendocrine cells and basal cells while the alveolar epithelium is comprised of two cell types, alveolar epithelial type 2 cells (AEC2) and alveolar epithelial type 1 cells (AEC1). AEC2 are responsible for surfactant formation which enables the alveoli to effectively expand and compress during ventilation and are the progenitor cells of AEC1. AEC1 cover 95% of the alveolar surface allowing for gas exchange to occur[12].

The epithelial lining fluid, which can be comprised of two layers within the large airways, contains the periciliary layer which enables the movement of cilia, and the mucus layer which enables unwanted inhaled particles to become trapped. Both the periciliary and mucus layer act to remove particles in a process called mucociliary clearance. The alveolar surface liquid contains pulmonary surfactant to protect the alveoli against inhaled particles. In addition to these fluid layers production of protective substances such as antimicrobial peptides and protein and lipid mediators also occurs[12].

While the airway epithelium is known to alter in its composition dependent on its location within the lungs it is also known to possess an altered composition within

diseased states such as asthma where it has been documented that goblet cells are noted to increase whilst ciliated cells are present in decreased amounts[13].

Epithelial cell culture models

The use of *in vitro* models are vital to gain further knowledge with regards to the interplay present at the epithelium level in diseases such as asthma[14]. When developing an *in vitro* model system there are a number of culture models currently available to investigate lung epithelial cells including primary cells, immortalised or tumour epithelial cell lines, organ on a chip models, organoids and precision cut lung slices, all of which offer valid alternative or supplementary options to animal studies[12]. When choosing a model system all options offer advantages and disadvantages. For example primary lung epithelial cells, isolated from bronchial biopsies and bronchial brushings obtained during bronchoscopy offer the ability to investigate inter donor variations and the ability to culture primary airway epithelial cells on permeable mesh supports at air liquid interface (ALI) enables the study of fully differentiated airway epithelial cells, however, it can be a prohibitively expensive means of cell growth with a limited cell lifespan and is reliant on access to fresh bronchial biopsies or bronchial brushings and primary cells can be difficult to successfully culture[12]. Cell lines such as BEAS-2B and Calu-3 are often used as asthma model systems and are an attractive alternative to primary cell culture systems. Cell lines are usually cultured in a format whereby the cell monolayers are grown on a plastic substrate and are fully submerged[14]. The cell line model therefore does not represent fully differentiated cells and as a cell line is often developed from one donor, the cell model may not be truly representative of a population[12]. However cell lines are a relatively inexpensive means of model system when compared to primary cells and they offer the ability to create a high throughput screening system[12].

It was therefore decided due to the large scale number of cell stimulation experiments to be investigated the *in vitro* model system implemented in this study would be a cell line model system. The widely used and commercially available

BEAS-2B cell line, generated by the immortalisation of human bronchial epithelial cells using the AD12-SV40 virus, was chosen as the cell line of interest[15].

Effects of microbial compounds and cytokines upon the BEAS-2B cell culture

Studies have depicted strong correlations between asthma and respiratory pathogens, viruses, bacteria and fungi[10,11]. Therefore it was decided that the effects of microbial components on BEAS-2B cells and subsequent immune signalling would be investigated. Microbial components including including LPS derived from *Escherichia coli*, *Pseudomonas aeruginosa* and *Porphyromonas gingivalis* (TLR4 agonists) and Pam3CSK4 (TLR2 agonist) were investigated alone or in combination with cytokines of interest with regards to asthma, IL-1β, IL-4, IL-7 and IL-17A. It was decided that various bacterial sources of LPS would be investigated to observe the potential effects different LPS bacterial sources, from bacteria known to be prominent within different areas of the host, may have on BEAS-2B cells alone or in combination with the cytokines IL-1β, IL-4, IL-7 and IL-17A.

The interaction between pattern recognition receptors (PRR's) and pathogen associated molecular patterns (PAMP's) result in the activation of the hosts innate and adaptive immune response[16]. Toll-like receptors (TRL's) are a class of pattern recognition receptors (PRR's) and in humans there are 10 different Toll-like receptors (TLR's) in which each different TLR recognises a specific pathogen associated molecular pattern (PAMP)[16]. In this study the lipopolysaccharide (LPS) TLR-4 agonist was examined through the use of LPS derived from *Escherichia coli*, *Pseudomonas aeruginosa* and *Porphyromonas gingivalis*. The TLR-1/2 agonist Pam3CSK, a synthetic bacterial lipoprotein, was used to study the TLR-2 response.

The pleiotropic cytokine IL-1β is capable of both pro- and anti- inflammatory effects. It is believed that IL-1β is critical in the pathobiology of asthma and has been an important player in driving the inflammatory response and subsequent changes in airway smooth muscle (ASM) responsiveness making its modulation an attractive therapeutic target[17].

The cytokine IL-4 is known to be associated with the development of allergic inflammation by driving differentiation of naïve T helper type 0 (T_H0) lymphocytes to a T helper type 2 (T_H2) response[18]. IL-4 plays a role in the induction of IgE dependent mast cell activation resulting in sudden allergic reactions[18]. The cytokine IL-4 is also capable of inducing the expression of the gene mucin which results in the hypersecretion of mucus a well-known characteristic feature of asthma[18].

Recent studies have shown that the cytokine IL-7 may play a complex role in allergic fungal asthma[19]. Published work from our group has shown that in BAL examined from 69 well characterised asthmatic patients, fungi was detectable by qPCR in 86% of patients[20].

IL-17 is recognised for its important role in the pathobiology of asthma and has been documented for the role it plays in neutrophilic inflammation and asthma severity[21]. The pro-inflammatory cytokine IL-17 is known to promote the production of cytokines and chemokines in bronchial epithelial cells[21]. IL-17 has also been implicated in airway remodelling[21]

***Pseudomonas aeruginosa* (PA)**

P. aeruginosa (PA) is a gram negative bacteria commonly encountered in the environment, which in healthy individuals is not a cause for alarm as it is cleared by the host defence system[22]. However, in susceptible individuals *P. aeruginosa* is an opportunistic pathogen and its presence in susceptible individuals can lead to chronic lung infection[22]. *P. aeruginosa* derived LPS represents a TLR4 agonist.

***Porphyromonas gingivalis* (PG)**

P. gingivalis (PG) is a gram negative, obligate anaerobic oral pathogen which is implicated in periodontal disease existing within a complex biofilm on the surface of the teeth often as a secondary colonizer of dental plaque[23]. *P. gingivalis* derived LPS represent a TLR4 agonist ligand derived from the host oral environment.

Effects of the TLR-4 LPS agonist *P. aeruginosa* and *P. gingivalis* alone or in combination with the cytokines IL-1β, IL-4, IL-7 and IL-17A

BEAS-2B cells stimulated with *Pseudomonas aeruginosa* alone did not result in a significant change in IL-6 expression, however cells stimulated with a combination of *P. aeruginosa* (PA) LPS + IL-1β (P<0.01), a combination of LPS PA + IL-4 (P<0.05), a combination of LPS PA + IL-7 (P<0.05), and a combination of LPS PA + IL-17A (P<0.05) had a significant increase in IL-6 compared to US cells, n=3 (See Figure 1). The cytokine IL-6 was not significantly expressed upon stimulation with *Porphyromonas gingivalis* LPS alone, however, the combinations of *P. gingivalis* LPS + IL-4 (P <0.05), *P. gingivalis* LPS + IL-7 (P<0.005) and *P. gingivalis* LPS + IL-17A (P<0.005) did result in significant IL-6 expression levels (See Figure 1). IL-6 is a pleotrophic cytokine with the ability to act in an anti-inflammatory and pro-inflammatory manner. It is recognised that IL-6 is produced in response to the recognition of microbes by pattern associated molecular patterns[24]. It was interesting to note that *P. aeruginosa* or *P. gingivalis* only in combination with other cytokines resulted in an upregulation of the IL-6 cytokine. IL-6 is produced in response to infections and tissue injuries and in a host defence contributor whereby its expression triggers an alarm signal, activating the host defence mechanisms[25].

CXCL8 (IL-8) expression was not significantly affected by *Pseudomonas aeruginosa* LPS stimulation alone or in combination with IL-1β, IL-4 or IL-7, however a combination of *P. aeruginosa* LPS + IL-17A (P<0.05) did result in a significant change in CXCL8 expression (See Figure 2). Studies have shown that IL-17 activation can result in elevated levels of CXCL8 in bronchial epithelial cells[21]. CXCL8 was not significantly expressed upon stimulation with *P. gingivalis* LPS alone or in combination with IL-17A however the combination of *P. gingivalis* LPS + IL-1β (P<0.01) and *P. gingivalis* LPS + IL-7 (P<0.05) did result in significant expression of CXCL8 (See Figure 2).

EGR1 was not significantly expressed upon *P. aeruginosa* LPS stimulation or upon combination with IL-4, IL-7 or IL-17 however, *P. aeruginosa* LPS + IL-1β (P<0.05) did

result in a significant increase in EGR1 expression (See Figure 4). EGR1 was significantly expressed upon stimulation with *P. gingivalis* LPS + IL-1β (P<0.05) and *P. gingivalis* LPS + IL-17A (P<0.05) (See Figure 4). Recent studies involving *P. aeruginosa* infection in a mouse model of acute bacterial pneumoniae showed that EGR1 deficient mice had a decreased mortality rate and reduced pro-inflammatory cytokine levels including IL-1β cytokine levels. The findings of this study suggested that EGR1 may play a detrimental role in the ability of a host to defend against *P. aeruginosa* lung infection with a mouse model system[26]

IFN-γ is known to play a role in recognising and eliminating pathogen challenge in the host[27]. IFN-γ expression was not significantly altered upon stimulation with *P. aeruginosa* LPS alone, however when stimulated with a combination of *P. aeruginosa* LPS + IL-1β (P<0.005), *P. aeruginosa* LPS + IL-4 (P<0.01), *P. aeruginosa* LPS + IL-7 (P<0.005) and *P. aeruginosa* LPS + IL-17A (P<0.0005) significance in IFN-γ expression was observed. (See Figure 5) IFN-γ was significantly expressed upon cell stimulation with *P. gingivalis* LPS alone (P<0.05) and in combination of *P. gingivalis* LPS + IL-1β (P<0.005), *P. gingivalis* LPS + IL-4 (P<0.0005), *P. gingivalis* LPS + IL-7 (P<0.0005) and *P. gingivalis* LPS + IL-17A (P<0.005) (See Figure 5).

While BEAS-2B cells stimulated with *P. aeruginosa* LPS alone or in combination did not result in a significant TGFβ-1 or TGFβ-2 response *P. aeruginosa* + IL-17A resulted in a significant TGFβ-3 response (P<0.05) (See Figure 8). TGFβ-3 was significantly expressed upon *P. gingivalis* LPS (P<0.05) stimulation however when cells were stimulated with *P. gingivalis* LPS combined with IL-1β, IL-4, IL-7 or IL-17A no significance was observed (See Figure 8). Transforming growth factor (TGF)-β upregulation has been noted in many of the major pulmonary diseases including asthma where it plays a role in the response of the immune system and airway remodelling[28].

The cytokine thymic stromal lymphopoietin (TSLP) is a pleiotrophic cytokine believed to be involved in the pathogenesis of asthma[29]. TSLP expression was significant upon stimulation with *P. aeruginosa* LPS alone (P<0.05) and in combinations of *P. aeruginosa* LPS + IL-1β (P<0.05), *P. aeruginosa* LPS + IL-7

(*P*<0.05) and *P. aeruginosa* LPS + IL-17A (*P*<0.05) (See Figure 9). TSLP was significantly expressed upon *P. gingivalis* LPS (*P*<0.05) stimulation and also upon stimulation with *P. gingivalis* LPS + IL-1β (*P*<0.005), *P. gingivalis* LPS + IL-4 (*P*<0.05), *P. gingivalis* LPS + IL-7 (*P*<0.005) and *P. gingivalis* LPS + IL-17A (*P*<0.0005) (See Figure 9).

While HDAC6 expression was not altered significantly upon the cells exposure to *P. aeruginosa* alone or in combination with the cytokines IL-1β, IL-4 or IL-7, cells stimulated with *P. aeruginosa* LPS + IL-17A resulted in a significant change in HDAC6 expression (*P*<0.05) (See Figure 10). HDAC6 was not significantly expressed upon stimulation with *P. gingivalis* LPS alone, however, when stimulated with *P. gingivalis* LPS + IL-1β (*P*<0.01), *P. gingivalis* LPS + IL-4 (*P*<0.05), *P. gingivalis* LPS + IL-7 (*P*<0.0001) and *P. gingivalis* LPS + IL-17A (*P*<0.005) HDAC6 was significantly expressed (See Figure 10). A recent animal study using a mouse model revealed that HDAC6 deletion or inhibition of the HDAC6 deacetylase activity promotes the expression of IL-17 in γδ T cells[30].

The cytokine IL-36γ was significantly expressed upon stimulation of the BEAS-2 cells with *P. aeruginosa* LPS + IL-7 (*P*<0.05) and *P. aeruginosa* LPS + IL-17A (*P*<0.05) (See Figure 11). IL-36γ was not significantly expressed upon *P. gingivalis* LPS alone, however, when stimulated with *P. gingivalis* LPS + IL-1β (0.05), *P. gingivalis* LPS + IL-4 (*P*<0.05), *P. gingivalis* LPS + IL-7 (*P*<0.05) and *P. gingivalis* LPS + IL-17A (*P*<0.005) IL-36γ was significantly expressed (See Figure 11). The pro-inflammatory cytokine IL-36γ has been seen to be produced by lung epithelial cells in response to inflammatory stimuli in various models of asthma[31].

It is believed that fermentable fibre leading to short chain fatty acids can alter the microbial composition of both the lungs and gastrointestinal tract and infer protection against allergic inflammation in the lung[32]. While GPR41, GPR109A and GPR109B were studied with respect to metabolites and microbes it was decided that the microbial and cytokine cell stimulations would also undergo qRT-PCR examination for the relative expression of these G protein-coupled receptors. GPR41 expression has become of interest with respect to dietary fibres and the

production of short chain fatty acids (SCFA's) such as sodium acetate by bacteria in the gastrointestinal tract. SCFA's may activate the G protein-coupled receptor 41, which is believed to create an anti-inflammatory effect[33]. While GPR41 expression was not significantly altered upon cells exposure to *P. aeruginosa* LPS alone, when combinations of *P. aeruginosa* LPS + IL-1β ($P<0.05$), *P. aeruginosa* LPS + IL-4 ($P<0.05$), *P. aeruginosa* LPS + IL-7 ($P<0.05$) and *P. aeruginosa* LPS + IL-17A ($P<0.05$) were used to stimulate the BEAS-2B cells significance in GPR41 expression was observed (See Figure 12). GPR41 was not significantly expressed upon *P. gingivalis* LPS alone, however, when stimulated with *P. gingivalis* LPS + IL-1β (0.0005), *P. gingivalis* LPS + IL-4 ($P<0.001$), *P. gingivalis* LPS + IL-7 ($P<0.05$) and *P. gingivalis* LPS + IL-17A ($P<0.005$) GPR41 was significantly expressed (See Figure 12).GPR109A expression was significantly changed upon stimulation with the combination of *P. aeruginosa* LPS + IL-17A ($P<0.05$) (See Figure 13) GPR109A was not significantly expressed upon *P. gingivalis* LPS alone, however, when stimulated with *P. gingivalis* LPS + IL-1β (0.05), *P. gingivalis* LPS + IL-4 ($P<0.05$) and *P. gingivalis* LPS + IL-7 ($P<0.05$) GPR109A was significantly expressed (See Figure 13). BEAS-2B cells stimulated with a combination of LPS PA+ IL-4 resulted in a significant down regulation of GPR109B expression ($P<0.01$) (See Figure 14) but no significance was found upon stimulation with the various *P. gingivalis* combinations.

Pam3CSK

Pam3CSK is a synthetic bacterial lipoprotein and is classified as a TLR-2 ligand[34]. Toll-like receptor 2 (TLR-2) plays an important role in the recognition of gram positive bacteria, therefore Pam3CSK was implemented as a way of studying the effect a TLR-2 agonist may have on epithelial cells alone or when combined with the cytokines IL-1β, IL-4, IL-7 and IL-17A[16,34].

An interesting observation was that Pam3CSK alone in most cases was sufficient to result in a change in expression by qPCR for IL-6, CXCL8, EGR1, IFN-γ, TGFβ-3, TSLP, HDAC6, IL-36γ and GPR109B.

It is known that IL-6 levels are increased upon exposure of the pattern recognition receptors to microbial and damage associated molecular patterns[24]. Upon stimulation with Pam3CSK (P<0.05), Pam3CSK + IL-1β (P<0.01), Pam3CSK + IL-4 (P<0.0001), Pam3CSK + IL-7 (P<0.0005) and Pam3CSK + IL-17A (P<0.05) the cytokine IL-6 was significantly expressed (See Figure 1).

Pam3CSK (P<0.05) alone or the combinations of Pam3CSK + IL-1β (P<0.0005), Pam3CSK + IL-4 (P<0.005), Pam3CSK + IL-7 (P<0.01) and Pam3CSK + IL-17A (P<0.005) all resulted in a significant expression in the cytokine CXCL8 (See Figure 2).

Pam3CSK (P<0.05) alone or the combinations of Pam3CSK + IL-1β (P<0.05), Pam3CSK + IL-4 (P<0.05), Pam3CSK + IL-7 (P<0.05) and Pam3CSK + IL-17A (P<0.05) all resulted in a significant expression in EGR1 (See Figure 4).

IFN-γ was significantly expressed when the BEAS-2B cells were stimulated with Pam3CSK (P<0.05) alone or combinations of Pam3CSK + IL-1β (P<0.0005), Pam3CSK + IL-4 (P<0.0005), Pam3CSK + IL-7 (P<0.0001) and Pam3CSK + IL-17A (P<0.005) (See Figure 5).

TGFβ-3 was significantly expressed upon cell stimulation with Pam3CSK (P<0.05), Pam3CSK + IL-1β (P<0.05) or Pam3CSK + IL-4 (P<0.05) (See Figure 8).

TSLP was significantly expressed when the BEAS-2B cells were stimulated with Pam3CSK (P<0.0005) alone or combinations of Pam3CSK + IL-1β (P<0.005), Pam3CSK + IL-4 (P<0.05), Pam3CSK + IL-7 (P<0.001) and Pam3CSK + IL-17A (P<0.05) (See Figure 9).

HDAC6 was significantly expressed upon stimulation with Pam3CSK (P<0.05), Pam3CSK + IL-1β (P<0.001), Pam3CSK + IL-4 (P<0.001), Pam3CSK + IL-7 (P<0.01) and Pam3CSK + IL-17A (P<0.001) (See Figure 10).

IL-36γ was significantly expressed upon stimulation with Pam3CSK (P<0.05), Pam3CSK + IL-1β (P<0.001), Pam3CSK + IL-4 (P<0.05), Pam3CSK + IL-7 (P<0.001) and Pam3CSK + IL-17A (P<0.05) (See Figure 11).

GPR41 was not significantly expressed when cells were stimulated with Pam3CSK alone, however, Pam3CSK + IL-1β (P<0.005), Pam3CSK + IL-4 (P<0.05), Pam3CSK + IL-7 (P<0.05) and Pam3CSK + IL-17A (P<0.05) (See Figure 12) resulted in a significant GPR41 expression.

GPR109A was not significantly expressed when cells were stimulated with Pam3CSK alone, however it was significantly expressed when cells were stimulated with Pam3CSK + IL-1β (P<0.01), Pam3CSK + IL-4 (P<0.005), Pam3CSK + IL-7 (P<0.005) and Pam3CSK + IL-17A (P<0.005) (See Figure 13).

GPR109B was significantly expressed when cells were stimulated with Pam3CSK alone (P<0.05), however when Pam3CSK was combined with the cytokines IL-1β, IL-4, IL-7 and IL-17A no significant change in expression was calculated (See Figure 14).

Effects of metabolites and microbial compounds upon the BEAS-2B cell culture

Dietary, genetic, microbial and environmental factors can contribute to asthma risk[9]. Intestinal metabolites; small molecules derived from the host, microbiota or exogenous sources such as the diet; have been shown to play a part in diseases such as asthma. Clinically relevant metabolites can contribute to pathogenic changes and it has recently been shown that intestinal bacterial taxa correlate with intestinal metabolites and childhood asthma[9].

Indole Acetic Acid (IAA)

Indole Acetic Acid has been implicated in all aspects of plant growth and development, however IAA is not only associated with plants but IAA is also associated with many types of microorganisms, including bacteria and fungi. Many different bacterial species have the ability to produce the auxin phytohormone indole-3-acetic acid (IAA). While the majority of studies have focused on its role in bacteria-plant interactions studies have also revealed that IAA can be implemented by bacteria as a signalling molecule and as a microbial metabolite[35].

When cells were stimulated with Pam3CSK (*P*<0.005), the metabolite Indole Acetic Acid (IAA) (*P*<0.0001) and the combinations IAA + *P. aeruginosa* LPS (*P*<0.0001), IAA + *P. gingivalis* LPS (*P*<0.005), and IAA + Pam3CSK (*P*<0.0005) the relative expression of the cytokine IL-6 was statistically significant (See Figure 15).

Cells stimulated with Pam3CSK (*P*<0.005), the metabolite Indole Acetic Acid (IAA) (*P*<0.0001) and the combinations IAA + *P. aeruginosa* LPS (*P*<0.0005), IAA + *P. gingivalis* LPS (*P*<0.001), and IAA + Pam3CSK (*P*<0.0005) resulted in a significant CXCL8 expression (See Figure 16).

EGR1 was significantly expressed when cells were stimulated with Pam3CSK (*P*<0.05), however IAA alone or in combination did not result in a significant EGR1 expression (See Figure 18).

Cells stimulated with *P. aeruginosa* LPS did not result in significant IFN-γ expression, however, *P. gingivalis* LPS (*P*<0.05), Pam3CSK (*P*<0.05), Indole Acetic Acid (IAA) (*P*<0.001) and the combinations IAA + *P. aeruginosa* LPS (*P*<0.0001), IAA + *P. gingivalis* LPS (*P*<0.001), and IAA + Pam3CSK (*P*<0.0005) resulted in a significant IFN-γ expression (See Figure 19).

TGFβ-1 expression while not statistically significant upon stimulation with microbial components alone was found to be significantly expressed upon stimulation with the metabolite IAA (*P*<0.05) alone or in combination, IAA + *P. aeruginosa* LPS (*P*<0.05), IAA + *P. gingivalis* LPS (*P*<0.05), and IAA + Pam3CSK (*P*<0.05) (See Figure 20). TGFβ-2 expression was not significant upon stimulation with microbial and metabolite components (See Figure 21). TGFβ-3 expression was significantly expressed when cells were stimulated with *P. gingivalis* LPS (*P*<0.05), Pam3CSK (*P*<0.05), IAA (*P*<0.05), IAA+ *P. aeruginosa* LPS (*P*<0.05), IAA + *P. gingivalis* LPS (*P*<0.005), and IAA + Pam3CSK (*P*<0.05) (See Figure 22).

TSLP was significantly expressed upon stimulation with *P. aeruginosa* (*P*<0.05), *P. gingivalis* (*P*<0.05), Pam3CSK (*P*<0.0005), IAA (*P*<0.0005), IAA + *P. aeruginosa* LPS (*P*<0.0005), IAA + *P. gingivalis* LPS (*P*<0.0005), and IAA + Pam3CSK (*P*<0.0001) (See Figure 23).

HDAC6 was significantly expressed upon stimulation with Pam3CSK (*P*<0.05), IAA (*P*<0.0001), IAA + *P. aeruginosa* LPS (*P*<0.001), IAA + *P. gingivalis* LPS (*P*<0.001), and IAA + Pam3CSK (*P*<0.001) (See Figure 24).

IL-36γ was significantly expressed upon stimulation with Pam3CSK (*P*<0.05), IAA (*P*<0.0001), IAA + *P. aeruginosa* LPS (*P*<0.001), IAA + *P. gingivalis* LPS (*P*<0.005), and IAA + Pam3CSK (*P*<0.005) (See Figure 25).

GPR41 was significantly expressed upon stimulation with IAA (*P*<0.0001), IAA + *P. aeruginosa* LPS (*P*<0.0001), IAA + *P. gingivalis* LPS (*P*<0.01), and IAA + Pam3CSK (*P*<0.001) (See Figure 26).

GPR109A was significantly expressed upon stimulation with IAA (*P*<0.0001), IAA + *P. aeruginosa* LPS (*P*<0.001), IAA + *P. gingivalis* LPS (*P*<0.005), and IAA + Pam3CSK (*P*<0.001) (See Figure 27). GPR109B was significantly expressed upon stimulation with Pam3CSK (*P*<0.05) and IAA (*P*<0.01) (See Figure 28).

Sodium Acetate (SA)

The metabolite Sodium Acetate (SA) is a short chain fatty acid (SCFA) which is produced by the fermentation of dietary fibres[36]. In animal models SCFAs have been found to result in the creation of an anti-inflammatory effect via the activation of receptors such as G protein-coupled receptor 41 (GPR41)[33]. Studies have demonstrated that the consumption of soluble fibre by a stable asthma cohort resulted in a reduction of airway inflammation biomarkers[33]. Therefore the conclusion was reached that soluble fibre consumption may lead to anti-inflammatory effects within the asthmatic airway[33].

In this study BEAS-2B cells were stimulated with the short chain fatty acid, sodium acetate alone or in combination with TLR2 (Pam3CSK4) or TLR4 (LPS) agonists.

It was found that IL-6 was significantly expressed when cells were stimulated with Pam3CSK (*P*<0.005), Sodium Acetate (SA) (*P*<0.0001), SA + *P. aeruginosa* LPS

(*P*<0.005) and SA + Pam3CSK (*P*<0.05), however IL-6 levels were not significantly expressed upon stimulation with SA + *P. gingivalis* LPS (See Figure 15).

Similar findings were observed with respect to CXCL8 expression and SA + *P. gingivalis* LPS stimulation. CXCL8 (IL-8) was significantly expressed upon stimulation with Pam3CSK (*P*<0.005), Sodium Acetate (SA) (*P*<0.0005), SA + *P. aeruginosa* LPS (*P*<0.0001) and SA + Pam3CSK (*P*<0.05), however IL-6 levels were not significantly expressed upon stimulation with SA + *P. gingivalis* LPS (See Figure 16).

EGR1 was significantly expressed in cells stimulated with Pam3CSK (*P*<0.05) and Sodium Acetate (SA) (*P*<0.0001) and SA + *P*. gingivalis LPS (*P*<0.0001), however, SA + *P. aeruginosa* LPS and SA + Pam3CSK stimulation resulted in no significant change in EGR1 expression (See Figure 18).

IFN-γ expression was significant upon cell stimulation with *P. gingivalis* LPS (*P*<0.05), Pam3CSK (*P*<0.05), Sodium Acetate (SA) (*P*<0.0005), SA + *P. aeruginosa* LPS (*P*<0.0005), SA + *P*. gingivalis LPS (*P*<0.05) and SA + Pam3CSK (*P*<0.001) (See Figure 19).

TGFβ-1, TGFβ-2 and TGFβ-3 were not significantly expressed upon cell stimulation with the metabolite Sodium acetate alone or in combination with microbial components (See Figure 20, 21, 22).

TSLP was significantly expressed upon cell stimulation with the following components; *P. aeruginosa* LPS (*P*<0.05), *P. gingivalis* LPS (*P*<0.05) Pam3CSK (*P*<0.0005), Sodium Acetate (SA) (*P*<0.005), SA + *P. aeruginosa* LPS (*P*<0.0005), and SA + Pam3CSK (*P*<0.05) however SA + *P*. gingivalis LPS did not result in TSLP significance (See Figure 23).

Similarly, HDAC6 was significantly expressed upon cell stimulation with the following components; Pam3CSK (*P*<0.05), Sodium Acetate (SA) (*P*<0.01), SA + *P. aeruginosa* LPS (*P*<0.001), and SA + Pam3CSK (*P*<0.05) while SA + *P*. gingivalis LPS stimulated cells did not result in HDAC6 significance (See Figure 24).

IL-36G was significantly expressed upon stimulation with Pam3CSK (*P*<0.05), Sodium Acetate (SA) (*P*<0.0005), SA + *P. aeruginosa* LPS (*P*<0.0005) and SA + Pam3CSK (*P*<0.01) while SA + *P*. gingivalis LPS stimulated cells did not result in IL-36G significance (See Figure 25).

GPR41 was not significantly expressed upon stimulation with microbial components alone. When cells were stimulated with Sodium Acetate (SA) (*P*<0.0005), SA + *P. aeruginosa* LPS (*P*<0.0001) and SA + Pam3CSK (*P*<0.005) GPR41 was significantly expressed while SA + *P*. gingivalis LPS stimulated cells did not result in GPR41 significance (See Figure 26).

GPR109A not significantly expressed upon stimulation with microbial components alone however GPR109A was significantly expressed upon stimulation with Sodium Acetate (SA) (*P*<0.001), SA + *P. aeruginosa* LPS (*P*<0.0001), SA + *P*. gingivalis LPS (*P*<0.05) and SA + Pam3CSK (*P*<0.05) whereas GPR109B was not significantly expressed when cells were stimulated with microbial components or the metabolite Sodium Acetate (SA) (See Figure 27 and 28).

Overall the research aim to investigate the response of bronchial epithelial cells to microbial compounds, cytokines and metabolites individually and in combination and to investigate the resulting immune reaction upon stimulation was carried out. Microbial compounds including LPS derived from *Escherichia coli*, *Porphyromonas gingivalis* and *Pseudomonas aeruginosa* (TLR4 agonists) and Pam3CSK4 (TLR2 agonist), cytokines including IL-1β, IL-4, IL-7 and IL-17A and metabolites including Indole Acetic Acid and Sodium Acetate were utilised to investigate their effect upon asthmatic bronchial epithelial cells and the subsequent immune response was examined. Findings in this chapter are of interest and further investigation into the effects of such microbial, cytokine and metabolic components upon primary bronchial epithelial cells (PBECS) derived from asthmatic patients during bronchoscopy would be of interest.

6. Supplementary

Table S1. Table showing the NanoDrop ng/µl, A260/A280 and total ng yield per remaining RNA per sample extracted from the stimulated Beas-2B cells.

Sample	ng/µl	A260/A280	Total ng yield
Unstimulated	71.2	2.03	6408
Unstimulated	64.4	2.03	5796
Unstimulated	69.0	2.03	6210
LPS E. coli	71.1	2.00	6399
LPS E. coli	75.3	2.07	6777
LPS E. coli	72.5	2.11	6525
LPS P. aeruginosa	66.4	2.03	5976
LPS P. aeruginosa	68.4	2.09	6156
LPS P. aeruginosa	71.1	2.07	6399
LPS P. gingivalis	69.1	2.06	6219
LPS P. gingivalis	69.6	2.04	6264
LPS P. gingivalis	64.7	2.05	5823
Pam3CSK	74.9	2.05	6741
Pam3CSK	71.3	2.08	6417
Pam3CSK	82.2	2.04	7398
IL-1β	73.8	2.01	6642
IL-1β	71.6	2.01	6444
IL-1β	68.4	1.99	6156
IL-4	72.8	2.11	6552
IL-4	77.2	2.06	6948
IL-4	75.1	1.99	6759
IL-7	53.4	2.10	4806
IL-7	59.1	1.99	5319
IL-7	51.5	2.05	4635
IL-17A	72.8	1.99	6552
IL-17A	77.6	2.04	6984
IL-17A	78.1	1.97	7029
LPS PA + IL-1β	91.4	2.02	8226
LPS PA + IL-1β	91.4	1.92	8226
LPS PA + IL-1β	80.4	2.03	7236
LPS PA + IL-4	83.3	1.98	7497
LPS PA + IL-4	86.0	2.00	7740
LPS PA + IL-4	82.2	2.04	7398
LPS PA + IL-7	78.0	1.98	7020
LPS PA + IL-7	82.5	1.96	7425
LPS PA + IL-7	78.0	1.99	7020
LPS PA + IL-17A	83.8	1.97	7542
LPS PA + IL-17A	77.1	2.02	6939
LPS PA + IL-17A	61.8	1.98	5562
LPS PG + IL-1β	83.6	2.06	7524
LPS PG + IL-1β	83.0	2.01	7470
LPS PG + IL-1β	90.2	2.01	8118

LPS PG + IL-4	60.0	1.99	5400
LPS PG + IL-4	62.0	2.04	5580
LPS PG + IL-4	65.5	2.01	5895
LPS PG + IL-7	72.4	1.96	6516
LPS PG + IL-7	64.0	1.97	5760
LPS PG + IL-7	70.2	2.01	6318
LPS PG + IL17A	73.7	2.02	6633
LPS PG + IL17A	60.8	1.98	5472
LPS PG + IL17A	77.9	2.00	7011
Pam3CSK + IL1B	85.1	2.01	7659
Pam3CSK + IL1B	77.3	2.02	6957
Pam3CSK + IL1B	60.4	1.98	5436
Pam3CSK + IL4	73.7	1.99	6633
Pam3CSK + IL4	80.5	2.00	7245
Pam3CSK + IL4	68.2	2.00	6138
Pam3CSK + IL7	79.7	2.03	7173
Pam3CSK + IL7	83.5	2.02	7515
Pam3CSK + IL7	83.2	2.04	7488
Pam3CSK + IL17A	79.7	2.03	7173
Pam3CSK + IL17A	67.0	2.04	6030
Pam3CSK + IL17A	79.8	2.04	7182
Indole Acetic Acid	67.3	1.93	6057
Indole Acetic Acid	71.6	2.07	6444
Indole Acetic Acid	72.7	2.03	6543
IAA + LPS PA	85.6	2.05	7704
IAA + LPS PA	99.9	1.99	8991
IAA + LPS PA	89.5	2.03	8055
IAA + LPS PG	83.3	2.03	7497
IAA + LPS PG	93.4	2.03	8406
IAA + LPS PG	90.3	2.04	8127
IAA + Pam3CSK	60.8	2.06	5472
IAA + Pam3CSK	84.0	2.08	7560
IAA + Pam3CSK	67.4	2.03	6066
Sodium Acetate	64.0	2.01	5760
Sodium Acetate	75.7	2.01	6813
Sodium Acetate	59.9	2.01	5391
S. Acetate + LPS PA	84.0	2.04	7560
S. Acetate + LPS PA	83.6	2.05	7524
S. Acetate + LPS PA	96.6	2.03	8694
S. Acetate + LPS PG	70.4	2.02	6336
S. Acetate + LPS PG	95.0	2.05	8550
S. Acetate + LPS PG	71.7	2.02	6453
S. Acetate + Pam3CSK	87.6	1.97	7884
S. Acetate + Pam3CSK	81.7	2.01	7353
S. Acetate + Pam3CSK	82.2	2.02	7398

Table S2. Table showing the NanoDrop ng/µl, A260/A280 and total ng yield per remaining RNA per sample extracted from the second time the Beas-2B cells were stimulated using the same stimulants and conditions are the previous Beas-2B stimulations.

Sample	ng/µl	A260/A280	Total ng yield
Unstimulated	56.4	2.08	5076
Unstimulated	58.1	2.07	5229
Unstimulated	74.0	2.05	6660
LPS E. coli	75.1	2.04	6759
LPS E. coli	58.6	2.16	5274
LPS E. coli	47.7	2.09	4293
LPS P. aeruginosa	68.1	2.09	6129
LPS P. aeruginosa	71.2	2.09	6408
LPS P. aeruginosa	78.8	2.07	7092
LPS P. gingivalis	67.9	2.03	6111
LPS P. gingivalis	85.5	2.05	7695
LPS P. gingivalis	65.1	2.07	5859
Pam3CSK	80.3	2.05	7227
Pam3CSK	73.0	2.02	6570
Pam3CSK	87.7	2.08	7893
IL-1β	74.6	2.06	6714
IL-1β	86.9	2.03	7821
IL-1β	71.4	2.12	6426
IL-4	52.7	2.05	4743
IL-4	77.0	2.10	6930
IL-4	71.9	2.06	6471
IL-7	63.7	2.03	5733
IL-7	33.9	2.13	3051
IL-7	49.9	2.05	4491
IL-17A	57.4	2.00	5166
IL-17A	74.2	2.09	6678
IL-17A	63.7	2.06	5733
LPS PA + IL-1β	80.1	2.05	7209
LPS PA + IL-1β	76.5	2.04	6885
LPS PA + IL-1β	71.3	2.06	6417
LPS PA + IL-4	78.7	2.06	7083
LPS PA + IL-4	80.8	2.07	7272
LPS PA + IL-4	80.5	2.06	7245
LPS PA + IL-7	85.6	2.03	7704
LPS PA + IL-7	70.0	2.03	6300
LPS PA + IL-7	73.4	2.05	6606
LPS PA + IL-17A	73.0	2.09	6570
LPS PA + IL-17A	79.4	2.07	7146
LPS PA + IL-17A	75.9	2.06	6831
LPS PG + IL-1β	64.0	2.02	5760
LPS PG + IL-1β	83.9	2.05	7551

LPS PG + IL-1β	73.1	2.08	6579
LPS PG + IL-4	72.3	2.03	6507
LPS PG + IL-4	65.9	2.04	5931
LPS PG + IL-4	73.6	2.04	6624
LPS PG + IL-7	56.4	2.06	5076
LPS PG + IL-7	53.6	2.02	4824
LPS PG + IL-7	57.7	2.01	5193
LPS PG + IL17A	64.3	2.05	5787
LPS PG + IL17A	74.6	2.07	6714
LPS PG + IL17A	66.3	2.03	5967
Pam3CSK + IL1B	72.0	2.05	6480
Pam3CSK + IL1B	79.4	2.08	7146
Pam3CSK + IL1B	73.2	2.06	6588
Pam3CSK + IL4	75.4	2.00	6786
Pam3CSK + IL4	76.9	2.03	6921
Pam3CSK + IL4	66.8	2.04	6012
Pam3CSK + IL7	102.0	2.04	9180
Pam3CSK + IL7	77.7	2.09	6993
Pam3CSK + IL7	75.0	2.06	6750
Pam3CSK + IL17A	68.4	2.08	6156
Pam3CSK + IL17A	75.7	2.02	6813
Pam3CSK + IL17A	74.1	2.04	6669
Indole Acetic Acid	69.3	2.05	6237
Indole Acetic Acid	85.4	2.14	7686
Indole Acetic Acid	69.8	2.05	6282
IAA + LPS PA	89.9	2.01	8091
IAA + LPS PA	88.2	2.03	7938
IAA + LPS PA	64.4	1.97	5796
IAA + LPS PG	86.8	2.06	7812
IAA + LPS PG	87.2	2.06	7848
IAA + LPS PG	60.7	2.04	5463
IAA + Pam3CSK	95.0	2.04	8550
IAA + Pam3CSK	95.7	2.02	8613
IAA + Pam3CSK	77.5	2.03	6975
Sodium Acetate	85.4	2.07	7686
Sodium Acetate	90.3	2.05	8127
Sodium Acetate	83.1	2.02	7479
S. Acetate + LPS PA	82.6	2.02	7434
S. Acetate + LPS PA	88.6	2.05	7974
S. Acetate + LPS PA	78.6	2.07	7074
S. Acetate + LPS PG	82.5	2.04	7425
S. Acetate + LPS PG	56.1	1.97	5049
S. Acetate + LPS PG	91.3	2.00	8217
S. Acetate + Pam3CSK	78.6	2.03	7074
S. Acetate + Pam3CSK	81.9	2.04	7371
S. Acetate + Pam3CSK	53.0	1.93	4770

Table S3. Table showing the NanoDrop ng/µl, A260/A280 and total ng yield per remaining RNA sample extracted from the third time the Beas-2B cells were stimulated using the same stimulants and conditions as the previous Beas-2B stimulations.

Sample	ng/µl	A260/A280	Total ng yield
Unstimulated	64.1	2.04	5769
Unstimulated	63.9	2.00	5751
Unstimulated	79.9	2.02	7191
LPS E. coli	76.9	2.04	6921
LPS E. coli	78.9	1.98	7101
LPS E. coli	81.0	2.02	7290
LPS P. aeruginosa	90.2	2.05	8118
LPS P. aeruginosa	65.3	2.03	5877
LPS P. aeruginosa	69.4	2.02	6246
LPS P. gingivalis	67.4	1.99	6066
LPS P. gingivalis	69.1	2.09	6219
LPS P. gingivalis	73.6	2.03	6624
Pam3CSK	62.7	2.01	5643
Pam3CSK	72.3	2.05	6507
Pam3CSK	75.4	2.01	6786
IL-1β	72.4	2.02	6516
IL-1β	86.6	2.03	7794
IL-1β	59.3	1.99	5337
IL-4	63.9	2.01	5751
IL-4	71.9	2.01	6471
IL-4	78.2	2.01	7038
IL-7	63.8	2.04	5742
IL-7	69.1	2.01	6219
IL-7	55.8	2.01	5022
IL-17A	60.0	2.00	5400
IL-17A	62.6	2.01	5634
IL-17A	61.3	2.03	5517
LPS PA + IL-1β	66.8	2.02	6012
LPS PA + IL-1β	72.0	1.99	6480
LPS PA + IL-1β	76.7	2.03	6903
LPS PA + IL-4	59.5	2.05	5355
LPS PA + IL-4	61.3	2.12	5517
LPS PA + IL-4	78.8	2.09	7092
LPS PA + IL-7	80.9	2.03	7281
LPS PA + IL-7	56.6	2.03	5094
LPS PA + IL-7	69.5	2.06	6255
LPS PA + IL-17A	60.8	2.08	5472
LPS PA + IL-17A	80.6	2.08	7254
LPS PA + IL-17A	71.1	2.09	6399
LPS PG + IL-1β	68.8	2.05	6192
LPS PG + IL-1β	90.0	2.07	8100

LPS PG + IL-1β	74.6	2.09	6714
LPS PG + IL-4	55.3	2.07	4977
LPS PG + IL-4	66.8	2.08	6012
LPS PG + IL-4	65.8	2.06	5922
LPS PG + IL-7	51.3	2.10	4617
LPS PG + IL-7	39.0	2.00	3510
LPS PG + IL-7	46.8	2.14	4212
LPS PG + IL17A	67.5	2.01	6075
LPS PG + IL17A	72.9	2.04	6561
LPS PG + IL17A	84.7	2.03	7623
Pam3CSK + IL1B	69.1	2.03	6219
Pam3CSK + IL1B	86.6	2.04	7794
Pam3CSK + IL1B	71.1	2.04	6399
Pam3CSK + IL4	65.3	2.03	5877
Pam3CSK + IL4	72.9	2.04	6561
Pam3CSK + IL4	66.2	2.03	5958
Pam3CSK + IL7	72.6	2.03	6534
Pam3CSK + IL7	72.9	2.08	6561
Pam3CSK + IL7	79.1	2.06	7119
Pam3CSK + IL17A	65.2	2.04	5868
Pam3CSK + IL17A	82.1	2.04	7389
Pam3CSK + IL17A	67.8	2.07	6102
Indole Acetic Acid	64.6	2.12	5814
Indole Acetic Acid	73.2	2.02	6588
Indole Acetic Acid	68.2	2.04	6138
IAA + LPS PA	66.9	2.02	6021
IAA + LPS PA	53.8	2.03	4842
IAA + LPS PA	76.5	2.00	6885
IAA + LPS PG	72.6	2.03	6534
IAA + LPS PG	63.2	2.04	5688
IAA + LPS PG	74.4	1.97	6696
IAA + Pam3CSK	78.8	2.03	7092
IAA + Pam3CSK	77.0	2.02	6930
IAA + Pam3CSK	71.3	2.02	6417
Sodium Acetate	70.9	2.01	6381
Sodium Acetate	81.6	2.02	7344
Sodium Acetate	73.2	2.03	6588
S. Acetate + LPS PA	65.4	2.04	5886
S. Acetate + LPS PA	76.5	1.98	6885
S. Acetate + LPS PA	82.1	2.05	7389
S. Acetate + LPS PG	82.4	2.00	7416
S. Acetate + LPS PG	78.6	2.00	7074
S. Acetate + LPS PG	59.2	1.96	5328
S. Acetate + Pam3CSK	44.6	2.01	4014
S. Acetate + Pam3CSK	48.1	2.05	4329
S. Acetate + Pam3CSK	37.3	2.04	3357

Table S4. Primer sequences and the corresponding probe numbers. The housekeeping gene used was β-actin.

Gene		**Primer 5'-3'**		**Probe**
β-actin	ACTB	Right 5'-3'	5'-GGATGCCACAGGACTCCA-3'	11
		Left 5'-3'	5'-ATTGGCAATGAGCGGTTC-3'	
Interleukin-1β	IL-1β	Right 5'-3'	5'-TTGGGTAATTTTTGGGATCTACA-3'	78
		Left 5'-3'	5'-CTGTCCTGCGTGTTGAAAGA-3'	
Interleukin-5	IL-5	Right 5'-3'	5'-CCGTCTTTCTTCTCCACACTTT-3'	47
		Left 5'-3'	5'-CACTGAAGAAATCTTTCAGGGAAT-3'	
Interleukin-6	IL-6	Right 5'-3'	5'-CAGTGCTTTAGGAACCCAGAA-3'	16
		Left 5'-3'	5'-AACAATGTACAAGCTTCCAAACAA-3'	
Interleukin-17F	IL-17F	Right 5'-3'	5'-TGGGGTCCCAAGTGACAG-3'	39
		Left 5'-3'	5'-GGCATCATCAATGAAAACCA-3'	
Interleukin-36G	IL-36G	Right 5'-3'	5'-AGTGTTGTATGACTTCCCAAGTTCT-3'	54
		Left 5'-3'	5'-GACTGGTTCATTGCCTCCTC-3'	
Chemokine ligand 5	CCL5	Right 5'-3'	5'-CTTTCGGGTGACAAAGACG-3'	59
		Left 5'-3'	5'-TGCCCACATCAAGGAGTATTT-3'	
Chemokine (C-X-C motif) ligand 8	CXCL8	Right 5'-3'	5'-ATGGTTCCTTCCGGTGGT-3'	72

		Left 5’-3’	5’-GAGCACTCCATAAGGCACAAA-3’	
Chemokine ligand 11	CCL11	Right 5’-3’	5’-GGTGGTTGGGACAGAAGC-3’	5
		Left 5’-3’	5’-ATGAAGGTCTCCGCAGCA-3’	
Chemokine ligand 20	CCL20	Right 5’-3’	5’-TCAAAGTTGCTTGCTGCTTC-3’	39
		Left 5’-3’	5’-GCTGCTTTGATGTCAGTGCT-3’	
Early growth response 1	EGR1	Right 5’-3’	5’-GGTTTGGCTGGGGTAACTG-3’	22
		Left 5’-3’	5’-AGCCCTACGAGCACCTGAC-3’	
Interferon-γ	IFN-γ	Right 5’-3’	5’-TTTGGATGCTCTGGTCATCTT-3’	21
		Left 5’-3’	5’-GGCATTTTGAAGAATTGGAAAG-3’	
Thymic stromal lymphopoietin	TSLP	Right 5’-3’	5’-CCTGAGTAGCATTTATCTGAG-3’	SYBR
		Left 5’-3’	5’-CCGCCTATGAGCAGCCAC-3’	
Transforming growth factor β 1	TGFβ1	Right 5’-3’	5’-TGCTTGAACTTGTCATAGATTTCG-3’	31
		Left 5’-3’	5’-ACTACTACGCCAAGGAGGTCAC-3’	
Transforming growth factor β 2	TGFβ2	Right 5’-3’	5’-AGAGCACCTGGGACTGTCTG-3’	44
		Left 5’-3’	5’-CCTTCTTCCCCTCCGAAAC-3’	
Transforming growth factor β 3	TGFβ3	Right 5’-3’	5’-CGCACACAGCAGTTCTCC-3’	38
		Left 5’-3’	5’-AAGAAGCGGGCTTTGGAC-3’	

G protein coupled receptor 41	GPR41	Right 5’-3’	5’-GGCCACACTCACCAGACC-3’	43
		Left 5’-3’	5’-CACCCACTGTGGTACAAGACC-3’	
G protein coupled receptor 109A	GPR109A	Right 5’-3’	5’-ATGCCTCATAGAAGCCATCC-3’	23
		Left 5’-3’	5’-GTGGGACAATGGGGATAAAA-3’	
G protein coupled receptor 109B	GPR109B	Right 5’-3’	5’-AAGCCAGCAAGGCTCTTATG-3’	62
		Left 5’-3’	5’-TGTATGCCCAGGGGATTTT-3’	
Histone deacetylase 6	HDAC6	Right 5’-3’	5’-GGAACGGCTCCCTTTTTAAT-3’	47
		Left 5’-3’	5’-GTAGGCAGAACCCCCAGTC-3’	

7. References

1. Lambrecht BN, Hammad H. The airway epithelium in asthma. *Nat Med.* 2012;18(5):684-692.
2. Mills PR, Davies RJ, Devalia JL. Airway Epithelial Cells, Cytokines, and Pollutants. *Am J Respir Crit Care Med.* 1999;160(supplement_1):S38-S43.
3. Li Y, Wang Y, Liu X. The role of airway epithelial cells in response to mycobacteria infection. *Clinical & developmental immunology.* 2012;2012:791392.
4. Crystal RG, Randell SH, Engelhardt JF, Voynow J, Sunday ME. Airway Epithelial Cells. *Proceedings of the American Thoracic Society.* 2008;5(7):772-777.
5. Holtzman MJ, Byers DE, Alexander-Brett J, Wang X. The role of airway epithelial cells and innate immune cells in chronic respiratory disease. *Nat Rev Immunol.* 2014;14(10):686-698.
6. Bateman ED, Hurd SS, Barnes PJ, et al. Global strategy for asthma management and prevention: GINA executive summary. *European Respiratory Journal.* 2007;31(1):143-178.
7. Hammad H, Lambrecht BN. Dendritic cells and epithelial cells: linking innate and adaptive immunity in asthma. *Nat Rev Immunol.* 2008;8(3):193-204.
8. Kim HY, DeKruyff RH, Umetsu DT. The many paths to asthma: phenotype shaped by innate and adaptive immunity. *Nature immunology.* 2010;11(7):577-584.
9. Lee-Sarwar KA, Kelly RS, Lasky-Su J, et al. Integrative analysis of the intestinal metabolome of childhood asthma. *The Journal of allergy and clinical immunology.* 2019;144(2):442-454.
10. Huang YJ, Nelson CE, Brodie EL, et al. Airway Microbiota and Bronchial Hyperresponsiveness in Patients with Sub-optimally Controlled Asthma. *The Journal of allergy and clinical immunology.* 2011;127(2):372-381.e373.
11. Edwards MR, Bartlett NW, Hussell T, Openshaw P, Johnston SL. The microbiology of asthma. *Nat Rev Micro.* 2012;10(7):459-471.
12. Hiemstra PS, Grootaers G, van der Does AM, Krul CAM, Kooter IM. Human lung epithelial cell cultures for analysis of inhaled toxicants: Lessons learned and future directions. *Toxicology in Vitro.* 2018;47:137-146.
13. Hiemstra PS, McCray PB, Jr., Bals R. The innate immune function of airway epithelial cells in inflammatory lung disease. *The European respiratory journal.* 2015;45(4):1150-1162.
14. Stewart CE, Torr EE, Mohd Jamili NH, Bosquillon C, Sayers I. Evaluation of Differentiated Human Bronchial Epithelial Cell Culture Systems for Asthma Research. *Journal of Allergy.* 2012;2012:11.
15. Reddel RR, Ke Y, Gerwin BI, et al. Transformation of Human Bronchial Epithelial Cells by Infection with SV40 or Adenovirus-12 SV40 Hybrid Virus, or Transfection via Strontium Phosphate Coprecipitation with a Plasmid Containing SV40 Early Region Genes. *Cancer Research.* 1988;48(7):1904-1909.
16. Lee S-H, Park S-R. Toll-like Receptor 1/2 Agonist Pam3CSK4 Suppresses Lipopolysaccharide-driven IgG1 Production while Enhancing IgG2a Production by B Cells. *Immune Netw.* 2018;18(1):e10-e10.
17. Whelan R, Kim C, Chen M, Leiter J, Grunstein MM, Hakonarson H. Role and regulation of interleukin-1 molecules in pro-asthmatic sensitised airway smooth muscle. *The European respiratory journal.* 2004;24(4):559-567.
18. Steinke JW, Borish L. Th2 cytokines and asthma. Interleukin-4: its role in the pathogenesis of asthma, and targeting it for asthma treatment with interleukin-4 receptor antagonists. *Respiratory research.* 2001;2(2):66-70.

19. Reeder KM, Dunaway CW, Blackburn JP, et al. The common gamma-chain cytokine IL-7 promotes immunopathogenesis during fungal asthma. *Mucosal immunology.* 2018;11(5):1352-1362.
20. Sullivan A, Hunt EB, Ward C, et al. The presence of Aspergillus fumigatus in asthmatic airways is not clearly related to clinical disease severity. *Allergy.* 2019.
21. Chesne J, Braza F, Mahay G, Brouard S, Aronica M, Magnan A. IL-17 in severe asthma. Where do we stand? *Am J Respir Crit Care Med.* 2014;190(10):1094-1101.
22. Faure E, Kwong K, Nguyen D. Pseudomonas aeruginosa in Chronic Lung Infections: How to Adapt Within the Host? *Front Immunol.* 2018;9:2416-2416.
23. How KY, Song KP, Chan KG. Porphyromonas gingivalis: An Overview of Periodontopathic Pathogen below the Gum Line. *Front Microbiol.* 2016;7:53-53.
24. Poynter ME, Irvin CG. Interleukin-6 as a biomarker for asthma: hype or is there something else? *The European respiratory journal.* 2016;48(4):979-981.
25. Tanaka T, Narazaki M, Kishimoto T. IL-6 in inflammation, immunity, and disease. *Cold Spring Harb Perspect Biol.* 2014;6(10):a016295-a016295.
26. Pang Z, Raudonis R, McCormick C, Cheng Z. Early Growth Response 1 Deficiency Protects the Host against Pseudomonas aeruginosa Lung Infection. *Infect Immun.* 2019;88(1):e00678-00619.
27. Kak G, Raza M, Tiwari Brijendra K. Interferon-gamma (IFN-γ): Exploring its implications in infectious diseases. *Biomolecular Concepts.* Vol 92018:64.
28. Saito A, Horie M, Nagase T. TGF-β Signaling in Lung Health and Disease. *Int J Mol Sci.* 2018;19(8):2460.
29. West EE, Kashyap M, Leonard WJ. TSLP: A Key Regulator of Asthma Pathogenesis. *Drug Discov Today Dis Mech.* 2012;9(3-4):10.1016/j.ddmec.2012.1009.1003.
30. Yan B, Liu Y, Bai H, et al. HDAC6 regulates IL-17 expression in T lymphocytes: implications for HDAC6-targeted therapies. *Theranostics.* 2017;7(4):1002-1009.
31. Ding L, Wang X, Hong X, Lu L, Liu D. IL-36 cytokines in autoimmunity and inflammatory disease. *Oncotarget.* 2017;9(2):2895-2901.
32. Trompette A, Gollwitzer ES, Yadava K, et al. Gut microbiota metabolism of dietary fiber influences allergic airway disease and hematopoiesis. *Nat Med.* 2014;20(2):159-166.
33. Halnes I, Baines KJ, Berthon BS, MacDonald-Wicks LK, Gibson PG, Wood LG. Soluble Fibre Meal Challenge Reduces Airway Inflammation and Expression of GPR43 and GPR41 in Asthma. *Nutrients.* 2017;9(1):57.
34. De Luca K, Frances-Duvert V, Asensio MJ, et al. The TLR1/2 agonist PAM3CSK4 instructs commitment of human hematopoietic stem cells to a myeloid cell fate. *Leukemia.* 2009;23(11):2063-2074.
35. Spaepen S, Vanderleyden J, Remans R. Indole-3-acetic acid in microbial and microorganism-plant signaling. *FEMS Microbiology Reviews.* 2007;31(4):425-448.
36. Deehan EC, Yang C, Perez-Muñoz ME, et al. Precision Microbiome Modulation with Discrete Dietary Fiber Structures Directs Short-Chain Fatty Acid Production. *Cell Host & Microbe.* 2020.

Chapter 8

Bronchial Brushings and Inflammatory Stimuli

Examination of bronchial brushings as a method to investigate the inflammatory response of the asthmatic cohort

Author Contributions: Desmond Murphy, John MacSharry and Ashley Sullivan were responsible for the study design and concept. Desmond Murphy was responsible for patient recruitment, clinical characterisation and sample acquisition. Deirdre Flynn was responsible for spirometry and FeNO testing and ACQ-7 questionnaires. Sample processing and study assays were primarily performed by Ashley Sullivan with contribution from Bernie Crowley and John MacSharry. Statistical analysis was performed by the authors. Analysis and interpretation of data and manuscript preparation and approval was performed by Ashley Sullivan, John MacSharry and Desmond Murphy

1. Abstract 376
2. Introduction 377
3. Methods 379
    3.1. Patient recruitment 379
    3.2. Sample storage and processing 380
    3.3. RNA isolation 380
    3.4. RNA quantification and dilution 381
    3.5. Reverse transcriptase PCR 381
    3.6. Primers 383
    3.7. qRT-PCR – quantitative Reverse Transcription –Polymerase Chain Reaction 383
    3.8. Statistical analyses 384
4. Results 385
    4.1. Patient demographics 385
    4.2. Molecular detection of human genes of interest 389
5. Discussion 400
6. Supplementary 406
7. References 409

1. Abstract

Background: As the airway epithelium is a first line defensive mechanism of the host against stimuli such as allergens, microorganisms and environmental factors it is vital to the understanding of respiratory disorders such as asthma. It is noted that airway epithelial cells, the key controllers of inflammatory, immune and regenerative responses in the host can be challenged in asthma and the ensuing response may be distorted. Therefore experiments which examine the interplay of the airway epithelium may prove vital in understanding the pathophysiology of asthma.

Methods: Bronchial brushings were collected during bronchoscopy and stored in a sterile falcon containing a preserving agent. RNA was isolated, quantified and diluted to the required concentration. Reverse transcriptase qPCR was carried out order to obtain cDNA. qRT-PCR was carried out with respect to the primers of interest, β-actin, IL-1β, IL-5, IL-17, CCL5, CXCL8, CCL11, CCL20, EGR1, IFN-γ, TSLP, TGFβ-1, TGFβ-2, TGFβ-3.

Results: Patient bronchial cDNA revealed a patient specific immune profile by qRT-PCR with IL-1β detectable in 39%, IL-5 detectable in 15%, IL-17F detectable in 22%, CCL5 in 98%, CXCL8 in 98%, CCL11 7%, CCL20 in 7%, EGR1 in 98%, INF-γ in 76%, TSLP in 59%, TGFβ-1 in 93%, TGFβ-2 in 68% and TGFβ-3 in 85% of cDNA extracted from the patients bronchoscopy bronchial brush, n=41 with subsequent significance found to certain patient demographics upon further analysis.

Conclusions: The examination cDNA obtained from bronchial brushings (n=41) revealed a patient specific immune profile by qPCR with subsequent significance found to certain patient demographics upon further analysis, highlighting the possibility of implementing bronchial brush cDNA analysis as an adjunct means of analysing the patient epithelial immune profile.

2. Introduction

Asthma is comprised of many clinical phenotypes and is known to be influenced by a plethora of components from environmental factors to susceptibility genes[1,2]. The airway epithelium is a first line defence mechanism of the host against infection due to direct exposure present between the lungs and the environment[2,3]. Respiratory epithelial cells produce inflammatory cytokines, chemokines and growth factors in order to contain the offending microbial insult present in the airways[4].

The lower airways have revealed themselves to contain a unique microbiome[2]. It has been seen that microorganisms can affect the epithelium and if the interaction results in a compromised epithelium, subsequent allergen exposure, along with environmental exposure to pollutants, may result in further exacerbations, a heightened immune response and asthma development[2].

The role of the microbiome with respect to disease prognosis and progression is of increasing interest in numerous disease types with advances in sequencing technologies further propelling the research field in recent years[5]. While sequencing technologies are readily implemented with regards to the investigation of microbes present at sites of interest within the host, often it is the case that a further model system is required to be implemented, in order to investigate the effect microbes may play on aspects such as inflammation and disease prognosis. It is established in asthma research that in order to investigate the function of the epithelium with regards to asthma it is important to utilise *in vitro* model systems. It is often the case that immortalized cell lines are utilised in respiratory disorders, such as asthma, as they offer a relatively cost-effective means to investigate the potential immune response upon exposure to stimulants of interest; however there are inherent limitations in using such a model system. Primary epithelial cells award the best representation of a model system for epithelial research however limitations such as cost, specialist expertise in primary cell culture, specialist facilitates available for primary cell culture and the variations which exist at the

inter- and intra-donor level with respect to primary cell culture present difficulties in implementing this model system on a wide scale[6].

While model systems to elucidate the pathogenic mechanisms present in respiratory disorders such as asthma are an established means of investigation they can be costly on a larger scale[6]. Therefore RNA from patients' lungs obtained from bronchial brushings was analysed as a potential mechanism to investigate immune cell profiling in asthmatics, by examining the cDNA for a variety of genes of interest by performing qRT-PCR with respect to the genes of interest, circumventing the need to culture the primary cell cultures and performing subsequent cell stimulations.

3. Methods

3.1. Patient recruitment

The study was approved by the Clinical Research Ethics Committee of the Cork Teaching Hospitals. 41 patients with a history of asthma (either documented change in FEV1 ≥12%/200ml with bronchodilator or a positive inhalation challenge) were recruited through a dedicated asthma clinic in a tertiary referral centre; Cork University Hospital by my clinical supervisor, Dr Des Murphy.

Patients were scheduled for bronchoscopy with spirometry, ACQ-7 and blood sampling performed on the day of bronchoscopy. Written informed consent was obtained from patients on the day of bronchoscopy. Spirometry was performed according to ATS/ERS guidelines[7]. The cohort was stratified by both severity [mild (GINA 1+2), moderate (GINA 3) and severe (GINA 4+5)] and asthma control (ACQ-7)[8,9]. Patients underwent bronchoscopy according to standard guidelines[10].

Bronchoalveolar lavage (BAL) was obtained as a standardised 180ml (3x60ml) sample from either the right middle lobe or lingula as we have previously described[11]. In addition to the collection of bronchoalveolar lavage (BAL) bronchial brushings were collected during bronchoscopy, by passing a small brush through the sampling channel of the bronchoscope to collect cells from the airway lining of the lung. The bronchial brushings for the purpose of this experiment were not used to establish primary cell cultures', rather; they were used for qRT-PCR analysis to examine the immune signalling at play within the cohort.

Within the cohort of 41 patients where bronchial brushing were collected 2 patients were classified as mild (GINA 1+2), 4 patients were classified as moderate (GINA 3) and 35 patients were classified as severe (GINA 4+5).

The mild asthma cohort was not prescribed oral steroids or inhaled corticosteroids (ICS) at time of sampling. Moderate patients were not prescribed oral steroids but were prescribed inhaled corticosteroids (ICS) (min 500 – max 800 ICS FDP). Within the severe asthma cohort 32% were in receipt of oral steroids (11/34) (2.5 – 25 mg)

and all 35 patients in the severe asthma cohort were in receipt of inhaled corticosteroids (min 800 – max 2400 ICS FDP). For further patient information see patient demographics Table 1.

3.2. Sample storage and processing

Upon completion of the bronchoscopy the bronchoscope brush, containing the bronchial cells, was cut and added to a 15ml sterile falcon tube containing 5 mls of DNA/RNA Shield (Zymo Research, UK), a preservative for processing the sample. The tube was shaken to ensure thorough homogenisation of the DNA/RNA Shield with the bronchoscope brush sample. The tube containing DNA/RNA shield and bronchoscope brush was labelled and stored in a -80^{o}C freezer until RNA isolation steps were carried out.

3.3. RNA isolation

In order to isolate total RNA from the patient bronchoscope brush sample stored in DNA/RNA Shield a Quick-RNA MiniPrep R1054 kit (Zymo Research, UK) was used as it was compatible with samples stored in DNA/RNA Shield.

Reagent preparation occurred before the kit was used; 96ml of 100% ethanol was added to the 24ml RNA Wash Buffer concentrate. The first step involved the lysis and homogenisation of the sample stored in DNA/RNA Shield by bringing the samples from -80^{o}C to room temperature. 1ml of this sample was then aliquoted to a screwcap tube and an equal volume of RNA Lysis buffer (1:1) was added to the same tube which was then mixed before proceeding to the sample clearing step. In order to clear the sample it was centrifuged at 10,000g for 1 minute. Genomic DNA was removed by pipetting the supernatant into a Spin-Away filter in a collection tube and the tube was centrifuged at 10,000g for 1 minute. The flow through was added to a new sterile 15ml falcon tube and the remaining supernatant was centrifuged through the Spin-Away filter and the flow through added to the same 15ml falcon tube for RNA purification. 2mls of 100% ethanol was added to 15ml falcon tube containing the sample in RNA Lysis Buffer (1:1) and thorough mixing

occurred. This mixture was then transferred to a Zymo-Spin IIICG Column in a collection tube and was centrifuged at 16,000g for 30 seconds, discarding the flow-through and repeating until all of the mixture had been centrifuged through the Zymo-Spin IIICG column. The column was then washed with 400µl of RNA Prep Buffer and 700µl RNA Wash Buffer ensuring the column was centrifuged at 16,000g for 30 seconds and the flow through discarded each time. 400µl RNA Wash Buffer was then added and the column was centrifuged at 16,000g for two minutes in order to ensure the RNA Wash Buffer was completely removed. The column was then transferred to an RNase free tube and in order to elute a higher concentration of RNA, 50µl DNase/RNase-Free Water was added directly to the membrane and centrifuged at 16,000g for 30 seconds. The eluted RNA was then stored at -80^{o}C.

3.4. RNA quantification and dilution

The concentration and quality of the extracted RNA was analysed using a Nano Drop ND1000 spectrophotometer (Thermo Fischer Scientific). In order to analyse RNA purity and concentration the computer settings chosen were nucleic acid; RNA-40. The Nano Drop was calibrated using 1µl of DNase/RNase free water. The RNA extracted from the patient bronchoscopy brush was then analysed by pipetting 1µl of sample onto the lower measure platform of the machine, closing the sampling arm and initiating spectral measurement using the operating software. The sample column was drawn between the upper and lower platforms and a spectral measurement was made. After each measurement was made the ng/µl and 260:280 values and RNA curve graph were documented and the measurement platform was cleaned (Supplementary Table S1). In order to standardise the RNA a dilution step was performed where the undiluted RNA was diluted to ensure a standard value of 10ng/µl of RNA for each patient sample.

3.5. Reverse transcriptase PCR

The patient mRNA isolated from the bronchial brush was reversed transcribed to cDNA. RNA from the bronchoscope brush samples from 41 asthma patients was

diluted to 10ng/µl and RNA samples were kept on ice in order to maintain the integrity of the RNA sample. A mastermix was prepared for the 41 patient RNA samples and the RNA extraction kit control sample. Per reaction mastermix consisted of 4µl 5X Transcriptor Buffer, 2µl dNTP (ATGC) 10mM, 1µl Transcriptor RT/RNAsin mix which consisted of Reverse Transcriptase and Protector RNase Inhibitor in a 1:1 volume ratio and 3µl of Random Primer (Roche, Merck/Sigma Aldrich). A No RT mastermix consisted of 4µl 5X Transcriptor Buffer, 2µl dNTP (ATGC) 10mM, 3µl Random Primer and 1µl DEPC treated molecular biology grade water (Calbiochem, Sigma Aldrich).

10µl of mastermix was pipetted into corresponding wells of an un-skirted 96 well plate (Thermo Fisher Scientific). 10µl of the No RT mastermix was pipetted into a separate well and clearly labelled. 10µl of 10ng/µl (100ng per reaction) RNA from each patient was pipetted into wells containing mastermix, corresponding to the pre-designed 96 well plate layout, ensuring each well contained individual RNA from one of the 41 patients See Supplementary Table S2 for layout. DEPC treated molecular grade water was added to the well designated as the Negative RT sample. In the well containing the No RT mastermix 10µl of RNA from a pre-made pool of RNA from various patients was added in order to determine if the primers amplify genomic DNA.

The 96 well plate was then sealed with a foil plate seal and spun using a microplate centrifuge (VWR, Ireland) to ensure the mastermix and RNA was dispersed to the bottom of the wells. A benchtop 2720 Thermal Cycler machine (Applied Biosystems, Thermo Fisher Scientific) was programmed to include 10 minutes at 25^{o}C, 30 minutes at 55^{o}C and 5 minutes at 85^{o}C before cooling to 4^{o}C with the PCR Thermal Cycler machine lid programmed to be heated to 100^{o}C to prevent reagent loss. Once the Reverse Transcriptase PCR cycles were complete the cDNA was diluted by adding 80µl DEPC treated molecular biology grade water to each well. The cDNA was then stored at -20^{o}C for further downstream applications.

3.6. Primers

Primers were designed using the Universal Probe Library Assay Design Centre (Roche Life Sciences) programme (Supplementary Table S3). Primers were chosen based on scientific literature with an emphasis on cytokines and chemokines in relation to bronchial epithelial cells.

When designing the primers using the Universal Probe Library Assay Design Centre *Homo sapiens* was selected as the organism of choice and the target gene of interest was entered by name leading to the design of numerous primer pairs for that gene. Two primer pairs were designed for each gene of interest based on the software ranking system. Primers were supplied by Eurofins Genomics (Ireland) or Sigma Aldrich (Ireland).

Primers were centrifuged upon arrival to ensure the lyophilized pellet remained at the bottom of the 2ml screw-cap tube. Primers were re-suspended with molecular grade water according to individual primer specification (µl for 100µM). Once primers were re-suspended they were then vortexed and combined by adding 20µl of right primer and 20µl of left primer and 160µl of molecular grade water to a sterile labelled Eppendorf tube. Primers were then stored at -20^{o}C.

Universal Probe Library Probes set (Roche Life Sciences) was available within the laboratory. Primers for which there was not a corresponding probe available for underwent SYBR green qRT-PCR conditions. Primers were tested on a pool of bronchial cDNA and primers were considered viable depending on Absolute Quantification/2nd Derivative Max Cp values and Tm calling analysis.

3.7. qRT-PCR – quantitative Reverse Transcription –Polymerase Chain Reaction

qRT-PCR's were performed using a 384 well plate layout and LightCycler Probes Master (Roche) or LightCycler SYBR Green Master (Roche) reagent mix, dependent on the use of hydrolysis probe or SYBR Green primer sets. Water NTCs (No Template Control) were used in each reaction in order to identify reaction set up

contamination and to test for the propensity of primers to create primer dimers in the case of reactions which were carried out with SYBR Green Master.

Reactions were performed on a LightCycler 480 machine (Roche). qRT-PCR conditions were as follows; pre-incubation at 50^{o}C for 2 minutes, ramp rate 4.8^{o}C/s and 95^{o}C for 10 minutes, ramp rate 4.8^{o}C/s. Amplification at 95^{o}C for 10 seconds, ramp rate 4.8^{o}C/s, 60^{o}C for 45 seconds, ramp rate 2.5^{o}C/s and 75^{o}C for 1 second, ramp rate 4.8^{o}C for 45 cycles in total. A melt curve also occurred at 95^{o}C with a ramp rate of 0.11^{o}C/s for any primer which used LightCycler SYBR Green Master. A cooling stage then occurred at 40^{o}C, ramp rate 2^{o}C/s at the end of the process. Fluorescent readings were taken in single acquisition mode.

NTCs did not produce a product and melt curves produced clear peaks indicating that the products produced were not an artefact. qRT-PCR was carried out on bronchial brush cDNA with a focus on the following primers; β-actin (probe library (pl) 11), IL-1β (pl 78), IL-5 (pl 47), IL-6 (pl 16), IL-17F (SYBR), CCL5 (pl 59), CXCL8 (SYBR), CCL11 (SYBR), CCL20 (SYBR), EGR1 (SYBR), IFN-γ (SYBR), TSLP (SYBR), TGFβ1 (pl 31), TGFβ2 (pl 44) and TGFβ3 (pl 38).

3.8. Statistical analyses

Statistical analyses and graphical representations of data were performed using Graph Pad Prism 8 Software. The Shapiro-Wilk test was applied to the data to assess if the data was normally distributed or not. Normally distributed date was presented as the mean± standard deviation (SD) and non-normally distributed data which did not pass the Shapiro-Wilk test was presented as median ± interquartile range in the text and figures. For data which passed the Shapiro-Wilk test for normality it was assumed that the data was sampled from Gaussian distribution and therefore the data was analysed using Pearson correlation co-efficients. Non-normally distributed data was analysed by assuming that the data was not sampled from Gaussian distribution and the data was analysed using nonparametric Spearman correlation. Results were considered statistically significant when $P<0.05$.

4. Results

4.1. Patient demographics

Table 1 Patient demographics. Patient demographics broken into mild (GINA 1+2) moderate (GINA 3) and severe (GINA 4+5) asthmatics. Note † ACQ-7, Asthma Control Questionnaire; ‡ ICS, Inhaled Corticosteroids; § FeNO, Fractional exhaled Nitric Oxide; ¶ FEV-1, Forced Expiratory Volume in the first second; ¥ BMI, Body Mass Index.

		Mild (GINA 1-2)	**Moderate (GINA 3)**	**Severe (GINA 4-5)**
Patients	n=41 (%)	2 (5%)	4 (10%)	35 (85%)
Male		0 (0%)	1 (25%)	13 (37%)
Female		2 (100%)	3 (75%)	22 (63%)
Smoker	Current	0	0	3
	Ex-	1	2	14
	Never	1	2	18
ACQ-7 †	[Mean (SD)]	[0.5 (0.7)]	[1.4 (0.4)]	[2.3 (1.1)]
	[Median (IQR)]	[0.15(0.0-1.0)]	[1.4 (1.1-1.6)]	[2.6 (1.1-2.9)]
Oral Steroids (mg)	Positive	0	0	11
	[Mean (SD)]			[10.0 (7.7)]
	[Median (IQR)]			[5 (5-15)]
ICS (FDP 250) ‡	Positive	0	4	35
	[Mean (SD)]		[725 (150.0)]	[1080 (347.1)]
	[Median (IQR)]		[800 (575-800)]	[1000 (1000-1000)]
FeNO (ppb) §	[Mean (SD)]	No data	[30 (28.3)]	[34.6 (24.7)]
	[Median (IQR)]	No data	[30 (10-50)]	[26 (14.8-55.0)]
FEV-1 (Percent Predicted) ¶	[Mean (SD)]	[93.5 (13.4)]	[79.5 (3.9)]	[71.3 (23.3)]
	[Median (IQR)]	[93.5 (84-103)]	[78.5 (76.5-83.5)]	[71.0 (52-89)]
BMI (kg/m^2) ¥	[Mean (SD)]	[21.3 (3.2)]	[29.6 (11.5)]	[31.3 (8.1)]
	[Median (IQR)]	[21.3 (19.0-23.5)]	[26.4 (21.1-41.3)]	[29.7 (25.4-34.4)]
IgE (KU/L)	[Mean (SD)]	[9.5 (0)]	[858.9 (1477)]	[477.7 (761.9)]
	[Median (IQR)]	[9.5 (9.5-9.5)]	[180 (16-2381)]	[115.1 (34.2-701.5)]
BAL Monocyte % count	[Mean (SD)]	[10.6 (4.8)]	[7.6 (4.2)]	[11.6 (7.0)]
	[Median (IQR)]	[10.6 (7.2-14.0)]	[5.4 (5-12.5)]	[10.5 (6.7-15.0)]
BAL Macrophage % count	[Mean (SD)]	[68.8 (6.8)]	[81.6 (5.9)]	[69.1 (19.4)]
	[Median (IQR)]	[68.8 (64.0-73.6)]	[80.4 (76.4-88.0)]	[77.0 (58.4-83.0)]
BAL Lymphocyte % count	[Mean (SD)]	[18.8 (4.5)]	[3.7 (0.9)]	[7.0 (7.1)]
	[Median (IQR)]	[18.8 (15.6-22.0)]	[4.0 (2.7-4.5)]	[4.8 (2.6-10.0)
BAL Eosinophil % count	[Mean (SD)]	[0 (0)]	[2.7 (4.6)]	[2.0 (5.0)]
	[Median (IQR)]	[0 (0-0)]	[0 (0-8)]	[0.5 (0.0-2.5)]

		Mild (GINA 1-2)	Moderate (GINA 3)	Severe (GINA 4-5)
BAL Neutrophil % count	[Mean (SD)]	[1.8 (2.6)]	[4.4 (2.0)]	[10.2 (15.7)]
	[Median (IQR)]	[1.8 (0.0-3.6)]	[3.6 (3.0-6.7)]	[3.5 (1.0-14.5)]
mRNA Expression		**Mild (GINA 1-2)**	**Moderate (GINA 3)**	**Severe (GINA 4-5)**
β-actin (Cycle Threshold CT)	Positive	2 (100%)	4 (100%)	35(100%)
	[Mean (SD)]	[29.3 (1.8])	[24.3 (1.2)]	[25.5 (2.2)]
	[Median (IQR)]	[29.3 (28.0-30.5)]	[23.9 (26.5-25.6)]	[25.0 (24.1-26.1)]
IL-1β (CT)	Positive	1 (50%)	1 (25%)	14 (40%)
	[Mean (SD)]	[36.1 (0)]	[33.7 (0)]	[35.0 (2.0)]
	[Median (IQR)]	[36.1 (36.1-36.1)]	[33.7 (33.7-33.7)]	[35.4 (34.1-36.6)]
IL-5 (CT)	Positive	0 (0%)	1 (25%)	5 (14%)
	[Mean (SD)]		[38.4 (0)]	[38.2 (1.1)]
	[Median (IQR)]		[38.4 (38.4-38.4]	[38.1 (37.4-39.1)]
IL-17F (CT)	Positive	0 (0%)	1 (25%)	8 (23%)
	[Mean (SD)]		[36.4 (0)]	[36.6 (0.8)
	[Median (IQR)]		[36.4 (36.4-36.4)]	[36.4 (36.3-37.1)]
CCL5 (CT)	Positive	2 (100%)	4 (100%)	34 (97%)
	[Mean (SD)]	[35.1 (2.6)]	[34.6 (2.1)]	[35.1 (1.7)]
	[Median (IQR)]	[35.1 (33.3-37.0)]	[34.1 (32.9-36.6)]	[34.9 (33.9-35.9)]
CXCL8 (CT)	Positive	2 (100%)	4 (100%)	34 (97%)
	[Mean (SD)]	[32.8 (3.9)]	[29.6 (1.9)]	[30.4 (2.1)]
	[Median (IQR)]	[32.8 (30.1-35.5)]	[30.1 (27.7-31.1)]	[30.3 (28.9-31.7)]
CCL11 (CT)	Positive	0 (0%)	1 (25%)	2 (6%)
	[Mean (SD)]		[32.9 (0)]	[31.9 (0.8)]
	[Median (IQR)]		[32.9 (32.9-32.9)]	[31.9 (31.4-32.5)
CCL20 (CT)	Positive	0 (0%)	0 (0%)	3 (9%)
	[Mean (SD)]			[33.5 (1.0)]
	[Median (IQR)]			[34 (32.4-34.1)]
EGR-1 (CT)	Positive	2 (100%)	4 (100%)	34 (97%)
	[Mean (SD)]	[29.7 (1.1)]	[31.1 (1.1)]	[31.7 (1.3)]
	[Median (IQR)]	[29.7 (28.9-30.5)]	[30.8 (30.3-32.1)]	[31.6 (30.8-32.7)]
IFN-γ (CT)	Positive	2 (100%)	3 (75%)	26 (74%)
	[Mean (SD)]	[33.4 (0.1)]	[28.7 (3.8)]	[31.1 (2.0)]
	[Median (IQR)]	[33.4 (33.3-33.5)]	[27.5 (25.8-33.0)]	[31.3 (29.6-32.8)]
TSLP (CT)	Positive	0 (0%)	2 (50%)	22 (63%)
	[Mean (SD)]		[32.3 (0.3)]	[32.3 (0.7)]
	[Median (IQR)]		[32.3 (32.1-32.6)]	[32.5 (31.8-32.8)]
TGFβ-1 (CT)	Positive	1 (50%)	4 (100%)	33 (94%)
	[Mean (SD)]	[32.5 (0)]	[30 (1.2)]	[30.7 (1.5)]
	[Median (IQR)]	[32.5 (32.5-32.5)]	[29.6 (29.1-31.3)]	[30.7 (29.6-31.7)]
TGFβ-2 (C%)	Positive	0 (0%)	3 (75%)	25 (71%)
	[Mean (SD)]		[36.3 (1.1)]	[36.4 (1.5)]
	[Median (IQR)]		[36.3 (35.2-37.3)]	[36 (35.6-37.0)]
TGFβ-3 (CT)	Positive	1 (50%)	4 (100%)	30 (86%)
	[Mean (SD)]	[37.5 (0)]	[35.4 (1.8)]	[35.7 (1.0)]
	[Median (IQR)]	[37.5 (37.5-37.5)	[35.0 (34.0-37.3)]	[35.7 (34.9-36.6)]

Table 2 qPCR analysis of corresponding patient BAL microbiome. qPCR results of both the bacteria pellet (BP) fraction and the cellular pellet (CP) fraction of the patient BAL.

n=41		Mild (GINA 1-2) (n=2)	Moderate (GINA 3) (n=4)	Severe (GINA 4-5) (n=35)
Total bacteria BP (CT)	Positive	2	4	34
	[Mean (SD)]	[26.6 (5.1)]	[29.7 (1.7)]	[27.8 (2.9)]
	[Median (IQR)]	[26.6 (23.1-30.2)]	[29.8 (28.0-31.2)]	[27.9 (25.3-29.6)]
Total bacteria CP (CT)	Positive	2	4	34
	[Mean (SD)]	[25.3 (5.9)]	[22.9 (4.7)]	[23.4 (3.0)]
	[Median (IQR)]	[25.3 (21.2-29.5)]	[20.7 (20.3-27.7)]	[22.5 (21.6-25.0)]
***Firmicutes* BP (CT)**	Positive	2	4	35
	[Mean (SD)]	[26.4 (4.4)]	[27.4 (2.1)]	[26.3 (2.8)]
	[Median (IQR)]	[26.4 (23.3-29.4)]	[28.1 (25.2-29.0)]	[26.4 (24.7-28.6)]
***Firmicutes* CP (CT)**	Positive	2	4	34
	[Mean (SD)]	[24.9 (2.7)]	[20.4 (4.8)]	[21.4 (2.8)]
	[Median (IQR)]	[24.9 (23.0-26.9)]	[18.3 (17.6-25.3)]	[21.0 (19.3-23.2)]
***P. aeruginosa* BP (CT)**	Positive	0	1	3
	[Mean (SD)]		[40 (0)]	[34.3 (6.7)]
	[Median (IQR)]		[40 (40-40)]	[37.9 (26.7-38.4)]
***P. aeruginosa* CP (CT)**	Positive	2	4	17
	[Mean (SD)]	[39.0 (1.4)]	[37.3 (1.0)]	[38.0 (1.4)]
	[Median (IQR)]	[39.0 (38.1-40.0)]	[37.8 (36.3-37.8)]	[37.8 (37.2-39.5)]
***P. fluorescens* BP (CT)**	Positive	2	4	35
	[Mean (SD)]	[29.5 (3.2)]	[32.3 (0.6)]	[31.5 (2.3)]
	[Median (IQR)]	[29.5 (27.2-31.8)]	[32.4 (31.7-32.8)]	[32.0 (30.7-33.2)]
***P. fluorescens* CP (CT)**	Positive	2	4	32
	[Mean (SD)]	[29.7 (5.7)]	[27.5 (3.7)]	[28.2 (2.8)]
	[Median (IQR)]	[29.7 (25.7-33.7)]	[26.5 (24.6-31.4)]	[28.6 (26.3-30.6)]
***Escherichia* BP (CT)**	Positive	0	1	11
	[Mean (SD)]		[37.3 (0)]	[36.7 (2.9)]
	[Median (IQR)]		[37.3 (37.3-37.3)]	[36 (35.6-40.0)]
***Escherichia* CP (CT)**	Positive	0	2	9
	[Mean (SD)]		[38.3 (2.5)]	[36.5 (4.1)]
	[Median (IQR)]		[38.3 (30.5-40.0)]	[37 (35.6-40.0)]
***Bordetella* BP (CT)**	Positive	1	0	10
	[Mean (SD)]	[35.7 (0)]		[34.5 (1.3)]
	[Median (IQR)]	[35.7 (35.7-35.7)]		[34.5 (33.7-35.5)]
***Bordetella* CP (CT)**	Positive	1	3	31
	[Mean (SD)]	[34.2 (0)]	[31.9 (2.5)]	[31.1 (1.3)]
	[Median (IQR)]	[34.2 (34.2-34.2)]	[31.2 (29.7-34.7)]	[31 (30.2-32.0)]
***Prevotella* BP (CT)**	Positive	2	3	32
	[Mean (SD)]	[32.0 (7.1)]	[34.4 (2.3)]	[31.9 (2.7)]
	[Median (IQR)]	[32 (27-37)]	[33.2 (32.9-37.1)]	[32.3 (29.6-33.3)]
***Prevotella* CP (CT)**	Positive	2	4	33
	[Mean (SD)]	[30.1 (5.0)]	[29.1 (5.4)]	[29.6 (3.4)]
	[Median (IQR)]	[30.1 (26.6-33.6)]	[27.2 (25.5-34.6)]	[29.2 (27.5-31.0)]
***Veillonella* BP (CT)**	Positive	2	4	34
	[Mean (SD)]	[28.8 (6.9)]	[31.4 (2.7)]	[29.5 (3.5)]
	[Median (IQR)]	[28.8 (23.9-33.7)]	[31.9 (28.6-33.6)]	[29.5 (27.8-31.3)]
***Veillonella* CP (CT)**	Positive	2	4	34
	[Mean (SD)]	[26.7 (8.2)]	[23.1 (3.3)]	[24.4 (2.7)]
	[Median (IQR)]	[26.7 (21.0-32.5)]	[22.4 (20.5-26.6)]	[23.7 (22.1-26.9)]
***M. pneumoniae* BP (CT)**	Positive	1	3	21
	[Mean (SD)]	[30.2 (0)]	[39.4 (0.7)]	[35.9 (3.2)]
	[Median (IQR)]	[30.2 (30.2-30.2)]	[39.5 (38.6-40.0)]	[35.8 (33.5-39.5)]

		Mild (GINA 1-2)	Moderate (GINA 3)	Severe (GINA 4-5)
***M. pneumoniae* CP (CT)**	Positive	1	3	24
	[Mean (SD)]	[30.3 (0)]	[34.4 (5.1)]	[34.3 (3.4)]
	[Median (IQR)]	[30.3 (30.3-30.3)]	[33.2 (30.1-40.0)]	[34.4 (31.3-37.0)]
***C. pneumoniae* BP (CT)**	Positive	1	1	23
	[Mean (SD)]	[36.7 (0)]	[32.6 (0)]	[33.7 (2.2)]
	[Median (IQR)]	[36.7 (36.7-36.7)]	[32.6 (32.6-32.6)]	[34.5 (32.5-35.0)]
***C. pneumoniae* CP (CT)**	Positive	1	2	30
	[Mean (SD)]	[34.5 (0)]	[28.1 (0.7)]	[29.5 (2.3)]
	[Median (IQR)]	[34.5 (34.5-34.5)]	[28.1 (27.6-28.6)]	[29.1 (28.5-30.1)]
***S. aureus* BP (CT)**	Positive	2	4	20
	[Mean (SD)]	[27.2 (3.3)]	[30.7 (3.6)]	[31.6 (3.0)]
	[Median (IQR)]	[27.2 (24.9-29.5)]	[31.0 (27.3-33.9)]	[32.5 (29.0-34.4)]
***S. aureus* CP (CT)**	Positive	2	2	10
	[Mean (SD)]	[25.2 (4.5)]	[20.4 (0.1)]	[28.1 (3.5)]
	[Median (IQR)]	[25.2 (22.0-28.3)]	[20.4 (20.3-20.4)]	[27.6 (25.1-32.1)]
***N. bacilliformis* BP (CT)**	Positive	2	3	22
	[Mean (SD)]	[28.0 (5.2)]	[32.5 (2.8))]	[31.4 (2.7)]
	[Median (IQR)]	[28.0 (24.5-31.6)]	[30.9 (30.8-35.7)]	[31.5 (30.7-33.7)]
***N. bacilliformis* CP (CT)**	Positive	2	4	34
	[Mean (SD)]	[26.3 (5.7)]	[26.5 (4.2)]	[28.8 (3.7)]
	[Median (IQR)]	[26.3 (22.3-30.3)]	[26.6 (22.6-30.4)]	[28.4 (26.1-32.0)]
***M. catarrhalis* BP (CT)**	Positive	2	4	34
	[Mean (SD)]	[29.2 (3.8)]	[31.9 (0.7)]	[31.2 (2.2)]
	[Median (IQR)]	[29.2 (26.6-31.9)]	[31.8 (31.3-32.6)]	[32.0 (30.6-32.7)]
***M. catarrhalis* CP (CT)**	Positive	2	4	32
	[Mean (SD)]	[29.5 (5.7)]	[27.0 (3.5)]	[28.2 (2.8)]
	[Median (IQR)]	[29.5 (25.5-33.5)]	[25.8 (24.5-30.7)]	[28.1 (26.0-30.6)]
***N. meningitidis* BP (CT)**	Positive	1	3	28
	[Mean (SD)]	[29.6 (0)]	[34.6 (2.4)]	[31.9 (3.4)]
	[Median (IQR)]	[29.6 (29.6-29.6)]	[34.0 (32.5-37.2)]	[32.4 (30.5-33.9)]
***N. meningitidis* CP (CT)**	Positive	1	4	31
	[Mean (SD)]	[26.9 (0)]	[27.9 (3.6)]	[27.6 (3.7)]
	[Median (IQR)]	[26.9 (26.9-26.9)]	[28.2 (24.3-31.2)]	[27.2 (25.1-28.6)]
***S. pneumoniae* BP (CT)**	Positive	1	3	25
	[Mean (SD)]	[29.8 (0)]	[33.8 (2.3)]	[33.4 (2.3)]
	[Median (IQR)]	[29.8 (29.8-29.8)]	[33.8 (31.6-36.1)]	[33.7 (32.4-34.8)]
***S. pneumoniae* CP (CT)**	Positive	2	4	29
	[Mean (SD)]	[31.8 (4.7)]	[28.6 (5.5)]	[28.9 (2.7)]
	[Median (IQR)]	[31.8 (28.5-35.2)]	[28.1 (23.8-34.1)]	[29.7 (26.7-30.9)]
***H. influenzae* BP (CT)**	Positive	1	2	23
	[Mean (SD)]	[27.1 (0)]	[35.2 (0.4)]	[32.5 (3.4)]
	[Median (IQR)]	[27.1 (27.1-27.1)]	[35.3 (35.0-35.5)]	[33.2 (31.4-35.1)]
***H. influenzae* CP (CT)**	Positive	2	4	33
	[Mean (SD)]	[30.6 (6.2)]	[28.4 (4.6)]	[29.2 (3.9)]
	[Median (IQR)]	[30.6 (26.2-35.0)]	[28.4 (24.3-32.4)	[28.6 (26.5-32.1)]
***Rothia* BP (CT)**	Positive	2	2	30
	[Mean (SD)]	[33.2 (1.1)]	[34.9 (1.7)]	[31.8 (3.4)]
	[Median (IQR)]	[33.2 (32.4-33.9)]	[34.9 (33.7-36.1)]	[32.3 (29.8-34.5)]
***Rothia* CP (CT)**	Positive	2	4	34
	[Mean (SD)]	[30.5 (5.3)]	[25.7 (4.2)]	[25.9 (3.7)]
	[Median (IQR)]	[30.5 (26.8-34.2)]	[24.6 (22.5-30.1)]	[25.7 (23.1-27.8)]
***Micromonospora* BP (CT)**	Positive	2	1	20
	[Mean (SD)]	[37.1 (0.9)]	[35.0 (0)]	[36.2 (2.2)]
	[Median (IQR)]	[37.1 (36.5-37.8)]	[35.0 (35.0-35.0)]	[36.7 (35.6-37.2)]
***Micromonospora* CP (CT)**	Positive	2	4	29
	[Mean (SD)]	[35.6 (2.0)]	[32.2 (2.8)]	[33.5 (2.5)]
	[Median (IQR)]	[35.6(34.2-37.1)]	[32.2 (31.1-36.1)]	[33.3 (31.3-35.9)]

4.2. Molecular detection of human genes of interest

qRT-PCR was performed on the extracted bronchial brush cDNA (n=41) using validated human primers. β-actin was chosen as the housekeeping gene and the genes of interest were IL-1β, IL-5, IL-17F, CCL5, CXCl8, CCL11, CCL20, EGR1, INF-γ, TSLP, TGFβ-1, TGFβ-2 and TGFβ-3. (See Table S3). Melt curve analysis for primers which used SYBR Green mastermix was undertaken to ensure the product produced was correct and not an artefact. No template controls (NTCs) were implemented in all reaction runs and were used as a cut-off point for cycle threshold (CT)/ crossing point (Cp) results as any product which appeared in cycles after the appearance of water was disregarded. The resulting genes were seen at various abundance levels in the patient bronchial brush cDNA samples.

When analysed with regards to the presence of the gene in the patient bronchial brush cDNA (n=41), IL-1β was detectable in 39%, IL-5 was detectable in 15%, IL-17F was detectable in 22%, CCL5 was present in 98%, CXCL8 was present in 98%, CCL11 was present in 7%, CCL20 was present in 7%, EGR1 was present in 98%, INF-γ was present in 76%, TSLP was present in 59%, TGFβ-1 was present in 93%, TGFβ-2 was present in 68% and TGFβ-3 was present in 85% of cDNA extracted from the patients bronchoscopy bronchial brush, n=41. See Table 1 for numerical details and patient stratification by GINA stage. See Figure 1 for qRT-PCR detection of human genes of interest in patient bronchial brush cDNA

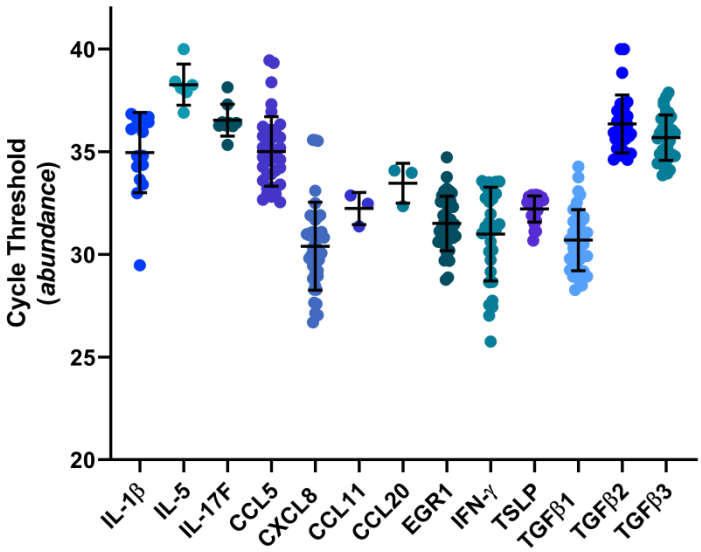


Figure 1. qRT-PCR detection of human genes of interest in patient bronchial brush cDNA. qPCR was performed on the extracted bronchial brush cDNA using validated human primers designed for the genes of interest IL-1β, IL-5, IL-17F, CCL5, CXCL8 CCL11, CCL20, EGR1, IFN-γ, TSLP, TGFβ-1, TGFβ-2 and TGFβ-3. n=41.

In order to investigate the relative expression of the genes of interest the qRT-PCR data was analysed using ddCT analysis. The housekeeper gene, beta (β) actin, raw qRT-PCR data was compared to the raw qRT-PCR Ct (Cycle threshold) data for each of the genes of interest. The delta delta CT (ΔΔCT) for each individual sample was calculated and the fold change of the samples was calculated by 2^-ΔΔCT. The relative changes in gene expression can be seen in Figure 2.

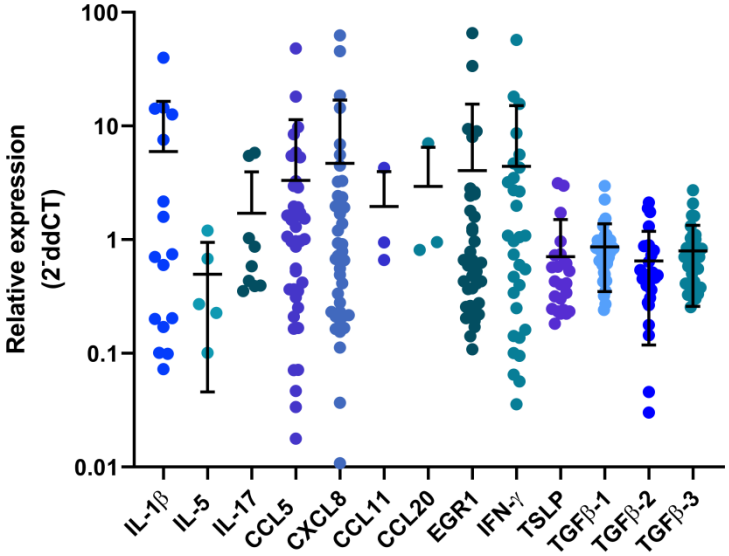


Figure 2. Relative changes in gene expression. The qRT-PCR CT (Cycle Threshold) data was analysed using delta delta CT (ΔΔCT) analysis to calculate the relative changes in gene expression by analysing the housekeeper gene (β-actin) against the genes of interest. n=41, log 10 graph.

The patient bronchial brush qPCR results, which highlighted the abundance of genes detectable from the bronchial brush cDNA sample, was further analysed against the patient demographics (n=41). Factors such as inhaled corticosteroids, smoking status, GINA, FeNO, ACQ-7, FEV-1, BAL % macrophages, BAL % monocytes, BAL % lymphocytes, BAL % eosinophils, BAL % neutrophils, microbiome qPCR analysis results, blood IgE levels, haemoglobin, white blood cells, blood lymphocytes, blood eosinophils and blood neutrophils were analysed. Microbiome qPCR was undertaken on both the bacteria pellet (BP) and the cellular pellet (CP) DNA isolated from the bronchoscopy BAL fluid; a detailed protocol of which can be found in *Chapter 5* and *Chapter 6.*

Statistical analysis and graphical representations of data was performed using Graph Pad Prism 8 Software. The Shapiro-Wilk test was applied to the data to

assess if the data was normally distributed or not. Normally distributed date was presented as the mean± standard deviation (SD) and non-normally distributed data which did not pass the Shapiro-Wilk test for normality was presented as median ± interquartile range in the text and figures. For data which passed the Shapiro-Wilk test for normality it was assumed that the data was sampled from Gaussian distribution and therefore the data was analysed using Pearson correlation coefficients. Non-normally distributed data was analysed by assuming that the data was not sampled from Gaussian distribution and the data was analysed using nonparametric Spearman correlation.

IL-1β was observed to correlate negatively with Total Bacteria (CP) (P<0.05; r_s=-0.5206), *Prevotella* (CP) (P<0.05; r_s=-0.5265), *Haemophilus influenzae* (BP) (P<0.01; r_s=-0.7273) and *Rothia* (CP) (P<0.05; r_s=-0.5383). IL-5 positively correlated with the percentage count of BAL eosinophils (P<0.05; r_s=0.8407). IL-17F negatively correlated with the percentage count of BAL lymphocytes (P<0.05; r_s=-0.7029). See Figure 3.

CCL5 positively correlated with inhaled corticosteroids (FDP) (P<0.005; r_s=0.4494), FeNO (P<0.05; r_s=0.4690) and the percentage count of BAL eosinophils (P<0.01; r_s=0.4344). CXCL8 positively correlated with qPCR *Bordetella* presence (P<0.05; r=0.3549) and negatively correlated with inhaled corticosteroids (FDP) (P<0.005; r_s=0.3792) and blood haemoglobin (HB) (g/L) levels (P<0.05; r_s=-0.6687). See Figure 4.

EGR1 positively correlated with inhaled corticosteroids (FDP) (P<0.01; r_s=0.4216) and *Staphylococcus aureus* (BP) presence by qPCR (P<0.05; r_s=0.4254). IFN-γ positively correlated with BAL monocyte percentage counts (P<0.05; r_s=0.3932). TSLP negatively correlated with qPCR Total Bacteria (BP) (P<0.05; r_s=-0.4471), *Pseudomonas fluorescens* (BP) (P<0.05; r_s=-0.4343) and *Prevotella* (BP) (P<0.05; r_s=-0.5055). See Figure 5.

TSLP also negatively correlated with qPCR *Veillonella* (BP) (P<0.05; r_s=-0.4566), *Chlamyodphila pneumoniae* (BP) (P<0.05; r_s=-0.5583), *Moraxella catarrhalis* (BP) (P<0.01; r_s=-0.5583), *Neisseria meningitidis* (BP)) (P<0.05; r_s=-0.5519), *Haemophilus*

influenzae (BP) (P<0.05; r_s=-0.6878) and *Rothia* (BP) (P<0.05; r_s=-0.5780). See Figure 6.

TGFβ-1 positively correlated with inhaled corticosteroids (FDP) (P<0.05; r_s=0.4153) and negatively correlated with the percentage of BAL monocytes (P<0.05; r_s=-0.3341), the presence by qPCR of *Pseudomonas fluorescens* (BP) (P<0.05; r_s=-0.3519), *Chlamydophila pneumoniae* (BP) (P<0.05; r_s=-0.4972) and *Neisseria meningitidis* (BP) (P<0.05; r_s=-0.4256). TGFβ-2 positively correlated with BAL eosinophil percentage counts (P<0.05; r_s=0.4244). See Figure 7.

TGFβ-2 negatively correlated with qPCR levels of *Pseudomonas fluorescens* (BP) (P<0.005; r_s=-0.5190), *Chlamydophila pneumoniae* (BP) (P<0.05; r_s=-0.5449), *Moraxella catarrhalis* (BP) (P<0.01; r_s=-0.5105) and *Neisseria meningitidis* (BP) (P<0.05; r_s=-0.5022). TGFβ-3 negatively correlated with total levels of blood IgE (KU/L) (P<0.05; r_s=-0.3736). See Figure 8.

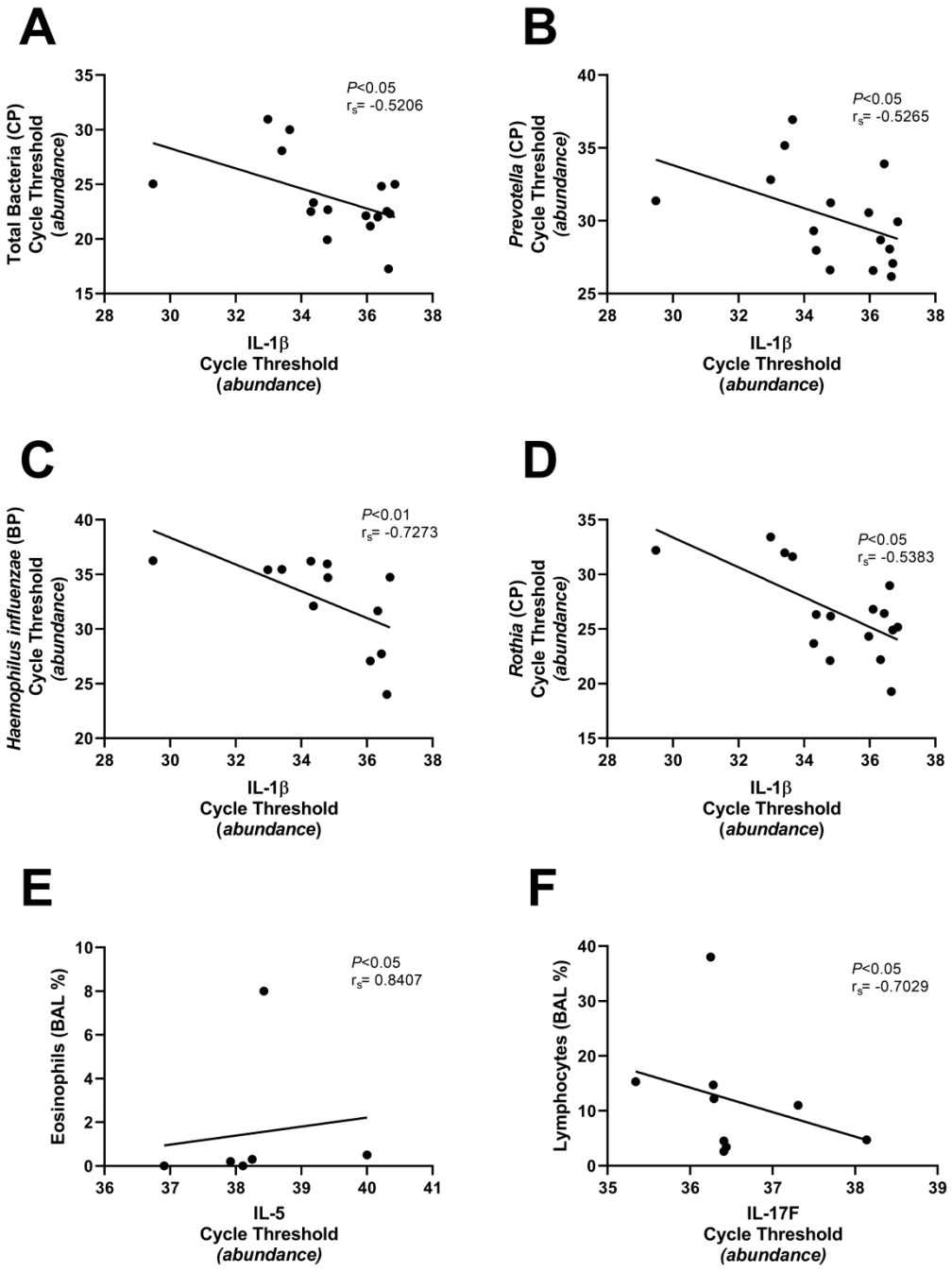


Figure 3. Correlations of brush mRNA detection to BAL BP and CP microbes and patient characteristics. IL-1β was observed to correlate negatively with Total Bacteria (CP) (P<0.05; r_s=-0.5206) (A), *Prevotella* (CP) (P<0.05; r_s=-0.5265) (B), *Haemophilus influenzae* (BP) (P<0.01; r_s=-0.7273) (C) and *Rothia* (CP) (P<0.05; r_s=-0.5383) (D). IL-5 positively correlated with the percentage count of BAL eosinophils (P<0.05; r_s=0.8407) (E). IL-17F negatively correlated with the percentage count of BAL lymphocytes (P<0.05; r_s=-0.7029) (F). n=41.

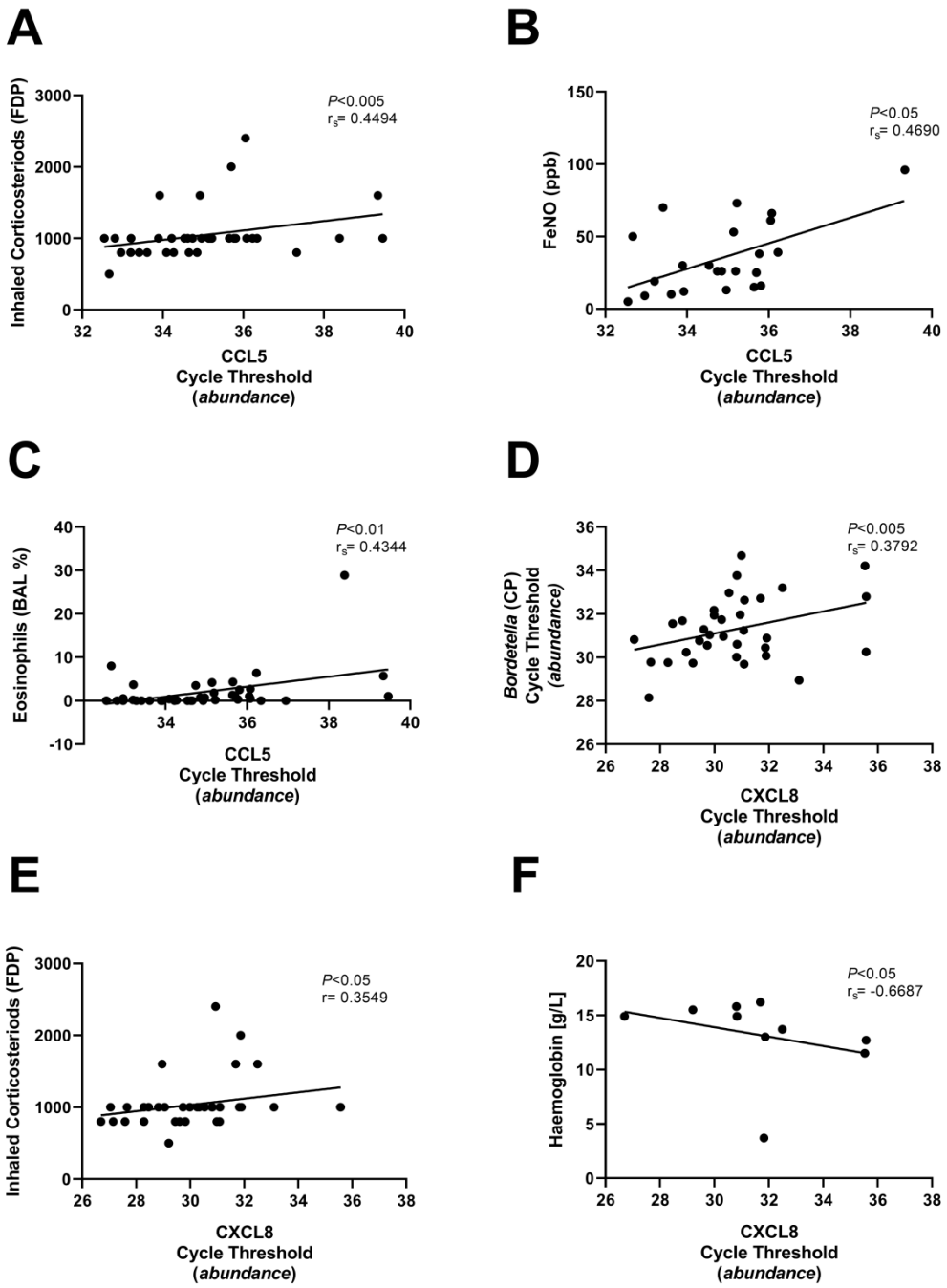


Figure 4. Correlations of brush mRNA detection, BAL CP microbes and patient characteristics. CCL5 positively correlated with inhaled corticosteroids (FDP) (*P*<0.005; r_s=0.4494) (A), FeNO (*P*<0.05; r_s=0.4690) (B) and the percentage count of BAL eosinophils (*P*<0.01; r_s=0.4344) (C). CXCL8 positively correlated with qPCR *Bordetella* presence (*P*<0.05; r=0.3549) (D) and negatively correlated with inhaled corticosteroids (FDP) (*P*<0.005; r_s=0.3792) (E) and blood haemoglobin (HB) (g/L) levels (*P*<0.05; r_s=-0.6687) (F). n=41.

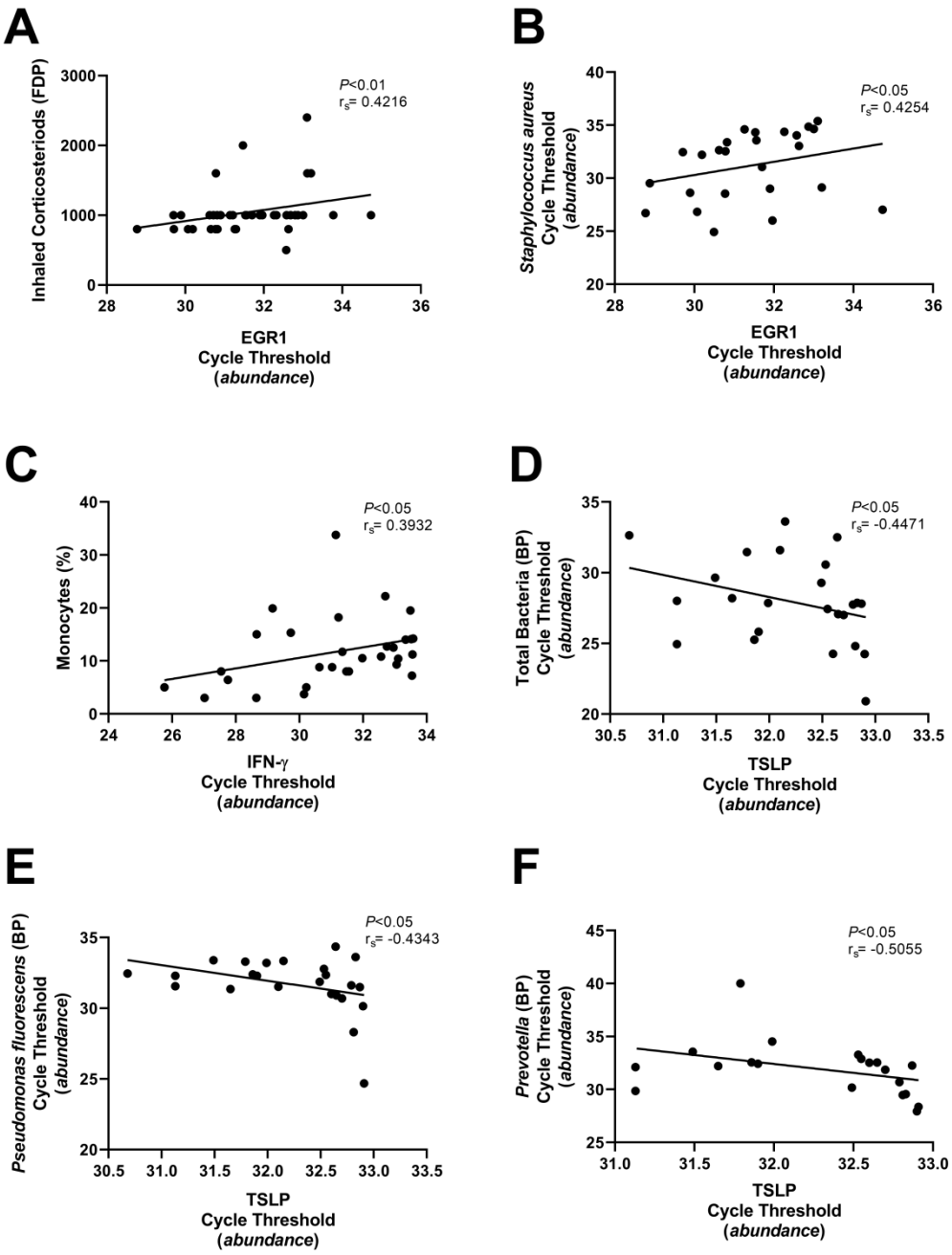


Figure 5. Correlations of brush mRNA detection to BAL BP microbes and patient characteristics. EGR1 positively correlated with inhaled corticosteroids (FDP) (*P*<0.01; r_s=0.4216) (A) and *Staphylococcus aureus* (BP) presence by qPCR (*P*<0.05; r_s=0.4254) (B). IFN-γ positively correlated with BAL monocyte percentage counts (*P*<0.05; r_s=0.3932) (C). TSLP negatively correlated with qPCR Total Bacteria (BP) (*P*<0.05; r_s=-0.4471) (D), *Pseudomonas fluorescens* (BP) (*P*<0.05; r_s=-0.4343) (E) and *Prevotella* (BP) (*P*<0.05; r_s=-0.5055) (F). n=41.

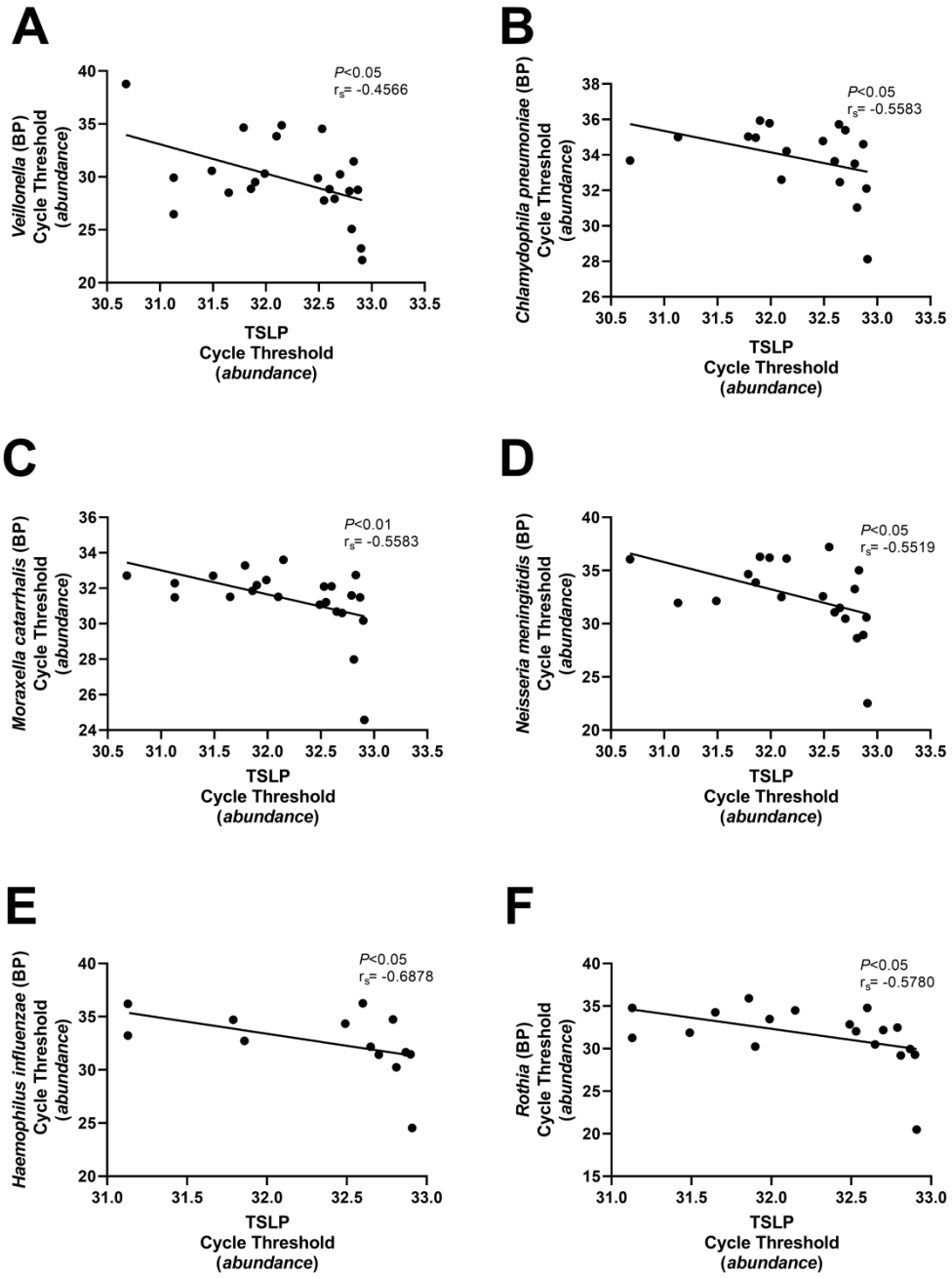


Figure 6. Correlations of brush mRNA detection to BAL BP microbes. TSLP negatively correlated with qPCR *Veillonella* (BP) (*P*<0.05; r_s=-0.4566) (A), *Chlamyodphila pneumoniae* (BP) (*P*<0.05; r_s=-0.5583) (B), *Moraxella catarrhalis* (BP) (*P*<0.01; r_s=-0.5583) (C), *Neisseria meningitidis* (BP)) (*P*<0.05; r_s=-0.5519) (D), *Haemophilus influenzae* (BP) (*P*<0.05; r_s=-0.6878) (E) and *Rothia* (BP) (*P*<0.05; r_s=-0.5780) (F). n=41.

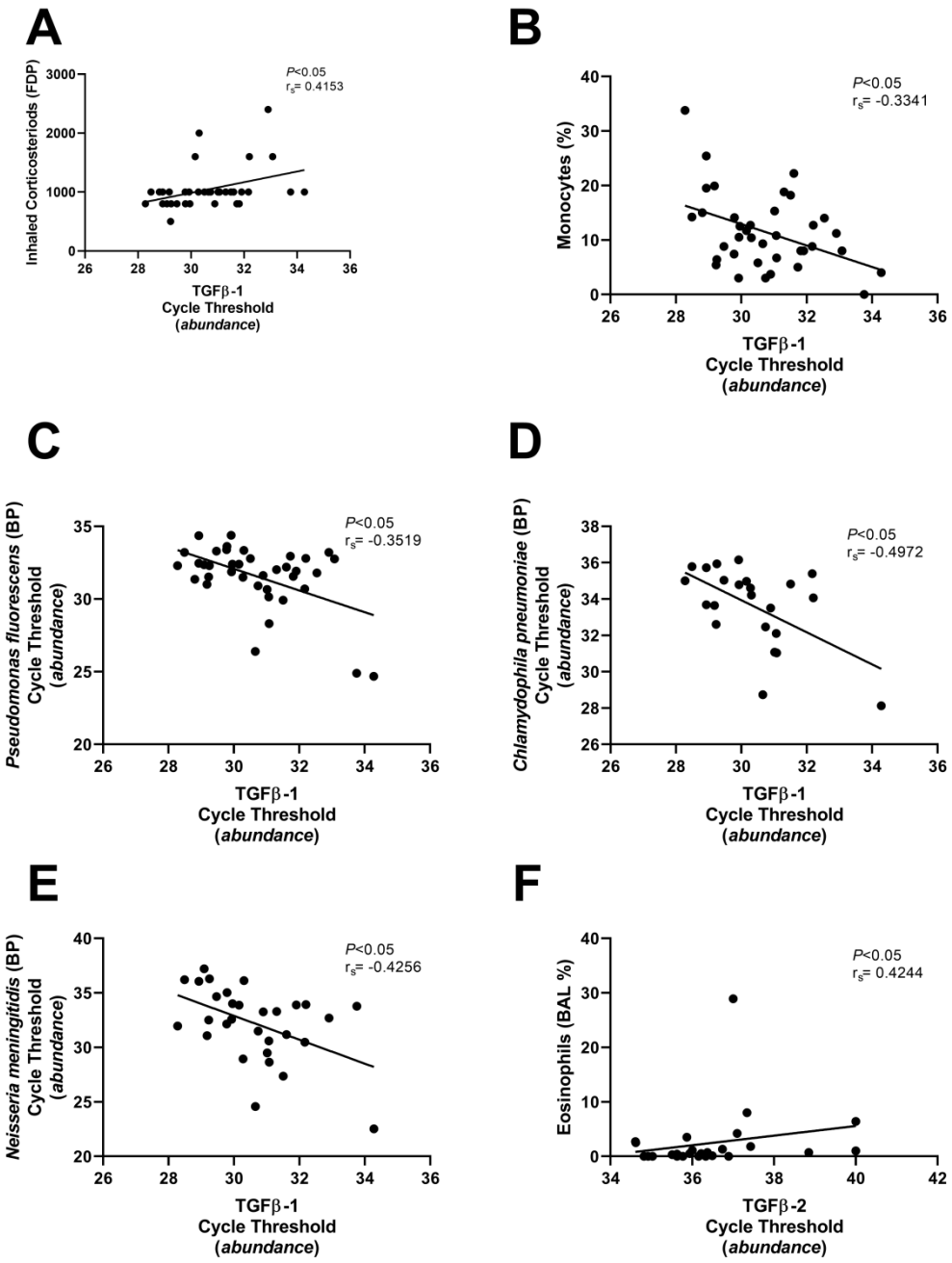


Figure 7. Correlations of brush mRNA detection to BAL BP microbes and patient characteristics. TGFβ-1 positively correlated with inhaled corticosteroids (FDP) (*P*<0.05; r_s=0.4153) (A) and negatively correlated with the percentage of BAL monocytes (*P*<0.05; r_s=-0.3341) (B), the presence by qPCR of *Pseudomonas fluorescens* (BP) (*P*<0.05; r_s=-0.3519) (C), *Chlamydophila pneumoniae* (BP) (*P*<0.05; r_s=-0.4972) (D) and *Neisseria meningitidis* (BP) (*P*<0.05; r_s=-0.4256) (E). TGFβ-2 positively correlated with BAL eosinophil percentage counts (*P*<0.05; r_s=0.4244) (F). n=41.

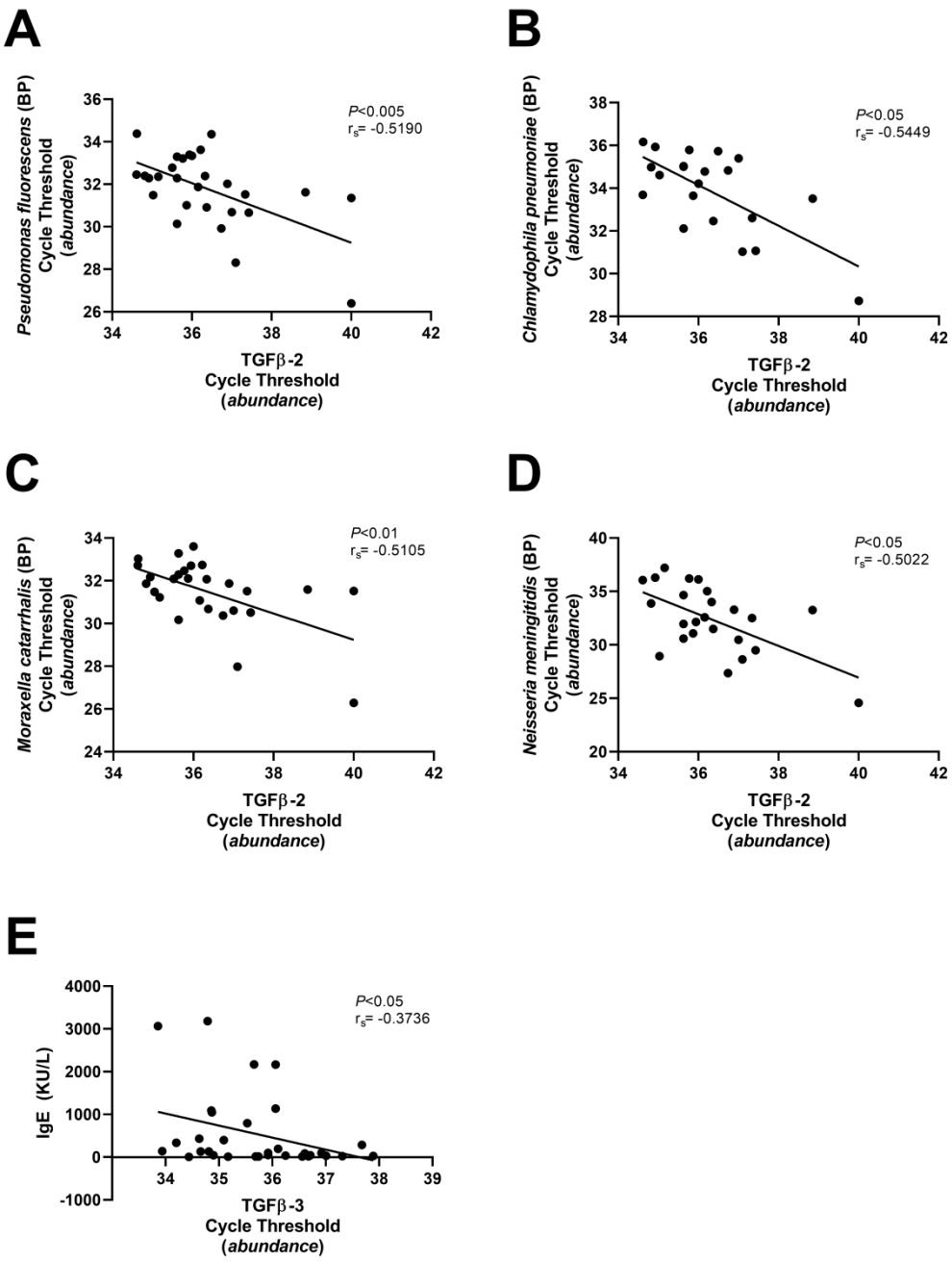


Figure 8. Correlations of brush mRNA detection to BAL BP microbes and patient characteristics. TGFβ-2 negatively correlated with qPCR levels of *Pseudomonas fluorescens* (BP) (*P*<0.005; r_s=-0.5190) (A), *Chlamydophila pneumoniae* (BP) (*P*<0.05; r_s=-0.5449) (B), *Moraxella catarrhalis* (BP) (*P*<0.01; r_s=-0.5105) (C) and *Neisseria meningitidis* (BP) (*P*<0.05; r_s=-0.5022) (D). TGFβ-3 negatively correlated with total levels of blood IgE (KU/L) (*P*<0.05; r_s=-0.3736) (E). n=41.

5. Discussion

Airway epithelium

Due to their anatomical location within the body the lungs possess a unique niche environment for microbial growth. The lungs are directly exposed to the environment and the epithelium is the first line of defence against infection[2,3]. The airway epithelium while offering protection against allergens, microorganisms and environmental stimuli in respiratory conditions such as asthma the inflammatory, immune and regenerative responses of the airway epithelium can be distorted[12,13]. In order to advance the understanding of asthma pathophysiology it is therefore important to further understand the airway epithelium interplay.

Model systems

Model systems to understand the epithelium are widely implemented, the most widespread being *in vitro* cell culture using immortalised cell lines however this system possesses inherent limitations. While primary epithelial cells grown at Air Liquid Interface (ALI) enable the creation of a *in vivo* physiologically relevant model system such a system requires expert knowledge, specialist materials and facilities and the replication of this model system on a large scale can be very costly[6].

Bronchial brush analysis

Therefore it was decided that instead of culturing primary bronchial epithelial cells from the asthma cohort (n=41), at bronchoscopy after the procedure was complete the attending physician would cut the bronchoscope brush approximately 1-2cm above the brush which contained patient cells from the procedure. This brush was then transferred to a 15ml falcon tube containing 5 mls of DNA/RNA Shield (Zymo Research, UK) and the tube was shaken to ensure thorough homogenisation of the DNA/RNA Shield with the bronchoscope brush sample. The tube containing DNA/RNA shield and bronchoscope brush was labelled and stored in a -80^{o}C freezer

until RNA isolation occurred. In doing this it was possible to create a bank of cDNA from the cohort which could be analysed for genes of interest by qRT-PCR using specific human primers with an initial focus on the following genes; β-actin, IL-1β, IL-5 , IL-6 , IL-17F , CCL5, CXCL8 , CCL11, CCL20, EGR1, IFN-γ, TSLP , TGFβ1, TGFβ2 and TGFβ3.

In doing this it was seen that patient bronchial cDNA revealed a patient specific immune profile by qRT-PCR with subsequent significance found to certain patient demographics upon further analysis. As a pilot study results show promise that bronchoscopy brush cDNA analyses could work in tandem with pre-established practices within the research group regarding patient sample collection and processing.

Interleukin 1β (IL-1β)

The pro-inflammatory cytokine IL-1β was detected in 39% of patients bronchial brush cDNA by qRT-PCR. Patient IL-1β levels was observed to correlate negatively with Total Bacteria (CP) (P<0.05; r_s=-0.5206), *Prevotella* (CP) (P<0.05; r_s=-0.5265), *Haemophilus influenzae* (BP) (P<0.01; r_s=-0.7273) and *Rothia* (CP) (P<0.05; r_s=-0.5383). IL-1β is recognised to have a key protective role in the host's defence system by activating responses such as endothelial adhesion, neutrophil recruitment and the activation of cytokines and chemokines. IL-1β has been shown to display a protective effect in several model systems upon bacterial, fungal or viral recognition[14].

Interleukin 5 (IL-5)

IL-5 positively correlated with the percentage count of BAL eosinophils (P<0.05; r_s=0.8407) which is of interest as the cytokine IL-5 is known to be highly specific to the eosinophil lineage, promoting growth and differentiation of eosinophils[15]. Anti-IL5 monoclonal antibody therapy as an adjunct therapy has shown promise for

specific cohorts of asthmatics as by targeting IL-5, selectively inhibiting its interaction with the receptor present on eosinophils resulting in the downregulation of its pathway[16 17]. It is thought that the reduction in eosinophil numbers would in turn reduce exacerbation risk in patients deemed appropriate for such therapy[16].

Interleukin 17 (IL-17)

The IL-17 family of cytokines are known to contribute to inflammatory responses and play a role in antimicrobial resistance in the lungs[18,19]. Research has documented that often the presence of IL-17 in asthma patients can be a sign of asthma severity[19,20]. Within the patient cohort it was seen that qRT-PCR IL-17F presence negatively correlated with the percentage count of BAL lymphocytes ($P<0.05$; $r_s=-0.7029$).

C-C motif chemokine ligand 5 (CCL5)

CCL5, also known as RANTES, was present by qRT-PCR in 98% of the asthma cohort. CCL5, a pro-inflammatory potent chemoattractant cytokine, is known to be produced by epithelial cells upon viral infection. CCL5 has been documented in asthma patient respiratory fluid. It is known to play a role in the recruitment of monocytes, T-cells and eosinophils[21]. Within this asthma cohort CCL5 positively correlated with inhaled corticosteroids (FDP) ($P<0.005$; $r_s=0.4494$), FeNO ($P<0.05$; $r_s=0.4690$) and the percentage count of BAL eosinophils ($P<0.01$; $r_s=0.4344$).

Chemokine (C-X-C motif) ligand 8 (CXCL8)/Interleukin 8 (IL-8)

CXCL8 (IL-8) cytokine is a neutrophil and mast cell chemoattractant which is known in asthma to function in inflammatory cell regulation[22]. *In vitro* experiments in non-diseased airways have shown that high dose inhaled corticosteroids can inhibit

CXCL8 production however in patients with severe persistent asthma poorly controlled by inhaled corticosteroids CXCL8 levels are not reduced[22] Within this asthma cohort 98% of patients tested positive for CXCL8 presence by qRT-PCR. CXCL8 by qRT-PCR detection was seen to positively correlated with qPCR *Bordetella* presence (*P*<0.05; r=0.3549) and negatively correlated with inhaled corticosteroids (FDP) (*P*<0.005; r_s=0.3792) and blood haemoglobin (HB) (g/L) levels (*P*<0.05; r_s=-0.6687).

Early growth response 1 (EGR1)

Early growth response (EGR) 1 is a zinc finger transcription factor, which acts as a transcriptional regulator playing in important role in cell physiology regulation, regulating host cell growth, differentiation and survival. Studies have demonstrated that EGR1 can by triggered into action in the host epithelial cells by environmental stimuli such as bacteria. Bacteria such as *Staphylococcus aureus* have been shown to upregulate EGR1 expression[23]. EGR1 was detectable by qRT-PCR within 98% of patients' bronchoscopy brush cDNA. Within this asthma cohort EGR1 positively correlated with inhaled corticosteroids (FDP) (P<0.01; r_s=0.4216) and *Staphylococcus aureus* (BP) presence by qPCR (P<0.05; r_s=0.4254).

Interferon-γ (IFN-γ)

Interferon (IFN) –γ was detectable in 76% of the asthma patients' cDNA by qRT-PCR. IFN-γ plays a vital role in pathogen recognition and elimination and is responsible for the mediation of a wide variety of biological activities[24]. IFN-γ positively correlated with BAL monocyte percentage counts (*P*<0.05; r_s=0.3932). TSLP negatively correlated with qPCR Total Bacteria (BP) (*P*<0.05; r_s=-0.4471), *Pseudomonas fluorescens* (BP) (*P*<0.05; r_s=-0.4343) and *Prevotella* (BP) (*P*<0.05; r_s=-0.5055)

Thymic stromal lymphopoietin (TSLP)

Thymic stromal lymphopoietin (TSLP), a pleiotropic cytokine, was detectable by qRT-PCR in 59% of patients. TSLP is recognised as an important factor in asthma pathogenesis with higher concentrations detectable within asthmatic lungs. TSLP can be induced by factors such as bacterial and viral infections[25]. TSLP was seen to negatively correlated with qPCR *Veillonella* (BP) (P<0.05; r_s=-0.4566), *Chlamydophila pneumoniae* (BP) (P<0.05; r_s=-0.5583), *Moraxella catarrhalis* (BP)) (P<0.01; r_s=-0.5583), *Neisseria meningitidis* (BP)) (P<0.05; r_s=-0.5519), *Haemophilus influenzae* (BP) (P<0.05; r_s=-0.6878) and *Rothia* (BP) (P<0.05; r_s=-0.5780).

Transforming growth factor-β (TGF-β)

Transforming growth factor (TGF) – β is known to be responsible for the regulation of a number processes such as tissue regeneration and immune reactions.[26]. TGFβ ligand upregulation has been documented in a number of pulmonary diseases including asthma[26].

Within the asthma cohort 93% had detectable TGFβ-1, 68% had detectable TGFβ-2 and 85% had detectable TGFβ-3 by qRT-PCR.Within the cohort TGFβ-1 positively correlated with inhaled corticosteroids (FDP) (P<0.05; r_s=0.4153) and negatively correlated with the percentage of BAL monocytes (P<0.05; r_s=-0.3341), the presence by qPCR of *Pseudomonas fluorescens* (BP) (P<0.05; r_s=-0.3519), *Chlamydophila pneumoniae* (BP) (P<0.05; r_s=-0.4972) and *Neisseria meningitidis* (BP) (P<0.05; r_s=-0.4256). TGFβ-2 positively correlated with BAL eosinophil percentage counts (P<0.05; r_s=0.4244).TGFβ-2 negatively correlated with qPCR levels of *Pseudomonas fluorescens* (BP) (P<0.005; r_s=-0.5190), *Chlamydophila pneumoniae* (BP) (P<0.05; r_s=-0.5449), *Moraxella catarrhalis* (BP) (P<0.01; r_s=-0.5105) and *Neisseria meningitidis* (BP) (P<0.05; r_s=-0.5022). TGFβ-3 negatively correlated with total levels of blood IgE (KU/L) (P<0.05; r_s=-0.3736).

Overall patient bronchial cDNA revealed a patient specific immune profile by qRT-PCR with subsequent significance found to certain patient demographics upon further analysis. The use of bronchial brush cDNA demonstrated a novel experimental method to reveal the real life response of epithelial cells within a well-defined asthma cohort and can provide key insights into the pathophysiology of asthma.

6. Supplementary

Table S1. Table showing the NanoDrop ng/µl, A260/A280, and total ng yield per remaining RNA extracted from the bronchoscope brush.

Patient ID	ng/µl	A260/A280	Total ng yield
AST01	24.8	1.6	1190.4
AST02	22.9	1.7	1099.2
AST04	19.7	1.6	945.6
AST05	23.0	1.5	1104.0
AST06	28.0	1.8	1344.0
AST07	16.9	1.4	811.2
AST08	14.5	1.4	696.0
AST09	22.3	1.6	1070.4
AST10	23.1	1.6	1108.8
AST11	21.9	1.8	1051.2
AST13	20.1	1.6	964.8
AST14	16.1	1.6	772.8
AST15	18.6	1.4	892.8
AST16	19.4	1.7	931.2
AST17	16.0	1.6	768.0
AST18	16.8	1.5	806.4
AST19	19.7	1.6	945.6
AST20	16.1	1.6	772.8
AST21	14.2	1.4	681.6
AST22	19.4	1.5	931.2
AST23	13.8	1.9	662.4
AST25	9.0	1.4	432.0
AST26	24.9	1.8	1195.2
AST28	7.7	1.6	369.6
AST29	5.1	1.2	244.8
AST30	30.7	2.0	1473.6
AST31	19.6	2.1	940.8
AST32	31.2	1.9	1497.6
AST33	13.5	1.9	648.0
AST35	13.1	1.7	628.8
AST36	34.9	1.9	1675.2
AST37	28.8	1.9	1382.4
A61_R	47.3	2.0	2270.4
A15_R	3.0	1.4	144.0
Severe 02	7.6	1.8	364.8
Severe 04	81.9	1.4	3931.2
Severe 05	41.8	2.0	2006.4
Severe 06	16.7	2.0	801.6
Severe 07	56.8	2.1	2726.4
Severe 09	52.4	2.0	2515.2

Table S2. Reverse Transcription PCR 96 well plate layout

	1	2	3	4	5	6	7	8	9	10	11	12
A	AST01	AST02	AST04	AST05	AST06	AST07	AST08	AST09	AST10	AST11	AST13	AST14
B	AST15	AST16	AST17	AST18	AST19	AST20	AST21	AST22	AST23	AST25	AST26	AST28
C	AST29	AST30	AST31	AST32	AST33	AST35	AST36	AST37	A61_R	A15_R	Severe 01	Severe 02
D	Severe 03	Severe 04	Severe 05	Severe 06	Severe 07	Severe 08	Severe 09	Severe 10	Severe 11	Kit control	No RT	Neg RT
E												
F												
G												
H												

Table S3. Primer sequences and corresponding probe numbers used in qRT-PCR analysis. The housekeeping gene used was β-actin.

Gene		**Primer 5'-3'**		**Probe**
β-actin	ACTB	Right 5'-3'	5'-GGATGCCACAGGACTCCA-3'	11
		Left 5'-3'	5'-ATTGGCAATGAGCGGTTC-3'	
Interleukin-1β	IL-1β	Right 5'-3'	5'-TTGGGTAATTTTTGGGATCTACA-3'	78
		Left 5'-3'	5'-CTGTCCTGCGTGTTGAAAGA-3'	
Interleukin-5	IL-5	Right 5'-3'	5'-CCGTCTTTCTTCTCCACACTTT-3'	47
		Left 5'-3'	5'-CACTGAAGAAATCTTTCAGGGAAT-3'	
Interleukin-6	IL-6	Right 5'-3'	5'-CAGTGCTTTAGGAACCCAGAA-3'	16
		Left 5'-3'	5'-AACAATGTACAAGCTTCCAAACAA-3'	
Interleukin-17F	IL-17F	Right 5'-3'	5'-TGGGGTCCCAAGTGACAG-3'	39
		Left 5'-3'	5'-GGCATCATCAATGAAAACCA-3'	
Interleukin-36G	IL-36G	Right 5'-3'	5'-AGTGTTGTATGACTTCCCAAGTTCT-3'	54
		Left 5'-3'	5'-GACTGGTTCATTGCCTCCTC-3'	
Chemokine ligand 5	CCL5	Right 5'-3'	5'-CTTTCGGGTGACAAAGACG-3'	59
		Left 5'-3'	5'-TGCCCACATCAAGGAGTATTT-3'	
Chemokine (C-X-C motif) ligand 8	CXCL8	Right 5'-3'	5'-ATGGTTCCTTCCGGTGGT-3'	72
		Left 5'-3'	5'-GAGCACTCCATAAGGCACAAA-3'	
Chemokine ligand 11	CCL11	Right 5'-3'	5'-GGTGGTTGGGACAGAAGC-3'	5
		Left 5'-3'	5'-ATGAAGGTCTCCGCAGCA-3'	
Chemokine ligand 20	CCL20	Right 5'-3'	5'-TCAAAGTTGCTTGCTGCTTC-3'	39
		Left 5'-3'	5'-GCTGCTTTGATGTCAGTGCT-3'	
Early growth response 1	EGR1	Right 5'-3'	5'-GGTTTGGCTGGGGTAACTG-3'	22
		Left 5'-3'	5'-AGCCCTACGAGCACCTGAC-3'	
Interferon-γ	IFN-γ	Right 5'-3'	5'-TTTGGATGCTCTGGTCATCTT-3'	21
		Left 5'-3'	5'-GGCATTTTGAAGAATTGGAAAG-3'	
Thymic stromal lymphopoietin	TSLP	Right 5'-3'	5'-CCTGAGTAGCATTTATCTGAG-3'	SYBR
		Left 5'-3'	5'-CCGCCTATGAGCAGCCAC-3'	
Transforming growth factor β 1	TGFβ1	Right 5'-3'	5'-TGCTTGAACTTGTCATAGATTTCG-3'	31
		Left 5'-3'	5'-ACTACTACGCCAAGGAGGTCAC-3'	
Transforming growth factor β 2	TGFβ2	Right 5'-3'	5'-AGAGCACCTGGGACTGTCTG-3'	44
		Left 5'-3'	5'-CCTTCTTCCCCTCCGAAAC-3'	
Transforming growth factor β 3	TGFβ3	Right 5'-3'	5'-CGCACACAGCAGTTCTCC-3'	38
		Left 5'-3'	5'-AAGAAGCGGGCTTTGGAC-3'	
G protein coupled receptor 41	GPR41	Right 5'-3'	5'-GGCCACACTCACCAGACC-3'	43
		Left 5'-3'	5'-CACCCACTGTGGTACAAGACC-3'	
G protein coupled receptor 109A	GPR109A	Right 5'-3'	5'-ATGCCTCATAGAAGCCATCC-3'	23
		Left 5'-3'	5'-GTGGGACAATGGGGATAAAA-3'	
G protein coupled receptor 109B	GPR109B	Right 5'-3'	5'-AAGCCAGCAAGGCTCTTATG-3'	62
		Left 5'-3'	5'-TGTATGCCCAGGGGATTTT-3'	
Histone deacetylase 6	HDAC6	Right 5'-3'	5'-GGAACGGCTCCCTTTTTAAT-3'	47
		Left 5'-3'	5'-GTAGGCAGAACCCCCAGTC-3'	

7. References

1. Murphy DM, O'Byrne PM. Recent advances in the pathophysiology of asthma. *Chest.* 2010;137(6):1417-1426.
2. Sullivan A, Hunt E, MacSharry J, Murphy DM. The Microbiome and the Pathophysiology of Asthma. *Respiratory Research.* 2016;17(1):163.
3. Gómez MI, Prince A. Airway epithelial cell signaling in response to bacterial pathogens. *Pediatric pulmonology.* 2008;43(1):11-19.
4. Proud D, Leigh R. Epithelial cells and airway diseases. *Immunological reviews.* 2011;242(1):186-204.
5. Sullivan A, Hunt E, MacSharry J, Murphy DM. 'The Microbiome and the Pathophysiology of Asthma'. *Respiratory Research.* 2016;17(1):163.
6. Stewart CE, Torr EE, Mohd Jamili NH, Bosquillon C, Sayers I. Evaluation of Differentiated Human Bronchial Epithelial Cell Culture Systems for Asthma Research. *Journal of Allergy.* 2012;2012:11.
7. Miller MR, Hankinson J, Brusasco V, et al. Standardisation of spirometry. *The European respiratory journal.* 2005;26(2):319-338.
8. GINA Report. Global strategy for asthma management and prevention. 2018.
9. Juniper EF, O'Byrne PM, Guyatt GH, Ferrie PJ, King DR. Development and validation of a questionnaire to measure asthma control. *The European respiratory journal.* 1999;14(4):902-907.
10. Du Rand IA, Blaikley J, Booton R, et al. British Thoracic Society guideline for diagnostic flexible bronchoscopy in adults: accredited by NICE. *Thorax.* 2013;68 Suppl 1:i1-i44.
11. Hunt EB, Ward C, Power S, et al. The Potential Role of Aspiration in the Asthmatic Airway. *Chest.* 2017;151(6):1272-1278.
12. Crystal RG, Randell SH, Engelhardt JF, Voynow J, Sunday ME. Airway Epithelial Cells. *Proceedings of the American Thoracic Society.* 2008;5(7):772-777.
13. Lambrecht BN, Hammad H. The airway epithelium in asthma. *Nat Med.* 2012;18(5):684-692.
14. Sahoo M, Ceballos-Olvera I, del Barrio L, Re F. Role of the inflammasome, IL-1β, and IL-18 in bacterial infections. *ScientificWorldJournal.* 2011;11:2037-2050.
15. Yang J, Hooper WC, Phillips DJ, Talkington DF. Cytokines in Mycoplasma pneumoniae infections. *Cytokine & Growth Factor Reviews.* 2004;15(2):157-168.
16. Edris A, De Feyter S, Maes T, Joos G, Lahousse L. Monoclonal antibodies in type 2 asthma: a systematic review and network meta-analysis. *Respiratory Research.* 2019;20(1):179.
17. O'Byrne PM. Role of monoclonal antibodies in the treatment of asthma. *Can Respir J.* 2013;20(1):23-25.
18. McGeachy MJ, Cua DJ, Gaffen SL. The IL-17 Family of Cytokines in Health and Disease. *Immunity.* 2019;50(4):892-906.
19. De Luca A, Pariano M, Cellini B, et al. The IL-17F/IL-17RC Axis Promotes Respiratory Allergy in the Proximal Airways. *Cell reports.* 2017;20(7):1667-1680.
20. Ota K, Kawaguchi M, Matsukura S, et al. Potential involvement of IL-17F in asthma. *Journal of immunology research.* 2014;2014:602846.
21. Culley FJ, Pennycook AMJ, Tregoning JS, et al. Role of CCL5 (RANTES) in viral lung disease. *J Virol.* 2006;80(16):8151-8157.
22. John AE, Zhu YM, Brightling CE, Pang L, Knox AJ. Human airway smooth muscle cells from asthmatic individuals have CXCL8 hypersecretion due to increased NF-kappa B p65, C/EBP beta, and RNA polymerase II binding to the CXCL8 promoter. *J Immunol.* 2009;183(7):4682-4692.

23. de Klerk N, Saroj SD, Wassing GM, Maudsdotter L, Jonsson A-B. The Host Cell Transcription Factor EGR1 Is Induced by Bacteria through the EGFR-ERK1/2 Pathway. *Front Cell Infect Microbiol.* 2017;7:16-16.
24. Kak G, Raza M, Tiwari Brijendra K. Interferon-gamma (IFN-γ): Exploring its implications in infectious diseases. *Biomolecular Concepts.* Vol 92018:64.
25. West EE, Kashyap M, Leonard WJ. TSLP: A Key Regulator of Asthma Pathogenesis. *Drug Discov Today Dis Mech.* 2012;9(3-4):10.1016/j.ddmec.2012.1009.1003.
26. Saito A, Horie M, Nagase T. TGF-β Signaling in Lung Health and Disease. *Int J Mol Sci.* 2018;19(8):2460.

Chapter 9

Primary Cell Culture Techniques

Future directions in primary cell culture techniques

Author Contributions: Desmond Murphy, John MacSharry, Chris Ward and Ashley Sullivan were responsible for the study design and concept. Primary cell cultures experiments were performed by Ashley Sullivan with significant contribution from Bernard Verdon and Chris Ward. Transepithelial Electrical Resistance, Ussing Chamber, ELISA and cell stimulation experiments were performed by Bernard Verdon and Ashley Sullivan with guidance from Chris Ward. Periodic Acid – Schiff assays were performed by Ashley Sullivan under the guidance of Bernard Verdon and Jeffery Pearson. Exosome isolation was performed by Ashley Sullivan with significant contribution from Emily Mavin. Transmission electron microscopy was performed by the Electron Microscopy Research Services at Newcastle University. Statistical analysis was performed by all the authors. Analysis and interpretation of data and manuscript preparation and approval were performed by Ashley Sullivan, Bernard Verdon, Emily Mavin, Chris Ward, John MacSharry and Desmond Murphy.

1. Abstract 413
2. Introduction 414
3. Methods 415
3.1. Primary cell culture techniques 415
3.2. Transepithelial electrical resistance (TEER) 418
3.3. Ussing chamber 418
3.4. Human IL-8/CXCL8 ELISA 419
3.5. Periodic acid – Schiff (PAS) assay 421
3.6. Primary epithelial cell LPS stimulation 422
3.7. Exosome isolation 422
3.8. Transmission electron microscopy (TEM) 423
3.9. Statistical analyses 423
4. Results 424
4.1. Primary nasal epithelial cell (PNEC) microscopy 424
4.2. Transepithelial electrical resistance (TEER) 426
4.3. Ussing chamber 427
4.4. Apical and basolateral IL-8 secretion in ALI culture using ELISA technology 435
4.5. NM37 Air Liquid Interface (ALI) primary nasal epithelial cell culture *Pseudomonas aeruginosa* LPS challenge and subsequent IL-8 (pg/ml) levels 437
4.6. Periodic acid – Schiff assay 440
4.7. Transmission electron microscopy (TEM) 442
5. Discussion 445
6. References 449

1. Abstract

Background: The airway epithelium, a key first line defence between the host and the environment, offers protection against allergens, microorganisms and environmental stimuli. However in respiratory disorders such as asthma this defence mechanism can be challenged and the airway epithelial cells, considered to be key controllers of inflammatory, immune and regenerative responses can be distorted. Therefore experiments to further elucidate the interplay of the airway epithelium could prove crucial in understanding the pathophysiology of asthma.

Methods: In order to gain a deeper insight into the various aspects of the airway epithelium a number of experiments were designed including; primary cell culture techniques such as Air Liquid Interface (ALI), Transepithelial Electrical Resistance (TEER), Ussing chamber analysis of barrier function, glycoprotein mucin analysis and electron microscopy analysis for extracellular vesicles.

Results: Primary nasal epithelial cells (PNEC) obtained from nasal polypectomy endoscopic sinus surgery from two asthmatic donors were successfully differentiated in Air Liquid Interface (ALI). Through the successful culturing of PNECs an *in vivo* model system was created. Primary epithelial differentiated ALI cells demonstrate novel insights as to how cell culture can be used for a variety of experiments to reveal the real life response of epithelial cells.

Conclusions: The establishment of protocols to successfully culture primary epithelial cell types offers the possibility of creating an *in vivo* model system using primary bronchial epithelial cells (PBEC) obtained from bronchial brushings from the asthmatic patient cohorts in the future. The airway epithelium can provide key insights into the pathophysiology of asthma and can potentially lead to the development of a system to improve the treatment of asthma.

2. Introduction

Asthma is a chronic inflammatory disease, characterised by airway hyper-responsiveness leading to intermittent, repeated bouts of wheezing, chest tightness, breathlessness and coughing[1,2]. Asthma has a complex heterogeneity with many clinical phenotypes which are affected by numerous factors including environmental factors and susceptibility genes[3-5]. The lungs are directly exposed to the environment and the epithelium is the first line of defence against infection[5,6]. The airway epithelium is a vital component of the inflammatory response of the host and is a major source of cytokines, chemokines and growth factors, produced in order to contain offending microbial insults which are present in the airways[3,5,7].

In order to further investigate the function of the epithelium with regards to asthma it is important to utilise *in vivo* and *in vitro* model systems. While immortalised cell lines are often utilized in respiratory disorders such as cystic fibrosis and asthma there are inherent limitations to such a model system. Primary epithelial cells, while variations exist at the inter- and intra- donor level, have been shown to be the best representation of a model system for epithelial research[8].

The advancement of primary Air Liquid Interface (ALI) cell culture allows for a more physiologically robust system whereby the primary human epithelial cells are fully differentiated in a pseudostratified and polarised manner, with differentiated cells including cilia and goblet cells. This ALI model enables primary epithelial cells to develop transepithelial electrical resistance (TEER) and represents a model system to elucidate the pathogenic mechanisms present in respiratory disorders such as asthma[8]. Such insights could afford the potential to create therapeutic targets for the treatment of the investigated disorder[9].

The establishment of protocols to successfully culture primary epithelial cell types offers the future possibility of creating an *in vivo* model system using primary epithelial cells obtained from the asthmatic patient cohorts. The airway epithelium can provide key insights into the pathophysiology of asthma and can potentially lead to the development of a system to improve the treatment of asthma.

3. Methods

Primary cell culture

All primary cell culture techniques took place under the supervision of Dr Bernard Verdon and Dr Chris Ward at Newcastle University, Newcastle upon Tyne, UK, as part of a European Respiratory Society (ERS) short-term research fellowship.

3.1. Primary cell culture techniques

Primary nasal epithelial cells were cultured from two asthmatic donors; AST01 and NM37 which were obtained under pre-existing ethics at Newcastle University.

AST01 primary cells were obtained from nasal polyps from an asthmatic donor and were frozen as part of a previous study carried out at Newcastle University. The AST01 cryovial was removed from a -150^{o}C cryogenic freezer and placed on dry ice before it was added to a 37^{o}C water bath to defrost. Cells were transferred to a 15ml falcon and the cryovial was washed with Pneuma Cult Ex Plus Basal Medium (Stem Cell Technologies) and added to the 15ml falcon before the total volume was brought to 12ml. Cells were centrifuged at 200g (1100rpm) for 7 minutes at 10^{o}C. The supernatant was removed and the cell pellet was re-suspended with warmed Pneuma Cult Ex Plus Basal Medium. Pneuma Cult Ex Plus Basal Medium was made in 50ml volumes to avoid contamination. Briefly 49ml of the basal medium was added to a falcon tube with 1ml Pneuma Cult 50x supplement and 50µl Hydrocortisone stock solution. T25 flasks (CellStar, Greiner Bio-One) were coated with 1% prepared Type 1 collagen (Pure Col 3mg, Advanced Biomatrix). The re-suspended cells were then transferred to the pre coated T25 flask and maintained in a 37^{o}C, 5% CO_2 incubator.

NM37 primary cells were obtained from a nasal polypectomy endoscopic sinus surgery carried out at the Freeman Hospital, Newcastle upon Tyne, as part of an existing study, with ethics granted. The polyp was placed in a petri dish and any bone fragments were removed using a fine tweezers. The polyp was finely minced using a scalpel and tweezers and was suspended using 2ml of Pneuma Cult Ex plus

Basal Medium. 1 ml of Pneuma Cult Ex Plus Basal Medium was added to the T25 flasks coated with 1% Type 1 collagen, the number of flasks required dependant on polyp size. The minced polyp suspension was transferred to the T25 flasks and Primocin (Invitrogen) was added in accordance with manufacturer's instructions to prevent Gram positive and negative bacterial and fungal growth. Upon microscopy examination rafts of ciliated cells were observed. T25 flasks were maintained in a 37^{o}C, 5% CO_2 incubator. After 2 days the cells were cleaned and fed by adding an additional 2ml of Pneuma Cult Ex Plus Basal Medium to the flask using a Pasteur pipette to forcefully pipette the medium around the larger polyp/cell matter to ensure the matter is explanted to other areas of the flask to ensure further cell growth. The cells also underwent further washes with PBS as larger fragments of polyp explant remained which would compromise the mesh membranes of the transwell plates (Corning, Sigma Aldrich) upon transfer. A Pasteur pipette was used to forcefully pipette the PBS in order to remove any large polyp fragments, and smaller fragments were removed from the cell lawn using a pipette tip attached to a Pasteur pipette to scrap the cell mass explants. This was repeated as many times as necessary to remove the cell mass explants and cells were then fed with 5ml of Pneuma Cult Ex Plus Basal Medium and incubated at 37^{o}C, 5% CO_2.

Once the primary nasal epithelial cells reached 60-70% confluence they were passaged. Briefly this involved detaching the primary cells by adding 2ml (per T25 flask) Trypsin 0.5% EDTA 0.25% (Sigma Aldrich) and incubating until cells are detached. Neutralising media; consisting of RPMI media (Sigma Aldrich) with 10% Fetal Calf Serum –FCS (Sigma Aldrich) and 10% Penicillin Streptomycin – Pen Strep solution was added at 2.5ml per T25 flask. The contents of the flask was then transferred to a 15ml falcon and centrifuged at 200g (1100rpm) for 7 minutes at 10^{o}C, supernatant removed and pellet re-suspended by trituration with 3ml Pneuma Cult Ex Plus Basal Medium. Cell numbers were obtained using a haemocytometer. Trypan Blue (Invitrogen) was utilised to determine cell viability and cell numbers. Healthy cells have ability to exclude Trypan Blue however non-viable cells cannot and are stained blue. Briefly 10µl of cell suspension and 10µl of Trypan Blue was combined in an Eppendorf tube and 10µl of this suspension was

pipetted uniformly into one of the two chambers of the cover-slipped Brightline Haemocytometer (Sigma Aldrich) and 4 squares per chamber are counted under an inverted microscope (Olympus) at 10x objective. When counting a system was employed whereby cells were only counted when they were within the set of 16 squares and on the right hand boundary line of the overall large square. The average cell count from each of the 4 sets of the 16 corner squares was calculated. This value was then multiplied by the volume of the cell suspension, the trypan blue dilution factor of 2 and 10,000. The value obtained from this calculation was then divided by 4 to account for the 4 squares of the haemocytometer chamber counted to obtain the total cells per ml value.

Primary nasal epithelial cells were then transferred to 6.5mm diameter, 0.4µm pore size, 10µm polyester membrane pre-treated with 80µl 1% Type 1 collagen per membrane well, Transwell plates, at a seeding density of 50,000 cells per well.

Primary nasal epithelial cells were also transferred to 12mm diameter, 0.4µm pore, polycarbonate Snapwell membranes (Corning, Sigma Aldrich) pre-treated with 200µl Type 1 collagen, at a seeding density of 150,000 cells per well, ensuring AST01 and NM37 primary cells had 3 Snapwells each for future cell diffusion chamber analysis.

Submerged Transwell cells were fed every two days by removing the apical and basolateral medium and replacing it with 600µl Pneuma Cult Ex Plus Basal Medium on the basolateral side and 100 µl on the apical side. Submerged Snapwell cells were fed in a similar manner with 2ml added to the basolateral side and 500µl added to the apical side.

Once the submerged cells reached confluence they were ready to be taken to Air Liquid Interface (ALI). Pneuma Cult ALI Basal Medium (Stem Cell Technologies) was prepared as follows; 5ml Penicillin Streptomycin (Pen Strep) solution, 2.5ml Hydrocortisone, ALI 5x1ml maintenance supplement (100x), 1ml Heparin and 5ml Supplement V2 was added to 500ml Pneuma Cult ALI Basal Medium and the prepared medium transferred to 50ml aliquots to prevent contamination. The submerged Transwell and Snapwell cells were brought to ALI by removing the apical

medium and debris and then removing the basolateral medium. The cells were subsequently only fed basolaterally with Pneuma Cult ALI Basal Medium with 600µl for Transwell and 2ml for Snapwell inserts, ensuring cells were monitored daily and potential leaks removed as cells became accustomed to ALI.

3.2. Transepithelial electrical resistance (TEER)

Weekly serial transepithelial resistance (TEER) measurements were performed to assess tight junction integrity according to the manufacturer's instructions (STX2 electrodes, EVOM2TM Epithelial Voltohmmeter, World Precision Instruments (WPI)). Pre-warmed PBS was added to the apical compartments of the Transwell membranes at a volume of 100µl and cultures were incubated to equilibrate at 37^{o}C for 20 minutes. TEER measurements were obtained within 1 minute of the removal of the cells from the incubator in order to prevent temperature related resistance changes. TEER measurement was also performed on a 'blank' membrane in order to obtain the background level of resistance which is the subtracted from each measurement. The overall TEER ($\Omega.cm^2$) = (TEER Value – blank value) x culture insert surface area. The apical PBS and basolateral medium was removed and stored at -80^{o}C for future analysis.

3.3. Ussing chamber

The Ussing chamber was developed by Hans Ussing as a technique to measure short circuit current (I_{SC}) as an indicator of net transepithelial ion transport[10]. All experiments were performed using non-perfussing Ussing chambers, controlled by the VCC MC8 (Voltage Current Clamp Multi Channel, Physiologic Instruments, Inc.) In order to offset the potential difference and fluid resistance between the two chambers a 'blank' semi-permeable membrane was mounted into the system prior to each experiment. Differentiated ALI Snapwell cultured cells grown on semi-permeable supports were mounted to the Ussing chambers and bathed apically and basolaterally with 7.5ml Krebs – Henseleit (KH) solution consisting of 25mM NaHCO3, 115mM NaCl, 5mM KCl, 1mM $CaCl_2$, 1mM MgCl with 10mM D glucose

added to the solution on the day of experiments. The Ussing chambers were gassed with 5% CO_2/95% O_2 and maintained at 37^{o}C, pH 7.4. An Ag/AgCL voltage sensing electrode and an Ag wire current sensing electrode were connected to each chamber by agar bridges in 3M KCl. In order to measure short circuit current (I_{SC}) the transepithelial voltage (V_{te}) was clamped and the injected current which was required to maintain V_{te} at 0mV was continuously measured and recorded using the Acquire and Analyze Software (Harvard Apparatus). The injected I_{sc} under these conditions is a direct measure of the net transport across the epithelial cell monolayer. After 20 minutes to allow the system to stabilise, pharmacological reagents of interest were added to the apical or basolateral compartment dependent on the pharmacological reagents mechanism of action, and the resulting effect on I_{sc} was documented. Amiloride (10µM, Torcris) was added to the apical chamber to inhibit ENaC activity, followed by the apical addition of forskolin (10µM, Torcris) a cAMP activator of CFTR and the apical inhibitor $CFTR_{inh}$-172 (20µM, Tocris) and apically added ATP (100µM Sigma Aldrich) a Ca^{2+} mobilising agonist and the trace was allowed to run until the time to half max decay was reached. Ussing chamber traces of short circuit current I_{sc} and transepithelial electrical resistance responses were analysed and the transepithelial electrical resistance calculated using Ohm's Law (I=V/R) and adjusted for the surface area of the membrane (1.13cm^2) to give the transepithelial electrical resistance in $\Omega.cm^2$.

3.4. Human IL-8/CXCL8 ELISA

A sandwich ELISA for Human IL-8/CXCL8 (R&D Systems) was performed on the basolateral medium collected at days 4, 11, 18 and 25 and apical washes collected from when TEERs was performed at days 4, 11, 18 and 25. The basolateral medium samples were diluted 1:5 and 1:10 with Reagent Diluent and the apical washes were diluted 1:10 and 1:20 with Reagent Diluent.

Reagents were prepared as follows; Reagent Diluent: 0.1% BSA, 0.05% Tween 20 in Tris-buffered Saline (20mM Trizma base, 150mM NaCl) pH 7.2-7.4, 0.2µm filtered; Wash Buffer 0.05% Tween-20 in PBS, pH 7.5-7.4; Block Buffer: 1% BSA in PBS, pH

7.2-7.4, filtered; Streptavidin-HRP: 2ml streptavidin conjugated to horseradish-peroxidase diluted to a working concentration of 1:40; Human IL-8 Capture Antibody: 480µg/ml of mouse anti-human IL-8 antibody when reconstituted with 500µl PBS diluted to a working concentration of 1:120 and Human IL-8 Detection Antibody: 1.2µg/ml of biotinylated goat anti-human IL-8 antibody when reconstituted with 1ml Reagent Diluent and diluted to a working concentration of 20ng/ml in Reagent Diluent. Human IL8 Standards were created by reconstituting 100ng/ml of recombinant human IL-8 with 500µl of deionised water, creating a seven point standard curve using two fold serial dilutions in Reagent Diluent to achieve standards 2000pg/ml, 1000pg/ml, 500pg/ml, 250pg/ml, 125pg/ml, 62.5pg/ml and 31.3pg/ml and a blank.

The 96 well microplate (Greiner, Sigma Aldrich) was coated with 100µl diluted Human IL-8 Capture Antibody, the plate was sealed and incubated overnight at room temperature. The wells were then aspirated and washed a total of 3 times with 400µl Wash Buffer per well per wash. The plate was blocked by adding 300µl Block Buffer to each well and the plate was incubated for 1 hour 30 minutes at room temperature. The plate was washed 3 times as previously described and the plate was then ready for sample addition.

100µl of standard or sample was added in duplicate to the 96 well plate, the plate was sealed and incubated for 2 hours at room temperature. The plate underwent 3 washes and 100µl of the diluted Detection Antibody was added to each well and the plate was sealed and incubated for 2 hours. The plate was then washed a total of 4 times before 100µl of the working solution of Streptavidin-HRP was added to each well, the plate was sealed and incubated for 20 minutes at room temperature in a dark environment. The plate was then washed a total of 4 times before 100µl of Substrate Solution was added to each well and the plate was sealed and incubated at room temperature in a dark environment for 20 minutes. 50µl Stop Solution was added to each well and the plate was read immediately using a Tecan i control Infinite 200 Pro (Tecan Trading AG) microplate reader, 450nm absorbance wavelength with a wavelength correction of 570nm.

3.5. Periodic acid – Schiff (PAS) assay

Periodic acid – Schiff (PAS) assay is a staining method used by Dr Ward and Prof. Pearson's group in Newcastle University to detect for glycoprotein. Apical washes from day 4, 11, 18, 25 diluted 1:5 and 1:25 and undiluted basolateral medium from day 4, 11, 18 and 25 were tested in duplicate. Two standard curves from porcine mucin (1mg/ml); 500µg/ml, 250µg/ml, 125µg/ml, 62.5µg/ml, 31.25µg/ml, 15.63µg/ml, 7.82µg/ml, blank and 300µg/ml, 200µg/ml, 100µg/ml, 80µg/ml, 60µg/ml, 40µg/ml, 20µg/ml, blank. Controls included PBS and Pneuma Cult ALI Basal Medium. The PAS assay is dependent on the number of hydroxyl groups in the molecule. The mechanism of the assay is divided into three steps. The initial phase involved the preparation of the basic fuchsin with metabisulphate, which decolourises the solution forming sulphonic acid groups. The apical and basolateral samples (100µl) and mucin standards (100µl) were added to a clear 96 well plate in duplicate. 10µl of periodic acid solution (50%) was mixed with 5ml of 7% acetic acid solution and 10µl of the periodic/acetic acid solution was added to each well and mixed. The next phase involved mixing periodic acid and acetic acid which are then added to the sample which resulted in oxidisation. The oxidation splits the rings between adjacent hydroxyl groups, converting them to adjacent aldehydes. Sodium metabisulphate ($Na_2S_2O_5$) at 16.6mg/ml in Schiffs reagent was prepared. The sample and the reagent were then incubated at 37^{o}C for 45 minutes. After incubation 20µl of the Schiffs reagent was added to each well and mixed. The plate was incubated at room temperature for 30 minutes for colour to develop. Upon addition of the Schiffs reagent the adjacent sulphonic acids group combines with the adjacent aldehydes, producing a red colour. The absorbance was read at 550nm using a spectrophotometer (Tecan i control Infinite 200 Pro Microplate Reader, Tecan Trading AG). The mean of the blank standards were subtracted from the whole plate values. The basolateral medium samples then required the subtraction of the blank basolateral cell medium control (PneumaCult ALI Basal Cell Medium) signal values from the basolateral signals.

3.6. Primary epithelial cell LPS stimulation

Primary nasal epithelial cells NM37 ALI differentiated cultures, 20 transwell membranes in total, were stimulated with various concentrations of *Pseudomonas aeruginosa* LPS. The ALI cell cultures were initially rested for 24 hours in Pneuma Cult Ex Plus Basal medium without growth factors added. 1mg *Pseudomonas aeruginosa* LPS was diluted using PBS with Calcium and Magnesium (Sigma Aldrich) to 0.1µg/ml, 1µg/ml, 10µg/ml and 100µg/ml concentrations. The cells were then challenged by adding 30µl of the LPS concentrations in duplicate and duplicate unstimulated ALI cells acted as a control. One transwell plate with 10 ALI differentiated cell culture membranes was incubated for 24 hours, and the second plate was incubated for 48 hours at 37^{o}C, 5% CO_2. The apical supernatant and the basolateral medium was then removed and Human IL-8/CXCL8 ELISAs (R&D Systems) were performed according to manufacturer's protocols and as described in *Methods 3.4 Human IL-8/CXCL8 ELISA* with apical supernatant samples diluted 1:20 and 1:40 and basolateral medium samples diluted 1:5 and 1:10.

3.7. Exosome isolation

Exosome isolation took place under the guidance of Dr Emily Mavin at Newcastle University, UK. In order to effectively isolate potential exosomes from the apical cell wash and basolateral cell medium from NM37 day 18 cells three spin steps occurred. A 2K spin occurred whereby the supernatant saved from the apical and basolateral cell wash was transferred to centrifuge tubes. These tubes were then spun at 2000g for 20 minutes at 4^{o}C to generate the 2K pellet. After the 2K spin the supernatant was transferred into clean centrifuge tubes, leaving a little media so as to not disturb the pellet. The 10K spin occurred whereby the 2K spin supernatant underwent a 45 minute spin at 10,000g at 4^{o}C. The supernatant was transferred to new ultra-centrifuge tubes (Beckman Coulter, Indianapolis, USA) ensuring the pellet was not disturbed. The 10K pellet was then re-suspended in 100µl PBS taking time to ensure the pellet was fully re-suspended. To obtain a 100K spin sample the supernatant collected from the 10K spin was ultra-centrifuged at 100,000g for 90 minutes at 4^{o}C, ensuring the 10K supernatant samples were fine balanced

beforehand. The supernatant was discarded and the pellet was re-suspended in 100µl PBS to obtain the 100K spin sample. The 10K and 100K spin samples was then stored on ice until the transmission electron microscopy step which was carried out on the same day. For long term storage the samples could also have been stored at -80^{o}C.

3.8. Transmission electron microscopy (TEM)

Transmission electron microscopy was carried out on the isolated apical and basolateral exosome samples with the aid of the Electron Microscopy Research Services at Newcastle University, UK. A negative staining 'on-grid' droplet procedure was implemented. Grids (Glider Grids, Lincolnshire, UK) were filmed with pioloform, carbon coated and plasma etched before use. 5-10µl of the biological material was directly applied from a pipette to the support film on 300- or 400-mesh grids held in forceps. After a few seconds the edge of the droplet was touched to the edge of a hardened filter paper, leaving a thin aqueous film containing the absorbed and freely suspended biological material. A 10µl droplet of 2% aqueous uranyl acetate (Agar Scientific, Stansted, UK) was applied to the grid and after a few seconds the edge of the droplet was touched to the edge of a hardened filter paper, leaving a thin aqueous film. This was allowed to dry completely before transmission electron microscope viewing. The grids were examined on a Hitachi HT7800 transmission electron microscope using an Emsis Xarosa camera with Radius software (Electron Microscopy Research Services, Newcastle University, UK)

3.9. Statistical analyses

Microsoft Excel was used to calculate final absorbance spectrophotometer readings and Ussing chamber readings. Graph Pad Prism 5 and 8 Software was used to perform all statistical analyses and to prepare graphical representation of the data.

4. Results

4.1. Primary nasal epithelial cell (PNEC) microscopy

Primary nasal epithelial cells (PNEC) were first cultured in submerged culture flasks in order to allow the primary nasal epithelial cells to establish and grow. Submerged cells were monitored daily by microscopy in order to avoid possible cell death or infection. Once cells were transferred from the T25 culture flasks to snapwell culture plates or ALI culture membranes monitoring by microscopy continued daily. See figures 1-3 for standard cell growth under submerged conditions.

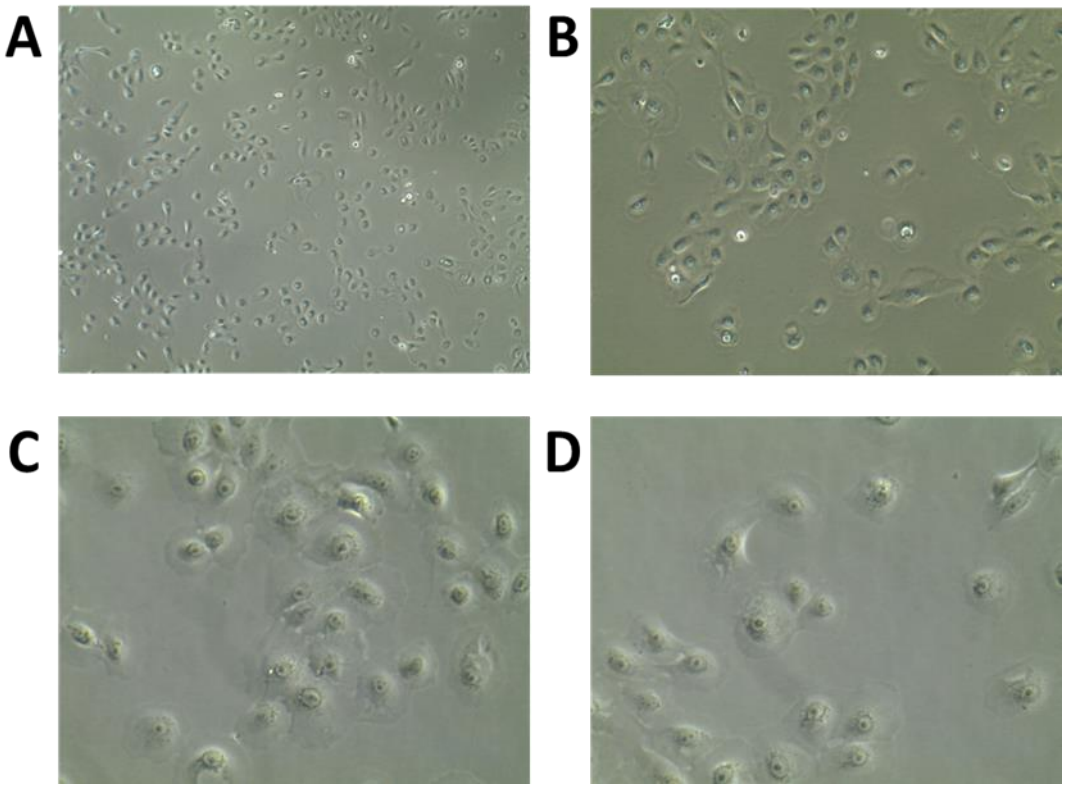


Figure 1 Primary nasal epithelial cell (PNEC) microscopy. AST01 Primary Nasal Epithelial Cells (PNECs) P2 submerged in a T25 flask at 10x magnification (A), 20x magnification (B) and 40x magnification (C-D).

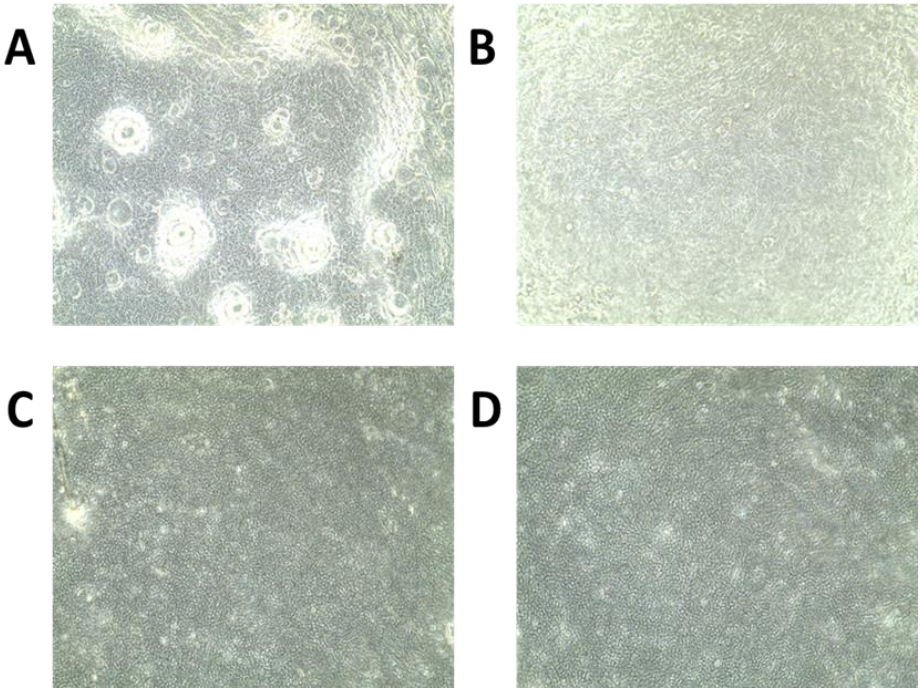


Figure 2. Primary nasal epithelial cell culture in snapwell plates. AST01 Snapwell 1 PNEC culture under submerged growth conditions at 10x magnification (A). AST01 Snapwell 2 PNEC culture under submerged growth.

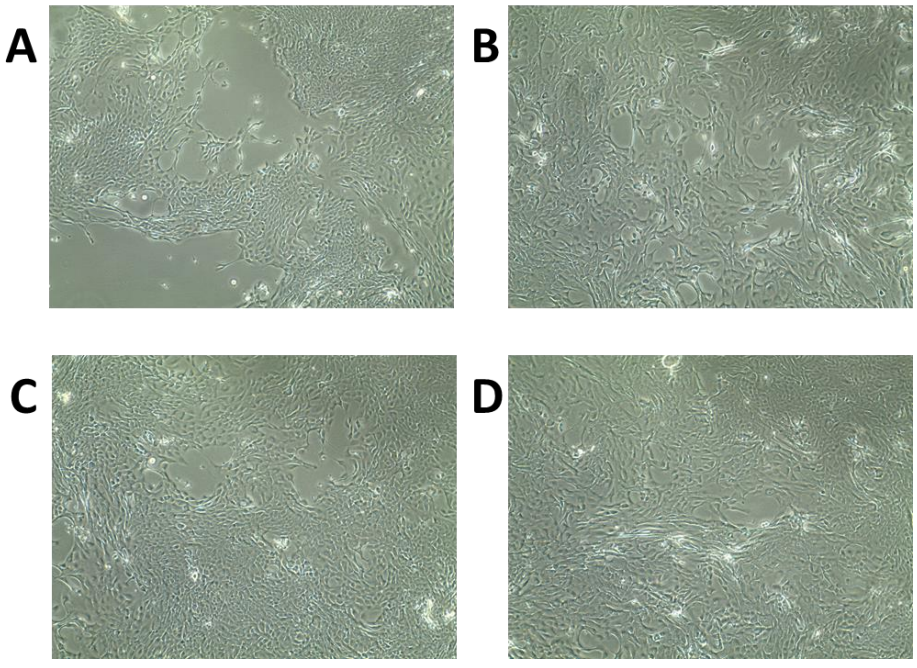


Figure 3. NM37 PNEC Microscopy. Representative images of NM37 PNEC under submerged culture conditions in T25 flasks at 10x magnification (A-D).

4.2. Transepithelial electrical resistance (TEER)

The Transepithelial Electrical Resistance (TEER) of the AST01 and NM37 primary nasal epithelial cell (PNEC) ALI cultures was obtained weekly from 4 Transwells of the AST01 and NM37 cells as a representative measure of the Transepithelial Electrical Resistance (TEER) changes over cell growth time. The TEER measurement was also performed on a 'blank' membrane without seeded cells to provide the background level of resistance and this value was subtracted from each PNEC measurement. The readings were converted to $\Omega.cm^2$ to account for the culture insert surface area. The mean with standard deviation was calculated for each ALI time point to give a representative measure of the Transepitheial Electrical Resistance (TEER) for both AST01 and NM37 donor PNEC's over days at ALI. See figure 4.

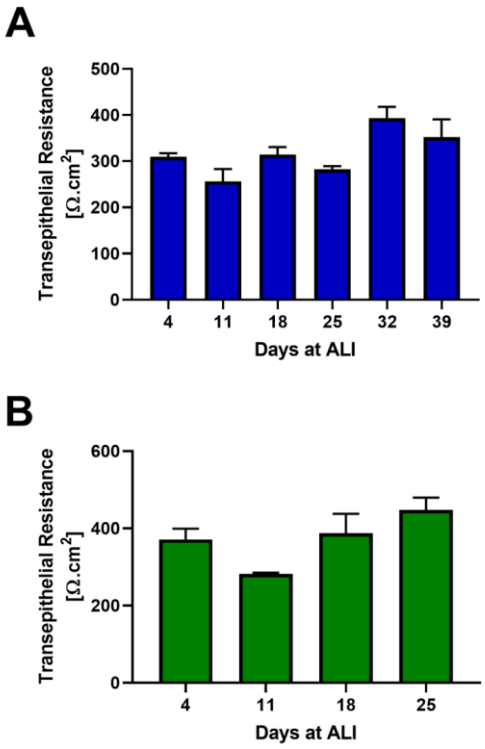


Figure 4. Transepithelial electrical resistance (TEER) measurements of primary nasal epithelial cell (PNEC) cultures at Air Liquid Interface (ALI). Transepithelial electrical resistance (TEER) of PNEC cultures AST01 (A) and NM37 (B) represented as the mean TEER value of the four Transwells monitored per PNEC culture in order to obtain a representative TEER value over days at ALI. n=4.

4.3. Ussing chamber

Ussing chamber experiments are important in order to measure the short circuit current as an indicator of net transepithelial ion transport. For all Ussing chamber experiments carried out primary nasal epithelial cells ALI differentiated cultures at day 29 from donors AST01 and NM37 underwent the following conditions. Amiloride (10μM) was added apically to inhibit ENaC. Forskolin (10μM) was apically added to act as a cAMP activator of CFTR, which was subsequently inhibited by the apical addition of $CFTR_{inh}$-172 (20μM). Finally ATP, a calcium mobilising agonist was added to the apical side and the Ussing trace continued until the time to half max decay was reached.

AST01 day 29 snapwell 1 cells had an initial transepithelial voltage (V_{TE}) of -5.6mV and an initial short circuit current (I_{sc}) of 11.6μA. The change in current in response to the applied 5mV step voltage returned a transepithelial resistance (R_{TE}) of 483Ω.cm^2. Amiloride addition resulted in a -3.3μA decrease. Forskolin addition resulted in a peak of 1.7μA in 89 seconds. $CFTR_{inh}$-172 addition resulted in a decrease of -6μA in the Ussing chamber trace. ATP addition resulted in a trace peak of 6.5μA in 108 seconds. The ATP time for half max decay (t50) was 6.5 minutes. See figure 5.

AST01 day 29 snapwell 2 cells had an initial transepithelial voltage (V_{TE}) of -5.1mV and an initial short circuit current (I_{sc}) of 11.5μA. The change in current in response to the applied 5mV step voltage returned a transepithelial resistance (R_{TE}) of 444Ω.cm^2. Amiloride addition resulted in a -2.6μA decrease. Forskolin addition resulted in a peak of 3.2μA in 111 seconds. $CFTR_{inh}$-172 addition resulted in a decrease of -6.2μA in the Ussing chamber trace. ATP addition resulted in a trace peak of 3.9μA in 117 seconds. The ATP time for half max decay (t50) was 8.6 minutes. See figure 6.

AST01 day 29 snapwell 3 cells had an initial transepithelial voltage (V_{TE}) of -20.8mV and an initial short circuit current (I_{sc}) of 38μA. The change in current in response to the applied 5mV step voltage returned a transepithelial resistance (R_{TE}) of 547Ω.cm^2. Amiloride addition resulted in a -30.7μA decrease. Forskolin addition

resulted in a peak of 19.5µA in 210 seconds. $CFTR_{inh}$-172 addition resulted in a decrease of -20.4µA in the Ussing chamber trace. ATP addition resulted in a trace peak of 7.2µA in 108 seconds. The ATP time for half max decay (t50) was 8 minutes. See figure 7.

NM37 day 29 snapwell 1 cells had an initial transepithelial voltage (V_{TE}) of -20.2mV and an initial short circuit current (I_{sc}) of 57.7µA. The change in current in response to the applied 5mV step voltage returned a transepithelial resistance (R_{TE}) of 350Ω.cm^2. Amiloride addition resulted in a -51.2µA decrease. Forskolin addition resulted in a peak of 14.8µA in 142 seconds. $CFTR_{inh}$-172 addition resulted in a decrease of -23µA in the Ussing chamber trace. ATP addition resulted in a trace peak of 27µA in 106 seconds. The ATP time for half max decay (t50) was 5.9 minutes. See figure 8.

NM37 day 29 snapwell 2 cells had an initial transepithelial voltage (V_{TE}) of -7.5mV and an initial short circuit current (I_{sc}) of 38µA. The change in current in response to the applied 5mV step voltage returned a transepithelial resistance (R_{TE}) of 197Ω.cm^2. Amiloride addition resulted in a -23.7µA decrease. Forskolin addition resulted in a peak of 15.8µA in 210 seconds. $CFTR_{inh}$-172 addition resulted in a decrease of -30.6µA in the Ussing chamber trace. ATP addition resulted in a trace peak of 30.4µA in 66 seconds. The ATP time for half max decay (t50) was 7.2 minutes. See figure 9.

NM37 day 29 snapwell 3 cells had an initial transepithelial voltage (V_{TE}) of -16.5mV and an initial short circuit current (I_{sc}) of 54µA. The change in current in response to the applied 5mV step voltage returned a transepithelial resistance (R_{TE}) of 306Ω.cm^2. Amiloride addition resulted in a -39.7µA decrease. Forskolin addition resulted in a peak of 17.7µA in 174 seconds. $CFTR_{inh}$-172 addition resulted in a decrease of -31.4µA in the Ussing chamber trace. ATP addition resulted in a trace peak of 32.7µA in 78 seconds. The ATP time for half max decay (t50) was 5.6 minutes. See figure 10.

Overall, both AST01 and NM37 cells displayed barrier function and confluence.

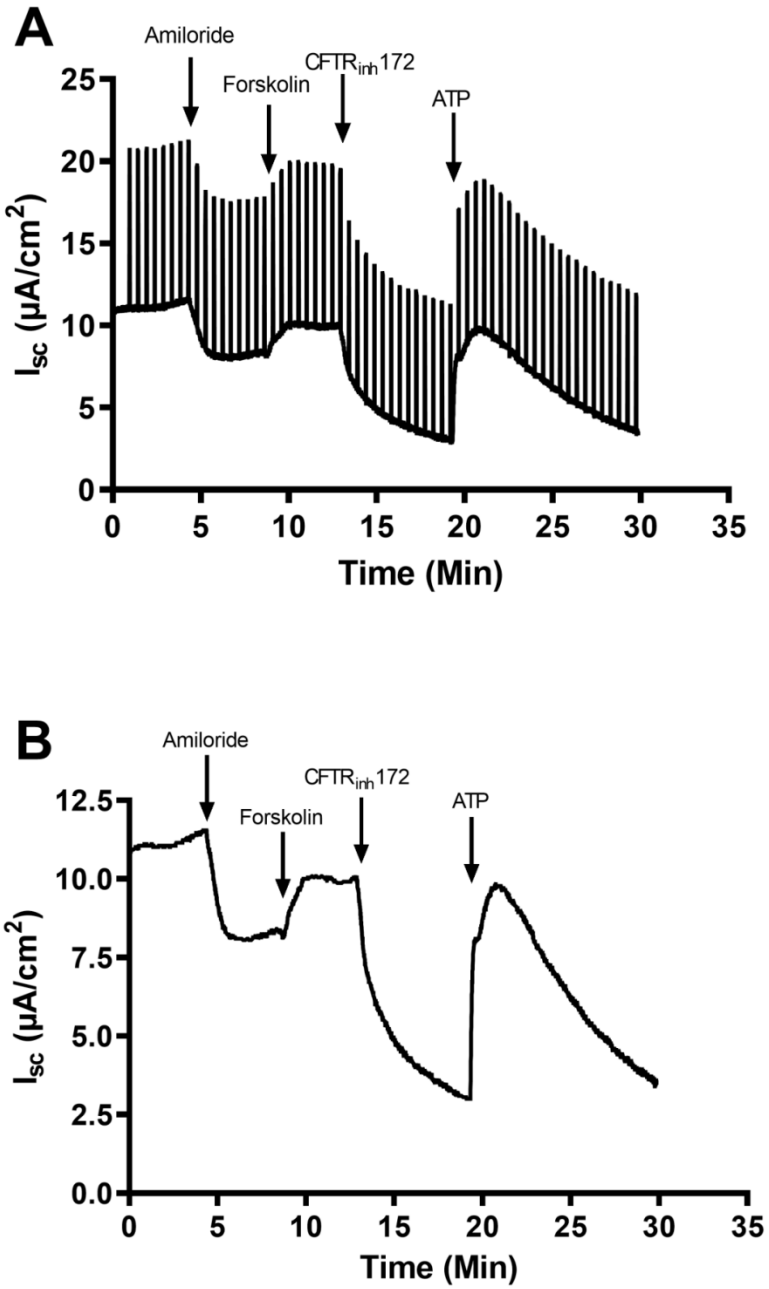


Figure 5. Ussing chamber analysis of AST01 PNEC cells. AST01 day 29 snapwell 1 cells had an initial transepithelial voltage (V_{TE}) of -5.6mV and an initial short circuit current (I_{sc}) of 11.6µA. The change in current in response to the applied 5mV step voltage returned a transepithelial resistance (R_{TE}) of 483Ω.cm^2. Amiloride addition resulted in a -3.3µA decrease. Forskolin addition resulted in a peak of 1.7µA in 89 seconds. $CFTR_{inh}$-172 addition resulted in a decrease of -6µA in the Ussing chamber trace. ATP addition resulted in a trace peak of 6.5µA in 108 seconds. The ATP time for half max decay (t50) was 6.5 minutes.

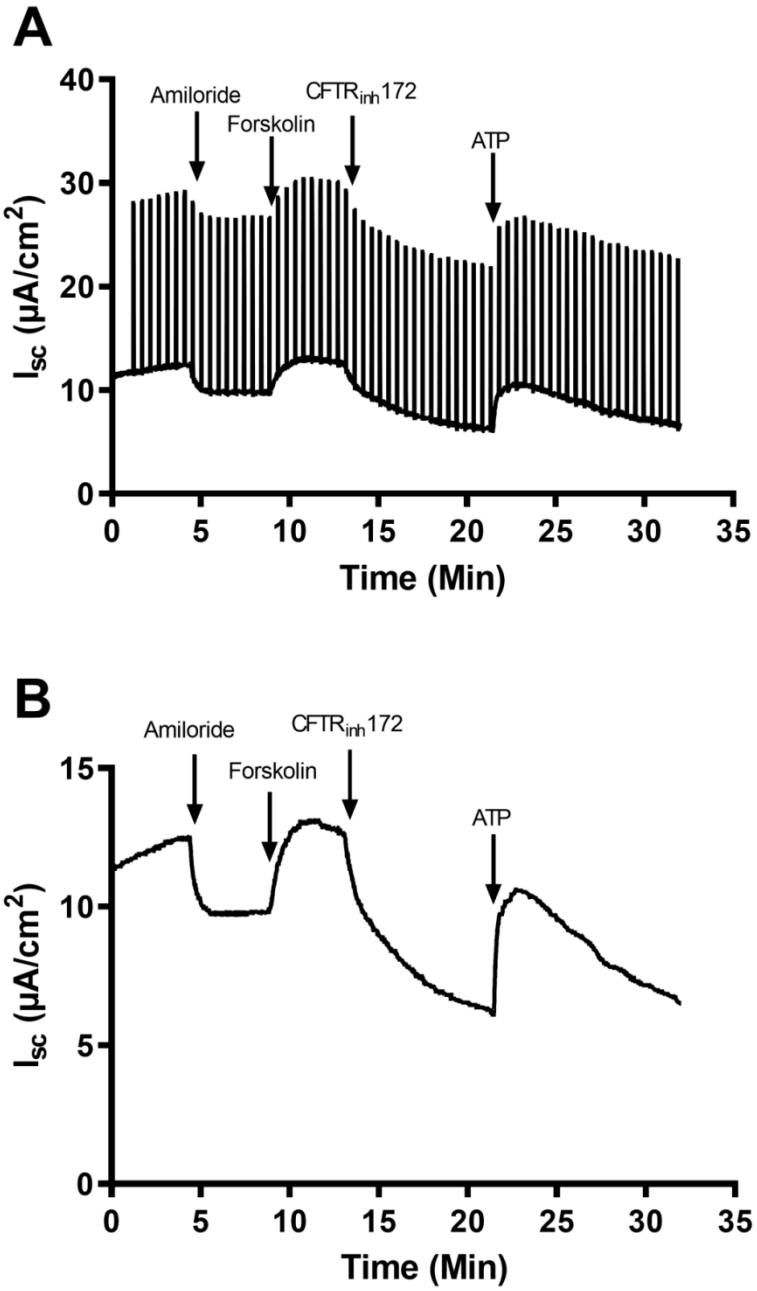


Figure 6. Ussing chamber analysis of AST01 PNEC cells. AST01 day 29 snapwell 2 cells had an initial transepithelial voltage (V_{TE}) of -5.1mV and an initial short circuit current (I_{sc}) of 11.5µA. The change in current in response to the applied 5mV step voltage returned a transepithelial resistance (R_{TE}) of 444Ω.cm^2. Amiloride addition resulted in a -2.6µA decrease. Forskolin addition resulted in a peak of 3.2µA in 111 seconds. $CFTR_{inh}$-172 addition resulted in a decrease of -6.2µA in the Ussing chamber trace. ATP addition resulted in a trace peak of 3.9µA in 117 seconds. The ATP time for half max decay (t50) was 8.6 minutes.

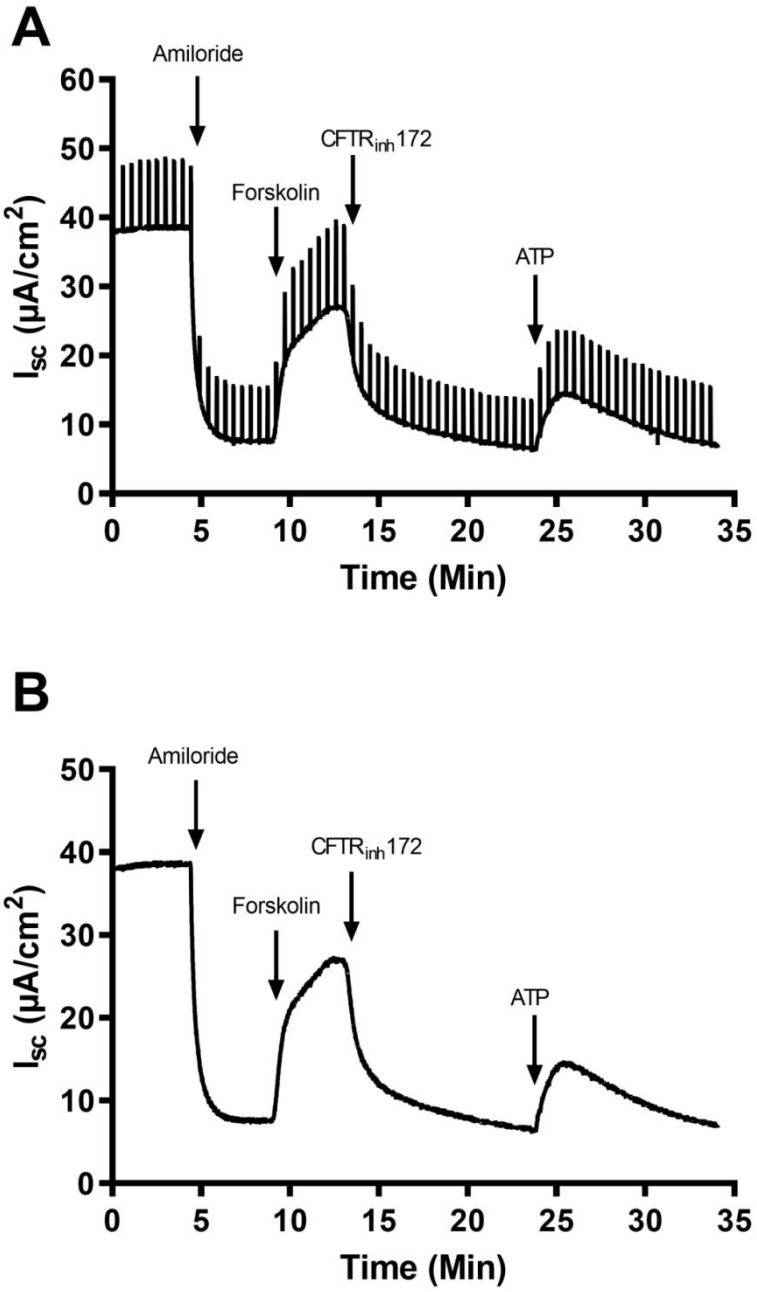


Figure 7. Ussing chamber analysis of AST01 PNEC cells. AST01 day 29 snapwell 3 cells had an initial transepithelial voltage (V_{TE}) of -20.8mV and an initial short circuit current (I_{sc}) of 38µA. The change in current in response to the applied 5mV step voltage returned a transepithelial resistance (R_{TE}) of 547Ω.cm^2. Amiloride addition resulted in a -30.7µA decrease. Forskolin addition resulted in a peak of 19.5µA in 210 seconds. $CFTR_{inh}$-172 addition resulted in a decrease of -20.4µA in the Ussing chamber trace. ATP addition resulted in a trace peak of 7.2µA in 108 seconds. The ATP time for half max decay (t50) was 8 minutes.

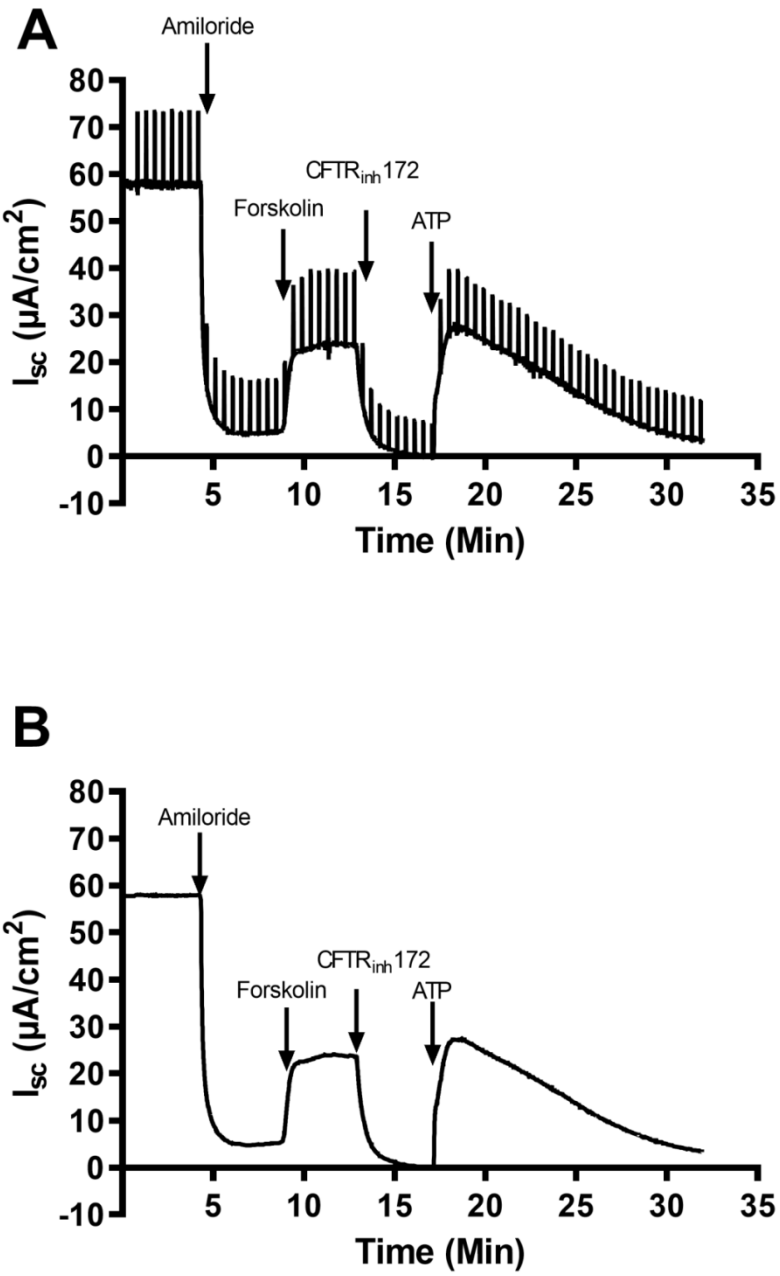


Figure 8. Ussing chamber analysis of NM37 PNEC cells. NM37 day 29 snapwell 1 cells had an initial transepithelial voltage (V_{TE}) of -20.2mV and an initial short circuit current (I_{sc}) of 57.7µA. The change in current in response to the applied 5mV step voltage returned a transepithelial resistance (R_{TE}) of 350Ω.cm^2. Amiloride addition resulted in a -51.2µA decrease. Forskolin addition resulted in a peak of 14.8µA in 142 seconds. $CFTR_{inh}$-172 addition resulted in a decrease of -23µA in the Ussing chamber trace. ATP addition resulted in a trace peak of 27µA in 106 seconds. The ATP time for half max decay (t50) was 5.9 minutes.

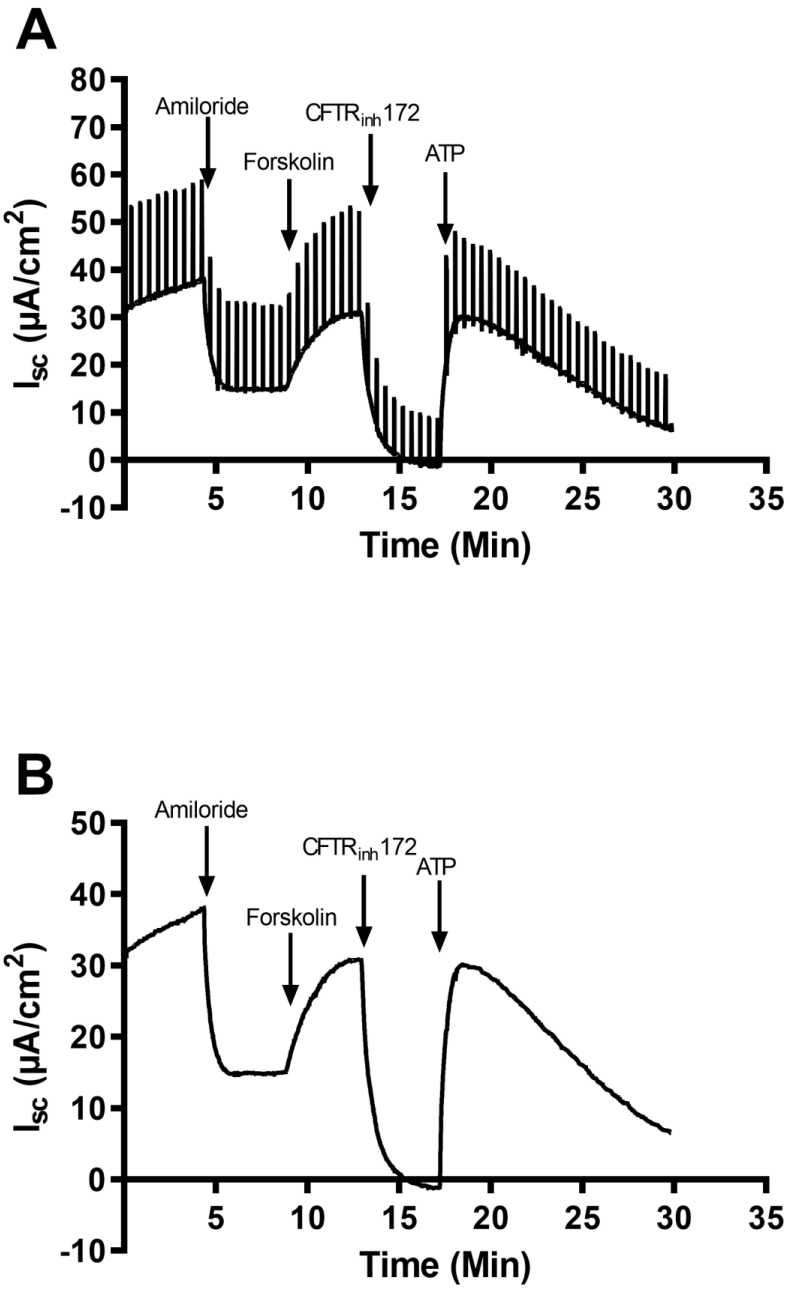


Figure 9. Ussing chamber analysis of NM37 PNEC cells. NM37 day 29 snapwell 2 cells had an initial transepithelial voltage (V_{TE}) of -7.5mV and an initial short circuit current (I_{sc}) of 38µA. The change in current in response to the applied 5mV step voltage returned a transepithelial resistance (R_{TE}) of 197Ω.cm^2. Amiloride addition resulted in a -23.7µA decrease. Forskolin addition resulted in a peak of 15.8µA in 210 seconds. $CFTR_{inh}$-172 addition resulted in a decrease of -30.6µA in the Ussing chamber trace. ATP addition resulted in a trace peak of 30.4µA in 66 seconds. The ATP time for half max decay (t50) was 7.2 minutes.

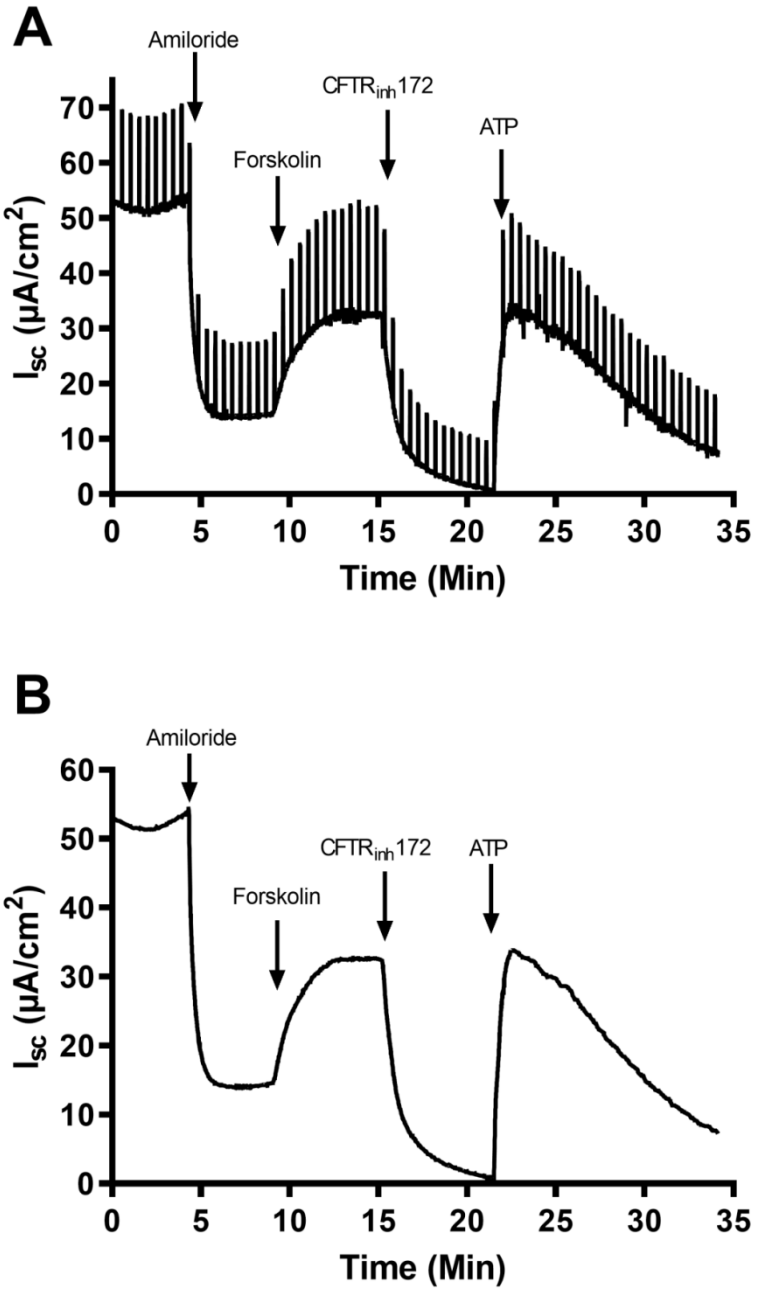


Figure 10. Ussing chamber analysis of NM37 PNEC cells. NM37 day 29 snapwell 3 cells had an initial transepithelial voltage (V_{TE}) of -16.5mV and an initial short circuit current (I_{sc}) of 54µA. The change in current in response to the applied 5mV step voltage returned a transepithelial resistance (R_{TE}) of 306Ω.cm^2. Amiloride addition resulted in a -39.7µA decrease. Forskolin addition resulted in a peak of 17.7µA in 174 seconds. $CFTR_{inh}$-172 addition resulted in a decrease of -31.4µA in the Ussing chamber trace. ATP addition resulted in a trace peak of 32.7µA in 78 seconds. The ATP time for half max decay (t50) was 5.6 minutes.

4.4. Apical and basolateral IL-8 secretion in ALI culture using ELISA technology

Absorbance was read at 450nm using a Tecan i control microplate reader to obtain the dual wavelength measurement with measurement wavelength, the dual wavelength measurement with reference wavelength and the calculated difference between the measurement and the reference measurement. This calculated difference was then adjusted to ensure the blank controls are corrected for by subtracting the mean of the two blank controls from the plate. These values were then log transformed to obtain the mean log value of the absorbance readings. The log values were interpolated using a sigmoidal dose response variable slope and the log X interpolated readings were converted to their anti-log and the dilution factor was accounted to reveal the pg/ml IL-8 value per apical and basolateral samples from NM37 donor ALI cells.

The calculated mean apical and basolateral IL-8 pg/ml per days at ALI were analysed and significance was found between basolateral IL-8 levels at day 4 compared to day 11 ($P<0.005$), day 18 ($P<0.0005$) and day 25 ($P<0.0001$) and also with apical IL-8 levels at day 4 compared to day 11 ($P<0.05$), day 18 ($P<0.05$) and day 25 ($P<0.05$). See figure 11 A-B. Apical IL-8 secretion was also observed to be consistently higher than basolateral secretions.

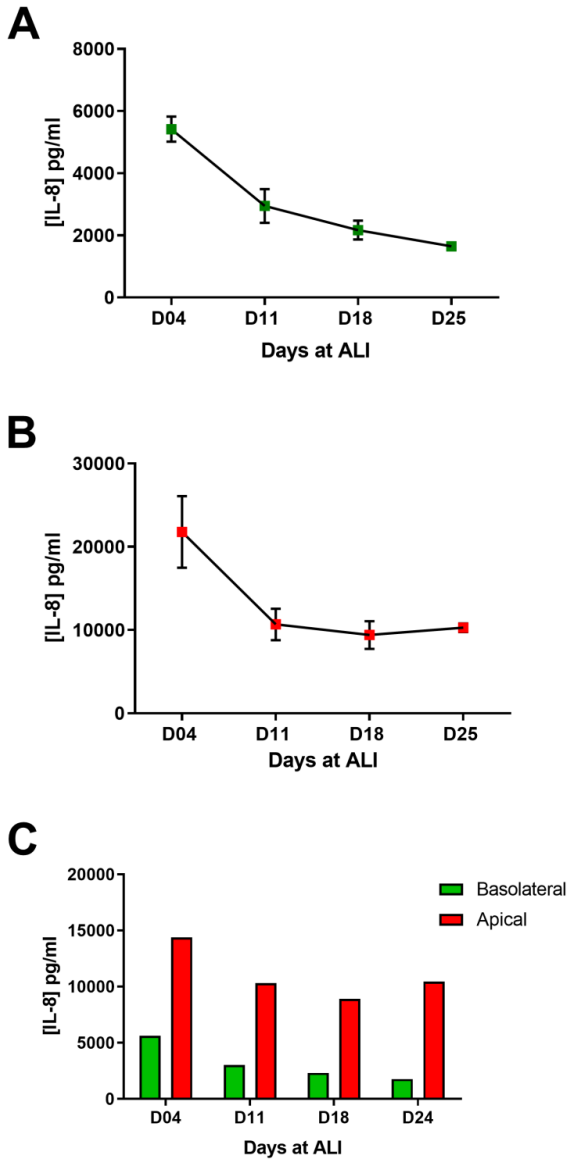


Figure 11. IL-8 secretion in the apical and basolateral compartments of NM37 cells at ALI. IL-8 levels were quantified in basolateral medium and apical TEER washes from NM37 donor PNEC cultures at ALI. A significant difference was observed between the mean IL-8 values at day 4 compared to the mean of day 11 ($P<0.005$), day 18 ($P<0.0005$) and day 25 ($P<0.0001$) using ordinary one-way ANOVA with Tukey analysis (A). The mean IL-8 levels were significantly different at day 4 compared to the mean IL-8 levels at day 11 ($P<0.05$), day 18 ($P<0.05$) and day 25 ($P<0.05$) (B). Apical wash samples had higher levels of IL-8 in comparison to basolateral IL-8 levels (C). n=4.

4.5. NM37 Air Liquid Interface (ALI) primary nasal epithelial cell culture *Pseudomonas aeruginosa* LPS challenge and subsequent IL-8 (pg/ml) levels.

NM37 primary nasal epithelial cell culture challenged with 0.1µg/ml, 1µg/ml, 10µg/ml and 100µg/ml *Pseudomonas aeruginosa* derived LPS per transwell ALI culture (n=2) in duplicate carried out over two time points, 24 hours and 48 hours before the basolateral medium was collected and the apical cells were washed with PBS containing Ca^+ and Mg^+ before collection. The Human IL-8/CXCL8 ELISA (R&D Systems) once complete was analysed as previously described in *Results 4.4. Apical cell wash and basolateral cell medium IL-8 ELISA*.

No statistically significant difference was observed in the basolateral and apical IL-8 levels post 24 hour (Figure 12) and 48 hour (Figure 13) LPS stimulation using ordinary one-way ANOVA with Dunnett multiple comparisons test to compare the mean of each column with the mean of the control column.

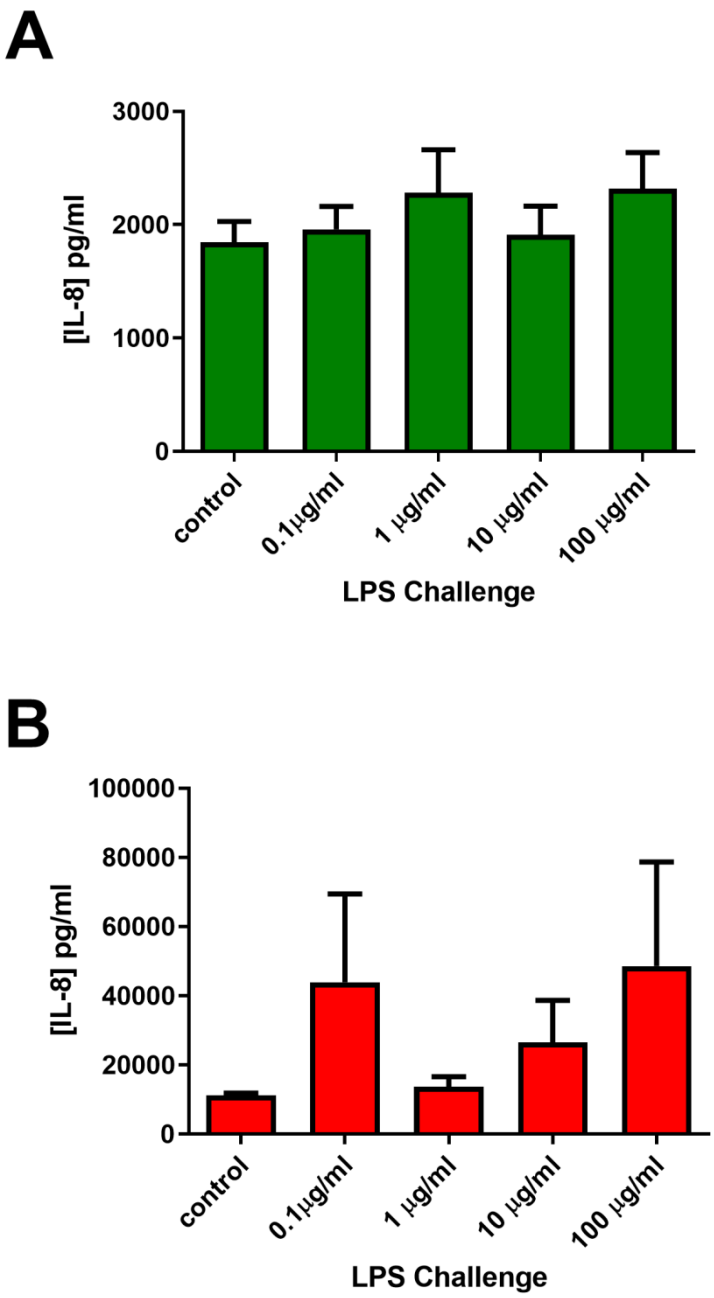


Figure 12. IL-8 secretion of ALI culture following LPS challenge. NM37 Transwell cultures at ALI were stimulated with *Pseudomonas aeruginosa* derived LPS and IL-8 levels after 24 hours of LPS stimulation were analysed. No statistically significant difference was observed in the basolateral (A) and apical (B) IL-8 levels post LPS stimulation using ordinary one-way ANOVA with Dunnett multiple comparisons test. n=2.

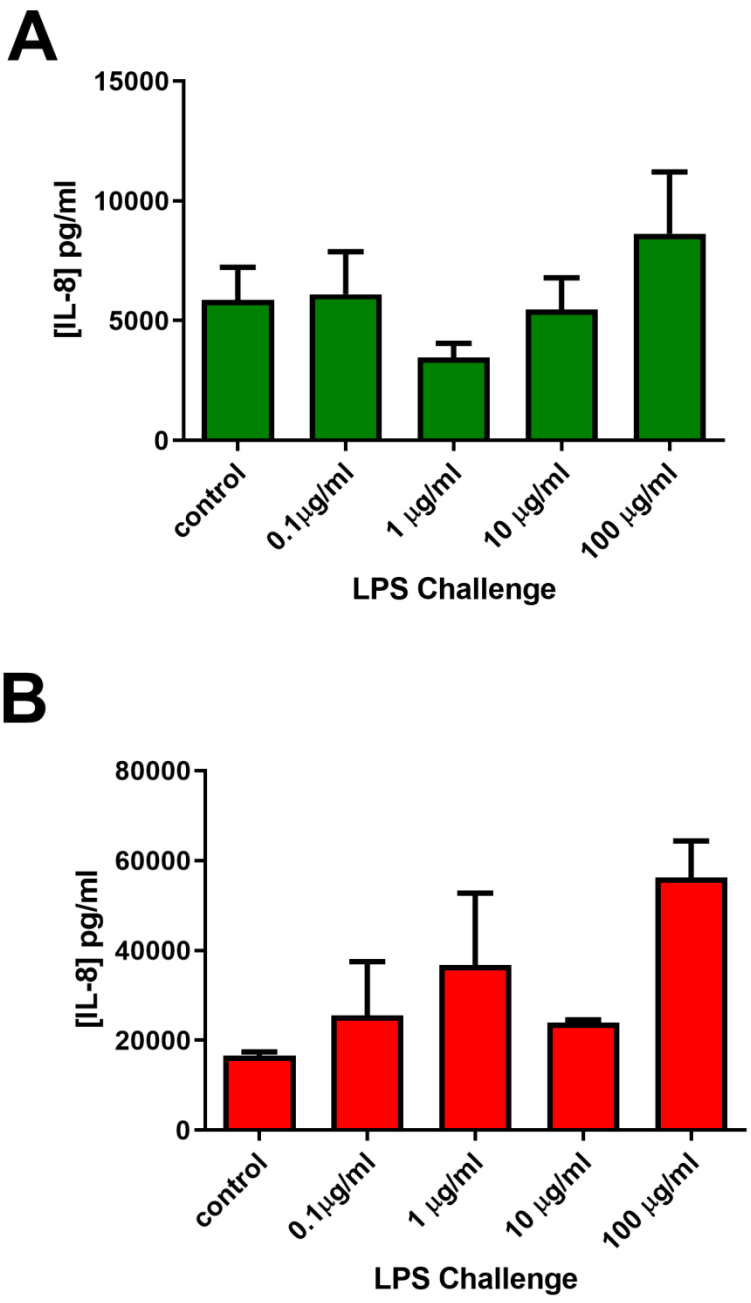


Figure 13. IL-8 secretion of ALI culture following LPS challenge. NM37 Transwell cultures at ALI were stimulated with *Pseudomonas aeruginosa* derived LPS and IL-8 levels after 48 hours of LPS stimulation were analysed. No statistically significant difference was observed in the basolateral (A) and apical (B) IL-8 levels post LPS stimulation using ordinary one-way ANOVA with Dunnett multiple comparisons test. n=2.

4.6. Periodic acid – Schiff assay

To assess mucus secretion by the PNEC cells at ALI a Periodic acid –Schiff assay was performed. The mean value of the blank standards was subtracted from the plate absorbance values and an additional subtraction of the mean control blank, which contained cell medium, from the basolateral absorbance readings was carried out in order to compensate for the glucose contained in cell medium which can give a positive PAS signal. The standard curve was then utilised using linear regression analysis to calculate the interpolated glycoprotein (μg/ml) values for the apical and basolateral duplicate samples using Graph Pad Prism Software and the mean of the interpolated glycoprotein (μg/ml) values was obtained (figure 14 A). The dilution factors of 5 and 25 were then corrected for with regards to the apical samples. The basolateral and apical glycoprotein (μg/ml) levels at ALI day 4, 11, 18 and 25 were investigated (figure 14 B-C). A significant difference in glycoprotein (μg/ml) levels in ALI NM37 cell washes at day 25 in comparison to day 4 (P<0.0001), day 11 (P<0.0001) and day 18 (P<0.0001) using an Ordinary one-way ANOVA with a Tukey's multiple comparisons test to compare the mean of each column with the mean of every other column was observed (figure 14 C). When apical and basolateral mean glycoprotein (μg/ml) values were compared it was observed that the apical wash samples had higher glycoprotein (μg/ml) detectable, demonstrating apical mucus secretion reaching a maximum at day 25 of ALI culture. n=2 in duplicate.

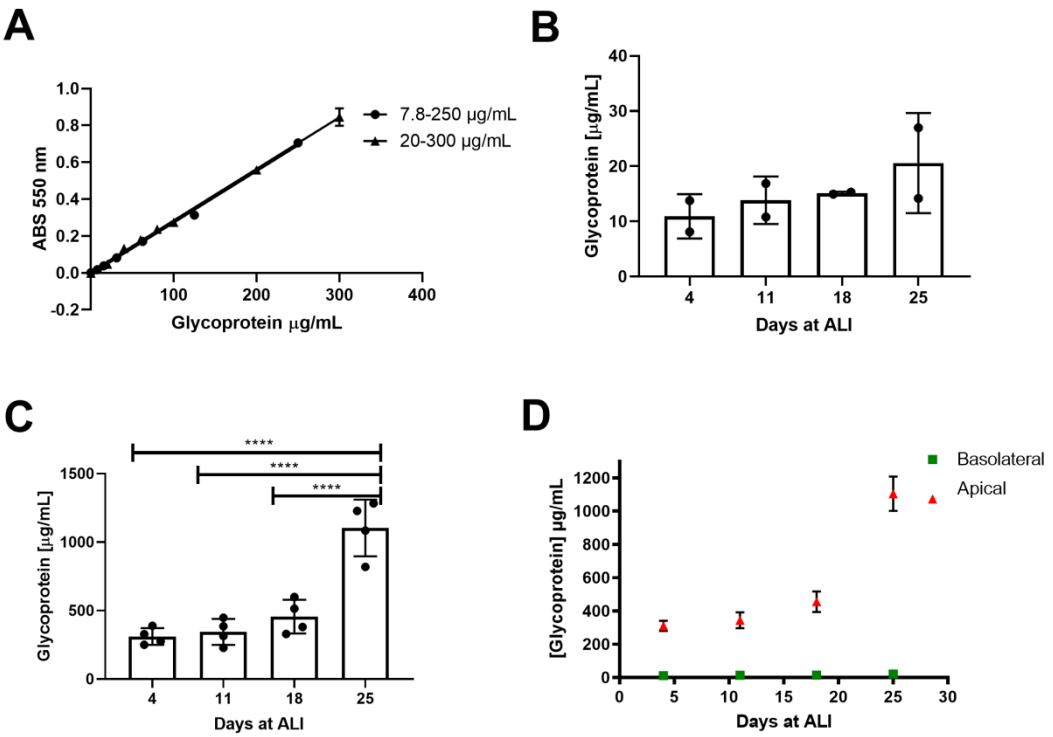


Figure 14. Analysis of mucus secretion within PNEC cells at ALI using a Periodic acid – Schiff assay. Porcine mucin standard curves were utilised to calculated glycoprotein (µg/ml) in basolateral and apical samples (A). Glycoprotein (µg/ml) in basolateral samples revealed no significant difference with respect to time of sampling (B). However apical (C) samples at ALI day 4, 11, 18 and 25 revealed a significant difference with respect to apical wash samples at ALI day 25 and ALI day 4, 11 and 18 using an Ordinary one-way ANOVA and Tukey multiple comparisons test. There was an observable higher level of glycoprotein (µg/ml) in apical wash samples in comparison to basolateral samples (D). n=2, in duplicate.

4.7. Transmission electron microscopy (TEM)

Transmission electron microscopy (TEM) revealed the presence of exosomes within the apical cell wash post exosome isolation. See figure 15 and figure 16. Exosome isolation was also performed on the basolateral cell medium and transmission electron microscopy (TEM) was utilised to investigate if it was possible to identify exosomes within the basolateral cell medium. However due to the presence of cell medium after exosome isolation it was not possible to clearly view exosomes by transmission electron microscopy (TEM) as the presence of the cell medium created a cloudy appearance upon visualisation by transmission electron microscopy. Therefore in order to investigate potential exosomes within the basolateral cell medium further wash steps would be required during the exosome isolation procedure

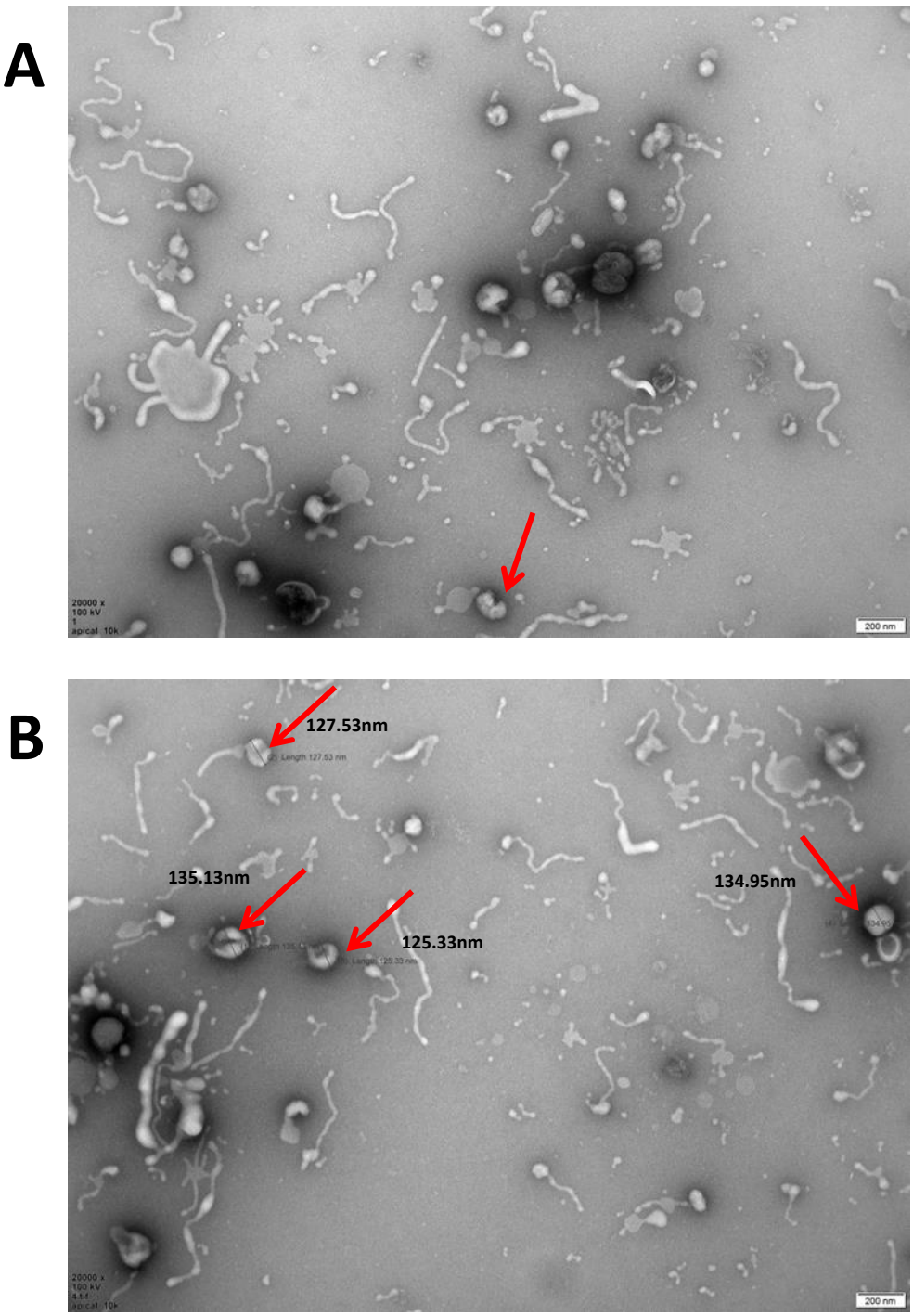


Figure 15. Apical exosome secretion. Electron microscopy images of the apical PBS obtained post TEER measurement from day 18 ALI NM37 cells isolated from nasal polyps. The apical wash was centrifuged at 10.000g for exosome pellet isolation (A-B). Red arrows indicate representative exosome presence at 20000x magnification (A-B) with exosome size highlighted in (B).

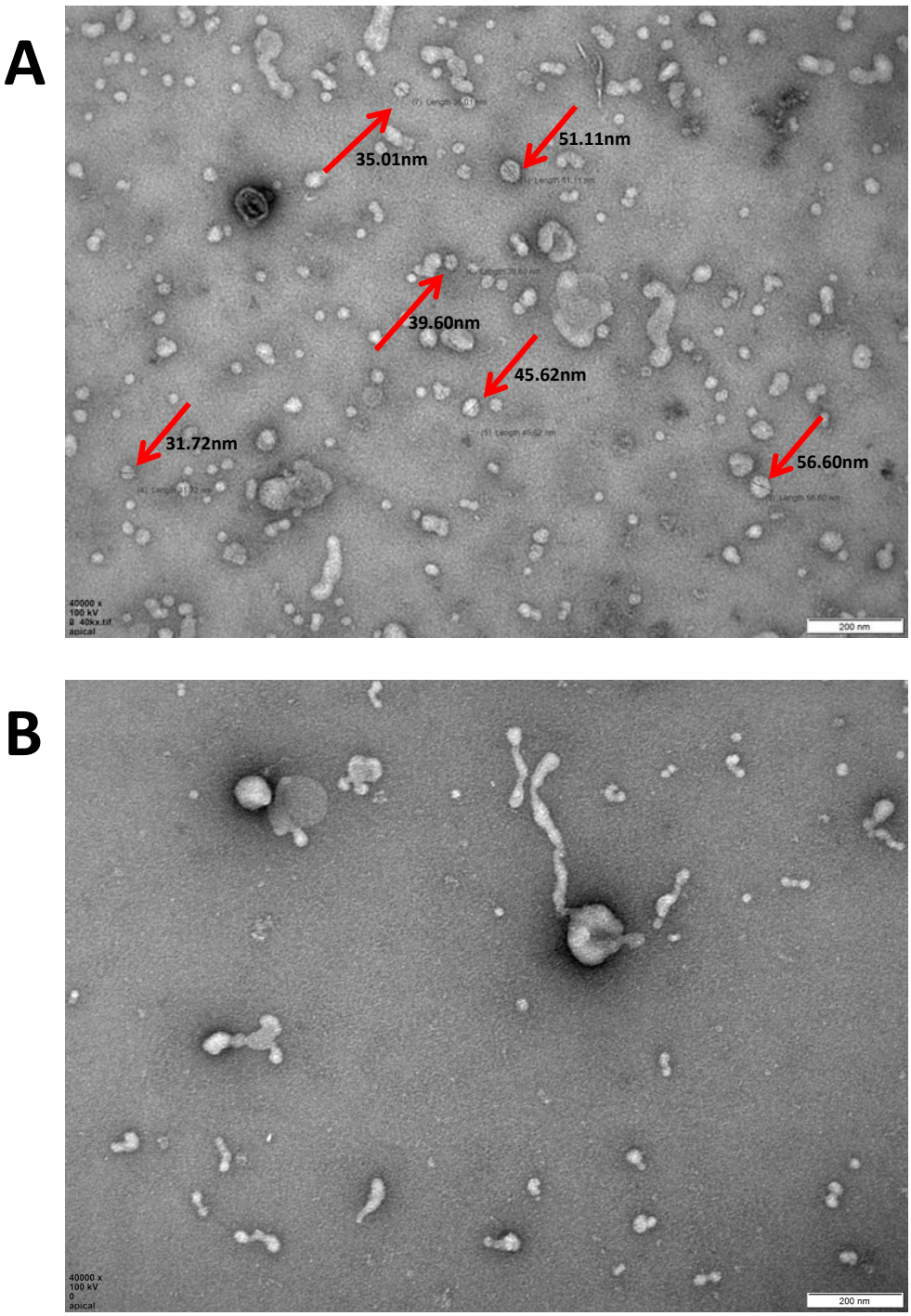


Figure 16. Apical exosome secretion. Electron microscopy images of exosome presence in apical ALI cell wash obtained post TEER measurement at day 18 ALI which underwent a 100,000 ultracentrifugation step in order to isolate the exosome pellet (A-B). Red arrows indicate representative exosomes isolated from the 100,000g pellet with corresponding nm size (A). Images were obtained at 40,000x magnification (A-B).

5. Discussion

The airway epithelium offers a first line defence for the host in relation to exposure of the respiratory system to the environment and the airway epithelium is known to offer protection against allergens, microorganisms and environmental stimuli[11]. However in respiratory disorders such as asthma this defence mechanism can be challenged and the airway epithelial cells, considered key controllers of inflammatory, immune and regenerative responses can be distorted[12]. Therefore experiments to further elucidate the interplay of the airway epithelium could prove crucial in understanding the pathophysiology of asthma.

In order to further investigate the function of the epithelium with regards to asthma it is important to utilise *in vitro* model systems. While immortalized cell lines are often utilised in respiratory disorders such as cystic fibrosis and asthma there are inherent limitations in using such a model system[8]. Primary epithelial cells, while variations exist at the inter- and intra- donor level, have been shown to be the best representation of a model system for epithelial research[8].

However, while primary epithelial cells are a representation of real life epithelial airway responses and when grown at Air Liquid Interface they closely replicate an *in vivo* physiologically relevant model system culturing such a model system requires expert knowledge, specialist materials and facilities and replicating such a model system on a large scale can be costly[8].

Therefore through a European Respiratory Society (ERS) short term research fellowship it was possible to gain a deeper understanding of the procedures required to implement a primary bronchial epithelial cell model system at Cork University Hospital and University College Cork and develop a deeper understanding of various protocols which can be implemented in tandem with the growth of primary cells to best investigate the pathophysiological aspect of respiratory diseases such as asthma. Through the ERS short term research fellowship it was possible to develop primary cell culture techniques and experimental best practice procedures for primary cell culture at a dedicated cell culture facility in Newcastle University, Newcastle upon Tyne, UK, under the

supervision of Dr Chris Ward and Dr Bernard Verdon. Primary nasal epithelial cells were cultured to Air Liquid Interface (ALI). ALI cell culture models are physiologically relevant model systems for respiratory research[8,9].

While cell culture model systems often utilise submerged cultured cell monolayers to investigate respiratory disorders advances in culture techniques now allow for the representation of airway epithelial cells at Air Liquid Interface (ALI). This advancement allows for a more physiologically robust system whereby the primary human epithelial cells are fully differentiated in a pseudostratified and polarised manner, with differentiated cells including cilia and goblet cells. This ALI model enables primary epithelial cells to develop transepithelial electrical resistance (TEER) and represents a model system to elucidate the pathogenic mechanisms present in respiratory disorders such as asthma[8].

Transepithelial electrical resistance (TEER) measurements were obtained weekly and TEER development was measured over 39 days for the AST01 cell cultures and 25 days for the NM37 cell cultures (see figure 4). TEER measurements were used to assess the tight junction integrity of primary epithelial cells at Air Liquid Interface (ALI). The TEER was best at day 32 for the AST01 cells and remained at respectable levels at day 39. The NM37 cells TEER values increased weekly and at the final reading at day 25 the mean TEER value was at its highest. It is accepted that patient variability exists in relation to the tight junction integrity transepithelial resistance readings[8]. It has also been shown that to compensate for intra-donor variability within cell culture at ALI at least 5-6 ALI membranes should ideally be cultured per donor[13].

Ussing chamber experiments have been shown as a valuable technique to measure short circuit current (I_{sc}) as an indicator of net transepithelial ion transport[10]. This technique allows for the examination of pharmacological reagents of interest by their addition to the apical or basolateral compartments of the chambers. Within this study the asthma donor epithelial cells were tested with a variety of components of interest in Cystic Fibrosis as these asthma cells were to later be used as a control comparison for subsequent CF experiments, however it is also possible

to probe other pharmacological agents of interest using the Ussing chamber system[14]. Amiloride was used to inhibit ENaC activity, Forskolin was used as a cAMP activator of CFTR, $CFTR_{inh}$-172 as an apical inhibitor and ATP as a Ca^{2+} mobilising agent. The Ussing chamber allows for transepithelial electrical resistance responses for specific pharmacological reagents of interest and an overall transepithelial electrical resistance to be calculated using Ohms Law. See figures 5-10.

Periodic acid –Schiff assay is a useful experimental procedure to include when analysing primary cell cultures at Air Liquid Interface. The assay is used to detect for the presence of glycoproteins (mucus) and it can be used simply as a staining method or it can be used as a quantitative method for glycoprotein detection when used with a spectrophotometer. Airway obstruction is an important pathophysiological feature in asthma with heightened secretion of airway glycoproteins an common occurrence in severe asthma, with the risk of glycoprotein accumulation and glycoprotein plug formation posing serious risks of leading to airflow obstruction in patients[15].

A significant difference in glycoprotein (µg/ml) levels in ALI NM37 cell washes at day 25 in comparison to day 4 (P<0.0001), day 11 (P<0.0001) and day 18 (P<0.0001) using an Ordinary one-way ANOVA with a Tukey multiple comparisons test to compare the mean of each column with the mean of every other column was observed (see figure 14) showing an accumulation in glycoproteins within the asthma cell washes. When apical and basolateral mean glycoprotein (µg/ml) values were compared it was observed that the apical wash samples had higher glycoprotein (µg/ml) detectable.

The periodic-acid –Schiff assay could also be a useful protocol addition when analysing Bronchoalveolar lavage from asthma patients as it could aid in the quantification of glycoproteins in the BAL.

The IL-8 (CXCL8) cytokine is a neutrophil and mast cell chemoattractant which is known in asthma to function in inflammatory cell regulation[16]. IL-8 cytokine levels were calculated from the apical and basolateral wash samples at various time points. The calculated mean apical and basolateral IL-8 pg/ml per days at ALI were

analysed and significance was found between basolateral IL-8 levels at day 4 compared to day 11 ($P<0.005$), day 18 ($P<0.0005$) and day 25 ($P<0.0001$) and apical IL-8 levels at day 4 compared to day 11 ($P<0.05$), day 18 ($P<0.05$) and day 25 ($P<0.05$). See figure 11. When basolateral levels were compared to apical IL-8 levels, samples received from apical PBS washes at TEER readings had higher levels of detectable IL-8. When cells at ALI day 36 were stimulated with various concentrations of *Pseudomonas aeruginosa* LPS no statistically significant difference was observed in LPS challenge at various concentrations regardless of time stimulated (24 hours and 48 hours). See figure 12 and figure 13. As cells were fully differentiated at time of stimulation it may be possible that apical stimulation of cells with LPS in liquid form may not fully translocate the cell membrane so future experiments investigating this challenge should be investigated.

Overall primary epithelial differentiated ALI cells demonstrated novel insights as to how cell culture can be used for a variety of experiments to reveal the real life responses of epithelial cells. The airway epithelium can provide key insights into the pathophysiology of asthma and can potentially lead to the development of a system to improve the treatment of asthma, therefore it is a hope that in the future through the expertise gained during the ERS fellowship it would be possible to develop primary bronchial epithelial cell (PBEC) culture facilities and culture PBEC cells obtained from patient bronchial brushings during bronchoscopy procedures at Cork University Hospital.

6. References

1. Hammad H, Lambrecht BN. Dendritic cells and epithelial cells: linking innate and adaptive immunity in asthma. *Nat Rev Immunol.* 2008;8(3):193-204.
2. Levy ML, Fletcher M, Price DB, Hausend T, Halbert RJ, Yawn BP. International Primary Care Respiratory Group (IPCRG) Guidelines: Diagnosis of respiratory diseases in primary care. *Primary Care Respiratory Journal.* 2006;15:20.
3. Murphy DM, O'Byrne PM. Recent advances in the pathophysiology of asthma. *Chest.* 2010;137(6):1417-1426.
4. Kim HY, DeKruyff RH, Umetsu DT. The many paths to asthma: phenotype shaped by innate and adaptive immunity. *Nature immunology.* 2010;11(7):577-584.
5. Sullivan A, Hunt E, MacSharry J, Murphy DM. The Microbiome and the Pathophysiology of Asthma. *Respiratory Research.* 2016;17(1):163.
6. Gómez MI, Prince A. Airway epithelial cell signaling in response to bacterial pathogens. *Pediatric pulmonology.* 2008;43(1):11-19.
7. Proud D, Leigh R. Epithelial cells and airway diseases. *Immunological reviews.* 2011;242(1):186-204.
8. Stewart CE, Torr EE, Mohd Jamili NH, Bosquillon C, Sayers I. Evaluation of Differentiated Human Bronchial Epithelial Cell Culture Systems for Asthma Research. *Journal of Allergy.* 2012;2012:11.
9. Brodlie M, McKean MC, Johnson GE, et al. Primary bronchial epithelial cell culture from explanted cystic fibrosis lungs. *Experimental Lung Research.* 2010;36(2):101-110.
10. Ussing HH, Zerahn K. Active transport of sodium as the source of electric current in the short-circuited isolated frog skin. *Acta physiologica Scandinavica.* 1951;23(2-3):110-127.
11. Lambrecht BN, Hammad H. The airway epithelium in asthma. *Nat Med.* 2012;18(5):684-692.
12. Crystal RG, Randell SH, Engelhardt JF, Voynow J, Sunday ME. Airway Epithelial Cells. *Proceedings of the American Thoracic Society.* 2008;5(7):772-777.
13. Tosoni K, Cassidy D, Kerr B, Land SC, Mehta A. Using Drugs to Probe the Variability of Trans-Epithelial Airway Resistance. *PLoS ONE.* 2016;11(2):e0149550.
14. Fischer H, Illek B, Sachs L, Finkbeiner WE, Widdicombe JH. CFTR and calcium-activated chloride channels in primary cultures of human airway gland cells of serous or mucous phenotype. *American journal of physiology Lung cellular and molecular physiology.* 2010;299(4):L585-L594.
15. Lee S-H, Kiss A, Xu J, et al. Airway glycoprotein secretion parallels production and predicts airway obstruction in pulmonary allergy. *J Allergy Clin Immunol.* 2004;113(1):72-78.
16. John AE, Zhu YM, Brightling CE, Pang L, Knox AJ. Human airway smooth muscle cells from asthmatic individuals have CXCL8 hypersecretion due to increased NF-kappa B p65, C/EBP beta, and RNA polymerase II binding to the CXCL8 promoter. *J Immunol.* 2009;183(7):4682-4692.

Chapter 10

Immunoglobulins and Asthma

BAL and serum immunoglobulin profiling in a cohort of asthma patients

Author Contributions: Desmond Murphy, John MacSharry, Chris Ward and Paul O'Byrne were responsible for the initial study design and concept. Desmond Murphy and was responsible for patient recruitment, clinical characterisation and sample acquisition. Sample processing and study assays were primarily performed by Ashley Sullivan with contribution from John MacSharry. Immunoglobulin assays were performed by RayBiotech. Statistical analysis was performed by the authors. Analysis and interpretation of data, manuscript preparation and approval were performed by the authors.

1. Abstract 452
2. Introduction 453
3. Methods 456
    3.1. Patient recruitment 456
    3.2. Sample processing 457
    3.3. Immunoglobulins 458
    3.4. Cytokine measurement 460
    3.5. Statistical analyses 461
4. Results 462
    4.1. Patient demographics 462
    4.2. BAL immunoglobulins 466
    4.3. Serum immunoglobulins 470
    4.4. Comparison of the BAL and serum immunoglobulins 474
    4.5 BAL and plasma cytokine concentrations 475
    4.6 BAL antibody and BAL cytokine correlations 476
    4.7. Serum antibody and plasma cytokine correlations 477
5. Discussion 479
6. Supplementary 486
7. References 487

1. Abstract

Background: Immunoglobulins are heterodimeric glycoprotein molecules which can be divided into five main classes IgA, IgD, IgE, IgG and IgM. Immunoglobulins play a vital role in the host immune response. Insights into immunoglobulins present within a cohort of adult asthmatics may lead to further knowledge of the complex Ig immune response and may aid in the discovery of novel therapeutic avenues.

Methods: 76 well-defined adult asthmatics underwent venepuncture sampling for blood serum and plasma and bronchoscopy with bronchoalveolar lavage (BAL) on the same day. The total antibody IgA, IgD, IgE, IgG1, IgG2, IgG3, IgG4 and IgM levels were measured in the BAL) and serum samples using Quantibody Human Ig Isotype Array 1 technology. BAL and plasma cytokines were analysed using an MSD proinflammatory panel 1 containing targets for Interleukin (IL)-1β, IL-4, IL-6, IL-8, IL-10, IL-13 and tumour necrosis factor (TNF)-α and a custom MSD cytokine panel 1 containing targets for IL-5 and IL-17A.

Results: 100% of patients had detectable levels of IgA, IgG3 and IgM within the BAL and serum. IgD was detectable in 37% (28/76) of BAL and 97% (74/76) of serum samples. 28% (21/76) had IgE detectable within the BAL while IgE was undetectable in the serum. IgG1 was detectable in 86% (65/76) of BAL and 100% of serum samples. IgG2 was detectable in 95% (72/76) of BAL and 100% serum. IgG4 was detectable in 96% (73/76) of patient BAL and 100% of serum samples. BAL IgD correlated with BAL IL-17 levels ($P<0.05$; $r_s=-0.7857$). IgM correlated with BAL TNF-α levels ($P<0.05$; $r_s=0.2559$). IgG1 correlated with BAL IL-6 levels ($P<0.01$; $r_s=0.3251$) and BAL TNF-α levels ($P<0.05$; $r_s=0.3280$).Serum IgA negatively correlated with plasma IL-4 ($P<0.0005$; $r_s=-0.5126$) and IL-13 levels ($P<0.0005$; $r_s=-0.4519$). Serum IgM correlated with plasma IFN-γ levels ($P<0.05$; $r_s=-0.2518$). Serum IgG3 correlated with plasma IL-4 levels ($P<0.01$; $r_s=-0.3692$), IL-6 levels ($P<0.01$; $r_s=-0.3407$) and IL-13 levels ($P<0.05$; $r_s=-0.2523$).

Conclusions: Research which advances the current understanding of the immunoglobulin profile within the BAL and serum of asthmatic patients may offer real advances in potential treatment options for asthma patients.

2. Introduction

Composed of two heavy and two light chains and classified functionally into variable domains and constant domains, Immunoglobulins can be described as heterodimeric proteins[1]. The variable domains of immunoglobulins are tasked with binding antigens while the constant domains of immunoglobulins are responsible for specifying the effector functions. Created through a series of complex gene rearrangement events and the possibility of; after antigen presentation; undergoing somatic hyper-mutation in order to develop affinity maturation, the variable domains of immunoglobulins is complex structure[1]. The variable domains can contain three regions of complementarity-determining regions and four framework regions, which remain consistent[1]. Through the pairing of the complementarity-determining regions on both the heavy and light chain the antigen-binding site is formed[1]. The constant domains maintain antigen-specificity; however they can be switched allowing for an altered effector function[1]. IgA, IgD, IgE, IgG and IgM are the main classes of the heavy chain constant domains, with IgG further divided into the subclasses of IgG1, IgG2, IgG3 and IgG4[1,2].

Individual immunoglobulins can bind to antigen specific to the immunoglobulin in question; however as a population immunoglobulins can, bind to a vast set of antigens[1]. It is known that immunoglobulins function on two levels as they can both act as an antigen cell surface receptor allowing for cell signalling and activation and they can also act as soluble effector molecules whereby they can specifically bind to antigens resulting in antigen neutralisation[1].

IgM is the first immunoglobulin expressed during B cell development, where naïve B cells express IgM in its monomeric form within their surface. Upon maturation and antigenic stimulation IgM is usually expressed in its pentameric form making IgM highly successful in opsonizing antigens for elimination and fixing complement[1]. IgM can be considered as a primary immune response antibody and is often associated with immunogen or pathogen exposure[1]. IgM provides both the first initial response to an antigen and also upon subsequent exposure IgM plays a regulatory role in response to an antigen and can accelerate the production of IgG[3]

Due to its foundation within B cell development it is recognised that IgM in comparison to other immunoglobulins has undergone less somatic mutation in response to antigens and therefore IgM can be considered to be more reactive to antigens[1].

IgD is found at low levels in the serum in comparison to other immunoglobulins. It is believed that IgD in the serum may recognise and react to a specific group of bacterial proteins and the binding to these bacterial proteins may result in the stimulation and activation of Bcells[1]. IgD can also be found in its membrane bound form on B cells when the B cells populate secondary lymphoid organs[1]. On B cells which express IgD on their membrane it is often the case that the B cell can also express IgM and both are involved in B cell receptor signalling[1].

IgG consists of the subclasses IgG1, IgG2, IgG3 and IgG4 which are ranked by number based on the serum levels expected of these immunoglobulins within a healthy population whereby total IgG represents 75% of total serum immunoglobulin and IgG1 = 67%, IgG2=22%, IgG3=7% and IgG4 = 4%[1]. All are expressed as monomers and IgG key function is related to both the secondary immune response and as a neutralization agent to toxins and viruses within the host[1]

IgA levels within the serum is believed to be at 15%, slightly higher than IgM serum levels of 10%, however within mucosal surfaces IgA levels are significantly higher[1]. Expressed mainly in its monomeric form within the serum IgA is often expressed as a dimer within the mucosal environment. IgA plays a vital protective role at mucosal surfaces and through methods such as direct neutralisation or the prevention of binding, IgA protects the host from bacteria, viruses and toxins[1].

IgE is associated with hypersensitivity and allergic reactions and has also been noted to be linked to the exposure of parasitic worm infections[1]. While IgE is present at low concentrations (<0.01%) within the serum it acts as a very potent immunoglobulin[1]. IgE is expressed as a monomer and upon allergen exposure, circulating allergen specific IgE binds to the $F_{c\varepsilon}RI$ receptors, on immune cells such as mast cells and basophils, leading to crosslinking and release of inflammatory

mediators[1,4]. Omalizumab (Xolair®) (Novartis-Genentech), the recombinant humanised monoclonal antibody, binds to the IgE antibody at the Fc portion which reduces the amount of free IgE, stops IgE from binding to inflammatory cell IgE receptors and reduces IgE receptor ($F_{c\varepsilon}RI$ and $F_{c\varepsilon}RII$) density on effector cells, all of which prevent an inflammatory cascade from occurring[4,5]

Great advances have occurred in recent times with respect to immunoglobulins and such advances have enabled numerous immunoglobulin applications as diagnostic and therapeutic agents[2]. Monoclonal antibodies represent the highest growth segment within the biopharmaceutical field and monoclonal antibody therapies such as Omalizumab (Xolair®, Novartis-Genentech) which targets IgE offer real potential for treatment of severe asthmatic patients[2,4-7]. Therefore research which advances the current understanding of the immunoglobulin profile within the BAL and serum of asthmatic patients may offer real therapeutic insights into potential treatment options for asthma patients through the use of humanised monoclonal antibody therapy.

3. Methods

3.1. Patient recruitment

The following study was approved by the Clinical Research Ethics Committee of the Cork Teaching Hospitals. The study cohort consists of 76 adult patients with a history of asthma; either documented change in FEV1≥12%/200ml with bronchodilator or a positive inhalation challenge. The 76 adult asthma patients were recruited through a dedicated asthma clinic in a tertiary referral centre, Cork University Hospital, by my clinical supervisor, Dr Des Murphy.

Patients were scheduled for bronchoscopy, with spirometry, ACQ-7 and bloods taken on the day of bronchoscopy. Written informed consent was obtained from patients on the day of bronchoscopy. Spirometry was performed according to ATS/ERS guidelines immediately prior to bronchoscopy[8]. Spirometry is a widely used pulmonary function test which provides an aid in the diagnosis of lung diseases, differentiating between obstructive and restrictive airway disorders and the general monitoring of lung health[9]. Spirometry measures the maximal volume of air an individual can inspire and expire with maximal effort[9]. The Asthma Control Questionnaire (ACQ-7) was carried out on the day of bronchoscopy. The ACQ-7 consists of 7 items and all questions in the ACQ-7 are equally weighted and the mean of the 7 questions is used to calculate the patients ACQ-7 score which enables the measurement of patient asthma control[10]. Venepuncture was carried out prior to bronchoscopy using the Vacutainer System for blood drawing, with the order of the blood draw carried out in accordance with Cork University Hospital recommendations of blood draw order. For the purposes of this research project both serum and plasma samples were collected in serum specific red and yellow capped Vacuette tubes and plasma specific purple capped Vacuette tubes (Greiner Bio-One).

Patients underwent bronchoscopy according to standard guidelines[11]. Flexible bronchoscopy using video assisted imaging was performed under conscious sedation with local anaesthetic applied topically to the vocal cords, trachea and

endobronchial tree. Bronchoalveolar lavage (BAL) was achieved through the instillation of saline via the bronchoscope and this enabled the collection of specimen directly from the endobronchial lumen for subsequent immunoglobulin investigation. Bronchoalveolar lavage (BAL) was obtained as a standardised 180ml (3X60ml) sample from either the right middle lobe or lingula[12].

Further information with regards to asthmatic patient bronchoscopy and patient sample collection protocols can be found in Chapter 2 Study Cohort's.

3.2. Sample processing

Bronchoalveolar lavage (BAL)

Immediately after the bronchoscopy procedure was performed the patient samples were transported to the APC Microbiome Ireland for processing. Patient BAL was processed on the day of bronchoscopy in a laminar flow hood under the adherence of strict aseptic technique.

A portion (5ml) of the neat BAL was aliquoted and stored at -80^{o}C prior to the processing of the remaining patient BAL. The remaining BAL was transferred to 50ml sterile falcon tubes and centrifuged at 500g for 10 minutes. The supernatant was then aliquoted into labelled 2-5ml sterile tubes for future analysis. All samples were stored at -80^{o}C for future processing and analysis.

Bloods

The required blood samples were collected in serum specific red and yellow capped Vacuette tubes and plasma specific purple capped Vacuette tubes (Greiner Bio-One) at Cork University Hospital prior to bronchoscopy. The inner wall of the serum specific Vacuette tube was coated with silica particles which activated the coagulation process and a specific separator gel at the base of the tube formed a stable barrier during centrifugation to enable the serum and the blood to remain separated. The plasma specific purple capped Vacuette tube contained a coating of either K2EDTA or K3EDTA which acted as an anticoagulant by binding calcium ions to prevent the clotting cascade from taking place. Upon return to the laboratory

both tubes were centrifuged at 200rpm for 20 minutes and the serum and plasma was removed by pipetting and stored in screw-cap microcentrifuge tubes. All patient serum and plasma isolated samples were then stored at -80^{o}C for future processing and analyses.

3.3. Immunoglobulins

BAL and serum immunoglobulins IgA, IgD, IgE, IgG1, IgG2, IgG3, IgG4 and IgM were analysed by RayBiotech using a Quantibody Human Ig Isotype Array 1 (Catalog #: QAH-ISO-1) (RayBiotech, Georgia, USA) which utilised sandwich-ELISA based technology, quantifiably measuring the eight human isotype immunoglobulins. Testing was carried out according to in-house procedures at RayBiotech which consisted of the following protocol. Each RayBiotech Quantibody Human Ig Isotype glass slide array consists of 16 arrays of IgA, IgD, IgE, IgG1, IgG2, IgG3, IgG4 and IgM along with two positive controls, arranged in quadruplicate, allowing for the analysis of 16 samples per slide. The patient BAL was diluted to a dilution factor of 100 while the patient serum was diluted to a dilution factor of 40000.

The RayBiotech Quantibody Human Isotype Array 1 is based upon traditional Enzyme-Linked Immunosorbent Assay (ELISA) technology. Firstly the sealed glass slide was allowed to equilibrate for 20-30 minutes at room temperature before the plastic bag and cover film was removed and the glass slide was allowed to air dry for approximately 2 hours. Immunoglobulin standard dilutions were prepared by reconstituting the lyophilised standards by adding 500µl of the Sample Diluent to the vial containing the standard which had been spun briefly beforehand. Upon addition of the Sample Diluent the lyophilised standard was dissolved by gently mixing the two components creating Standard 1. 200µl of Sample Diluent was then added to 6 sterile labelled microcentrifuge tubes. 100µl of Standard 1 was added to the first tube, labelled Standard 2, and mixed gently. Serial dilutions were performed on the remaining 5 microcentrifuge tubes by adding 100µl of Standard 2 to the Standard 3 tube and so on. In order to create a negative control standard 100µl alone was added to a sterile microcentrifuge tube. See Supplementary Table 1 for the serial standard concentration (pg/ml) of the immunoglobulins.

100µl of the Sample Diluent was added to each well in the glass slide and incubation at room temperature for 30 minutes took place in order to block the slide. The buffer was then decanted from each well and 100µl of immunoglobulin standards or patient sample was added to each well before assays were covered with adhesive film and were incubated for 2+ hours at room temperature or overnight at 4^{o}C.

After incubation the samples were decanted from each well and the wells were washed 5 times in total for 5 minutes each wash with 150µl of 1X Wash Buffer I at room temperature ensuring the wash buffer was completely removed after each wash. The wells were then washed with 150µl of 1X Wash Buffer II two times for 5 minutes each wash ensuring the wash buffer was completely removed after each wash.

The Biotinylated Antibody Cocktail was reconstituted with 1.4ml of Sample Diluent before 80µl of which was added to each well. The glass slide was incubated at room temperature for 2+ hours. After incubation, the samples were decanted from each well and the glass slide was washed with 150µl of 1X Wash Buffer I, 5 times for 5 minutes each wash., then with 150µl of 1X Wash Buffer II twice for 5 minutes each wash, ensuring the wash buffer is completely removed after each wash.

The Cy3 equivalent dye-conjugated Streptavidin was reconstituted by adding 1.4ml of Sample Diluent to the tube and mixing gently. Upon reconstitution 80µl of Cy3 equivalent dye-conjugated Streptavidin was added to each well on the glass slide before the slide was covered with aluminium foil and incubated for 1 hour at room temperature. After incubation the samples were decanted from each well and the plate was washed 5 times (5 minutes each wash) with 150µl of 1X Wash Buffer I ensuring the wash buffer was removed completely after each wash.

The glass slide was added to a slide washer/dryer covering the whole slide with 1X Wash Buffer I and gently shaking the slide for 15 minutes at room temperature. The Wash Buffer I was then decanted before the glass slide was washed with 1X Wash Buffer II by covering the glass slide and gently shaking the slide for 5 minutes at room temperature. Fluorescence detection of immunoglobulins IgA, IgD, IgE, IgG1,

IgG2, IgG3, IgG4 and IgM took place using a Cy3 wavelength equipped laser scanner. The unknown immunoglobulin concentration of the BAL and plasma samples was calculated using the immunoglobulin standard curve.

The patient BAL limit of detection was as follows; IgA 107.4 pg/ml, IgD 342.5 pg/ml, IgE 359.4 pg/ml, IgG1 483.0 pg/ml, IgG2 926.4 pg/ml, IgG3 23.0 pg/ml, IgG4 21.7 pg/ml and IgM 134.3 pg/ml.

The patient serum limit of detection was as follows; IgA 13.0 pg/ml, IgD 94.4 pg/ml, IgE 307.6 pg/ml, IgG1 80.4 pg/ml, IgG2 1950.9 pg/ml. IgG3 112.2 pg/ml, IgG4 119.8 pg/ml and IgM 50.0 pg/ml.

Upon the detection of the immunoglobulin concentrations within the patient BAL and Serum the dilution factors of 100 for the BAL samples and 40000 for the serum samples were accounted for.

3.4. Cytokine measurement

BAL and plasma cytokines were analysed using a MSD proinflammatory panel 1 containing targets for Interleukin (IL)-1β, IL-4, IL-6, IL-8, IL-10, IL-13 and tumour necrosis factor (TNF)-α and a custom MSD cytokine panel 1 containing targets for IL-5 and IL-17A. Reagent preparation consisted of the following; calibrator standards were prepared by suspension of the lyophilised calibrator with 1000µl of the appropriate diluent (diluent 2 for proinflammatory panel 1 and diluent 43 for cytokine panel 1) and then transferring 100µl of the re-suspended calibrator with 300µl of appropriate diluent. This 4 fold serial dilution was repeated 5 additional times to generate 7 calibrators with the diluent alone used as a zero calibrator. Plasma samples were diluted as follows; 35µl of plasma and 35µl of appropriate diluent, while BAL samples were undiluted. A detection antibody solution was created for the proinflammatory panel by combining 60µl of each SULFO-TAG anti-human IL-1β, IL-4, IL-6, IL-8, IL-10, IL-13 IFN-γ and TNF-α antibody with 2520µl diluent 3 to bring to a final volume of 3000µl. A detection antibody solution for cytokine panel 1 consisted of 60µl each of SULFO-TAG Anti-human IL-5 and IL-17A with 2880µl of diluent 3 for a final volume of 3000µl. Wash buffer consisted of PBS

and 0.05% Tween 20. Read buffer for each plate consisted of 10ml of Read Buffer T (4X) and 10ml of deionised water for a 2X working solution. Step 1 of the assay involved washing the plate 3 times with 150µl/well wash buffer 50µl of prepared calibrators or samples was added per well, the plate was sealed before overnight incubation with shaking at 2-8^{o}C. Step 2 involved washing the plate a further 3 times with 150µl/well wash buffer before the addition of 25µl detection antibody solution to each well, the plate sealed and a two hour room temperature incubation with shaking occurred. Step 3; the plate was washed 3 times as before and 150µl of 2X Read Buffer T was added to each well before analysis of the plate using an electro-chemiluminescence QuickPlex SQ 120 imager from Meso Scale Discovery (Gaithersburg, MD, USA). The MSD lower limit of detection for the cytokines tested was as follows; IL-1β=0.04pg/ml, IL-4=0.02pg/ml, IL-5=0.22pg/ml, IL-6=0.06pg/ml, IL-8=0.04pg/ml, IL-10=0.03pg/ml, IL-13=0.24pg/ml, IL-17A=0.74pg/ml, TNF-α=0.04pg/ml and IFN-γ=0.20pg/ml.

3.5. Statistical analyses

Graph Pad Prism 8 software was used to perform all statistical analyses and to provide graphical representation of the data. All data was assessed using normality and lognormaility tests and the Shaprio-Wilk test was applied to assess the normality of the data.

Normally distributed data was presented as the mean ± standard deviation within the text and figures. Normally distributed data sets where both the X and Y values were normally distributed were analysed using Pearson correlation coefficient analysis. Data was considered statistically significant when $P<0.05$.

Non-normally distributed data was presented as median ± interquartile range (IQR) within the text and figures. Non-normally distributed data sets where both the X and Y values were not both normally distributed were analysed using the non-parametric Spearman correlation[13]. Data was considered statistically significant when $P<0.05$.

4. Results

4.1. Patient demographics

The patient cohort consisted of seventy six adult asthmatic patients in which the total antibody immunoglobulin IgA, IgD, IgE, IgG1, IgG2, IgG3, IgG4 and IgM levels were measured in the bronchoalveolar lavage (BAL) and in time and patient matched serum samples

Within the cohort of seventy six adult asthmatic patients there were 28 males and 48 females. 63% (48/76) of the asthmatic patients had never smoked, while 28% (21/76) were ex-smokers and 9% (7/76) were current smokers. 63% (48/76) of the cohort lived in a rural location while 37% (28/76) lived in an urban location.

When stratified by asthma severity 34% (26/76) were classified as mild (GINA 1+2), 22% (17/76) were moderate (GINA 3) and 44% (33/76) were classified as severe asthmatics (GINA 4+5). When stratified by level of asthma control (ACQ-7), 37% (28/76) were controlled (ACQ-7<1.5) while 63% (48/76) were uncontrolled (ACQ-7≥1.5).

Nine patients within the study cohort were in receipt of oral steroids (mg) at the time of bronchoscopy (min 5 – max 30 mg) of which all nine patients in receipt of oral steroids were classified as severe asthmatics (GINA 4+5). 14% (11/76) of asthmatics were steroid naïve at time of bronchoscopy. 86% (65/76) of patients were in receipt of inhaled corticosteroids (ICS) (FDP 250) (min 250 – max 2000 FDP) at time of bronchoscopy

See Table 1 for patient demographics at bronchoscopy

Table 1 Patient demographics at bronchoscopy. Note *ACQ-7, Asthma Control Questionnaire; ~ICS, Inhaled Corticosteroid; † FEV-1, Forced Expiratory Volume in the first second; § FeNO, Fractional exhaled Nitric Oxide; ¶ BMI, Body Mass Index; ¥ ESR, Erythrocyte Sedimentation Rate; ‡ CRP, C-reactive protein.

		Mild (GINA 1-2)	**Moderate (GINA 3)**	**Severe (GINA 4-5)**
Patients	n=76 (%)	26 (34%)	17 (22%)	33 (44%)
Male		10 (38%)	5 (29%)	13 (39%)
Female		16 (62%)	12 (71%)	20 (61%)
ACQ-7*	[Mean (SD)]	[1.1 (0.6)]	[1.9 (1.0)]	[3.2 (1.1)]
	[Median (IQR)]	[1.1 (0.6-1.6)]	[1.9(1.1-2.6)]	[3.1 (2.5-4.1)]
ICS (FDP 250)~	[Mean (SD)]	[442.3 (470.7)]	[926.5 (521.2)]	[1038 (464.0)]
	[Median (IQR)]	[375 (0-1000)]	[1000 (500-1000)]	[1000 (750-1250)]
IgE (KU/L)	[Mean (SD)]	[361.3 (643.2)]	[168.8 (237.8)]	[270.6 (436.3)]
	[Median (IQR)]	[96.1 (30.7-399.0)]	[138.0 (63.1-180.0)]	[100.1 (22.4-286.3)]
FEV-1 (Percent Predicted)†	[Mean (SD)]	[86.9 (13.1)]	[86.7 (20.7)]	[64.9 (22.7)]
	[Median (IQR)]	[88.0 (78.8-96.0)]	[81.6 (74.0-101.5)]	[67.0 (46.5-80.5)]
FeNO (ppb) §	Readings from	23	14	24
	[Mean (SD)]	[30.5 (27.4)]	[22.7 (11.4)]	[20.2 (25.1)]
	[Median (IQR)]	[21.0 (11.0-43.0)	[21.0 (15.5-32.0)]	[13.0 (19.3-23.8)]
BMI (kg/m^2) ¶	[Mean (SD)]	[26.0 (4.5)]	[27.5 (6.9)]	[30.0 (6.5)]
	[Median (IQR)]	[24.5 (22.4-30.0)]	[26.0 (22.5-31.2)]	[29.0 (25.1-33.8)]
Haemoglobin (Hb) (g/L)	[Mean (SD)]	[14.1 (1.2)]	[13.8 (0.9)]	[13.4 (1.4)]
	[Median (IQR)]	[14.0 (13.1-15.3)]	[14.1 (13.0-14.4)]	[13.5 (12.5-14.5)]
White cell count (WBC) (10^9/L)	[Mean (SD)]	[6.6 (1.6)]	[7.0 (1.6)]	[8.7 (3.5)]
	[Median (IQR)]	[6.6 (5.3-7.8)]	[6.7 (5.6-8.1)]	[8.2 (7.1-9.1)]
Blood Lymphocyte count (10^9/L)	[Mean (SD)]	[2.0 (0.6)]	[1.9 (0.7)]	[2.3 (1.0)]
	[Median (IQR)]	[2.0 (1.6-2.6)]	[1.9(1.5-2.3)]	[2.1 (1.5-2.9)]
Blood Eosinophil count (10^9/L)	[Mean (SD)]	[0.3 (0.2)]	[0.3 (0.4)]	[0.3 (0.3)]
	[Median (IQR)]	[0.2 (0.1-0.3)]	[0.2 (0.1-0.4)]	[0.2 (0.1-0.3)]
Blood Neutrophil count (10^9/L)	[Mean (SD)]	[3.8 (1.2)]	[4.5 (1.0)]	[5.5 (2.9)]
	[Median (IQR)]	[3.9 (3.0-4.6)]	[4.8 (3.6-5.4)]	[5.0 (4.0-6.0)]
ESR (mm/hr)¥	Readings from	25	15	27
	[Mean (SD)]	[6.3 (4.4)]	[9.8 (7.9)]	[11.8 (13.1)]
	[Median (IQR)]	[5.0 (2.0-9.5)]	[8.0 (3.0-16.0)]	[6.0 (2.0-14.0)]
CRP (mg/L)‡	Readings from	26	17	29
	[Mean (SD)]	[5.8 (2.0)]	[5.9 (2.7)]	[10.0 (15.9)]
	[Median (IQR)]	[5.0 (5.0-5.0)]	[5.0 (5.0-5.8)]	[5.0 (5.0-8.5)]

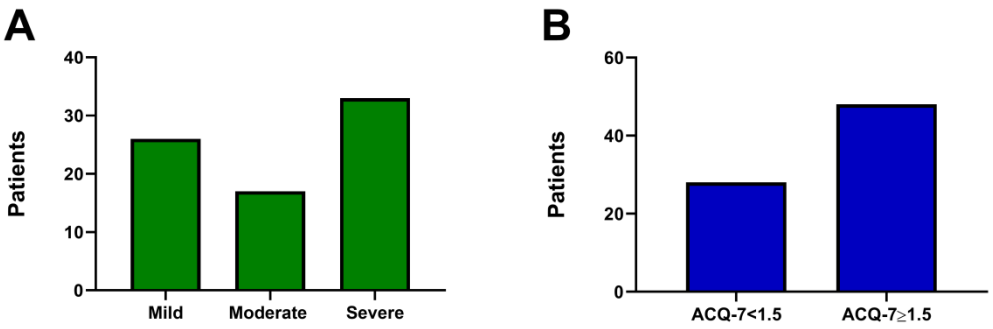


Figure 1. Patient asthma severity and level of control. The patient cohort was stratified by asthma severity (GINA). Upon grouping patients by GINA stage it was observed that 34% (26/76) were mild (GINA 1+2), 22% (17/76) were moderate (GINA 3) and 44% (33/76) were severe (GINA 4+5) (A). When patients were stratified by level of control (ACQ-7) 37% (28/76) were controlled (ACQ-7<1.5) while 63% (48/76) were uncontrolled (ACQ-7≥1.5) asthmatics (B). n=76

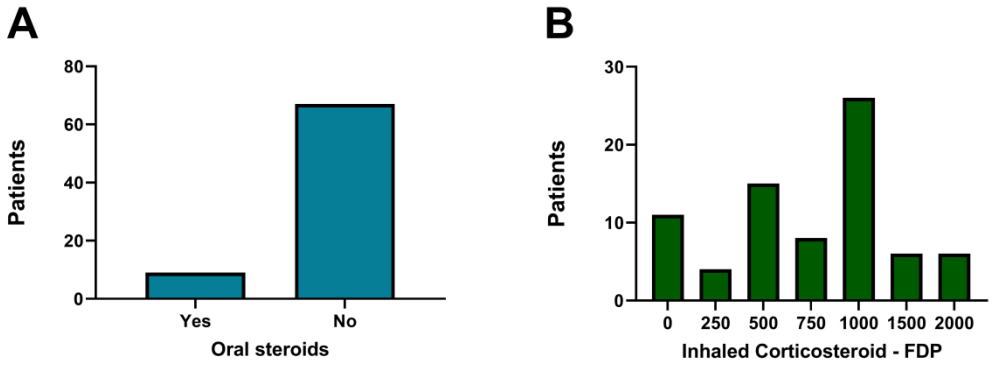


Figure 2. Patient oral steroids and inhaled corticosteroids. At time of bronchoscopy 9 patients were in receipt or oral steroids (5mg min – 30mg max) while 67 patients were not in receipt of oral steroid (A). Breakdown of patient inhaled corticosteroid (ICS) (FDP) dose at time of bronchoscopy. 86% (65/76) of patients were in receipt of ICS while 14% (11/76) of patients within the cohort were newly diagnosed and ICS naïve at the time of sampling. n=76

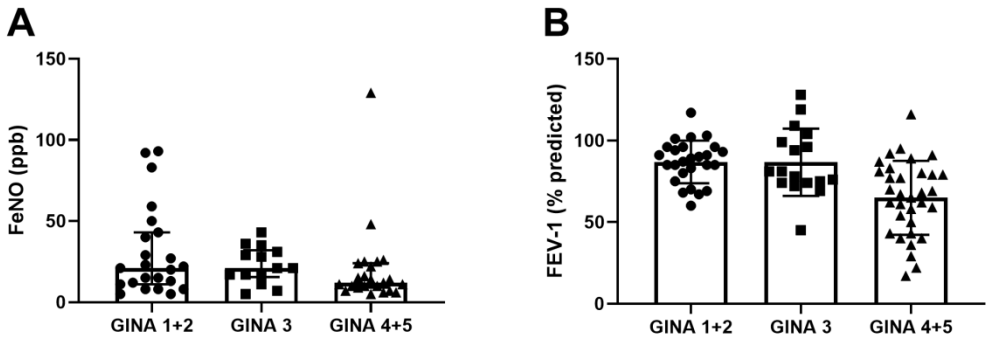


Figure 3. FeNO and FEV-1 at bronchoscopy. Fractional exhaled Nitric Oxide (FeNO) is a non-invasive marked of inflammation. Patients who were capable of undergoing the procedure underwent FeNO measurements prior to bronchoscopy whereby the level of nitric oxide in parts per billion (ppb) in the air which is exhaled slowly from their lungs was measured using a portable FeNO device (A). n=61. Patients underwent spirometry prior to bronchoscopy. Forced Expiratory Volume in the first second (FEV-1) is a measurement of the expiratory volume in the first second of the Forced Vital Capacity (FVC) maneuver whereby (B) depicts theFEV-1 % predicted measurements obtained from the cohort on the day of bronchoscopy. n=76.

4.2. BAL immunoglobulins

BAL immunoglobulins IgA, IgD, IgE, IgG1, IgG2, IgG3, IgG4 and IgM were analysed by RayBiotech using a Quantibody Human Ig Isotype Array 1 (RayBiotech, Georgia, USA) which utilised sandwich-ELISA based technology, quantifiably measuring the eight human isotype immunoglobulins. 100% (76/76) of patients had detectable levels of IgA within the BAL. 37% (28/76) of patients had detectable levels of IgD within the BAL. 28% (21/76) of patients had detectable levels of IgE within the BAL. 86% (65/76) of patients had detectable IgG1 within the BAL. 95% (72/76) of patients had detectable levels of IgG2 within the BAL. 100% (76/76) of patients had detectable levels of IgG3 within the BAL. 96% (73/76) of patients had detectable levels of IgG4 within the BAL. 100% (76/76) of patients had detectable levels of IgM within the BAL. See figure 4.

Looking specifically at Immunoglobulin presence in relation to asthma severity (GINA) there was an even distribution of IgA, IgG3 and IgM across patient GINA groups (100% detection). IgD was present at detectable levels within 31% (8/26) of mild asthmatics (GINA 1+2), 29% (5/17) of moderate asthmatics (GINA 3) and 45% (15/33) of severe asthmatics (GINA 4+5). IgE was present at detectable levels within 23% (6/26) of mild asthmatics (GINA 1+2), 29% (2/17) of moderate asthmatics (GINA 3) and 30% (10/33) of severe asthmatics (GINA 4+5). IgG1 was present at detectable levels within 77% (20/26) of mild asthmatics (GINA 1+2), 82% (14/17) of moderate asthmatics (GINA 3) and 94% (31/33) of severe asthmatics (GINA 4+5). IgG2 was present at detectable levels within 100% (26/26) of mild asthmatics (GINA 1+2), 94% (16/17) of moderate asthmatics (GINA 3) and 91% (30/33) of severe asthmatics (GINA 4+5). IgG4 was present at detectable levels within 96% (25/26) of mild asthmatics (GINA 1+2), 94% (16/17) of moderate asthmatics (GINA 3) and 97% (32/33) of severe asthmatics (GINA 4+5). See figure 5 for BAL immunoglobulins stratified by asthma severity and figure 6 for the differences in individual BAL immunoglobulins when patients are stratified by asthma severity. n=76 No statistically significant difference was found by GINA with respect to the levels of immunoglobulins.

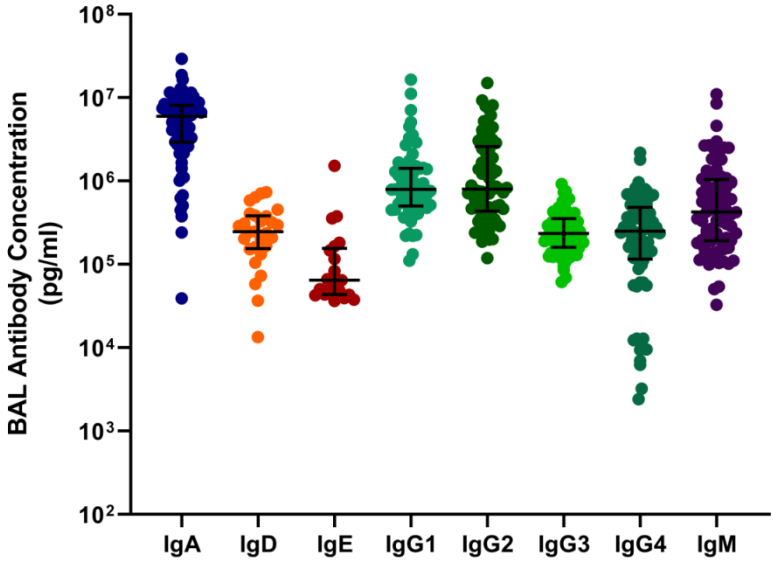


Figure 4. Total BAL immunoglobulin levels. The immunoglobulins IgA, IgD, IgE, IgG1, IgG2, IgG3, IgG4 and IgM were quantifiably measured in the patient BAL using a Quantibody Human Ig Isotype Array 1 (RayBiotech, Georgia, USA). Patient BAL immunoglobulin levels are represented in the form of a log10 graph with [Median (IQR)], n=76.

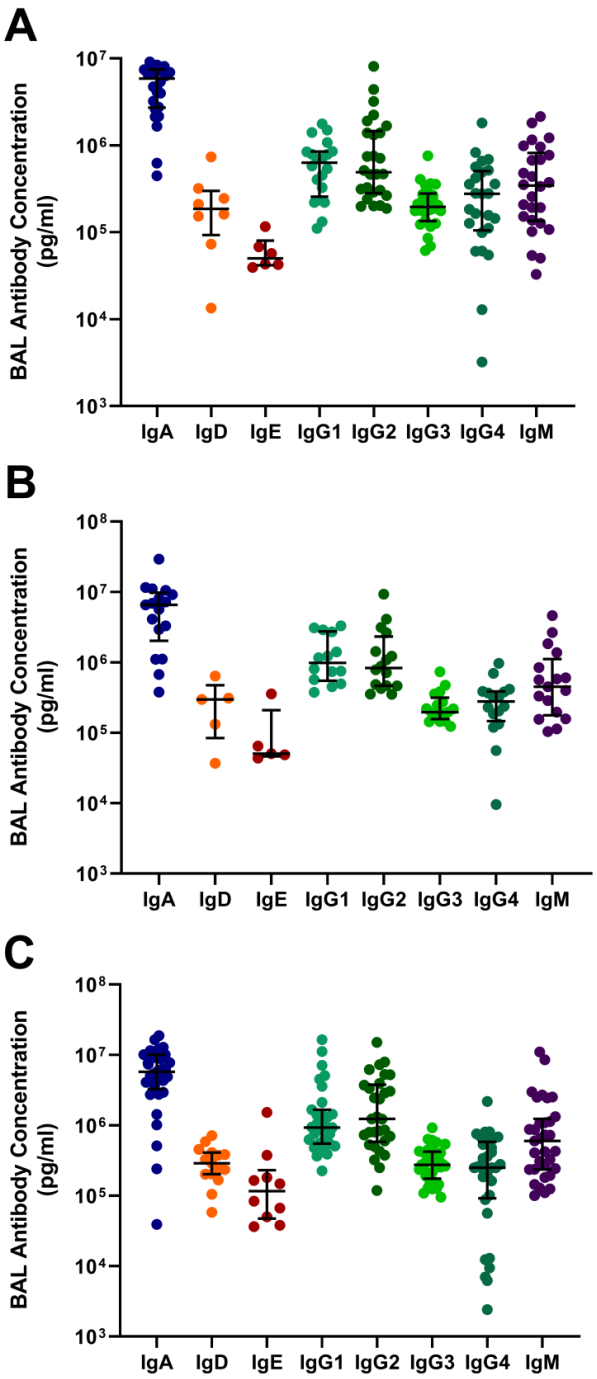


Figure 5. GINA grouped BAL immunoglobulins levels. The immunoglobulins IgA, IgD, IgE, IgG1, IgG2, IgG3, IgG4 and IgM were quantifiably measured in the patient BAL using a Quantibody Human Ig Isotype Array 1 (RayBiotech, Georgia, USA). The BAL immunoglobulin levels for patients grouped by asthma severity (GINA) are represented in the form of a log10 graph with [Median (IQR)] whereby (A) represents mild (GINA 1+2) asthmatics, n=26, (B) represents moderate (GINA 3) asthmatics, n=17, and (C) represents severe (GINA 4+5) asthmatics, n=33.

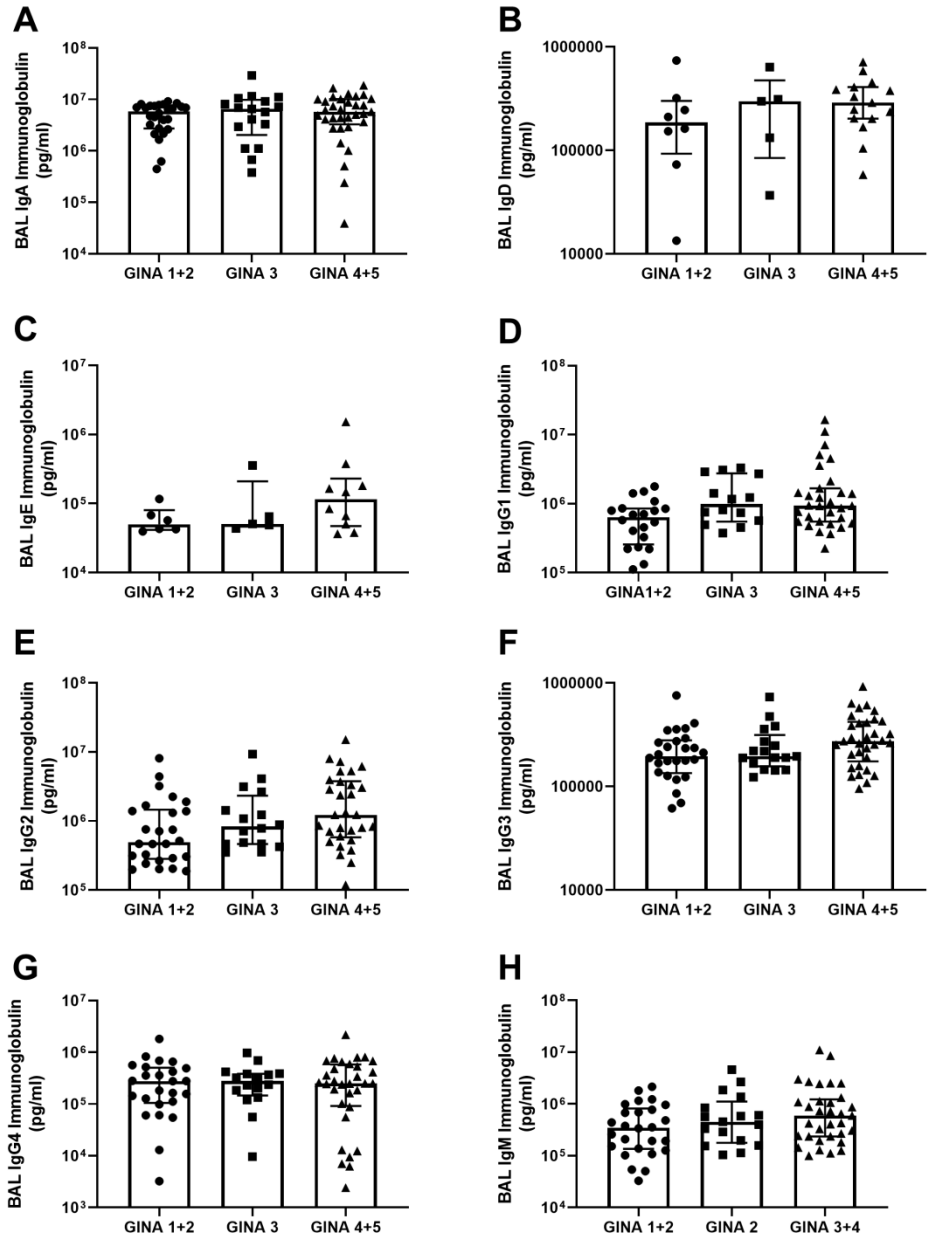


Figure 6. Differences in individual BAL immunoglobulin levels by GINA groupings. Potential differences in the individual immunoglobulins IgA(A), IgD (B), IgE (C), IgG1 (D), IgG2 (E), IgG3 (F), IgG4 (G) and IgM (H) when patients were stratified by asthma severity (GINA) was investigated. While there are clear visual differences in certain immunoglobulin levels when patients were stratified by GINA, in particular a higher level of immunoglobulins were observed in patients stratified as severe asthmatics (GINA 4+5) there was so statistically significant difference when patient immunoglobulin levels were analysed. The data is represented in the form of a log10 [Median (IQR) graphs, n=76.

4.3. Serum immunoglobulins

Serum immunoglobulins IgA, IgD, IgE, IgG1, IgG2, IgG3, IgG4 and IgM were analysed by RayBiotech using a Quantibody Human Ig Isotype Array 1 (RayBiotech, Georgia, USA) which utilised sandwich-ELISA based technology, quantifiably measuring the eight human isotype immunoglobulins.

100% (76/76) of patients had detectable levels of IgA within the serum. 97% (74/76) of patients had detectable levels of IgD within the serum. No patients had detectable levels of IgE within the serum. 100% (76/76) of patients had detectable IgG1 within the serum. 100% (76/76) of patients had detectable levels of IgG2 within the serum. 100% (76/76) of patients had detectable levels of IgG3 within the serum. 100% (76/76) of patients had detectable levels of IgG4 within the serum. 100% (76/76) of patients had detectable levels of IgM within the serum. See figure 7.

Looking specifically at Immunoglobulin presence in relation to asthma severity (GINA) there was an even distribution of IgA, IgG1, IgG2, IgG3, IgG4 and IgM across patient groups stratified by asthma severity (GINA) (100% detection). IgD was present at detectable levels within 100% (26/26) of mild asthmatics (GINA 1+2), 94% (16/17) of moderate asthmatics (GINA 3) and 94% (32/33) of severe asthmatics (GINA 4+5). No patients within the cohort had detectable levels of IgE within the serum. See figure 8 for serum immunoglobulin levels upon stratification of patients by severity (GINA).

Potential differences in the individual immunoglobulins IgA(A), IgD (B), IgE (C), IgG1 (D), IgG2 (E), IgG3 (F), IgG4 (G) and IgM (H) when patients were stratified by asthma severity (GINA) was investigated. Significant difference was found between IgA GINA 3 and GINA 4+5 ($P<0.05$). A Brown-Forsythe test to determine if the SD of the values was significantly different was used and as there was no significant difference an ordinary one way ANOVA with Tukey test for multiple comparisons was utilised. The mean difference between GINA 3 v GINA 4+5 was $2x10^9$ (2548237726) and the S.E of difference was $9x10^8$ (909338107).

IgG1 was also determined to be significantly different between GINA 3 and GINA 4+5 (P<0.05) where the mean difference was $8x10^8$ (864992847) and the S.E of difference was $3x10^8$ (337319407). The data is represented in figure 9 in the form of log10 [Median (IQR)] graphs, n=76

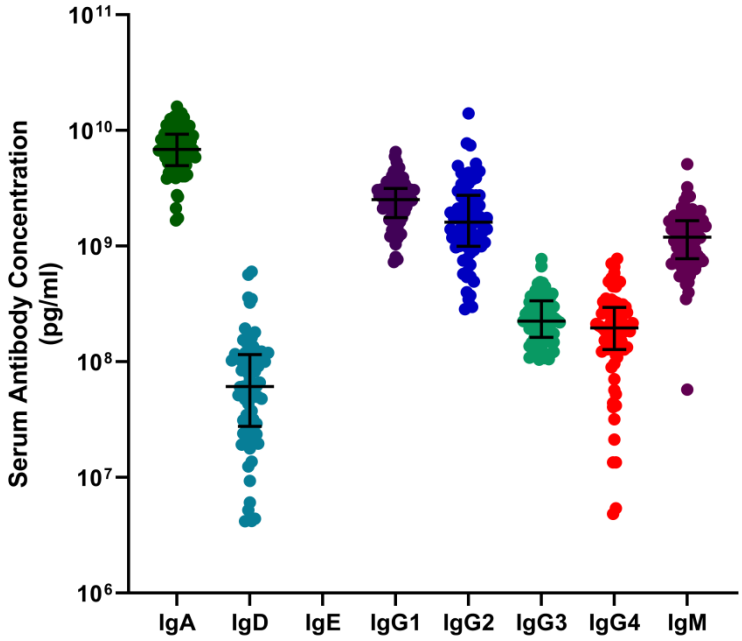


Figure 7. Total serum immunoglobulin levels. The immunoglobulins IgA, IgD, IgE, IgG1, IgG2, IgG3, IgG4 and IgM were quantifiably measured in the patient serum using a Quantibody Human Ig Isotype Array 1 (RayBiotech, Georgia, USA). Patient serum immunoglobulin levels are represented in the form of a log10 graph with [Median (IQR)], n=76.

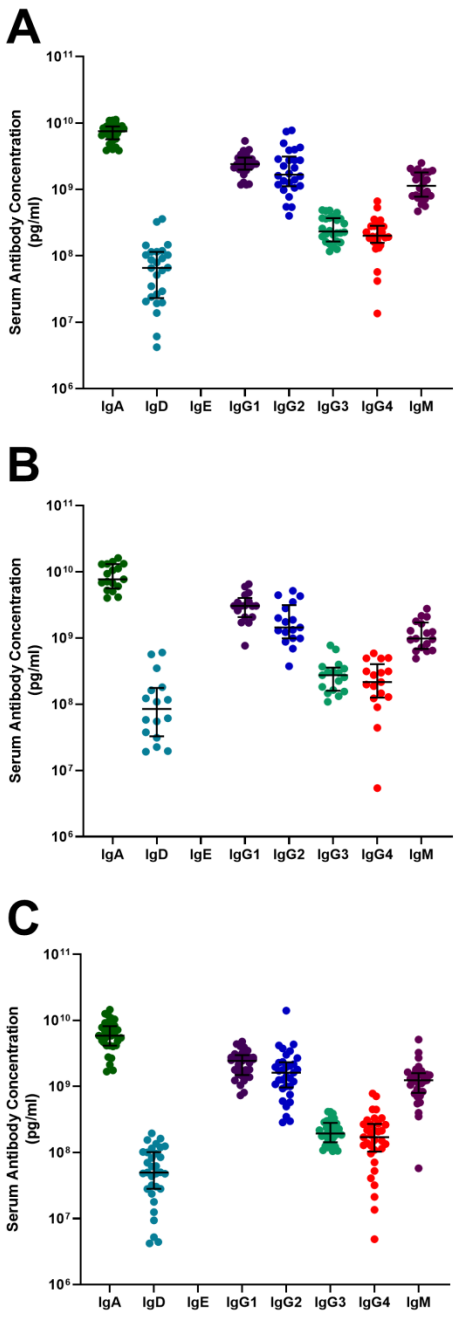


Figure 8. GINA grouped serum immunoglobulins levels. The immunoglobulins IgA, IgD, IgE, IgG1, IgG2, IgG3, IgG4 and IgM were quantifiably measured in the patient serum using a Quantibody Human Ig Isotype Array 1 (RayBiotech, Georgia, USA). The serum immunoglobulin levels for patients grouped by asthma severity (GINA) are represented in the form of a log10 graph with [Median (IQR)] whereby (A) represents mild (GINA 1+2) asthmatics, n=26, (B) represents moderate (GINA 3) asthmatics, n=17, and (C) represents severe (GINA 4+5) asthmatics, n=33.

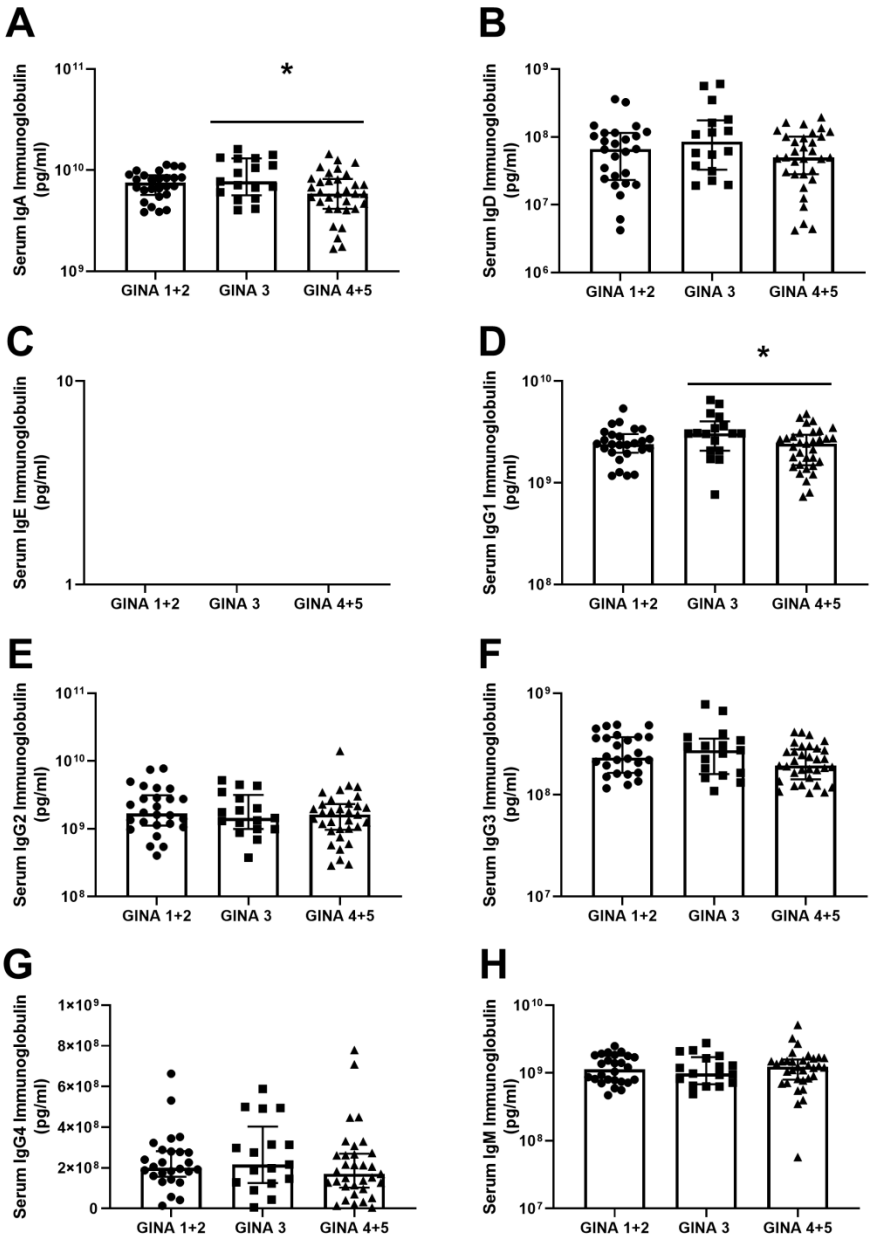


Figure 9. Differences in individual serum immunoglobulin levels by GINA groupings. Potential differences in the individual immunoglobulins IgA(A), IgD (B), IgE (C), IgG1 (D), IgG2 (E), IgG3 (F), IgG4 (G) and IgM (H) when patients were stratified by asthma severity (GINA) was investigated. Significant difference was found between IgA GINA 3 and GINA 4+5 (P<0.05) and IgG1 GINA 3 and GINA 4+5 (P<0.05). The data is represented in the form of a log10 [Median (IQR) graphs, n=76

4.4. Comparison of the BAL and serum immunoglobulins

The IgA, IgD, IgE, IgG1, IgG2, IgG3, IgG4 and IgM levels within the patient cohorts BAL and serum were compared using the t-test with Welch's correction. Significant differences were observed between all BAL and serum immunoglobulin levels. BAL IgA (mean=6255285) and serum IgA (mean=7367716755) were significantly different (*P*<0.0001). BAL IgD (mean=288710) and serum IgD (mean=93002950) were significantly different (*P*<0.0001). IgE was not present at detectable levels within the patient serum and so BAL and serum IgE levels could not be compared. BAL IgG1 (mean=1593259) and serum IgG1 (mean=2617043155) were significantly different (*P*<0.0001). BAL IgG2 (mean=1949990) and serum IgG2 (mean=2199076095) were significantly different (*P*<0.0001).BAL IgG3 (mean=275453) and serum IgA (mean=257423140) were significantly different (*P*<0.0001). BAL IgG4 (mean=351389) and serum IgG4 (mean=229551172) were significantly different (*P*<0.0001). BAL IgM (mean=985106) and serum IgM (mean=1291739719) were significantly different (*P*<0.0001). n=76

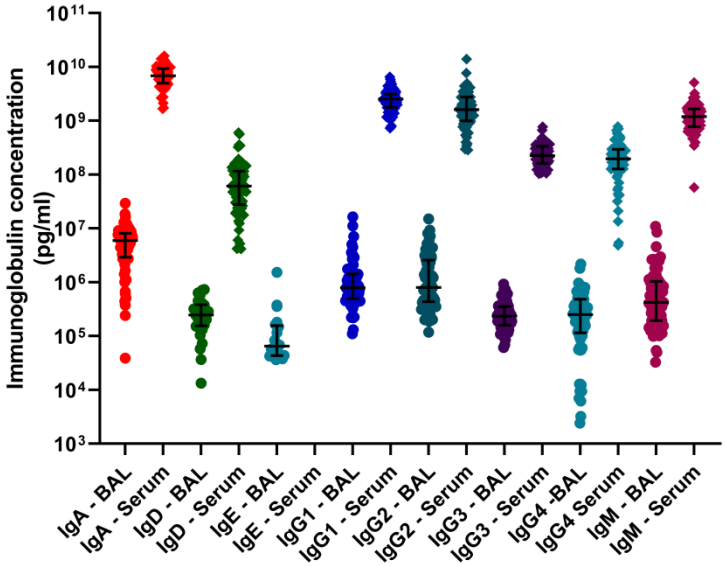


Figure 10. Comparison of the BAL and serum immunoglobulin concentrations. A comparison of the different immunoglobulin concentrations present within the patient BAL or serum sample. Log10 graph [Median (IQR)]. n=76

4.5 BAL and plasma cytokine concentrations

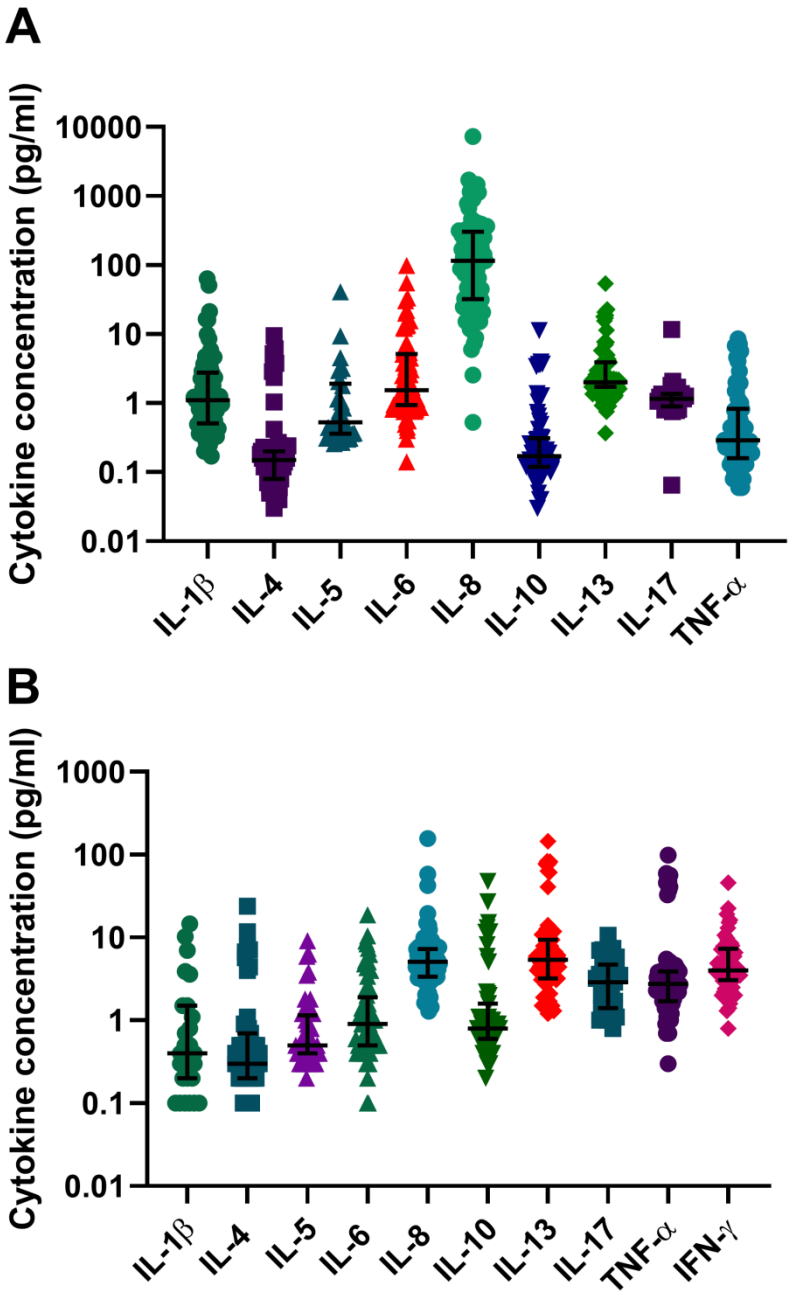


Figure 11. Cytokine levels in patient BAL and plasma. Measurement of secreted human cytokines interleukin- 1β (IL-1β), IL-4, IL-5, IL-6, IL-8, IL-10, IL-13, IL-17, tumour necrosis factor-α (TNF-α) and interferon-γ (IFN-γ) in patient BAL and plasma using an electro-chemiluminescence QuickPlex SQ 120 imager from Meso Scale Discovery (Gaithersburg, MD, USA) where antibodies labelled with SULFO-TAG™ reagents emitted light upon electrochemical stimulation. n=76

4.6 BAL antibody and BAL cytokine correlations

The immunoglobulins IgA, IgD, IgE, IgG1, IgG2, IgG3, IgG4 and IgM antibody concentration in the BAL from the patient cohort was analysed against the time matched BAL cytokines. The data was first analysed for normality using the Shapiro-Wilk test. All data was not considered to be normally distributed. Therefore Spearman correlations were used to examine the dataset with $P<0.05$ considered as statistically significant. No significant correlation was detected for the immunoglobulins IgA, IgE, IgG2, IgG3 or IgG4. IgD negatively correlated with BAL IL-17 levels ($P<0.05$; $r_s=-0.7857$). See figure 12 (A). IgM positively correlated with BAL TNF-α levels ($P<0.05$; $r_s=0.2559$) although the correlation was weak. See figure 12 (B). IgG1 positively correlated with BAL IL-6 levels ($P<0.01$; $r_s=0.3251$) and BAL TNF-α levels ($P<0.05$; $r_s=0.3280$). See figure 12 (C-D). n=76

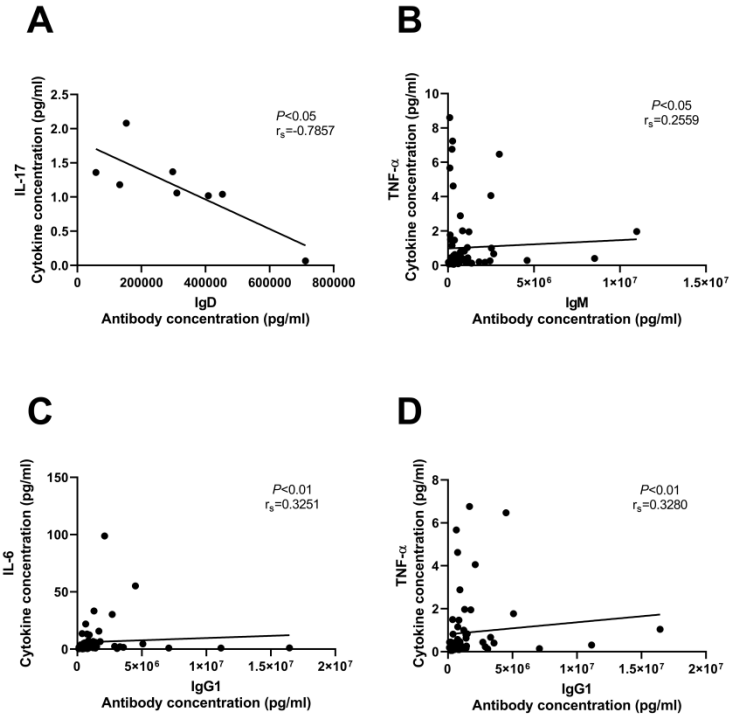


Figure 12. BAL antibody and cytokine correlations. IgD negatively correlated with BAL IL-17 levels ($P<0.05$; $r_s=-0.7857$) (A). IgM positively correlated with BAL TNF-α levels ($P<0.05$; $r_s=0.2559$) (B). IgG1 positively correlated with BAL IL-6 levels ($P<0.01$; $r_s=0.3251$) and BAL TNF-α levels ($P<0.05$; $r_s=0.3280$).(C-D). n=76

4.7. Serum antibody and plasma cytokine correlations

The immunoglobulins IgA, IgD, IgE, IgG1, IgG2, IgG3, IgG4 and IgM antibody concentration in the serum obtained from the patient cohort on the day of bronchoscopy was analysed against the time matched sample of plasma cytokine concentrations. The data was first analysed for normality using the Shapiro-Wilk test. All data was not considered to be normally distributed. Therefore Spearman correlations were used to examine the dataset with $P<0.05$ considered as statistically significant.

No significant correlation was detected for the immunoglobulins IgD, IgG1 and IgG2. IgE was undetectable within the patient serum and therefore could not be further analysed. IgG4 did appear to significantly correlated with the plasma cytokine TNF-α ($P<0.05$; $r_s=0.2468$) however the Spearman r value indicated this was a very weak correlation and so it was not included in figure 13.

Serum IgA negatively correlated with plasma IL-4 levels ($P<0.0005$; $r_s=-0.5126$). See figure 13 (A). Serum IgA negatively correlated with plasma IL-13 levels ($P<0.0005$; $r_s=-0.4519$). See figure 13 (B).

Serum IgM negatively correlated with plasma IFN-γ levels ($P<0.05$; $r_s=-0.2518$), although the correlation is weak. See figure 14 (C).

Serum IgG3 correlated negatively with plasma IL-4 levels ($P<0.01$; $r_s=-0.3692$), plasma IL-6 levels ($P<0.01$; $r_s=-0.3407$) and weakly with plasma IL-13 levels ($P<0.05$; $r_s=-0.2523$). See figure 13 (D-F). n=76

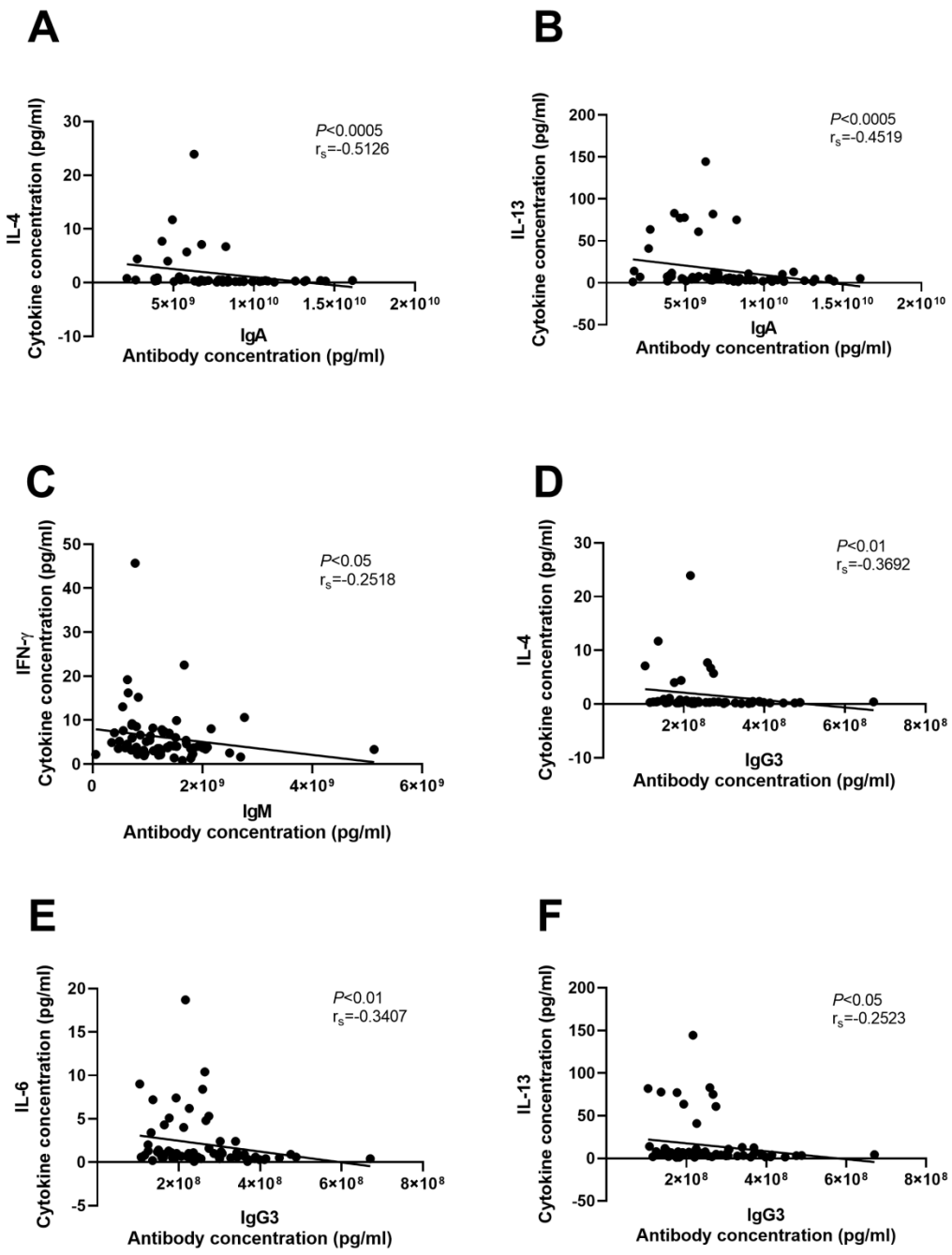


Figure 13. Serum antibody and plasma cytokine correlations. Serum IgA negatively correlated with plasma IL-4 levels (*P*<0.0005; r_s=-0.5126)(A). Serum IgA negatively correlated with plasma IL-13 levels (*P*<0.0005; r_s=-0.4519) (B). Serum IgM negatively correlated with plasma IFN-γ levels (*P*<0.05; r_s=-0.2518), although the correlation is weak(C).Serum IgG3 correlated negatively with plasma IL-4 levels (*P*<0.01; r_s=-0.3692), plasma IL-6 levels (*P*<0.01; r_s=-0.3407) and weakly with plasma IL-13 levels (*P*<0.05; r_s=-0.2523) (D-F). n=76

5. Discussion

Background

Immunoglobulins can be described as heterodimeric glycoproteins[1]. There are five main classes of immunoglobulins; IgA, IgD, IgE, IgG and IgM; with IgG further divided into the subclasses of IgG1, IgG2, IgG3 and IgG4[1,2]. Individual immunoglobulins can bind to antigen specific to the immunoglobulin in question; however as a population immunoglobulins can, bind to a vast set of antigens[1]. It is known that immunoglobulins function on two levels as they can both act as an antigen cell surface receptor allowing for cell signalling and activation and they can also act as soluble effector molecules whereby they can specifically bind to antigens resulting in antigen neutralisation[1].

Immunoglobulins and monoclonal antibodies

Immunoglobulin research has awarded the creation of numerous immunoglobulin applications as diagnostic and therapeutic agents[2]. Perhaps one of the greatest advances in implementing the knowledge gained through immunoglobulin research has been with respect to monoclonal antibodies. Monoclonal antibodies represent the highest growth segment within the biopharmaceutical field and monoclonal antibody therapies, such as Omalizumab (Xolair®, Novartis-Genentech) which targets IgE, offer real potential for treatment of severe asthmatic patients[2,4-7]. Therefore research which advances the current understanding of the immunoglobulin profile within the BAL and serum of asthmatic patients may offer real therapeutic insights into potential treatment options for asthma patients through the use of humanised monoclonal antibody therapy.

Demographics of the study cohort

The patient cohort in this study consisted of seventy six adult asthmatic patients in which the total antibody immunoglobulin IgA, IgD, IgE, IgG1, IgG2, IgG3, IgG4 and

IgM levels were measured in the bronchoalveolar lavage (BAL) and in time and patient matched serum samples. Within the cohort of seventy six adult asthmatic patients there were 28 males and 48 females. When stratified by asthma severity 34% (26/76) were classified as mild (GINA 1+2), 22% (17/76) were moderate (GINA 3) and 44% (33/76) were classified as severe asthmatics (GINA 4+5). When stratified by level of asthma control (ACQ-7), 37% (28/76) were controlled (ACQ-7<1.5) while 63% (48/76) were uncontrolled (ACQ-7≥1.5) asthmatics.

Nine patients within the study cohort were in receipt of oral steroids (mg) at the time of bronchoscopy (min 5 – max 30 mg) of which all nine patients in receipt of oral steroids were classified as severe asthmatics (GINA 4+5). 14% (11/76) of asthmatics were steroid naïve at time of bronchoscopy. 86% (65/76) of patients were in receipt of inhaled corticosteroids (ICS) (FDP 250) (min 250 – max 2000 FDP) at time of bronchoscopy. From this we are confident that the study group is robust and relatively unbiased to asthma factors such as asthma severity (GINA), asthma control (ACQ-7) and inhaled corticosteroid (ICS) treatment.

BAL and serum immunoglobulins

BAL and serum immunoglobulins IgA, IgD, IgE, IgG1, IgG2, IgG3, IgG4 and IgM were analysed by RayBiotech using a Quantibody Human Ig Isotype Array 1 which utilised sandwich-ELISA based technology, quantifiably measuring the eight human isotype immunoglobulins.

Immunoglobulin A (IgA)

Expressed mainly in its monomeric form within the serum IgA is often expressed as a dimer within the mucosal environment[1].IgA plays a vital protective role at mucosal surfaces and through methods such as direct neutralisation or the prevention of binding, IgA protects the host from bacteria, viruses and toxins[1]

It was discovered that 100% of patients had detectable levels of IgA in both the BAL and plasma samples. The IgA levels within the patient cohorts BAL and serum were

compared using the t-test with Welch's correction. Significant differences were observed between BAL IgA and serum IgA where the mean of the BAL IgA was 6255285 pg/ml and serum IgA mean was 7367716755 pg/ml and levels were significantly different (*P*<0.0001). IgA levels within the serum are believed to be at 15% of total immunoglobulins, however within mucosal surfaces IgA levels are significantly higher[1].Looking at potential correlations present between the BAL immunoglobulin A levels and the human cytokines interleukin- 1β (IL-1β), IL-4, IL-5, IL-6, IL-8, IL-10, IL-13, IL-17 and tumour necrosis factor-α (TNF-α) no significance was observed, n=76.

Similarly the serum immunoglobulin A levels were compared to the human cytokines interleukin- 1β (IL-1β), IL-4, IL-5, IL-6, IL-8, IL-10, IL-13, IL-17, tumour necrosis factor-α (TNF-α) and interferon-γ (IFN-γ) in the plasma samples a number of significant correlations were observed. Serum IgA negatively correlated with plasma IL-4 levels (*P*<0.0005; r_s=-0.5126). See figure 13 (A). Serum IgA negatively correlated with plasma IL-13 levels (*P*<0.0005; r_s=-0.4519). See figure 13 (B).

The significant correlation present between IgA and the plasma cytokine IL-4 is interesting as IL-4 plays a key role in allergic inflammation. The cytokine IL-4 is known to be associated with the development of allergic inflammation by driving differentiation of naïve T helper type 0 (T_H0) lymphocytes to a T helper type 2 (T_H2) response[14]. IL-4 plays a role in the induction of IgE dependent mast cell activation resulting in sudden allergic reactions[14]. The cytokine IL-4 is also capable of inducing the expression of the gene mucin which results in the hypersecretion of mucus a well-known characteristic feature of asthma[14].

The significant correlation existing between serum IgA and the plasma cytokine IL-13 is also of interest. IL-13 has been linked to many key asthma characteristics such as mucus hyper-secretion and airway hyper-responsiveness and IL-13 has been documented to be the central regulator in IgE synthesis[15].

Immunoglobulin D (IgD)

IgD was detectable in 37% (28/76) of BAL and 97% (74/76) of serum samples. IgD is found at low levels in the serum in comparison to other immunoglobulins. IgD can recognise and react to certain bacterial proteins and the binding to these bacterial proteins may result in the stimulation and activation of Bcells[1]. IgD can also be found in its membrane bound form on B cells when the B cells populate secondary lymphoid organs[1].

The IgD levels within the patient cohorts BAL and serum were compared using the t-test with Welch's correction. Significant differences were observed between levels of IgD in the BAL and IgD in the serum. BAL IgD (mean = 288710 pg/ml) and serum IgD (mean = 93002950 pg/ml) were significantly different (P<0.0001).

The levels of BAL IgD negatively correlated with the levels of IL-17 in the BAL (P<0.05; r_s=-0.7857). See figure 12 (A).

The cytokine IL-17 plays a key role in the pathobiology of asthma. The pro-inflammatory cytokine IL-17 is known to promote the production of cytokines and chemokines in bronchial epithelial cells[16]. IL-17 has also been implicated in airway remodelling, neutrophilic inflammation and asthma severity[16]. IL-17 is produced in high amounts by T helper type 17 (TH17) cells and TH17 cells have in *in vitro* studies been shown to induce a strong proliferative response within B cells[17].

Immunoglobulin E (IgE)

IgE is associated with hypersensitivity and allergic[1]. While IgE is present at low concentrations (<0.01%) within the serum it acts as a very potent immunoglobulin[1]. IgE is expressed as a monomer and upon allergen exposure, circulating allergen specific IgE binds to the $F_{c\varepsilon}$RI receptors, on immune cells such as mast cells and basophils, leading to crosslinking and release of inflammatory mediators[1,4]. Currently monoclonal antibody therapy exists with respect to IgE in asthma in the form of Omalizumab. Omalizumab (Xolair®) (Novartis-Genentech), the recombinant

humanised monoclonal antibody, binds to the IgE antibody at the Fc portion which reduces the amount of free IgE, stops IgE from binding to inflammatory cell IgE receptors and reduces IgE receptor ($F_{c\varepsilon}RI$ and $F_{c\varepsilon}RII$) density on effector cells, all of which prevent an inflammatory cascade from occurring[4,5].

Within this study cohort 28% (21/76) of patients had IgE detectable within the BAL while IgE was at undetectable levels in the serum under the Quantibody Immunoglobulin Array protocols for limits of detection.

No significant correlations were found to exist between IgE in the patient cohorts BAL and the cytokines interleukin- 1β (IL-1β), IL-4, IL-5, IL-6, IL-8, IL-10, IL-13, IL-17, tumour necrosis factor-α (TNF-α) present within the patient BAL.

Immunoglobulin G

IgG consists of the subclasses IgG1, IgG2, IgG3 and IgG4 which are ranked by number based on the serum levels expected of these immunoglobulins within a healthy population whereby total IgG represents 75% of total serum immunoglobulin and IgG1 = 67%, IgG2=22%, IgG3=7% and IgG4 = 4%[1]. All are expressed as monomers and IgG key function is related to both the secondary immune response and as a neutralization agent to toxins and viruses within the host[1].

IgG1 was detectable in 86% (65/76) of BAL and 100% (76/76) of serum samples. BAL IgG1 levels (mean = 1593259 pg/ml) and serum IgG1 levels (mean = 2617043155 pg/ml) were significantly different ($P<0.0001$) when compared using a t-test with Welch's correction, n=76. When BAL IgG1 was analysed against BAL cytokine levels it was found that IgG1 positively correlated with BAL IL-6 levels ($P<0.01$; $r_s=0.3251$) and BAL TNF-α levels ($P<0.05$; $r_s=0.3280$). See figure 12 (C-D). IL-6 is a pleotrophic cytokine with the ability to act in an anti-inflammatory and pro-inflammatory manner. It is recognised that IL-6 is produced in response to the recognition of microbes by pattern associated molecular patterns[18]. It is interesting that IL-6, known for its pro-inflammatory abilities produced in response to microbial

presence is significantly linked to IgG1 levels as the immunoglobulin IgG1 is known to function within the adaptive immune response[1]. TNF-α is also recognised for its response to the presence of microbes and plays a key role in the hosts immediate response to the presence of microbes before the adaptive immune response is activated[19].

IgG2 was detectable in 95% (72/76) of BAL and 100% (76/76) of patient serum. BAL IgG2 (mean = 1949990 pg/ml) and serum IgG2 (mean = 2199076095 pg/ml) were significantly different (P<0.0001). However with respect to BAL and plasma cytokine levels no correlations with respect to BAL and serum IgG2 levels were found to exist.

IgG3 was detectable in all of the patients BAL and serum samples (100%). BAL IgG3 (mean = 275453 pg/ml) and serum IgA (mean = 257423140 pg/ml) were significantly different (P<0.0001).No correlation was found to be present with respect to BAL IgG3 and BAL cytokine levels. However serum IgG3 correlated negatively with plasma IL-4 levels (P<0.01; r_s=-0.3692), plasma IL-6 levels (P<0.01; r_s=-0.3407) and weakly with plasma IL-13 levels (P<0.05; r_s=-0.2523). See figure 13 (D-F).

IgG4 was detectable in 96% (73/76) of patient BAL and 100% of serum samples. BAL IgG4 (mean = 351389 pg/ml) and serum IgG4 (mean = 229551172 pg/ml) were significantly different (P<0.0001). When IgG4 BAL and serum levels were analysed against the respective cytokine levels IgG4 did appear to significantly correlated with the plasma cytokine TNF-α (P<0.05; r_s=0.2468) however the Spearman r value indicated this was a very weak correlation and so it was not included in further analysis.

Immunoglobulin M (IgM)

IgM is the first immunoglobulin expressed during B cell development, where naïve B cells express IgM in its monomeric form within their surface. Upon maturation and antigenic stimulation IgM is usually expressed in its pentameric form making

IgM highly successful in opsonizing antigens for elimination and fixing complement[1]. IgM can be considered as a primary immune response antibody and is often associated with immunogen or pathogen exposure[1]. IgM provides both the first initial response to an antigen and also upon subsequent exposure IgM plays a regulatory role in response to an antigen[3].

IgM was detectable within all of the cohorts BAL and serum samples. BAL IgM (mean = 985106 pg/ml) and serum IgM (mean = 1291739719 pg/ml) were significantly different (P<0.0001). With respect to cytokine levels BAL IgM correlated with BAL TNF-α levels (P<0.05; r_s=0.2559). Serum IgM correlated with plasma IFN-γ levels (P<0.05; r_s=-0.2518). Interferon-γ (IFN-γ) plays a vital role in pathogen recognition and elimination and is responsible for the mediation of a wide variety of biological activities[20].As previously mentioned TNF-α is recognised for its response to the presence of microbes and plays a key role in the host immediate response to the presence of microbes before the adaptive immune response is activated[19]. It is interesting that both the BAL immunoglobulin levels of IgG1 and IgM correlated with the levels of the cytokine TNF-α. It is recognised that IgM can play a regulatory role in response to an antigen and can accelerate the production of IgG therefore it is interesting that both IgG1 and IgM appear to be linked to the cytokine TNF-α in the asthma patient cohorts immune response[1].

It should be noted that while there is a statistically significant difference between the BAL and serum levels this may in part be explained by the nature of the sample, whereby the antibodies present within the bronchoalveolar lavage are diluted whereas the serum levels are as would be detected in the blood.

Conclusions

Immunoglobulin research has awarded the creation of numerous immunoglobulin applications as diagnostic and therapeutic agents[2]. Research which advances the current understanding of the immunoglobulin profile within the BAL and serum of asthmatic patients may offer real advances in potential treatment options for asthma patients.

6. Supplementary

Supplementary Table 1: The serial standard concentration (pg/ml) of the immunoglobulin antigens of interest.

(pg/ml)	Ctrl	Std7	Std6	Std5	Std4	Std3	Std2	Std1
IgA	0	274	823	2469	7407	22222	66667	200000
IgD	0	69	206	617	1852	5556	16667	50000
IgE	0	69	206	617	1852	5556	16667	50000
IgM	0	137	412	1235	3704	11111	33333	100000
IgG1	0	549	1646	4938	14815	44444	133333	400000
IgG2	0	549	1646	4938	14815	44444	133333	400000
IgG3	0	69	206	617	1852	5556	16667	50000
IgG4	0	69	206	617	1852	5556	16667	50000

7. References

1. Schroeder HW, Jr., Cavacini L. Structure and function of immunoglobulins. *The Journal of allergy and clinical immunology.* 2010;125(2 Suppl 2):S41-S52.
2. Gautam S, Loh K-C. Immunoglobulin-M purification — Challenges and perspectives. *Biotechnology Advances.* 2011;29(6):840-849.
3. Louis AG, Gupta S. Primary selective IgM deficiency: an ignored immunodeficiency. *Clinical reviews in allergy & immunology.* 2014;46(2):104-111.
4. Thomson NC, Chaudhuri R. Omalizumab: clinical use for the management of asthma. *Clin Med Insights Circ Respir Pulm Med.* 2012;6:27-40.
5. Bang LM, Plosker GL. Spotlight on omalizumab in allergic asthma. *BioDrugs : clinical immunotherapeutics, biopharmaceuticals and gene therapy.* 2004;18(6):415-418.
6. Chung KF. Targeting the interleukin pathway in the treatment of asthma. *Lancet.* 2015;386(9998):1086-1096.
7. Al Said A, Cushen B, Costello RW. Targeting patients with asthma for omalizumab therapy: choosing the right patient to get the best value for money. *Ther Adv Chronic Dis.* 2017;8(2-3):31-45.
8. Miller MR, Hankinson J, Brusasco V, et al. Standardisation of spirometry. *The European respiratory journal.* 2005;26(2):319-338.
9. Graham BL, Steenbruggen I, Miller MR, et al. Standardization of Spirometry 2019 Update. An Official American Thoracic Society and European Respiratory Society Technical Statement. *Am J Respir Crit Care Med.* 2019;200(8):e70-e88.
10. Juniper EF, Bousquet J, Abetz L, Bateman ED. Identifying 'well-controlled' and 'not well-controlled' asthma using the Asthma Control Questionnaire. *Respir Med.* 2006;100(4):616-621.
11. Du Rand IA, Blaikley J, Booton R, et al. British Thoracic Society guideline for diagnostic flexible bronchoscopy in adults: accredited by NICE. *Thorax.* 2013;68 Suppl 1:i1-i44.
12. Hunt EB, Ward C, Power S, et al. The Potential Role of Aspiration in the Asthmatic Airway. *Chest.* 2017;151(6):1272-1278.
13. Kowalski CJ. On the Effects of Non-Normality on the Distribution of the Sample Product-Moment Correlation Coefficient. *Journal of the Royal Statistical Society Series C (Applied Statistics).* 1972;21(1):1-12.
14. Steinke JW, Borish L. Th2 cytokines and asthma. Interleukin-4: its role in the pathogenesis of asthma, and targeting it for asthma treatment with interleukin-4 receptor antagonists. *Respiratory research.* 2001;2(2):66-70.
15. Rael EL, Lockey RF. Interleukin-13 signaling and its role in asthma. *The World Allergy Organization journal.* 2011;4(3):54-64.
16. Chesne J, Braza F, Mahay G, Brouard S, Aronica M, Magnan A. IL-17 in severe asthma. Where do we stand? *Am J Respir Crit Care Med.* 2014;190(10):1094-1101.
17. Mitsdoerffer M, Lee Y, Jäger A, et al. Proinflammatory T helper type 17 cells are effective B-cell helpers. *Proceedings of the National Academy of Sciences.* 2010;107(32):14292-14297.
18. Poynter ME, Irvin CG. Interleukin-6 as a biomarker for asthma: hype or is there something else? *The European respiratory journal.* 2016;48(4):979-981.
19. Brightling C, Berry M, Amrani Y. Targeting TNF-alpha: a novel therapeutic approach for asthma. *The Journal of allergy and clinical immunology.* 2008;121(1):5-12.
20. Kak G, Raza M, Tiwari Brijendra K. Interferon-gamma (IFN-γ): Exploring its implications in infectious diseases. *Biomolecular Concepts.* Vol 92018:64.

Thesis Summary

Within this thesis we have reported novel findings which will contribute to a better understanding of the role the microbiome plays within the lungs of clinically diagnosed asthmatic patients. The prevalence of asthma is increasing in the western world with more than 300 million people worldwide believed to affected by this chronic respiratory disorder. Through this thesis we have dissected the immune microbe dialogue at play within the asthmatic lung. The findings within this thesis are novel, and we feel add to recent discoveries within the field of microbiome research, with an emphasis on the potential contribution the lung microbiome may play in the pathogenesis of asthma.

Within this study we were fortunate to have access to a large well-defined and stratified asthma patient cohort thanks to Dr Des Murphy and his asthma clinic at Cork University Hospital. As discussed in *Chapter 2 – Study Cohorts'* this thesis consisted of a number of clinical sampling components. We believe the possession of such a cohort adds greatly to lung microbiome studies as through the thorough analysis of patient demographics such as asthma severity (GINA), asthma control (ACQ-7), patients habitual residence (Rural or Urban), patients spirometry. FeNO, BMI, ICS usage and hospital blood analysis it is possible to investigate a multitude of questions with respect to the asthmatic immune microbe dialogue hypothesis posed in this thesis. Through the availability such data it was possible to stratify patients by GINA type (severity) or ACQ-7 (level of control) and in doing so we not only investigated the immune microbe dialogue at play within asthmatics in general but also within various subgroups of asthma such as controlled or uncontrolled asthmatics (ACQ-7) or mild, moderate or severe asthmatics based on severity of disease (GINA). Through this we believe greater insights have been gained.

Chapter 3 – Fungi in Asthma involved a published study of the mycobiome in the airways of 69 adult asthmatics. This included the striking finding that fungal spores and hyphae were detected microscopically in 70% of the cohort. Molecular analysis demonstrated that 86% of patients had evidence of fungal presence within their

BAL and almost half had detectable *Aspergillus fumigatus* in the airways by qPCR analysis. Asthma severity was associated with BAL neutrophils and the detection of fungal DNA correlated with BAL neutrophil counts. Fungal β-glucans represent the most abundant cell wall polysaccharides found in fungi and can be used *in vitro* in order to model its pathophysiology in asthma, representing an exciting future direction that this research could take. Our work in *Chapter 3 – Fungi in Asthma* resonates well with emergent studies showing that exposure to bacterial and fungal components may imprint epigenetic memory in inflammatory cells of the innate immune system.

Chapter 4 – The Microbiome in Asthma implemented both Next Generation Sequencing and qPCR technology in order to investigate the lung microbiome. In doing this we fell a defined picture of the lung microbiome can be discovered as the techniques are complementary of each other. We confirmed the presence of previously published findings with respect to a number of bacteria while at the same time we discovered new species by both qPCR and NGS. The implementation of both qPCR and NGS offered a deeper insight into the microbes present within the lungs of a cohort of asthmatic patients than the implementation of only one of the techniques would have revealed. For example, during NGS analysis it was determined that *Micromonospora* was dominant at the genus level, a finding not currently associated with the microbiome of the lung. Through the use of qPCR this finding was confirmed and 85% (49/73) of patients had detectable levels of *Micromonospora* within the BAL by qPCR. Another exciting finding upon further analysis of the NGS dataset was the prevalence of *Ralstonia* by NGS, a genus which has been linked to the Cystic Fibrosis lung. While *Ralstonia* was not also determined by qPCR family members such as *Pseudomonas aeruginosa* (34%) and *Pseudomonas fluorescens* (88%) were detected by qPCR. Indeed *Ralstonia* and *Pseudomonas* are closely related genetically and this overlap could be investigated at the genome level. In the future it would also be possible to design specific qPCR for *Ralstonia* species to differentiate these and also apply culture specific means. While *Chapter*

4 – The Microbiome in Asthma mainly focused on the bacterial kingdom subsequent analysis of the fungal, viral and other eukaryote reads present within the dataset.

Chapter -5 – The Effect of Immunomodulation Therapy on the Microbiome of the Adult Asthmatic Lung investigated the effects of anti-IgE (Omalizumab) treatment on the lung microbiome in a subset of nine severe adult asthmatic patients. *Chapter 6 – The Microbiome of the Lung* investigated the effect of anti-IL5 therapy on the lung microbiome in a cohort of eight severe adult asthmatic patients. While both groups of patients received monoclonal antibody therapy the interaction of the monoclonal antibodies in question with the host is very different. Within these studies patient cytokines and immune cells have been linked to certain bacterial species and clinical data. It would therefore be of interest to investigate this phenomenon further.

Monitoring of the lung microbiota during treatment may allow for identification of therapeutic benefit but also susceptibility to respiratory tract infections. In the future it would be of interest to investigate the two asthma cohorts over a longer period of time, analysing BAL from various treatment time-points may help pinpoint changes to the lung microbiota with respect to therapy. It would also be of interest to investigate other asthma approved monoclonal antibodies such as Mepolizumab and Benralizumab, two other anti-IL-5 monoclonal antibodies, in order to investigate potential difference such drugs may have on the patients' lung microbiome. Novel treatment protocols such as those implemented in *Chapter 5* and *Chapter 6* offer a lifeline to severe, difficult asthmatic therefore further understanding the microbiome changes may aid the treatment of such patients.

Within *Chapter 7 – Epithelial Response to Inflammatory Stimuli* the response of asthmatic airway bronchial epithelial cells (BEAS-2B) to microbial compounds, cytokines and metabolites was investigated. The stimulation of cells with microbial compounds including LPS derived from *Escherichia coli*, *Porphyromonas gingivalis* and *Pseudomonas aeruginosa* and Pam3CSK4, cytokines including IL-1β, IL-4, IL-7 and IL-17A and metabolites including Indole Acetic Acid and Sodium Acetate alone

or in combination resulted in a significant change in the relative expression of an array of targets of interest including IL-6, CXCL8, EGR1, IFN-γ, TGFβ, TSLP, HDAC6, IL-36γ, GPR41, GPR109A and GPR109B**.** Many facets of allergic sensitisation are controlled by the airway epithelium and it in turn plays a key role in allergic inflammation, remodelling and bronchial hyper-reactivity. Therefore, experiments targeting the airway epithelium with the goal of further understanding the pathophysiology of asthma could have many beneficial ramifications in terms of targets for new therapies and advancements in general asthma understanding and management. Overall, the research aim to investigate the response of bronchial epithelial cells to microbial compounds, cytokines and metabolites individually and in combination and to investigate the resulting immune reaction upon stimulation was carried out. In the future this research aim could be expanded to include both the use of primary bronchial epithelial cell culture models and also the addition of further stimulants of interest.

Chapter 8 – Bronchial brushings and inflammatory stimuli consisted of an investigation as to the effectiveness of using bronchial brushings as a potential method to investigate the inflammatory response of the asthmatic cohort. Patient bronchial cDNA revealed a patient specific immune profile by qRT-PCR with IL-1β detectable in 39%, IL-5 detectable in 15%, IL-17F detectable in 22%, CCL5 in 98%, CXCL8 in 98%, CCL11 7%, CCL20 in 7%, EGR1 in 98%, INF-γ in 76%, TSLP in 59%, TGFβ-1 in 93%, TGFβ-2 in 68% and TGFβ-3 in 85% of cDNA from the patients bronchoscopy bronchial brush, n-=41 with subsequent significance found to certain patient demographics upon further analysis. This is an exciting finding as bronchial brush cDNA analysis could easily be implemented within lung microbiome study protocols as an adjunct means of analysing the patient epithelial cell profile.

Chapter 9 – Primary Cell Culture Techniques is an exciting chapter in that it highlights potential future avenues this research can take. The implementation of various experiments such as ALI culture, Transepithelial Electrical Resistance (TEER)

analysis, Ussing chamber analysis of barrier function, glycoprotein mucin analysis and electron microscopy analysis of extracellular vesicles all offer exciting new experimental additions to existing research protocols. Overall primary epithelial differentiated ALI cells demonstrated novel insights as to how cell culture can be used for a variety of experiments to reveal the real-life responses of epithelial cells. The airway epithelium can provide key insights into the pathophysiology of asthma and can potentially lead to the development of a system to improve the treatment of asthma; therefore, it is a hope that in the future through the expertise gained during the ERS fellowship it would be possible to develop primary bronchial epithelial cell (PBEC) culture facilities and culture PBEC cells obtained from patient bronchial brushings during bronchoscopy procedures at Cork University Hospital.

Chapter 10 – Immunoglobulins and Asthma investigated the immunoglobulins IgA, IgD, IgE, IgG1, IgG2, IgG3, IgG4 and IgM within the BAL and serum of 76 adult asthmatic patients. This is an exciting study as immunoglobulins play a vital role in the host immune response and insights into immunoglobulins present within the an asthmatic cohort may lead to further knowledge of the complex immunoglobulin immune response at the mucosal and systemic level and may aid in the discovery of novel therapeutic avenues.

Overall I believe this thesis contains novel insights into many different facets of asthma research from the host to the microbial perspective and the combination of these areas is the future for therapy development. I am looking forward to building on these findings in future works.

Future Directions

As highlighted within the thesis summary the findings contained within this thesis pave the way for exciting and novel research to be continued and key discoveries made during the course of this PhD will be further interrogated by the research group.

Future research directions envisioned by the group include further investigations with respect to the exciting and novel finding, the presence of *Micromonospora*, within the lungs of the asthmatic patient cohort. The presence of *Micromonospora* within the lungs of asthmatic patients has, to the best of our knowledge, been unreported. While linked to conditions such as 'Farmers Lung', clinically referred to as extrinsic allergic alveolitis or hypersensitivity pneumonitis, *Micromonospora* has not been examined to date in lung microbiome sequencing studies.

Micromonospora is widely distributed in nature and is known to produce both antimicrobial and antifungal agents which is of great excitement to the group and poses the question as to the effect the presence of this bacteria may have upon the overall lung microbiome in asthmatic patients. As a bacteria, *Micromonospora* possesses a complex lifecycle, with the ability to differentiate into both substrate mycelia and spores. Given the high number of patients who, in Chapter 3, displayed visible hyphae and spores by microscopy (70%) it would be exciting in the future to investigate the lifecycle of *Micromonospora* within the lungs of the asthmatic patients and further interrogate if its presence is linked to the high number of patients, 70%, who displayed visible signs of spores by microscopy.

Looking back the Next Generation Sequencing data it was exciting that *Micromonospora aurantica* was the most dominant microbe present in 51/70 patients. The Next Generation Sequencing findings of high abundance of *Micromonospora* species within the BAL of the asthmatic cohort lead to the investigation of its presence by qPCR within all asthma cohorts present within this PhD thesis. It was exciting that upon confirmation of its presence by qPCR within 85% of the cohort, further analysis of data revealed correlations present between

the presence of *Micromonospora* by qPCR and Next Generation Sequencing findings of *Micromonospora aurantiaca* ($P<0.05$) and *Micromonospora globosa* ($P<0.05$).

Micromonospora globosa was found subsequently to correlate with BAL IL-13 ($P<0.05$), plasma IL-1β ($P<0.05$) and plasma IL-8 ($P<0.0001$) and *Micromonospora aurantiaca* was found to correlate with plasma IL-1β ($P<0.05$) and plasma IL-8 ($P<0.0005$) levels. Given its high abundance within the asthma cohort by both qPCR and Next Generation Sequencing techniques and its correlation to immune cytokines such as IL-1β and IL-8 and given the exciting fact that there is little research present with respect to the presence of *Micromonospora* within the lungs of asthmatic patients we are most interested to continue researching this novel and exciting finding.

We relish the opportunity to implement the model systems discussed within Chapter 7, which would implement a high throughput cell culture model system and Chapter 9, which through the use of primary cell culture and Air Liquid Interface culture systems which would enable the utilisation of a *in vivo* model system in future studies of *Micromonospora* enabling us to research the interplay present between the airway epithelium and *Micromonospora.*

Through culture independent techniques *Micromonospora* has been found within the BAL of asthmatic patients. In the future we would like to implement culture dependent techniques to investigate the microbe *Micromonospora.* Building on this aim we also would like to investigate the interaction of *Micromonospora* within the airway epithelium.

The advancement of primary Air Liquid Interface (ALI) cell culture allows for a physiologically robust system whereby the primary human epithelial cells are fully differentiated in a pseudostratified and polarised manner, with differentiated cells including cilia and goblet cells. This ALI model enables primary epithelial cells to develop Transepithelial Electrical Resistance (TEER) and represents a model system to elucidate the pathogenic mechanisms present in respiratory disorders such as asthma and would also enable us to study the potential effects of *Micromonospora* upon the airway epithelium.

It is interesting that from our findings *Micromonospora* presence ensues an immune reaction. Through the implementation this *in vivo* modelling technique in the future there is huge potential for novel findings.

Overall, through the various chapters of this thesis we have uncovered a number of exciting and novel research findings to which a great number of future research avenues exist. As highlighted by our future plans with respect to *Micromonospora* we hope to build upon the findings of this thesis, adding to the growing body of evidence published with respect to the importance of the microbiome with regards to the human host. We look forward to building upon the findings of this thesis to advance the knowledge base with respect to the microbiome and asthma.

Appendix

Academic achievements during this PhD

Publications

Sullivan A, Hunt E, MacSharry J, Murphy DM. The Microbiome and the Pathophysiology of Asthma. *Respiratory Research.* 2016;17(1):163.

Hunt EB, Ward C, Power S, **Sullivan A**, Pearson JP, Lapthorne S, O'Byrne PM, Eustace J, Plant BJ, Maher MM, MacSharry J, Murphy DM. The Potential Role of Aspiration in the Asthmatic Airway. *Chest.* 2017;151:1272-1278.

Hunt EB, **Sullivan A**, Gavin J, MacSharry J, Murphy DM. Gastric Aspiration and its Role in Airway Inflammation. *The Open Respiratory Medicine Journal.* 2018;12:1-10.

Sullivan A, Hunt EB, Ward C, Lapthorne S, Eustace J, Fanning LJ, Plant BJ, O'Byrne PM, MacSharry J, Murphy DM. The Presence of *Aspergillus fumigatus* in asthmatic airways is not clearly related to clinical disease severity. *Allergy.* 2019 In press.

Manuscripts in preparation

Immunoglobulins and Asthma

Epithelial Cell Stimulation with Cytokine, Microbial and Metabolite compounds.

The Microbiome and Asthma

The Microbiome and Aspiration

Oral Presentations

'A combination of cytokines and LPS increase pro-inflammatory chemokine expression in bronchial epithelial cells'. APC Microbiome Ireland – Imperial College London Postgraduate Symposium, September 2015, Cork, Ireland.

'Aiming at asthma – the asthmatic immune microbe dialogue'. APC Microbiome Ireland Research Forum, December 2016, Cork, Ireland.

‘Aiming at asthma – the asthmatic immune microbe dialogue’. APC Microbiome Ireland Innovation Forum, May 2017, Cork, Ireland.

‘A study to define microbiome subtypes in the adult asthmatic airway’. Notable Abstracts in Asthma – European Respiratory Society Congress, September 2017, Milan, Italy.

‘Detecting the presence of Aspergillus in the asthmatic airway and its relationship to disease severity’. Irish Thoracic Society Annual Scientific Meeting, November 2017, Limerick, Ireland.

‘Detecting the presence of Aspergillus in the asthmatic airway and its relationship to disease severity’. New Horizons Medical Conference, December 2017, Cork, Ireland.

Poster Presentations

‘A combination of cytokines and LPS increase pro-inflammatory chemokine expression in bronchial epithelial cells’. New Horizons Medical Conference, December 2015, Cork, Ireland.

‘A study to define the microbiome of the asthmatic airway’. APC Microbiome Ireland – Imperial College London Postgraduate Symposium, October 2016, London, UK.

‘A study to define the microbiome of the asthmatic airway’. New Horizons Medical Conference, December 2016, Cork, Ireland.

‘Presence of Aspergillus in the asthmatic airway and its relationship to disease severity’. European Respiratory Society Congress, September 2017, Milan, Italy.

‘An investigation into adult asthma to define the microbiome subtypes present’. Irish Thoracic Society Annual Scientific Meeting, November 2017, Limerick, Ireland.

‘An investigation into adult asthma microbiota subtypes and the association with disease severity’. International Human Microbiome Congress, June 2018, Killarney, Ireland.

‘Detecting the presence of fungal signals in the asthmatic airway’. European Respiratory Society Congress, September 2018, Paris, France.

‘Detecting the presence of fungal signals in the asthmatic airway’. New Horizons Medical Conference, December 2018, Cork, Ireland.

Additional Conferences Attended

British Thoracic Society Winter Meeting, December 2017, London, UK.

North East Postgraduate Conference, November 2018, Newcastle upon Tyne, UK.

Future Conference Presentations

Two abstracts chosen for the 2020 ERS Congress which will take place online in September 2020

Awards Received

Poster prize winner – New Horizons Medical Conference December 2016, Cork, Ireland.

European Respiratory Society Young Scientist Sponsorship – European Respiratory Society September 2017, Milan, Italy.

ITS–GSK-BTS Travel Bursary – British Thoracic Society Winter Meeting December 2017, London, UK.

ITS-GSK-ERS Travel Bursary – European Respiratory Society Congress September 2018, Paris, France.

ERS International Short Term Research Training Fellowship – Institute of Cellular Medicine, Newcastle University, October – December 2018, Newcastle upon Tyne, UK.

European Respiratory Society Young Scientist Sponsorship – European Respiratory Society. September 2020

Modules

PG6001 – STEPS Scientific Training for Enhanced Postgraduate Studies

PG6015 – An Introduction to Research Ethics

Postgraduate Cert in Innovation Commercialisation and Entrepreneurship

AC6301 – Innovation Finance

MG6705 – Marketing for Technology Entrepreneurs

IS6306 – Technology Business Planning

IS6307 – Creativity and Opportunity Recognition

LW6104 – Intellectual Property Law for Entrepreneurs

MG6704 – Internationalisation and Sales

Certificates

GDPR Compliance in the Republic of Ireland Workplace Fundamentals – 2018

ERS International Short Term Research Training Fellowship – 2018/2019

Research Integrity – 2019

Postgraduate Cert – Innovation, Commercialisation and Entrepreneurship – 2019